Green Energy and Technology

Atul Sharma
Amritanshu Shukla
Lu Aye *Editors*

Low Carbon Energy Supply

Trends, Technology, Management

Springer

Green Energy and Technology

Climate change, environmental impact and the limited natural resources urge scientific research and novel technical solutions. The monograph series Green Energy and Technology serves as a publishing platform for scientific and technological approaches to “green”—i.e. environmentally friendly and sustainable—technologies. While a focus lies on energy and power supply, it also covers “green” solutions in industrial engineering and engineering design. Green Energy and Technology addresses researchers, advanced students, technical consultants as well as decision makers in industries and politics. Hence, the level of presentation spans from instructional to highly technical.

More information about this series at http://www.springer.com/series/8059

Atul Sharma · Amritanshu Shukla
Lu Aye
Editors

Low Carbon Energy Supply

Trends, Technology, Management

Springer

Editors
Atul Sharma
Rajiv Gandhi Institute of Petroleum Technology
Amethi, Uttar Pradesh
India

Lu Aye
Melbourne School of Engineering
University of Melbourne
Melbourne, VIC
Australia

Amritanshu Shukla
Division of Sciences and Humanities
Rajiv Gandhi Institute of Petroleum Technology
Amethi, Uttar Pradesh
India

ISSN 1865-3529 ISSN 1865-3537 (electronic)
Green Energy and Technology
ISBN 978-981-10-7325-0 ISBN 978-981-10-7326-7 (eBook)
https://doi.org/10.1007/978-981-10-7326-7

Library of Congress Control Number: 2018941993

© Springer Nature Singapore Pte Ltd. 2018
This work is subject to copyright. All rights are reserved by the Publisher, whether the whole or part of the material is concerned, specifically the rights of translation, reprinting, reuse of illustrations, recitation, broadcasting, reproduction on microfilms or in any other physical way, and transmission or information storage and retrieval, electronic adaptation, computer software, or by similar or dissimilar methodology now known or hereafter developed.
The use of general descriptive names, registered names, trademarks, service marks, etc. in this publication does not imply, even in the absence of a specific statement, that such names are exempt from the relevant protective laws and regulations and therefore free for general use.
The publisher, the authors and the editors are safe to assume that the advice and information in this book are believed to be true and accurate at the date of publication. Neither the publisher nor the authors or the editors give a warranty, express or implied, with respect to the material contained herein or for any errors or omissions that may have been made. The publisher remains neutral with regard to jurisdictional claims in published maps and institutional affiliations.

Printed on acid-free paper

This Springer imprint is published by the registered company Springer Nature Singapore Pte Ltd.
The registered company address is: 152 Beach Road, #21-01/04 Gateway East, Singapore 189721, Singapore

Foreword

The heat-trapping nature of carbon dioxide and other gases was found in the mid of nineteenth century. The current global warming trend is of particular significance because most of it is extremely likely to be the result of the man-made activity since the mid-twentieth century and proceeding at a rate that is recorded over several decades. Due to the latest development in the earth-orbiting satellites and other technological advances, which have enabled scientists to understand the image, collecting many different types of data about our globe and its climate on a global scale. Ice cores drawn from the mountain glaciers showed that the Earth's climate responds to changes in greenhouse gas levels. There is no question that increased levels of greenhouse gases in the earth atmosphere must cause the earth to warm in response.

Global demand for energy is increasing too fast due to the population and economic growth, especially in emerging market economies around the globe. While accompanied by greater prosperity, rising demand creates a lot of new challenges to manage their energy demand in the entire world. Energy security concerns can emerge as more consumers require ever more energy resources to fulfil their energy demand. The higher consumption of fossil fuels leads to higher greenhouse gas emissions, particularly carbon dioxide (CO_2), which contribute to global warming. At the same time, the number of people without access to electricity remains too high.

This climate objective (<2 °C/<450 ppm) is confirmed at every subsequent annual United Nations climate conference, and the global climate targets are further refined in the 2015 Paris Agreement. The Paris climate agreement is an agreement within the United Nations Framework Convention on Climate Change (UNFCCC) dealing with greenhouse gas emissions mitigation, adaptation and finance starting in the year 2020. This was based on the latest scientific insights, which demonstrate that the severity of a 2 °C rise in the average global temperature is even more crucial than previously thought. Since the adoption of the Paris Agreement, the consensus is that in order to avoid detrimental climate change, global warming must be limited to well below 2 °C and preferably to 1.5 °C. This also implies a need to remain well below 450 ppm.

The Intergovernmental Panel on Climate Change (IPCC) had reported that the world will have to totally phase out fossil fuels in power generation by the end of the century and reduce their use to 20% by 2050.

These developments have, obviously, led to the search for commercially exploitable other sources of energy that while meeting human needs do not cause further damage to the environment for the sustenance of our planet. The return to renewables will help mitigate climate change is an excellent way, however, needs to be sustainable in order to ensure a sustainable future and bequeath future generations to meet their energy needs. It is also expected that energy mix of the planet will change substantially in the coming years.

It is, indeed, a very timely effort by the editors, known to me for over ten years now, from the Rajiv Gandhi Institute of Petroleum Technology (RGIPT) and University of Melbourne, to have come out with a book that discusses the myriad ways in which the natural resources of our well-endowed country can be made use of for meeting the energy needs of our millions of citizens without damage to the environment.

In the course of my interactions with the professors of RGIPT during their visit to Kun Shan University, Tainan, Taiwan, R.O.C., we had often discussed the likely energy scenarios in the days ahead. During such discussions, the need to publish a book on low carbon energy supply was felt. I congratulate the editors for having come out with the book which will be of immense help to students, practicing managers and policymakers alike.

Tainan, Taiwan, R.O.C.

Prof. H. M. Chou
Professor and Dean
Department of Mechanical Engineering
Kun Shan University

Preface

The major greenhouse gas (GHG) emissions have been released by the usage of fossil-based primary fuels to produce electricity, heat or motion. This means that it is almost certainly impossible to reduce GHG concentrations in upper atmosphere to sustainable levels unless large quantities of low carbon energy resources can be taken on-stream to substitute primary fossil fuels. Today, in the context of the decent agenda of sustainable economic growth, including concerns about the global warming, climate change are very important issues. These include environmental and social impacts and the question of the electricity generation and fuel production processes as well as associated emissions. The earth’s environment has been negatively impacted during the production, distribution and consumption of energy through the usage of non-renewable energy resources. Low carbon energy supply-based criteria have been promoted in several years into the front line of energy policy, which also showed that how we address our energy needs on a more sustainable basis. At this moment, the whole world is continuing consuming fossil-based energy for social upliftment, economic development, the advancement of knowledge and improvement of the human condition.

The energy originated from various energy resources and sources have been consumed for human's activities across every single domestic, commercial, industrial and transport sector, across every country. The world total energy demand is also expected to increase and the share of energy supplied in the form of electricity is likely to rise rapidly. Meeting the needs of the present energy demand without compromising the needs of the future, the humanity has to pay attention to the low carbon energy supply-based technologies which harness non-exhaustible environmentally friendly renewable energy sources.

The main renewable energy sources and resources include solar, wind, hydro, geothermal, biomass, biogas and biofuels. They are available and distributed worldwide to meet the expanding energy demands without negative environmental impacts. However, the current renewable energy share is small in the worldwide energy production. The renewable energy also offers a method to increase the income, improves the trade balances, contributes to industrial development and creates jobs. It is an acknowledged fact that the renewable energy share should have been much higher than that of current in favour of the environment, which is an important issue globally. Almost every country pays much attention to renewable energy sources, due to the ongoing environmental challenges, which may be solved only by the usage of renewables. Many countries are making significant efforts to increase renewable energy share as much as they can within economic and political constraints.

The aim of this book is to share the latest developments and advances in materials and processes involved in the energy generation, transmission, distribution, storage and policies, and the chapters were contributed by researchers in the energy and materials field, using original materials. This book may be used as a reference for college/university/training institute/professionals. It may also be referred in green energy-related laboratories, industries and academic libraries as well as used as a reference book for the "Alternative Energy Sources, Renewable Energy Resources, Climate Change, Energy Sustainability, Energy Policies, etc". for undergraduate and graduate students. The book presents a timely combination of research and practice explained in a simple and comprehensive manner.

Jais, Amethi, UP, India Atul Sharma
Jais, Amethi, UP, India Amritanshu Shukla
Melbourne, Australia Lu Aye

Acknowledgements

Before the start of this project in late 2017, we were not fully aware of the time and effort that go into editing a book. We thought of bringing an edited book to share knowledge, development and scientific advancement in the field of green energy with a large group of interested readers. Therefore, we thought we can simply get connected with the researchers around the world and request them to share their recent leading-edge research in the form chapters for an edited volume. To us it was feeling so simple at the beginning, however, we were wrong. Now we understood it in a better way. Since the authors contributed to this book are from the scientific and academic community with their prior commitments, our deadlines for submitting chapter proposal, first drafts of the chapters, peer reviews of all manuscripts and submission of final revisions of the contributions have frequent challenges. Throughout, however, we received remarkable encouragement and enthusiasm from our authors and reviewers. We are really honoured to have all the contributors who have been very supportive, dedicated and responsive throughout our interactions. We are really thankful to all our passionate authors and reviewers!

We would like to express our gratitude to the many persons who saw us through this book; to all those who provided support, talked things over, read, wrote, offered comments and allowed us to quote their remarks. This book would never have taken off without the generous support of authors of the chapters and our colleagues at Rajiv Gandhi Institute of Petroleum Technology (RGIPT) and the University of Melbourne. It would never have been completed without the cooperation, administrative and editorial assistance of Ms. Swati Meherishi, Ms. Aparajita Singh and Ms. T. C. A. Avni of Springer. Our heartfelt thanks to all these dedicated and cooperative individuals!

We would like to thank our families, who supported and encouraged us in spite of the time it took us away from them. There is no doubt that we are very excited, enthusiastic and gratified about the final outcome, we also feel sorry about unwittingly neglecting them on many occasions, especially during weekends. For all their patience and moral support, we dedicate this book to our families.

Atul Sharma
Amritanshu Shukla
Lu Aye

Contents

About the Editors

Dr. Atul Sharma completed his M.Phil. in Energy and Environment (August 1998) and Ph.D. on the topic "Effect on Thermophysical Properties of PCMs due to Thermal Cycles and Their Utilization for Solar Thermal Energy Storage Systems" (June 2003) from the School of Energy and Environmental Studies, Devi Ahilya University, Indore (MP), India. He has worked as a Scientific Officer at the Regional Testing Centre Cum Technical Backup Unit for Solar Thermal Devices, School of Energy and Environmental Studies, Devi Ahilya University, Indore, funded by the Ministry of Non-Conventional Energy Sources of the Government of India. He also worked as a Research Assistant at the Solar Thermal Research Center, New and Renewable Energy Research Department at the Korea Institute of Energy Research, Daejon, South Korea (1 April 2004–31 May 2005), and as a Visiting Professor at the Department of Mechanical Engineering, Kun Shan University, Tainan, Taiwan, R.O.C. (1 August 2005–30 June 2009). He is currently an Associate Professor at the Rajiv Gandhi Institute of Petroleum Technology (RGIPT), which has been set up by the Ministry of Petroleum and Natural Gas, Government of India through an Act of Parliament (RGIPT Act 54/2007) along the lines of the IITs with an "Institute of National Importance" tag. The institute is co-promoted as an energy domain-specific institute by six leading PSUs—ONGC Ltd., IOCL, OIL, GAIL, BPCL and HPCL in association with OIDB. The mission of the institute is to work towards promoting energy self-sufficiency in the country through its teaching and R&D efforts. Recently, He published an edited book, *Energy Sustainability Through Green Energy* published by Springer (Pvt.) Limited, India, and *Energy Security and Sustainability* published by CRC Press, Taylor and Francis Group. He has published several research papers in various international journals and conferences. He has also published several patents related to the phase change materials (PCM) technology in the Taiwan region. He is working on the development and applications of phase change materials, green building, solar water heating system, solar air heating system, solar drying systems, etc. He is conducting research at the Non-Conventional Energy Laboratory (NCEL), RGIPT, and is currently engaged with the Council of Science and Technology, UP, sponsored project at his laboratory. Further, he served as an editorial board member and was a reviewer for many national and international journals, project reports and chapters.

Dr. Amritanshu Shukla did his Masters in Physics and completed his Ph.D. from IIT Kharagpur in January 2005. He did his postdoctoral research work from some of the premier institutes across the globe, namely at the Institute of Physics, Bhubaneswar (Department of Atomic Energy, Government of India), University of North Carolina Chapel Hill, USA, University of Rome/Gran Sasso National Laboratory, Italy, and Physical Research Laboratory Ahmedabad (Department of Space, Government of India). He is currently working as an Associate Professor in Physics at the Rajiv Gandhi Institute of Petroleum Technology (RGIPT) (set up through an Act of Parliament by the Ministry of Petroleum and Natural Gas, as an "Institute of National Importance" on the lines of IITs). His research interests include nuclear physics and physics of renewable energy resources. He has published more than hundred research papers in various international journals and in various international and national conferences. He has delivered invited talks at various national and international institutes. Currently, he is having several national as well as international projects and active research collaborations from India and abroad on the topics of his research interests.

Dr. Lu Aye is an Associate Professor in the Department of Infrastructure Engineering at the University of Melbourne, Melbourne, Australia. He obtained his Bachelor of Mechanical Engineering at the Rangoon Institute of Technology and Graduate Certificate in Computing Rangoon Institute of Computer Science, Rangoon, Myanmar (Burma). He received his Masters of Engineering Science (Mechanical), Ph.D. (Advanced Energy Systems) and Graduate Certificate in University Teaching at the University of Melbourne. He has over 36 years of engineering experience in university teaching. His research interests are renewable energy, energy efficiency technologies, biomass gasification, green buildings, energy system simulation and optimization, thermal storage, advanced energy systems, heat pumps and life cycle analysis of energy systems. He is a leading expert in modelling, simulation and optimization of energy systems. He has an international collaboration in Exchange programs, Research, Technical Assistance/Training with the Chiang Mai University, Thailand. He is also a member of the University of Melbourne Energy Institute Energy Efficiency and Smart Grids research groups.

Applications of Solar Thermal Technologies in the Built Environment

Lu Aye and Amitha Jayalath

Abstract Solar radiation reaching the Earth surface is the most abundant renewable energy. Solar energy can be harnessed in two types of technologies: Solar Photovoltaics (PV) and Solar Thermal. This chapter deals with the applications of solar thermal technologies in the built environment. The applications presented are electricity generation, hot water production, product drying, cooking, clean water production, space heating, space cooling and refrigeration. Fundamental principles and recent developments and trends of these applications are presented and discussed.

Keywords Electricity · Hot water · Drying · Cooking · Clean water
Refrigeration

1 Introduction

Solar radiation is naturally occurring and the most abundant energy source arriving on the Earth both in direct and indirect forms. The annual solar radiation reaching the Earth is approximately 3,400,000 EJ and nearly 7,500 times more than the current global energy demand (Dhall 2013). The maximum magnitude of solar energy available on earth is at the equator with an annual average of 22 MJ m^{-2}. However, 80% of worldwide energy consumption is currently based on fossil fuels (Thirugnanasambandam et al. 2010) with rising concerns on climate change as a consequence of greenhouse gas emissions and depletion of cheap fossil fuel resources. Thus, as a solution renewable energy sources have attracted considerable attention worldwide. Considerable efforts have been made and are on progress for promotion of renewable and sustainable energy among energy policy makers.

L. Aye (✉) · A. Jayalath
Renewable Energy and Energy Efficiency Group,
Department of Infrastructure Engineering, Melbourne School of Engineering,
The University of Melbourne, Melbourne, VIC 3010, Australia
e-mail: lua@unimelb.edu.au

A. Sharma et al. (eds.), *Low Carbon Energy Supply*, Green Energy and Technology,
https://doi.org/10.1007/978-981-10-7326-7_1

Solar energy has been proven to be reliable, cost effective and low environmental impact source to cater for most of the built environment applications.

Solar thermal technologies can be applied for various applications as an alternative to fossil energy that includes electricity generation, hot water production, product drying, cooking, clean water production, space heating, space cooling and refrigeration. Seasonal or short term thermal energy storage systems are required in operation as solar energy is intermittent and can differ hourly, daily or seasonally. Space heating and cooling of buildings can be achieved with passive or active methods. Passive solar buildings are one of the oldest applications of solar energy in buildings. Solar hot water is another promising application and becoming a legislative requirement among construction of residential buildings and also in industry applications. For example, European Solar Thermal Technology Platform recommend that to increase the supply of solar hot water up to 50% of all heating applications that require temperatures up to 250 °C by 2030 in European Union (EU) (Mills and Schleich 2009). Furthermore, solar drying is proven to be an effective and economical method used for drying and preservation of agricultural and food products especially in developing counties and has been able to overcome the drawbacks faced with sun drying in the past. Water purification with solar stills is another example for use of renewable sources in thermal desalination to obtain portable fresh water. Due to rapid population growth and industrial developments, an imbalance has been created between portable water supply and consumption. Thus, environment friendly, energy efficient desalination systems has been sought after at present and is on high demand. Moreover, solar cooking can be considered as an environmental and economical friendly option for heavily used wood and fossil fuel based cooking in residential sector. Solar cookers provide many advantages that includes fuel economy, reduction of greenhouse gas emissions and help in preservation of forest and fossil fuels. Electricity generation is one of the heavily investigated applications of solar energy and can be achieved through solar thermal options or solar photovoltaics (PV). Concentrating solar power (CSP) plants have become attractive in producing electricity due to its benefits including high efficiency, scale-up opportunities, and low operating costs. It is estimated by IEA that the contribution of CSP in global electricity production will reach up to 11% by 2050 (Pelay et al. 2017). This chapter presents fundamental principles, current applications of solar thermal technology, and their trends.

2 Electricity Generation

Solar thermal electricity (STE) generates electricity with zero operational greenhouse gas emissions and has attracted interest recently around the world. STE industry has gained a robust growth since 2009 mainly in Spain and United States as one of the potential technologies in mitigating climate change (IEA 2015). The generation of electricity using solar thermal energy mainly achieved using concentrating solar power (CSP) systems. In CSP, concentrated solar rays are used to heat working fluid which directly or indirectly turns a turbine to generate electricity. Main types of CSP includes linear Fresnel reflector (LFR), solar power tower (SPT), paraboloidal dish system (PDS) and parabolic trough collector (PTC) (Fig. 1). CSP plants need to have thermal storage capacity for later conversion into electricity and auxiliary fossil fuel backup system for delivering additional heat to the system.

PTCs are most widely used CSP technology with a system efficiency about 11%. The system uses single axis sun tracking linear receiver and concentrates solar rays on evacuated tube collector. Paraboloid dish system uses double axis tracking system and a central receiver with concentration ratio from 100 to 1000. High concentration ratios of dishes facilitate efficient generation of electricity with minimal energy losses. However, lack of heat storage which is essential requirement for operation in winter is a major drawback of dish concentrator (Trainer 2014). SPT has also attracted attention in recent years and possess a concentration ratio from 150 to 1500 (Pelay et al. 2017). In SPT, heliostats focus on central receiver and high temperature fluid heats boiler water for steam turbine-generator. Compared with trough and disk systems, central receiver systems perform better in direct normal irradiation (DNI) and storage capacity (Trainer 2014). LFR uses single axis tracking system and system efficiency is less than 10%. They use long rows of flat or slightly curved mirrors and show greater optical losses compared with troughs in winter (IEA 2015).

Due to built-in storage capabilities, STE offers significant advantage over solar PV and it is estimated that STE's share of global electricity will reach 11% by 2050. Most of the CSP components are coming to commercial maturity with increased efficiency and lower costs. Furthermore, integration of efficient thermal energy storage facilitates dispatchability of CSP systems. Currently sensible heat storage is most widely used with CSP plants in operation and latent and thermochemical storage technologies bear future promise with increased energy storage capacity (Pelay et al. 2017).

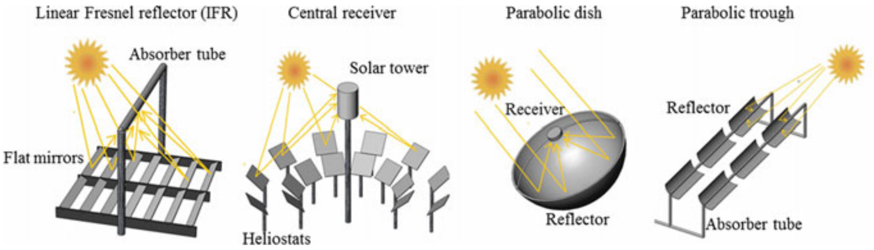

Fig. 1 Main CSP technologies

3 Hot Water Production

Solar hot water systems potentially play a major role in reducing household energy use. The main components of a water heating system include tank, pump and controller. Either a horizontal tank or a vertical tank could be used with relative merits attached to them. Horizontal tanks have low profile on roof while thermosiphon vertical tank extends above roof if it is external or requires high ceiling space if it is internal. Thermal stratification in the storage tank is vital for efficiency of the solar heating system. It is a natural process where hot water ascends to the top of the tank due to its low density compared with cold water and helps in effective utilization of heat. Thus, the heat exchanger will be mounted near to the bottom of the tank where the water is relatively cold and the hot water outlet will be near the top of the tank. In a horizontal tank hot and cold water can be mixed more quickly where vertical tank maintains temperature stratification. Stratification benefits from low flow system, but high flow rates can be used if mixed store is of beneficial.

In a closed coupled system (Fig. 2), roof mounted tank is situated above the collectors. The heated water moves by convection from the collector to the tank, thus requires no pump or controller to operate. Pipework needs to be consistent upward and downward the slope of the roof and overheating can be issue in operation.

Split type system (Fig. 3) consists of roof mounted solar collectors and ground mounted water storage tank, thus requires a hot water circulation pump. This configuration facilitates improved access for installation and maintenance, but heat losses can be evident due to long pipe runs. Electric or gas booster can be added to the system to ensure continuous hot water supply year around.

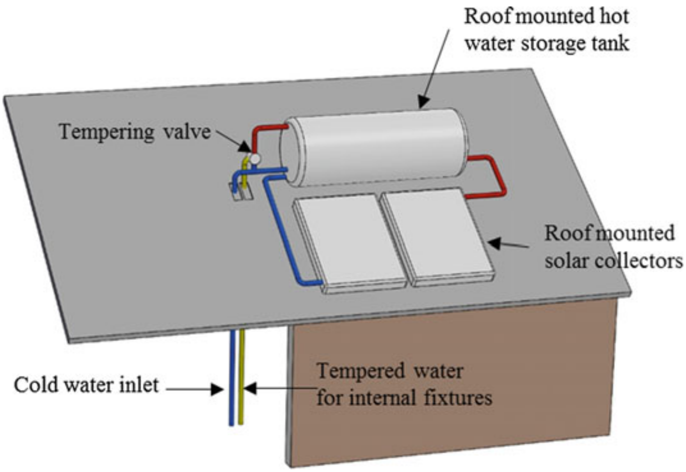

Fig. 2 Solar hot water—closed couple. Adapted from MPMSAA (2009)

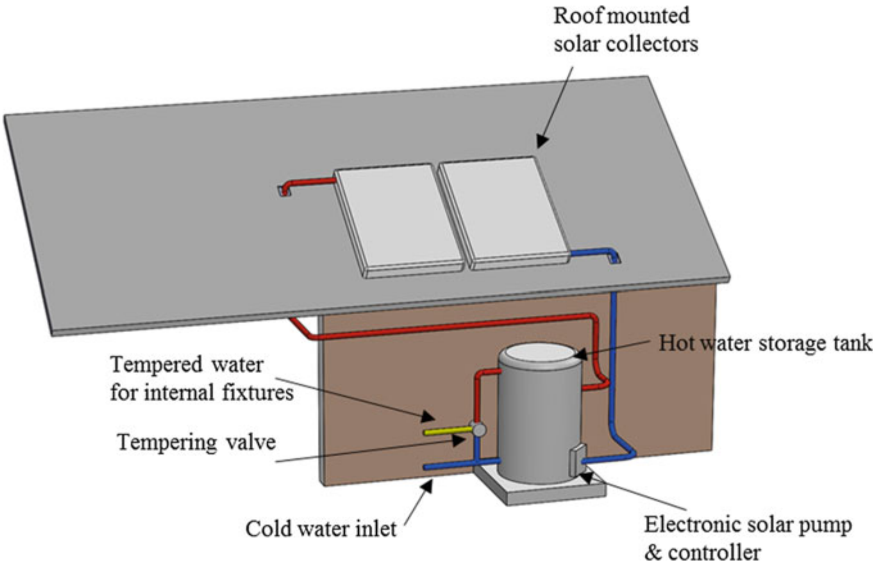

Fig. 3 Solar hot water—split type. Adapted from MPMSAA (2009)

Roof mounted thermosiphon system with electricity for auxiliary boosting is widely used in Australia (Moore et al. 2017). The collector performance is not the sole contributor for solar hot water system performance, but depend on number of factors including storage tank performance, booster and collector efficiency, flow rate, applied hot water loads, inclination and orientation of the collector. Care should be taken to reduce the damage to the system from freezing and stagnation. High-grade insulation (evacuated tubes, double glazing), glycol antifreeze in the collector loop, circulation of water and drain down can be considered as some measures for freezing protection of the system. Furthermore, extreme high temperatures can be build up due to stagnation and can cause collector damage. Stagnation may be caused by pump failure and the storage tank and piping should be able to withstand high operating temperatures. Pressure valves can be used to allow for unwanted increase in pressure as a result of boiling and solar collectors should be tested for high temperature resistance in deterioration due to stagnation. Flow into the storage tank is controlled to minimize the mixing and increase stratification.

Solar heat pump systems can also be used for provision of hot water in domestic applications. Heat pump is a heat energy transformer from lower to higher temperatures. Thus, solar heat pumps harness low temperature sources of energy stored in the environment to achieve required temperature level for specific operations. A vapour compression heat pump unit consists of four major components; compressor, condenser, expansion device and evaporator with a working fluid suitable for evaporation and condensation. The heat pump requires additional mechanical energy input in upgrading the thermal energy output from low energy input stored in the environment. If the use of solar input is to indirectly raise evaporator temperature, it is recognized as solar assisted heat pumps (SAHP) (Fig. 4). If the evaporator performs as an evaporator/collector unit for direct capture of the solar radiation, it is termed as solar boosted heat pump (SBHP) (Fig. 5).

SBHP capture energy from both ambient air and solar, and upgrade to a higher temperature level for useful applications. Solar access is a necessity for operation of SBHP and it costs more compared with standalone heat pumps due to additional complexity. However, system does not require auxiliary back-up heating and increased efficiency in heat collection is one of the advantages of the system. Furthermore, location of installation plays a very significant role in the selection of hot water heaters. Thermosyphon water heaters are most appropriate for geographical areas with high uniform solar radiation. The domestic applications of the heat pump include space heating and swimming pool heating apart from hot water. Commercial applications of heat pump further include drying and dehumidification, evaporation, boiling and desalination compared with domestic applications.

4 Product Drying

Growing global population, food shortages, finite land area for food production and increased wastage are growing concerns at current time. Drying of food and agricultural products can preserve crops for out-of-season consumption, create new products and can even be pre-processing requirement in some food categories. Solar drying is effective and economical method of drying and preservation of food, agricultural and many other products. Drying involves removal of bound moisture in the product. The increase in heat during thermal drying increases moisture vapour pressure in the product above that of surrounding air. This built-up pressure and thermal gradients cause moisture to move to the surface of the product, and finally water vapour transferred to surrounding air.

The traditional methods of sun drying involved increase in product temperature by direct absorption of solar radiation. Crops are surrounded by air at ambient

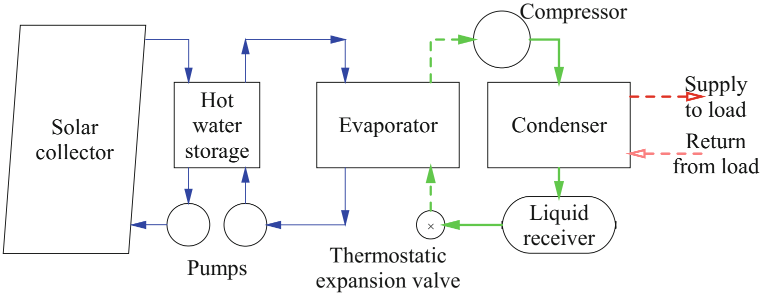

Fig. 4 Solar assisted heat pumps (SAHP). Adapted from Aye et al. (2006)

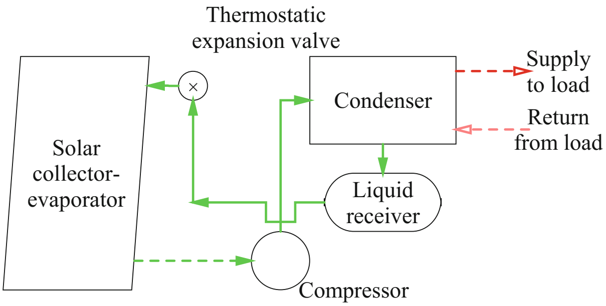

Fig. 5 Solar boosted heat pump (SBHP). Adapted from Aye et al. (2006)

temperature, thus process parameters including heat input, moisture content, temperature and air flow are difficult to control. This led to degraded product with undesirable drying periods and quality of product was further affected by wind-blown debris (Kumar et al. 2016). Thus, solar dryers were developed to overcome these issues related to sun drying. It involves a devise to enhance the capture of solar energy to increase the drying rate (Fig. 6). The air surrounding product is higher than ambient air temperature.

Three main types of solar dryers include direct type, indirect type and mixed mode type (Mustayen et al. 2014). In direct type the drying chamber is produce with an insulated box covered by a transparent cover for direct impregnation of solar radiation on the products. Holes are created to facilitate natural air circulation. The temperature of the product is raised by absorption and convection. These are simplest and cheapest to construct, but some of the drawbacks of direct type involves lack of process controllability, overheating, poor product quality and limited drying capacity.

Indirect solar driers have separate solar collector and a drying unit. Initially the air is heated in separate solar collector and send into the drying chambers. Indirect type is more suitable for crops that can be deteriorate in exposure to the sunlight and

Fig. 6 Direct solar dryer. Adapted from Kumar et al. (2016)

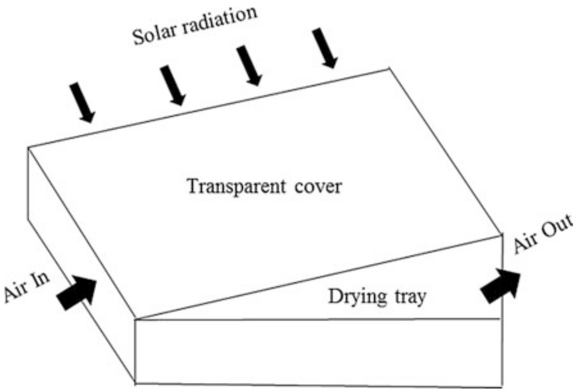

the solar collector unit is helpful in achieving higher temperatures. Compared with direct type solar driers, the construction cost is higher for indirect type, but provides better control over process temperature required. In mixed mode method, direct and indirect methods are combined where direct solar radiation heating is used with preheating of air using auxiliary energy. Though mixed types are expensive, they are the most effective and best alternative for the products require fast solar drying to achieve required product quality.

5 Cooking

Solar cookers can be considered as one of the most promising thermal applications of solar energy. In developing countries, wood is used predominantly used for cooking along with fossil fuel based energy sources (Yettou et al. 2014). However, difficulties in collection and shortage of fuelwood have driven the need to search for solutions that includes improved cooking stoves, firewood plantation and solar cookers. A solar cooker converts solar energy into heat energy which is used to cook the food in the cooking utensil. There are different types of solar cookers; box type, concentrating type and indirect type or steam generating (Panwar et al. 2012). A box type solar cooker (Fig. 7, photos on the left) consists of an insulated box with transparent glass cover. Booster mirrors are used to reflect the solar radiation into the box. Box type solar cookers are slow to heat up, but reaches up to 100–120 °C with heat transfer by absorption, conduction and convection. Several pots can be heated at one time and the cookers are easy to operate. No stirring is needed and it helps to keep food warm. Compared with other solar cookers, box type is relatively inexpensive and easy to make and repair. Some of the disadvantages include long cooking time, incapability to grilling or frying and restrictions for day time cooking only.

Concentrating solar cookers (Fig. 7, photos on the right) use Fresnel lens, parabolic or spherical collectors to focus solar radiation to the cookpot. These are capable of achieving high temperatures about 120–180 °C that suits for most cooking types. Heat is transferred only through absorption and facilitate faster cook times compared with box type. Due to high temperatures, concentrating type cookers can be used for frying, grilling and boiling. Some of the disadvantages include high heat losses, danger of injuries, unsuitability in windy conditions and difficulty in operation. Furthermore, concentrating type solar cookers can be used only in day time and need constant realignment. The indirect type relates to the non-focusing type solar cookers where flat-plate or vacuum-tube is used most of the time. These cookers use a heat transfer fluid to carry thermal energy, thus they are suitable for indoor applications. However, these are more complex compared to previous categories and expensive in construction. Thermal storage has also been used with solar cookers to facilitate cooking during insufficient sunshine.

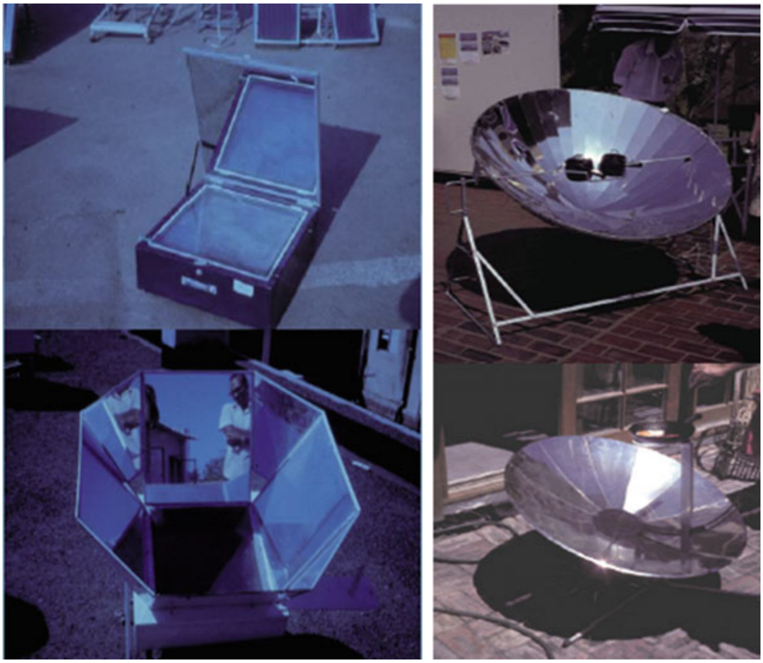

Fig. 7 Solar cooker; box type (left) and concentrating type (right). Photos by Bob Fuller, The University of Melbourne

6 Clean Water Production

Portable or fresh water is a prime necessity for human beings and scarcity of fresh water is expected to outweigh oil crisis in future. Seawater contains 35 kg of salt per 1000 kg (~35,000 mg per litre), but drinking water should have less than 600 mg total dissolved solids (TDS) per litre. Distillation and reverse osmosis can be considered as the two main clean water production technologies widely used in practise today. Distillation achieves 2–50 mg per litre (TDS) and more than 17,000 desalination plants are currently in operation in 120 countries. In distillation, heat is applied for the evaporation of water. Reverse osmosis gives 10-500 mg per litre (TDS) and electricity is the source of power for the process. Solar still is one of the promising applications of solar energy that can be used to convert impure water into fresh water (Sharshir et al. 2017).

The basic solar still (Fig. 8) consists of enclosed insulated glazed box, sloping transparent roof and black absorber base. The black absorber base holds the impure water supplied through the inlet pipe and the water is evaporated due to the solar radiation transmitted through the glazed surface. Then the evaporated vapour is condensed on the inner side of the sloped surface and collected using distillate channels (Panchal and Patel 2017).

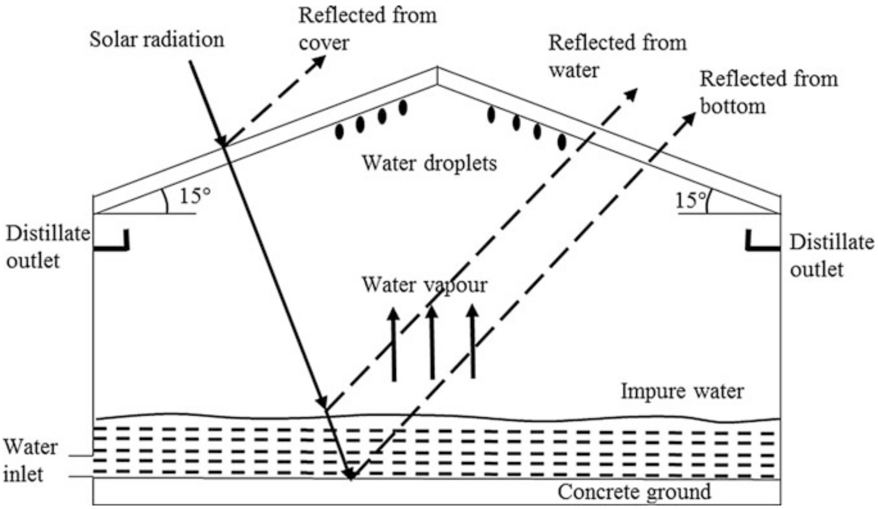

Fig. 8 Desalination using solar still

In a solar still, captured solar energy is mainly dissipated by evaporation, convection and radiation. Water production rate in the solar still is a function of water temperature and temperature difference between water and cover. Generally, in operation, it is aimed to maintain water temperature above 40 °C by maintaining shallow water depth, low heat losses and maximum solar radiation input and absorption. The basin solar still is easy and inexpensive to construct and incur low maintenance cost also. However large areas are usually required for construction and usage is limited due to low productivity. Research has been carried out to further reduce costs and improve the productivity of solar stills. Inclined and multi effect solar stills provide more output but at more cost and added complexity.

7 Space Heating

Space heating using solar power can be considered as one of the fist applications of solar thermal power used by humans that can be dated back to centuries. Applications of space heating systems can be divided into two main categories, active and passive systems. A passive system is defined as one in which thermal energy flow is by natural means (i.e. conduction, free convection and radiation) and integrate solar collection, storage and distribution into the building design. Passive solar system may require minimal supply of external energy in some instances to make the system function. In some cases, the performance can be enhanced by the use of a fan or pump. The average temperature of the space over a day is determined by, the amount of solar radiation collected (the quantity of equator facing glazing, e.g. north wall glazing in southern hemisphere), the degree of insulation (to reduce the heat loss of the building) and the outdoor climate conditions. The daily temperature fluctuation of the space is determined by the size, distribution, material, and radiation properties of the thermal mass. The main design issues of a passive system include the storage of heat and the control of heat flows. The ultimate aim of a passive heating system is to maintain the space at a relatively uniform temperature in spite of the intermittent heat inputs and the varying temperatures of the storage material. Direct gain systems, thermal storage walls, thermal storage roofs (heating & cooling), attached sunspaces and thermosyphoning (convective loop) rock bed are some of the passive heating systems used in practise. In direct gain system, large areas of equator facing glass, that allow solar radiation to enter the house during the winter, is used. The summer sun is generally excluded by the use of shading devices and provision has been made for thermal mass. When thermal storage wall or Trombe wall (Fig. 9) is used, incident radiation is absorbed by the dark surface of the wall. Heat transfer to the room is achieved by two processes, free convection in the gap between the glass and the wall where warm air is fed into the room via the top vents. The second process is conduction through the wall, but introduces a large time delay.

The components of the thermal storage roofs include metal roof, water ponds, movable insulating covers ad optional glazing. It can be used for both winter heating and summer cooling. In winter, insulating covers are pulled back when the sun is shining. Then the solar radiation is absorbed by the dark plastic layer beneath the water and heat is partially transmitted through the roof and stored in the water. The covers are moved over the pond at night. During summer, the process is reversed. Attached sunspaces relates to attachment of a greenhouse to the side of a house. Heated air can be delivered directly to the building or may be indirectly transferred by a thermal storage wall between the greenhouse and the living space.

An active system is a system that relies on pumps or blowers to transport the heated working fluid from the solar collectors to either the load or a thermal storage unit. It uses either liquid or air as the collector heat transfers fluid and must have a continuous availability of external energy supply, in the form of mechanical power

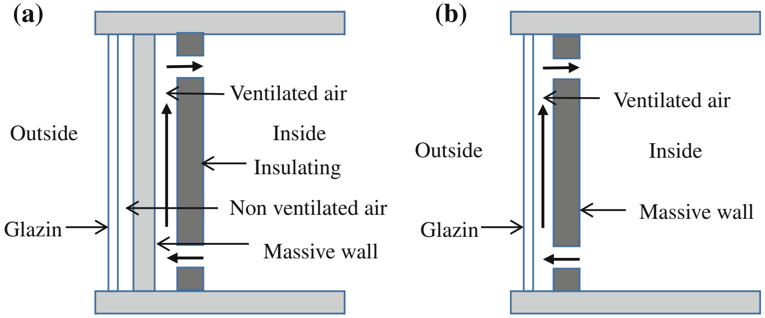

Fig. 9 **a** Composite solar wall, **b** Trombe wall. Adapted from Zalewski et al. (2002)

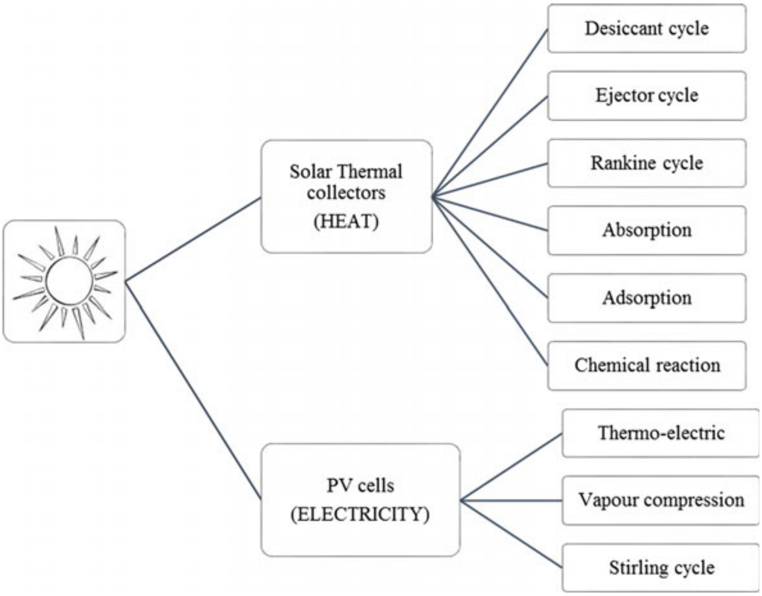

Fig. 10 Solar cooling options

or electricity to operate pumps or fans. A complete active system consists of solar collectors, thermal storage units, pumps or blowers and transfers energy either to the storage or to the load.

8 Space Cooling

Solar cooling systems are a promising alternative for conventional vapour compression air-conditioning and have attracted considerable interest worldwide. The coincidence of solar irradiation and high demand for cooling in summer periods places solar cooling with lowest energy consumptions compared with other technologies. Solar cooling is an active system that is driven by heat generated with solar thermal collectors or electricity generated by PV arrays (Fig. 10). Though air-conditioning is one of the prime applications of solar cooling, other applications include food/vaccine storage and freezing.

In solar cooling systems, heat can be generated using variety of solar collectors. This includes flat-plate collector (FPC), evacuated tube collector (ETC) and parabolic trough collector (PTC) (Mahesh 2017). Out of different solar driven options for cooling, Absorption chillers (Fig. 11), Adsorption chillers and Desiccant-evaporative cooling systems are widely used in practice (Kohlenbach and Jakob 2014). Mode of delivery could be either using air or water. In an absorption chiller, the continuous cycle process is based on two liquids; the refrigerant and the

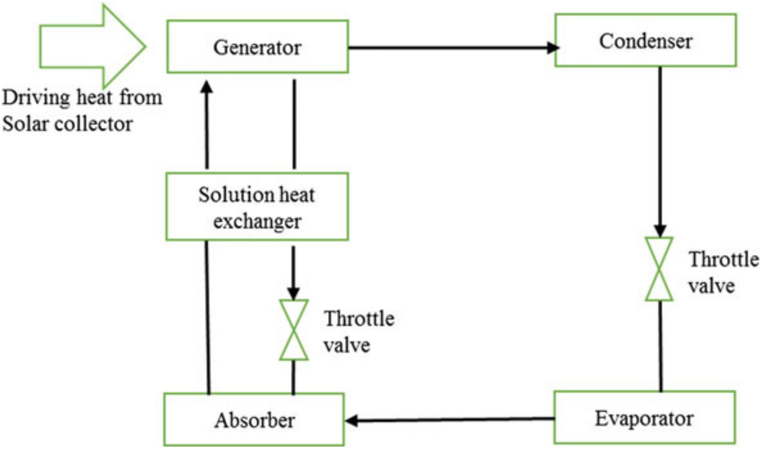

Fig. 11 Absorption cycle for a solar cooling system

carrier fluid. During absorption the refrigerant ipermeates or dissolves into carrier fluid. Adsorption is a surface phenomenon where molecules of solid carrier medium adhered to the liquid surface of refrigerant. In a desiccant- evaporative system either solid or liquid is used to remove humidity of air and then the air is chilled using evaporation of water.

Solar energy is one of the heat sources for thermally driven cooling processes and sometimes termed as solar air-conditioning. The two main physical principles used in thermally driven cooling system include either evaporation of refrigerant by removal of heat from liquid flow or evaporation of water by removal of heat from airflow. Desiccant-evaporative cooling systems are categorized under solar cooling system that provides conditioned air in an open system. Ambient air is continuously employed to cool the building and usually flows once through the building. Furthermore, it provides building. Consequently the ventilation at the same time. Absorption chillers and Adsorption chillers uses water to remove the building heat in a closed system. The heat from the building is removed using heat transfer into water and then cooled in a water chiller. The chiller rejects the building heat to the environment and as there is no air is drawn into the building. Consequently the ventilation of the building need to be considered separately.

9 Refrigeration

Solar refrigeration is one of the main applications in solar cooling systems. This deals with refrigeration in warm weather regions and remote areas for storage of life-sustaining materials such as medicine, food and beverages. Main refrigeration technologies include vapour compression system (Fig. 12), absorption system and

Fig. 12 Schematic of a simple vapour compression refrigerator

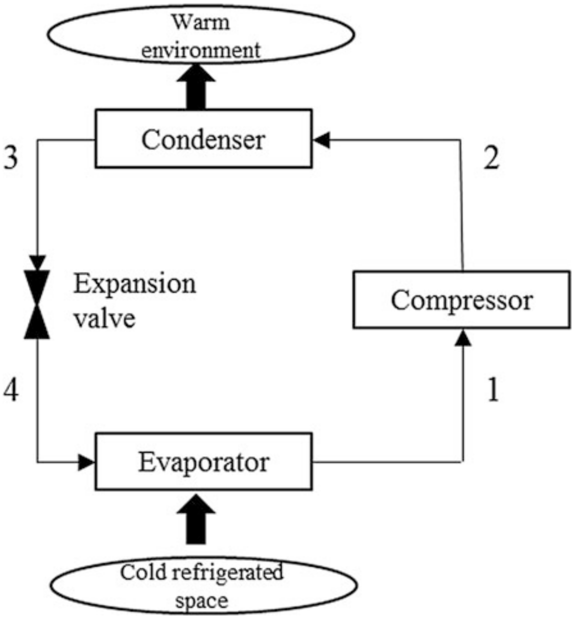

thermoelectric system. In solar thermal cooling technologies, generally an auxiliary heating unit is used in operation as a backup for low solar radiation and night time (Ghafoor and Munir 2015).

Solar PV can be used to generate electricity and converted DC fed into the DC motor to drive the compressor of the vapour compression refrigerate system. The vapour compression systems are widely used for refrigeration, and they have very high performances (Kalkan et al. 2012). The technology is relatively simple and refrigeration system components available at low prices. Furthermore, little maintenance is required in operation and relatively low heat loss occurred compared with other technologies. However, for standalone applications, requirement of electricity that being fulfilled using solar PV arrays and batteries can increase the cost of the system and the working fluid need to be sealed.

As discussed in the earlier section, absorption system for solar refrigeration use heat collected through solar thermal collectors. Thus, in general, they incur lower cost than PV-driven systems and require less maintenance compared with vapour compression systems. However high collector temperatures are required and due to higher heat rejections, the coefficients of performance (COPs) can be low. Moreover, requirement of mechanical energy for the systems with pumps is also a drawback of the solar absorption refrigeration.

10 Summary/Conclusion

This chapter presents some of the main applications of solar thermal energy and their practices. Undoubtedly the potential and benefits of using solar thermal power in applications presented have been realized and is on high demand compared with conventional fossil based fuels. Solar building architecture, solar hot water, solar cooling and STE can be recognized as rising fields for solar thermal applications. Passive solar architecture has promising benefits for heating and cooling of buildings. The availability of solar radiation at the time that is most needed acts favourably in development of solar cooling technologies. Due to built-in complementary thermal storage capabilities, STE shows significant benefits over solar PV. However supportive government policies and appropriate regulatory frameworks will positively reinforce these solar thermal applications. Furthermore, strengthening of research and development efforts to reduce cost, improve storage and maximize output with minimal losses are key for sustainable development of solar thermal applications.

References

Aye L, Charters WWS, Chaichana C (2006) Solar boosted heat pump (SBHP). In: Hough TP (ed) Solar energy: new research. Nova Science Publishers, New York, pp 239–54

Dhall V (2013) India's energy security. Vij Books India Pvt Ltd, New Delhi

Ghafoor A, Munir A (2015) Worldwide overview of solar thermal cooling technologies. Renew Sustain Energy Rev 43:763–774

IEA (2015) Technology Roadmap Solar Thermal Electricity [electronic resource]. OECD Publishing, IEA Technology Roadmaps, Paris

Kalkan N, Young EA, Celiktas A (2012) Solar thermal air conditioning technology reducing the footprint of solar thermal air conditioning. Renew Sustain Energy Rev 16:6352–6383

Kohlenbach P, Jakob U (2014) Solar cooling [electronic resource]. The Earthscan Expert Guide to Solar Cooling Systems. Earthscan Expert, Taylor and Francis, Florence

Kumar M, Sansaniwal SK, Khatak P (2016) Progress in solar dryers for drying various commodities. Renew Sustain Energy Rev 55:346–360

Mahesh A (2017) Solar collectors and adsorption materials aspects of cooling system. Renew Sustain Energy Rev 73:1300–1312

Mills BF, Schleich J (2009) Profits or preferences? Assessing the adoption of residential solar thermal technologies. Energy Policy 37(10):4145–4154

Moore AD, Urmee T, Bahri PA, Rezvani S, Baverstock GF (2017) Life cycle assessment of domestic hot water systems in Australia. Renew Energy Int J 103:187–196

MPMSAA (2009) Household solar hot water and heat pump installation and maintenance handbook. The Master Plumbers and Mechanical Services Association of Australia (MPMSAA), Melbourne

Mustayen AGMB, Mekhilef S, Saidur R (2014) Performance study of different solar dryers: A review. Renew Sustain Energy Rev 34:463–470

Panchal HN, Patel S (2017) An extensive review on different design and climatic parameters to increase distillate output of solar still. Renew Sustain Energy Rev 69:750–758

Panwar NL, Kaushik SC, Kothari S (2012) State of the art of solar cooking: an overview. Renew Sustain Energy Rev 16(6):3776–3785

Pelay U, Luo L, Fan Y, Stitou D, Rood M (2017) Thermal energy storage systems for concentrated solar power plants. Renew Sustain Energy Rev 79:82–100

Sharshir SW, Elsheikh AH, Peng G, Yang N, El-Samadony MOA, Kabeel AE (2017) Thermal performance and exergy analysis of solar stills—a review. Renew Sustain Energy Rev 73: 521–544

Thirugnanasambandam M, Iniyan S, Goic R (2010) A review of solar thermal technologies. Renew Sustain Energy Rev 14:312–322

Trainer T (2014) The limits to solar thermal electricity. Energy Policy 73:57–64

Yettou F, Azoui B, Malek A, Gama A, Panwar NL (2014) Solar cooker realizations in actual use: an overview. Renew Sustain Energy Rev 37:288–306

Zalewski L, Lassue S, Duthoit B, Butez M (2002) Study of solar walls—validating a simulation model. Build Environ 37(1):109–121

Perspective of Solar Energy in India

Atul Sharma, Amritanshu Shukla and Karunesh Kant

Abstract The renewable energy resources have high impending to offer the way out to the long-standing energy shortage difficulties being confronted through the emerging countries like India. The solar energy obtained from the sun can be an imperative part of India's plan not only to add new capability but also to upsurge energy security, address ecological concerns, and lead to the huge market for renewable energy. The electricity generated by solar thermal which is also known as concentrating solar power is emerging renewable energy technologies and can be developed as a future potential option for electricity generation in India. In this chapter, authors have been summarizing the accessibility, present status, promotion policies, strategies, viewpoints, major achievements barriers and future perspective of solar energy opportunities in India.

Keywords Solar energy · CST

1 Introduction

India as the second largest populated nation is now subjected to a steep evolution of the economy and successively, a rapidly rising energy demand. In 2015, India was placed as the third highest energy (882 Mton) and electricity (1,027 TWh) consumers in the world (Enerdata 2016). The yearly growing electricity demand and overall energy consumption are presented in Fig. 1 and yearly growth of electricity generation in Fig. 2. The economic progress and growth of any nation be governed by the accessibility of energy resources and its consumptions. Energy resources deliver not only financial power but also play a vital role in any present-day society. The global energy demand in succeeding two decades is expected to upsurge by

---

A. Sharma · A. Shukla · K. Kant (✉)
Non-Conventional Energy Laboratory, Rajiv Gandhi Institute of Petroleum
Technology, Jais, Amethi 229304, UP, India
e-mail: k1091kant@gmail.com

A. Sharma et al. (eds.), *Low Carbon Energy Supply*, Green Energy and Technology,
https://doi.org/10.1007/978-981-10-7326-7_2

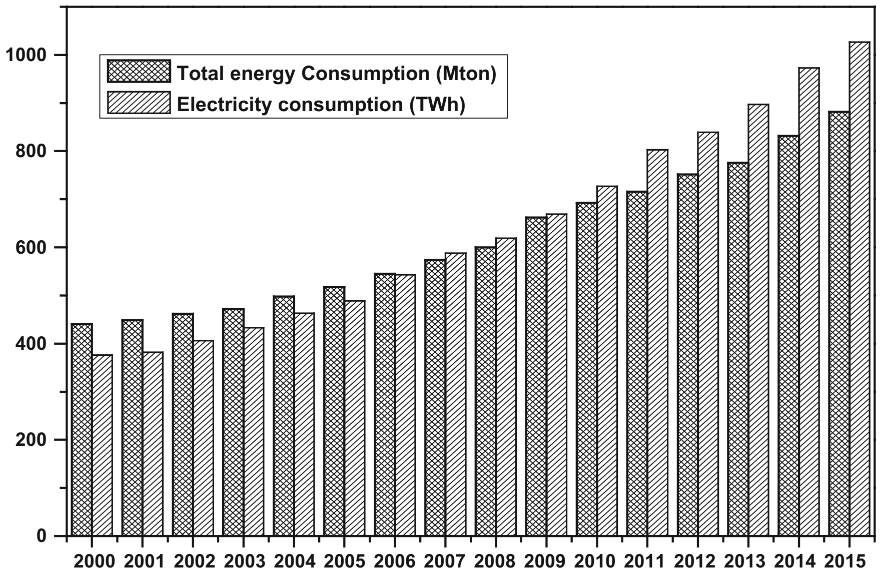

Fig. 1 Total energy and electricity consumption per capita in India (MoP 2017)

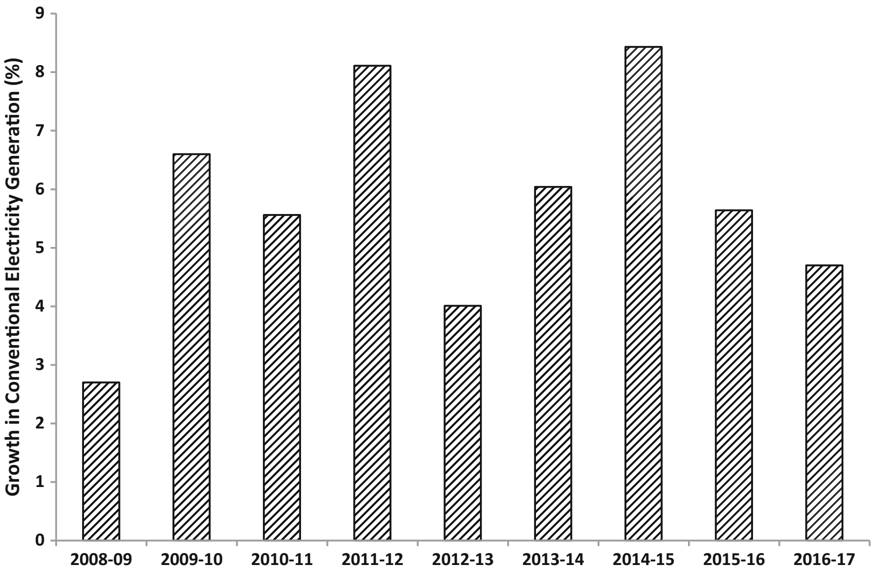

Fig. 2 The growth of conventional electricity generation (MoP 2017)

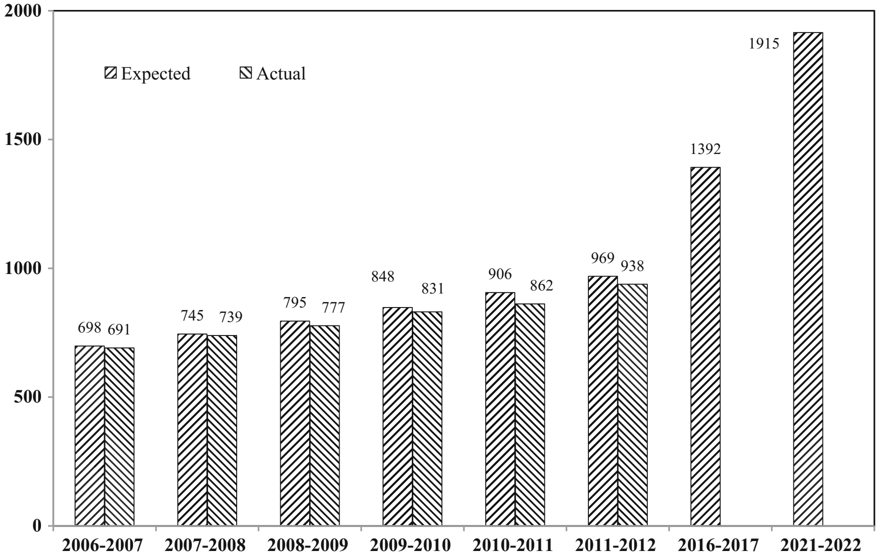

Fig. 3 The electricity demand in India (expected and actual) 2006–2022 (Ministry of Power 2011)

nearly 50%, attaining around 778 EJ by 2035 (Van der Hoeven 2013; Teske et al. 2012). The financial growth of society, the growth of industry and the increase in new services have contributed to a sharp intensification in electricity demand. The electricity demand is anticipated to rise even further in the near future (see Fig. 3). The electric power generation by fossil fuel is the widespread beginnings of greenhouse gas emissions. To reduce the greenhouse gas production, diverse policies have made known to power sector throughout the world. The consumption of renewable energy as sources of electrical power is one of the most operational policies taken by the power sectors of all over the world. India lies in the good sunniest areas where around 250–300 rich sunny days in the year. The solar energy, if utilized, can play an energetic role in decreasing India's power deficit. Solar energy is cost-effective and operationally best feasible energy resource and one of the principal power sources in terms of renewable energy sector. Numerous technologies are applied to transform solar irradiation into a usable form of energy identical thermal and electricity (Goel 2016; Suresh and Rao 2017).

2 Potential of Solar Energy in India

India is one of the prominent countries which have good Direct Normal Irradiance (DNI). The DNI primarily depends on the geographical location, movement of sun–earth, the angle of earth rotational axis and atmospheric dilution due to suspended particles. The potential of solar power is assessed numerous times of the energy

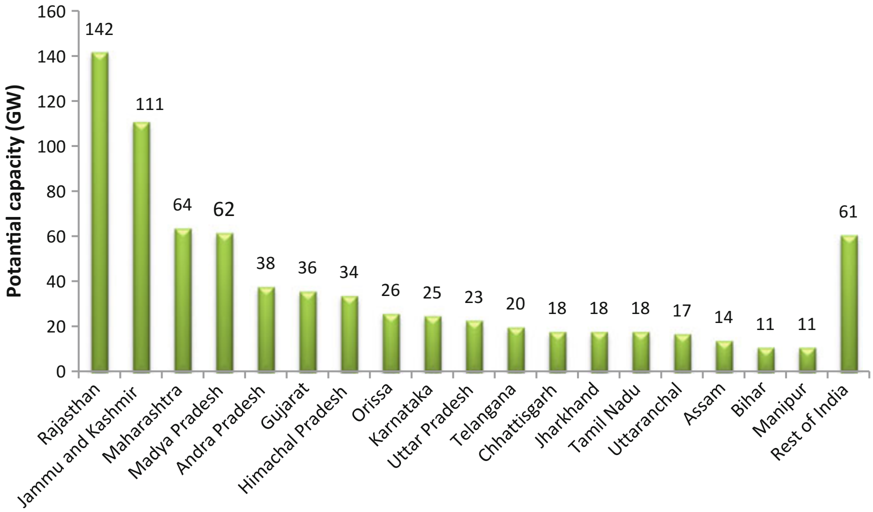

Fig. 4 Solar potential in leading states in India (Kar et al. 2016)

requirement which is about 5,000 trillion kWh per year. The solar radiation incident over India is equal to 4–7 kWh (Kumar et al. 2010) per metre square every day have a yearly radiation varying from 1,200 to 2,300 kWh per m^2. India is benefited with an average of 250–300 rich sunny days and 2,300–3,200 sunshine hours per year. The electricity needs of India's can be encountered in a total land area of 3,000 km^2 which is the same to 0.1% of entire land in the country (Veeraboina and Ratnam 2012; Pandey et al. 2012; Kapoor et al. 2014). India has an expected potential of solar energy which is about to 749 GW to be utilized for decreasing energy deficiency in the country (Kar and Gopakumar 2015). The Rajasthan leads in the table with 142 GW as shown in Fig. 4 trailed by Jammu and Kashmir with 111 GW in terms of the potential capacity of solar energy. India gets sufficient solar energy to produce in excess of 500,000 TWh per year of electricity, considering 10% efficiency of photovoltaic (PV) modules for converting solar radiation to electricity. It is three times higher than the electricity needed to India by the year 2015 (Muneer et al. 2005). Figure 5 displays a map of India with incident solar radiation with levels in different parts of the country. It can be perceived that even though the maximum yearly global solar radiation is incident in Rajasthan, northern Gujarat and portions of the Ladakh region, the parts of Maharashtra, Andhra Pradesh and Madhya Pradesh also obtain a fairly enormous quantity of solar irradiation as compared to many regions of the world mainly Japan, Europe and the US where the growth and deployment of solar technologies are supreme (Garud and Purohit 2012).

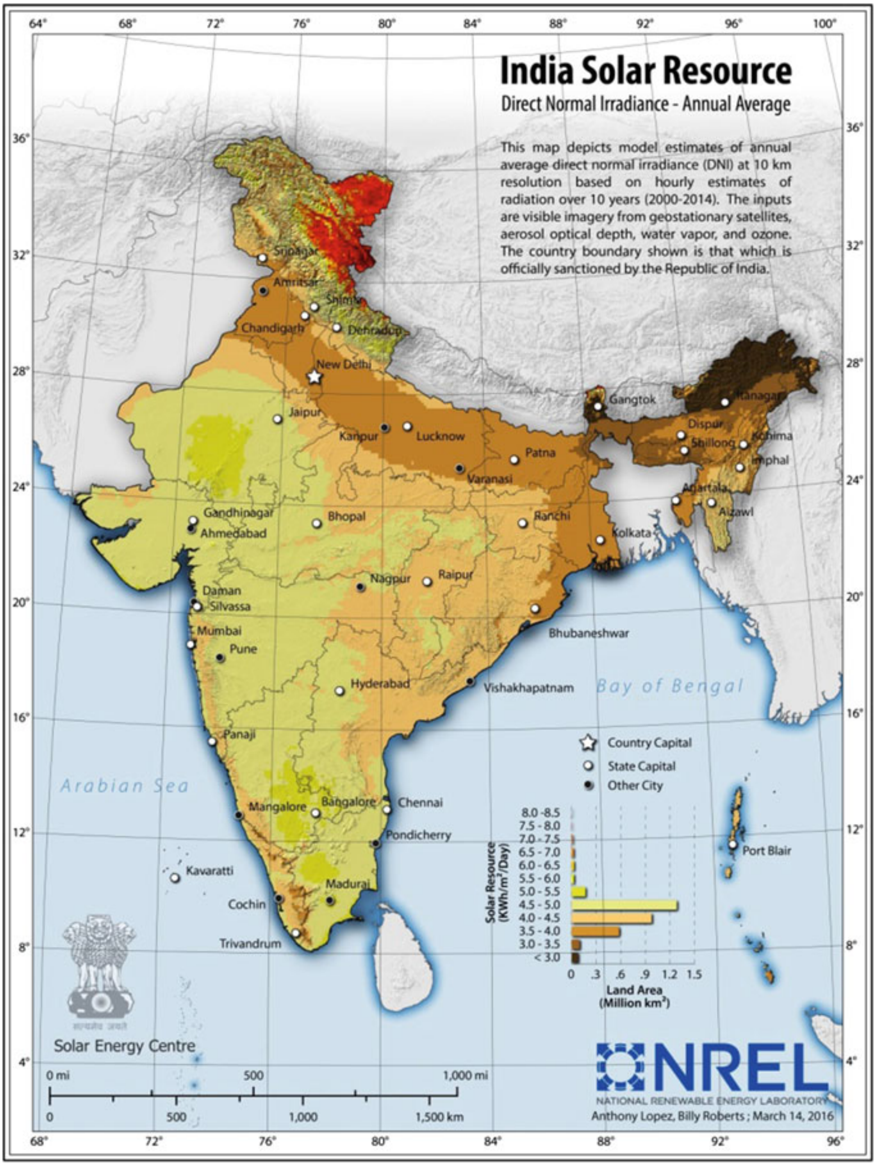

Fig. 5 Solar potential map of India (http://www.nrel.gov/international/ra_india.html)

3 Solar Energy Status and Current Scenario in India

Till the month of January 2017, around 272,687 MW power produced in India by means of renewable and non-renewable energy resources, and 35,776.96 MW power produced through renewable sources, which is only 13.12% of the country's total power generation (Kar et al. 2016). The ministry of new and renewable energy (MNRE), functioning with the conjunction of Indian Renewable Energy Development Agency (IREDA) to stimulate the consumption of all forms of solar power in addition to upsurge the portion of renewable energy in the Indian market. This upgrade is being accomplished through R&D, demo projects, government funding platforms, and also private sector schemes. The Prime Minister of India released the National Action Plan on Climate Change (NAPCC) on 30 June 2008. The proposed plan was started at eight assignments; among one of them is the National Solar Mission (Kumar et al. 2010). The solar thermal and solar photovoltaic, both technologies, are included by the solar energy programme that is being executed by the Ministry (observed as one of the biggest in the world) to exploit India's projected solar power potential of 20 and 35 MW/km^2 solar thermal. India's general perspective of water heating systems by solar energy has been projected to be 140 million m^2 of collector area.

3.1 An Overview of Solar Power Technologies

There are various techniques that have been exploited to convert solar energy into power. There are two kinds of technologies that have been applied to utilized solar energy, i.e. solar photovoltaic and solar thermal.

3.1.1 Solar Photovoltaic Technology

Solar photovoltaic is the technology used for the conversion of solar radiation into electricity directly. This implies that the solar PV systems are only effective during the availability of sunlight due to which electricity storage is not a cost-efficient process. The thermal energy is also known as heat energy is a far easier and effective method, which makes solar thermal technology enchanting for large-scale energy generation. The thermal energy can be stored throughout the day in thermal energy storage devices and then converted into electricity by suitable conversion devices at night in the absence of sunlight. The solar thermal power plants that have storage capacities can significantly increase both the economics and the dispatch ability of solar electricity. The productivity of solar cell mainly depends on the operating conditions, such as solar radiation intensity, wind speed, operating temperature, and ambient temperature. The following types of solar photovoltaic technology are used to convert solar energy into direct electricity:

- Grid-connected solar photovoltaic (PV) systems,
- Off-grid solar photovoltaic (PV) systems,
- Hybrid solar photovoltaic (PV) systems,
- Solar- and wind-powered water pumps, and
- Battery-less solar photovoltaic (PV) systems.

3.1.2 Solar Thermal Technology

It is essential to comprehend that solar thermal technology is not the same as a solar panel, or photovoltaic, technology. The electric energy generation by solar thermal energy concentrates the light using the sun to produce heat, and that produced heat is used to run a heat engine, which turns a generator to generate power. By the concentrated sunlight, the working fluid includes water, oil, salts, air, nitrogen, helium, etc., which is in liquid or a gas medium. The various heat engine types include gas turbines, steam engines, sterling engines, etc. These types of engines are very efficient, often between 30 and 40%, and are proficient at generating 10s to 100s of megawatts of power. Application-based solar thermal technologies are hot water, cooking, steam generation, space heating, swimming pool heating, drying, etc. Medium-based solar thermal technologies are water heating, air heating, etc.

3.2 Solar Power Scenario of India

The economic growth of any developing nation depends on energy supplied to the nation. India is the developing nation, and therefore, it requires the energy for the day-to-day use and also for the running industries. Though the relation concerning the economic evolution and augmented energy plea is not every time linear, in the current situation, the 7.5% increase in India's GDP would cause an augmented energy plea of 9% in the Indian energy sector. The 60% of electricity in India is produced by coal which influences the energy mix in India. The difference has happened in the total electrical network if the huge dissimilarity concerning the energy supply and demand is found.

Based on a comprehensive assessment on the power and energy development in India, it was decided that the amount of power shortage is reduced in 2015 as compared to 2014; however, the quantity of power shortage is not insignificant. Owing to the high power shortage between demand and supply of power, there is a chance for shutdowns in Indian electricity generation sectors. For the reduction of this big power shut down related to the electrical energy demand, it is necessary to upsurge the power production. The renewable energy technology is a superior option for setting up of new power generation source in India that have ecological, social and commercial benefits. Table 1 shows region and resource-wise power developments scenarios of India. The key source in India for power generation is coal, nuclear gas, diesel, hydro and renewable energy sources. The overall electricity generation capacity of India till 30 April 2017 is 329,204.53 MW, out of which 22,0569.88 MW of electricity power was produced from thermal power plants. The highest electricity is generated from Western Region among the five different electricity boards. Around 74.4% of electricity generated in the western region is by the thermal power plant. The nuclear power plants produced around 6,780.00 MW, and all the nuclear power plant is located in the southern, western and northern region of India. The hydropower plants in India were producing about 42,473.42 MW electricity, while 36,470.64 MW power is generated from the renewable energy resources.

3.2.1 State-Wise Solar Power Installed Capacity in India

Grid-connected solar power generation method is generally categorized into two kinds, i.e. (i) standalone photovoltaic systems and (ii) rooftop photovoltaic. The Indian government has executed several solar power projects, counting ultra-mega solar energy power generation project under Jawaharlal Nehru national solar mission (JNNSM). The power generation based on solar energy has played most important role towards the fulfilment of energy supply of India. The rooftop solar photovoltaic technology is not only producing electrical energy for its individual electricity load but also adding supplementary electrical energy generation into the grid. Table 2 shows the commissioning prominence of a solar power generation project in India at the end of January 2017. With 1,269.93 MW capacities, Rajasthan has the uppermost quantity of installed solar power capacity (MNRE 2017a). Asia's biggest solar park has been set up in Gujarat; however, biggest concentrating solar power (CSP) plant has been installed in Rajasthan. These days, several state governments in India have hurled rooftop solar power generation arrangement, to sustain the rapid growth of solar power production.

3.2.2 Jawaharlal Nehru National Solar Mission (JNNSM)

JNNSM was hurled on 11 January 2010, by the Prime Minister of India under the banner of renewable energy.[1] JNNSM is the part of India's NAPCC, which centres on India's reaction to climate change and reports miscellaneous policy matters such as energy security and the formation of new capabilities (Sharma et al. 2015). The goal of JNNSM is to build India as global front-runner in terms of solar energy generation, by creating strategies for its larger scale dissemination all over the country immediately. The JNNSM had set the motivated aim to setup 20,000 MW of grid-connected solar power by 2022 and intended to drop the price of solar power production in the country through (i) long-term policy; (ii) large-scale

---

[1] http://mnre.gov.in/file-manager/UserFiles/jnnsm_gridconnected_24082011.pdf.

Table 1 The power scenarios in India as on 30 April 2017 (region- and resource-wise)

Region	Thermal (in MW)				Nuclear (in MW)	Hydro (in MW)	RES (in MW)	Total (in MW)
	Coal	Gas	Diesel	Total				
Northern Region	51,989.2	5,781.26	0	57,770.46	1,620	19,311.77	11,539.36	90,241.59
Western Region	69,623.62	11,203.41	0	80,827.03	1,840	7,447.5	18,304.43	108,418.96
Southern Region	43,382.02	6,473.66	761.58	50,617.26	3,320	11,739.03	26,132.07	91,808.36
Eastern Region	28,828.02	100	0	28,928.02	0	4,834.12	990.74	34,752.87
North-Eastern Region	580.02	1,771.05	36	2,387.07	0	1,262	281.12	3,930.19
Islands	0	0	40.05	40.05	0	0	12.52	52.57
All India (Total)	194,402.88	25,329.38	837.63	22,0569.9	6,780	44,594.42	57,260.24	32,9204.54

Source Central Electricity Authority, Ministry of Power, Government of India

Table 2 State-wise installed capacity of solar power projects as on 31 January 2017 (MNRE 2017a) Solar Power Projects Commissioning Status as on 31 January 2017

Sr. No.	State/UT	Total cumulative capacity till 31 March 2016 (MW)	Capacity commissioned in 2016–17 till 31 January 2017 (MW)	Total cumulative capacity till 31 January 2017 (MW)
1.	Manipur	0	0.01	0.01
2.	Meghalaya	0	0.01	0.01
3.	Sikkim	0	0.01	0.01
4.	Puducherry	0.03	0	0.03
5.	Goa	0	0.05	0.05
6.	Mizoram	0.1	0	0.1
7.	Arunachal Pradesh	0.27	0	0.27
8.	Himachal Pradesh	0.2	0.13	0.33
9.	Nagaland	0	0.5	0.5
10.	Dadra & Nagar Haveli	0	0.6	0.6
11.	Lakshadweep	0.75	0	0.75
12.	J&K	1	0	1
13.	Daman & Diu	4	0	4
14.	Tripura	5	0.02	5.02
15.	Andaman & Nicobar	5.1	0.3	5.4
16.	Assam	0	11.18	11.18
17.	Kerala	13.05	2.81	15.86
18.	Chandigarh	6.81	9.4	16.2
19.	Jharkhand	16.19	1.33	17.51
20.	West Bengal	7.77	15.3	23.07
21.	Delhi	14.28	24.5	38.78
22.	Uttarakhand	41.15	3.95	45.1
23.	Other/MoR/PSU	58.31	3.39	61.7
24.	Haryana	15.39	57.88	73.27
25.	Odisha	66.92	10.72	77.64
26.	Bihar	5.1	90.81	95.91
27.	Chhattisgarh	93.58	41.61	135.19
28.	Uttar Pradesh	143.5	125.76	269.26
29.	Karnataka	145.46	196.46	341.93
30.	Maharashtra	385.76	44.7	430.46
31.	Punjab	405.06	187.29	592.35
32.	Madhya Pradesh	776.37	73.98	850.35

(continued)

Table 2 (continued)

Sr. No.	State/UT	Total cumulative capacity till 31 March 2016 (MW)	Capacity commissioned in 2016–17 till 31 January 2017 (MW)	Total cumulative capacity till 31 January 2017 (MW)
33.	Andhra Pradesh	572.97	406.68	979.65
34.	Telangana	527.84	545.57	1,073.41
35.	Gujarat	1,119.17	40.58	1,159.76
36.	Rajasthan	1,269.93	47.71	1,317.64
37.	Tamil Nadu	1,061.82	529.15	1,590.97
Total		6,762.85	2,472.39	9,235.24

Table 3 JNNSM target of capacity additions (http://seci.gov.in/content/innerinitiative/jnnsm.php)

S. No.	Section	Target for phase 1	Cumulative target for phase 2	Target for phase 3
1.	Utility grid power including rooftop	1,000–2,000 MW	4,000–10,000 MW	20,000 MW
2.	Off-grid solar applications	200 MW	1,000 MW	2,000 MW
3.	Solar collectors	7 million m^2	15 million m^2	20 million m^2

deployment goals; (iii) aggressive R&D and (iv) in-house production of critical raw materials, components and products, in order to achieve grid tariff parity by 2022 (Sharma et al. 2015). The mission will produce a permitting policy framework to attain this impartial and make India as worldwide leader in the solar energy generation sector. The JNNSM was set up with a three-phase method, traversing from the period 2011–2022. The period from 2010 to 2013 is known as I Phase, the 12th Plan, i.e. 2013–2017 as II Phase, and 2017–2022 the 13th Plan as III Phase.[2] The target of the mission under each phase is given in Table 3.

3.3 Target of Solar Power in India by 2022

In line with the Ministry of Power, 581,397 numbers of villages were electrified, out of 597,464 numbers of villages in India in 2015 at the ending of October month. The target of Indian government is to electrify all villages by the year 2022. By reason of the restriction in power production from conventional sources, the Indian government has enthused towards non-conventional energy sources, i.e. renewable energy sources for achieving the energy demand of customers. Recently, uses of solar photovoltaic and thermal technology have augmented considerably in all over

---

[2] http://mnre.gov.in/file-manager/UserFiles/draft-jnnsmpd-2.pdf.

India. The government has fixed an objective to reach the total electric power production of 175,000 MW from renewable energy resources by the year 2022, out of which around 100,000 MW of electricity will be generated by solar energy (MNRE 2017b).

3.4 Solar Power Institution and Association in India

The Indian government had been allied with some private and semi-government organizations for the promotion of solar power in India. The details of institutions are as follows:

3.4.1 Ministry of New and Renewable Energy (MNRE)

The Ministry of New and Renewable Energy (MNRE) is the nodal Ministry of the Government of India for all matters concerning to new and renewable energy. Creation CASE and Ministry are as follows: (I) Commission for Additional Sources of Energy (CASE) in 1981, (II) Department of Non-Conventional Energy Sources (DNES) in 1982, (III) Ministry of Non-Conventional Energy Sources (MNES) in 1992 and (IV) Ministry of New and Renewable Energy (MNRE) in 2006. The role of the ministry has been presumptuous growing importance in current times with the growing apprehension for the country’s energy security. The self-sufficiency of energy was recognized as the main driver for renewable energy in the country in the wake of the two oil tremors of the 1970s. The unexpected upsurge in the cost of oil, uncertainties related with its supply and the contrary influence on the stability of payments position directed to the founding of the Commission for Additional Sources of Energy in the Department of Science and Technology in March 1981 (MNRE 2017c).

3.4.2 Indian Renewable Energy Development Agency (IREDA)

Indian Renewable Energy Development Agency (IREDA) is a Mini Ratna (Category-I) Indian Government enterprise under the managerial control of Ministry of New and Renewable Energy. IREDA is a public sector government corporation recognized as a Non-Banking Financial Institution in 1987 involved in encouraging, increasing and spreading monetary support for setting up projects relating to renewable sources of energy and energy efficiency. The main objective of IREDA is (i) to provide monetary support to the specific projects and schemes for generating electricity, (ii) to endeavour to be economical institution through customer gratification, (iii) to preserve its situation as a leading association to offer effective and effective financing in renewable energy and energy efficiency projects, and (iv) to enhancement in the efficiency of services provided to consumers through continual advance of systems, methods and resources (IREDA 2017).

3.4.3 Solar Energy Corporation of India (SECI)

'Solar Energy Corporation of India Ltd' (SECI) is a CPSU under the organizational control of the Ministry of New and Renewable Energy (MNRE), set up on 20 September 2011 to facilitate the operation of JNNSM and accomplishment of targets fixed in that. This organization is the only CPSU devoted to the solar energy area. It was originally integrated as a Section 25 (not for profit) company under the Companies Act, 1956.

In the present outlook of the renewable energy sector, especially solar energy, SECI has a key role to play in the solar energy sector growth. This organization is responsible for execution of a number of orders of MNRE, foremost ones being the VGF schemes for significant grid-connected projects under JNNSM, solar park scheme and grid-connected solar rooftop scheme, along with a host of other specialized arrangements such as defence scheme, canal top scheme, Indo–Pak border scheme, etc. (SECI 2017).

3.4.4 National Institute of Solar Energy (NISE)

National Institute of Solar Energy (NISE) is a self-governing organization of MNRE, which is the top National R&D organization in the field solar energy in India. The Indian government has converted 25-year-old Solar Energy Centre (SEC) under MNRE to a self-governing organization in September 2013 to support the Ministry in executing the National Solar Mission and to manage research, technology and other associated works. National Institute of Solar Energy as an apex institute of the Ministry of New and Renewable Energy, in the area of solar energy, is undertaking activities related to research and development, testing, certification, standardization, skill development, resource assessment and awareness in the field of solar energy and associated technologies (CERC 2012).

4 Concentrating Solar Power (CSP)

The CSP technologies only utilize direct sunlight which incident on the solar concentrator surface. The incident solar irradiation focused on heat transfer fluid by solar concentrator and thus produces higher temperatures when the light is absorbed by some material surface. Presently, the CSP systems have four main categories which can be classified by the way, that is, they focus the sun's rays and the technology castoff to collect the sun's energy. The CSP systems are categorized by their focus geometry as either line-focus concentrators (which includes parabolic trough collectors and linear Fresnel collectors) or as point-focus concentrators (which includes central receiver systems, parabolic dishes and Scheffler systems).

4.1 Godawari CSP Plant

The power production by Godawari CSP Plant has started in June 2013, coinciding with World Environment Day. Godawari CSP Plant is the nation's first Solar Thermal Power Plant under JNNSM, Phase-I. This solar thermal power plant has used parabolic trough CSP technology with state-of-the-art SKAL-ET 150 trough structure. Upon reaching full capacity, the project featuring a solar field aperture area of almost 400,000 m^2, produces up to 118,000 MW hours of electricity per year. Godawari plant is one of the finest examples of successful installation and operation of CSP technology in India. Being a first-ever CSP plant in India, it had created assurance among industries to implement cleaner and highly proficient technology.

4.2 Thermal Energy Storage and Applications

Thermal energy storage (TES) systems allow the storage of heat or cold for later use. TES is useful for applications where there is a mismatch between supply and demand of energy. TES systems can be extremely useful for integration with renewable energy sources which are intermittent and whose availability is further reduced by weather perturbation. Solar thermal energy is available only during the day, and hence, its application requires efficient thermal energy storage so that the excess heat collected during sunshine hours can be stored for later use during the night.

4.2.1 Phase Change Materials and Their Properties

In the recent times, a lot of research is being conducted in the high-temperature thermal energy storage system. They can be primarily divided into three types, namely sensible, latent and thermochemical energy storage system. The traditional two-tank sensible heat storage system (sensible heat storage), which uses molten salts, are not as efficient as latent heat energy storage system (LHES), which store a greater amount of heat per unit volume. The materials used for LHES are called phase change materials (PCM). They store a large amount of heat as the heat of fusion and can provide the stored heat when required by the system.

4.3 Integrated Solar Thermal Power Plant at DADRI (U.P.) India

National Thermal Power Corporation (NTPC) Dadri is the power project to come across the power plea of National Capital Region (NCR) in India. It has 1,820 MW coal-fired thermal power plant and 817 MW gas-fired plants. This power plant is installed in Gautam Budh Nagar in Uttar Pradesh, which is 9 km from Dadri and about to 25 km from Ghaziabad. The project at NTPC DADRI is the first integrated solar thermal power plant project in India. In this project, a solar field is going to supply heat to the existing power plant. The heat will be supplied to the high-pressure heater which will offset the steam which is currently being used for this purpose. This steam which is saved will go through the high-pressure and the low-pressure turbine and deliver work with a high efficiency of 42%.

4.4 CST Plant for Cloth Processing at Navkar Textiles

Navkar Textiles is a process industry, wherein they purchase grey material (cloths) prepared in various looms, the cloth is then stitched together and sent for bleaching and various chemical processes so as to remove impurities during the cloth-making process. After various bleaching and chemical processes, the cloth is passed through a closed chamber where it is passed through the steam to clean various chemical agents during the bleaching process. Further, the cloth is coloured as per required order before dispatch.

5 The Initiatives and Acts for Promotion Solar Energy

To encourage solar energy generation and utilization in India, with wind, biomass, small hydro, etc., the government of India has started numerous electricity policies as well as missions in the recent past like National Electricity Policy 2005, National Rural Electrification Policy 2006, Electricity Act 2003, National Tariff Policy 2006, etc. The particulars of guidelines brought by State and Central Government to develop renewable energy are discussed as follows:

5.1 National Electricity Policy 2005

The ‘National Electricity Policy 2005’ shapes that constantly the part of electricity from renewable energy technology would need to be augmented in terms of sustainable growth; such procurement by scattering corporations will be done by bidding process. Proportion of purchased power from renewable energy sources essentially finished substantially for the prices to be resolute by SERC. The following sections of National Electricity Policy 2005 aim to enhance generation and utilization of electricity produces from renewable energy sources.

- Section 5.2.20 encourages private contribution in renewable energy electricity generation sector.
- Section 5.12.1 aims to reduce the capital cost of renewable energy technology through competition.
- Section 5.12.2 shapes that SERCs must recognize suitable charges to encourage renewable energy and identify goals for this technology.

5.2 National Rural Electrification Policy 2006

India is gifted with the prosperity of rich natural resources, i.e. gas, coal, oil, etc. and some non-conventional energy resources like wind, solar, biomass, small hydro, tidal, geothermal, etc. These energy resources can be appropriately and effectively used to make accessible consistent source of electricity to each and every ménage. The supply of electricity at worldwide reasonable tariffs would also make economic movement in the nation reasonable in the globalized atmosphere. Users, predominantly individuals who are prepared to pay a price which imitates effective costs, have the right to get continuous 24 h supply of quality power.

6 Obstructions and Challenges

India is one of the developing countries in relation to the solar energy industries by developing large solar power plant to meet the current energy demands. The obstructions and challenges related to the solar energy development have been divided into several factors, that is, further extended into different variables and their opinions.

6.1 Technical Obstructions

The solar energy technology is bounded by numerous technical matters and uncertainties, such as energy storage issues, the hazard related to technology and the system, the deficiency and reliability of the direct normal irradiation (DNI) data available, and many others that have always been a matter of debate. The technical obstacles to solar energy vary across the type of technology used (Kumar 2016). The main drawback of photovoltaic systems is its low electrical conversion efficiencies, performance limitations of system elements such as batteries and inverters, and inadequate supply of raw materials.

6.2 Policy and Regulatory Obstructions

To develop steadily solar energy sector needs compassionating policies and promising conventions. The financiers show unwillingness and insecurity if they observe high risk in the sector, which can only be guaranteed by durable and attractive policies for emerging a market. The lack of clearness in the policies and guidelines can unfavourably affect the long-standing growth planning of nations.

6.3 Socio-economic Challenges

The socio-economic challenges have a strong influence on the growth of solar electricity generation in India, as these challenges can tend to less implementation and acceptance of the technology. It is a hard fact that solar energy technology needs huge capital cost which alone cannot be satisfied through independent funds, so there is a need to inducement of private investments, which can only be fascinated when there are favourable incentives to capitalize in this type of technology.

7 Conclusions

India has a severe electricity deficiency. It needs considerable trappings in ability to meet the demand of its rapidly growing economy of the country. The progress of solar energy, which is original and scattered and has the low peripheral cost of generation, can upsurge energy security by expanding supply, decreasing import requirement and justifying fuel price instability. Solar energy growth in India can also be a significant tool for encouraging local economic growth, mainly for numerous underdeveloped states, that have the highest possible for emerging solar power systems which is an unconstrained and clean source of energy. It can provide secure power supply to substitute national industrial growth. Consequently, it can be established that photovoltaic power generation systems will have a significant contribution to the electricity generation of the future not only in India but all over the world.

References

CERC (2012) Central Electricity Regulatory Commission (CERC)

Enerdata (2016) Global energy statistical yearbook 2016. https://yearbook.enerdata.net/#energy-Consumption-Data.html

Garud S, Purohit I (2012) Making solar thermal power generation in India a reality—overview of technologies, opportunities and challenges. http://www.solarthermalworld.org/sites/gstec/files/Solar%20Power%20India%20a%20Reality.pdf, pp 1–9

Goel M (2016) Solar rooftop in India: policies, challenges and outlook. Green Energy Environ 1:129–137. https://doi.org/10.1016/j.gee.2016.08.003

IREDA (2017) Indian Renewable Energy Development Agency Ltd. http://www.ireda.gov.in. Accessed 23 Apr 2017

Kapoor K, Pandey KK, Jain AK, Nandan A (2014) Evolution of solar energy in India: a review. Renew Sustain Energy Rev 40:475–487. https://doi.org/10.1016/j.rser.2014.07.118

Kar SK, Gopakumar K (2015) Progress of renewable energy in India. Adv Energy Res 3:97–115. https://doi.org/10.12989/eri.2015.3.2.097

Kar SK, Sharma A, Roy B (2016) Solar energy market developments in India. Renew Sustain Energy Rev 62:121–133. https://doi.org/10.1016/j.rser.2016.04.043

Kumar S (2016) Renewable and sustainable energy reviews solar photovoltaic energy progress in India: a review. Renew Sustain Energy Rev 59:927–939. https://doi.org/10.1016/j.rser.2016.01.049

Kumar A, Kumar K, Kaushik N, Sharma S, Mishra S (2010) Renewable energy in India: current status and future potentials. Renew Sustain Energy Rev 14:2434–2442. https://doi.org/10.1016/j.rser.2010.04.003

Ministry of Power (2011) Growth of electricity sector in India from 1947–2011, pp 1–63

MNRE (2017a) State wise installed solar power capacity. Ministry of New and Renewable Energy, Govt. of India, http://mnre.gov.in/file-manager/UserFiles/grid-Connected-Solar-Power-Project-Installed-Capacity.pdf

MNRE (2017b) Tentative State-wise break-up of Renewable Power target to be achieved by the year 2022, 1–2. http://mnre.gov.in/file-manager/UserFiles/Tentative-State-wise-break-up-of-Renewable-Power-by-2022.pdf

MNRE (2017c) Ministry of New and Renewable Energy. http://mnre.gov.in/. Accessed 23 Apr 2017

MoP (2017) Growth in conventional electricity generation. Government of India, Ministry of Power, (http://powermin.nic.in/en/content/overview)

Muneer T, Asif M, Munawwar S (2005) Sustainable production of solar electricity with particular reference to the Indian economy. Renew Sustain Energy Rev 9:444–473. https://doi.org/10.1016/j.rser.2004.03.004

Pandey S, Singh VS, Gangwar NP, Vijayvergia MM, Prakash C, Pandey DN (2012) Determinants of success for promoting solar energy in Rajasthan, India. Renew Sustain Energy Rev 16:3593–3598. https://doi.org/10.1016/j.rser.2012.03.012

SECI (2017) Solar Energy Corporation of India Limited (SECI), A Government of India Enterprise, Under Ministry of New and Renewable Energy. http://www.seci.gov.in/content/. Accessed 23 Apr 2017

Sharma A, Srivastava K, Kar SK (2015) Jawaharlal Nehru National Solar Mission in India. In: Sharma A, Kar SK (eds), Energy sustainability through green energy, 1st edn. Springer, India, pp 47–67. https://doi.org/10.1007/978-81-322-2337-5_3

Suresh NS, Rao BS (2017) Solar energy for process heating: a case study of select Indian industries. J Cleaner Prod. https://doi.org/10.1016/j.jclepro.2017.02.190

Teske S, Muth J, Sawyer S, Pregger T, Simon S, Naegler T, O'Sullivan M, Schmid M, Pagenkopf J, Frieske B (2012) Energy [r] evolution-a sustainable world energy outlook. Greenpeace International, EREC and GWEC

Van der Hoeven M (2013) World energy outlook 2013. International Energy Agency, Tokyo

Veeraboina P, Ratnam GY (2012) Analysis of the opportunities and challenges of solar water heating system (SWHS) in India: estimates from the energy audit surveys & review. Renew Sustain Energy Rev 16:668–676. https://doi.org/10.1016/j.rser.2011.08.032

Fundamentals and Performance Evaluation Parameters of Solar Dryer

Mukul Sharma, Om Prakash, Atul Sharma and Anil Kumar

Abstract Solar energy is freely available clean and renewable energy, and available to all. Researchers have developed various technologies to utilize it in various ways such as solar PV technology to generate electricity from solar radiation, solar dryers for drying crops, solar desalination, and solar thermal technology for electricity generation, cooking, etc. This chapter focuses on the utilization of solar energy for vegetable/crop drying. Crop drying is essential for developing countries so that they can provide food security to their citizen in adverse climatic conditions. The solar drying technology is economical and useful for all the developing nations. It has various advantages over open sun drying practices, which are generally performed in various developing nations from an ancient era. This piece of work provides access to various factors and parameters such as dryer efficiency, collector efficiency, moisture ratio, drying period, SMER, etc., which are important in the evaluation of the performance of different types of solar dryers.

Keywords Solar drying · Crop · Performance · Food security
Dryer efficiency

M. Sharma · A. Kumar (✉)
Department of Energy (Energy Centre), Maulana Azad
National Institute of Technology, Bhopal 462003, India
e-mail: anilkumar76@gmail.com

O. Prakash
Department of Mechanical Engineering, Birla Institute
of Technology, Mesra, Ranchi 835215, India

A. Sharma
Non-Conventional Energy Laboratory, Rajiv Gandhi Institute
of Petroleum Technology, Jais, Amethi 229304, UP, India

A. Sharma et al. (eds.), *Low Carbon Energy Supply*, Green Energy and Technology,
https://doi.org/10.1007/978-981-10-7326-7_3

1 Introduction

Sun is the center of our solar system. It is a source of light and heat energy for the residents of the planet earth. The solar energy is used for various natural processes like photosynthesis, evaporation, etc., and some other processes like electricity generation and drying. Human beings had explored the use of solar energy from the ancient era for cloth drying, water desalination, navigation, drying of fruits and vegetables, preparation of spices, etc. These practices are being carried out presently. Energy crisis also encouraged humans to explore new ways of utilizing solar energy for their purposes like electricity generation, food drying, etc.

Food drying is an energy-intensive process and can be costly in case, if electrical and mechanical equipment are used for food drying. The cost of electricity is the main factor which made the conventional technology to be replaced by some other cost-effective technologies of food drying. Researchers have developed some new ways to overcome this factor. They had analyzed and redeveloped the ancient method of food drying, i.e., solar food drying.

The technology of solar food drying is very economical and efficient. In developing countries like India, it has been practiced from the ancient period. The solar food drying is used for drying of spices, vegetables, and fruits so that they can be used in the season in which they are not available. Open sun drying is the most economical method of solar drying in underdeveloped countries to evaporate moisture content from the food products which in turn increase their shelf life and decrease moisture activity (Vijayan et al. 2016). But open sun drying has various demerits such as degradation of food product due to dust, rain, and insects, over or under drying of food, contamination of food products due to human and animals, labor-intensive process, poor quality of drying, large area requirement for drying, etc. (Prakash et al. 2016). To remove these disadvantages, the researchers had developed various solar dryers which can be used for domestic as well as industrial purposes. These solar dryers are classified into various types, viz., indirect type, direct type, and mixed type solar dryers (Prakash et al. 2016). These dryers can also be divided into two types on the basis of mode of operation, viz., active type (forced convection) and passive type dryer (natural convection). The various classifications are shown in Fig. 1.

2 Types of Solar Dryers

Solar dryers are divided into three types on the basis of utilization of solar radiation for the purpose of food drying. The various types of solar dryers are discussed below.

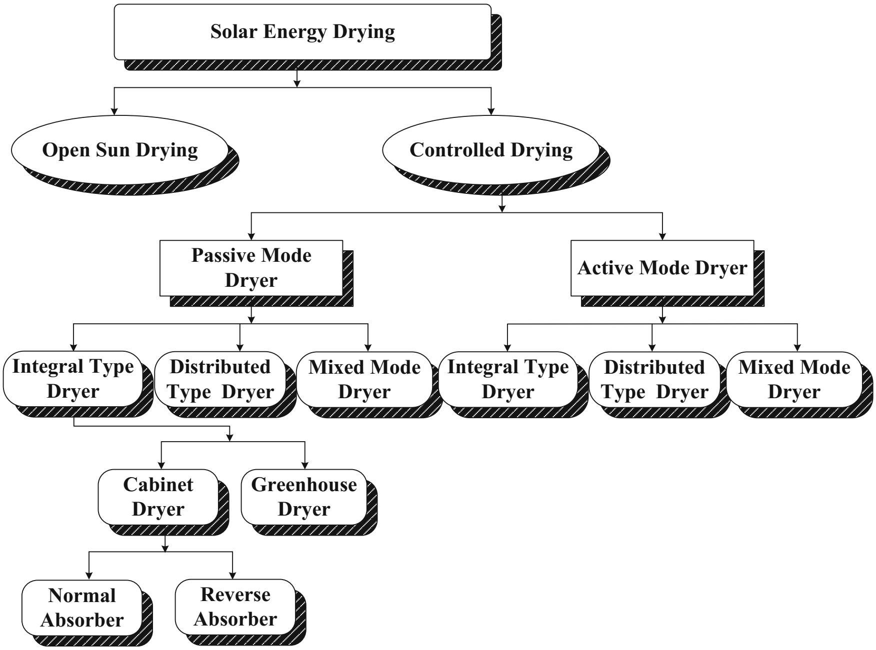

Fig. 1 Classification of solar dryers (Kumar 2006)

2.1 *Direct Type Solar Dryer*

Direct type solar dryers use direct solar radiation for drying. In these, two prominent types of dryers are being used all around the world. First one is cabinet type dryer, and another is greenhouse dryer (Prakash et al. 2016). These dryers are economic as well as these are easy to manufacture. The material of construction is easily locally available. Both the dryers can be operated in both the modes of heat transfer, i.e., active and passive modes. These dryers are most suitable for low-level thermal drying as their inside temperature reaches to 45–70 °C, and the relative humidity inside the dryer is very low (<50%) (Prakash et al. 2016) (Fig. 2).

2.2 *Indirect Type Solar Dryers*

In the indirect type solar dryer, a separate box which is known as drying chamber is used to keep food products. The collector of the dryer is kept under the solar radiation, and with the help of air, the heat is transferred to the drying chamber where the drying of food products is carried out by air through the removal of moisture when it comes in contact with food product. The indirect type solar dryers

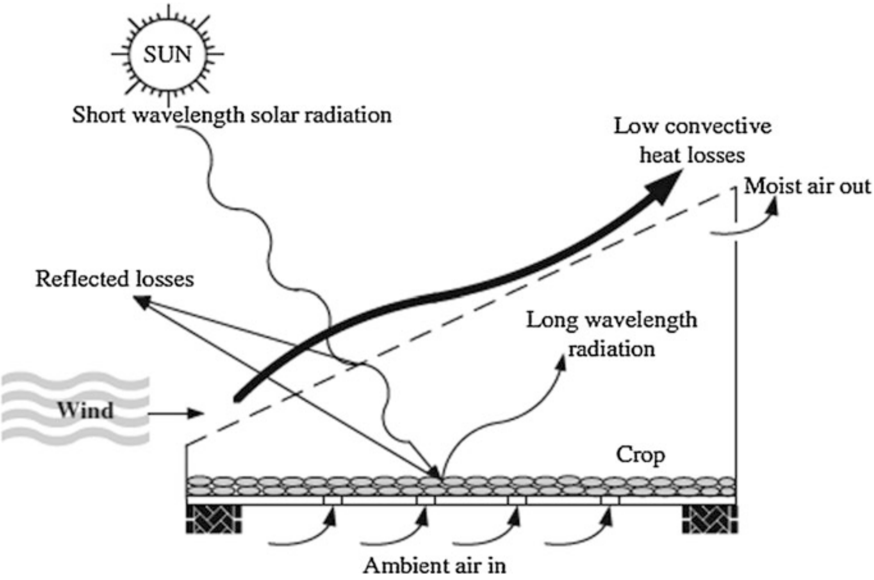

Fig. 2 Direct sun drying (Prakash et al. 2016)

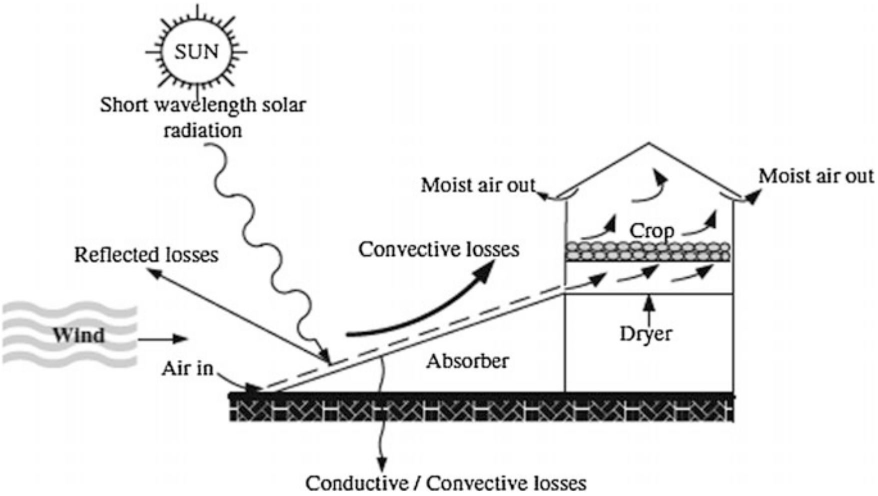

Fig. 3 Indirect sun drying (Prakash et al. 2016)

can be operated in passive as well as active mode. The crops with low moisture content are dried with passive indirect solar dryer while the crops with higher moisture content are dried using the active indirect solar dryer (Prakash et al. 2016) (Fig. 3).

2.3 Mixed Mode Type Solar Dryers

Mixed mode type solar dryers work on both drying mode concepts, i.e., indirect and direct mode. In this, the food products are directly exposed to sunlight as well as it also gets heat from solar air heating collector, which reduces the drying period. The drying chamber is exposed to solar radiation, and solar thermal energy is transferred to it by air using either forced or passive convection mode.

3 Performance Evaluation Parameters of Various Solar Dryers

The performance of solar dryers depends on various factors such as moisture content, drying period, dryer efficiency, etc. For the different types of solar dryers, there are different parameters which affect the performance of these dryers. The different factors which are essential to evaluate the performance of various solar dryers are discussed below.

3.1 Direct Solar Dryer

Wankhade et al. (2014) discussed the method to evaluate the performance of direct type solar dryer. The performance of direct type solar dryer is evaluated by various factors. These factors are moisture content, moisture ratio, drying efficiency, and drying rate. The factors are given as follows.

3.1.1 Moisture Content

The quantity of water present in a material, such as fruits, is known as moisture content or water content. The moisture content in percentage can be determined using the following relation (Wankhade et al. 2014):

$$M_c = \frac{M_\mathrm{i} - M_\mathrm{d}}{M_\mathrm{i}} \times 100$$

where

M_i mass of food product before drying, and
M_d mass of food product after drying.

3.1.2 Moisture Ratio

The moisture ratio of the food product is calculated by using equilibrium moisture content and initial moisture content. The relation of the moisture ratio is given as follows (Wankhade et al. 2014):

$$\mathrm{MR} = \frac{M - M_\mathrm{e}}{M_\mathrm{o} - M_\mathrm{e}}$$

where

MR moisture ratio,
M moisture content at any time,
M_e equilibrium moisture content, and
M_o initial moisture content of the food material.

3.1.3 Drying Rate

Drying rate is indicated using the graphical representation with time and moisture content as its coordinates. The drying rate of the food sample will be determined as (Wankhade et al. 2014)

$$R_\mathrm{d} = \frac{(M_\mathrm{i} - M_\mathrm{d})}{t}$$

where

t time interval of readings taken during the drying period.

3.1.4 Drying Efficiency

The ratio of total heat consumed by the product for evaporating the moisture present inside it to the total amount of solar radiation on the collector surface is known as drying efficiency (Wankhade et al. 2014). It can be written as

$$\eta_d = \frac{(W \times \Delta H_\mathrm{l})}{A_\mathrm{c} \times I_\mathrm{c}}$$

where

W moisture evaporated from food product in kg,
ΔH_l latent heat of vaporization of water, 2320 kJ/kg,
I_c total hourly isolation upon collector, Wm^2, and
A_c area of the collector, m^2.

3.2 Indirect Solar Dryer

The performance of the indirect type solar dryer is evaluated on the basis of following factors: moisture content, drying rate, drying efficiency, collector efficiency, flow velocity of air, and drying period. The factors moisture content and drying rate were already discussed. The other factors are determined as follows.

3.2.1 Drying Period

It is the duration during which drying of the food product is carried out inside the dryer. It is a most important parameter which is considered for evaluation of dryers. The drying time is taken into estimation from the time when the food product is kept in the dryer until when it dries to a certain moisture content level. The drying period is estimated in hours or days.

3.2.2 Flow Velocity of Air

It is the velocity of air (in m/s) which is provided inside the drying chamber by active (Forced flow) or passive (natural flow) medium. In active indirect type solar dryer, the food product is dried in higher air velocity than passive indirect type solar dryer.

3.2.3 Collector Efficiency

The collector efficiency is described by conversion of sun's radiation into usable heat gain and losses. The heat gain and losses are calculated by performing thermal analysis. In this analysis, heat gain and losses for top flow (between absorber plate and glass cover) and bottom flow (between absorber plate and bottom insulation) are calculated (Hegde et al. 2015). The relation for collector efficiency is as follows (Gatea 2011):

$$\eta = \frac{\rho V C_{\mathrm{p}} \Delta T}{A I_{\mathrm{c}}}$$

where

ρ air density, kg/m^3,
I_{c} insolation on the collector,
ΔT difference of temperature, K,
C_{p} specific heat capacity of air at constant pressure, J/kgK,
V volumetric flow rate, m^3/s, and
A collector's effective area facing the sun, m^3.

3.2.4 Dryer Efficiency (η_d)

The dryer efficiency gives the performance of the dryer. It shows that how effectively the energy input is used to dry the food product. Dryer efficiency is given as (Gatea 2011)

$$\eta_\mathrm{d} = \frac{\boldsymbol{ML}}{\boldsymbol{I_c A t}}$$

where

L latent heat of vaporization of water,
M mass of food material, and
t drying period.

3.3 *Mixed Mode Solar Dryer*

Mixed mode solar dryer works on the principle of direct and indirect solar dryer. Various factors calculated for evaluating the performance of solar dryers are as follows: pressure drop calculation, mass flow measurement, velocity measurement, Reynolds number, heat gained by air, thermal efficiency, drying rate, and moisture content.

3.3.1 Pressure Drop Calculation

The pressure drop is defined as the difference in pressure between two points of a fluid carrying network. The pressure drop across the orifice plate has measured by the following relationship (Pardhi and Bhagoria 2013):

$$\Delta P_o = \Delta h \times 9.81 \times \rho_\mathrm{m} \times \frac{1}{5}$$

where

ΔP_o pressure difference,
Δh difference of liquid head in manometer, and
ρ_m density of mercury, 13.6×10^3.

3.3.2 Mass Flow Measurement

Mass flow rate of air is the mass of airflow per unit of time, and it is calculated by measuring pressure difference across the orifice plate by following relation (Pardhi and Bhagoria 2013):

$$m = C_\mathrm{d} \times A_\mathrm{o} \times \left[\frac{2\rho \Delta P_o}{1-\beta^4}\right]^{0.5}$$

where

m mass flow rate of air, kg/s,
C_d coefficient of discharge of orifice, 0.62,
A_o area of orifice plate in m^2,
ρ density of air, 1.157 $\mathrm{kg/m}^3$, and
β ratio of diameter (Do/Dp).

3.3.3 Reynolds Number

Reynolds number is determined as the ratio of viscous force and inertia force. It is given as (Pardhi and Bhagoria 2013):

$$R_e = \frac{VD}{\vartheta}$$

where

V air velocity, m/s,
D hydraulic diameter in meter, and
ϑ kinematic viscosity, $16.70 \times 10^{-6}\ \mathrm{m}^2/\mathrm{s}$.

3.3.4 Heat Gained by Air

The heat gained by the air is calculated using inlet and outlet temperature of the air. The heat transfer rate inside solar air heat collector is given by the following relations (Pardhi and Bhagoria 2013):

$$Q_\mathrm{a} = mC_\mathrm{p}(T_\mathrm{o} - T_\mathrm{i})$$

where

m mass flow rate of air, kg/s,
C_p specific heat of air, kJ/kg,
T_o outlet temperature, °C, and
T_i inlet temperature, °C.

3.3.5 Thermal Efficiency

It is the ratio of heat gained by the air inside collector to the product of the area of collector and solar insolation. It is a dimensionless parameter. The thermal efficiency of a mixed mode dryer is given as (Pardhi and Bhagoria 2013)

$$\eta = \frac{Q_a}{IA_p}$$

where

Q_a heat gain by air, watts,
A_p area of collector plate, m^2, and
I solar insolation, W/m^2.

4 General Parameters Considered for Performance Evaluation of Solar Dryers

Leon et al. (2002) described various general parameters which are considered for performance evaluation of solar dryers. The commonly measured parameters are as follows:

- Physical parameters of dryer
  - Type, size, and shape of dryer,
  - Drying capacity/loading density of dryer, and
  - Area of tray and number of trays (as per dryer).
- Thermal performance parameters
  - Drying rate,
  - Drying air temperature,
  - Airflow rate, and
  - Dryer efficiency.

- Quality of dried product
    - Sensory quality (taste, color, aroma, etc.),
    - Nutritional attributes, and
    - Rehydration capacity.
- Payback period and cost of dryer

4.1 *Physical Parameters of the Dryer*

This refers to the physical features of the solar dryers, i.e., its type, dimensions, the material used for fabrication, and weight of the dryer. Some common materials for construction of dryer are wood, metals, fiber sheets, etc. Apart from these materials, cement and mortar are also used for the construction of solar dryer (Ekechukwu and Norton 1999). Solar collectors are usually fabricated with GI or steel, aluminum, and painted with a matt finish (non-reflecting) black paint. Common glazing materials which are used for the construction of solar dryer are glass, transparent plastic sheet, polyethylene, etc. Insulating materials include glass wool, rock wool, plywood, etc. Trays are fabricated from stainless steel, GI steel, and nylon wire mesh.

The size of the dryer is a measure of its capacity, i.e., the quantity of food product which can be loaded in the dryer in a single batch for drying. For a particular dryer, the drying capacity varies with the type and shape of food material which is kept in it for drying. For efficient drying of the food product, the food material should be spread in a single layer. So in this case, total tray area available is the most important factor in the calculation of capacity. In cabinet type and shelf type dryers which consist of more than one tray, the no. of layers of the tray and their area are considered in determining the capacity of the solar dryer. The capacity of the dryer also depends on the size of collector and size of drying chamber in indirect and mixed mode solar dryers (Leon et al. 2002).

Loading density is defined as the total capacity of the dryer (with total tray area and drying time). The concept of placing the food material one over another tends to limit the exposure of the food product to drying air, and this results in poor drying of the food product. Overloading of the food product also results in poor quality of drying. Apart from this, part loading leads to non-optimal utilization of the dryer area which results in low dryer efficiency. The loading density depends on product type, its moisture content, and rate of airflow.

4.2 Thermal Performance Parameters of the Dryer

The drying duration is most important parameter considered in the evaluation of a dryer. The drying duration (in hours or minutes) is estimated from the time of loading of the dryer to the time when the moisture content of the product is reduced to a certain defined (depends on food crop) level. The time duration when sun's radiation is not obtained is also included in the drying time. Higher temperature can reduce the drying duration but could also lead to deterioration of the food product quality (loss of flavor, vitamins, and color). Drying time also reduced by reducing the dimensions of the food material, i.e., by slicing the product (Sodha et al. 1985).

Drying rate can be increased significantly by increasing the air temperature in two ways: First, it results in increasing the ability to dry air to hold moisture content. Second, the vapor pressure can be increased by in heating the food product by hot air. But the temperature of air in a dryer can increase up to a certain limit. The thermal sensitivity of most food products (fruits and vegetables) is the common constraint to the operation of dryers at high temperature. If the air temperature is very high at the beginning of drying process, then the food material can develop hard shell on the outside, and the moisture will remain trapped inside the food material (Leon et al. 2002).

Another important factor for drying process is relative humidity of drying air. Heating of air before entering the drying chamber can result in increase in the ability to hold the moisture from the food materials. To improve dryer's thermal efficiency, the exit hot air from drying chamber can be mixed with some warm air and then again recirculate it in the drying chamber. Soponronnarit et al. (1992) observe a reduction of 50% in drying energy consumption in banana drying. About 95% of the air gets recycled.

Airflow rate is an important thermal parameter which affects the performance of a dryer. As there is an increase in the airflow rate, there will be significant reduction in the conduction and radiation losses due to small temperature rise. But this can also reduce the evaporating capacity of air due to the contact time of air with the food material is significantly reduced and hence results in reduction of drying efficiency.

The efficiency of dryer system consists of dryer efficiency, collector efficiency, pickup efficiency, and SMER (specific moisture extraction rate). The collector efficiency is the measure of the performance of collector of a solar dryer.

The pickup efficiency is the measure of the efficiency of moisture removal by the air from the food material (Tiris et al. 1995). Pickup efficiency decreases with the reduction in moisture content in the food material.

$$\eta_p = \frac{h_o - h_i}{h_{as} - h_i} = \frac{W}{\rho V t (h_{as} - h_i)}$$

Dryer efficiency is the measure of throughout effectiveness of the drying system. It usually represents the performance of dryer by showing how the food drying process effectively utilized the input energy (Vijayan et al. 2016). Leon et al. (2002) mentioned that major factors which affect the dryer efficiency are air temperature rise in drying chamber, wind speed, airflow rate, and dryer/collector design.

SMER is the total amount of moisture (water) removed from the food product per unit energy consumed during the drying process (Vijayan et al. 2016). SMER is the inverse of specific energy consumption (Leon et al. 2002). It is given by following relation (Fudholi et al. 2014; Vijayan et al. 2016):

$$\mathrm{SMER} = \frac{\text{Total moisture removed from the product}}{\text{Total energy input}}$$

4.3 *Quality of Dried Products*

The physical properties are basically affected by the drying process, and these result in a change in shape, size, texture, and color of food material. Dehydration during drying of food products causes various enzymatic and chemical conversions in them (Leon et al. 2002). Some of these conversions can make the food unpleasant in taste but not all the changes are undesirable. Quality of drying totally depends upon the type of dryer used, dryer temperature, drying period, and mode of drying. Assessment of nutritional and sensory parameters and rehydration capacity is considered in the quality assessment of dried food products.

Sensory assessment includes assessment of shape, size, taste, smell, and absence of defects. Loss of flavors in the dried food material occurs due to unpredictable losses and chemical reactions (oxidation, browning, etc.) (Leon et al. 2002).

Nutritional attributes contain chemical parameters such as vitamin C, ash and sugar content, and acidity content before and after drying. Contamination of food products by dust indicates higher ash content; lower level of vitamin C indicates loss of nutrients due to high-temperature drying; and fermentation in food products indicates the higher acidity level in dried food products.

Some food products are consumed after rehydration. The original flavor, texture, and appearance of food products are regained when water is added to the food products. However, the food products cannot attain its original moisture level after rehydration. Drying process affects the tissues of the food products which affect their rehydration capacity (Oliveira and Ilincanu 1999).

5 Conclusion

Solar drying technologies are economic as well as efficient food drying technologies developed by various researchers. These technologies can be used in any season and in various climatic conditions by performing minor changes in the structure and orientation of the dryer. The performance evaluation parameters and the factors affecting performance of solar dryers are discussed in this chapter. The performance parameters such as dryer efficiency, collector efficiency, drying period, etc., can be calculated using relations discussed in the chapter for different types of solar dryers. Based on these results, further graphs can be drawn using simulation software.

References

Ekechukwu O, Norton B (1999) Review of solar-energy drying systems II: an overview of solar drying technology. Energy Convers Manage 40(6):615–655. https://doi.org/10.1016/S0196-8904(98)00093-4

Fudholi A, Sopian K, Yazdi MH, Ruslan MH, Gabbasa M, Kazem HA (2014) Performance analysis of solar drying system for red chili. Sol Energy 99:47–54. https://doi.org/10.1016/j.solener.2013.10.019

Gatea AA (2011) Performance evaluation of a mixed-mode solar dryer for evaporating moisture in beans. J Agric Biotechnol Sustain Dev 3(4):65–71. https://doi.org/10.1080/07373939708917254

Hegde VN, Hosur VS, Rathod SK, Harsoor PA, Narayana KB (2015) Design, fabrication and performance evaluation of solar dryer for banana. Energy, Sustain Soc. https://doi.org/10.1186/s13705-015-0052-x

Kumar A (2006) Thermal modeling of greenhouse dryer. PhD Thesis, Indian Institute of Technology, Delhi. TH 3349. http://www.eprint.iitd.ac.in/bitstream/2074/6174/1/TH-3349.pdf

Leon MA, Kumar S, Bhattacharya SC (2002) A comprehensive procedure for performance evaluation of solar food dryers. Renew Sustain Energy Rev 6(4):367–393. https://doi.org/10.1016/S1364-0321(02)00005-9

Oliveira AR, Ilincanu L (1999) Rehydration of dried plant tissues: basic concepts and mathematical modelling. In: Oliveira Fernanda AR, Oliveira Jorge C (eds) Processing foods: quality optimisation and process assessment. CRC Press. http://www.crcnetbase.com/doi/pdfplus/10.1201/9781420049008.ch12

Pardhi CB, Bhagoria JL (2013) Development and performance evaluation of mixed-mode solar dryer with forced convection, pp 1–8

Prakash O, Kumar A, Sharaf-Eldeen YI (2016) Review on Indian solar drying status. Curr Sustain/Renew Energy Rep 3(3–4):113–120. https://doi.org/10.1007/s40518-016-0058-9

Sodha MS, Dang A, Bansal PK, Sharman SB (1985) An analytical and experimental study of open sun drying and a cabinet tyre drier. Energy Convers Manage 25(3):263–271. https://doi.org/10.1016/0196-8904(85)90042-1

Soponronnarit S, Dussadee N, Hirunlabh J (1992) Computer simulation of solar-assisted fruit cabinet dryer. RERIC Int Energ J 14(1). http://archive.lib.kmutt.ac.th/doc/objects/20100120143941/ar_6651/2011092313514512000223.pdf

Tiris C, Tiris M, Dincer I (1995) Investigation of the thermal efficiencies of a solar dryer. Energy Convers Manage 36(3):205–212. https://doi.org/10.1016/0196-8904(94)00051-Z

Vijayan S, Arjunan TV, Kumar A (2016) Mathematical modeling and performance analysis of thin layer drying of bitter gourd in sensible storage based indirect solar dryer. Innov Food Sci Emerg Technol 36:59–67. https://doi.org/10.1016/j.ifset.2016.05.014

Wankhade PK, Sapkal RS, Sapkal VS (2014) Design and performance evaluation of solar dryer, 2014, pp 70–73

Role of Solar Drying Systems to Mitigate CO_2 Emissions in Food Processing Industries

K. Rajarajeswari, B. Hemalatha and A. Sreekumar

Abstract This chapter sheds light on the role of solar drying systems in food processing industries to mitigate carbon dioxide emissions. The industrializing world is encircled by scads of environmental problems. Greenhouse gas emission leading to climate change is a major concern for which there are many policies emerging among the countries. India, ranking sixth in the world in energy-related carbon dioxide emission, pledged to decrease the emission in Nationally Determined Contributions (NDC). Industries gobble major portion of the energy produced in a country. Food processing is the largest sector in India, which has segments like dairy, fruit and vegetable processing, grain processing, meat processing, poultry processing, fisheries, etc. Drying is an important processing method for food preservation. A conventional type of drying process in industries uses electricity and fossil fuels. Replacing the existing drying systems to alternate energy-driven drying systems helps to reduce the total energy consumption. Solar drying system is remarkable in energy efficiency and product quality. A considerable amount of carbon dioxide emission reduction can be attained by using solar drying systems since they derive energy from the sun, a freely available source of energy. Details on energy consumed by food sectors, energy consumed by other drying systems, and solar drying systems are discussed in this chapter.

Keywords Solar dryer · Greenhouse gas · Carbon dioxide · Food quality
Energy

K. Rajarajeswari · A. Sreekumar (✉)
Centre for Green Energy Technology, Pondicherry University, Puducherry 605014, India
e-mail: sreekmra@gmail.com

B. Hemalatha
Department of Biotechnology, Bharathidasan University, Tiruchirappalli 620024, India

A. Sharma et al. (eds.), *Low Carbon Energy Supply*, Green Energy and Technology,
https://doi.org/10.1007/978-981-10-7326-7_4

1 Energy-Related CO_2 Emission

Global warming is a widely spoken problem since last few decades. The emission of greenhouse gases like CO_2, N_2O, CH_4, CO, etc., into the atmosphere resulted in heating up the Earth. The infrared absorption per molecule is more for greenhouse gases (GHG). The increase in temperature of the globe provides away to climate change and melting of glaciers. Out of all the GHG, 80% of contribution to global warming is by carbon dioxide (Lashof and Ahuja 1990). To mitigate CO_2 emission the world countries have adopted the global warming limit of 2 °C or below. But the probability of exceeding 2 °C is 53–87% if the emission of GHGs is increasing more (Meinshausen et al. 2009). The fossil fuel resource that accumulates carbon for years together, when burnt releases an enormous amount of carbon into the atmosphere. Combustion of coal is the major source of electricity across the globe which is also the source of carbon dioxide emissions into the atmosphere. India relies on coal reserves for its 70% of electricity generation. The carbon dioxide emission factor for electricity production in India was 901.7 gCO_2/kWh in 2005 and increased to 926 gCO_2/kWh in 2012. The emission factor is much higher than the global average energy-related CO_2 emission which was 542 and 533 gCO_2/kWh in the year 2005 and 2012, respectively (IEA 2015). The growing population and energy demand may increase the trace of carbon in the atmosphere. India pledged to reduce the overall emission intensity by 35% in its NDC (Nationally Determined Contributions) (Shearer et al. 2017).

The average carbon dioxide emission factor for different parts of the world is given in Table 1. In India, the emission factor varies with different states, among which Jharkhand has the highest emission factor of 1.21 $kgCO_2e$/kWh and the average electricity generation emission factor of India is 0.89 $kgCO_2e$/kWh (cBalance Solutions Pvt. Ltd. 2009). The emission factor varies with different energy sources. It is obvious from Table 2 that the emission is high for lignite and coal-based thermal power plants. The renewable energy resources emit less carbon into the atmosphere compared to conventional energy resources.

The major energy consumption is by industrial and transport sectors. The industries use different forms of energy like heat, light, water, etc. The heating

Table 1 Carbon dioxide emission factor (IEA 2015)

	CO_2 emission factor from electricity ($kgCO_2e$/kWh)
Africa	0.70
Asia	0.77
Europe	0.36
Latin America	0.18
Middle East	0.67
North America	0.567
Pacific	0.46
Former USSR	0.36

Table 2 Carbon dioxide emission of different sources (World Nuclear Association 2011)

Source	Carbon dioxide emission (tons CO_2e/GWh)
Lignite	1,054
Coal	888
Oil	733
Natural gas	499
Solar PV	85
Biomass	45
Nuclear	29
Hydroelectric	26
Wind	26

sector is one of the potential consumers of energy. Heat generation consumes more than 50% of global energy consumption. Heating sector uses a considerable percentage of total energy and it is met with the fossil fuel reserves. This production of heat accounts for one-third of energy-related carbon dioxide emissions according to International Energy Agency (IEA). One-third of energy accounts for 10 Gtonne emission of carbon dioxide per year (Eisentraut and Adam 2014). Despite its huge energy consumption, the heating sector receives less attention. Heat production using alternative energy provides a way to boost energy security and turn down energy-related CO_2 emissions in the economically viable way. Heat generation is a very important process in many industries for processing, melting, boiling, evaporation, etc., among which food processing industries rely on heat generation for producing quality food products.

2 Energy Consumed by Food Sector

Industrial sector uses more energy amounting to 54% of world's total energy consumption. Industries are classified into two according to their energy usage, namely, energy-intensive manufacturing, non-energy-intensive manufacturing, and nonmanufacturing (U.S. Energy Information Administration 2014). Industrial sector uses energy for different applications such as assembly, cogeneration, steam, lighting, heating, air-conditioning, process heating, and cooling. Food and beverage production falls under energy-intensive manufacturing sector. The different food processing industries in India are dairy, fruits, vegetables, grain, meat, poultry processing, and fisheries. The country produces a large number of food products out of which only 2% undergoes processing (I. Brand Equity Foundation). This is due to lack of food processing techniques and the high cost of existing techniques. A packed food or processed food undergoes many stages from the day of cultivation till it reaches consumers. Each and every stage requires energy in the form of electricity, thermal energy, and water. The food industry in Taiwan is the largest consumer of electricity among the manufacturing sectors. 95% of total energy used is petroleum and electricity. The intensity of GHG emission is increased due to large amount energy consumption among of food sectors. The energy consumption of 76 food sectors in Taiwan is 685,002 MWh of electricity, 69,540 L of fuel oil, 2,136 ton of LPG and 2,853 km^3 of natural gas (Ma et al. 2012). The food industry was the fifth largest energy-consuming sector in the USA in the year 1994 (Drescher et al. 1997). The energy requirement was mainly met with electricity. Food sector depends on energy for food processing, safe package, and storage. Heating processes such as roasting, cooking, frying, and boiling use fuels and electricity. Cooling and refrigeration process depend on electricity. Packaging is a very important step, which is more energy-consuming process. Freezing and drying are the most pivotal methods of food storage. Freezing requires more energy and drying is mostly met with fossil fuel reserves.

Atmospheric forced hot air dryers are the commonly used method for drying food products. The major problem that deals with the hot air drying is the large energy requirement and low drying efficiency. During the drying process, the evaporation occurs at a rapid rate and the outer skin gets dried faster with wet interior leading to case-hardening which is a quality defect. If the products are exposed to high temperature for longer time, the color and flavor of the product degrade. So the conventional method of drying does not result in good quality. The methods that result in high-quality food products consume more energy and the traditional open sun drying consumes zero energy but suffers from food loss and low quality.

3 Fundamentals of Drying

Drying is one of the oldest methods of food preservation. Drying prevents the growth of microbes in the food and helps the food for longer storage. This is because the microbial growth and multiplication get deteriorated in the absence of water. Drying of the food product is removing excess moisture content by vaporizing the water present in the product. This process of drying requires energy to vaporize the water. There are two processes that are responsible for the unit operation of energy required for drying:

- The energy required to remove the bound water from the product, i.e., heat transfer to provide necessary latent heat of fusion.
- The energy required to remove the water vapor from the product, i.e., flow of hot air to remove the moisture.

The drying systems are mostly provided with electricity and another fossil fuel has driven systems to generate the heat required for drying. There are many types of drying. They are:

Hot air drying: In this type of drying the moisture is removed by supplying hot air.

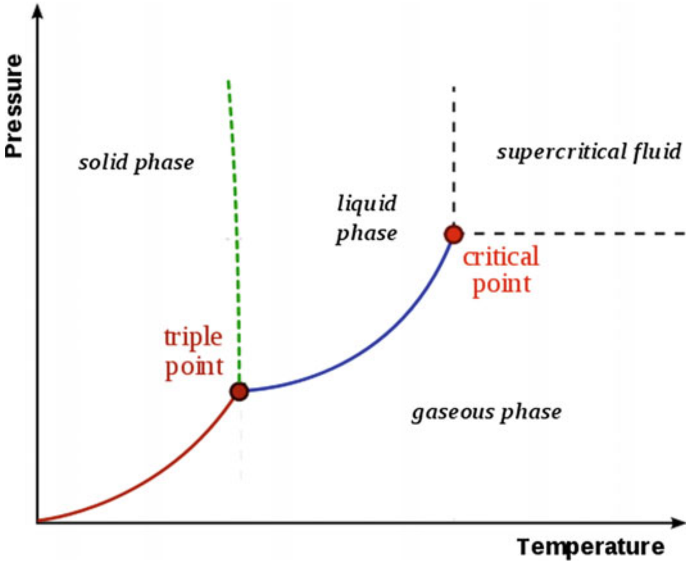

Fig. 1 Phase diagram of water

Freeze drying: This is the process in which the product is frozen and the moisture is removed by the process of sublimation. The food structure is maintained superior in this type of drying.
Vacuum drying: In this type, the pressure is reduced by means of the vacuum pump, and the heat transfer is done by conduction by passing the steam over the products.

The phase diagram of water shown in Fig. 1 gives the physical states at different temperatures and pressures. At room temperature and pressure, it takes the liquid form. It becomes solid when the temperature is lowered below 273 K and above 373 K, it gets vaporized at the same pressure. The point at which all the three phases coexist is called triple point. The energy required to evaporate a particular mass of water (m_w) is given as

E (kJ) = m_w × Latent heat of vaporization of water

$$m_w = \frac{M(m_i - m_f)}{100 - m_f}$$

where m_w is the mass of water to be removed (kg), m_i is the initial moisture content (%), m_f is the final moisture content (%), and M is the total mass of product (kg).

The percentage moisture content of a sample can be given as

$$\%\,\text{moisture} = \frac{\text{weight of wet sample} - \text{weight of dried sample}}{\text{weight of wet sample}} \times 100$$

Drying of food products is more energy consuming due to the high moisture content. The moisture content varies with different products. The product has to be dried to equivalent moisture content for storage. Low moisture content tends to prevent the microbial attack and preserve the product for a longer duration. The major parameters that are concerned about drying process are:

Time period: The products with high moisture content require more time to be dried. This may invite the microbial attack during the process of drying.
Energy: It requires more energy to remove water that is bound to the food products than the liquid water due to the high latent heat of vaporization. Hence, drying is a more energy-consuming process.
Economics: The storage process is most expensive than the cost required for producing the food products, particularly the food producers cannot afford.
Quality: The quality of dried products enables the consumer to attract toward the market. So quality is the most important parameter which cannot be compromised.

The drying technology must be able to meet the above parameters of the drying process. There are many technological advances in recent times to produce high-quality products.

4 Energy Consumed by Different Drying Technology

Microwave drying is a technique in which microwave energy is applied to the products to increase the temperature of the product which increases the rate of water removal. Soysal et al. used microwave convective drying to enhance the quality of dried red pepper. Color, texture, and sensory properties were analyzed and presented. The drying system comprised of two 900 W microwave oven, a 100 W radial fan with volume flow rate 180 m^3 h^{-1} (Soysal et al. 2009). If the operation of the equipment is for 2 h, then it requires 1.8 kWh of energy. This process releases 1.6 kg of carbon dioxide into the atmosphere for 2 h if the average emission is considered to be 0.89 $kgCO_2e/kWh$. If the equipment is operated continuously in a food processing industry, it leads to 529 kg of CO_2 emissions per year for drying single product. The energy-related carbon dioxide emission changes with different products. Mortaza et al. developed a laboratory-scale hot air dryer for drying berberis fruit and compared it to the sun drying. The specific energy requirement for thin drying of berries is given as 20.93–1,110.07 (kWh/kg) (Aghbashlo et al. 2008). The energy-related carbon dioxide emission is 17 kg to 910 kg per kg of fresh product.

Lucio et al. investigated the energy consumption and analysis of industrial drying plants for fresh pasta process. They discussed the energy needs and CO_2 emissions resulting from a small factory producing fresh pasta located in Molise, Italy. According to the study, 50% of electricity is consumed by two processes, namely, pasteurization, and drying. There are five steps in processing before the product is packed: (i) picking up and storage of raw materials, (ii) mixing of ingredients, (iii) shaping, (iv) pasteurization and pre-drying of pasta, and (v) drying. Energy resources like electricity, thermal, and water were used. Electrical energy is used in the whole plant and thermal energy is used for pasteurization and drying. Monthly pasta production consists of 5,846 kg of pasta, 175 kg of dry pasta. The amount of energy used is (i) 1,100 kWh of electricity, 44.77 kWh of which was used for dry pasta, (ii) 6,231.8 kWh of thermal energy, 366.2 kWh was used for the production of dry pasta. Every kg of monthly produced pasta requires 0.18 kWh of electricity, equivalent to almost 78 g of CO_2 emission and 1.1 kWh thermal energy equivalent to almost 220 g of CO_2 emissions.

Firouzi S et al. analyzed energy consumption for drying paddy using the newly designed horizontal rotary dryer. Two types of the dryers, namely, industrial horizontal rotary dryer (IHRD) and industrial batch type bed dryer (IBBD), are analyzed in terms of energy consumption and drying performance. Specific energy is defined as the energy used to evaporate unit mass of water from the bulk grain in a dryer. Specific electrical energy consumption (SEEC) and specific thermal energy consumption (STEC) are studied for both the dryers. SEEC varied between 2.64 and 7.48 MJ/kg for IBBD and 5.50 and 17.41 MJ/kg for IHRD for different levels of moisture content. It was reported that the energy requirement increased with decreasing moisture content. It required more energy to remove the moisture from the inside of grains that is bound to the solid. Specific thermal energy consumption varied from 7.78 to 22.09 MJ/kg and 11.5 to 36.44 MJ/kg of water removed while drying with IBBD and IHRD, respectively. The total specific energy consumption is given in Fig. 2, which shows that the energy consumption varied between 10.41 and 29.58 MJ/kg and 17.00–53.86 MJ/kg while drying with IBBD and IHRD, respectively. In this case, the CO_2 emission is a maximum of 7,289 gCO_2e per kg of water removed using IBBD and 13,261 gCO_2e/kg of water removed using IHRD.

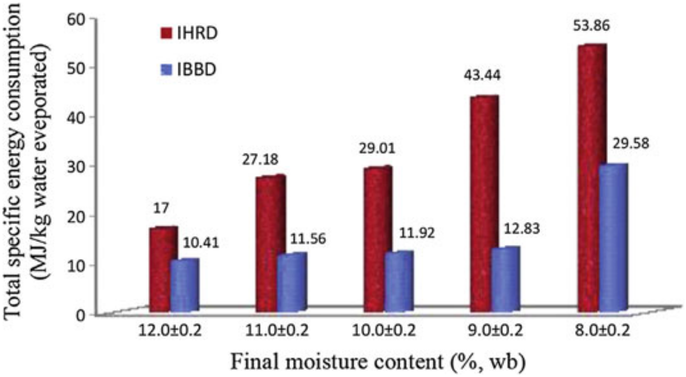

Fig. 2 Total energy consumption during drying of paddy with industrial batch dryer and industrial horizontal rotary dryer in Northern Iran (Firouzi et al. 2017)

A laboratory-scale microwave-vacuum oven was developed for drying cranberries by Yongswatdigul and Gunasekaran. Cranberries were pretreated and dried to bring down the moisture to 15% (wet basis). Drying efficiency was calculated using the parameters: total energy input which is the multiplication of microwave power and total power-on time, energy absorbed which is calculated by changes in sensible and latent heat, and heat of vaporization of water. The drying process was operated in continuous mode and a pulsed microwave-vacuum drying mode. Drying efficiency in continuous mode ranges from 3.59 to 5.02 MJ/kg of water which emits a maximum of 1,237 gCO_2e/kg of water removed and drying efficiency in pulsed microwave-vacuum drying is 2.51–4.49 MJ/kg which contributes a maximum of 1,103 gCO_2e/kg of water removed. Pulsed microwave-vacuum drying consumes less energy than the continuous mode drying (Yongsawatdigul and Gunasekaran 1996). The specific energy consumption for batch drying, spray drying, freeze drying, fluidized bed drying is 40, 5,300, 18,000, and 11,400 kJ/kg, respectively (Huang et al. 2017).

Tohidi et al. studied energy and quality aspects of deep bed drying of paddy grains. Drying experiment of paddy with different temperatures and velocities was performed. The total energy consumption ranged between 0.37 and 1.85 kWh at temperatures 80 and 40 °C, respectively. The corresponding carbon dioxide emissions would be between 329.3 and 1,646 gCO_2. It was found that energy efficiency was more at higher drying temperatures, lower velocity, and lower relative humidity (Tohidi et al. 2017).

Microwave, vacuum, and convective drying of nettle leaves were compared in terms of energy consumption and color characteristics. The energy consumption at different conditions and different drying methods is shown in Fig. 3. The maximum energy consumed during convective drying is 0.35 kWh at the lowest temperature which corresponds to 311.5 gCO_2 emission. The maximum energy consumed during vacuum drying is 0.9 kWh at highest pressure and lowest temperature which corresponds to 801 gCO_2 emissions. The maximum energy consumed during microwave drying is 0.06 kWh which corresponds to 53 gCO_2 emissions. Among different drying methods, microwave drying is energy efficient for drying nettle leaves. The color change was less in microwave drying followed by vacuum and convective drying methods (Alibas 2007).

Solar Drying

Sun is the major source of energy for the Earth. The solar intensity outside the atmosphere is 1,367 W/m^2. On an average, the radiation falling on the ground is between 800 and 1,000 W/m^2. This huge amount of energy can be more effectively utilized by the intervention of appropriate technology (Rajarajeswari and Sreekumar 2016; Aravindh and Sreekumar 2016). The solar energy sector is growing rapidly with innovative technology and materials in recent years for generating electrical energy and thermal energy from Sun. Solar drying technology is the one that utilizes heat radiation from the sun for drying variety of food products, marine products, agricultural products, meat, poultry products, etc. This method of food drying is a better replacement for the traditional method of drying

Fig. 3 Energy consumption for nettle leaves drying at three different drying methods (Alibas 2007)

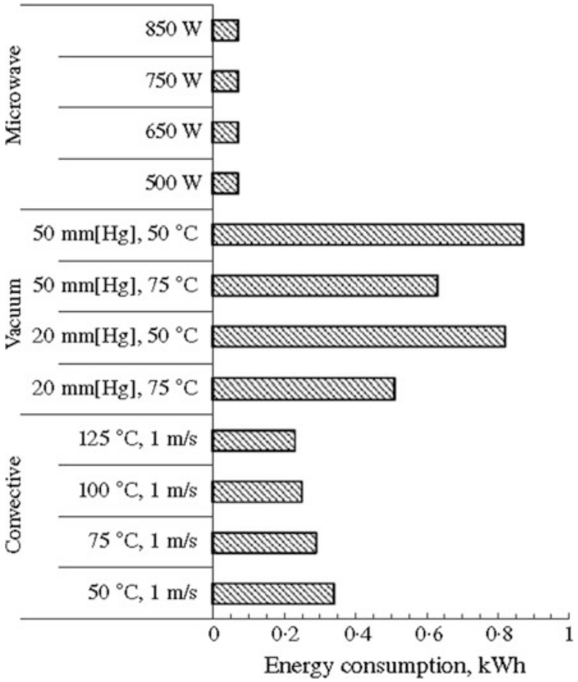

which suffers from poor quality of dried products. Electrical drying results in a good quality product, but it consumes more energy even though. The energy consumption is almost zero in a solar dryer.

Advantages of solar drying over open sun drying are

- Higher temperature and lower humidity increase the rate of drying.
- The casing protects the food from weathering, dust, and birds, and hence, the postharvest loss is low.
- The drying area is small as compared to open sun drying area due to high drying rate.
- The shelf life is longer due to complete drying.
- The product quality is very high as compared to the branded products.

The three important parts of a solar collector are glazing that transmits the solar radiation, absorber plate which absorbs the incoming radiation, and insulation that suppresses the heat losses. Solar dryers are classified into

Direct solar dryer: In this type, the food products are exposed to solar radiation. The moisture is removed by the incoming solar radiation and also by the hot air that is allowed to pass through the drying chamber.

Indirect solar dryer: In indirect solar drier, the moisture is removed only by passing hot air through the drying chamber. The atmospheric air is passed through the solar collector; the absorber plate which is heated by the solar radiation transfers the heat to the flowing fluid. The air temperature thus increases and passed on to drying chamber (Aravindh and Sreekumar 2014; Aravindh and Sreekumar 2015; Sreekumar and Aravindh 2014; Rajarajeswari and Sreekumar 2014).

Mixed mode dryer: In this type, food is dried by both the solar radiation and by the hot air.

Hybrid dryer: Both solar energy and conventional energy are used for drying in the hybrid dryer.

5 Solar Dryers—A Case Study

Commercial solar dryers

SEED (Society for Energy, Environment and Development) developed various solar food processing dryers.

The dehydrated food products using developed solar dryers include fruits, vegetables, green leafy vegetables, spices, forest products, medicinal products, herbal products, food items, and chemicals. The products can be dehydrated with pretreatment for longer shelf life with zero energy cost using the developed solar dryers. The specifications of various capacity solar dryers are shown in Table 3. All the dryers are completely solar driven with electrical energy backup that can be utilized during nonsolar hours. The photograph of the commercially developed solar dryer is shown in Fig. 4.

Frito lay, a chip manufacturing company in the USA, uses concentrated solar collectors for five acres, which consist of 384 solar collectors. The solar collectors are designed to absorb sunlight which produces steam that is used to heat the cooking oil used for frying chips. This predominantly reduced the use of natural gas. The company contributes in mitigating 1.7 million pounds of CO_2 emissions every year (Eswara and Ramakrishnarao 2012).

Abhay et al. developed an indirect solar dryer for drying banana slices. Solar air heater with corrugated absorber plate connected with the drying chamber forms the drying system. The moisture content of banana reduced from 56% (db) to 16.3%, 19.4%, 21.15%, 31.15%, and 42.3% in tray 1, tray 2, tray 3, tray 4, and open sun. The drying time was more in the open sun than the solar dryer. It was concluded that the solar drying was more efficient than open sun drying (Lingayat et al. 2017; Rajarajeswari 2016).

Table 3 Specification of solar dryers developed by SEED (TERI 2014)

Model	Loading capacity (kg)	Drying area (m^2)	Solar photovoltaic panel 12 VDC (W)	Electrical backup (kW)
SDM-8	8	0.56	3.5	1
SDM-50	50	3.6	20	4
SDM-100	100	7.2	50	8
SDM-200	200	14.4	100	16

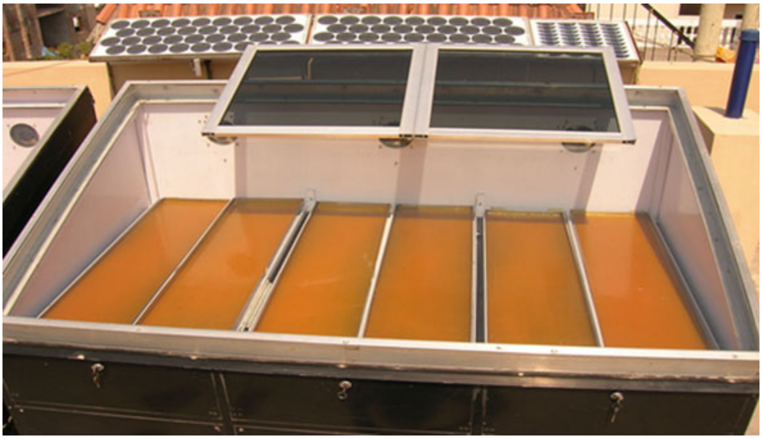

Fig. 4 Commercial solar dryer developed by SEED (Eswara and Ramakrishnarao 2012)

Fig. 5 Direct type solar dryer (Castillo-Téllez et al. 2017)

Direct and indirect dryer
Solar dryers for chili drying shown in Figs. 5 and 6 were designed and installed in Mexico. Drying experiment was carried at solar radiation between 200 and 950 W/m^2 with the ambient air temperature ranging from 26 to 33 °C and drying temperature ranged from 31 to 45 °C. Drying air velocity ranged between 0.7 and 2.6 m/s. The initial moisture content of chilies varied between 80.65 and 88.83%. The final moisture content of dried chilies varied between 5.46 and 8.29% wet basis. The total drying time was 16 h. The thermal efficiency of solar dryer ranged from 67 to 72%. The energy required for drying was taken from solar radiation.

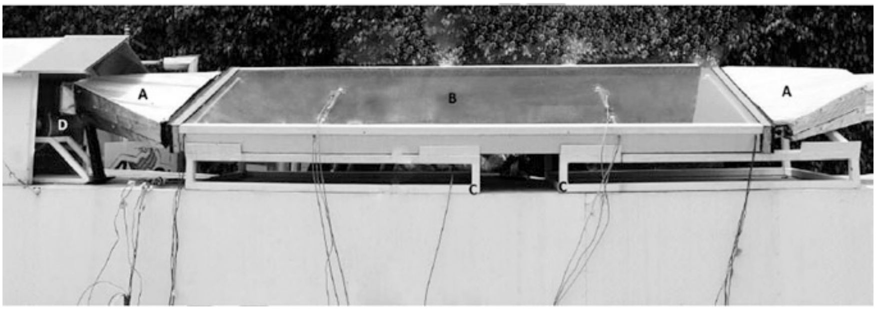

Fig. 6 Indirect type solar dryer (Castillo-Téllez et al. 2017)

Fig. 7 Chilli in solar dryer at different drying stages (Castillo-Téllez et al. 2017)

The energy consumed was only for running centrifugal blowers. The product at different stages of drying is shown in Fig. 7 (Castillo-Téllez et al. 2017).

Greenhouse type solar dryer

The greenhouse type solar dryer shown in Fig. 8 is installed at a small-scale food industry in Thailand. The loading capacity is 1,000 kg of fruits. The size of the dryer is 20 m length, 8 m width, and 3.5 m height. DC fans with three 50 W solar panels were used to circulate the air. A 100 kW LPG burner was present to heat the air during nonsolar hours. Tomatoes were chosen for drying experiment. The moisture content of 57% (wet basis) reduced to 17% (wet basis) in 4 days while in the open sun drying it was 29% for the same period. The drying time is reduced in a solar dryer. Retention of original color in the solar dryer was appreciable as compared to open sun drying which had a pale yellow color whereas in the solar dryer it occurred in reddish brown color. The total electricity consumed was 252 kWh per year (Janjai 2012). The carbon dioxide emissions will be 148 kg CO_2 per year if conventional fuel was used. Since the fuel consumed is zero, the CO_2 emission due to the fuel consumption is zero. For drying 1,000 kg of tomatoes, the electricity required would emit 269.67 kgCO_2. For a year, it would emit 53,934 kg CO_2 if 200 days of operation and 0.89 kgCO_2e per kWh is considered.

Direct type solar tunnel dryer

A prototype of solar tunnel dryer of 12 kg capacity of fresh product shown in Fig. 9 was installed in the Centre for Green Energy Technology, Pondicherry University. The dryer is of direct type, where the products are exposed to sunlight. The energy

Fig. 8 Greenhouse solar drying system (Janjai 2012)

Fig. 9 Solar tunnel dryer (Rajarajeswari et al. 2016)

for vaporization of water is taken directly from solar radiation and also from the heated air inside the chamber. The DC fans that circulate air inside the chamber are powered by solar panels. The drying experiments were carried at latitude 11.91°N and longitude 79.81°E between 9:30 a.m. and 5:30 p.m. in the month of April where the solar radiation ranged between 300 and 900 W/m^2. The temperature profile of solar dryer is shown in Fig. 10. The drying temperature was between 35 and 48 °C. The ambient temperature ranged from 30 to 35 °C.

The products selected for drying are apple, tapioca, pineapple, and tomato. The initial moisture content of each product was found by hot air oven method. The products were kept for drying in the hot air oven at 110 °C for 24 h. The difference in the initial and final weight gives the percentage water content present in the products. The initial moisture content of apple, onion, and tomato are 86.2, 82.7, and 93.1%, respectively. Three types of drying were compared in terms of drying efficiency, energy consumed, and quality of dried products. The moisture content of apple dried in solar drier got reduced to 10.3% from 86.2% in three solar hours.

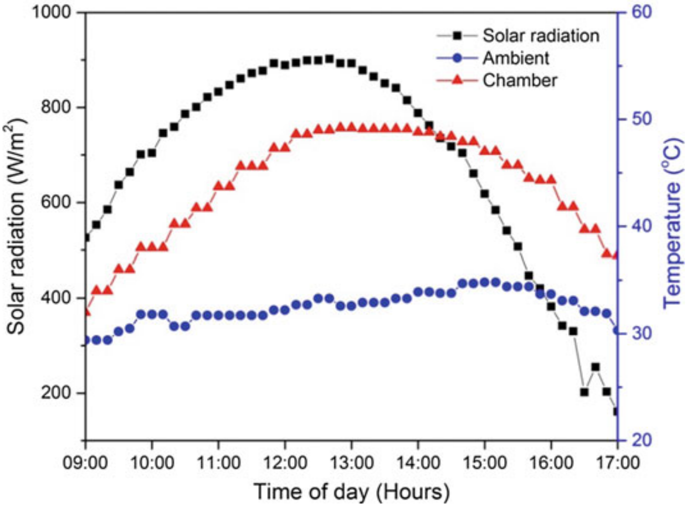

Fig. 10 Drying temperature and solar radiation on day of experiment

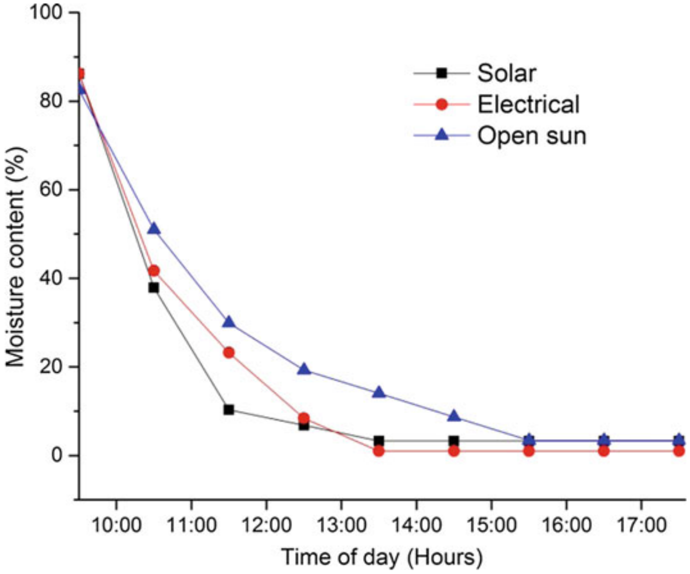

Fig. 11 Moisture reduction curve for apple

The same time was taken in the electrical drier. In open sun drying, it took a little longer for drying as shown in Fig. 11. The moisture content of onion got reduced to 10.4% from 82.7% in four solar hours in a solar tunnel dryer. The drying was faster

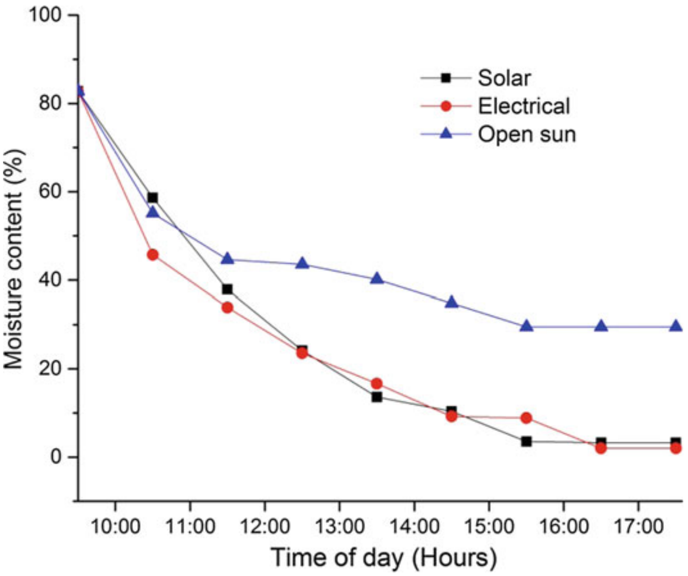

Fig. 12 Moisture reduction curve for onion

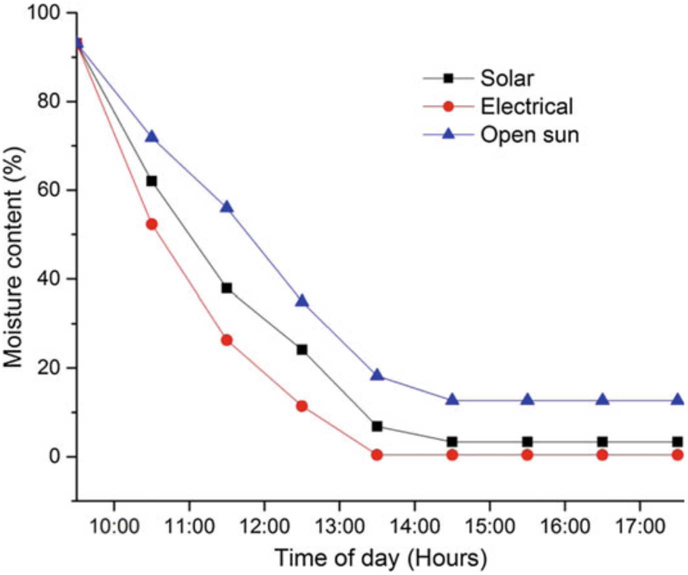

Fig. 13 Moisture reduction curve for tomato

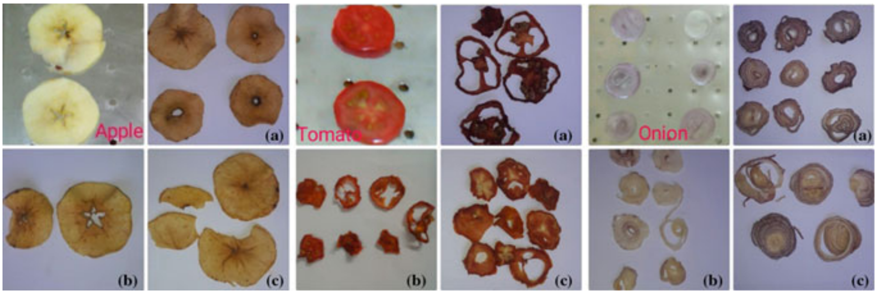

Fig. 14 Images of fresh and dried products: **a** solar dryer, **b** electric dryer, and **c** open sun

in electrical drying and in four hours the moisture percentage in open sun drying was 45%. The drying duration was longer in open sun drying as shown in Fig. 12. The moisture content of tomato reduced to 20% in three drying hours in the solar dryer. In electrical drying, the drying was faster as compared to the solar dryer as shown in Fig. 13. The drying duration was reduced in solar dryer comparing to open sun drying while in the electric dryer, it was faster than solar dryer due to a constant temperature. The images of fresh and dried products are shown in Fig. 14.

6 Reduction of CO_2 Emission

The solar dryer uses the energy from the solar radiation to vaporize the water present in the products. In the electric dryer, the energy is supplied by electricity. The energy required to remove per kg of water from each product is given in Table 4. Using solar dryers prevents 434 gCO_2e/kg of drying fresh apple, 467 gCO_2e/kg of fresh tomato, 410 gCO_2e/kg of onion, 480 gCO_2e/kg of pineapple, and 382 gCO_2e/kg of tapioca.

Table 4 Carbon dioxide mitigation using solar dryer

Product	Initial moisture content (%)	Final moisture content (%)	Energy required per kg (kWh)	CO_2 mitigation (g)
Apple	86.2	10.3	0.53	434
Tomato	93.1	20	0.57	467
Onion	82.7	10.4	0.50	410
Pineapple	86.5	23.5	0.54	480
Tapioca	72.4	6.8	0.43	382

7 Conclusion

Realizing the adverse impact of climate change each country must tread toward in mitigating the emission of greenhouse gases. This can be done by adopting clean and green energy resources that are less harmful to the environment. Since food industry is a major consumer of electricity and other conventional fuels, it is endorsed to stick to technology that is run by alternate energy. Solar dryer is an intriguing, ancient, and alternate technology that consumes zero fuel for the drying process. Large-scale promotion of solar drying technology helps to reduce CO_2 emissions up to a certain extent in food processing industries. The environmental cost of fuel also should be considered while making the economics of conventional and renewable energy systems. Influential amount of energy-related carbon dioxide emissions can be mitigated by proclaiming the technology among the food processing industries and small-scale food producers.

Acknowledgements The authors acknowledge SERB, Department of Science and Technology, Govt. of India for the financial support through a research project awarded under the scheme "Fast Track Young Scientist award".

References

Aghbashlo M, Mohammad H, Samimi-akhijahani H (2008) Influence of drying conditions on the effective moisture diffusivity, energy of activation and energy consumption during the thin-layer drying of berberis fruit (Berberidaceae), vol 49, pp 2865–2871

Alibas I (2007) Energy consumption and colour characteristics of nettle leaves during microwave, vacuum and convective drying. Biosyst Eng 96(4):495–502

Aravindh MA, Sreekumar A (2014) Experimental and economic analysis of a solar matrix collector for drying application. Curr Sci 107(3):350–355

Aravindh M, Sreekumar A (2015) Design and techno-economic analysis of a solar matrix collector for drying application. Res Civil Environ Eng 3(April 2014):160–171

Aravindh MA, Sreekumar A (2016) Efficiency enhancement in solar air heaters by modification of absorber plate-a review. Int J Green Energy 13(12):1209–1223

Castillo-Téllez M, Pilatowsky-Figueroa I, López-Vidaña EC, Sarracino-Martínez O, Hernández-Galvez G (2017) Dehydration of the red chilli using an indirect-type forced convection solar dryer. Appl Therm Eng 114:1137–1144

cBalance Solutions Pvt. Ltd. (2009) GHG inventory report for electricity generation and consumption in India

Drescher S, Rao N, Kozak J, Okos M (1997) A review of energy use in the food industry. In: 1997 Summer study on energy efficiency in industry, pp 29–40

Eisentraut A, Adam B (2014) Heating without global warming. Feature Insight 92

Eswara AR, Ramakrishnarao M (2012) Solar energy in food processing—a critical appraisal. J Food Sci Technol 50(April):209–227

Firouzi S, Alizadeh MR, Haghtalab D (2017) Energy consumption and rice milling quality upon drying paddy with a newly-designed horizontal rotary dryer. Energy 119

Huang S et al (2017) Spray drying of probiotics and other food-grade bacteria: a review. Trends Food Sci Technol 63:1–17

I. brand equity Foundation (2016) Food processing Market & Opportunities, pp 1–28

IEA (2015) Energy and climate change. World Energy Outlook Spec. Rep., pp 1–200

Janjai S (2012) A greenhouse type solar dryer for small-scale dried food industries: development and dissemination. Int J Energy Environ 3(3):383–398

Lashof DA, Ahuja DR (1990) Relative contributions of greenhouse gas emissions to global warming. Nature 344(6266):529–531

Lingayat A, Chandramohan VP, Raju VRK (2017) Design, development and performance of indirect type solar dryer for banana drying. Energy Proc 109(November 2016):409–416

Ma C-M, Chen M-H, Hong G-B (2012) Energy conservation status in Taiwanese food industry. Energy Policy 50:458–463

Meinshausen M et al (2009) Greenhouse-gas emission targets for limiting global warming to 2 °C. Nature 458(7242):1158–1162

Rajarajeswari ASK (2016) Solar energy-an effective tool for value addition of foodstuffs. Energy Secur Sustain 1–24

Rajarajeswari K, Sreekumar A (2014) Performance evaluation of a wire mesh solar air heater. Voice Res 3(3):46–53

Rajarajeswari K, Sreekumar A (2016) Matrix solar air heaters—a review. Renew Sustain Energy Rev 57:704–712

Rajarajeswari K, Sunooj KV, Sreekumar A (2016) Thermal investigation and food quality analysis on a solar tunnel drier. Curr Sustain Energy Rep 2–6

Shearer C, Fofrich R, Davis SJ (2017) Future CO_2 emissions and electricity generation from proposed coal-fired power plants in India

Soysal Y, Ayhan Z, Eştürk O, Arıkan MF (2009) Intermittent microwave–convective drying of red pepper: drying kinetics, physical (colour and texture) and sensory quality. Biosyst Eng 103(4): 455–463

Sreekumar A, Aravindh MA (2014) Spice India 2014

TERI (2014) Innovative solar technology 100(August 2014):34–37

Tohidi M, Sadeghi M, Torki-Harchegani M (2017) Energy and quality aspects for fixed deep bed drying of paddy. Renew Sustain Energy Rev 70:519–528

U.S. Energy Information Administration (2014) International energy outlook 2016; with projections to 2040, pp 113–126

World Nuclear Association (2011) Comparison of lifecycle greenhouse gas emissions of various electricity generation sources

Yongsawatdigul J, Gunasekaran S (1996) Microwave-vacuum drying of cranberries: part I. Energy use and efficiency. J Food Process Preserv 20(2):121–143

Low-Cost Systems for Agriculture Energy Management in Tunisia

Salwa Bouadila and Rim Ben Ali

Abstract Tunisia is one of the several countries where the agricultural greenhouses are used for maintaining the inside climate on its favorable environmental condition for production and plant growth. The agricultural greenhouse presents a complicated procedure because of the strong perturbations and the important number of its input parameters, which have a great potential and capacity to influence the climate inside it. A Fuzzy Logic Controller (FLC) is developed in order to promote a suitable microclimate by acting on the appropriate actuators installed inside the greenhouse such as the ventilation, the heating system, the humidifying, and the dehumidifying systems with the appropriate rate. The dynamic modeling of the studied greenhouse is presented and experimentally validated in the Research and Technology Center of Energy (CRTEn) in Tunisia and it is simulated using MATLAB/Simulink environment. Agricultural greenhouse presents an important number of its inputs; which have a great potential and capacity to influence the variation of the output parameters such as the internal temperature and the relative humidity. For this purpose, a contribution to combine a small wind turbine system to a greenhouse in order to power the actuators allows reducing the cost of the agricultural production.

Keywords Agricultural greenhouse · Temperature · Relative humidity
Controller

S. Bouadila (✉)
The Thermal Processes Laboratory, The Research and Technology Center
of Energy, Hammam Lif, B.P. 95, 2050 Tunis, Tunisia
e-mail: salwa.bouadila@crten.rnrt.tn

R. Ben Ali
Department of Physics Organization, Faculté des Sciences de Tunis,
Université de Tunis El Manar, Campus Universitaire Farhat Hached
B.P. n° 94 - Rommana, 1068 Tunis, Tunisia

A. Sharma et al. (eds.), *Low Carbon Energy Supply*, Green Energy and Technology,
https://doi.org/10.1007/978-981-10-7326-7_5

Nomenclature

C_a	Specific heat of air (J kg^{-1} K^{-1})
d_a	Air density (kg m^{-3})
H	Relative humidity
h	Heat transfer coefficient (W m^{-2} K^{-1})
I	Solar radiation (W m^{-2})
LAI	Leaf area index
l	Characteristic length of the leaf canopy (m)
m	Measured parameters
n	Number of variables
N_h	Number of heaters
T	Temperature (K)
r_a	Aerodynamic resistance (s m^{-1})
r_s	Stomatal resistance (s m^{-1})
RE	Rate of air infiltration (m^3 s^{-1})
S	Surface area (m^2)
$P(T)$	Water vapor pressure at temperature T (kPa)
Q	Heat rate (W)
V	Volume (m^3)
V_r	Ventilation rate (m s^{-1})
W	Wind velocity (m s^{-1})
Z	Depth of the soil

Greek Symbols

β	Pitch angle
α	Absorptivity for solar radiations
α_t	Absorptivity for thermal radiations
ε	Emissivity
γ	Psychometric constant (kPa K^{-1})
λ	Thermal conductivity (W m^{-1} K^{-1})
ρ	Reflectivity
σ	Stefan–Boltzmann constant 5.670×10^{-8} W m^{-2} K^{-4}
τ	Transmissivity

Subscripts

av	Average
c	Cover
ca	Canopy
i	Inside
o	Outside
s	Soil
sky	Sky

inf	Infiltration
ventilation	Ventilation
heating	Heating

Exponents

A	Absorbed heat
C	Convective heat
Cd	Conductive
L	Latent heat
R	Radiation heat

1 Introduction

By 2050, the global demand of energy will approximately double, while food and water demand is set to increase by over 50%, where the International Renewable Energy Agency (IRENA) (I. Renewable and E. Agency 2015) has projected that food production will be increased by 60%, water availability by 55%, and energy production by 80%. Food security is a global issue in order to meet the future global demand, which is defined as being achieved "when all people at all times have access to sufficient, safe, nutritious food to maintain a healthy and active life" (World Health Organization (WHO) 2014); It is a "complex sustainable development issue", linked to water and energy through the Water-Energy-Food Security Nexus; and to issues such as economic development, the environment, and health (World Health Organization (WHO) 2014). The issue of food security is gaining momentum around the world, especially for the developing countries in sunbelt or arid regions have strong population and consumption growth requiring expansion of food production. The scarcity of arable land and water limits crop production, and climate change is reducing the productivity of traditional agriculture.

All MENA countries have to cope with a water deficit, while they strive to achieve a self-sustaining agriculture at the same time. Furthermore, water is becoming a major source of concern in this region, as the exploitation of freshwater has surpassed the available renewable surface and groundwater sources, and the deficit is poorly covered by overexploiting the groundwater resources.

The relationship between water and food systems is among the most widely covered elements of the nexus. Generally, the accessibility and availability of water resources have greatly influenced the evolution of agricultural practices globally. The type of crops grown, the crop cycles, and the irrigation method adopted all vary from arid to wet parts of the MENA region.

Today, the fossil energy situation indicated several weakness aspects due to its limited and pollutant character. Therefore, the investment in the renewable energy sector seems to be one of the potential solutions. Because energy costs often account for the largest share of a water operation budget reliance on expensive energy sources, several utilities are introducing renewable energy solutions along different stages of the supply chain.

2 Integration of Renewable Energy in Greenhouse Applications

A greenhouse is an enclosure that allows owners to control climatic, nutrition, biotic, and cultural variables that influence crop growth. The greenhouses recognized as off-season horticultural solution to protect the canopy against diseases and develop the optimal conditions at different stages of crop growth. Cultivation in greenhouses can continually provide vegetable produces of high quality.

The control of the climate inside the greenhouse is an important step to provide cultivation with less risk and to reach a comfortable microclimate for the plant growth. Several control strategies have been technologically advanced to enhance the climate inside the greenhouse, such as adaptive predictive control, the neural network, nonlinear adaptive control, optimal control, genetic algorithm, adaptive neuro-fuzzy controller, and the fuzzy logic controller (Fourati 2014; Taki et al. 2016; Pawlowski et al. 2016; Zeng et al. 2012; van Beveren et al. 2015; Hasni et al. 2011; Mohamed and Hameed 2016; Khoshnevisan et al. 2014). The control of the microclimate inside the greenhouse by fuzzy logic controller membership represents useful tools to solve the nonlinearity problem of the greenhouse. Many researchers studied, developed, and demonstrated the controller membership of the actuators related to the inside greenhouse optimization (such as, ventilation actors, heating/cooling system and humidifying/dehumidifying system) and presented its advantages and disadvantages (Lafont et al. 2015; Lafont and Balmat 2002; Revathi and Sivakumaran 2016; Márquez-Vera et al. 2016; Atia and El-madany 2016; Salgado and Cunha 2005; Fitz-Rodríguez et al. 2010; Longo and Gasparella 2015; Joudi and Farhan 2015; Abdel-Ghany and Kozai 2006; Fatnassi et al. 2013; Mesmoudi et al. 2010).

Today, the fossil energy situation indicated several weakness aspects due to its limited character. Thus, the needs for energy alternatives become inevitable. The exploitation of different renewable energy resources seems to be one of the potential solutions. Alternate sources of energy like the solar energy, geothermal energy, or wind energy have been proposed for conditioning greenhouses and providing the optimum climatic conditions.

Solar energy is a universally available source, but its practical use still presents some technical, and most importantly, economic problems. Some solar systems have been developed but they are too expensive for commercial use. Several experimental studies presented in the Research and Technology Centre of Energy (CRTEn) in Tunisia, we can mention Lazaar et al. (2015) evaluate an experimental comparison between two tunnel greenhouses, the first one is equipped with a buried and suspended heat exchanger and the other not. They used two heating sources in order to increase the nocturnal air temperature under greenhouse. An electrical heating system, and a solar heating system. An economic analysis shows that the use of a system of 3 evacuated tube solar collectors for greenhouse heating is rentable since the payback period of the solar system is 3 years. Also, Kooli et al. (2015) also presented an experimental comparison between two identical greenhouses to examine the effect of the nocturnal shutter on reducing the energy consumption in the greenhouse during the night. The results show that the nocturnal variations of temperature inside the greenhouses with shutter exceed 2 °C the one without nocturnal shutter. Bouadila et al. (2014a, b) conducted an experimental study to evaluate the nighttime recovered heat of the performance of a new solar air heater collector using a packed bed of spherical capsules with a latent heat storage system in the east–west-oriented greenhouse.

The solar system is used for storing the excess of the transmitted solar irradiation in the packed bed absorber and to provide it at night. As a result of this system, the amount of the nighttime recovered heat of this system attains 31% of the total requirements of heating. The relative humidity was found to be on average 10–20% lower at night time inside the heated the greenhouse. The nocturnal variation of temperature inside the heated greenhouse exceeds the temperature inside conventional one with a difference of 5 °C. The solar collector remains a uniform useful heat all the night varied between 550 and 300 W.

Photovoltaics come along as the most prospective solar energy conversion system, the solar energy shining is converted into usable electricity. The photovoltaic systems can be a more economic choice to provide the solar electrical energy needs of the equipment installed in an agricultural greenhouse to improve plants productivity and energy efficiency. PV systems applications are more developed in many countries in the world like Italy, China, India, Norway, and Thailand such as electric fencing, area or building lighting, and water pumping either for livestock watering or crop irrigation (Marucci and Cappuccini 2016; Li et al. 2017; Nayak and Tiwari 2010; Nookuea et al. 2016; Kristjansdottir et al. 2016; Maher et al. 2016; Hassan et al. 2016).

Geothermal energy is present everywhere, it is one of the numerous renewable energies that could be very useful in farming and agriculture production. The exploitation of the geothermal surface energy usually requires the use of a geothermal heat pump. In Tunisia, Boughanmi et al. (2015) examine experimentally the performance of a novel buried conic geothermal basket heat exchanger for greenhouse cooling. The configuration typically consists of a series of parallel coil implanted in 3-m depth. The experimental system can be used in the Mediterranean regions for greenhouse cooling. The maximum obtained cooling capacity of the transferred heat quantity to the ground for the system is 8 kW. The coefficients of the performances of the ground-source heat pumps, COPhp, and the overall system, COPsys, are, respectively 3.9 and 2.82 for basket heat exchanger.

Other renewable energy sources such as wind energy are less commonly used in agriculture sector. Small wind systems can be provided to improve the agricultural productivity in the windy regions.

Wind turbine has significant benefit in the areas where there is a shorter rainy season and hence there is a demand for pumped water. Díaz-Méndez et al. (2014) studied the economic feasibility of the three systems to produce energy for pumping irrigation water in commercial greenhouses in Spain, Cuba, and Pakistan: wind pump technology, solar photovoltaic pumping, diesel generators, and connection to the electrical grid. The results reveal that the energy management decisions differ between countries. Cuce et al. (2016) analyzed a review on cost-effective, energy-efficient, and environmentally friendly technologies for potential utilization in greenhouses. They considered in this research renewable technologies solutions and concluded that up to 80% energy saving can be achieved through appropriate retrofit of conventional greenhouses with a payback period of 4–8 years depending on climatic conditions and crop type.

Ozgener (2010) evaluated the hybrid solar-assisted geothermal heat pump and a small wind turbine system utilization for heating greenhouse in Turkey. This study displayed that 3.13% of the total electricity energy consumption of the greenhouse during the year can be theoretically supplied by a small wind turbine system. The author suggested that the renewable combined systems can be economically used for space heating/cooling systems in agricultural in a windy region. Peillóna et al. (2013) presented a case study of a wind pumps for crop irrigation under several factors which include three-hourly wind velocity, flow supplied by the wind pump as a function of the elevation height, and daily greenhouse evapotranspiration as a function of crop planting date. The result shows that November is the optimum period of wind pump driven irrigation for 0.2 ha cultivated areas and using wind pumps at 15 m of height elevation. The wind turbine system has several environmental and economic advantages, Rasheed et al. (2016) evaluated the wind energy as an alternative energy source for the irrigation of greenhouse crops at four different locations in Asia; Shouguang (China), Sargodha (Pakistan), Buan and Gimhae (South Korea). The results indicate that the wind resources for Shouguang and Buan achieve the irrigation requirement of the large area. The internal return rate of using a wind pumping system at each location, Gimhae, Buan, Shouguang and Sargodha are 4.4, 10.0, 5.2% and below 1.0% respectively.

3 Geographical Situation and Agriculture Greenhouses Potential of Tunisia

Tunisia is the smallest and northernmost country in Africa along the Atlas mountain range. It is bordered by Algeria to the west and Libya to the southeast, with the following coordinates: Latitude 36° 43′N and Longitude 10° 25′E with a surface of 163,610 km^2. It is divided into three zones: the shoreline of Tunisia which extends to the East from Bizerte to the Sahel (Sfax) gives Tunisia two faces on the Mediterranean Sea (with 1298 km coastline), composed primarily of hills and plains; the interior of Tunisia composed essentially of mountains and valleys; the Tunisian desert, which represents 55% of the whole of the Tunisian territory.

Surrounded by the Mediterranean, Tunisia has a Mediterranean climate to the North of the country and desert to the South. The climate is generally soft. The annual temperature varies between 10° and 20° in winter and between 20° and 36° in summer. The temperature can reach 45° in summer for the Tunisian South area.

The wind speed values during March to June, in Tunisia exceed 7 m/s and the maximum wind speed reaches 20.6 m/s measured at the altitude of 30 m. However, in September and October, the wind speed attains its minimum values. The assessment of wind energy potential in Tunisia was evaluated by Dahmouni et al. (2011) with a comparative simulation in order to facilitate the choice of the best wind turbine system adapted to the studied site conditions. They have evaluated the characteristics of wind speed and the potential of wind power at a height of 30, 20 and 10 m above ground level. They confirm also that the Gulf of Tunis has promising wind energy potential (Dahmouni et al. 2010). We can found also the investigation of Maatallah et al. (2013), which is focused on the determination of the available wind speed and the assessment of the capacity factor and the generated electricity at different hub heights for eight commercial turbines on the central coast of the Gulf of Tunis.

The agricultural production is a moderate contributor to the economy in Tunisia and the use of the agricultural greenhouse continues to rise in order to increase the agricultural production yield, which are installed in all regions in Tunisia at varying degrees and are distributed at 36% in the northern region, 46% in the central region and 18% in the south (Ministère de l'Agriculture et des Ressources Hydrauliques (Hrsg.) 2006).

4 Thermal Modeling of an Agricultural Greenhouse

The greenhouse environment is generally divided into four homogeneous parts: the cover, the internal air, the canopy, and the soil. The various thermodynamic exchanges between the components of the greenhouse contribute to determining the inside climate evolution. The energy balance of each component of the greenhouse includes the conduction, the convection, the short and long wave radiation fluxes, and the infiltration.

The following assumptions are made for the heat exchange between greenhouse components:

- Radiation heat exchange between the greenhouse walls and the roofs are neglected.
- Storage capacity of the walls and roof material is neglected.
- Absorptivity and heat capacity of the enclosed air is neglected.
- Conduction heat exchange between air and walls of the greenhouse is neglected.

Figure 1 presents the heat transfer interaction between greenhouse components.

The thermal balance is developed to describe the dynamic evolution of the air temperature inside the greenhouse by taking into account the interaction between

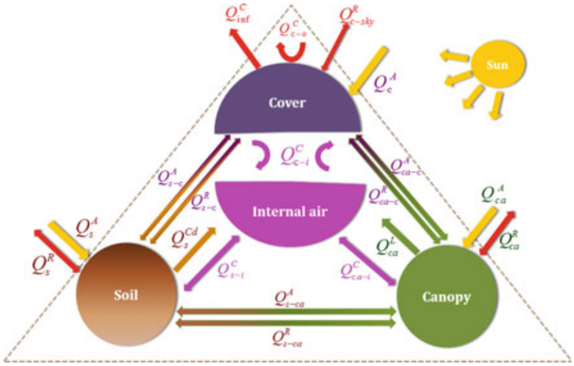

Fig. 1 Heat transfer interaction between greenhouse components

the different components. That ensures the heat transfer of the internal air, which is computed using the following equation.

$$\frac{\mathrm{d}T_\mathrm{i}}{\mathrm{d}t} = \left(Q^\mathrm{C}_\mathrm{c-i} + Q^\mathrm{C}_\mathrm{ca-i} + Q^\mathrm{C}_\mathrm{s-i} - Q^\mathrm{C}_\mathrm{inf}\right)/d_\mathrm{a}C_\mathrm{a}V \tag{1}$$

The term $Q^\mathrm{C}_\mathrm{c-i}$ in Eq. (1) is the convective heat transfer between the cover and the internal air, which is defined by

$$Q^\mathrm{C}_\mathrm{c-i} = Q^\mathrm{A}_\mathrm{c} + Q^\mathrm{A}_\mathrm{ca-c} + Q^\mathrm{A}_\mathrm{s-c} - Q^\mathrm{C}_\mathrm{c-o} + Q^\mathrm{R}_\mathrm{c-sky} + Q^\mathrm{R}_\mathrm{s-c} + Q^\mathrm{R}_\mathrm{ca-c} \tag{2}$$

Q^A_c is the heat absorbed by the cover, $Q^\mathrm{A}_\mathrm{ca-c}$ and $Q^\mathrm{A}_\mathrm{s-c}$ are, respectively, the reflected solar radiations by the canopy and absorbed by the cover and the reflected solar radiations by the soil surface of the greenhouse and absorbed by the cover. $Q^\mathrm{C}_\mathrm{c-o}$ is the convective heat transfer from the cover to the outside air. $Q^\mathrm{R}_\mathrm{c-sky}$, $Q^\mathrm{R}_\mathrm{s-c}$ and $Q^\mathrm{R}_\mathrm{ca-c}$ are, respectively, the radiation heat transfer from the cover to the sky, the radiation heat transfer from the soil to the cover, and the radiation heat transfer from the canopy to the cover.

The convective heat transfer between the inside air and the cover can be written using Eq. (3).

$$\begin{aligned} Q^\mathrm{C}_\mathrm{c-i} = {} & IS_\mathrm{c}\alpha_\mathrm{c} + I\tau_\mathrm{c}\alpha_\mathrm{c}\rho_\mathrm{ca}S_\mathrm{ca} + I\tau_\mathrm{c}\alpha_\mathrm{c}\rho_\mathrm{s}S_\mathrm{s} + h^\mathrm{C}_\mathrm{c-o}S_\mathrm{c}(T_\mathrm{o} - T_\mathrm{c}) + \sigma\varepsilon_\mathrm{c}S_\mathrm{c}(T^4_\mathrm{sky} - T^4_\mathrm{c}) \\ & + S_\mathrm{s}\sigma\alpha_\mathrm{t,c}\varepsilon_\mathrm{s}T^4_\mathrm{s} + S_\mathrm{ca}\sigma\alpha_\mathrm{t,c}\varepsilon_\mathrm{ca}T^4_\mathrm{ca} \end{aligned} \tag{3}$$

where τ_c is the cover transmissivity and I is the solar irradiation.

T_sky is the sky temperature that is suggested by Swinbank and calculated using Eq. (4), as cited in (Abdel-Ghany and Kozai 2006).

$$T_{\mathrm{sky}} = 0.0552\,T_{\mathrm{o}}^{1.5} \tag{4}$$

$h^{\mathrm{C}}_{\mathrm{c-o}}$ is the coefficient of the convective heat transfer between the outside greenhouse cover and the outside wind velocity is given by the empirical relation of Hottel and Woertz cited by Duffie and Beckman (1991). It is determined using Eq. (5).

$$h^{\mathrm{C}}_{\mathrm{c-o}} = 5.7 + 3.8\,\mathrm{W} \tag{5}$$

The terms $Q^{\mathrm{C}}_{\mathrm{ca-i}}$ in the Eq. (1), $Q^{\mathrm{C}}_{\mathrm{ca-i}}$, is the convective heat transfer between the canopy and the indoor air. It is calculated using Eq. (6).

$$Q^{\mathrm{C}}_{\mathrm{ca-i}} = Q^{\mathrm{A}}_{\mathrm{ca}} + Q^{\mathrm{R}}_{\mathrm{c-ca}} - Q^{\mathrm{R}}_{\mathrm{ca}} - Q^{\mathrm{R}}_{\mathrm{ca-s}} - Q^{\mathrm{L}}_{\mathrm{ca}} \tag{6}$$

where $Q^{\mathrm{A}}_{\mathrm{ca}}$ is the heat absorbed by the canopy, $Q^{\mathrm{C}}_{\mathrm{ca-i}}$ is the convective heat transfer from the canopy to the indoor air, $Q^{\mathrm{R}}_{\mathrm{c-ca}}$, and $Q^{\mathrm{R}}_{\mathrm{ca}}$ are, respectively, the thermal radiations radiated by the cover to the canopy and the thermal radiation emitted from the canopy. $Q^{\mathrm{R}}_{\mathrm{ca-s}}$ is the solar radiations reflected by the canopy and absorbed by the soil and $Q^{\mathrm{L}}_{\mathrm{ca}}$ is the latent heat emitted from the canopy, $Q^{\mathrm{C}}_{\mathrm{ca-i}}$ can be written as

$$\begin{aligned} Q^{\mathrm{C}}_{\mathrm{ca-i}} = {} & I\tau_{\mathrm{c}}\alpha_{\mathrm{ca}}S_{\mathrm{ca}} + \varepsilon_{\mathrm{c}}\sigma T_{\mathrm{c}}^{4}S_{\mathrm{c}}\alpha_{\mathrm{t,ca}} - \varepsilon_{\mathrm{ca}}\sigma T_{\mathrm{ca}}^{4}S_{\mathrm{ca}} - \tau_{\mathrm{ca}}\alpha_{\mathrm{s}}\tau_{\mathrm{s}}S_{\mathrm{s}}I \\ & - \frac{d_{\mathrm{a}}C_{\mathrm{a}}\mathrm{LAI}}{\gamma}\frac{(P^{*}(T_{\mathrm{ca}}) - P(T_{\mathrm{i}}))}{r_{\mathrm{a}} + r_{\mathrm{s}}}S_{\mathrm{ca}} \end{aligned} \tag{7}$$

where C_{a} is the specific heat of air, d_{a} is the density of air, and LAI is the Leaf Area Index.

The saturated water vapor pressure $P^{*}(T_{\mathrm{ca}})$ at the temperature of the canopy is calculated using Eq. (8) (Boulard and Wang 2000).

$$P^{*}(T_{\mathrm{ca}}) = 0.6108\ \exp\left(\frac{17.27\,T_{\mathrm{ca}}}{T_{\mathrm{ca}} + 237.3}\right) \tag{8}$$

The aerodynamic resistance r_{a} and the stomatal resistance r_{s} of the canopy are determined using Eqs. (9) and (10) (Boulard and Wang 2000).

$$r_{\mathrm{a}} = 220\,\frac{l^{0.2}}{W_{\mathrm{i}}^{0.8}} \tag{9}$$

$$r_{\mathrm{s}} = 200 + \left(\frac{1}{\exp(0.05\,(\tau_{\mathrm{c}}I - 50))}\right) \tag{10}$$

with, l is the characteristic length of the leaf canopy and W_{i} is the speed of the inside air.

The terms $Q^{\mathrm{C}}_{\mathrm{s-i}}$ in the Eq. (1) are the convective heat transfer between the soil surface and the indoor air. It is computed using Eq. (11).

$$Q^{\mathrm{C}}_{\mathrm{s-i}} = Q^{\mathrm{A}}_{\mathrm{s}} - Q^{\mathrm{Cd}}_{\mathrm{s}} - Q^{\mathrm{R}}_{\mathrm{s}} + Q^{\mathrm{R}}_{\mathrm{c-s}} \tag{11}$$

where $Q^{\mathrm{A}}_{\mathrm{s}}$ is the heat absorbed by the soil, $Q^{\mathrm{R}}_{\mathrm{s}}$ and $Q^{\mathrm{R}}_{\mathrm{c-s}}$ are, respectively, the radiation heat transferred from the soil and the radiation heat transfer from the cover to the soil.

$Q^{\mathrm{C}}_{\mathrm{s-i}}$ can be written as

$$Q^{\mathrm{C}}_{\mathrm{s-i}} = IS_{\mathrm{s}}\tau_{\mathrm{c}}\alpha_{\mathrm{s}} - \frac{\lambda_{\mathrm{s}}}{Z}S_{\mathrm{s}}(T_{\mathrm{s}} - T_{\mathrm{z}}) - \varepsilon_{\mathrm{s}}\sigma S_{\mathrm{s}}T^4_{\mathrm{s}} + \varepsilon_{\mathrm{c}}\sigma S_{\mathrm{c}}\alpha_{\mathrm{s}}T^4_{\mathrm{c}} \tag{12}$$

where λ_{s} is the thermal conductivity of soil and Z is the soil depth.

The terms $Q^{\mathrm{C}}_{\mathrm{inf}}$ in Eq. (1) are the thermal energy loss by infiltration:

$$Q^{\mathrm{C}}_{\mathrm{inf}} = d_{\mathrm{a}}C_{\mathrm{a}}\mathrm{RE}(T_{\mathrm{i}} - T_{\mathrm{o}}) \tag{13}$$

The dynamic model of the relative humidity inside the greenhouse can be determined using Eq. (14) (Fitz-Rodríguez et al. 2010).

$$\frac{\mathrm{d}H_{\mathrm{i}}}{\mathrm{d}t} = \frac{1}{d_{\mathrm{a}}V}(E - V_{\mathrm{r}}(H_{\mathrm{i}} - H_{\mathrm{o}})) \tag{14}$$

with, H_{i} and H_{o} are, respectively, the inside and outside relative humidity and E is the evapotranspiration rate resulting by the evaporation of soil and the crop transpiration.

In case to control the internal air of the greenhouse and to activate of the actuators inside the greenhouse (activate the heating system or/and the ventilation system), Eq. (1) becomes:

$$\frac{\mathrm{d}T_{\mathrm{i}}}{\mathrm{d}t} = \frac{1}{d_{\mathrm{a}}C_{\mathrm{a}}V}\left(Q^{\mathrm{C}}_{\mathrm{c-i}} + Q^{\mathrm{C}}_{\mathrm{ca-i}} + Q^{\mathrm{C}}_{\mathrm{s-i}} - Q^{\mathrm{C}}_{\mathrm{inf}} - Q_{\mathrm{ventilation}} + Q_{\mathrm{heating}}\right) \tag{16}$$

$Q_{\mathrm{ventilation}}$ (W m^{-2}) is the rate of heat loss from the greenhouse by activating the ventilation and it is expressed in Eq. (17) (Fitz-Rodríguez et al. 2010).

$$Q_{\mathrm{ventilation}} = V_{\mathrm{r}}C_{\mathrm{a}}d_{\mathrm{a}}(T_{\mathrm{o}} - T_{\mathrm{i}}) \tag{17}$$

where V_{r} is the ventilation rate.

Q_{heating} (W m^{-2}) is the thermal energy provided by the heating system and is defined as in Eq. (18) (Fitz-Rodríguez et al. 2010).

$$Q_{\mathrm{heating}} = \frac{N_{\mathrm{h}} R_{\mathrm{h}}}{S_{\mathrm{s}}} \tag{18}$$

where N_{h} is the number of heaters and R_{h} is the capacity of the heating system.

Furthermore, the humidity rate R_{hum} provided by the humidifying system and the rate of humidity loses by the dehumidifying system R_{dehum} will be taken into account in the dynamic model of the relative humidity, which can be rewritten using the following equation:

$$\frac{\mathrm{d}H_{\mathrm{i}}}{\mathrm{d}t} = \frac{1}{d_{\mathrm{a}} V}\left(E - V_{\mathrm{r}}(H_{\mathrm{i}} - H_{\mathrm{o}})\right) + R_{\mathrm{hum}} - R_{\mathrm{dehum}} \tag{19}$$

5 Materials and Methods

The studied agricultural greenhouse is a small chapel-shaped greenhouse designed and implemented at the Research and Technology Center of Energy of Borj Cedria in Tunisia. The external view of the greenhouse is presented in Fig. 2. The experimental greenhouse occupied a floor area equal to 14.8 m^2 (length = 4 m, width = 3.7 m and height = 3 m). The specific design of the insulated greenhouse maximizes the input of solar irradiation and reduces the heat losses, which is used to plant a tomato crop. It is built by a sandwich panel with 0.4 m of thickness at the

Fig. 2 External view of the greenhouse

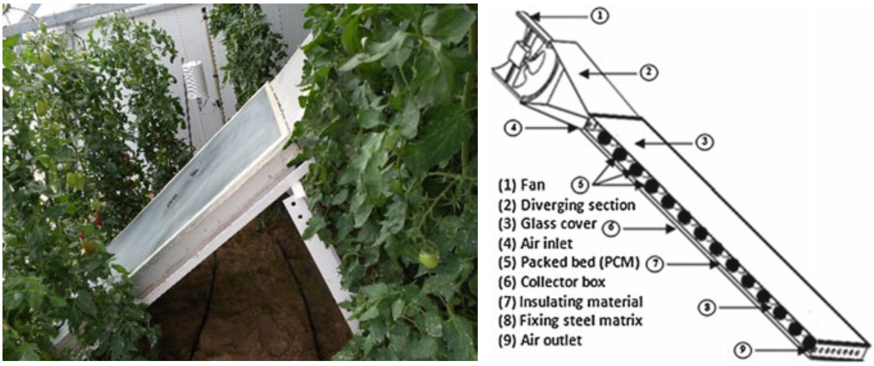

(a) Real photo **(b)** Schematic view

Fig. 3 Solar heating system

sidewalls and 0.6 m of thickness at the northern roof. It is specified by a wall and roof oriented to the south and covered by plexiglass with 0.003 m of thickness.

The heating system Fig. 3 is installed inside the greenhouse which is used to provide an additional heat to inside air of the greenhouse during the night. This system consists of a packed bed absorber with spherical capsules with a black coating and fixed with steel matrix. The nodules have an outer diameter of 0.077 m and are blow molded from a blend of polyolefin with an average thickness of 0.002 m. The nodule is filled with the phase change materials. The absorber is the most important component of this solar system which absorbs the sun radiations and stores the solar thermal energy as sensible heat and latent heat.

The studied agricultural greenhouse is equipped with the following actuators: One (1) water pump; One (1) small extractor is used to extract the stored heat from the solar air collector with phase change materials and two (2) identical exhaust extractors are used to refresh the inside climate by exchanging the air between the inside and outside the greenhouse. The exhaust fan is located at 2 m height from the soil in the east wall of the greenhouse and the second one is installed at 0.5 m in the west wall.

Several *K*-type thermocouples are used to measure the variation of temperatures, at the top, the bottom of the cover, and at the sandwich panel inside and outside the greenhouse.

- (2) two *HMP155A* sensors were used: the first one is installed at a height of 1.5 m above the roof of the greenhouse to measure the ambient parameters. The second sensor is installed at a height of 1.5 m above the soil into the greenhouse to measure the inside parameters such as the temperature and the relative humidity. They are protected and designed with a louvered construction to allow the air spread out freely through the shield.

- Kipp and Zonen pyranometer is used to measure the solar irradiation, which is situated at 1.5 m above the soil into the greenhouse and an anemometer is used to measure the wind velocity at 3 m above the ground.
- Three *PT-107* sensors, located under the soil, are used to measure the soil temperature inside the greenhouse at the surface of the soil, 0.25 m at depth and 0.5 m at depth. The surface temperature of the canopy is measured using an infrared temperature sensor *IR120*, which is protected by the *IR-SS* Solar Shield from direct solar irradiation.
- *NRG* weather station is located in the Research and Technology Center of Energy which is used in order to provide the internal and external weather conditions.
- *CR5000* data logger (Campbell Scientific Inc) which is used to measure the inside and outside climatic parameters with a sample time equal to 10 min.

The outside parameters such as the solar irradiation, wind speed, temperature, and the relative humidity are measured with appropriate instruments to carry out the experimental measurements. The uncertainty analysis of the various measured and calculated parameters are estimated according to Holman correlation (Holman 1993). The sensitiveness was obtained from datasheets of the instruments. The experimental results are highly acceptable if they presented very small values of uncertainties.

The reflectivity and transmissivity spectra recorded in the wavelength range (380–900 nm) of the soil, cover and canopy layer are plotted in Fig. 4. They are realized using LAMBDA950 UV–vis–NIR spectrometer equipped with an integrating sphere.

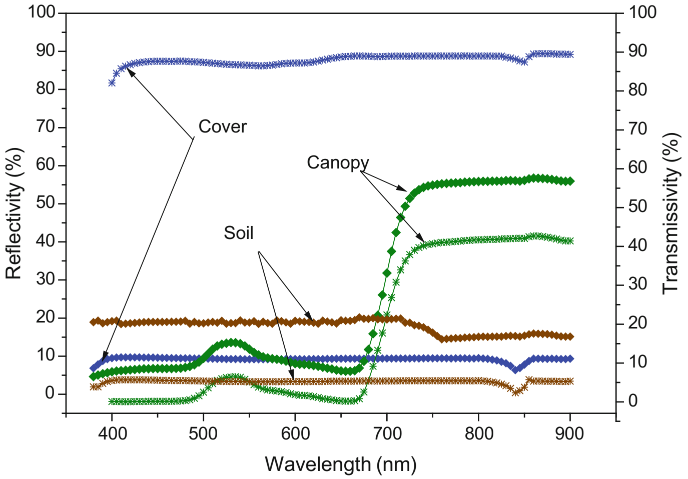

Fig. 4 Physical characteristics of the greenhouse

6 Control Strategies

An FLC controller is used to hold the internal temperature at its set point value by turning on/off the actuators installed inside the greenhouse, with the appropriate rate and at the right time. This technique is characterized by its simplicity, where it is necessary to create a membership function based on the expertise of a human deep as well the knowledge of the indoor climate conditions of the greenhouse and the various decisions to activate the greenhouse actuators to achieve the optimal microclimate. Thus, its user instructions depend on the set point value and the inside and outside weather conditions. The membership functions of the used FLC controller are given in Table 1.

The input variables of the temperature fuzzy controller are the temperature error ΔT.

$$\Delta T = T_{\text{setpoint}} - T_{\text{inside}} \tag{20}$$

where

BN	negative big
MN	negative medium
Z	zero
MP	positive medium
BP	positive big.

The output variables are the ventilation and the heating rate, where

Z	zero
M	medium
H	high.

The rules present the decisions will be applied to the air temperature inside the greenhouse in order to have a desirable internal temperature. The membership function of the input variable (the temperature error) is plotted in Fig. 5 and the membership functions of the output variables (the ventilation and the heating rates) are shown in Fig. 6.

The temperature error ΔT presents the input parameter of the FLC controller and the actuators started to work when its value is different to *zero*.

Table 1 Fuzzy rules of the air temperature

Temperature error	Ventilation rate	Heating rate
BN	H	Z
MN	M	Z
Z	Z	Z
MP	Z	M
BP	Z	H

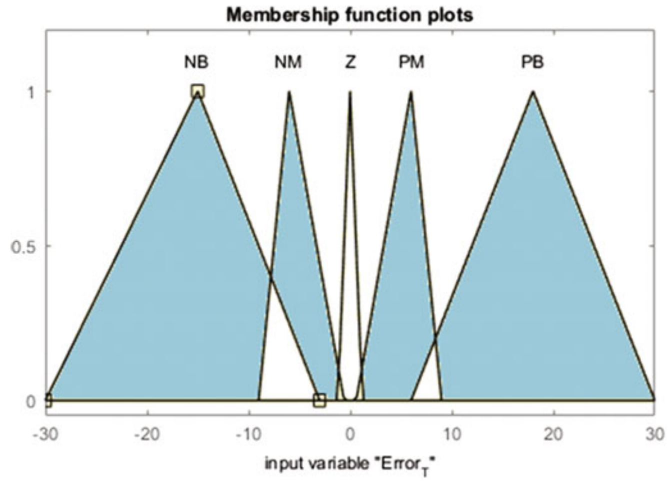

Fig. 5 Membership function of the temperature error

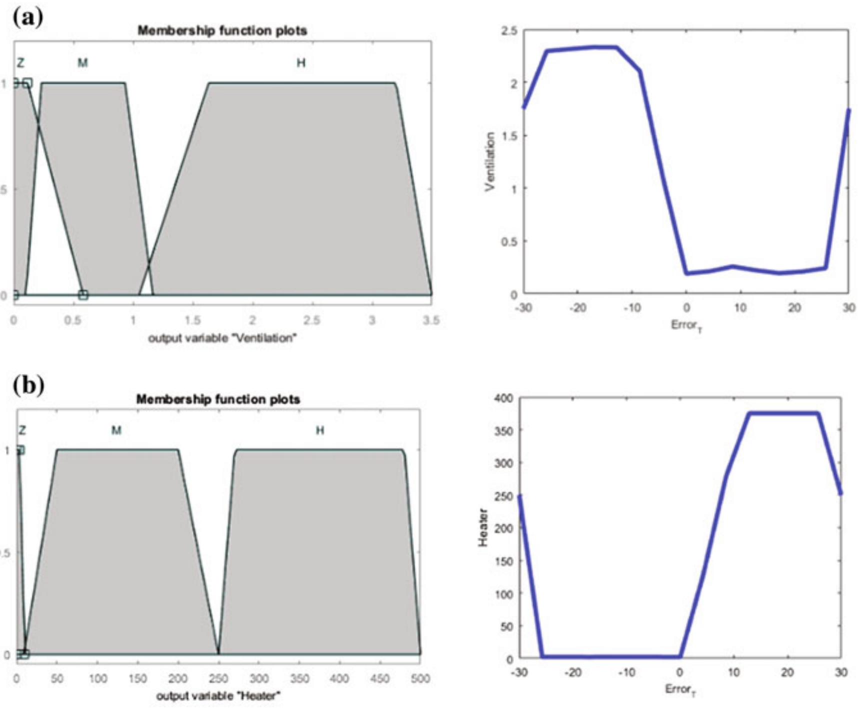

Fig. 6 Membership functions of the ventilation rate

The dynamic model of the agricultural greenhouse was performed using MATLAB/Simulink environment (Fig. 7). The fuzzy rules of the inside air temperature are selected in order to ensure the desired internal temperature. The ventilation system will be activated when the inside temperature exceeds the fixed favourable value Fig. 6a and the heating system will be activated if the inside temperature is lower than the set-point value Fig. 6b.

The MATLAB/Simulink environment is used in several studies to predict the microclimate inside the greenhouse (Kıyan et al. 2013; Ben Ali et al. 2015) and it is used in this study to perform a comparative analysis between the measured and predicted values of the internal air temperature (Fig. 8), where the predicted temperature can be calculated by applying Eq. (1).

As can be seen in Fig. 8, there is a fair agreement between the inside predicted and measured temperature, which are varied, respectively, between 10 and 44 °C and between 13 and 40 °C. That proves the effectiveness of the proposed physical model to predict the temperature inside the agricultural greenhouse with a low percentage error of the Root Mean Squared Error (*RMSE*), which is equal to

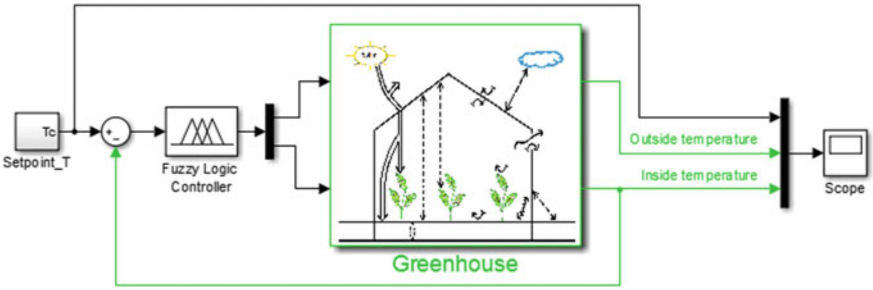

Fig. 7 Simulink model of the controlled greenhouse

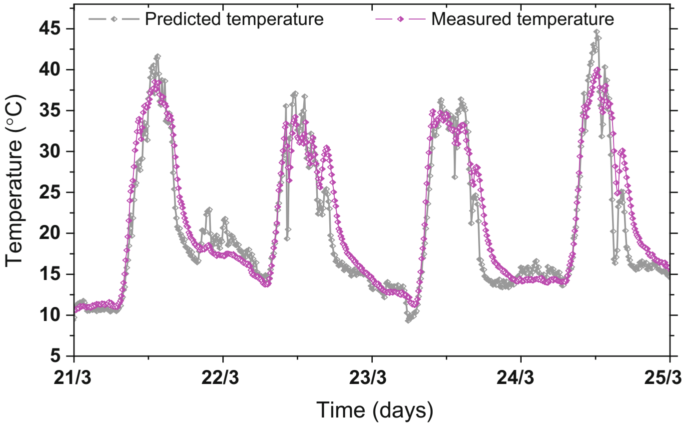

Fig. 8 Predicted and measured air temperatures into the greenhouse

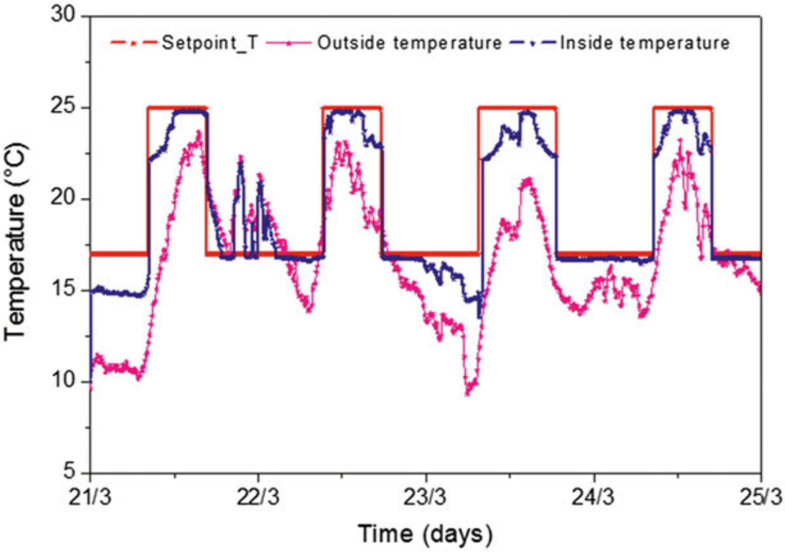

Fig. 9 The evolution of the air temperature with the FLC controller

0.02 °C and a high coefficient of determination (R^2) equal to 1. They were also calculated using MATLAB environment. However, the temperature inside the greenhouse is not always favourable for the canopy growth. For this reason, an FLC controller is applied to reach the predefined set point value by activating the appropriate actuator installed inside the greenhouse (ventilation or heating system). Thus, the simulation results of the air temperature inside the studied greenhouse with the FLC controller is presented in Fig. 9.

7 Modeling of the Wind Turbine System

Figure 10 presented schematically the mathematical model of the small wind turbine system linked to PMSG generator which is simulated using MATLAB/Simulink environment.

The wind turbine is considered as one of the important renewable energy systems (Grisales and Lemus 2014). Generally, it is composed by

- Wind turbine.
- PMSG generator.
- Power electronic converter.
- Load.

AC load is applied that is why the studied wind turbine is linked to a PMSG generator without power electronic converter.

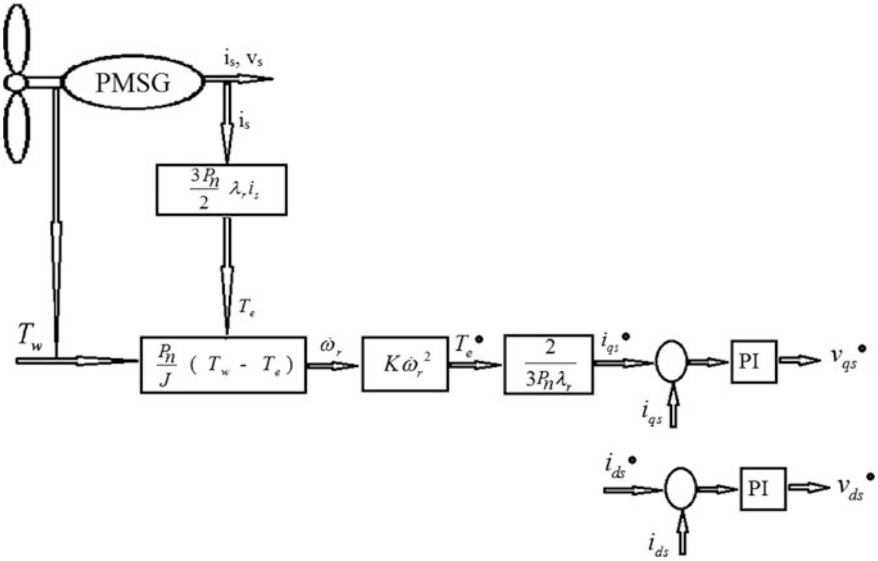

Fig. 10 Control scheme of the PMSG generator using ZDC control

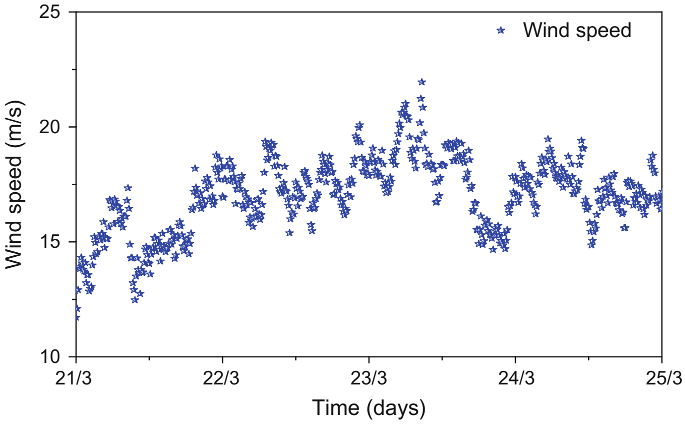

Fig. 11 Variation of the wind speed

It is simulated using MATLAB/Simulink environment with a database carried out in the CRTEn center in Tunisia during 4 days in spring.

The wind speed velocity presents the most important parameter and the sustainable source of energy for the wind turbine system. Its variation is shown in Fig. 11.

The variation of the torque T_w (N m) generated by the wind turbine is plotted in Fig. 12.

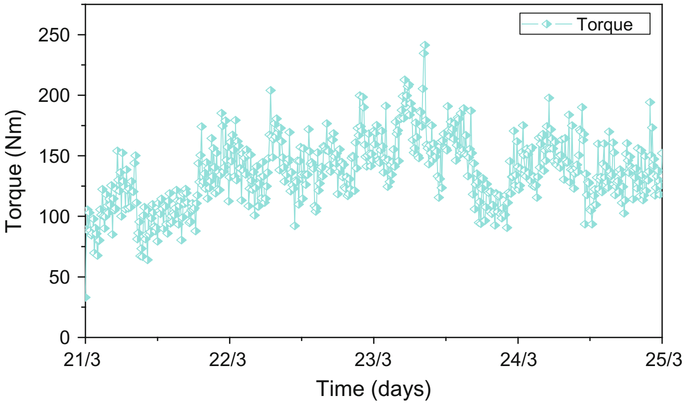

Fig. 12 Variation of the torque supplied by the Wind turbine

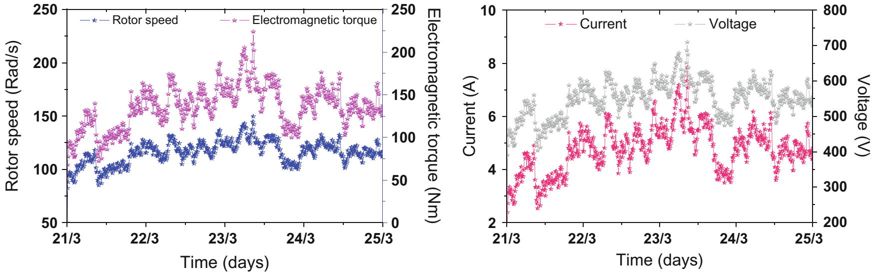

(a) Variation of the rotor speed and the electromagnetic torque.

(b) Variation of the output current and voltage.

Fig. 13 Variation of the output parameters delivered by the PMSG generator

Figure 13 presents the variation of the output parameters delivered by the PMSG generator such as the rotor speed and the electromagnetic torque (Fig. 13a); the variation of the current and the voltage generated (Fig. 13b).

In addition, the variation of the output mechanical, active, and reactive power is shown in Fig. 14.

The simulation results show that the voltage is increased to achieve 700 V and the variation of the mechanical, active and reactive power, and current vary according to the variation of the wind velocity. They reach their maximum value during 23/03 when the wind velocity achieves 22 m s^{-1}. Thus, the current varies between 0 and 6 A. Nonetheless, the mechanical and active power varies between 0 and 16 KW and the reactive power varies between 0 and 1.5 KW, for which the AC voltage generated by the Wind turbine system reaches 800 V.

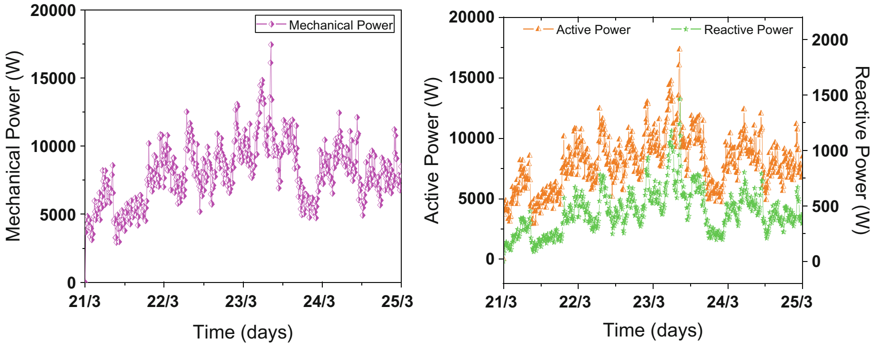

Fig. 14 Variation of the output mechanical, active and reactive power

8 Conclusion

Actually, the exploitation of the renewable energy is the aim of several research studies regarding its advantages in terms of efficiency, cost, and reliability. The wind turbine system is one of several power supply systems that can be used not only to produce the electricity but also to reduce the pollution. This paper aims to develop a dynamic model of a small wind turbine system by estimating its dynamic behaviors, in addition to the modeling and the experimental validation of the agricultural greenhouse. They are modeled using the MATLAB/Simulink environment. The simulation results of the numerical validation showed the effectiveness of the proposed model of the greenhouse to predict the temperature inside the greenhouse which is instilled in the Research and Technology Center of Energy (CRTEn) in Tunisia. Moreover, in order to reach a suitable microclimate inside the greenhouse, it is necessary to equip it by actuators such as the heating and the cooling systems, controlled by a fuzzy logic controller (FLC). Furthermore, the wind turbine system can be used to power these actuators.

References

Abdel-Ghany AM, Kozai T (2006) Dynamic modeling of the environment in a naturally ventilated, fog-cooled greenhouse. Renew Energy 31(10):1521–1539

Atia DM, El-madany HT (2016) Analysis and design of greenhouse temperature control using adaptive neuro-fuzzy inference system. J Electr Syst Inf Technol

Ben Ali R, Aridhi E, Mami A (2015) Dynamic model of an agricultural greenhouse using Matlab-Simulink environment, pp 346–350

Bouadila S, Lazaar M, Skouri S, Kooli S, Farhat A (2014a) Assessment of the greenhouse climate with a new packed-bed solar air heater at night, in Tunisia. Renew Sustain Energy Rev 35:31–41

Bouadila S, Kooli S, Skouri S, Lazaar M, Farhat A (2014b) Improvement of the greenhouse climate using a solar air heater with latent storage energy. Energy 64:663–672

Boughanmi H, Lazaar M, Bouadila S, Farhat A (2015) Thermal performance of a conic basket heat exchanger coupled to a geothermal heat pump for greenhouse cooling under Tunisian climate. Energy Build 104:87–96

Boulard T, Wang S (2000) Greenhouse crop transpiration simulation from external climate conditions. Agric For Meteorol 100(1):25–34

Cuce E, Harjunowibowo D, Cuce PM (2016) Renewable and sustainable energy saving strategies for greenhouse systems: a comprehensive review. Renew Sustain Energy Rev 64:34–59

Dahmouni AW, Ben Salah M, Askri F, Kerkeni C, Ben Nasrallah S (2010) Wind energy in the Gulf of Tunis, Tunisia. Renew Sustain Energy Rev 14(4):1303–1311

Dahmouni AW, Ben Salah M, Askri F, Kerkeni C, Ben Nasrallah S (2011) Assessment of wind energy potential and optimal electricity generation in Borj-Cedria, Tunisia. Renew Sustain Energy Rev 15(1):815–820

Díaz-Méndez R, Rasheed A, Peillón M, Perdigones A, Sánchez R, Tarquis AM, García-Fernández JL (2014) Wind pumps for irrigating greenhouse crops: comparison in different socio-economical frameworks. Biosyst Eng 128:21–28

Duffie J, Beckman W (1991) Solar engineering of thermal processes, 2nd edn. Wiley, New York, USA

Fatnassi H, Boulard T, Bouirden L (2013) Development, validation and use of a dynamic model for simulate the climate conditions in a large scale greenhouse equipped with insect-proof nets. Comput Electron Agric 98:54–61

Fitz-Rodríguez E, Kubota C, Giacomelli GA, Tignor ME, Wilson SB, McMahon M (2010) Dynamic modeling and simulation of greenhouse environments under several scenarios: a web-based application. Comput Electron Agric 70(1):105–116

Fourati F (2014) Multiple neural control of a greenhouse. Neurocomputing 139:138–144

Grisales LT, Lemus CG (2014) Overall description of wind power systems 10(19):99–126

Hasni A, Taibi R, Draoui B, Boulard T (2011) Optimization of greenhouse climate model parameters using particle swarm optimization and genetic algorithms. Energy Proc 6:371–380

Hassan GE, Salah AH, Fath H, Elhelw M, Hassan A, Saqr KM (2016) Optimum operational performance of a new stand-alone agricultural greenhouse with integrated-TPV solar panels. Sol Energy 136:303–316

Holman JP (1993) Experimental methods for engineers/J. P. Holman. Version details—Trove, 6th edn

I. Renewable and E. Agency (2015) Renewable energy in the water, energy & food nexus. no. January, 2015

Joudi KA, Farhan AA (2015) A dynamic model and an experimental study for the internal air and soil temperatures in an innovative greenhouse. Energy Convers Manage 91:76–82

Khoshnevisan B, Rafiee S, Omid M, Mousazadeh H, Clark S (2014) Environmental impact assessment of tomato and cucumber cultivation in greenhouses using life cycle assessment and adaptive neuro-fuzzy inference system. J Clean Prod 73:183–192

Kıyan M, Bingöl E, Melikoğlu M, Albostan A (2013) Modelling and simulation of a hybrid solar heating system for greenhouse applications using Matlab/Simulink. Energy Convers Manage 72:147–155

Kooli S, Bouadila S, Lazaar M, Farhat A (2015) The effect of nocturnal shutter on insulated greenhouse using a solar air heater with latent storage energy. Sol Energy 115:217–228

Kristjansdottir TF, Good CS, Inman MR, Schlanbusch RD, Andresen I (2016) Embodied greenhouse gas emissions from PV systems in Norwegian residential Zero Emission Pilot Buildings. Sol Energy 133:155–171

Lafont F, Balmat JF (2002) Optimized fuzzy control of a greenhouse. Fuzzy Sets Syst 128(1):47–59

Lafont F, Balmat JF, Pessel N, Fliess M (2015) A model-free control strategy for an experimental greenhouse with an application to fault accommodation. Comput Electron Agric 110:139–149

Lazaar M, Bouadila S, Kooli S, Farhat A (2015) Comparative study of conventional and solar heating systems under tunnel Tunisian greenhouses: thermal performance and economic analysis. Sol Energy 120:620–635

Li C, Wang H, Miao H, Ye B (2017) The economic and social performance of integrated photovoltaic and agricultural greenhouses systems: case study in China. Appl Energy 190:204–212

Longo GA, Gasparella A (2015) Three years experimental comparative analysis of a desiccant based air conditioning system for a flower greenhouse: assessment of different desiccants. Appl Therm Eng 78:584–590

Maatallah T, El Alimi S, Dahmouni AW, Ben Nasrallah S (2013) Wind power assessment and evaluation of electricity generation in the Gulf of. Sustain Cities Soc 6:1–10

Maher A, Kamel E, Enrico F, Atif I, Abdelkader M (2016) An intelligent system for the climate control and energy savings in agricultural greenhouses. Energy Effi 1–15

Márquez-Vera MA, Ramos-Fernández JC, Cerecero-Natale LF, Lafont F, Balmat J-F, Esparza-Villanueva JI (2016) Temperature control in a MISO greenhouse by inverting its fuzzy model. Comput Electron Agric 124:168–174

Marucci A, Cappuccini A (2016) Dynamic photovoltaic greenhouse: energy efficiency in clear sky conditions. Appl Energy 170:362–376

Mesmoudi K, Soudani A, Zitouni B, Bournet PE, Serir L (2010) Experimental study of the energy balance of unheated greenhouse under hot and arid climates: Study for the night period of winter season. J Assoc Arab Univ Basic Appl Sci 9(1):27–37

Ministère de l'Agriculture et des Ressources Hydrauliques (Hrsg.) (2006) Enquête sur les Structures des Exploitations Agricoles 2004–2005, pp 1–77

Mohamed S, Hameed IA (2016) A GA-based adaptive neuro-fuzzy controller for greenhouse climate control system. Alexandria Eng J

Nayak S, Tiwari GN (2010) Energy metrics of photovoltaic/thermal and earth air heat exchanger integrated greenhouse for different climatic conditions of India. Appl Energy 87(10):2984–2993

Nookuea W, Campana PE, Yan J (2016) Evaluation of solar PV and wind alternatives for self renewable energy supply: case study of shrimp cultivation. Energy Proc 88:462–469

Ozgener O (2010) Use of solar assisted geothermal heat pump and small wind turbine systems for heating agricultural and residential buildings. Energy 35(1):262–268

Pawlowski A, Beschi M, Guzmán JL, Visioli A, Berenguel M, Dormido (2016) Application of SSOD-PI and PI-SSOD event-based controllers to greenhouse climatic control. ISA Trans 65:525–536

Peillóna M, Sánchezb R, Tarquisc AM, García-Fernández JL (2013) The use of wind pumps for greenhouse microirrigation: a case study for tomato in Cuba. Agric Water Manage 120(1): 107–114

Rasheed A, Lee JW, Lee HW (2016) Feasibility evaluation of the wind energy as an alternative energy source for the irrigation of greenhouse crops. Int J Renew Energy Res 6(4):1–25

Revathi S, Sivakumaran N (2016) Fuzzy based temperature control of greenhouse. IFAC-PapersOnLine 49(1):549–554

Salgado P, Cunha JB (2005) Greenhouse climate hierarchical fuzzy modelling. Control Eng Pract 13(5):613–628

Taki M, Ajabshirchi Y, Ranjbar SF, Rohani A, Matloobi M (2016) Heat transfer and MLP neural network models to predict inside environment variables and energy lost in a semi-solar greenhouse. Energy Build 110:314–329

van Beveren PJM, Bontsema J, van Straten G, van Henten EJ (2015) Optimal control of greenhouse climate using minimal energy and grower defined bounds. Appl Energy 159:509–519

World Health Organization (WHO) (2014) http://apps.who.int/iris/bitstream/handle/10665/170620/WPR_RC065_10_Progress_Report_2014_en.pdf?sequence=2&ua=1

Zeng S, Hu H, Xu L, Li G (2012) Nonlinear adaptive PID control for greenhouse environment based on RBF network. Sensors (Basel) 12(5):5328–5348

Design and Selection Criteria of Biogas Digester

Anirshu Dev Roy, Om Prakash, Anil Kumar, A. K. Kaviti and Anukul Pandey

Abstract Biogas, produced from animal or kitchen waste, is possibly the only energy source that allows farmers to produce their own electricity. There is an added advantage of reducing the contamination and pollution of water, bad odor, and global warming emissions caused due to animal waste. Biogas is generated when bacteria decompose organic waste anaerobically. The biogas is a combination of gases containing about 60–70% CH_4, 20–30% CO_2, and few of other gases like CO, H_2S, NH_3, O_2, H_2, N_2, and water vapor, etc. The gas produced can be used not only for cooking but also for rural electrification where grid connection is not viable. The remaining digested slurry can be used as manure. The idea behind this chapter is to prepare a document which can help in the installation of biogas units and reduce the size of the biogas plant. This communication discusses the various design aspects of the most common types of biogas digesters used today. It takes into account the design aspects of Fixed dome type and Floating drum type.

A. D. Roy
Department of Mechanical Engineering, Jalpaiguri Government Engineering College,
Jalpaiguri 735102, India
e-mail: anirshu95@gmail.com

O. Prakash
Department of Mechanical Engineering, Birla Institute of Technology,
Mersa, Ranchi 835215, India
e-mail: 16omprakash@gmail.com

A. Kumar (✉)
Department of Energy (Energy Centre), Maulana Azad National Institute
of Technology, Bhopal 462003, India
e-mail: anilkumar76@gmail.com

A. K. Kaviti
Department of Mechanical Engineering, VNR Vignana Jyothi Institute
of Engineering and Technology, Hyderabad 500090, India
e-mail: ajaykaviti@gmail.com

A. Pandey
Department of Electronics and Communication Engineering,
Dumka Engineering College, Dumka 814101, India

A. Sharma et al. (eds.), *Low Carbon Energy Supply*, Green Energy and Technology,
https://doi.org/10.1007/978-981-10-7326-7_6

Mathematical equations for measuring the amount of biogas digester volume have been discussed. The selection criterion for biogas digesters has also been discussed.

Keywords Biogas · Digester types · Selection · Design · Parameter

1 Introduction

The production of biogas takes place by the anaerobic digestion of the bio-degradable materials with the help of bacteria. The biogas is an important source of renewable/non-conventional energy (Martins das Neves et al. 2009). The energy obtained from biogas has some advantages over other energy sources. Optimizing the use of biogas technology can result not only in the production of energy resources and fertilizers production but also other economic and environmental profit counting sanitation, reforestation, and decrease the demand of natural gas and oil (Walekhwa et al. 2009). Like many developing countries of the world, India also faces major problem due to the petroleum products price hike in the international market. Also, the rising demand for energy from urban as well as rural sector implies that newer sources of energy need to be focused on. Not only this, but these newer and alternative sources of energy have to be made available to the common people at a sustainable amount and at an affordable price. For this reason, conversion of agricultural, cattle, and kitchen wastes into biogas will provide a scope for solving some of the mentioned energy crisis. Most of the developing countries face the problem of the dearth of adequate access to cooking gas and electricity for their rural and suburban population (Beall et al. 2002). Conventional stoves generally made of cow dung cause the major producers of greenhouse gases (GHG) (Smith 1994). Generally, there is the formation of CO, methane, and other nitrogen compounds such as nitric oxide and nitrogen dioxide (Ndiema et al. 1998). In developed countries when rising convenience and lessening prices of fossil fuel during 1950–1970, the attractiveness of biogas got down and made less attractive biogas energy (Deublein and Steinhauser 2008). From the 1970s and continuing, there are now 27 million biogas plants in India and China (Bond and Templeton 2011). Production of methane by anaerobic digestion of bio-degradable materials has been experienced since early times of civilization. In the 10 BC, the usage of biogas was for heating tubs in Assyria (Deublein and Steinhauser 2008). In the twentieth century, Louis Pasteur produced 100 L of the gas by fermenting horse dung. The establishment of biogas (methane) plants in these communities is expected to greatly ameliorate these problems and help preserve the environment. Biogas is composed of CH_4 (40–75%) and CO_2 (15–60%) and the rest is other gases in small quantities, i.e., N_2 (0–2%), CO (<0.6%), H_2S (0.005–2%), O_2 (0–1%), NH_3 (<1%), traces of siloxanes (0–0.02%), halogenated hydrocarbons (<0.65%), and other hydrocarbons which have no methane content like aromatic hydrocarbons, alkanes, alkenes, etc. (Bailón Allegue et al. 2012). The waste generated from this has high levels of inorganic elements like nitrogen and phosphorus which are essential for growth of plants and also improves the process, commonly called bio-fertilizer which increases the soil quality and provides no harmful property to the surroundings (Purwono et al. 2013). A biogas plant is an airtight storage place where biogenic wastes when diluted with water are fermented by bacteria in the absence of oxygen (Weiland 2010). Municipal solid waste can be the input raw material of the biogas digester. A detailed study on the anaerobic-based biogas digester was presented (Appels et al. 2008; Hilkiah et al. 2008). The cattle dung digesters can be improved by adding soya sludge/mustard cake. It increases the amount of gas generated and nitrogen and phosphorus content, and further improves the time for capillary suction. The study shows that the performance of digester was enhanced. Methane content in biogas was also risen by adding of soya sludge/mustard cake. Manorial value (N_2 and PO43-) denoted enhancement in the quality of sludge. The addition does not have any negative effect on the digester performance (Satyanarayan et al. 2008, 2010). Simultaneous anaerobic digestion of press water and food products in a biogas digester improves its buffer capacity (Nayono et al. 2010). A performance of the anaerobic process used mixed fruit and vegetable wastes as substrates in a single stage fed-batch anaerobic digester for biogas production has been carried out (Sitorus et al. 2013). Anaerobic digestion of a mix of fruit and vegetable wastes was done in a 200-L digester within 14 weeks at ambient temperature. Chemical analyses based on standard methods were conducted for the initial waste and for the bio-reactor slurry. The biogas was having a methane content of 65% which is the maximum, with the biogas flow of 20–40 ml/min. The biogas plants are taken into consideration, i.e., the family size plants (capacity from 1 to 6 m^3), where there are generally three models like KVIC, Janta, and Deenbandhu, where the comparison had taken place, based on cost. However, by comparison, Deenbandhu model was found to be the most economic and useful model (Singh and Sooch 2004). Investments in domestic bio-digester had overall profit and variety of discounts available. It is projected that domestic bio-digester implementation at the national level could be a good source for accessing significant amount in carbon emissions reduction (CER) yearly financing through the Clean Development Mechanism (Laramee and Davis 2013). The plants are generally made of plastic, concrete sometimes steel, and even bricks materials. They could also be in shapes like silos, troughs, basins, or ponds and may be placed underground (pit) or on the surface. Many countries such as India, China, Taiwan, and Nigeria among others have built biogas plants (bio-digesters) based on cow dung. However, the sizes, shapes, constructional materials, etc., vary. Hence there is need to characterize the different bio-digesters with objectives of; to generate energy and provide rich-nutrients manure (EIS et al. 2011).

In this chapter; Sect. 1 deals with the introduction part, Sects. 2 and 3 present the studies about components of a biogas plant, biogas production methodology, under biogas production methodology Hydrolysis, Acidogenesis, Acetogenesis, and Methanogenesis. Sections 4 present the design of biomass digester Sects. 5 and 6 present the effect of working parameters on the performance of biogas digester, under the effect of working parameters on the performance of biogas digester various parameters, required for a successful digester. In Sects. 7–9, the studies

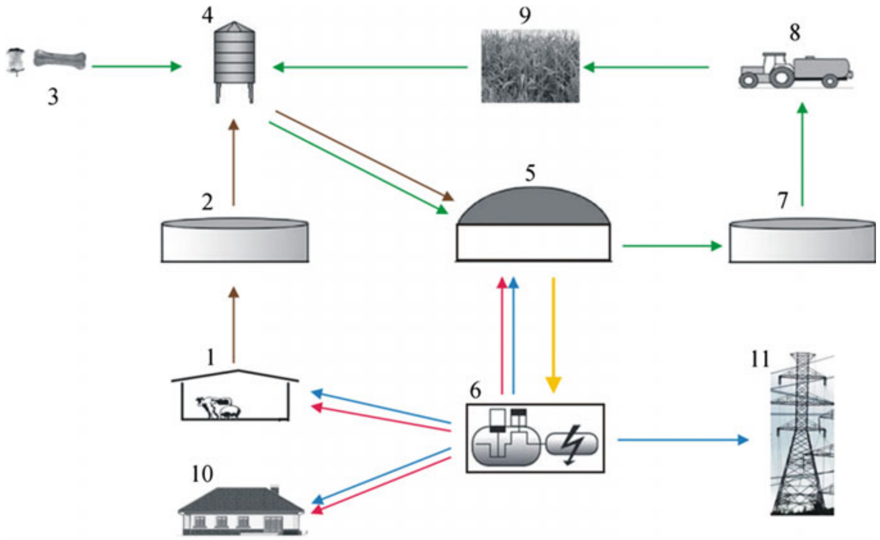

Fig. 1 A simple diagram of the biogas and its utilities 1: livestock house, 2: initial tank, 3: waste from agriculture and livestock, 4: mixing tank, 5: bio-reactor, 6: accumulation of the co-generation, 7: tank for keeping the remaining materials after fermentation, 8: fertilizer obtained from the post-fermentation, 9: maize silage, 10: offices, and 11: Electrical grid for energy supply. Igliński et al. (2012)

about biogas development in some developed countries, biogas development in some developing countries is discussed. A diagrammatic representation of the biogas plant is given in Fig. 1.

2 Components of a Biogas Plant

To produce the biogas, an air-tight enclosed chamber is required. This chamber is called a biogas digester. Digestion process takes place anaerobically inside the digester. The major components of bio-digester are: Waste inlet, Digester chamber, Gas collecting chamber, Gas outlet and tube, Slurry outlet. The brief discussion of each component is as follows:

(a) **Waste inlet**: The organic solid waste is mixed with water in a 1:1 ratio to achieve a homogenous mixture and poured in through this inlet. For obtaining the right bacteria to digest this waste, a one-time dumping of cow dung is required and the bacteria within is allowed to multiply after which the organic waste can be put in everyday.

(b) **Digester chamber**: Anaerobic decomposition takes place and methane gas rises within the chamber while the solid and liquid settle at the bottom.

(c) **Gas collecting chamber**: In case of the floating drum type biogas digester, the gas rises into a fiber drum or fiber-coated metal drum placed above the digestion chamber that constantly floats in a small pool of water. As the gas rises into the dome, the dome also rises and exerts pressure on the internal gas and slurry. It is a constant pressure type biogas digester. In case of the fixed dome type biogas digester, the chamber is static, and it is a constant volume type biogas digester. The pressure varies, and care should be taken that pressure build-up should not exceed permissible limit.

(d) **Gas outlet and tube**: The pressure from the dome causes the gas to pass through the gas outlet into a tube which is connected to a gas stove placed in a kitchen.

(e) **Slurry outlet**: The solid and liquid waste that collects in the digester chamber will rise into the slurry outlet and can be collected with a buck (Tanskanen 2016).

3 Biogas Production Methodology

The pH value of the digester slurry is an important parameter. This should be monitored on weekly basis and should lie between 5.93 and 7.73. Slurry temperature, slurry pressure, and ambient temperature are needed to observed on daily basis for proper functioning of digester. The slurry temperature and ambient temperature should lie between 20 and 45 °C. The slurry pressure should lie between the 0–0.6 bar and the pressure of the outlet biogas is varying 0–0.25 bar (Ezekoye and Okeke 2006). Batch anaerobic digestion experiments using manure from dairy products as feedstocks were experimented at psychrophilic (20–25 °C), mesophilic (37 °C), and thermophilic (52.5 °C) temperatures (Pandey and Soupir 2011). The mesophilic reactors (37–45 °C) produced a less than 30% biogas from the actual rate and less than 23.3% methane, followed by psychrophilic (20–25 °C) which given output of less than 41% biogas and 39.7% less methane (Vanegas and Bartlett 2012). The methane gas obtained is a form of energy which can be utilized and stored for different domestic purposes.

3.1 Hydrolysis/Liquefaction

Hydrolysis is the first step in the process of conversion of the biomass/bio-waste to the biogas. It is also called liquefaction process. In this stage, with the help of the fermentative bacteria, the unsolvable complex organic substance is being converted to the soluble substance. The common unsolvable complex organic substance is cellulose, and common soluble substances are; sugars, amino acids, and fatty acids. In order to enhance the process, some chemical is being used to reduce the digestion time and increase the methane yield (Bansal et al. 2013). The governing chemical reaction of this stage is given below (Arsova 2010):

$$C_6H_{10}O_4 + 2H_2O = C_6H_{12}O_6 + 2H_2$$

3.2 Acidogenesis

Acidogenesis process also known as the first process of fermentation. In this process, there is a continuous breakdown of small sub-units from larger unit due to hydrolysis process. This leads to forms varieties of acids of organic nature along with H_2 and CO_2. This part is the generally the fastest part in the digestion process and has high output energy for the microorganisms (Beam 2011). Degradation to methane and carbon occurs with a short or no time lag when the additional substrate is fed to the respective cultures. On the other hand, some time is needed normally for the acclimation of every aromatic compound, nevertheless, when the culture is used to process one aromatic compound and another similar is feed, it may not need any acclimation time (Peris et al. 2011). The acidogenic fermentation resulted in the formation of fermented products of maize silage as the main substrate in a leach bed process was determined by gas and liquid chromatography. The dynamics of bacterial community was monitored by terminal restriction fragment length polymorphism analysis (Sträuber et al. 2012).

The main output of acidogenesis is acetic (lactic, and propionic acids). The pH of the slurry falls as the rate of the generation of these compound increases. In order to accomplish this process, acidogenic bacteria, organic acid, alcohol, and other compounds are required in the biogas digester (Bansal et al. 2013).

3.3 Acetogenesis

Acetogenesis is a process of production of acetate by anaerobic bacteria obtained from a variety of sources of energy and carbon. The species of bacteria that are capable of acetogenesis are collectively termed acetogenesis. Acetogenic bacteria which produces H_2 are capable of producing acetate and H_2 from heavier fatty acids (Merlin Christy et al. 2014). Acetogenic bacteria employing the Wood–Ljungdahl pathway act as biocatalysts in syngas fermentation during the production of biofuels such as ethanol or butanol as well bio-products such as acetate, lactate, butyrate, 2, 3 butanediol, and acetone (Bertsch and Müller 2015). The ability of such processes can be obtained by the global syngas output, which was 70,817 MW thermal in 2010 and is expected to rise to 72% in 2016. Till date, for acetogen is used for the syngas fermentation for industrial purpose and demonstration. The potential for a number of fermentative products obtained is promising. Synthetic biology will now play a major role in constructing a pathway for commercial operations. In such way, a cheap and abundant carbon producing material will mostly replace, processes where it is obtained from crude oil or sugar in the upcoming future (Bengelsdorf et al. 2013).

3.4 Methanogenesis

Methanogenesis process involves the production of methane from the waste material during the final stage. The production of methane is by acetate-degrading methanogen in two ways: either by means of cleavage of acetic acid molecules to generate carbon dioxide and methane or by reduction of carbon dioxide with hydrogen. Methane produced is higher when obtained by reduction of carbon dioxide and is limited when hydrogen is present in digesters resulting in acetate reaction is the primary producer of methane. Methanogens can also be divided into two groups: acetate and H_2/CO_2 consumers. The reactions of methanogenesis are shown below:

$$CH_3COOH \rightarrow CH_4 + CO_2$$
$$2C_2H_5OH + CO_2 \rightarrow CH_4 + 2CH_3COOH$$
$$CO_2 + 4H_2 \rightarrow CH_4 + 2H_2O$$

Methanogenesis is sensitive to pH, it is in the mildly acidic range (6.6–7.0) (Bansal et al. 2013). Biogas technology among other processes has made their way into emerging sustainable technologies for waste treatment since waste disposal is a major issue in the developing countries. The matter obtained from this process is a material rich in highly useful inorganic elements like nitrogen and phosphorus required for the growth of plants commonly known as the bio-fertilizer, this increases the soil quality without affecting other components in the soil (Ofoefule et al. 2010).

4 Biogas Plants Types

Biogas plants are mainly of three types based on their shapes (Sasse et al. 1988). They are (1) Balloon plants (2) Fixed dome plants (3) Floating drum plants. As represented in Fig. 2.

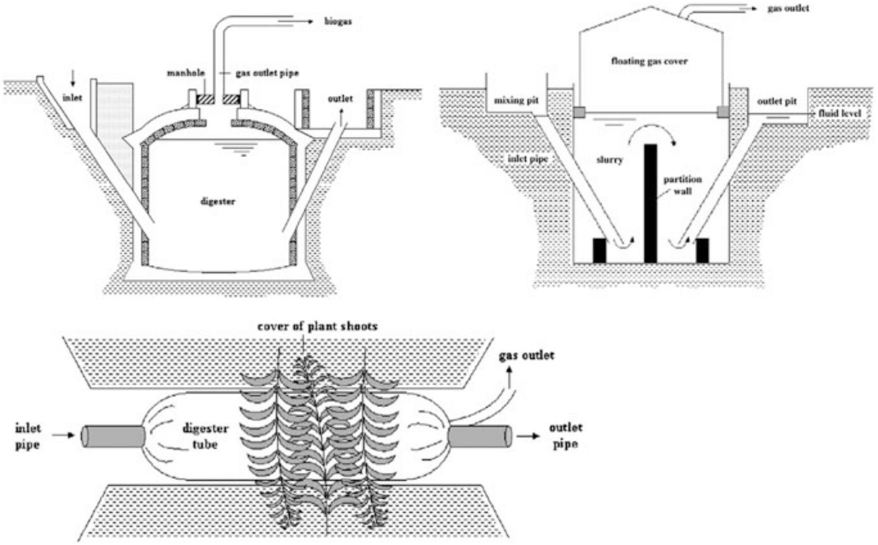

Fig. 2 Fixed dome (top left), floating cover (top right), and balloon type (bottom). Bond et al. (2011)

4.1 Balloon Plants

This digester is made of plastic in the upper region of the digester where the gas is stored. The inlet and the outlet are directly attached to the balloon skin. When the space for holding the gas is full, it works like a fixed dome plant. The fermentation of slurry gets activated due to the movement of the skin of the balloon. This helps in the digestion process. Even different materials for feed such as water hyacinths can be used. The materials of the balloon plant should be UV resistant. Red Mud Plastic material (RMP) is also used in fabrication of this type of digester.

The advantages of the balloon plant are: low cost, can be easily transported from one place to another and easy in construction. Also, it has less complexity of cleaning and maintenance issues. The disadvantages associated with this plant are: has a very small life span and is prone to damage. It is mainly used where it is less prone to damage.

4.2 Fixed Dome Plant

A fixed dome plant consists of a digester enclosed with a fixed, non-movable gas space. The upper part contains the gas of the digester. When gas production is stopped, the slurry is sent into the compensating tank. Gas pressure rises according to the volume of gas stored, hence the digester volume should not be more than 20 m^3. The gas pressure becomes low if there is some gas present in the holder.

The advantages of this plant are: it is very cheap and has no moving parts hence there is less chance of oxidation and so the lifespan is very long. It also creates a source of employment. The disadvantages associated with this are: it is full of porosity and cracks, there is a pressure drop of the gas. This plant is usually used where easy availability of supervising members or technicians.

4.3 Floating Drum Plants

Floating drum plants contain a container for holding the moving gas and the digester. The holder stays float due to the fermentation slurry or due to a water jacket. The gas collects in the drum, resulting in the rising of the drum. If gas is taken away, it falls again. The drum is prevented from tilting by a guiding frame.

The advantages of these types of plants are: easy to operate due to their simple design and very few errors in construction. However, the disadvantages are being the high cost of construction of the floating drum, also steels parts have chance of corrosion, hence a shortage of lifespan. It also has a constant maintenance cost due to repeated painting.

Further, the anaerobic digesters again can be classified into (Appels et al. 2008):

(1) Standard rate (cold digester)—It is a very simple type digester which can be used for a lengthy period of digestion of 30–60 days. It has four stages (a) scum layer (b) a liquid layer (c) a region of digesting solid (d) a region of digested solid.
(2) Higher rate digester—It is a modified version of the generalized rate digester. In such digester, there is continuous feeding. The sludge is mixed and thickened. All the mixing creates a uniformity reducing the tank volume and casing a stable efficient process. There are heat exchangers included in this type of digester it is because of maintenance of constant temperature.
(3) Two-stage digester—In this type of digester a secondary digester is attached with the high rate digester. The purpose of the secondary digester is to store the digested solid. Sometimes the secondary and the primary digester both have heat exchangers and are of similar design to serve as a standby digester.
(4) Mesophilic and Thermophilic digestion—The high rate digesters are operated at a particular range of temperature. It is said to be a mesophilic digester if the temperature is around 30–38 °C. When the temperature is in the range of 50–57 °C, it is known as thermophilic.

5 Effect of Operational Parameters on Biogas Digester

A study on the effect of operational parameters on anaerobic digestion based biogas digester was being studied (Appels et al. 2008). In this study, pH value, temperature of the solid and the hydraulic retention time were considered for observation. Each bacteria function better at certain range of pH such as the methanogenic bacteria functions at a pH range of 6.5–7.2. The fermentative bacteria functions at 4.5–8.2. Acetic and butyric are produced at low pH. However, at high pH value such as 8, the propionic and acetic acid are produced.

Temperature affects the growth rate and the metabolism of the microorganism in the digester. It also affects the production of the acid (propionate and butyrate). The increase in temperature is very useful in the digester as it increases the rate of the reaction, kills pathogens, and increases the solubility of few organic compounds. However, too much increase in temperature can cause the production of ammonia which inhibits the functioning of microorganisms. Solid retention time (SRT) is the average stay time of activated-sludge solids in the system. The reduction in the SRT decreases the reaction. Retention time less than 5 days is not healthy for as proper digestion. For 5–8 days the volatile fatty acid (VFA) concentration is quite high. For 8–10 a proper digestion is obtained. Hence, SRT is a very important factor.

Various design parameters were taken into account during design of municipal solid waste based anaerobic digester (Hilkiah et al. 2008). The first parameter considered was temperature. The temperature had direct impacts on the decomposition rate and the amount of the gas produced. It was seen that higher temperature has a high impact on the digester. However, too much increase in temperature caused instability. Moreover, if the bacteria used were thermophilic then it is very sensitive to small change in temperature. Hence mesophilic bacterium is being proposed to use in practice. Researchers have recommended that a constant temperature should be kept inside the digester for optimum production. After temperature, pH is taken into consideration. The pH value of 6–8 is the best for continuing production. But during the long process, the pH gets unstable hence it was proposed that lime or sodium bicarbonate is to be used for increasing the pH. The carbon–nitrogen (C/N) ratio is another factor which affects the production of biogas. The carbon–nitrogen content should be in the ratio of 30:1 for any material. To increase the decomposition process, moisture should be present hence it plays an important role in the production of the biogas. For municipal solid waste (MSW), material is also an important factor for the biogas production. The MSW provide in the digester should be small in nature. Due to small size, the surface area increases, which increasing the decomposition for MSW because decomposition entirely takes place on the surface of the material. Finally, the last part which is taken into account is the mixing. It creates a uniform concentration, temperature, and other factors such as regaining of any valuable gases lost etc.

A serious monitoring of the biogas digester was done (Ward et al. 2011). The various concentrations of the gases such as H_2, CO_2, H_2S, CH_4 and N_2 were monitored. Figure 3 shows the results of monitoring of various gases of the digester.

Figure 4 illustrates a variation of CH_4 and H_2S concentration in µ-GC and MIMS for 33 days of operational time. Figure 5 shows the variation of dimethyl sulfide and methanethiol measured in MIMS during the operational time.

A review on household-based biogas plant was being presented by authors (Rajendran et al. 2012). The authors took an account of few parameters which affect the biogas production. The materials used in the digester plant had an important part

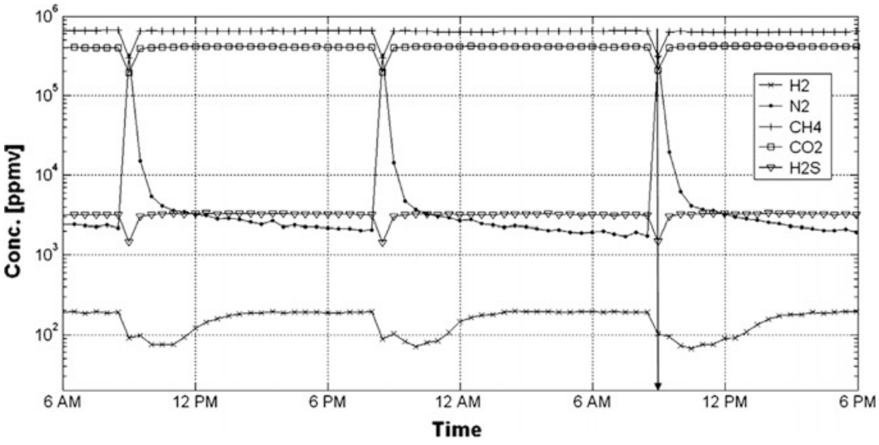

Fig. 3 Results of monitoring of the gases using μ-GC as a function of time. Ward et al. (2011)

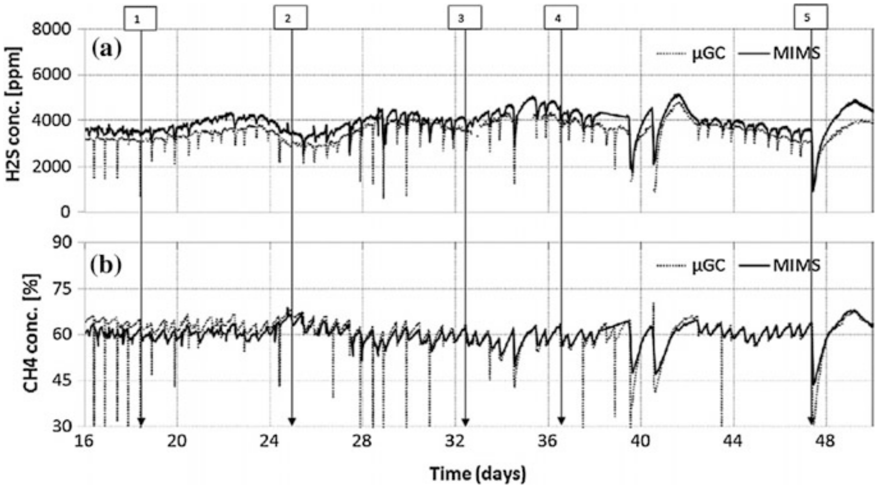

Fig. 4 Concentration of CH_4 and H_2S using μ-GC and MIMS for 33 days. Ward et al. (2011)

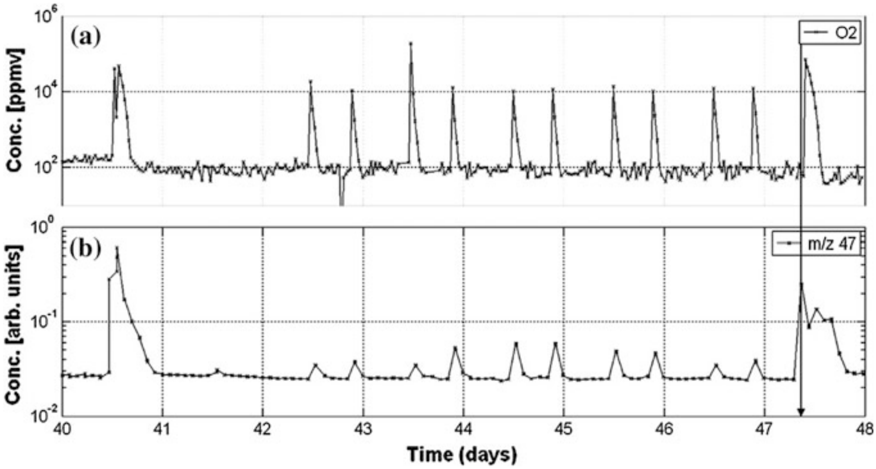

Fig. 5 Variation of dimethyl sulfide and methanethiol measured in MIMS during the operational time. Ward et al. (2011)

in the production of the biogas. Previously biogas digesters were made of stone and bricks but now with technological advancements, PVC and polyethylene are used which are light in weight and economic. The next important parameter to be considered is the temperature. High temperatures are useful for increase the production, but it is not applicable for all cases as with increasing temperature there is a decrease in production in some cases. The substrate selection primarily depends on the type of digesters used and its raw materials. The kitchen waste is a useful substrate as it contains a high amount of fat which increase the productivity of the biogas. Solid concentration and the material of the feedstock are also important parameters. The increase in solid concentration decreases the biogas production. The feedstock material C/N ratio and digestion time together affects the biogas production.

6 Productivity Enhancement of Biogas Digester

A study on the effects of the parameters and the substrates of a biogas digester in presence of sulfate-reducing bacteria was conducted (Moestedt et al. 2013). Study revealed that the temperature and the sulfate concentration significantly affected the productivity when there are any changes due to any of these two parameters.

An enhancement of biogas production using solid substrates is carried out using different technique (Sreekrishnan et al. 2004). The different techniques used for biogas production are:

(i) Use of additional materials to enhance the process of digestion.
(ii) Reusing of the slurry obtained and its filtrate.
(iii) Varying the working parameters such as the temperature, size of the particles, etc.
(iv) Use of films or biofilters.

Increase the production of the biogas, by adding various additives of the biological and chemical composition. At first, green biomass was used where the production rate increased in the range of 18–40%. On using the microbial strains, the production rate increased about 8.4–44%. The maximum production was obtained for inorganic additives which was around 54%. The recycling of slurry filtrate takes place. The slurry shows a 10% rise in obtained biogas. Any change in working parameters had drastic changes in the productivity of the biogas. For films and biofilters, various modifications are being made till now and the latest results show a 17% rise in the obtained biogas.

A study on the optimization of the biogas for anaerobic digestion was conducted in Zimbabwe (Jingura and Matengaifa 2009). The following techniques were adopted for the improvement of the biogas production.

(a) Anaerobic digestion of MSW—As MSW is produced in large quantities in Zimbabwe hence it is useful material.
(b) Anaerobic digestion of sewage sludge and wastewater—In Zimbabwe, the gases produced in the sewage plants are mostly lost. Hence in order to reduce the loss and to increase the power generation, this product should be used for the biogas production. This will lead to increase in overall production of the biogas in the country.
(c) Co-digestion—Co-digestions helps in the places where an adequate amount of resources are not available for the biogas production.
(d) Centralized anaerobic digestion—This is also a useful technology for improving the biogas production by decreasing the raw materials and enhancing the process.

7 Enhancement of Biogas Production

A test was conducted for a semi-continuously mixed tubular digester (Bouallagui et al. 2003). Fruits and vegetable waste was used for the preparation of biogas. There was a reduction in performance due to the change in concentration of the feed from 8–10%. The final conversion of the fruit and vegetable waste was 75% and methane content of 64% in the produced biogas.

An investigation of the digestion process from products based on fat, oil, and grease were conducted (Li et al. 2015). A two-stage thermophilic semi-continuous flow co-digestion system was used. Among the digesters, one of the two-stage co-digestion was made, using a pretreatment based on thermo-chemical process having pH 10 at 55 °C. Another two-stage digestion have no pretreatment process. Each of the two systems had a hydraulic retention time of 24 days. The result showed that the process involved pretreatment had a better yield than the second one which did not include any pretreatment.

Biogas productivity of cassava peels mixed with various types of livestock waste was compared (Adelekan and Bamgboye 2009). The livestock waste were poultry, piggery, cattle waste according to the input of 1:1, 2:1, 3:1, 4:1 by mass in anaerobic digesters. There was a significant influence of the mixing of the waste from the livestock with the tapioca peels. The obtained value had increased to 13.7, 12.3, 10.4, 9.0 L/kg-TS on mixing with poultry waste for the ratio of 1:1, 2:1, 3:1, 4:1. The yield on piggery waste had increased to 35.0, 26.5, 17.1, 9.3 L/kg-TS for the ratio of 1:1, 2:1, 3:1, 4:1. The yield on mixing cattle waste had increased to 21.3, 19.5, 15.8, 11.2 L/kg-TS for the ratio of 1:1, 2:1, 3:1, 4:1. Hence, the results show that the mixing the livestock waste in the ratio of 1:1 produced the maximum yield.

An experiment was conducted to increase biogas productivity by using *Brassica compestris* (mustard oil cake) in cattle dung digesters (Satyanarayan et al. 2008). The mustard oil cake was added to the digester in different ratios. The result showed a 12.2–13.08% increase which 30% mustard cake. Hence, there is a 63.44% increase in comparison to only cattle dung. The biogas production increased 13.38, 25.27, 39.16, 52.26, 63.44% with 10, 15, 20, 25, 30% of mustard cake respectively.

Neves et al. have developed the methods to increase the production of methane from industrial waste composed of 100% barley (2006). In the first process, the barley waste was treated with alkaline solution resulting in water formation pre-treatment before activated-sludge co-digestion process. The methane production was 224 L. The second process involved co-digestion with 40% barley waste and 60% kitchen waste. The result methane obtained was 363 L.

An enhancement process of digestion in anaerobic process of waste activated-sludge (WAS) using bio-cremation process was examined (Jih-Gaw et al. 1997). The WAS pretreated with NaOH and its examination occurred. There were 4 reactors A, B, C, D. A was given untreated WAS and total solid (1% TS). The other 3 reactors B, C and D were given WAS which was pretreated but of different percentage of TS with 20 meq/l NaOH and WAS (1% TS), 40 meq/l NaOH and WAS (1% TS), 20 meq/l NaOH with WAS (2% TS). The production of the B, C, and D reactors increased to 33, 30 and 163%.

8 Development of Biogas in Developed Countries

The development of biogas was mostly seen in the northern European countries like Sweden, Denmark, Germany, Austria, and Switzerland (Plöchl and Heiermann 2006). Initially, the idea of biogas plant was to clear the odor of, livestock waste and a supply of electricity to the farms. Later, the main idea of the biogas plant was to generate electricity. In Europe, the digester was made of concrete and steel. The digesters have insulation and heating system to control the temperature. Propellers are installed for the stirring of the materials.

The technology used was for wet anaerobic digestion, but recent developments have made in for dry anaerobic digestion. Also, the feedstock used in biogas plants was another factor. In countries like Germany and Austria, agricultural biogas plants only used agricultural waste as feedstock in the biogas plants. Some the materials of the feedstock are maize, sugar beet, barley, etc. Each crop has a different amount of yield for biogas.

The setting of biogas plants in countries like Denmark started during early 1970 (Raven and Gregersen 2007). The development and the usage of biogas had started during the 1970s. The first type of biogas plants was at farm scale levels. These plants were not constructed on technical knowledge hence the plants failed. This lead to another development which was the centralized biogas plants took place in the 1980s. After 1980 there was no new type of plants until the mid of 1990 when the centralized plants and the farm scale plants were improved in technology.

A case study conducted on the Dutch biogas plants (Geels and Raven 2006). The case study shows that previous biogas plants had a single usage but after 1990 the biogas plants were constructed with the idea of multiple usages such as (1) increasing the agricultural sustainability by reducing artificial fertilizers. (2) decrease the amount of methane emitted into the atmosphere. (3) good source of alternative energy. Many improvements were made during the mid of the 1990s. The learning are:

- Co-digestion can increase biogas production.
- New purification system can remove the hydrogen sulfide.
- Process manure was more homogenous and can be used for fertilizer application.
- Process manure was much more feasible for crops hence reduction in the artificial fertilizer.
- The manure which was processed had less affecting germs or pathogens and weed.
- The accumulation and usage of the methane reduced the methane quantity in the air reducing greenhouse effect.

Finally, two changes in government policy made the way for developing new projects for the next 10 years.

The countries like Ukraine and Poland technical aspects of biogas plants were studied (Chasnyk et al. 2015). The beginning of biogas plant in Poland was in 1928. Since then there were many technological changes. The latest biogas plants from 2011 to 2015 produced methane under mesophilic conditions. In 2014 the biogas plants produced 222, 856, 466-m^3 of biogas, 59.6 MW electric power and 61.26 MW of thermal power. In Ukraine, it all started in 1933. Now there exist ten landfill plants, six agricultural plants, and three plants of sewage treatment.

9 Development of Biogas in Developing Countries

In the developing countries, three types of biogas digesters are used (Plöchl and Heiermann 2006). They are Chinese fixed dome, Indian floating drum, and the tube digesters. The floating digesters are manufactured using steel and materials of concrete. The Chinese digester is made of local materials. The Tube digesters are made of polyethylene foils. The inlet and the outlet are made of porcelain. Even though their design is different, but all are based on the same idea. The feedstock enters through an inlet after mixing with the digester.

The tube shape digester, floating over digester, Chinese dome digester have many advantages such as: inexpensive, locally available, can be handled easily and less moving parts hence less prone to failure. China and India have a massive impact on domestic biogas technology (Bond and Templeton 2011). As per surveys, the working biogas plant in India are 40 to 81%. The floating drum plants have better working than the fixed dome biogas plants. The reasons for massive developments in the biogas technology were because of government support providing free servicing, maintenance and provids subsidies. Also, many other factors were involved as: an abundance of cattle manure and other materials for feedstock for the biogas plant. As per the survey in Bangladesh, only 3% biogas plants were properly functioning. 76% of the plants were defective and 21% were not functions. In rural China, only 19% of the biogas potential is used (Chen et al. 2010). In China, Luo Guo Rui type biogas digester was used. This is a hydraulic type biogas digester made of concrete and brick. After 2000 commercial household biogas digester came into action. These were made of glass reinforced plastic. These have several advantages over the previously biogas digesters such as low maintenance cost, less time in construction and a long period of operation. As per survey in Sri Lanka there survey in 1986 and 1996, only 303 and 369 plants were functioning out of 5000 (de Alwis 2002). This shows that there is not much development in the biogas area. In Pakistan, the reports show that presently there are 5357 biogas plants throughout the country. The estimated production biogas production is 12–16 million m^3 per day (Mirza et al. 2008). In Nepal, fixed dome digesters are used (Gautam et al. 2009). It was a modification of the Indian and the Chinese model. As per the survey, Nepal uses only 9% of its biogas potential (Akinbami et al. 2001).

10 Biogas Development in the Underdeveloped Countries

In the Sub-Saharan countries, very less development in the biogas technology. The reason for such low development is due to the lack of basic research and awareness (Mshandete and Parawira 2009).

Nigeria does not have much developments in the biogas gas technology, but the design and research activities were conducted. For instance, a plastic bio-digester plant was designed, constructed and tested (Ezekoye and Okeke 2006).

Various digester were designed based on different type of waste to be treated (Hilkiah et al. 2008). A covered lagoon digester is used for the treatment of liquid manures. The semi-solid digester was used for partly solid manure. Plug flow digesters are used for materials which have solid contents of 11–13%. Also, high solid digesters are being implemented for non-fluid and solid materials.

In Sudan, the biogas technology is very much used (Mshandete and Parawira 2009). It is because of Sudan is widely dependent on agriculture. Mainly anaerobic digesters are used for the biogas production. A suggestion was made to use water hyacinth as a feedstock material. In Tanzania, due to government involvement, there is a usages of biogas technology. In 1993 polythene tubular digesters were used which is continued till now. Since there is lack of research in this area there is no such development in the biogas production.

Another study of biogas use in Nigeria was conducted (Akinbami et al. 2001). The country has very less production of biogas due to the poor financial condition of the country. If proper steps are not taken then biogas will be another fuel for high-income groups. Proper planning is needed for entering biogas in the Nigerian energy market.

11 A Case Study on Biogas Digester

A horizontal continuous based digester was used for conducting experiments of 12″ ID PVC pipe having length 4, 5, 6 m (Budhijanto et al. 2012). Mathematical model was developed to obtain the rate of production.

11.1 Mechanism

The first stage of making biogas is the conversion of organic matter into carboxylic acids. After this, the carboxylic acids get converted into CH_4 or into CO. However, proper carbon dioxide and methane ratio are required. The digesters are designed to increase the amount of CH_4 and decrease the amount of CO_2. Now the organic matter, CH_4 and CO_2 are obtained at a rate of k_1, k_2, and k_3 respectively. These rates are entirely dependent on the concentration of the nutrients, temperature, pH, etc. Optimization of these properties leads to an increase in the production of methane. The mathematical equations used for the simulation are as follows:

The following equation is the mass balance equation for the digester:

$$Q.O_Y - Q.O_{Y+\Delta Y} - \mu_0 C \frac{1}{Z_{\mathrm{c/o}}} \Delta V_0 - p_{\mathrm{r}} C \frac{1}{Z_{\mathrm{p/o}}} \Delta V_0 \tag{1}$$

Here, Q = amount of feed flow by volume (m^3/day), O = organic content in the feed expressed as volatile solids (kg/m^3), μ_0 = specific rate of growth of bacteria (1/day), C = amount of microorganism of the basis of mass per unit volume (kg/m^3), $Z_{\mathrm{c/o}}$ = the amount of cell obtained per unit mass of bio-degradable materials consumed (kg cell/kg mass), V_0 = digester volume (m^3), p_{r} = Is a constant denoting the amount of products formed (1/day), $Z_{\mathrm{p/o}}$ = product obtained per unit mass of bio-degradable materials consumed (kg obtained/kg mass).

Equation (1) can be written as below

$$\frac{\mathrm{d}O}{\mathrm{d}y} = -\frac{k_1 O^n}{M_{\mathrm{s}}} \tag{2}$$

Equation (2) is an empirical equation, does not take into the consideration of microorganisms' population during the process and the mechanisms behind the conversion of the organic matter. Here, k_1 is a constant denoting the rate constants of O conversion to new cells and biogas (1/day), M_{s} is the rate of flow of mass at a linear rate of digester materials (m/s), and n is a constant denoting the order of a reaction of O consumption (dimensionless).

The expression for the amount of CO_2 and CH_4 formation is being represented by Eqs. (3) and (4).

$$\frac{\mathrm{dCH_4}}{\mathrm{d}t} = k_2 \mathrm{N}^{\mathrm{c1}} \tag{3}$$

$$\frac{\mathrm{dCO_2}}{\mathrm{d}t} = k_3 \mathrm{N}^{\mathrm{c2}} \tag{4}$$

Here, Eqs. (3) and (4) $\frac{\mathrm{dCO_2}}{\mathrm{d}t}$ is the rate of CO_2 formation (kmol/day). $\frac{\mathrm{dCH_4}}{\mathrm{d}t}$ is the rate of CH_4 (kmol/day). N is the volatile fatty acid concentrations. The c1 and c2 are the value of the constant representing the reactions of empirical order.

Equation (5) represents the selectivity

$$\frac{k_2}{k_3} \tag{5}$$

11.2 Experiment

The experiments were conducted on six digesters. The inlet was fed with slurry consisting of cattle manure mixed with water. It filled 80% of the digester by volume. The surface of the mixture did not have any holes to avoid the contact of air getting into the digester. The gas valve is open after this and was kept for 20 days which was the intermediate period since there was no input or output of the gas. A regular measurement was done for taking in account of the volume of the gas produced. A sample of the gas was taken to find the amount of methane present. At first, the gas obtained was mainly composed of carbon dioxide. The feed concentrations were varied for every 2 months. Again, after one month, after changing the feed concentration the methane content was obtained. The data obtained from the experiments had fitted in the mathematical model.

11.3 Results and Discussions

The results showed that the digester consumed good amount of organic matter. From the experimental data and the mathematical model, a simulation of the digester was conducted. The simulation results revealed that the amount of CH_4 and CO_2 obtained was less. 50% of the organic matters were digested initially. The biogas production was dependent on the various types of microorganism present in the manure. Hence, an increase the amount of manure would increase the microorganisms which increase in the production. Another simulation result showed that even with the increase in the feed there would be very fewer changes in the production rate. Hence, the alternative pathway was taken which was increasing the remaining time and also increasing the stability of digester. There was 30% increase in the CH_4 compared to the previous case. It was noticed that drastic decrease in the residence time after three times recycling the organic matter.

The rate constants k_1 is need to increase for increasing biogas production. However, the slight increase in k_1 will not affect the biogas production rate. The increase in k_1 can be done by increasing the amount of organic matter, but, too much increase in the organic matter would result in a drawback in a continuous digester. Therefore, to increase the production rate of a biogas digester a combination of increasing the rate constant and a method of recycling is to be done.

12 Overall Conclusion

Global increase in energy demand is leading to efficient management of energy. The continue rise in the LPG price and other fuel made it necessary substitute for cooking and other domestic purposes. In developing countries, implementation of biogas digester plants as a renewable source of energy has great potential. An inclusive review of the various designs, details of structure, and operational philosophy of the wide variety of biogas digesters designs have been described. Two major groups of biogas digester can be identified, viz., fixed dome and floating drum. The introduction of low-cost plastic drum type biogas digesters has made it very attractive for domestic application. The retention period is low and gas yield is also higher than the conventional types. Its portability is an added advantage. Some digester easy to construct and user-friendly that can be suitably employed at small as well as the large scale at rural domestic purposes. Scientifically designed biogas digesters are found to be more effective and controllable than the ordinary installation. It makes rural population independent from the dependency over fossil fuel/ electricity. Therefore, biogas digester is agreed to be suitable for remote rural village cooking lighting and other applications in most developing countries. Considerable research and field level design of the biogas digester has been done in all over the world. Mathematical equations for fixed and floating drum types of biogas digester are developed to design the optimal digester. As per observations, the size of biogas digester increases and the production cost decreases. The aim in the future is to decrease the production cost to a very affordable level. Hence, it is important to design, development, high-tech, and low-cost biogas digester.

References

Adelekan BA, Bamgboye AI (2009) Comparison of biogas productivity of cassava peels mixed in selected ratios with major livestock waste types. African J Agric Res 4(7):571–577

Akinbami J-F, Ilori M, Oyebisi T, Akinwumi I, Adeoti O (2001) Biogas energy use in Nigeria: current status, future prospects and policy implications. Renew Sustain Energy Rev 5(1): 97–112

Appels L, Baeyens J, Degrève J, Dewil R (2008) Principles and potential of the anaerobic digestion of waste-activated sludge. Prog Energy Combust Sci 34(6):755–781

Arsova L (2010) Anaerobic digestion of food waste: current status, problems and an alternative product. M.S. Degree dissertation, Department of earth and Environmental Engineering foundation of Engineering and Applied Science, Columbia University

Bailón Allegue L, Hinge J (2012) Biogas and bio-syngas upgrading. In: DTI report no. December, pp 1–97

Bansal AK, Kapoor S, Agrawal M (2013) The road to zero waste : anaerobic digestor. Int J Environ Sci 3(5):1390–1397

Beall J, Crankshaw O, Parnell S (2002) Victims, Villains and Fixers: the Urban environment and Johannesburg's poor. J South Afr Stud 26(4):5–11

Beam RG (2011) Enhanced biogas production through the optimization of the anaerobic, M.Sc. thesis

Bengelsdorf FR, Straub M, Dürre P (2013) Bacterial synthesis gas (syngas) fermentation. Environ Technol 34(13–14):1639–1651

Bertsch J, Müller V (2015) Bioenergetic constraints for conversion of syngas to biofuels in acetogenic bacteria. Biotechnol Biofuels 8(1):210

Bond T, Templeton MR (2011a) History and future of domestic biogas plants in the developing world. Energy Sustain Dev 15(4):347–354

Bond T, Templeton MR (2011) Energy for sustainable development history and future of domestic biogas plants in the developing world. Energ Sustain Dev Int Energy Initiative 15(4):347–354. https://doi.org/10.1016/j.esd.2011.09.003

Bouallagui H, Ben Cheikh R, Marouani L, Hamdi M (2003) Mesophilic biogas production from fruit and vegetable waste in a tubular digester. Bioresour Technol 86(1):85–89

Budhijanto W, Purnomo CW, Siregar NC (2012) Simplified mathematical model for quantitative analysis of biogas production rate in a continuous digester. Eng J 16(5):167–176

Chasnyk O, Sołowski G, Shkarupa O (2015) Historical, technical and economic aspects of biogas development: case of Poland and Ukraine. Renew Sustain Energy Rev 52:227–239

Chen Y, Yang G, Sweeney S, Feng Y (2010) Household biogas use in rural China: a study of opportunities and constraints. Renew Sustain Energy Rev 14(1):545–549

de Alwis A (2002) Biogas—a review of Sri Lanka's performance with a renewable energy technology. Energy Sustain Dev 6(1):30–37

Deublein D, Steinhauser A (2008) Biogas from waste and renewable resources. Choice Curr Rev Acad Libr 443

Eze IS et al (2011) Characterization and performance evaluation of 11 m^3 biogas plant constructed at National Center for Energy Research and Development. Cont J Renew Energy 2(1): 1–6. https://doi.org/10.1504/IJRET.2011.037978

Ezekoye Va, Okeke CE (2006) Design, construction, and performance evaluation of plastic biodigester and the storage of biogas. Pacific J Sci Technol 7(2):176–184

Gautam R, Baral S, Herat S (2009) Biogas as a sustainable energy source in Nepal: present status and future challenges. Renew Sustain Energy Rev 13:248–252

Geels F, Raven R (2006) Non-linearity and expectations in niche-development trajectories: ups and downs in dutch biogas development (1973–2003). Technol Anal Strateg Manag 18(3–4):375–392

Hilkiah IA, Ayotamuno MJ, Eze CL, Ogaji SOT, Probert SD (2008) Designs of anaerobic digesters for producing biogas from municipal solid-waste. Appl Energy 85(6):430–438

Igliński B, Buczkowski R, Iglińska A, Cichosz M, Piechota G, Kujawski W (2012) Agricultural biogas plants in Poland: investment process, economical and environmental aspects, biogas potential. Renew Sustain Energy Rev 16(7):4890–4900

Jih-Gaw L, Chang CN, Chang SC (1997) Enhancement of anaerobic digestion of waste activated sludge by alkaline solubilization. Bioresour Technol 62(3):85–90

Jingura RM, Matengaifa R (2009) Optimization of biogas production by anaerobic digestion for sustainable energy development in Zimbabwe. Renew Sustain Energy Reviews 13:1116–1120

Laramee J, Davis J (2013) Economic and environmental impacts of domestic bio-digesters: evidence from Arusha, Tanzania. Energy Sustain Dev 17(3):296–304

Li C, Champagne P, Anderson BC (2015) Enhanced biogas production from anaerobic co-digestion of municipal wastewater treatment sludge and fat, oil and grease (FOG) by a modified two-stage thermophilic digester system with selected thermo-chemical pre-treatment. Renew Energy 83:474–482

Martins das Neves LC, Converti A, Vessoni Penna TC (2009) Biogas production: new trends for alternative energy sources in rural and urban zones. Chem Eng Technol 32(8):1147–1153

Merlin Christy P, Gopinath LR, Divya D (2014) A review on anaerobic decomposition and enhancement of biogas production through enzymes and microorganisms. Renew Sustain Energy Rev 34:167–173

Mirza UK, Ahmad N, Majeed T (2008) An overview of biomass energy utilization in Pakistan. Renew Sustain Energy Rev 12(7):1988–1996

Moestedt J, Nilsson S, Schnürer A (2013) Bioresource technology the effect of substrate and operational parameters on the abundance of sulphate-reducing bacteria in industrial anaerobic biogas digesters. Bioresour Technol 132:327–332

Mshandete AM, Parawira W (2009) Biogas Technology Research in Selected Sub-Saharan African Countries—a Review. African J Biotechnol 8(2):116–125

Nayono SE, Winter J, Gallert C (2010) Anaerobic digestion of pressed off leachate from the organic fraction of municipal solid waste. Waste Manag 30(10):1828–1833

Ndiema CKW, Mpendazoe FM, Williams A (1998) Emission of pollutants from a biomass stove. Energy Convers Manag 39(13):1357–1367

Neves L, Ribeiro R, Oliveira R, Alves MM (2006) Enhancement of methane production from barley waste. Biomass Bioenergy 30(6):599–603

Ofoefule AU, Nwankwo JI, Ibeto CN (2010) Biogas production from paper waste and its blend with cow dung. Adv Appl Sci Res 1(2):1–8

Pandey PK, Soupir ML (2011) Escherichia coli inactivation kinetics in anaerobic digestion of dairy manure under moderate, mesophilic and thermophilic temperatures. AMB Express 1(1):18

Peris RS (2011) Biogas process simulation using aspen plus. Dep Chem Eng Biotechnol Environ Technol Syddansk Univ 1–88

Plöchl M, Heiermann M (2006) Biogas farming in Central and Northern Europe : a strategy for developing countries ? Agric Eng Int VIII(8):1–15

Purwono BSA, Suyanta, Rahbini (2013) Biogas digester as an alternative energy strategy in the marginal villages in Indonesia. Energy Proc 32:136–144

Rajendran K, Aslanzadeh S, Taherzadeh MJ (2012) Household biogas digesters—a review. Energies 5(8): 2911–2942. https://doi.org/10.3390/en5082911

Raven RPJM, Gregersen KH (2007) Biogas plants in Denmark: successes and setbacks. Renew Sustain Energy Rev 11(1):116–132

Sasse L (1988) Biogas plants. Dtsch. Zent. für Entwicklungstechnologien 1–66

Satyanarayan S, Murkute P, Ramakant (2008) Biogas production enhancement by Brassica compestries amendment in cattle dung digesters. Biomass Bioenergy 32(3):210–215

Satyanarayan S, Ramakant, Shivayogi (2010) Biogas production enhancement by soya sludge amendment in cattle dung digesters. Biomass Bioenergy 34(9):1278–1282

Singh KJ, Sooch SS (2004) Comparative study of economics of different models of family size biogas plants for state of Punjab, India. Energy Convers Manag 45(9–10):1329–1341

Sitorus B, Sukandar, Panjaitan SD (2013) Biogas recovery from anaerobic digestion process of mixed fruit–vegetable wastes. Energy Proc 32:176–182

Smith KR (1994) Health, energy, and greenhouse-gas impacts of biomass combustion in household stoves. Energy Sustain Dev 1(4):23–29

Sreekrishnan TR, Kohli S, Rana V (2004) Enhancement of biogas production from solid substrates using different techniques — a review. Bioresour Tech 95(1):1–10. https://doi.org/10.1016/j.biortech.2004.02.01

Sträuber H, Schröder M, Kleinsteuber S (2012) Metabolic and microbial community dynamics during the hydrolytic and acidogenic fermentation in a leach-bed process. Energy Sustain Soc 2(1):13

Tanskanen M (2016) World TMs largest science, technology & medicine. In: Amyloid–historical aspects smoothing, filter. Prediction—Estimation Past, Present Future

Vanegas C, Bartlett J (2012) Anaerobic digestion of laminaria digitata: the effect of temperature on biogas production and composition. Waste Biomass Valorization 4(3):509–515

Walekhwa PN, Mugisha J, Drake L (2009) Biogas energy from family-sized digesters in Uganda: critical factors and policy implications. Energy Policy 37(7):2754–2762

Ward A, Feilberg A, Adamsen APS, Poulsen AK (2011) Real time monitoring of a biogas digester with gas chromatography, near-infrared spectroscopy, and membrane-inlet mass. Bioresour Technol 102(5):4098–4103

Weiland P (2010) Biogas production: current state and perspectives. Appl Microbiol Biotechnol 85(4):849–860

Biofuels in Transport Sector

Renu Singh

Abstract In the developing nations, biofuels emerge as a best possible alternative fuel option. Energy obtained from biomass is an attractive source of energy due to several numbers of reasons such as it is a renewable source of energy and a large amount of biomass are available on the Earth's surface, it is cheap and may be utilized using environmentally friendly solutions. With the help of biochemical or thermochemical processes, raw materials or feedstocks can be converted into biofuels such as ethanol, methanol, biodiesel, bio-crude, and methane which can be used as transportation fuels. The energy use in the transport sector is mainly governed by fossil fuels. In order to reach sustainability targets, it is important to replace the use of fossil fuels by renewables.

Keywords Biomass · Biofuels · Fossil fuels · Transportation

1 Introduction

Biomass is defined as living or dead organisms or any byproducts of those organisms, plant, or animal. It can be utilized to produce renewable energy, biofuels, or thermal energy, which is used as transportation fuels. Utilization of biofuels in transportation instead of traditional fossil fuels (Oil, petroleum, and coal) helps in reducing the dependency on these traditional fuels; minimizes climate change impact; reduce the emissions coming from the transportation sector. In the developing nations, biofuels emerge as a best possible alternative fuel option. Biofuels are of the three types first, second and third generation. The first-generation biofuels mainly rule the market of biofuels and include ethanol production from rapeseed, oil palm, corn, and sugarcane. But with the advancement in technologies a number of improved second-generation biofuels are obtained from

---

R. Singh (✉)
Centre for Environmental Science and Climate Resilient Agriculture,
Indian Agricultural Research Institute, New Delhi 110012, India
e-mail: renu_icar@yahoo.com

A. Sharma et al. (eds.), *Low Carbon Energy Supply*, Green Energy and Technology,
https://doi.org/10.1007/978-981-10-7326-7_7

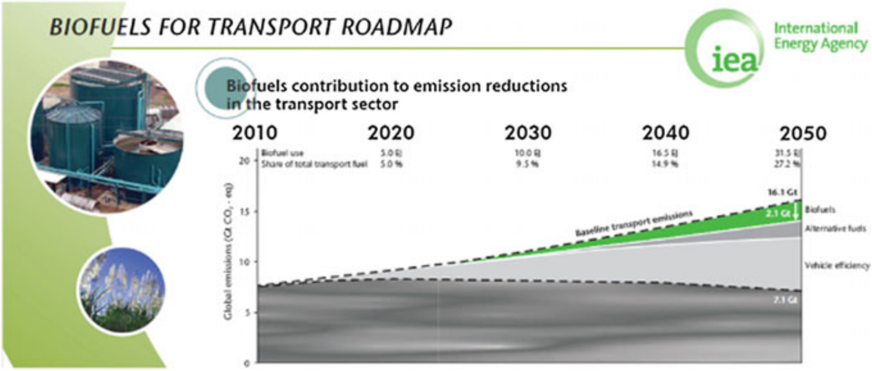

Fig. 1 Biofuels contribution to emission reductions in the transport sector (http://www.iea.org/publications/freepublications/publication/technology-roadmap-biofuels-for-transport.html)

nonfood feedstocks, e.g., algae, municipal waste, perennial grasses, and wood chips and several companies are doing a great work towards developing market for these second-generation biofuels. Second-generation biofuels mainly involve bio-butanol, cellulosic ethanol, methanol and a number of synthetic equivalents of the gasoline/diesel. First-generation biofuels have many limitations due to food-fuel issues, pressure on land use, higher resource consumption, high particulates emissions, and others. Besides having number of other benefits, e.g., energy security and reduced carbon footprint (Pant et al. 2011). IEA technology roadmap on the future use of biofuels stated that by 2050 biofuels will provide 27% of total transport fuel. I will be able to reduce around 2.1 Gt CO_2 emissions per year if production is sustainable (Fig. 1).

Algae can grow very fast, are able to produce many times higher biomass with compare to terrestrial trees and crops, require little land and other resources, producing more lipid and carbohydrate biofuels. Therefore, algal biofuels are very much beneficial and could be an alternative for first-generation biofuels (Singh et al. 2012). With the increase in population, demands for fossil fuels also increasing day by day so in order to replace these fossil fuels with biofuels, there is a requirement to research a range of sustainable biofuel resources and also, there is a demand to produce a large amount of electric vehicles which can run smoothly using these energy sources or necessary modifications can be done in vehicle's engine according to the biofuels, with these implementations, biofuels can be exploited in the transportation sector and thus, we get a clean, pollution free environment and also reduces over-exploitation of natural resources, i.e., coal and petroleum.

Energy obtained from biomass is an attractive source of energy due to several numbers of reasons such as it is a renewable source of energy and a large amount of biomass are available on the Earth's surface, it is cheap and can be utilized using more environment-friendly solutions. It provides the option for increased self-sufficiency locally as well as across the planet. With the help of biochemical or thermochemical processes, raw materials or feedstocks can be converted into biofuels such as ethanol, methanol, biodiesel, bio-crude, and methane which can be used as transportation fuels.

2 Ethanol

Different types of crop residues like wheat straw, rice straw, corn cob, corn stover, bagasse are used for the production of ethanol through the process of fermentation. This is an anaerobic biological process which requires sugars to be converted to alcohol through the action of microorganisms, e.g., yeast. Finally, the distilled form is used in the engines. Ethanol made from cellulosic biomass materials as an alternative of traditional feedstocks (starch crops) is called bioethanol (Singh et al. 2014). Ethanol may be used in its pure form, as a blend with gasoline, or as a fuel for fuel cells. In the United States each year, more than 1.5 billion gallons are supplementary to gasoline as an oxygenate agent, to improve vehicle performance and decrease air pollution.[1]

3 Methanol

Methanol is also an alcohol that can be utilized as a transport fuel and it is obtained through thermochemical process firstly, gasification of biomass is done to obtained hydrogen and carbon monoxide and then, these gases are retorted to produce methanol. It can be employed in its pure form, as a feedstock for the gasoline additive methyl tertiary butyl ether (MTBE), or as fuel for fuel cells. In the United States, approximately 1.2 billion gallons of methanol is produced annually, out of which 38% is consumed in the transport sector.

4 Biodiesel

One of the best alternatives that can be used as a diesel in vehicles is biodiesel. It is gained by the breakdown of plant oils obtained from plants or are transformed synthetically. The biodiesels have the same composition is just like mineral diesel. Biodiesel is a renewable fuel and a best diesel fuel substitute that can be derived chemically through combining any natural oil or fat with an alcohol (usually methanol). Blended biodiesel derives from lipids (fats) from both grains as well as from animals, chemically reacted with an alcohol. Biodiesel can be mixed with

---

[1] www.ott.doe.gov/biofuels.

petroleum products without processing, making it a practical transition fuel. Biodiesel can be utilized as a diesel additive and mainly consumed as a fuel additive in 20% blends (B20) with petroleum diesel in compression ignition (diesel) engines. Blending levels of biodiesel usually depend on the cost of the fuel and the desired benefits (www.ott.doe.gov/biofuels).

5 Bio-crude

Bio-crude is very similar to petroleum crude and can be derived from biomass through fast pyrolysis process. Bio-crude is produced by condensation of the biomass-derived oil vapors. It is further converted into fuel through the process of catalytic cracking (www.ott.doe.gov/biofuels).

6 Methane

Methane is an important component of compressed natural gas and it is one of the best alternative transportation fuels. In 2000, approximately 100 million gallons will be sold in the United States. It can be produced from biomass by a biochemical process called anaerobic digestion, in a blend with other gases (www.ott.doe.gov/biofuels).

7 Need for Environment

In any country, due to dependency on traditional fuels, the transportation sector is a main reason to a number of environmental difficulties. Harmful gases such as nitrogen dioxide, sulfur dioxide, carbon monoxide, carbon dioxide, etc., releases from the vehicles lead to a bad impact on plants, human beings, and environment. Increase in the emission of Greenhouse gases causes global warming which in turn causes climate change. In the present scenario, every nation is dealing with the issues related to the excessive exploitation of natural resources, pollution, and climate change. In the United States, one-third of CO_2 emission is only from the transportation sector (www.ott.doe.gov/biofuels). CO_2 is a major greenhouse gas which may lead to global climate change. Employment of biofuels in transportation sector not only offers substitutes to fossil fuels but also help in providing answers to many environmental difficulties. Biofuels are cheap, sustainable, and renewable and pollution free source of energy. Biofuels address global concern by mitigating carbon emissions as compared to fossil fuels. Biofuels on combustion emit reduced pollutants like, e.g., 99% reduction of SO_x, 20% of CO, 32% of HC, 59% of soot, 39% of particulate matter (Sams 1996), CO_2 (78%) (Srivastava et al. 2007) etc.

Application of biofuels for transport can help in minimizing CO_2 buildup meaningfully. Fossil fuels lead to the emission of CO_2, by displacing the use of fossil fuels, this emission can be avoided, and the CO_2 content of fossil fuels is allowed to remain in storage. Biofuels emit a very small amount of CO_2 which is further absorbed by the plants and trees that serve as feedstocks for biofuels and required CO_2 during the process of photosynthesis. Biofuels usage reduces public health risks and other environmental factors borne diseases. Bioethanol has been utilized very effectively as an oxygenate additive in gasoline so as to minimize emissions from vehicles. In the coming up years, as biofuels come to the forefront as substitutes for gasoline, we anticipate additional improvements in air quality; whether these fuels are used in internal combustion engines or in new clean automobile technologies such as fuel cells. Usage of biofuels also leads to the employment regeneration and improvement in the economy (especially rural/agriculture area that is prone to land degradation and natural calamities).

8 Transportation Sector Energy Consumption by Fuel

Today, the world mainly depends on petroleum and other fuels for the sources of transport energy, although their contributions in total transport energy turns downcast over the IEO (2016) projection period, from 96% in 2012 to 88% in 2040. Every nation mainly depends mainly on petroleum, coal, and oil in order to fulfill their transportation energy demands. A study depicted that liquid fuels consumption in transportation sector all over the world raises by 36 quadrillion Btu in the reference case forecast, with diesel (including biodiesel) presenting the largest increase (13 quadrillion Btu), jet fuel intake increasing by 10 quadrillion Btu, and motor gasoline (including ethanol blends) increasing by 9 quadrillion Btu (Fig. 2) (IEO 2016). Although, automobile gasoline is the principal transport fuel, its share

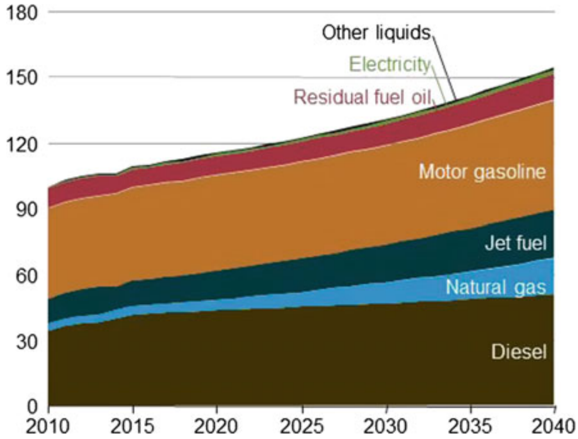

Fig. 2 World transportation sector delivered energy consumption by energy source 2010–2040 (quadrillion Btu) (IEO 2016)

of total transportation energy consumption reduces from 39% in 2012 to 33% in 2040. Diesel fuel is the second-largest transportation fuel, the total transport market share of diesel fuel (including biodiesel), turn down from 36 to 33% from 2012 to 2040 respectively and the jet fuel share increases from 12 to 14% in 2040. The natural gas consumption as a transportation fuel grows from 3% in 2012 to 11% in 2040. In 2012, pipelines reported for 66% of transportation sector natural gas use, light-duty automobiles 28%, and buses 4%. Due to the promising fuel economics, the share of natural gas used for transport types of travel other than pipelines are cumulative and the strong increase is found for the natural gas portion of total energy use by large trucks in the base case, from 1% in 2012 to 15% in 2040. It is expected in 2040 intake of natural gas will be 50% in the bus, as well as 17% freight rail, 7% light-duty vehicles and 6% domestic marine vessels respectively. For the world's transportation energy use, electricity is relatively an insignificant fuel, although it is essential in passenger rail transportation system and for this, its requirement remains high, about 40% of the total passenger rail energy consumption requirement is fulfilled through electricity in 2040. The electricity contribution of total light-duty automobile energy consumption grows to 1% in 2040 in the reference case; due to the increased sales of new plug-in electric automobiles enter the total light-duty stock (IEO 2016).

9 Transport Sector Energy Consumption by Type

The transport sector consists of both freight and passenger. The passenger modes involved light-duty trucks, airplanes, cars and buses, two- and three-wheel vehicles, and passenger trains. The freight modes, which are utilized in the movement of raw, intermediate, and finished goods to consumers, involved trucks (heavy-, medium-, and light-duty), marine vessels (international and domestic), rail, and pipelines. For all transportation modes, energy consumption rises from 2012 to 2040 world widely. For passenger travel modes, total energy consumption increases by an average of 1.4%/year, from 63 quadrillions Btu in 2012 to 94 quadrillion Btu in 2040 (Fig. 3) (IEO 2016). Light-duty vehicles depict the largest absolute increase (15 quadrillions Btu) from 2012 to 2040 among the passenger modes of travel but the slowest growth (1.0%/year) among all the transport modes. In the world, from 2012 to 2040, energy consumption for aircraft growths by a total of 10 quadrillion Btu, however, the combined energy use for buses, two- and three-wheel vehicles and rail grows by 6 quadrillions Btu (IEO 2016).

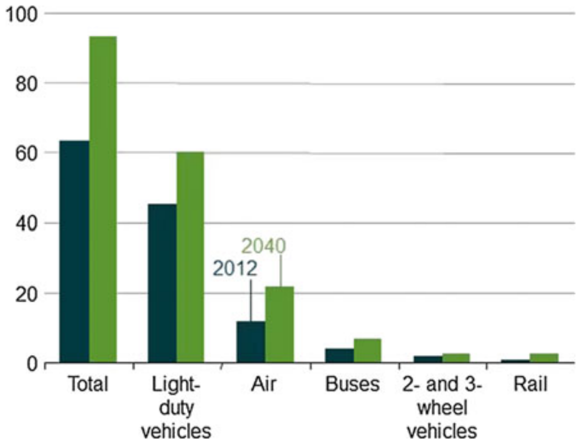

Fig. 3 World transportation sector energy consumption by passenger modes, 2012 and 2040 (IEO 2016)

10 Application of Biofuels in Transport Sector in Different Countries

Currently, the European Commission published a package for climate and energy in the period from 2020 to 2030 (COM (2014) 15 final), to supplement the current 2020 policy goals. The new framework endorses a global EU policy based on a 40% decrease in total greenhouse gas emissions in 2030 compared to 1990 and this is assisted up by the target to reach a 27% indicative share of renewables in the total energy mix. These stimulating goals help in improving the energy security and controlling the impact of Europe towards climate change. The transport sector is one of the critical element on which more emphasis is given in this new policy plan. The transport sector is mainly ruled by liquid fossil fuels and therefore, replacement of these fuels with renewable energy will significantly contribute in success the overarching energy and sustainability goals. Biofuels have played the utmost important role in the substitution of fossil fuels, accounting for 4% of total energy usages in transport by 2010, their contribution in transportation sector rises by each year. The need of essential investments with respect to the production of feedstock, processing, and distribution of biofuels, advancement in technologies and innovations has already done. Thus, the whole area has been developed and has been competently working for a several years.

China is also facing the challenges regarding how to decarbonize its transport area. Biofuels projects as one of the decarbonization choices and will reduce 0.43 Gt of CO_2 emissions in 2050 in the CM30 (Cumulative CO_2 emissions in 2010–2050 reduced by 30% scenario) and contribute to 35% of the total decrease (Zhang and Chen 2015). However, the growth of biofuels in China will still be examined by food safekeeping concern and facing the land readiness issues and the extent to which the biomass potential can be transformed into energy still involve more argumentation to be determined (Zhang and Chen 2015).

The government in Sweden had confirmed that the automobile fleet should be free of fossil fuels by 2030 while Swedish total emissions of GHGs should be zero by 2050 (Swedish Government 2008). Ong et al. (2012) described that there is steady need to adopt appropriate energy policy so as to balance energy demand and reduces emissions in Malaysia transportation sector. Kemausuor et al. (2015) reported the extent to which upcoming energy demands in Ghana that could fulfill by energy from biomass sources, through the creation of biogas, liquid biofuels, and electricity and an investigation was done based on the moderate and high use of bioenergy for transportation, electricity generation, and residential fuel. Tsita and Pilavachi (2013), examined next generation biomass-derived fuels for the transport sector ultimate that a stable, economically sound and environmentally friendly source of transport fuel can potentially be a mix of bio-synthetic natural gas and electricity from biomass burning.

11 Current Scenario in India

India has inadequate reserves of fossil fuels and relies on import oil in order to achieve its energy demands. In 2012, imports 75% of India’s oil demand is coming from import; it is expected that the import dependency will rise to 92% of demand in 2035 (IEA 2012). Out of total oil demand, about 50% is used up in the transport sector trailed by 18% in agriculture and 11% in the industry sector. In recent years, the economic growth rate of India has been improved; the commercial energy usages of the country have also been growing fast, keeping pace with its economic growth. Therefore, it is essential to reduce dependency on oil for minimizing its energy import bill, improving energy security and reducing greenhouse gas (GHG) emissions. Endorsing the use of biofuels in the transport sector is thus very significant for the sustainable growth of India.

In 2001, India started 5% ethanol blending (E5) trial program and formulated the National Mission on Biodiesel in 2003 to realize 20% biodiesel blends by 2011–2012 (Blanchard et al. 2015). This initiative differs from other nations’ in its choice of raw material for biofuel creation molasses for bioethanol and nonedible oil for biodiesel. There are numerous issues such as cyclicality of sugar, molasses, and ethanol production that resulted in a fuel ethanol program which suffered from unreliable making and supply. The preventive policies, availability of molasses, and cost hampered the fuel ethanol program. Inconsistent policies, availability of land, selection of nonnative crops, yield, and market value have been major obstructions for biodiesel implementation. However, a clear, reliable, and dedicated policy with long-term vision can endure India’s biofuel effort and this will ensure energy security, economic development, and success and ensure a higher quality of life for people.

There are a several challenges in the development of biofuels as a transport fuel in India as well as other parts of the world. The major market limitations explicit to biofuels can be reviewed by eight main market hurdles, which are economic barriers, technical barriers, trade barriers, infrastructure barriers, ethical barriers, knowledge barriers, political barriers, and conflict of interests (Blanchard et al. 2015). Economic barrier mostly deals with the production of biofuels which are still costly, beneficial externalities are not costed. Technical obstacles include quality of fuel which is not yet continuous and preservation expertise for certain biofuels are still in very primary stages (e.g., for synthetic biofuels). Trade hurdles involved that in the market, for some biofuels still, no quality criteria exists. Infrastructure, challenge the issues of the obligation of new or adapted infrastructures depending on the type of biofuels, especially the use of bio-hydrogen and bio-methane. Ethical barriers comprise a rivalry of biomass feedstock sources with the food supply. Knowledge barriers include that not only the general community but also decision makers and representatives are absent knowledge on biofuels. Political obstacles include that the governments continuing subsidy to kerosene promoting is the inefficient and occasionally illegal use of this fossil fuel through with the use of available technologies the target people could have been likewise or more benefitted with the use of biofuels but for political will and policy. Lastly, conflict of interest which includes that variance between "promoters" of first and second-generation biofuels may deteriorate the overall growth of biofuels (Blanchard et al. 2015).

12 Conclusion

Biomass can play a big and significant part in future sustainable energy resource for modern energy carriers as electricity and transport fuels. The introduction of biofuels from biomass is good because it is one of the very few choices for low CO_2 emission systems against (eventually) reasonable costs and it reductions or spreads fuel reliance. The justification for taking up main program for the production of biofuels for blending with gasoline and diesel originates from a variety of issues i.e., firstly, nonavailability of ready-to-use alternative to the petroleum-based fuels (gasoline/HSD/motor spirit); secondly, biofuels are environmentally superior fuels and policymakers should compel government for stringent emission norms and regulations and for a necessary usage of biofuels; thirdly global concern for climate change and ensuring energy security. There is a requirement that in planning the energy and transport strategies importance should be given on the contribution of all stakeholders, taking into account the connections with the economy, society, environment, and policy. Policy development procedure must be participating and complete to be accepted and promoted by all. For each country, a possible preparation should be done for the safeguard of natural resources and a sustainable development, without harmfully disturbing the next generations.

References

Blanchard R, Bhattacharya SC, Chowdhury M, Chowdhury B, Biswas K, Choudhury BK (2015) A review of biofuels in India: challenges and opportunities. 2015. In: World energy engineering congress 2015, Orlando, Florida, USA

IEA (2012) Understanding energy challenges in India—policies, issues and players. International Energy Agency, Paris, France

International Energy Outlook 2016 (IEO 2016) Report Number: DOE/EIA-0484(2016)

Kemausuor F, Nygaard I, Mackenzie G (2015) Prospects for bioenergy use in Ghana using long-range energy alternatives planning model. Energy 93:672–682

Ong HC, Mahlia TMI, Masjuki HH (2012) A review on energy pattern and policy for transportation sector in Malaysia. Renew Sustain Energ Rev 16:532–542

Pant D, Singh A, Bogaert GV, Diels L, Vanbroekhoven K (2011) An introduction to the life cycle assessment (LCA) of bioelectrochemical systems (BES) for sustainable energy and product generation: relevance and key aspects. Renew Sustain Energ Rev 15:1305–1313

Sams T (1996) Use of biofuels under real world engine operation. In: 2nd european motor biofuels forum, Graz, Austria, 225–231

Singh A, Pant D, Olsen SI, Nigam SP (2012) Key issues to consider in microalgae based biodiesel production. Energ Educ Sci Technol Part A 29:687–700

Singh R, Shukla A, Tiwari S, Srivastava M (2014) A review on delignification of lignocellulosic biomass for enhancement of ethanol production potential. Renew Sustain Energ Rev 32:713–728

Srivastava A, Biswas AK, Sanyal PB, Chakraborty A, Chakraborty R (2007) Environmental concerns of biodiesel use. In: National workshop on biofuels: production methodologies, utilization techniques and challenges ahead, March 22–23, 2007, MERADO-CSIR, Ludhiana

Swedish Government (2008) En sammanhållen klimat-och energipolitik – Proposition 2008/09:163 (A cohesive climate and energy policy—Government bill 2008/09:163). Government Offices Sweden, Stockholm (in Swedish)

Tsita KG, Pilavachi PA (2013) Evaluation of next generation biomass derived fuels for the transport sector. Energ Policy 62:443–455

Zhang H, Chen W (2015) The role of biofuels in China's transport sector in carbon mitigation scenarios. Energ Proc 75:2700–2705

Biodiesel: Sources, Production, Emissions, and Policies

Arun Kumar Sharma and Prashant Baredar

Abstract A major part of energy generated is being consumed by transport sector creating an imbalance in the atmosphere by releasing the emissions resulting in global warming which is the biggest threat to living beings and the environment. Therefore, it is importance and need of biodiesel as a replacement for diesel and other conventional fuels. The various sources of biodiesel production comprise of obtaining raw oil from the seeds and are converted to biodiesel through various techniques of transesterification that utilizes catalysts to increase the yield. The newly available techniques have been discussed with primarily focusing on the various catalysts that affect the yield keeping in view the policies related to curtail down the global warming.

Keywords Biodiesel · Oil · Sources · Extraction · Catalysts · Methods
New technologies · Policies

Abbreviations

AC	Air conditioned
AEOE	Aqueous enzymatic oil extraction
Al_2O_3	Aluminium oxide
ASTM	American Society for Testing and Materials
Ba	Barium
$BaCO_3$	Barium carbonate
BaO	Barium oxide
BP	Boiling point
BSFC	Brake specific fuel consumption
BTE	Brake thermal efficiency
C	Carbon

A. K. Sharma · P. Baredar (✉)
Energy Centre, Maulana Azad National Institute of Technology, Bhopal, India
e-mail: prashant.baredar@gmail.com

A. K. Sharma
e-mail: sharmaarunkumar@rediffmail.com

A. Sharma et al. (eds.), *Low Carbon Energy Supply*, Green Energy and Technology,
https://doi.org/10.1007/978-981-10-7326-7_8

°C	Degree centigrade
Ca	Calcium
CaO	Calcium oxide
$CaCO_3$	Calcium carbonate
$_1Ca_1Ce$	Calcium oxide–cerium oxide catalyst
CALB	Candida Antarctica lipase B
CeO_2	Cerium oxide
CH	Hydro carbon
CH_2	Methylene
CH_3ONa	Sodium methoxide
CH_3OK	Potassium methoxide
CI	Compression ignition
Conc.	Concentrated
COP	Conference of parties
CR	Conservative review
CSTR	Continuous flow stirred-tank reactor
CuO	Copper oxide
CO_2	Carbon dioxide
CSO	Central statistics office
Fig.	Figure
Hetero.	Heterogeneous
Homo.	Homogeneous
min	Minute
mol	Mole
MS	Motor spirit
MW	Microwave
nPAH	Nitrated polycyclic aromatic hydrocarbons
NaX	Faujasite zeolites
$NaOCH_3$	Sodium methoxide
NaOH	Sodium hydroxide
NBB	National biodiesel board
OH	Hydroxide
Pb	Lead
PFAD	Palm fatty acid distillate
PAH	Polycyclic aromatic hydrocarbons
rpm	Revolutions per minute
RCOO	Carboxylate
SCF	Supercritical fluid
SiO_2	Silicon dioxide
Sn	Tin
CV	Countervailing
CZO	Critical zone observatories
DG	Diesel generator
DI	Direct ignition

DMC	Data Monitoring Committee
E_a	Activation energy (kJ/mol)
EBB	European biodiesel board
EGT	Exhaust gas temperature
EN	European nation
ETS-10	Titanosilicate structure-10 zeolite
FFA	Free fatty acids
g	Grams
h	Hours
H^+	Anion
H^-	Cation
HC	Hydrodynamic cavitation
HCL	Hydro chloric acid
HF	Hydrogen fluoride
HPA	Hetropoly acid
H_3PO_4	Phosphoric acid
H_2SO_4	Sulfuric acid
kJ	Kilo Joules
$KOCH_3$	Potassium methoxide
KOH	Potassium hydroxide
La_2O_3	Lanthanum oxide
MAE	Microwave-assisted extraction
Mg	Magnesium
$MgCO_3$	Magnesium carbonate
MgO	Magnesium oxide
MG	Motor generator
Sr	Strontium
$SrCO_3$	Strontium carbonate
SrO	Strontium oxide
SVO	Sraight vegetable oil
t	Time
TAGs	Triacylglycerol
TG	1-hexadecanoyl-2,3-di-(9Z-octadecenoyl)-sn-glycerol
TDI	Turbocharged direct injection
UC	Ultrasonic cavitation
UHC	United health care
WC	World Council
WCO	Waste cooking oil
w/w	Weight per weight
Zn	Zinc
ZnO	Zinc oxide
ZSM-5	Zeolite socony mobil–5

1 Introduction

The energy plays an important role and its demand is increasing for the fulfillment of the basic needs and sustainment of life, almost at 1.8% since 2011, in developing nations as compared to developed country (World Energy Outlook 2017). Energy is being consumed either in the form of electricity and fuel and for cooking and transport. The transport industry alone is accounted for 25% consumption (EASAC 2012) (Fig. 1).

In the rapidly developing countries like China and India, the demand for energy is growing rapidly (Darzins et al. 2010). The new millennium has set up the challenge by generating biofuel for developed as well as developing nations to solve the problem of global warming and generating new opportunities for the peoples to meet up the demand of fossil fuel (supplied by limited countries) (ABN 2010; Tadele et al. 2013). The mixing of available biodiesel, liquid biofuels, and ethanol to existing fossil fuels is being done as a renewable fuel, with United States and Brazil being the leader in producing about nearly 80% (Miguel et al. 2010). Global energy demand in transport accounts for about 28% of overall energy consumption and emitting 23% of related greenhouse gases.

The impact on environment of a locality depends upon social, cultural, topographic, political, and economic issues. All of these factors decide the energy supplied and energy consumed. At present, energy production is quite easy but more emphasis is being laid on its conservation and proper utilization as the energy required produces an adverse impact on climate resulting in global warming. This global warming is the biggest threat as it causes the sea level to rise due to melting of ice from glaciers. Keeping all these views in mind, most of the governments are making policies so as to protect the environment from global warming. These targets are being monitored on regular basis.

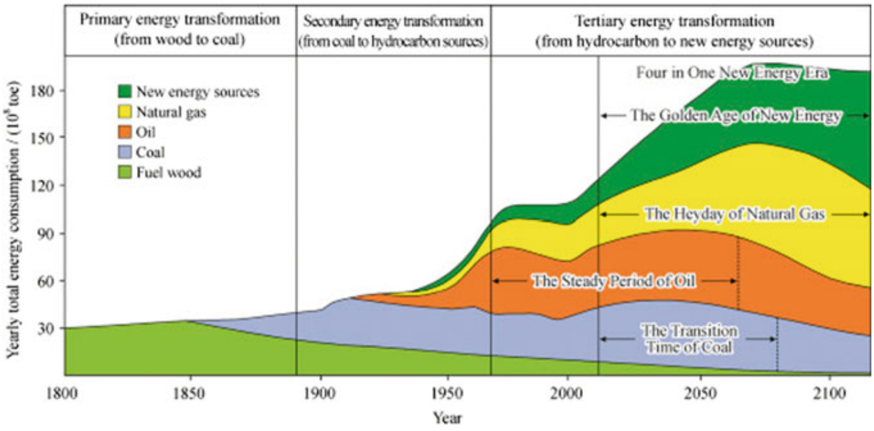

Fig. 1 Trends and forecasts of global energy consumption (Zou et al. 2016)

The transport sector is responsible up to a greater extent by emitting carbon dioxide (CO_2), carbon monoxide (CO), NO_x, CH_4, C_6F_6, and heat. As a result, the use of renewable fuels is being promoted such as biofuels, biodiesel, etc.

2 Biodiesel

The biodiesel is obtained from edible oil, nonedible oil, and waste cooking oil. The process used is centrifugation or transesterification. The mono-alkyl esters derived from lipid feedstocks such as vegetable oils or animal fats are termed as biodiesel (Marchetti 2010).

The triglycerides are the esters of fatty acid and glycerol consists of different fatty acids that influence both chemical and physical properties of plant oils and animal fats along with the quality of biodiesel. The saturated (carbon–carbon single bond) and unsaturated (carbon–carbon single bond or more) are the kinds of fatty acids. The most common fatty acids found in the lipid feedstocks are linoleic, palmitic, stearic, oleic, and linolenic acid. Various plant oils include myristic, arachidic, palmitoleic, and erucic acid. They also contain phospholipids, carotenes, tocopherols, sulfur compounds, and water (Marchetti 2012; Ong et al. 2013). Figure 2 shows the categorization of variously available fuels.

3 Extraction of Oil

Consistent performance and high oil yield were the criteria for using chemical oil extraction was used (Bhuiya et al. 2016). Various Extraction methods are shown in Fig. 3.

3.1 Chemical Methods

3.1.1 Solvent Extraction

Leaching is a solvent extraction process, *n*-hexane method yields are high, and uses liquid solvent for extracting constituent from solid mass. The type of liquid, particle size, agitation of solvent, temperature, and particle size affects the rate of extraction. The small particle size is preferred for greater contact area between liquid and solid. The solvent extraction from the seeds *Jatropha curcas* and *Pongamia pinnata* using *n*-hexane (viscosity is low) can produce up to 50 t of biodiesel per day (Bhuiya et al. 2016). The preparatory of seed for biodiesel is shown in Fig. 4 and the transesterification process is shown in Fig. 5.

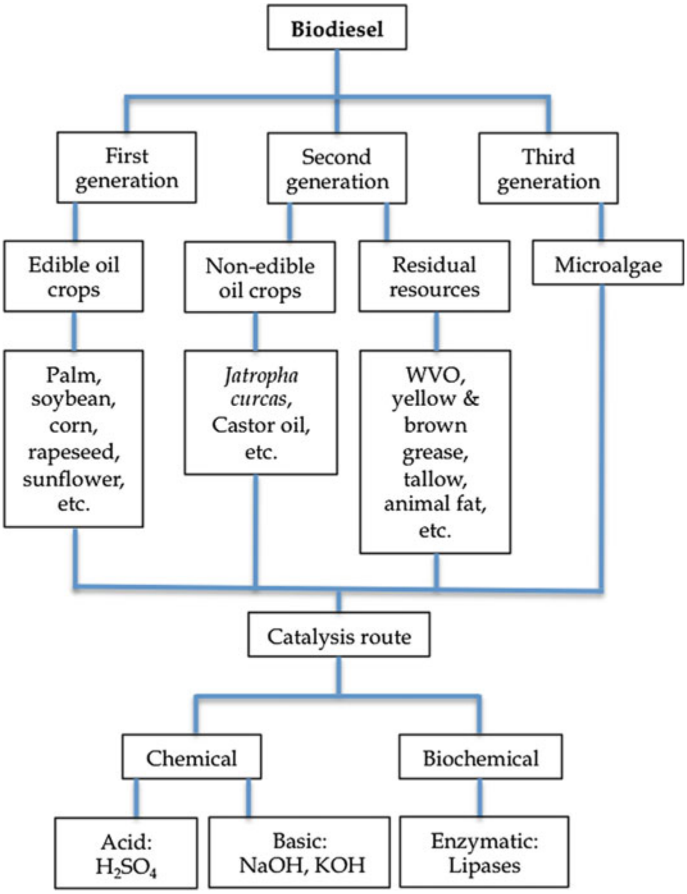

Fig. 2 Classification of biodiesel and catalysis routes for its production (Montero et al. 2015)

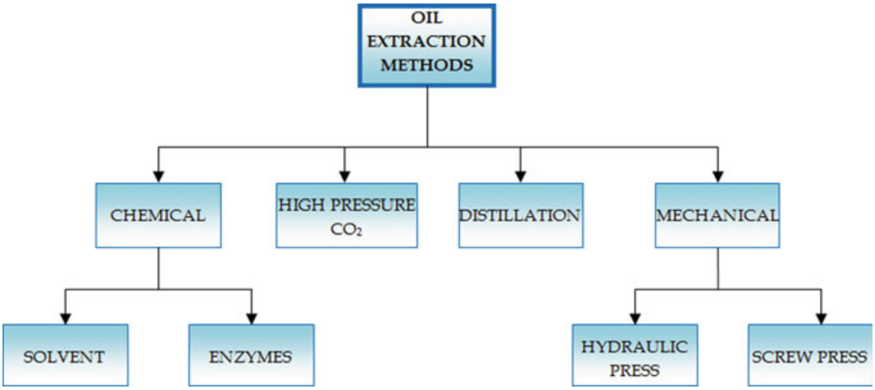

Fig. 3 Oil extraction methods (Stefan et al. 2013)

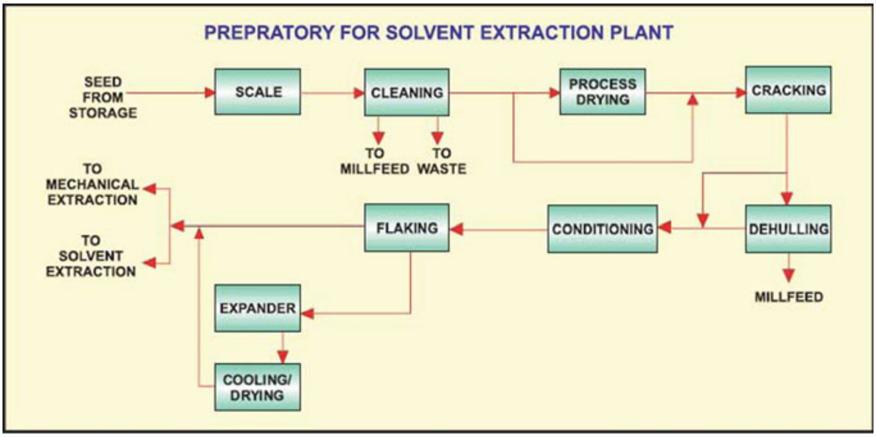

Fig. 4 Preparatory for solvent extraction (Spectec Techno Projects 2010)

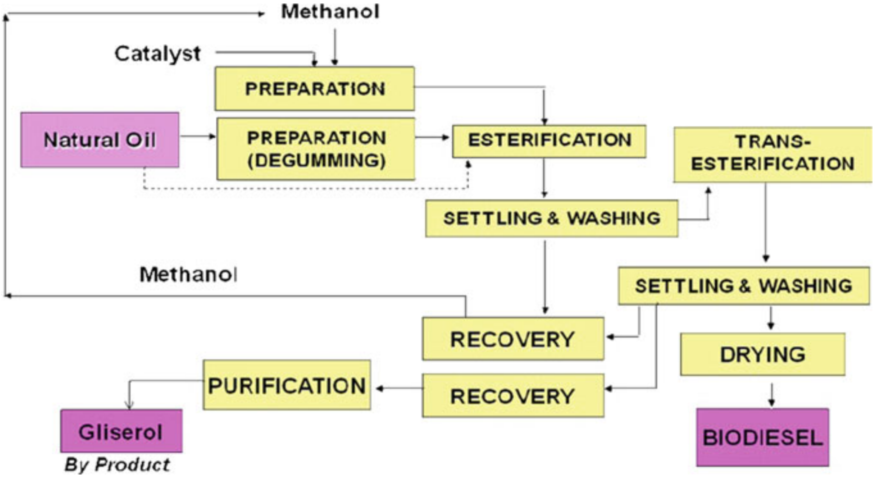

Fig. 5 Generation of biodiesel (Paryanto et al. 2017)

3.1.2 Enzymatic Oil Extraction

Although the time consumed being high in aqueous enzymatic oil extraction (AEOE), from plant, method is being used as it is eco-friendly without producing volatile organic compound and reduces the problems of solvent extraction technique (Bhuiya et al. 2016).

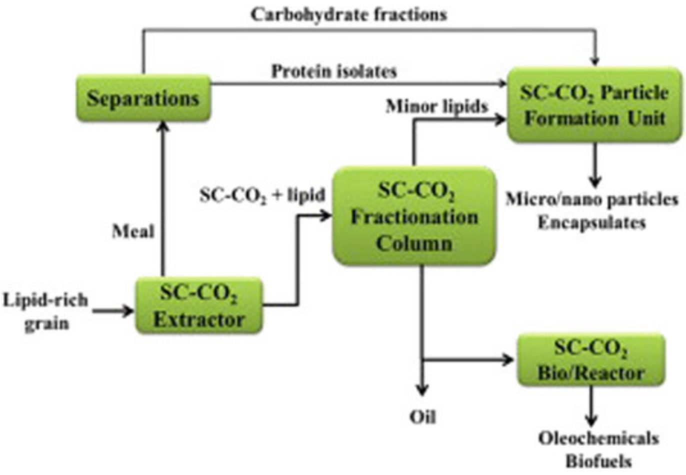

Fig. 6 Supercritical (using CO_2) for biodiesel extraction (Temelli and Ciftci 2015)

3.2 High Pressure CO_2

The supercritical-fluid (SCF) extraction is a process in which fluid is considered supercritical when it presents diffusivity similar to gas and density comparable to liquids. The results showed that the oil yields were 38.8% to solvent extraction, 35.3% for the supercritical extraction, and 25.5% for expelling. In terms of extracting the components omega-6-fatty acid and omega-3-fatty acid, supercritical extraction was more efficient than solvent and expelling extractions. The chemical composition of oil obtained from expelling is similar to that obtained by supercritical extraction, although the yield was lower. The quality of oil was lower in terms of its acid value and peroxide values using extraction with hexane but resulted higher in yield and presenting a lower concentration of omega fatty acids (Pradhan et al. 2010). Figure 6 shows the supercritical process of biodiesel extraction using CO_2.

3.3 Distillation

The design of a continuous reactive distillation process for biodiesel production comparing the homogeneous and heterogeneous catalyst was prepared. Sodium hydroxide (the homogeneous catalyst) and magnesium methoxide (the heterogeneous catalyst) are used for the transesterification of triglycerides with methanol into the reactive distillation column. The conclusions from these simulations were that the reactive distillation process with the heterogeneous catalyst offers advantages over the conventional process because it could eliminate the requirement of postprocessing separation and purification at cost-effective column design and operating conditions. Despite these relevant results, a pure vegetable oil is assumed to perform the simulations and a waste vegetable oil could not be managed. In distillation process, extraction of oil depends upon sensitivity, volatility and water solubility (Boon-Anuwat et al. 2015).

3.4 Mechanical Press

The mechanical presses, manual ram press, or engine drive screw press are capable of extracting oil within the range of 60–80% because seeds are subjected to repeated extractions through the expeller. The extracted oil is subjected to further treatment of filtering process and degumming. The yield can be increased by cooking of seeds and then pressed up to 89% after single press and 91% after dual press depending upon the design of the mechanical press (Bhuiya et al. 2016).

3.4.1 Hydraulic Press

Figure 7 shows a labeled diagram of hydraulic press and in hydraulic pressing, there are three stages:

- Initial stage
- Dynamic stage
- Final stage (Mrema and McNulty 1985; Owolarafe et al. 2008).

3.4.2 Screw Press

The food products use raw vegetable oil (Soybean oil, corn oil, sunflower oil, canola oil, peanut oil, olive oil, and safflower oil, etc.), either as food product or an industrial product for dressing, pan frying, and deep frying. These are obtained from screw press as shown in Fig. 8.

The screw press produces oil and meal (residual left after oil extraction). The oil to meal ratio varies from seed to seed. The presses are categorized as per the seeds processed per hour (Schaufler and Schaufler 2013).

3.5 Sources of Biodiesel Production

There are numerous sources of production of biodiesel. They are categorized under three categories, edible oil, nonedible oil, and other oils and are listed in Table 1.

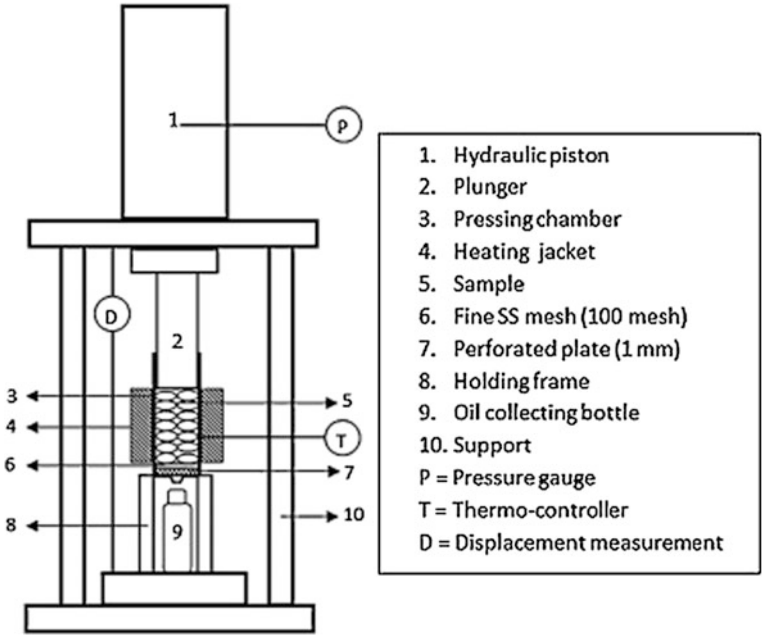

Fig. 7 Hydraulic press (Subroto et al. 2015)

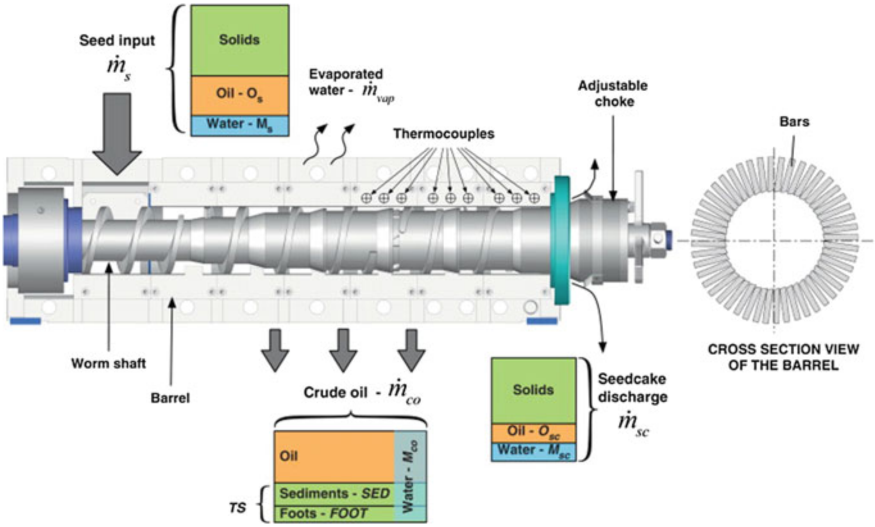

Fig. 8 Expeller press (Chapuis et al. 2014)

Table 1 Oil sources for biodiesel production (Verma and Sharma 2016)

Oils	Edible oils	Nonedible oil	Other oils
Sources	Cottonseed, Coconut, Sunflower, Canola, Soybean, Castor, Mustard, Peanut, Palm, Rapeseed	Jatropha, Karanja (Pongamia), Mahua, Neem, Eucalyptus, Linseed, Rubber seed, Polanga, Yellow oleander	Microalgae, Spirulina platensis algae, Waste cooking, Animal fats, Beef tallow, Poultry fat, Fish, Chicken fat, Chlorella protothecoides microalgae

3.6 Various Parameters Used for Biodiesel Production

Various parameters are shown in Table 2.

4 Biodiesel Production

Biodiesel is produced by centrifugation or transesterification process. In which methanol is added before the base catalyst. Methanol is mixed with starting oil stirring and heating. After this heating, the mixture is being added by catalyst such as NaOH, KOH, and H_2SO_4 (Priambodo et al. 2015).

4.1 Straight Vegetable Oil (Nonedible Oil)

Straight vegetable is obtained from plants that are inconsumable by humans. The oil is extracted from different kernels of seeds of nonedible crops by the processes discussed above. The various sources for biodiesel production from nonedible oils are Jatropha (*Jatropha curcas*), Karanjaorhongeor Korochseed (*Pongamia pinnata* or Pongamiaglabra), *Aleurites moluccana*, tobacco seed (*Nicotiana tabacum*), Pachiraglabra, desert date (*Balanites aegyptiaca*), Nagchampa (*Calophylluminophyllum*), rubber tree (*Hevea brasiliensis*), Jojoba (*Simmondsia chinensis*), *Croton megalocarpus*, rice bran, sea mango (*Cerbara odollam*), *Terminalia belerica*, Neem (*Azadirachta indica*), Mahua (*Madhuca indica* and *Madhuca longifolia*), soapnut (*Sapindus mukorossi*), *Sterculia feotida*, Chinese tallow (Sapium sebiferum Roxb.), silk-cotton tree (*Ceiba pentandra*), Babassu tree, *Euphorbia tirucalli*, and microalgae (Bhuiya et al. 2016).

Table 2 Variation of parameters in production of biodiesel

S. No.	Variety of oil	Catalyst used transesterification	Concentration and catalyst	Temp. at stirring (°C)	Stirring speed (RPM)	Duration (min)	Output (%)	Source
1	Soybean oil	Homo. base	$KOCH_3$	30–60	400	5.8–26.5	–	Tubino et al. (2014)
		Hetero. catalyst	6% CaFeAl	60	270	60	90	Lu et al. (2015)
2	WCO	Homo. (acid and base)	1% H_2SO_4	65	400	180	21.5	Jain et al. (2010)
			1% NaOH	50	400	180	21.5	
		Hetero.	10% Hetero poly acid	65	–	8400	88.6	Talebian-Kiakalaieh et al. (2013)
			–	255	–	45	97.6	Caldas et al. (2016)
		Hetero. catalyst	12% CZO	55	–	50	97.9	Baskar and Aishwarya (2016)
3	Jatropha oil	Homo. acid and base	1% H_2SO_4	65	400	180	21.2	Jain et al. (2010)
				50	400	180	90.1	
4	Linseed oil	Homo. base	0.5–1.0% NaOH	50	750	180	88–96	Kumar et al. (2013)
5	Mustard oil	Homo. base	KOH	40–60	600	30	–	Issariyakul et al. (2012)
6	Spirulina plagtensis alage		60	55	450	90	75	Nautiyal et al. (2014)
7	Canola oil	Homo. base	0.2–1.2% KOH	30–70	100–600	25–75	–	Likozar and Levec (2014b)
8	Sunflower oil	Hetero.	0.2–1.2% CaO	60–120	–	90–330	91	Vujicic et al. (2010)
		Homo. base	–	23–60	400	–	99	Reyero et al. (2015)
9	Karanja oil (Pongamia)	Homo. base	9% KOH	60–80	–	480	97.2	Rathore et al. (2015)
			1–2% KOH	30–60	–	120	64.11–98.8	Karmee et al. (2004)
			1.43% KOH	56.5	–	81.43	98.4	Dwivedi and Sharma (2015)

(continued)

Table 2 (continued)

S. No.	Variety of oil	Catalyst used transesterification	Concentration and catalyst	Temp. at stirring (°C)	Stirring speed (RPM)	Duration (min)	Output (%)	Source
10	Jatropha oil	Homo. base	9% KOH	60–80	–	480	96.8	Rathore et al. (2015)
11	Waste frying oil		1–4%	50–65	–	300–480	87.28	Birla et al. (2012)
12	Palm oil	Homo. base	KOH	40–60	600	30	–	Issariyakul et al. (2012)
			1% KOH	60	600	60	88	Shahbazi et al. (2012)
			1% NaOH	60	600	60	93	Shahbazi et al. (2012)
			8.5% KOH	65–75	–	480	96.2	Zhang et al. (2010)
			0.4% KOH	70–110	–	–	98	Yunus et al. (2004)
			1% KOH	60	–	90	–	Darnoko et al. (2000)
		Supercritical	–	200–400	–	0.5–20	–	Song et al. (2012)
13	Microalgae oil	Supercritical		270–350	–	10–50	90.8 For methanol 87.8 for ethanol	Nan et al. (2015)
14	Rice bran oil	Homo. base	0.5, 0.75, 1, 1.25% NaOH	55	–	60	35–99%	Sinha et al. (2008)
15	WCO	Homo. base	1% NaOH	60	–	120	95	Rabu et al. (2013)
16	Used olive oil	homo. base	1.26% KOH	10–50	1100	60	94	Dorado et al. (2004)
17	Rapeseed oil	Supercritical	–	200–500	–	–	95	Kusdiana and Saka (2001)
		Homo. base catalyzed with cosolvent	0.7% KOH	30	700	120	97–98	Encinar et al. (2016)

(continued)

Table 2 (continued)

S. No.	Variety of oil	Catalyst used transesterification	Concentration and catalyst	Temp. at stirring (°C)	Stirring speed (RPM)	Duration (min)	Output (%)	Source
18	Peanut oil	Supercritical	–	250–310	500	30–360	>90	Cheng et al. (2008)
19	Waste frying oil	Hetero. base	3% CaO	50	–	180	>89	Nair et al. (2012)
20	Castor oil	Homo. base	0.25–0.50% $NaOCH_3$ NaOH, KOH, $KOCH_3$	25–80	250–600	120	68.3–87.30	Ramezani et al. (2010)
21	Canola oil	Homo. base	0.5% KOH	45	–	–	–	Clark et al. (2013)
22	Used frying oil	Homo. base	0.55% KOH	60–100	–	120	–	Berrios et al. (2010)
23	Neem oil	Hetero. catalyst	10% CZO	55	–	60	97.18	Baskar and Aiswarya (2016)
24	Palm kernel oil (waste plum stores)	Homo. acid	2% H_2SO_4	45	–	60	–	Kostić et al. (2016)
		Hetero. base	5% CaO	60		180	98.2	
25	Waste lard	Ultrasonic assisted enzymatic	4–6 wt% enzyme (wt % of fat)	50	–	20	96.8	Adewale et al. (2016)
26	*Silybum marianum* L. Seed	Carbon acid (esterifications)	6.0% w/w sulfonated carbonic acid catalyst	68	–	180		Fadhil et al. (2016)
		Homo. base		60	600	75	96.98	

4.2 Edible Oil

Refined edible oils with less than 1 wt% free fatty acids (FFA) are mainly used as feedstocks for industrial biodiesel production and the feedstock price is one of the important factors affecting fuel production. The by-products, such as soapstock, acid oils, and deodorized distillates obtained during the refining of edible oils have been suggested as alternative and cheaper feedstocks for biodiesel The main components of acid oils are FFA, the remaining comprise of triglycerides, and hence the oils are almost solid at room temperature owing to the higher melting points of FFA (Kitakawa et al. 2015).

4.3 Waste Vegetable Oil

Mostly, the biodiesel is not in practice as the raw material is not continuous, the search is on for substitutes with low prices and continuous. In case if waste vegetable oil/ waste cooking oil are released in the running water or sewage water, it can kill the useful bacteria and the fisheries. Figure 9 shows extraction of biodiesel obtained from waste vegetable oil. This utilization of waste cooking oils instead of virgin oils for the production of biodiesel can solve the problems mentioned above which will be cheaper (Nurfitri et al. 2013). Some of the WCO is used in soap preparation, but mostly is illegally dumped into landfills and rivers. The cost of waste frying oil is estimated as half the price of virgin oil (Encinar et al. 2005). The cost of production is reduced using these wastes as a reactant for biodiesel synthesis (Canakci and Gerpen 2001). The biofuels are biogenic and renewable and thus help in maintaining greenhouse gases along with the reduction of CO_2 using WCO as a biodiesel (Chhetri et al. 2008). Figure 9 shows the extraction of biodiesel obtained from waste vegetable oil.

4.4 Algae

The comparative evaluation of heterogeneous tungstated zirconia catalyst has yielded 94.58% conversion and less conversion efficiency for synthesis of microalgal biodiesel. The study revealed that heterogeneous catalyst the advantage of higher conversion than enzyme catalyst and lower reaction time, reusability and low methanol requirement over the homogeneous catalyst. The process of extraction of biodiesel from algae is shown in Fig. 10. The fuel properties of microalgal biodiesel are in accordance with the specifications set by ASTM 6751 and EN 14214 for standard biodiesel with tungstated zirconia as a heterogeneous catalyst (Guldhe et al. 2017).

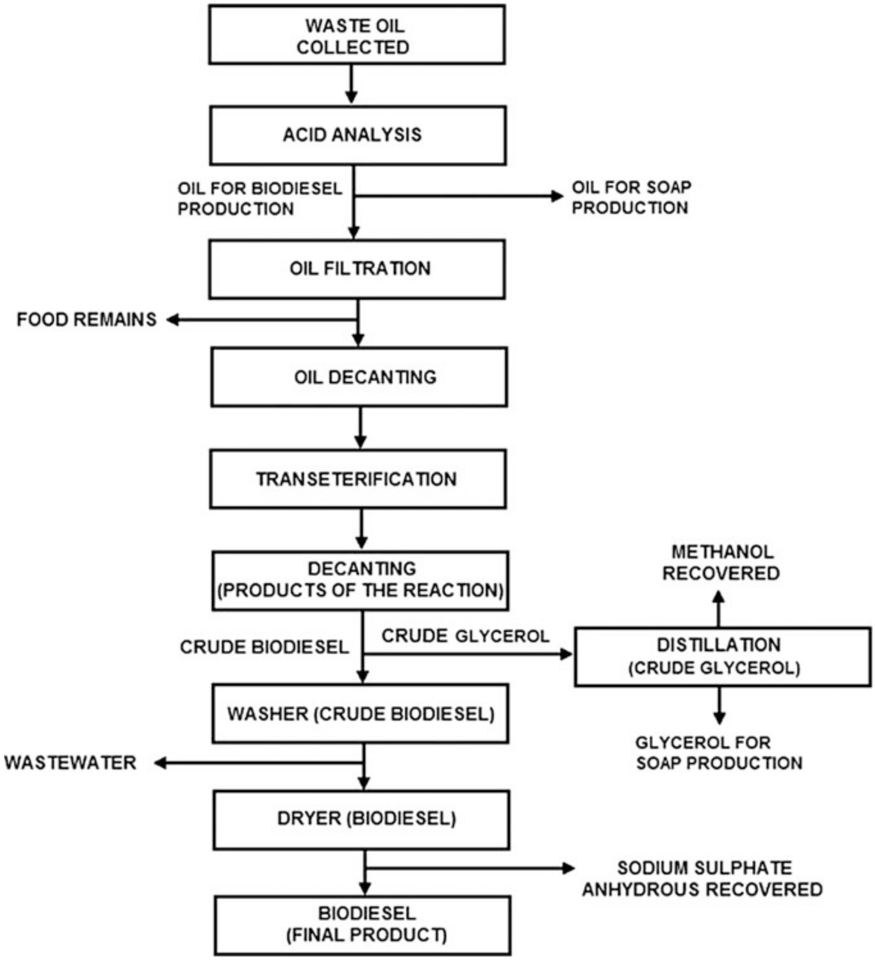

Fig. 9 Biodiesel obtained from waste vegetable oil (Moecke et al. 2016)

The transesterification of edible vegetable oils and animal fats using homogeneous acids is considered unsustainable by industries, food versus fuel competition, environmental challenges and economics for feedstocks, and catalyst systems. Figure 10 shows flowchart for the production of biodiesel from micro- and macroalgae.

The algae species capable of producing high-grade biodiesel abundant and can be cultivated with limited environmental challenges and are comparable to those of regular edible crops. Algae can be grown in salty environments and is known for CO_2 consumption during their growth period. Zeolite catalysts must possess desirable porosity and acidity/basicity properties. Avoid pore blockage while

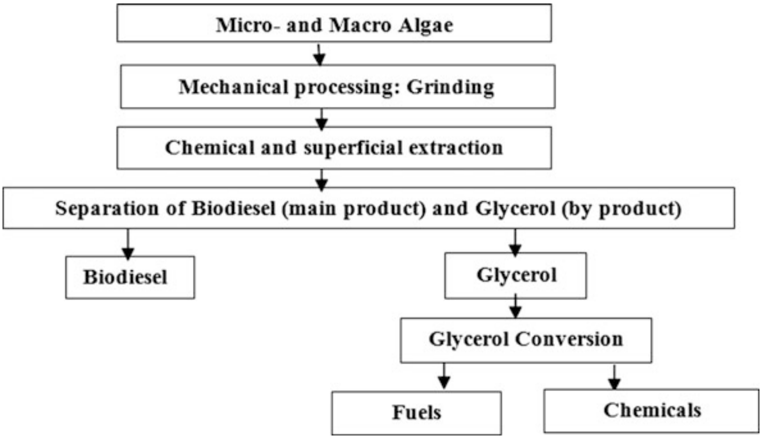

Fig. 10 Flowchart for production of biodiesel from algae (Galadima and Muraza 2014)

doping which can result in competitive transesterification versus cracking process. Heteropoly acids are also promising due to free fatty acid tolerance.

The heterogeneous transesterification of algae oil yielding high purity glycerol has strong potential to reduce industrial dependence on nonrenewable petrochemicals as raw materials.

Capability of oxides and zeolites for the formulation of many liquids and gaseous products such as formaldehyde, allyl alcohols, olefins, methane, diols, and hydrogen fuel, as well as other liquid hydrocarbons like diesel and light naphtha (Galadima and Muraza 2014).

5 Catalyst

5.1 Homogeneous Catalysts

Transesterification is a kind of acid or base-catalyzed intermolecular reaction. Liquid mineral acid and base have been first used for the production of liquid biodiesel.

5.1.1 Homogeneous Acid Catalysts

According to Bronsted and Lowry, an acid is a molecule or ion that is able to lose, or “donate”, a proton (H^+) and according to Lewis which can take an electron lone pair from another molecule in attaining stability. The great number of free fatty acids of waste vegetable oil increases its suitability of acid catalysts which is more for biodiesel production. In transesterification reactions carried out with homogeneous acid catalysts, there are two reagents, like alcohol and a free acid (FFA), reacting to form an ester as the product of the reaction. Therefore, acid catalysts were preferred in cases when FFA content of vegetable oil is greater than 1 wt%. The most commonly used homogeneous acid catalysts in biodiesel production process include HCl, BF_3, H_2SO_4, H_3PO_4, and $FeSO_4$ (Maity 2015). Biodiesel production from the transesterification of animal fats (dairy cow and beef) yields were 94.1 ± 2.43 and 98.4 ± 2.3%, respectively, for the dairy cow and beef tallow. 2.5 g of concentrated (conc.) H_2SO_4, 24 h of reaction time and 50 °C for dairy cow fat and 2.5 g of concentrated H_2SO_4, 6 h of reaction time and 60 °C for beef fat were the optimum conditions.

Several times, the acid-catalyzed transesterification initiated slower than the base-catalyzed one due to the formation of intermediate molecules which are susceptible to nucleophilic attack. Whereas, the base-catalyzed reaction proceeds created initially and directly as a strong nucleophile on the straight route at which alkoxide ion is.

The protonation of the carbonyl group of the ester leads to the carbonation and producing tetrahedral intermediate proceeded by acid-catalyzed esterification reactions. This, in turn, regenerates the catalyst when glycerol is eliminated to form a new ester and may be extended to di and triglycerides. The utilization of Bronsted acids like H_2SO_4 has some common drawbacks, such as their corrosive nature, difficult laborious removal from the mixture by neutralization, and low reaction rates results in higher cost of biodiesel production process (Doyle et al. 2016; Likozar and Levec 2014a). Figure 11 shows mechanism of transesterification via acid catalysis.

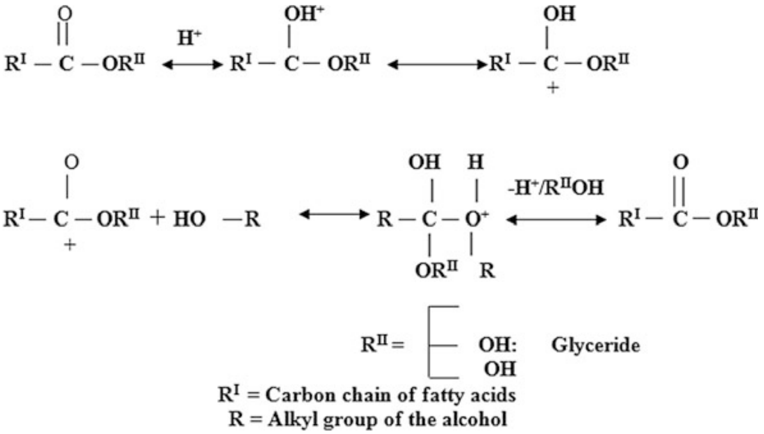

Fig. 11 Mechanism of Transesterification via acid catalysis (Doyle et al. 2016; Likozar and Levec 2014a)

5.1.2 Homogeneous Base Catalysts

A base is a species which accepts a proton or the ability to gain as per Bronsted–Lowry theory, and Lewis theory, a base is one that can provide an electron lone pair to help other molecules from the stable group of atoms. For faster, less corrosive, more effective and reliable biodiesel production, homogeneous base catalysts (sodium hydroxide, potassium hydroxide, barium hydroxide and potassium carbonate and so on) are preferred to homogeneous acid catalysts. The most commonly used base catalysts in biodiesel production include alkaline metal hydroxides and carbonates. (Kumar et al. 2013).

The transesterification reaction with homogeneous base catalysts occurs in four consecutive steps:

- Base reacts with alcohol.
- Alkoxide attacks the carbonyl group of the triglyceride forming tetrahedral intermediate.
- The formation of alkyl ester and diglyceride anion.
- Finally, the catalyst is deprotonated and thus the active species which react with another molecule of the respective alcohol are regenerated and then another catalytic cycle is started.

Free fatty acids present in the vegetable oil might react with the catalysts (NaOH, KOH and/or their methoxide) and result in the formation of soap that causes a loss in biodiesel yield. The water molecule so produced interfered with the transesterification reaction.

The NaOH or KOH catalyzed transesterification reaction is also affected by reaction temperature and time, the molar ratio of oil to methanol, catalyst type, and concentration, and the stirring intensity. The major loss in biodiesel yield was due to saponification of triglycerides and dissolution of alkyl esters in glycerol phase. To avoid this saponification of triglycerides in base-catalyzed transesterification reaction, a two-step reaction was investigated. In the first phase, the triglycerides were treated with acid catalysts to produce methyl esters of FFAs in the vegetable oil and in the second phase, the same base-catalyzed reaction was preceded. However, the utilization of liquid acid catalysts along with base catalysts further leads to a higher cost of biodiesel production and the process becomes further complicated because the homogeneous acid catalyst has to be removed prior to base-catalyzed transesterification.

5.1.3 Biocatalysts for Biodiesel Production

To make biodiesel production process more economical and sustainable, enzyme lipase was focused on transesterification of vegetable oil for limitations associated with homogeneous acid and base catalysts. Both extracellular and intracellular lipases were utilized for methanolysis of vegetable oil. Lipases are more suitable for transesterification of waste vegetable oil because they can also work with free fatty acids. The mechanism of lipase-mediated alcoholysis of triglycerides involves two steps: in the first step, ester bond is hydrolyzed with the release of an alcohol moiety. Esterification took place during the second step, esterification of second substrate takes place (Guo et al. 2015).

Compared with classical homogeneous catalysts, heterogeneous solid catalysts are used for biodiesel production as it gets separated easily with fewer wastes. However, the yield of methyl esters is lower compared with commonly utilized homogeneous catalysts catalyzed with biodiesel production reactions. The deactivation with the passage of time is due to many reasons, like poisoning, leaching, and coking. Therefore, it is essential for the development of heterogeneous catalysts with better stability, selectivity, activity at a low temperature and pressure during the reaction, which is also economical and sustainable (Yang et al. 2015).

5.2 Heterogeneous Solid Acid Catalysts

During transesterification preventing of saponification, waste vegetable oil (high FFA), the solid waste catalyst is used. They are normally less active at a lower temperature, and to obtain higher conversion rates, reaction temperature above 170 °C is needed.

5.2.1 Strong Acid Resins

The acid resins are composed of exchangeable H^+ cations which impart the resins to become insoluble but highly acidic. They are composed of cross-linked polystyrene matrix with active sites for esterification as sulfonic acid groups. These resins easily get ionized not only in acidic but also a salt form of the sulfonic acid group and are therefore nowadays utilized as strong acid catalysts in a number of reactions in place of common homogeneous acids like H_2SO_4.

The conversion rate of the cation exchange resin was not higher compared with its anion exchange counterparts. The main reason was the efficient adsorption of alcohol on anion exchange resins which was not achieved for cation exchange resins.

5.2.2 Heteropoly Acids

Heteropoly acids (HPAs) for the operations of liquid phase esterification reactions are important solid acids. It is observed that strong Bronsted acidity was exhibited compared with conventional acid catalysts, like acidic resins and H_2SO_4. It depends on three factors, the acidity, the structure of heteropoly anion, and the nature of reagents used in the reaction, heterogeneous and homogeneous phase.

5.2.3 Acidic Zeolites

The inorganic solid catalysts are more suitable for biodiesel production than ion exchange resins. Among these inorganic solid acid catalysts, the zeolite is highly important as it has been widely used in current chemical industry as it is microporous (<2 nm) material composed of silicon and aluminum linked by oxygen atoms in crystal framework. When single aluminum ($Al_3{}^+$) replaces single silicon ($Si_4{}^+$) in the framework, oxygen shows negative charge. When one proton contacts this oxygen, the Bronsted acid site is produced. The acidity, acidic strength, and density can be controlled by its SiO_2/Al_2O_3. The advantages of zeolites for catalytic reactions are the shape and size of pores, acid site strength, and their distribution as well as surface hydrophobicity, which can be obtained by the synthesis of a variety of crystal structures and Si/Al ratios with the various exchange levels of proton. Zeolites with large pores have been used successfully for transesterification of vegetable oil for large molecular size FFAs. Based on zeolites Y, beta, mordenite, and ZSM-5, the reaction pathways have been significantly changed due to their various pore sizes. Zeolites with large pores give significant amounts of bicyclic reaction products, whereas the medium pore size ZSM-5 gives almost no bicyclic products. The formation of undesirable by-products also happens because zeolites catalyzed reactions occur at high temperatures (Zhong et al. 2016) (Fig. 12).

The efficiency of zeolites in transesterification is highly dependent on strength of acid sites and hydrophobicity along with adsorption characteristics, geometrical factors, the dimensionality of the channel system, and aluminum content of the

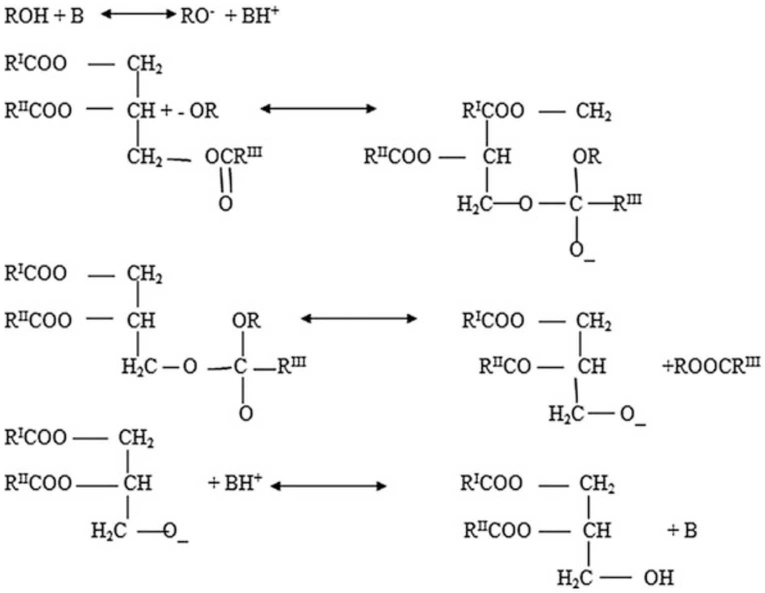

Fig. 12 Mechanism of base-catalyzed transesterification (Galadima and Muraza 2014)

zeolites framework which affect the catalytic activity and the performance for esterification. For the reaction of the large molecular size oil on small pore zeolites, the transesterification was limited and the cracking started.

5.3 Heterogeneous Solid Basic Catalysts

The mechanism of reaction in the conversion of fatty acids into alkyl esters is the same as that of the reaction carried out with homogeneous basic catalysts. These types of solid catalysts are categorized as alkaline earth metal hydroxides, alkaline metal carbonates, alumina loaded with different compounds, hydrotalcites, basic zeolites, and many other compounds with high basic properties, like SnO.

5.3.1 Metal Oxides

Low toxicity, price, and easy availability make CaO to be widely used. The manufacturing cost of CaO was lower compared with traditional basic catalyst KOH. Industrial waste eggshells, golden apple snails, and meretrix venus utilized solid oxide catalysts for formation of biodiesel from palm oil. The waste materials at 80 °C for 2–4 h calcined in air, 90% of biodiesel, transformed Ca species into active CaO catalysts and with sunflower at 60 °C for 2 h, 98% of biodiesel was obtained (Likozar et al. 2016).

Due to the presence of bi-catalytic sites of CaO and MgO, the combined effect of CaO and MgO on transesterification was more encouraging with the great conversion of vegetable oil into esters. However, it was observed that the by-products, like glycerol, were contaminated by the production of soap catalyzed by MgO and the dissolution of surface species into the reaction mixture. The CaO and La_2O_3 mixed metal oxide catalyst showed quite interesting and promising results, but structural changes of the catalyst happened after its exposure to air. The application of nanocrystalline CaO and MgO in transesterification as heterogeneous catalysts attracted much interest these days. The oxide support of nanocrystalline CaO and MgO played an important role in the basicity, surface area, mechanical strength, and cost of the catalyst. CaO–CeO_2 catalyst for transesterification of palm oil among which there are CaO–CeO_2 catalysts, and the best result was obtained with the $_1Ca_1Ce$ coded catalyst (calcined at 650 °C) with a methyl ester yield (>90%) after 2 h of reaction. The catalyst possessed high base strength with a negligible leaching of catalyst components into the reaction mixture. The cerium species and calcium's great interaction and negligible leaching of catalyst components into reaction mixture were further reduced by increasing the calcinations temperature. After 18 cycles, there is a decrease in yield of methyl esters and its basicity at higher calcinations temperatures is lost (Avhad and Marchetti 2015a, b).

5.3.2 Hydrotalcites

Hydrotalcites with general formula $[\mathrm{M}^{2+}_{(1-x)}\mathrm{M}^{3+}x(\mathrm{OH})_2](\mathrm{A}x/n)^{n-}\cdot y\mathrm{H_2O}\cdot y\mathrm{H_2O}$ are environmentally friendly in nature, and hydrotalcite $\mathrm{Mg_6Al_2(OH)_{16}CO_3\cdot 4H_2O}$ displayed a high activity in the transesterification reaction, the catalyst with medium basic strength was highly effective in transesterification (Konwar et al. 2014).

Maximum catalytic activity was observed for catalysts calcined at 400 °C. Interestingly, the samples calcined at this temperature had lower basicity and possessed a bigger surface area and pore volume than those calcined at 200 °C.

The Mg + Al hydrotalcites were examined for the production of canola oil methyl esters. A 71.9% conversion of vegetable oil to methyl esters was obtained when carried out with a 6:1 molar ratio of methanol to oil, 9 h of reaction, and a 3% (w/w) catalyst concentration at 60 °C. The particle size of catalysts was 125–150 mm. It has been observed that it was suitable for catalysts with strongest basic sites to be operated at low temperatures (100 °C) in the transesterification reaction. In contrast, those catalysts with basic sites in medium strength were operated at higher temperatures to promote the same type of reaction. Transesterification reactions were carried out with magnetic stirring at 64 °C under atmospheric pressure coupled to a condenser, by changing molar ratio of methanol/oil and the reaction time.

5.3.3 Basic Zeolites

The physical and chemical properties of basic zeolites, like adsorption, ionic interchange, and catalytic activity also render their commercial application for biodiesel production as zeolites can serve as basic catalysts and generate weak active centers by decreasing the silica/alumina ratio or interchanging with alkaline cations.

The increase in negative charge of oxygen atoms, basicity of zeolites improved, by the occlusion of sodium metal clusters, a positive correlation between the number of basic sites on zeolites and the yield of methyl esters. The calcination temperature is also important for determining the activity of basic zeolites in a transesterification reaction. Various zeolites, such as mordenite, beta, and X with different metal loadings were investigated for the transesterification of sunflower seed oil. The zeolite X was agglomerated with sodium bentonite as a binder to investigate how the catalytic performance of zeolites changed with a binder. The 93.5 and 95.1% (w/w) yields of methyl esters were achieved at 60 °C by utilizing zeolite X in the presence or absence of sodium bentonite, respectively.

The transesterification reaction of soybean oil with various catalysts, like NaO_x occluded in NaX (faujasite zeolite), K occluded in ETS-10 (titanosilicate structure-10 zeolite) and ETS-10 (titanosilicate structure-10 zeolite) were studied with molar ratio of 1:6, oil to methanol, for 24 h at different temperatures. ETS-10 catalysts were more effective than zeolite X type catalysts with a more than 90% yield of methyl esters. This increased conversion ratio of vegetable oil to methyl esters was due to the greater basicity of ETS-10 zeolites and their larger pore structures. By the introduction of alkali earth oxides, number of basic sites increased in NaX zeolites and it depended on the molecular size of the metal oxide, which led to the utilization of nanocrystalline metal oxides as heterogeneous basic catalysts for biodiesel production. It was observed that methyl ester content is greatly dependent on basicity of catalysts. The most effective catalyst was the one with 16% (w/w) CaO nanoparticles and a more than 93.5% conversion rate was achieved. However, the catalytic activity of the catalyst was lost on reuse and only 5% of methyl esters content was achieved in the third cycle (Bryant and Romijn 2014).

5.4 Limitations of Heterogeneous Solid Catalysts

In a heterogeneous solid catalyst catalyzed reaction system, the rate of reaction is dependent on the diffusion between gaseous and/or liquid phases. In order to overcome, this mass transfer problem in transesterification, catalyst support, or structure promoters were introduced to provide large specific surface areas and pores for active species. Alumina with a high thermal and mechanical stability, $NaOH/Al_2O_3$ catalyst which was prepared with different concentrations of aqueous sodium hydroxide solution by impregnation method and calcined for 3 h for palm oil's transesterification, a 99% conversion of oil into biodiesel was obtained with 3% (w/w) catalyst concentration. The optimum yield (99%) was observed, where methanol to oil ratio of 15:1 with 3% (w/w) catalyst concentration and 8 h reaction at 60 °C. Similarly, a KI/Al_2O_3 catalyst was prepared for the conversion of soybean seed oil to biodiesel. Other limitations of heterogeneous catalysts include high-temperature requirements, the low conversion rate of reaction, and the production of some unwanted by-products whose removal further adds the cost of biodiesel production technology. The utilization of metal oxides results in the leaching of metal into methyl esters and then decreases the quality of glycerol which is an important side byproduct in biodiesel industry (Sangeeta et al. 2014). Table 3 shows various advantages and disadvantages of catalyst used.

6 Known Problems, Probable Cause, and Potential Solutions for Using Straight Vegetable Oil in Diesel Engine

See Table 4.

Table 3 Table showing various advantages and disadvantages of catalysts (Hanis et al. 2017)

Types of catalysts	Examples	Advantages	Disadvantages
Homogeneous			
Alkali's	NaOH, KOH	High catalytic activity	(<1 wt%) FFA requirement
		Faster reaction time	Highly susceptible to water and FFA
		Low Cost	Saponification takes place
		Favorable Kinetics	Formation of soap
		Modest operational conditions	High quantity of wastewater
			Catalyst cannot be recycled
			Equipments corrode away
Acid's	HCL, HF, H_3PO_4, ρ-sulphonic acid H_2SO_4	Ineffective to free fatty acids and water content	Slow reaction rate
			A long reaction time
		Simultaneous catalyzed esterification and transesterification reactions	Equipment corrode
			High reaction temperature and pressure
			High (alcohol/oil) ratio
		Avoid soap formation	Poor catalytic activity
			Recycling of catalyst is difficult
Heterogeneous			
Alkali's	CaO, MgO, SrO, mixed oxide hydrotalcite	Noncorrosive	Negligible reaction rate compared to homogeneous ones
		Environmentally benign	(<1 wt%) FFA required
		Recyclable	Highly sensitive to water and FFA
		Fewer disposable problems	Saponification takes place
		Easy separation	Wastewater obtained is more
		Higher selectivity	Extraction of active catalyst sites
		Longer catalyst life	Restricted diffusion
			Costly and complicated synthesis route
			Catalytic synthesis is expensive

(continued)

Table 3 (continued)

Types of catalysts	Examples	Advantages	Disadvantages
Acids	ZrO, TiO, ZnO, HPA, zeolites, ion exchange resin, sulfonic acid, mesostructured silica, sulfonated carbon-based catalyst	Insensitive to FFA and water content in oil	Slow reaction rate
			A long reaction time
		Simultaneous catalyzed esterification and transesterification	The higher reaction temperature and pressure
			High ratio (alcohol/ oil requirement)
			Catalytic activity is less
			Low acidic sites
		Recyclable, eco-friendly	Low microporosity
		Noncorrosive for reactor and its parts	Solvent extraction active catalyst sites
			Limited diffusions
			Expensive complex synthesis route
			Catalyst synthesis is too expensive
Enzyme's	Candida Antartica fraction B lipase, *Rhizomucor miehei* lipase	FFA and water content does not hinders activity	Negligible reaction rate
			Highly expensive
		Avoid soap formation	Highly sensitive to alcohol
		Nonpolluting	Denaturation of enzyme
		Easy purification	
		Possible reuse	

7 New Technologies Frequently Used for Biodiesel Production

The drawback of the transesterification reaction is limited by mass transfer resulting in much lower reaction rate and also much higher cost compared to diesel fuel. Therefore, the need arises for the development of new technologies such as

1. Microwave-assisted extraction (MAE)
2. Ultrasonic cavitation (UC)
3. Hydrodynamic cavitation (HC).

Table 4 Difficulties associated with SVO and solutions for diesel engines (Fanguri and Hanna 1999)

Difficulties	Reason	Solutions
Short-term		
Starting at low temperature	High viscosity, low cetane and flash point of oils	Heating fuel before injection Convert fuel to an ester
Choking of filters, lines and injectors	Presence of phosphatides (natural gums) and ash in oil	Gum removal by partially refining the oil
Knocking	Longer ignition delay and Irregular injection timing	Use higher compression engines and Adjust injection timing Preheat fuel prior to injection. Chemically alter fuel to an ester
Long-term		
Coking of injectors on piston and head of engine	Viscosity is high, incomplete combustion of fuel at part load with vegetable oils	Heating fuel before injection Convert fuel to an ester
Deposits of carbon on piston and head	Viscosity is high, incomplete combustion of fuel at part load with vegetable oils	Heating fuel before injection Starting engine with diesel fuel at part load Convert vegetable oil to an ester
High engine wear	Viscosity is high, incomplete combustion of fuel at part load with vegetable oils Presence of free fatty acids in the vegetable oil Loss in lubricating oil due to blow-by of vegetable oil	Heating fuel before injection Starting engine at the beginning Convert vegetable oil to an ester Frequent oil changes to inhibit oxidation
Engine oil Failure due to polymerization	Collection of polyunsaturated oil blow-by at crankcase where polymerization takes place, conversion of oil to an ester Frequent changes of motor oil Addition of Motor oil additives for oxidation	Heating fuel before injection Starting engine with diesel fuel at part load

7.1 Microwave-Assisted Extraction (MAE)

The microwave-assisted extraction is being displayed in Table 5 (Fig. 13).

Origin of MW power can be traced back to 1940, where it is generated from a very high power generator called the magnetron. A magnetron that could generate a high power output (≈100 kW on a pulse basis) was initially developed at the University of Birmingham by Randall and Booth.

This led to the invention of the first prototype MW oven by P. L. Spencer from Raytheon band and this investigation led to establishing commercial scale MW food processing technology in 1960. Decades of 1970–80s witnessed the bulk production of domestic ovens. A comparison of the MW assisted biodiesel production is shown in Table 5.

This has led to the production of MW oven after years and years of modification and improvement (Lam et al. 2016). Biodiesel production via transesterification assisted MW has increased since 2007. MW usage for chemical reactions enhancement and energy efficiency has garnered significant attention in recent years. A major obstacle in its commercial use is due to the small penetration depth of the MW in the reactive media (Mazubert et al. 2014).

7.2 Ultrasonic Cavitation

Optimal conditions for ultrasonically assisted biodiesel production were 1:4 M ratio of oil to methanol, 6 wt% catalyst loading, 20 min of reaction time (30 fold lower than MS), and 40% of ultrasonic amplitude at 5 Hz. A comparison of the UC assisted transesterification is illustrated in Table 6.

7.3 Hydrodynamic Cavitation

Hydrodynamic cavitation can broadly be classified as

- Inertial (or transient) or
- Noninertial.

Inertial cavitation is the process where a void of bubble or cavities collapses due to the recovery of pressure and releases great amount of energy (Shockwaves at high temperature) causing molecules to fragment and generate highly reactive radical species favoring forward reaction (Sajjadi et al. 2015). Noninertial cavitation is often employed in ultrasonic cleaning baths and can also be observed in pumps

Table 5 Microwave-assisted biodiesel production

Oil	Catalyst	Catalyst amount (wt%)	Reactant	Oil:alcohol (molar ratio)	Reaction condition	Ester yield/ conversion (wt%)	Source
Refined cotton seed oil	KOH	1.5	Methanol	1:6	60 °C, 7 min	92.4 (yield)	Azcan and Danisman (2007)
Jatropha oil	KOH	1.5	Methanol	1:7.5	65 °C, 2 min	97.4 (yield)	El Sherbiny et al. (2010)
Used vegetable oil	BaO	0.75	Methanol	1:6	2 min	91 (yield)	Martinez-Guerra and Gude (2014)
						83.5 (yield)	
						93.5 (yield)	
Palm oil	CH_3ONa	0.75	Methanol	1:6	65 °C, 600 rpm, 3 min	99.5 (yield)	Lin et al. (2014)
	NaOH					99.0 (yield)	
Pongamia pinnata seed oil	KOH	1	Methanol	1:6	60 °C, 5 min	97(yield)	Kumar et al. (2011)
	NaOH	0.5				96 (yield)	
FFA stearic acid	D418	9	Ethanol	1:11	80 °C, 7 h	>90 (conversion)	Liu et al. (2013)
Waste cooking oil	CH_3ONa	1	Methanol	1:6	60 °C, 5 min	98.87 (conversion)	Azcan and Yilmaz (2013)
Palm oil	CaO derived from waste eggshells	15	Methanol	1:18	122 °C, 4 min	96.7 (yield)	Khemthong et al. (2012)
Soybean	SrO	1.8	Methanol	1:6	60 °C, 40 s	97 (conversion)	Koberg et al. (2011)
	KOH	1				81 (conversion)	
	$Sr(OH)_2$	2.1				97 (conversion)	

(continued)

Table 5 (continued)

Oil	Catalyst	Catalyst amount (wt%)	Reactant	Oil:alcohol (molar ratio)	Reaction condition	Ester yield/ conversion (wt%)	Source
Cooked oil	SrO	1.8	Methanol	1:6	60 °C, 20 s	93.2 (conversion)	Perin et al. (2008)
Castor oil	KOH	1	Methanol	1:6	60 °C, 30 min	99.4 (conversion)	Venkatesh Kamath et al. (2011)
	SiO_2/50% H_2SO_4	10				95 (conversion)	
Cooked oil	Al_2O_3/50% KOH	1.8	Methanol	1:6	60 °C, 5 min	95 (conversion)	
Karanja oil	H_2SO_4 (esterification)	3.73	Methanol	1:9.4	300 rpm, 190 s	87.5 (FFA reduction)	
Ceiba pentandra	KOH	1.33	Methanol	1:9.3	300 rpm, 150 s	89.9 (yield)	Bokhari et al. (2015)
	H_2SO_4 (esterification)	1.5		1:6	500 rpm, 5 min, 60 °C	86.4 (FFA reduction)	
Waste frying palm oil	KOH	2.15	Ethanol	1:9.85	500 rpm, 3.29 min 57.09 °C	89.9 (conversion)	Lertsathapornsuk et al. (2008)
	NaOH	3		1:12	78 °C, 30 s	97 (conversion)	
Pretreated Jatropha oil	$NaOCH_3$	1	Methanol	1:6	67–78 °C, 30 s	96.5 (yield)	Tippayawong and Sittisun (2012)
Used vegetable oil	KOH	1	Methanol	1:6	50 °C, 30 s	97.9 (conversion)—2 L/min 98.9 (conversion)—7.2 L/min	Barnard et al. (2007)

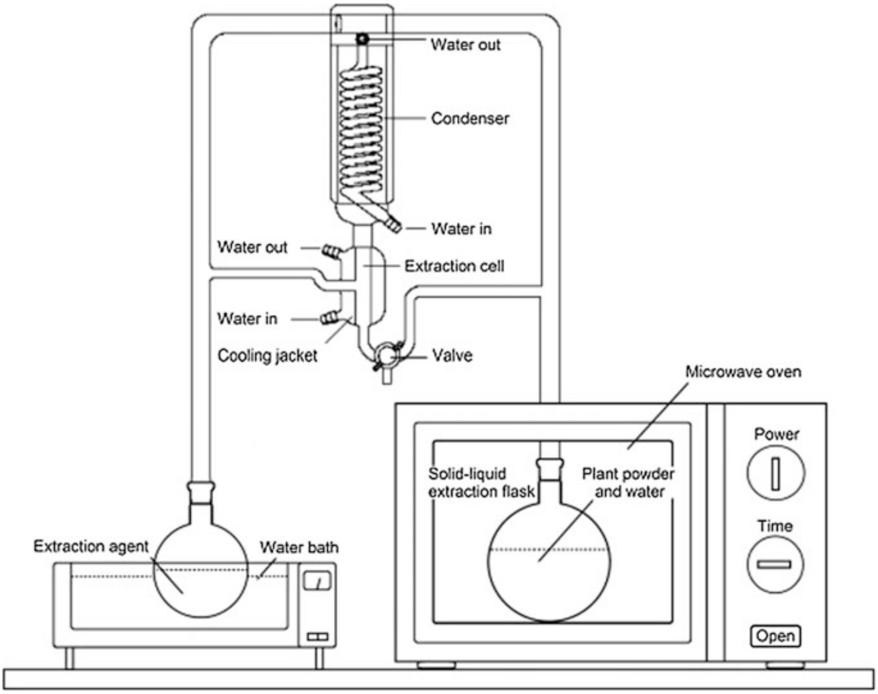

Fig. 13 Microwave-assisted simultaneous distillation process (Chen et al. 2016)

and propellers due to bubble formed in a fluid is forced to oscillate (Shah et al. 1999). Table 7 shows comparison of frequently used microwave-assisted extraction (MAE), ultrasonic cavitation (UC), and hydrodynamic cavitation (HC).

8 Biodiesel Emissions

Table 8 shows the emissions from the various fuels that are being used for the production of biodiesel.

9 Global Policies

On October 2014, National Biodiesel Board (NBB, U.S. industry group) filed comments with the EC for import duties that were introduced in 2009. Till 2016, EU’s had planned to extend the duty imposed on U.S. produced biodiesel until

Table 6 A comparison of the UC assisted transesterification

Oil	Catalyst	Catalyst amount (wt%)	Reactant	Oil to alcohol molar ratio	Reaction condition	Ester yield/ conversion (wt%)	Source
Vegetable oil	NaOH	0.5	Methanol	1:6	30 °C, 40 min	98 (yield)	Stavarache et al. (2005)
					30 °C, 20 min		
Jatropha oil	HPA/AC	3.5	Methanol	1:25	65 °C, 40 min, 60% amplitude	91 (yield)	Badday et al. (2013)
Vernicia fordii	KOH	1	Methanol	1:6	20–30 °C, 10 min	91.15 (yield)	Manh et al. (2011)
Palm oil	waste ostrich egg shell—derived CaO	8	Methanol	1:9	60 °C, 60 min	92.7 (yield)	Chen et al. (2014)
Treated waste fish oil	KOH	1	Methanol	1:6	55 °C, 30 min	79.86 (yield)	Maghami et al. (2015)
Vegetable oil	KOH	1	Methanol	1:6	45 °C, 10 min	85 (yield)	Ji et al. (2006)
Palm oil	KOH	1	Methanol	1:6	50 °C, 90 min	92 (yield)	Pukale et al. (2015)
Waste cooking oil	K_3PO_4	3	Methanol	1:6	50 °C, 90 min	92 (yield)	Pukale et al. (2015)
Waste cooking oil	CH_3OK	1	Methyl acetate	1:12	40 °C, 30 min	90 (yield)	Maddikeri et al. (2013)
Palm oil	BaO	2.8	Methanol	1:9	65 °C, 50 min	95 (yield)	Salamatinia et al. (2010)
	SrO						
Palm oil	CaO	3	Methanol	1:9	65 °C, 60 min, 50% amplitude	77.3 (yield)	Mootabadi et al. (2010)
	SrO					95.2 (yield)	
	BaO					95.2 (yield)	

(continued)

Table 6 (continued)

Oil	Catalyst	Catalyst amount (wt%)	Reactant	Oil to alcohol molar ratio	Reaction condition	Ester yield/ conversion (wt%)	Source
Jatropha oil	H_2SO_4 (esterification)	4	Methanol	1:11	60 °C, 60 min	89 (FFA reduction)	Deng et al. (2010)
	NaOH	1.4		1:6.6	60 °C, 30 min	96.4 (yield)	
Corn oil, canola oil, sunflower oil, used palm oil	SrO	0.08	Methanol	1:15	pulse on (10 s), pulse off (3 s), 60 min, 57 °C	76.45 (yield)	Anuar and Abdullah (2016)
Waste cooking oil	Hydrotalcite	0.08	Methanol	1:15	pulse on (10 s), pulse off (3 s), 60 min, 57 °C	76.45 (yield)	Anuar and Abdullah (2016)
Pistacia tlantica Desf. oil	KOH	1	Methanol	1:5e1:6	pulse on (10 s), pulse off (3 s), 5–7 min, 55 °C	96.6 (conversion)	Samani et al. (2016)
Waste tallow oil	Candida Antarctica lipase B (CALB)	6	Methanol	1:4	20 min, 5 Hz ultrasonic cycle	76.45 (yield)	Adewale et al. (2015)

Table 7 Comparison microwave-assisted extraction (MAE) ultrasonic cavitation (UC) and hydrodynamic cavitation (HC)

Raw material	Method	Process	Alcohol	Catalyst	Parameters				Results		Source
					Oil to alcohol molar ratio	Temp. (°C)	Catalyst (wt%)	Time (min)	Ester yield/ conversion (wt%)	Yield efficiency 10^{-4} (g/J)	
Vegetable oil	HC	Trans.	Methanol	KOH	1:6	45	1.0	10	98 (Yield)	15.18	Ji et al (2006)
	UC							30	98 (Yield)	0.11	
	MS							45	90(Yield)	0.06	
Vegetable oil	HC	Trans.	Methanol	NaOH	1:20	N/A	1	15	98 (yield)	33.27	Gogate. (2008)
	UC							10	99 (yield)	0.86	
	MS							180	98 (yield)	0.23	
Fatty acid (C9–C10)	HC	Ester.	Methanol	H_2SO_4 Caprylic acid	1:10	28	1.0 2.0	90	92 (conversion)	–	Kelkar et al. (2008)
	UC							125	98 (conversion)		
	MS							75	98 (conversion)	–	
Thumba oil	HC	Trans.	Methanol	NaOH	1:4.5	50	1.0	30	80 (yield)	N/A	Pal et al. (2010)
Frying oil	HC	Trans.	Methanol	KOH	1:6	60	1.0	10	95 (conversion)	12.8	Ghayal et al. (2013)
Nagchampa oil	HC	Trans.	Methanol	KOH	1:6	60	1.0	20	92.1 (conversion)	8.7	Gole et al. (2013)
	UC	Trans.						40	92.5 (conversion)	0.1	
	MS	Trans.						90	90.6 (conversion)	0.05	

(continued)

Table 7 (continued)

Raw material	Method	Process	Alcohol	Catalyst	Parameters				Results		Source
					Oil to alcohol molar ratio	Temp. (°C)	Catalyst (wt%)	Time (min)	Ester yield/ conversion (wt%)	Yield efficiency 10^{-4} (g/J)	
Waste cooking oil	HC	Interester.	Methyl acetate	CH_3OK	1:12	40	1.0	30	89.2 (yield)	12.2	Maddikeri et al. (2014)
	UC								90.0 (yield)	0.5	
	MS								70.0 (yield)	0.3	
Waste cooking oil	HC	Trans.	Methanol	KOH	1:6	60	1	15	98 (conversion)	12.5	Chuah et al. (2016)
	MS							90	97 (conversion)	1.5	
Rubber seed oil	HC	Inter ester.	Methanol	CH_3ONa	1:6	55	8	30	96.4 (conversion)	2.2	Bokhari et al. (2016a)
	MS							90	92.8 (conversion)	0.5	
Rubber seed oil	HC	Trans.	Methanol	KOH	1:6	55	1	18	97.0 (conversion)	9.1	Bokhari et al. (2016b)
	MS							90		1.4	
Jathropa oil	MW	Trans.	Methanol	KOH	1:75	65	1.5	2	97.4(yield)	6.9	El herbiny et al. (2010)
Palm oil	MW	Trans.	Methanol	CH_3ONa	1:6	65	0.75	3	99.5 (yield)	6.9	Lin et al. (2014)
				NaOH					99.0 (yield)		
Waste cooking oil	MW	Trans.	Methanol	CH_3ONa	1:6	65	0.75	3	96.2(yield)	6.9	Chen et al. (2012)
				NaOH					97.4(yield)		
Pongamia pinnata seed oil	MW	Trans.	Methanol	KOH	1:6	60	1	5	97(yield)	4.4	Kumar et al. (2011)
				NaOH			0.75		96 (yield)		

Table 8 Emissions from the various fuels used for the production of biodiesel

Biodiesel fuel	Engine type	Emission	Source
Pongamia, jatropha and neem methyl esters	No. of cylinder 1,4 stroke, WC, DI,CR: 16.5:1, RP: 3.7 kW	Decrease in Smoke, HC and CO emissions for biodiesel blends	Rao et al. (2008)
Neem and mixed pongamia-coconut methyl esters	No. of cylinder 1,4stroke, WC, DI, CR: 16:1–25:1, RP: 3.75 kW	–	Nithyananda et al. (2013)
Preheated cottonseed oil methyl ester (CSOME)	No. of cylinder 1,4 stroke, WC, DI,CR: 17.5:1, RP: 5.2 kW	Decrease in CO and HC by 34 and 16% respectively for CSOME80	Augustine et al. (2012)
Cottonseed oil methyl ester (CSOME)	No. of cylinder 1,4stroke, WC, DI, CR: 6.5:1, RP: 4.476 kW	Decrease in NO_x by 11% for CSOME80 CO and PM for CSOME blends	Nabi et al. (2009)
Cottonseed oil methyl ester (CSOME)	No. of cylinder 1,4 stroke, AC, DI, CR: 18/1, RP: 10 HP		Aydin and Bayindir (2010)
Cottonseed oil (CSO)	No. of cylinder 1,4 stroke, AC, DI, CR:18:1, maximum torque: 38.5 N m	Increase in CO emission for CSO blends Decrease in NO_x emission for CSO blends No change in CO_2 emission	Daho et al. (2013)
Cottonseed oil methyl ester (COME)	No. of cylinder 1,4 stroke, DI, CR: 18:1	Increase in NO_x emission for COME fuel Decrease in CO for COME fuel	Karabektas et al. (2008)
Jatropha oil	No. of cylinder 1,4stroke, WC, DI, CR: 17.5, RP: 7.4 kW	CO, CO_2, HC and smoke opacity of preheated blends are close to the diesel fuel	Agarwal (2007)
Jatropha methyl ester	No. of cylinder 1,4 stroke, WC, DI, CR:17.5:1, RP: 3.5 kW	Increase in CO and CO_2 by 38% and 2% respectively Decrease in HC, NO_x emissions and smoke opacity by 50, 25, and 10%, respectively	Jindal et al. (2010)
Jatropha oil biodiesel	No. of cylinder 1,4 stroke, WC, DI,CR: 18	Increase in NO_x emission with the addition of biodiesel blends	EL-Kasaby et al. (2013)

(continued)

Table 8 (continued)

Biodiesel fuel	Engine type	Emission	Source
		Decrease in CO emission for biodiesel blends	
Jatropha biodiesel	No. of cylinder 1,2-cylinder, 4 stroke, WC, DI,RP: 7.35 kW	Increase in CO_2 and NO_x emission for methyl Decrease in CO, unburned hydrocarbon and smoke intensity for methyl ester	Paul et al. (2014)
Karanja oil	No. of cylinder 1, 4 stroke, WC, DI,CR: 17.5:1, RP: 7.4 kW	Increase in NO and CO_2 emission for Karanja oil blends Decrease in HC and smoke emissions for up to K50	Agarwal (2013)
Pongamia pinnata methyl ester (PPME)	No. of cylinder 1,4 stroke, WC, CR:16.5:1, RP: 3.68 kW	Decrease in CO2for medium blends of PPME Decrease in CO, HC and NO_x with the addition of PPME	Suresh kumar et al. (2008)
Pungam oil methyl ester (PGME) and rice bran oil methyl ester (RBME)	No. of cylinder 1, 4 stroke, AC, DI, CR: 17.5:1, RP: 4.4 kW	Increase in CO_2 and NO_x emission for methyl esters Decrease in CO, unburned hydrocarbon and smoke intensity for methyl esters	Rao and Ajayamohan (2008)
Koroch seed oil methyl ester (KSOME)	No. of cylinder 1,4 stroke, WC, DI, CR: 12–18, RP: 3.5 kW	–	Gogoi et al. (2011)
Biodiesel–diesel blends	No. of cylinder 1, 4 stroke, AC, DI, CR: 19.5:1, RP: 7.4 kW	Increase in NO_x emission with the addition of biodiesel in the blend decrease in CO, HC and smoke opacity for biodiesel blends	Lahane and Subramanian (2015)
Turpentine oil	No. of cylinder 1, 4 stroke, WC, DI, CR: 17.5:1, RP: 5.2 kW	Increase in CO_2 emission for turpentine oil blends Decrease in CO, HC and NO_x emissions with the addition of turpentine oil	Anand et al. (2010)

(continued)

Table 8 (continued)

Biodiesel fuel	Engine type	Emission	Source
Turpentine direct injection (TDI)	No. of cylinder 1,4 stroke, AC, DI, RP: 4.4 kW	Increase in CO and NO_x for TDI Decrease in HC and smoke intensity for TDI	Karthikeyan et al. (2010)
Mahua oil methyl ester	No. of cylinder 1,4 stroke, WC, DI, CR: 17.5:1, RP: 5.2 kW	Increase in CO, CO_2 and NO_x for methyl ester blends Decrease in HC emission with the addition of methyl ester	Lenin et al. (2012)
Mahua oil ethyl ester (MOEE)	No. of cylinder 1,4 stroke, WC, DI, CR: 16.5:1, RP: 3.7 kW	Increase in CO_2 emission for MOEE Decrease in CO, HC and NO_x emission for MOEE	Puhan et al. (2005)
Methyl ester mahua (*Madhuca indica*) oil	No. of cylinder 6, WC, DI, CR: 17.6:1	For B100 at full load Increase in 12% of EGT Increase in 11.6% of NO_x Decrease in CO and HC for all the blends	Godiganur et al. (2009)
Waste fish fat	No. of cylinder 1, 4 stroke, AC, DI, CR: 18:1, RP: 4.5 kW	Increase in CO_2 and NO_x emission with the addition of biofuel Decrease in CO, UHC and PM with the addition of biofuel	Varuvel et al. (2012)
Fish oil biodiesel	No. of cylinder 1,4 stroke, WC, DI,CR: 17.5, RP: 5.2 kW	Increase in Smoke, NO_x, CO and HC emissions	Savariraj et al. (2013)
Fish oil methyl ester	No. of cylinder 3, 4 stroke, AC, DI, CR:17:1, RP: 20 kW	Increase in NO_x emission for biodiesel blends Decrease in CO and HC emission with the addition of methyl ester	Godiganur et al. (2017)
Waste cooking oil methyl ester	No. of cylinder 1,4 stroke, WC, CR: 5:1–22:1, RP: 3.7 kW	Increase in NO_x emission for B40 at CR:21 Decrease in CO and CO_2 emissions at compression ratio of 21 Decrease in HC emission for other blends except B40	Muralidharan and Vasudevan (2011)

(continued)

Table 8 (continued)

Biodiesel fuel	Engine type	Emission	Source
Waste cooking oil methyl ester (WCME)	No. of cylinder 1,4 stroke, AC, DI, CR:17.5:1, RP: 4.4 kW	Increase in NO_x emission with the addition of WCME Decrease in unburned hydrocarbon, CO and smoke opacity for WCME blends at full load	Gopal et al. (2014)
Canola (COME) and waste palm oil methyl esters (WPOME)	No. of cylinder 6, 4 stroke, WC, DI, CR: 15.9:1, maximum power 81 kW at 2600 rpm	Decrease in unburned HC, CO, CO_2 and smoke opacity by 26, 67, 8% and 63% respectively for WPOME Decrease in unburned HC, CO, $CO_2$and smoke opacity by 17, 59, 5% and 56% respectively for COME	Ozsezen and Canakci (2011)
Waste cooking oil biodiesel	No. of cylinder 4, 4 stroke, WC, CR: 21.6:1	Increase in CO_2 for B50 blend Increase in NO_x with the addition of biodiesel Increase in PM for B100 Decrease in CO and SO_2 for biodiesel blends	Lin et al. (2007)
Waste frying oil methyl ester	No. of cylinder 1, 4 stroke, WC, DI, turbocharged, CR: 17:1, Power (kW/rpm) 85/2800	Increase in NO_x emission for methyl ester blends Decrease in HC, CO and CO_2 emission with the addition of methyl ester	Shirneshan et al. (2013)
Waste cooking oil biodiesel	No. of cylinder 4, 4 stroke, WC, DI, Turbocharged, CR: 18.5:1, RP:75 kW	Increase in CO emission for biodiesel blends Decrease in HC and CO_2 emission with the addition of biodiesel Decrease in NO_x emission for B100	An et al. (2013)

(continued)

Table 8 (continued)

Biodiesel fuel	Engine type	Emission	Source
Waste frying oil	No. of cylinder 6, 4 stroke, WC, DI, CR: 16.4:1	Increase in CO_2 and NO_X emissions for esters Decrease in CO and THC	Sanli et al. (2015)
Diesel–microalgae biodiesel–butanol blends	No. of cylinder 4, 4 stroke, WC, DI, RP: 89 kW (power)	Decrease in CO and smoke opacity for all blends Decrease in NO_x emission with the addition of butanol in the blend	Tuccar et al. (2011)
Microalgae oil methyl esters (AME)	No. of cylinder 3, DI, maximum power 30 kW	Decrease in Smoke and HC emission by 10–75 and 5–25% respectively for AME blends Decrease in CO emission with the addition of AME	Makareviciene et al. (2014)
Rubber seed oil methyl ester	No. of cylinder 1, 4 stroke, DI, RP:5.5 kW	Increase in CO_2 emission for B100 Decrease in CO emission and smoke density for biodiesel blends	Ramadhas et al. (2005)
Neat orange oil	No. of cylinder 1, AC, CR: 17.5:1, RP:4.4 kW	Increase in NO_X for orange oil Decrease in CO, HC and smoke emission for orange oil	Purushothaman and Nagarajan (2009)
Castor seed oil methyl ester	No. of cylinder 1,4 stroke, WC, VCR, CR: 17.5, RP: 3.5 kW	Increase in NO_x emission for higher percentage of methyl ester	Panwar et al. (2010)
castor oil biodiesel	No. of cylinder 4, 4 stroke, WC, DI, CR: 17.25:1, max power: 82 hp in 2000 rpm	Increase in NO_x emissions Decrease in CO, HC and PM for the blends	Shojaeefard et al. 2013
Ceiba pentandra biodiesel (CPB)	No. of cylinder 1,4 stroke, WC, DI, CR: 17.7:1, RP: 7.7 kW	Decrease in HC, smoke opacity and ↑ NO_x with the addition of CPB Decrease in CO and CO_2 for CPB10 and CPB50 respectively	Silitonga et al. (2013)

(continued)

Table 8 (continued)

Biodiesel fuel	Engine type	Emission	Source
Clove stem oil (CSO)	No. of cylinder 4, 4 stroke, WC, DI, CR: 18.4:1, RP: 43 kW	Increase in CO_2 with the addition of CSO Increase in NO_x emission for 50% of CSO Decrease in CO, HC and smoke opacity for CSO blends at all speeds	Mbarawa (2010)
Croton megalocarpus (musine) methyl ester (CME)	No. of cylinder 3, 4 stroke, WC, DI, CR: 18.5:1, RP: 33.56 kW	Increase in CO, CO_2 and HC emissions for CME blends Decrease in Smoke emission with the addition of CME	Aliyu and Bala (2011)
Jojoba methyl ester (JME)	No. of cylinder 2, 4 stroke, WC, DI, EGR, CR: 16.4, RP: 26 HP	Increase in CO, HC and NO_x emission for JME Increase in NO for MB blends Increased EGR rate causes ↓ NO_x and EGT for JME	Saleh (2009)
Mustard Biodiesel (MB)	No. of cylinder 4, WC, CR: 21:1	Decrease in HC, CO and sound level with the addition of MB	Sanjid et al. (2014)
Coconut oil based hybrid fuels	No. of cylinder 1,4 stroke, AC, DI, RP:3.8 hp	Increase in CO emission Decrease in NO, SO_2 and CO_2 emission with addition of hybrid fuels	Singh et al. (2010)
Beef tallow methyl ester	No. of cylinder 1,4 stroke, WC, DI, CR: 17.5:1, RP: 5.2 kW	Decrease in CO, HC emissions and smoke density by 24.7, 32.5 and 63% respectively for neat biodiesel Increase in NO_x by 5.5% for neat biodiesel	Selvam et al. (2012)
Hazelnut kernel oil methyl ester(HOME)	No. of cylinder 1,4 stroke, AC, DI, CR: 18:1, RP: 8 kW	Decrease in emissions for B50 and neat HOME biodiesel blends	Gumus (2008)

(continued)

Table 8 (continued)

Biodiesel fuel	Engine type	Emission	Source
Pine oil	No. of cylinder 1,4 stroke, WC, DI, CR: 17.5:1, RP: 5.2 kW	For 100% pine oil at full load Increase in CO_2 and NO_x emissions for all pine oil blends Decrease in 65% of CO Decrease in 30% of HC Decrease in 70% of smoke Decrease in 25% of NO_x	Vallinayagam et al. (2013)
Pine oil	No. of cylinder 1,4 stroke, AC, DI, CR:17.5:1, RP: 4.4 kW	Decrease in CO and HC emissions for all pine all blends at full load	Tamilselvan and Nallusamy (2015)
Annona methyl ester (AME)	No. of cylinder 1,4 stroke, WC, DI, CR: 17.5:1, RP: 5.9 kW	Decrease in CO and smoke emission for AME blends Increase in HC and NO_X emission for AME blends	Senthil and Silambarasan (2015)
Paradise oil methyl ester-eucalyptus oil blends	No. of cylinder 1,4 stroke, AC, DI, CR: 17.5:1, RP: 4.4 kW	Increase in NO_X by 2.7% for Me50-Eu50 blend Decrease in CO, HC and smoke by 37, 34 and 49% respectively for Me50–Eu50 blend	Devan and Mahalakshmi (2009)
Pine oil-kapok methyl ester (KME) blends	No. of cylinder 1,4 stroke, WC, DI, CR: 17.5:1, RP: 5.2 kW	Increase in CO, HC and smoke by 18.9, 8.1 and 12.5% respectively for B50P50 blend	Vallinayagam et al. (2014)
Palm and Jatropha	No. of cylinder 1,4 stroke, AC, DI, CR: 17.5:1, RP: 5.2 hp	Decrease in CO, CO_2 and EGT for the blends Increase in 28% NO_x emissions	Nalgundwar et al. (2016)
Blends of biodiesel and ethanol fuel	No. of cylinder 1,4 stroke, AC, DI, CR: 18:1	Increase in CO_2 for BE20 blend Increase in NO_x for BE20 at lower loads Decrease in CO and SO_2 emission for both fuels	Aydin and Bayindir (2010)

(continued)

Table 8 (continued)

Biodiesel fuel	Engine type	Emission	Source
Eucalyptus biodiesel/natural gas	No. of cylinder 1,4 stroke, AC, DI, CR:18:1, RP: 4.5 kW	Increase in UHC and CO for biodiesel Decrease in NO_x and CO_2 for dual fuel mode Decrease in PM for dual fuel mode at full load	Tarabet et al. (2014)
Diesel-biodiesel-bioethanol emulsions	No. of cylinder 1,4 stroke, AC, DI, RP: 7.08 kW	Increase in NO_x for the blends at lower and high speed Decrease in CO and CO_2 for all the blends	Tan et al. (2017)
Kutkura (Meyna spinosa Roxb. Ex.) fruit seed oil	No. of cylinder 1,4 stroke, WC, DI, CR: 18:1, RP: 3.5 kW	Decrease in Smoke emission for the blended fuels	Kakati and Gogoi (2016)

September of 2020, with the renewal of the U.S. tax credit for biodiesel and European based biodiesel on equal footing with U.S. made fuel. The focus issue of COP 22 in Marrakechwas, Morocco, on 7–18 November 2016 were:

- Scarcity, cleanliness, and water-related sustainability.
- Greenhouse emission reduction utilizing low-carbon energy sources (UNCC, 2016).

Biofuel blend mandates and financial incentives policies were adopted throughout 2016 overcoming debates related to production and sustainability concerns for transport sector in Argentina, India, Malaysia, Panama, Zimbabwe, United States, and Denmark's advanced biofuels mandate (USDA, EU-28 2016).

10 Conclusion

As the worlds primary energy demand has grown around 1.8% since 2011, there is an urgent need for changes for a reduction in global warming. The communities are emphasizing for a eco-friendly development. Transportation sector is among the leader in polluting the environment by releasing the Greenhouse gases. The conventional fuels, especially diesel, left for around 150 years from now need to be replaced by diesel. The recent researches have shown substantial reductions in unburned hydrocarbons (67% lower), carbon monoxide (48% lower than that of diesel), particulate matter (47% lower) and smog-forming is 50% less than diesel fuel. Biodiesel eliminates sulfur oxides and sulfates (major components of acid rain) and NO_x emissions from biodiesel increase (nearly 10%). The above reductions are welcomed as the human health is of prime concern. The policies nowadays are being framed keeping in mind of not letting the temperature rise beyond 2 °C by the end of this century.

References

Adewale P, Dumont MJ, Ngadi M (2015) Enzyme-catalyzed synthesis and kinetics of ultrasonic-assisted biodiesel production from waste tallow. Ultrason Sonochem 27:1–9

Adewale K, Olabisi O (eds) (2016) Handbook of thermoplastics, vol 41. CRC press

African Biodiversity Network (ABN) (2010) Biofuels: a failure for Africa. The Ethiopian Society for Consumer Protection, and the Gaia Foundation

Agarwal AK (2007) Biofuels (alcohols and biodiesel) applications as fuels for internal combustion engines. Prog Energy Combust Sci 33(3):233–271

Agarwal BK (2013) X-ray spectroscopy: an introduction, vol 15. Springer

Aliyu S, Bala M (2011) Brewer's spent grain: a review of its potentials and applications. Afr J Biotechnol 10(3):324–331

An H, Yang WM, Maghbouli A, Li J, Chou SK, Chua KJ (2013) Performance, combustion and emission characteristics of biodiesel derived from waste cooking oils. Appl Energy 112:493–499

Anand BP, Saravanan CG, Srinivasan CA (2010) Performance and exhaust emission of turpentine oil powered direct injection diesel engine. Renew Energy 35:1179–1184

Anuar MR, Abdullah AZ (2016) Ultrasound-assisted biodiesel production from waste cooking oil using hydrotalcite prepared by combustion method as catalyst. Appl Catal A General 514:214–223

Augustine A, Marimuthu L, Muthusamy S (2012) Performance and evaluation of DI diesel engine by using preheated cottonseed oil methyl ester. Proc Eng 38:779–790

Avhad MR, Marchetti JM (2015a) A review on recent advancement in catalytic materials for biodiesel production. Renew Sustain Energy Rev 50:696–718. https://doi.org/10.1016/j.rser.2015.05.038

Avhad MR, Marchetti JM (2015b) A review on recent advancement in catalytic materials for biodiesel production. Renew Sustain Energy Rev 50:696–718

Aydin H, Bayindir H (2010) Performance and emission analysis of cottonseed oil methyl ester in a diesel engine. Renew Energy 35(3):588–592

Azcan N, Danisman A (2007) Alkali catalyzed transesterification of cottonseed oil by microwave irradiation. Fuel 86:2639–2644

Azcan N, Yilmaz O (2013) Microwave assisted transesterification of waste frying oil and concentrate methyl ester content of biodiesel by molecular distillation. Fuel 104:614–619

Barnard TM, Leadbeater NE, Boucher MB, Stencel LM, Wilhite BA (2007) Continuous-flow preparation of biodiesel using microwave heating. Energy Fuels 21:1777–1781

Baskar G, Aiswarya R (2016) Trends in catalytic production of biodiesel from various feedstocks. Renew Sustain Energy Rev 57:496–504

Berrios M, Martín MA, Chica AF, Martín A (2010) Study of esterification and transesterification in biodiesel production from used frying oils in a closed system. Chem Eng J 160(2):473–479

Birla A, Singh B, Upadhyay SN, Sharma YC (2012) Kinetics studies of synthesis of biodiesel from waste frying oil using a heterogeneous catalyst derived from snail shell. Bioresour Technol 106:95–100

Bhuiya MMK, Rasul MG, Khan MMK, Ashwath N, Azad AK (2016) A prospects of 2nd generation biodiesel as a sustainablefuel—Part: 1 selection of feedstocks, oil extraction techniques and conversion technologies. Renew Sustain Energy Rev 55:1109–1128

Boon-anuwat NN, Kiatkittipong W, Aiouache F, Assabumrungrat S (2015) Process design of continuous biodiesel production by reactive distillation: comparison between homogeneous and heterogeneous catalysts. Chem Eng Process: Process Intensification 92:33–44

Bokhari A, Chuah LF, Suzana Y, Ahamd J, Shamsuddin MR, Teng MK (2015) Microwave-assisted methyl esters synthesis of Kapok (*Ceiba pentandra*) seed oil: parametric and optimization study. Biofuel Res J 7:281–287

Bokhari A, Chuah LF, Yusup S, Klemeš JJ, Kamil RNM (2016a) Optimisation on pretreatment of rubber seed (*Hevea brasiliensis*) oil via esterification reaction in a hydrodynamic cavitation reactor. Bioresour Technol 199:414–422

Bokhari A, Chuah LF, Yusup S, Klemeš JJ, Akbar MM, Kamil RNM (2016b) Cleaner production of rubber seed oil methyl ester using a hydrodynamic cavitation: optimisation and parametric study. J Clean Prod. https://doi.org/10.1016/j.jclepro.2016.04.091

Bryant ST, Romijn HA (2014) Not quite the end for Jatropha? Assessing the financial viability of biodiesel production from Jatropha in Tanzania. Energy Sustain Dev 23:212–219

Caldas SS, Rombaldi C, de Oliveira Arias JL, Marube LC and Primel EG (2016) Multi-residue method for determination of 58 pesticides, pharmaceuticals and personal care products in water using solvent demulsification dispersive liquid–liquid microextraction combined with liquid chromatography-tandem mass spectrometry. Talanta 146:676–688

Canakci M, Gerpen JV (2001) Biodiesel production from oils and fats with high free fatty acids. Trans ASAE 44:1429–1436

Carriquiry M, Dong F, Du X, Elobeid A, Fabiosa JF, Chavez Ed, Pan S (2010) World market impacts of high biofuel use in the European Union. Center for Agricultural and Rural Development, Iowa State University

Chapuis A, Blin J, Carré P, Lecomte D (2014) Separation efficiency and energy consumption of oil expression using a screw-press: the case of *Jatropha curcas* L. seeds. Ind Crops Prod 52:752–761

Chen Y, Cheng JJ Creamer KS (2008) Inhibition of anaerobic digestion process: a review. Bioresour Technol 99(10):4044–4064

Chen KS, Lin YC, Hsu KH, Wang HK (2012) Improving biodiesel yields from waste cooking oil by using sodium methoxide and a microwave heating system. Energy 38(1):151–156

Chen G, Shan R, Shi J, Yan B (2014) Ultrasonic-assisted production of biodiesel from transesterification of palm oil over ostrich eggshell-derived CaO catalysts. Bioresour Technol 171:428–432

Chen F, Dua X, Zu Y, Yang L, Wang F (2016) Microwave-assisted method for distillation and dual extraction in obtaining essential oil, proanthocyanidins and polysaccharides by one-pot process from Cinnamomi Cortex. Sep Purif Technol 164:1–11

Chhetri AB, Watts KC, Islam MR (2008) Waste cooking oil as an alternate feedstock for biodiesel production. Energies 1:3–18

Chuah LF, Yusup S, Abd Aziz AR, Bokhari A, Abdullah MZ (2016) Cleaner production of methyl ester using waste cooking oil derived from palm oleinusing a hydrodynamic cavitation reactor. J Clean Prod 112:4505–4514

Clark ID, Fritz P (2013) Environmental isotopes in hydrogeology. CRC press

Daho T, Vaitilingom G, Ouiminga SK, Piriou B, Zongo AS, Ouoba S (2013) Influence of engine load and fuel droplet size on performance of a CI engine fueled with cottonseed oil and its blends with diesel fuel. Appl Energy 111:1046–1053

Darnoko D, Cheryan M (2000) Kinetics of palm oil transesterification in a batch reactor. J Am Oil Chem Soc 77(12):1263–1267

Darzins A, Pienkos P, Edye L (2010) Current status and potential for algal biofuels production. A report to IEA bioenergy task 39. Commercializing 1st and 2nd generation liquid biofuels from biomass

Deng X, Fang Z, Liu Yh (2010) Ultrasonic transesterification of Jatropha curcas L. oil to biodiesel by a two-step process. Energy Convers Manag 51:2802–2807

Devan PK Mahalakshmi NV (2009) Performance, emission and combustion characteristics of poon oil and its diesel blends in a DI diesel engine. Fuel 88(5):861–867

Dorado MP, Ballesteros E, López FJ Mittelbach M (2004) Optimization of alkali-catalyzed transesterification of Brassica C arinata oil for biodiesel production. Energ Fuel 18(1):77–83

Doyle AM, Albayati TM, Abbas AS, Alismaeel DT (2016) Biodiesel production by esterification of oleic acid over zeolite Y prepared from kaolin. Renew Energy 97:19–23

Dwivedi G, Sharma MP (2015) Application of Box–Behnken design in optimization of biodiesel yield from Pongamia oil and its stability analysis. Fuel 145:256-262, Energy 38:151e156

EASAC (2012) Sustainable biofuels

EL Kasaby M, Nemitallah MA (2013) Experimental investigations of ignition delay periodand performance of a diesel engine operated with Jatropha oil biodiesel. Alex Eng J 52:141–149

El Sherbiny SA, Refaat AA, El Sheltawy ST (2010) Production of biodiesel using the microwave technique. J Adv Res 1:309–314

Encinar JM, Gonzalez JF, Rodriguez-Reinares (2005) A biodiesel from used frying oil: variables affecting yield and characteristics of the biodiesel. Ind Eng Chem Res 44:5491–5499

Fadhil AB, Aziz AM, Al-Tamer MH (2016) Biodiesel production from Silybum marianum L. seed oil with high FFA content using sulfonated carbon catalyst for esterification and base catalyst for transesterification. Energ Convers Manage 108:255–265

Galadima A, Muraza O (2014) Biodiesel production from algae by using heterogeneous catalysts: a critical review. Energy 78:72–83. https://doi.org/10.1016/j.energy.2014.06.018

Ghayal D, Pandit AB, Rathod VK (2013) Optimization of biodiesel production in a hydrodynamic cavitation reactor using used frying oil. Ultrason Sonochem 20:322–328

Godiganur S, Murthy CHS, Reddy RP (2009) 6BTA 5.9 G2-1 Cummins engine performance and emission tests using methyl ester mahua (*Madhuca indica*) oil/diesel blends. Renew Energy 34:2172–2177

Godiganur S, Srikanth HV, Venkatesh J, Venkateswaran S, Manne B (2017) Biobased diluents improve cold flow properties of dairy washed milk-scum biodiesel. Renew Energ 111:168–174

Gogate PR (2008) Cavitational reactors for process intensification of chemical processing applications: a critical review. Chem Eng Process Process Intensif 47:515–527

Gogoi P, Bhattacharyya DK, Borah B, Kalita JK (2011) A survey of outlier detection methods in network anomaly identification. Comput J 54(4):570–588

Gole VL, Naveen KR, Gogate PR (2013) Hydrodynamic cavitation as an efficient approach for intensification of synthesis of methyl esters from sustainable feedstock. Chem Eng Process Process Intensif 71:70–76

Gopal KN, Pal A, Sharma S, Samanchi C, Sathyanarayanan K, Elango T (2014) Investigation of emissions and combustion characteristics of a CI engine fueled with waste cooking oil methyl ester and diesel blends. Alex Eng J 53:281–287

Guldhe A, Singh P, Ansari FA, Singh B, Bux F (2017) Biodiesel synthesis from microalgal lipids using tungstated zirconia as a heterogeneous acid catalyst and its comparison with homogeneous acid and enzyme catalysts. Fuel 187:180–188

Gumus M (2008) Evaluation of hazelnut kernel oil of Turkish origin as alternative fuel in diesel engines. Renew Energy 33:2448–2457

Guo Y, Yeh T, Song W, Xu D, Wang S (2015) A review of bio-oil production from hydrothermal liquefaction of algae. Renew Sustain Energy Rev 48:776–790

Hanis S, Abdullaha YS, Hanis N, Hanapia M, Azida A, Umara R, Juahira H, Khatoon H, Enduta A (2017) A review of biomass-derived heterogeneous catalyst for a sustainable biodiesel production. Renew Sustain Energy Rev 70:1040–1051

Issariyakul T, Dalai AK (2012) Comparative kinetics of transesterification for biodiesel production from palm oil and mustard oil. Can J Chem Eng 90(2):342–350

Jain AK (2010) Data clustering: 50 years beyond K-means. Pattern Recognit Lett 31(8):651–666

Ji J, Wang J, Li Y, Yu Y, Xu Z (2006) Preparation of biodiesel with the help of ultrasonic and hydrodynamic cavitation. Ultrasonics 44:411–414

Jindal S, Nandwana BP, Rathore NS, Vashistha V (2010) Experimental investigation of the effect of compression ratio and injection pressure in a direct injection diesel engine running on Jatropha methyl ester. Appl Therm Eng 30:442–448

Kakati J, Gogoi TK (2016) Biodiesel production from Kutkura (Meyna spinosa Roxb. Ex.) fruit seed oil: its characterization and engine performance evaluation with 10% and 20% blends. Energy Convers Manag 121:152–61

Karabektas M, Ergen G, Hosoz M (2008) The effects of preheated cottonseed oil methyl ester on the performance and exhaust emissions of a diesel engine. Appl Therm Eng 28:2136–2143

Karmee SK, Mahesh P, Ravi R, Chadha A (2004) Kinetic study of the base-catalyzed transesterification of monoglycerides from pongamia oil. J Am Oil Chem Soc 81(5):425–430

Karthikeyan R, Nallusamy N, Alagumoorthi N, Elangovan V (2010) A detailed experi-mental investigation on hot air assisted turpentine direct injected compression ignition engine. Int J Eng Sci Technol 2:5034–5049

Kelkar MA, Gogate PR, Pandit AB (2008) Intensification of esterification of acids for synthesis of biodiesel using acoustic and hydrodynamic cavitation. Ultrason Sonochem 15:188–194

Khemthong P, Luadthong C, Nualpaeng W, Changsuwan P, Tongprem P, Viriyaempikul N, Faungnawakij K (2012) Industrial eggshell wastes as the heterogeneous catalysts for microwave-assisted biodiesel production. Catal Today 190:112–116

Kitakawa NS, Hiromori K, Ihara T, Nakashima K, Yonemoto T (2015) Production of high quality biodiesel from waste acid oil obtained duringedible oil refining using ion-exchange resin catalysts. Fuel 139:11–17

Koberg M, Abu-Much R, Gedanken A (2011) Optimization of bio-diesel production from soybean and wastes of cooked oil: combining dielectric microwave irradiation and a SrO catalyst. Bioresour Technol 102:1073–1078

Konwar LK, Boro J, Deka D (2014) Review on latest developments in biodiesel production using carbon-based catalysts. Renew Sustain Energy Rev 29:546–564

Kostić MD, Veličković AV, Joković NM, Stamenković OS, Veljković VB (2016) Optimization and kinetic modeling of esterification of the oil obtained from waste plum stones as a pretreatment step in biodiesel production. Waste Manag 48:619–629

Kumar R, Ravi Kumar G, Chandrashekar N (2011) Microwave assisted alkali catalyzed transesterification of *Pongamia pinnata* seed oil for biodiesel production. Bioresour Technol 102:6617–6620

Kumar S, Cho JH, Park J, Moon I (2013) Advances in diesel–alcohol blends and their effects on the performance and emissions of diesel engines. Renew Sustain Energy Rev 22:46–72

Kusdiana D, Saka S (2001) Kinetics of transesterification in rapeseed oil to biodiesel fuel as treated in supercritical methanol. Fuel 80(5):693–698

Lahane S, Subramanian KA (2015) Effect of different percentages of biodiesel–diesel blends on injection, spray, combustion, performance, and emission characteristics of a diesel engine. Fuel 139:537–545

Lam SJ, O’Brien-Simpson NM, Pantarat N, Sulistio A, Wong EH, Chen YY, Lenzo JC, Holden JA, Blencowe A, Reynolds EC, Qiao GG (2016) Combating multidrug-resistant gram-negative bacteria with structurally nanoengineered antimicrobial peptide polymers. Nat Microbiol 1(11):16162

Lenin AH, Ravi R, Arumugham S, Thyagarajan K (2012) Performance, emission and combustion evaluation of diesel engine using methyl esters of mahua oil. Int J Environ Sci 3:639–649

Lertsathapornsuk V, Pairintra R, Aryusuk K, Krisnangkura K (2008) Microwave assisted in continuous biodiesel production from waste frying palm oil and its performance in a 100 kW diesel generator. Fuel Process Technol 89:1330–1336

Likozar B, Levec J (2014a) Effect of process conditions on equilibrium, reaction kinetics and mass transfer for triglyceride transesterification to biodiesel: experimental and modeling based on fatty acid composition. Fuel Process Technol 122:30–41

Likozar B, Levec J (2014b) Transesterification of canola, palm, peanut, soybean and sunflower oil with methanol, ethanol, isopropanol, butanol and tert-butanol to biodiesel: modelling of chemical equilibrium, reaction kinetics and mass transfer based on fatty acid composition. Appl Energ 123:108–120

Likozar B, Pohar A, Levec J (2016) Transesterification of oil to biodiesel in a continuous tubular reactor with static mixers: Modelling reaction kinetics, mass transfer, scale-up and optimization considering fatty acid composition. Fuel Process Technol 142:326–336

Lin Y, Wu YG, Chang CT (2007) Combustion characteristics of waste-oil produced biodiesel/diesel fuel blends. Fuel 86:1772–1780

Lin YC, Hsu KH, Lin JF (2014) Rapid palm-biodiesel production assisted by a microwave system and sodium methoxide catalyst. Fuel 115:306–311

Liu W, Yin P, Liu X, Chen W, Chen H, Liu C, Qu R, Xu Q (2013) Microwave assisted esterification of free fatty acid over a heterogeneous catalyst for biodiesel production. Energy Convers Manag 76:1009–1014

Lu X, Wang P, Niyato D, Kim DI, Han Z (2015) Wireless networks with RF energy harvesting: a contemporary survey. IEEE Commun Surv Tutor 17(2):757–789

Ma F, Hanna MA (1999) Biodiesel production: a review. Bio Resour Technol 7:01–15

Maddikeri GL, Pandit AB, Gogate PR (2013) Ultrasound assisted interesterification of waste cooking oil and methyl acetate for biodiesel and triacetin production. Fuel Process Technol 116:241–249

Maddikeri GL, Gogate PR, Pandit AB (2014) Intensified synthesis of biodiesel using hydrodynamic cavitation reactors based on the interesterification of waste cooking oil. Fuel 137:285–292

Maghami M, Sadrameli SM, Ghobadian B (2015) Production of biodiesel from fishmeal plant waste oil using ultrasonic and conventional methods. Appl Therm Eng 75:575–579

Maity SK (2015) Opportunities, recent trends and challenges of integrated biorefinery: PartII. Renew Sustain Energy Rev 43:1446–1466

Makareviciene V, Lebedevas S, Rapalis P, Gumbyte M, Skorupskaite V, Zaglinskis J (2014) Performance and emission characteristics of diesel fuel containing microalgae oil methyl esters. Fuel 120:233–239

Manh DV, Chen YH, Chang CC, Chang MC, Chang CY (2011) Biodiesel production from Tung oil and blended oil via ultrasonic transesterification process. J Taiwan Inst Chem Eng 42:640–644

Marchetti JM (2010) Biodiesel production technologies, 1st edn. Nova Science publisher Inc., NewYork

Marchetti JM (2012) A summary of the available technologies for biodiesel production based on a comparison of different feedstock's properties. Process Safe Environ Prot 90:157–163. https://doi.org/10.1016/j.psep.2011.06.010

Martinez-Guerra E, Gude VG (2014) Transesterification of used vegetable oil catalyzed by barium oxide under simultaneous microwave and ultrasound irradiations. Energy Convers Manag 88:633–640

Mazubert A, Taylor C, Aubin J, Poux M (2014) Key role of temperature monitoring in interpretation of microwave effect on transesterification and esterification reactions for biodiesel production. Bioresour Technol 161:270–279

Mbarawa M (2010) The effect of clove oil and diesel fuel blends on the engine performance and exhaust emissions of a compression-ignition engine. Biomass-Bioenergy 34:1555–1561

Moecke EHS, Feller R, dos Santos HA, de Medeiros Machado M, Cubas ALV, de Aguiar Dutra AR, Santos LLV, Soares SR (2016) Biodiesel production from waste cooking oil for use as fuel in artisanal fishing boats: integrating environmental, economic and social aspects. J Clean Prod 135:679–688

Montero G, Stoytcheva M, Coronado M, Garcia C, Cerezo J, Toscano L, Vazquez AM, Leon JA (2015) An overview of biodiesel production in Mexico. In: Biofuels—status and perspective. ISBN: 978-953-51-2177-0

Mootabadi H, Salamatinia B, Bhatia S, Abdullah AZ (2010) Ultrasonic-assisted biodiesel production process from palm oil using alkaline earth metal oxides as the heterogeneous catalysts. Fuel 89:1818–1825

Mrema GC, McNulty PB (1985) Mathematical-model of mechanical oil expression from oilseeds. J Agricult Eng Res 31:361–370. ISSN: 1095-9246

Muralidharan K, Vasudevan D (2011) Performance, emission and combustion characteristics of a variable compression ratio engine using methyl esters of waste cooking oil and diesel blends. Appl Energy 88(11):3959–3968

Nair RR, Wu HA, Jayaram PN, Grigorieva IV, Geim AK (2012) Unimpeded permeation of water through helium-leak–tight graphene-based membranes. Science 335(6067):442–444

Nabi MN, Rahman MM, Akhter MS (2009) Biodiesel from cotton seed oil and its effect on engine performance and exhaust emissions. Appl Therm Eng 29:2265–2270

Nalgundwar A, Paul B, Sharma SK (2016) Comparison of performance and emissions characteristics of DI CI engine fueled with dual biodiesel blends of palm and Jatropha. Fuel 173:172–179

Nan CW, Zhang X, Shen Y, Zhang Q, Gu L, Hu Y, Du J, Lin Y (2015) Ultrahigh energy density of polymer nanocomposites containing $BaTiO_3$@ TiO_2 nanofibers by atomic scale interface engineering. Adv Mater 27(5):819–824

Nautiyal CS (1999) An efficient microbiological growth medium for screening phosphate solubilizing microorganisms. FEMS Microbiol Lett 170(1):265–270

Nithyananda BS, Anand A, Prakash GVN (2013) Experimental investigation of neem and mixed pongamia-coconut methyl esters as biodiesel on C.I engine. Int J Mech Eng Technol 4: 232–242

Nurfitri I, Maniam GP, Hindryawati N, Yusoff MM (2013) Potential of feedstock and catalysts from waste in biodiesel preparation: a review. Energy Convers Manage 74:395–402

Ong HC, Silitonga AS, Masjuki HH, Mahlia TMI, Chong WT, Boosroh MH (2013) Production and comparative fuel properties of biodiesel from non-edible oils: *Jatropha curcas*, *Sterculia foetida* and *Ceiba pentandra*. Energy Convers Manag 73:245–255

Owolarafe OK, Osunlekeb AS, Odejobic OA, Ajadid SO, Faborodea MO (2008) Mathematical modeling and simulation of the hydraulic expression of oil from oil palm fruit. Biosyst Eng 101:331–340. ISSN: 1537-5129

Ozsezen AN, Canakci M (2011) Determination of performance and combustion characteristics of a diesel engine fueled with canola and waste palm oil methyl esters. Energy Convers Manag 52 (1):108–116

Pal A, Verma A, Kachhwaha SS, Maji S (2010) Biodiesel production through hydrodynamic cavitation and performance testing. Renew Energy 35:619–624

Panwar NL, Shrirame HY, Rathore NS, Jindal S, Kurchania AK (2010) Performance evaluation of a diesel engine fueled with methyl ester of castor seed oil. Appl Therm Eng 30:245–249

Paryanto I, Kismanto A, Amri K, Solikhah MD (2017) Some technical aspects for sustainable biodiesel production. Scientific Figure on Research Gate. Available from: https://www.researchgate.net/274082546_fig3_Fig-3-Biodiesel-production-process-via-esterification-followed-by-trans-esterification. Accessed 16 Aug 2017

Paul G, Datta A, Mandal BK (2014) An experimental and numerical investigation of the performance, combustion and emission characteristics of a diesel engine fueled with jatropha biodiesel. Energy Proc 54:455–467

Perin G, Alvaro G, Westphal E, Viana LH, Jacob RG, Lenardão EJ, D'Oca MGM (2008) Transesterification of castor oil assisted by microwave irradiation. Fuel 87:2838–2841

Pradhan RC, Meda V, Rout PK, Naik S, Dalai AK (2010) Supercritical CO_2 extraction of fatty oil from flaxseed and comparison with screw press expression and solvent extraction processes. J Food Eng 98:393–397. ISSN: 0260-8774

Priambodo R, Chen TC, Lu MC, Gedanken A, Liao JD, Huang YH (2015) Novel technology for bio-diesel production from cooking and waste cooking oil by microwave irradiation. Energy Proc 75:84–91

Puhan S, Vedaraman N, Sankaranarayanan G, Ram BVB (2005) Performance and emission study of Mahua oil (madhuca indica oil) ethyl ester in a 4-strokenatural aspirated direct injection diesel engine. Renew Energy 30:1269–1278

Pukale DD, Maddikeri GL, Gogate PR, Pandit AB, Pratap AP (2015) Ultrasound assisted transesterification of waste cooking oil using heterogeneous solid catalyst. Ultrason Sonochem 22:278–286

Purushothaman K, Nagarajan G (2009) Performance, emission and combustion characteristics of a compression ignition engine operating on neat orange oil. Renew Energy 34:242–245

Ramadhas AS, Muraleedharan C, Jayaraj S (2005) Performance and emission evaluation of a diesel engine fueled with methyl esters of rubber seed oil. Renew Energy 30:1789–1800

Rao LNG, Nallusamy N, Sampath S, Rajagopal K (2008) Combustion and emission characteristics of diesel engine fuelled with methyl esters of pungam oil and rice bran oil. Int J Glob Energy Issues 29:314–327

Rao SA, Ajayamohan RS (2008) Indian Ocean dipole modulates the number of extreme rainfall events over India in a warming environment. J Meteor Soc Japan. Ser. II 86(1):245–252

Rabu RA, Janajreh I, Honnery D (2013) Transesterification of waste cooking oil: process optimization and conversion rate evaluation. Energ Convers Manage 65:764–769

Ramezani K, Rowshanzamir S, Eikani MH (2010) Castor oil transesterification reaction: a kinetic study and optimization of parameters. Energy 35(10):4142–4148

Rathore MMU, Paul A, Ahmad A, Chen BW, Huang B, Ji W (2015) Real-time big data analytical architecture for remote sensing application. IEEE Journal Sel Top Appl Earth Obser Remote Sens 8(10):4610–4621

Reyero I, Arzamendi G, Zabala S, Gandía LM (2015) Kinetics of the NaOH-catalyzed transesterification of sunflower oil with ethanol to produce biodiesel. Fuel Process Technol 129:147–155

Salamatinia B, Mootabadi H, Bhatia S, Abdullah AZ (2010) Optimization of ultrasonic-assisted heterogeneous biodiesel production from palm oil: a response surface methodology approach. Fuel Process Technol 91:441–448

Saleh HE (2009) Effect of exhaust gas recirculation on diesel engine nitrogen oxide reduction operating with jojoba methyl ester. Renew Energy 34:2178–2186

Samani BH, Zareiforoush H, Lorigooini Z, Ghobadian B, Rostami S, Fayyazi E (2016) Ultrasonic-assisted production of biodiesel from *Pistacia atlantica* Desfontainia oil. Fuel 168:22–26

Sangeeta MS, Pande M, Rani M, Gakhar R, Sharma M, Rani J, Bhaskarwar AN (2014) Alternative fuels: an overview of current trends and scope for future. Renew Sustain Energy Rev 32: 697–712

Sajjadi SM, Haghighi M, Rahmani F (2015) Sol–gel synthesis of Ni–Co/Al2O3–MgO–ZrO2 nanocatalyst used in hydrogen production via reforming of CH4/CO2 greenhouse gases. J Nat Gas Sci Eng 22:9–21

Sanjid A, Masjuki HH, Kalam MA, Abedin MJ, Rahman SMA (2014) Experimental investigation of mustard biodiesel blend properties, performance, exhaust emis-sion and noise in an unmodified diesel engine. APCBEE Proc 10:149–153

Sanli H, Canakci M, Alptekin E, Turkcan A, Ozsezen AN (2015) Effects of waste frying oil based methyl and ethyl ester biodiesel fuels on the performance, combustion and emission characteristics of a DI diesel engine. Fuel 159:179–187

Savariraj S, Ganapathy T, Saravanan CG (2013) Performance, emission and combustion characteristics of fish-oil biodiesel engine. Eur J Appl Eng Sci Res 2:26–32

Schaufler D, Schaufler R (2013) Small-scale oilseed processing guide. University of Vermont

Selvam T, Machoke A, Schwieger W (2012) Supported ionic liquids on non-porous and porous inorganic materials—a topical review. Appl Catal A: General 445:92–101

Senthil R, Silambarasan R (2015) Annona: a new biodiesel for diesel engine: a comparative experimental investigation. J Energy Inst 88:459–469

Shah MM, Gill KS, Baenziger PS, Yen Y, Kaeppler SM, Ariyarathne HM (1999) Molecular mapping of loci for agronomic traits on chromosome 3A of bread wheat. Crop Sci 39(6):1728–1732

Shahbazi MR, Khoshandam B, Nasiri M, Ghazvini M (2012) Biodiesel production via alkali-catalyzed transesterification of Malaysian RBD palm oil–characterization, kinetics model. J Taiwan Inst Chem Eng 43(4):504–510

Shojaeefard MH, Etgahni MM, Meisami F, Barari A (2013) Experimental investigation on performance and exhaust emissions of castor oil biodiesel from a diesel engine. Environ Technol 34:2019–2026. https://doi.org/10.1080/09593330.2013.777080

Silitonga AS, Masjuki HH, Mahlia TMI, Ong HC, Chong WT (2013) Experimental study on performance and exhaust emissions of a diesel engine fuelled with *Ceiba pentandra* biodiesel blends. Energy Convers Manag 76:828–836

Singh PJ, Khurma J, Singh A (2010) Preparation, characterization, engine performance and emission characteristics of coconut oil based hybrid fuels. Renew Energy 35:2065–2070

Sinha S, Agarwal AK, Garg S (2008) Biodiesel development from rice bran oil: transesterification process optimization and fuel characterization. Energ Convers Manag 49(5):1248–1257

Song Q, Nataraj SK, Roussenova MV, Tan JC, Hughes DJ, Li W, Bourgoin P, Alam MA, Cheetham AK, Al-Muhtaseb SA, Sivaniah E (2012) Zeolitic imidazolate framework (ZIF-8) based polymer nanocomposite membranes for gas separation. Energ Environ Sci 5(8): 8359–8369

Spectec Techno Projects (2010) Private Limited

Stavarache C, Vinatoru M, Nishimura R, Maeda Y (2005) Fatty acids methyl esters from vegetable oil by means of ultrasonic energy. Ultrason Sonochem 12:367–372

Stefan BS, Ionescu M, Voicu G, Ungureanu N, Vladut V (2013) Calculus elements for mechanical presses in oil industry, agricultural and biological sciences. In: Muzzalupo I (ed) Food industry. ISBN 978-953-51-0911-2 (Published: 16 Jan 2013)

Subroto E, Manurung R, Heeres HJ, Broekhuis AA (2015) Mechanical extraction of oil from *Jatropha curcas* L. kernel: effect of processing parameters. Ind Crops Prod 63:303–310

Sureshkumar K, Velraj R, Ganesan R (2008) Performance and exhaust emission characteristics of a CI engine fuelled with *Pongamia pinnata* methyl ester (PPME) and its blends with diesel. Renew Energy 33:2294–2302

Tadele F, Zenebe G, Alem M, Fantu G (2013) Biofuels, economic growth, and the external sector in Ethiopia. Environment for Development

Talebian-Kiakalaieh A, Amin NAS, Mazaheri H (2013) A review on novel processes of biodiesel production from waste cooking oil. Appl Energ 104:683–710

Tamilselvan P, Nallusamy N (2015) Performance combustion and emission characteristics of a compression ignition engine operating on pine oil. Biofuels 6:273–281. https://doi.org/10.1080/17597269.2015.1096152

Tan YH, Abdullah MO, Nolasco-Hipolito C, Zauzi NSA, Abdullah GW (2017) Engine performance and emissions characteristics of a diesel engine fueled with diesel-biodiesel-bioethanol emulsions. Energy Convers Manag 132:54–64

Tarabet L, Loubar K, Lounici MS, Khiari K, Belmrabet T, Tazerout M (2014) Experimental investigation of DI diesel engine operating with eucalyptus biodie-sel/natural gas under dual fuel mode. Fuel 133:129–138

Temelli F, Ciftci ON (2015) Developing an integrated supercritical fluid biorefinery for the processing of grains. J Supercrit Fluids 96:77–85

Tippayawong N, Sittisun P (2012) Continuous-flow transesterification of crude jatropha oil with microwave irradiation. Sci Iran 19:1324–1328

Tubino M, Junior JGR, Bauerfeldt GF (2014) Biodiesel synthesis with alkaline catalysts: a new refractometric monitoring and kinetic study. Fuel 125:164–172

Tuccar G, Ozgur T, Ozcanli M, Aydin K (2011) Prediction of emissions of a diesel engine fueled with soybean biodiesel using artificial neural networks. Energ Educ Sci Technol Part A: Energ Sci Res 27(2):301–312

USDA Foreign Agricultural Services (2016) EU biofuels annual EU biofuels annual

Vallinayagam R, Vedharaj S, Yang WM, Lee PS, Chua KJE, Chou SK (2013) Combustion performance and emission characteristics study of pine oil in a diesel engine. Energy 57:344–351

Vallinayagam R, Vedharaj S, Yang WM, Lee PS, Chua KJE, Chou SK (2014) Pine oil–biodiesel blends: a double biofuel strategy to completely eliminate the use of diesel in a diesel engine. Appl Energy 130:466–473

Varuvel EG, Mrad N, Tazerout M, Aloui F (2012) Experimental analysis of biofuel as an alternative fuel for diesel engines. Appl Energy 94:224–231

Venkatesh Kamath H, Regupathi I, Saidutta MB (2011) Optimization of two step karanja biodiesel synthesis under microwave irradiation. Fuel Process Technol 92:100–105

Verma P, Sharma MP (2016) Review of process parameters for biodiesel production from different feedstocks. Renew Sustain Energy Rev 62:1063–1071

Vujicic D, Comic D, Zarubica A, Micic R, Boskovic G (2010) Kinetics of biodiesel synthesis from sunflower oil over CaO heterogeneous catalyst. Fuel 89(8):2054–2061. Waste cooking oil by using sodium methoxide and a microwave heating system. Waste cooking oil. Fuel 137:285e292

Yang Z, Kumar A, Huhnke RL (2015) Review of recent developments to improve storage and transportation stability of bio-oil. Renew Sustain Energy Rev 50:859–870

Yunus R, Fakhru'l Razi A, Ooi TL, Iyuke SE, Perez JM (2004) Lubrication properties of trimethylolpropane esters based on palm oil and palm kernel oils. Eur J Lipid Sci Technol 106(1):52–60

Zhang Z, Yao X, Zhu H (2010) Potential application of geopolymers as protection coatings for marine concrete: II. Microstructure and anticorrosion mechanism. Appl Clay Sci 49(1–2):7–12

Zhong W, Xuan T, He T, Wang Q, Li D, Zhang X, Yin HY (2016) Experimental study of combustion and emission characteristics of diesel engine with diesel/second-generation biodiesel blending fuels. Energy Convers Manag 121:241–250

Zou C, Zhao Q, Zhang G, Xiong B (2016) Energy revolution: from a fossil energy era to a new energy era. Natural Gas Industry B 3(1):1–11

Thermo-chemical Conversion of Solid Biomass

R. N. Singh and D. Asha

Abstract Due to rapid depletion of natural resources and continuous increase in energy demand, the utilization of biomass has attracted global attention. Biomass being so versatile and scattered in nature in the form of plant-derived and animal-derived. The efficient use of biomass as energy offers certain advantages in terms of energy, environment, economy, and society. In India, about 30% of energy comes from biomass. It can be used for different purposes such as cooking, process heating, electricity generation, steam generation, and mechanical and shaft power applications by using a number of the conversion process. Several technologies are available for biomass conversion such as physical, chemical, thermo-chemical, bio-conversion, etc. However, this chapter focused only on thermo-chemical conversion of solid biomass. Thermo-chemically biomass could be converted to energy by three ways named as Combustion, Gasification, and Pyrolysis. Direct combustion is the most common way of converting biomass to energy in presence of stoichiometric oxygen. Gasification is the partial oxidation process of converting solid biomass into the gaseous fuel. Pyrolysis is the thermal decomposition of biomass in the absence of oxygen. Compared to the other technologies, thermo-chemical primary conversion (gasification, pyrolysis) is the simplest and most developed technology.

Keywords Biomass · Combustion · Gasification · Pyrolysis

Biomass is a biological material derived from living or non-living organisms. In other words, biomass is a natural substance which can store energy during the process of photosynthesis in the presence of sunlight.

Chemically biomass is carbon-based and is composed of a mixture of organic molecules containing hydrogen, oxygen, nitrogen, and small quantities of other atoms. Unbalance chemical formula for biomass is: $CH_{1.44}O_{0.66}$, however, balance formula is $C_{50}H_{72}O_{33}$. It has a wide range of energy content varied from 3100 to

R. N. Singh (✉) · D. Asha
School of Energy & Environmental Studies, Devi Ahilya Vishwavidayala, Indore, India
e-mail: rnsingh.seema@gmail.com

A. Sharma et al. (eds.), *Low Carbon Energy Supply*, Green Energy and Technology,
https://doi.org/10.1007/978-981-10-7326-7_9

Fig. 1 Solid biomass (Singh 2013)

4700 kCal/kg. This wide variation is just because of different range of ash content in biomass. For examples rice husk has ash content about 20%, db however, firewood has only about 2%, db (Fig. 1).

1 Sources of Biomass

Biomass being so versatile and scattered in nature, sufficient database, and documentation are not always available. Still, it could be grouped into two categories; plant-derived biomass and animal-derived biomass. Plant-derived biomass further could be classified as (1) Forestry Biomass (fuel wood, oil, leaves) (2) Agricultural residue such as crop waste (3) Agro-industrial residue such as ground nutshell, rice husk, seed oil cake, etc. Animal-derived biomass includes waste of slaughterhouse, poultry house, aquatic, and marine biomass.

Plant-derived biomass is being called environmental-friendly fuel (Fig. 2), which could be understood easily from Fig. 2. Through a number of the process such as hydrolysis, fermentation, gasification, etc., biomass could be converted into useful industrial products. After application of these products, it would release CO_2 to the atmosphere; however, it would be taken back by the plant with photosynthesis process. Hence, leaves no effect in the atmosphere.

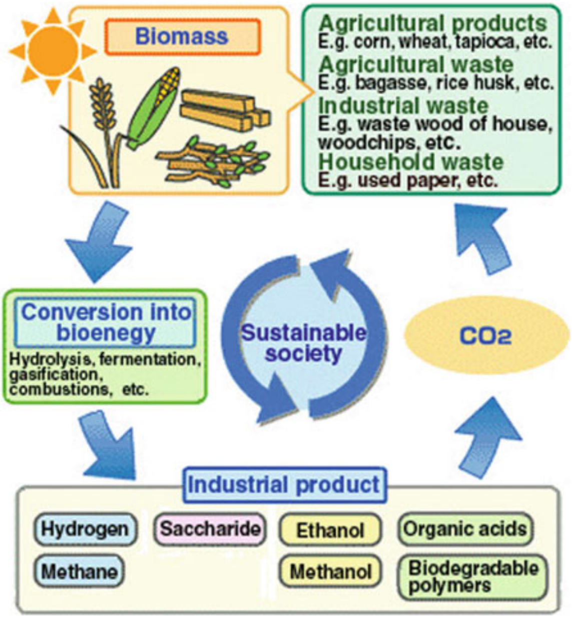

Fig. 2 Biomass-environmental friendly fuel (Singh 2014)

2 Availability of Biomass

Several estimations have been made by the different organization as well researcher. As per one of the estimate made by IISC, Bangalore (Table 1), If only half of the surplus biomass available in the country (Considering the year 2010–11) used for power generation, about 90 million Unit/year or 90000 MW/year electricity could be generated, which is about more than 66% of electrical power demand in India. The electrical power demand of India by March 2013 was 1, 35,453 MW (Energy Statistics 2013). It shows that, if all the surplus biomass used for power generation,

Table 1 Availabilities of biomass in India

Biomass availability estimates (million tons)			
Year	Ravindranath	Biomass atlas IISC, Bangalore	
		Production	Surplus
1996–97	626.5	–	–
1998–99	653.4	546.4	139.4
2004–05	741.0	619.0	157.9
2010–11	840.6	701.2	178.8
2024–25	1127.3	938.0	239.2

Source http://lab.cgpl.iisc.ernet.in/CropReport/Default.aspx. Accessed on 15 Sept 2007

Fig. 3 Burning rice straw in Punjab and Cotton sticks in Gujarat. *Source* Image taken by Author

India need not see any other sources of power generation. Now the question arises if that much potential is available with biomass then why India is not able to utilize it. One of the possible answers is that density of biomass is extremely poor and it is always in scatter nature. Resulting in worst collection economic and further processing to make it useable product. Therefore in India, it is being burnt in the field itself (Fig. 3). By burning the biomass in the field, we are inviting risk for our health apart from losing the energy content of biomass. As the ambient aerosol after burning of biomass consists of particulate matter of size normally 0.01 µm, which would never settle down on the earth and during breathing it will enter in our respiratory system and may have deposited on lungs. Therefore result in blockage of airflow in parts of lungs, a collection of fluid around the lungs or the spread of tumor throughout the lungs and causes many respiratory diseases. However, the particulates having size more than 100 µm generally do not remain suspended in the air for sufficient length of time; hence do not have sufficient impact on human health.

3 Uses of Biomass

In India, about 30% of energy comes from biomass. It can be used for different purposes such as cooking, process heating, electricity generation, steam generation and mechanical and shaft power applications using Biomass Conversion Process. Such as Physical (Chopping, shredding, pulverizing & densification/briquetting); Thermo-chemical (Combustion, Pyrolysis, Gasification, Liquefaction and Ammonia production); Chemical (Acid Hydrolysis, trans-esterification); Bio-conversion (Anaerobic digestion, Ethanol fermentation and composting), etc. However, this chapter only focuses on thermo-chemical conversion of solid

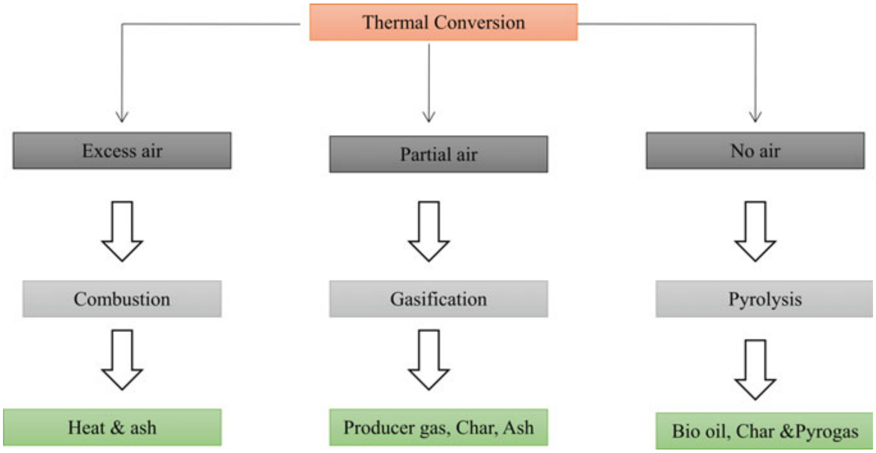

Fig. 4 Thermo-chemical conversion of biomass

biomass. Thermo-chemically biomass could be converted to energy through Combustion, Gasification, and Pyrolysis. The potential ability of thermal routes to accept a wider range of biomass feedstocks than biological/bio-conversion routes. These routes can use lingo-cellulosic (woody) feedstocks, and wastes, which cannot be converted by current biofuel production technologies. The resource availability of these feedstocks is very large. Basically, in thermal routes biomass decomposed due to heat and energy and some by-product is obtained at the end of the process. It can be done by three ways, i.e., by Combustion, Gasification, and Pyrolysis (Fig. 4).

3.1 Combustion

Technically when biomass oxidized in presence of stoichiometric oxygen (oxygen required for complete degradation of biomass) at the end of the process, hot combustion products (CO_2 and Water) are obtained. Direct combustion is the most common way of converting biomass to energy—both heat and electricity. Worldwide it already provides over 90% of the energy generated from biomass.

Compared to the other thermo-chemical primary conversion technologies (gasification, pyrolysis), it is the simplest and most developed technology. Apart from that biomass combustion systems can easily be integrated with existing infrastructure. Basically, three combustion technologies named as fixed-bed combustion systems, Fluidized bed combustion systems, and Pulverized fuel are commercially available in the markets. In fixed-bed combustion systems (Fig. 5a, b), primary air supplied below the grate, and initial combustion of solid fuel takes place on the grate and some gasification occurs. To improve the

Fig. 5 **a** Fixed-bed combustion of biomass (Singh 2014), **b** fixed-bed combustion (Singh 2008) Fig. 5, **c** metal cook stove (Singh 2017)

combustion efficiency, modern combustors have provision for the supply of primary and secondary air. Secondary air takes to care for combustion of gaseous fuel generated during combustion. For example Combustion, studies of Mahua shell and husk were carried out in the metal cook stove (Fig. 5c), which has provision for secondary air. It increases the thermal efficiency of fuel about 30% (Singh 2015). The combustible gases produced are burned after secondary air addition has taken place, usually in a combustion zone separated from the fuel bed.

However, in fluidized bed combustion system, a bed of an inert mineral such as sand or limestone is created through which air is blown from below the grate. The air is pumped through the bed in sufficient volume and at a high enough pressure to entrain the small particles of the bed material so that they behave much like a fluid.

Although combustion is very old technology, however, its efficiency is very poor (ranges from 10–35%). Apart from that its application is also limited.

3.2 Gasification

Gasification is nothing but the thermo-chemical conversion of solid biomass into a gaseous fuel usually known as producer gas (consisting of a mixture of CO, CO_2, N_2, CH_4, and H_2), which takes place under a sub-stoichiometric air supply condition. Generally, the requirement of air for gasification is one-third or less than that of stoichiometric air of biomass (Table 2). The producer gas production process is known as gasification and the equipment used to obtain this gas is known as a gasifier. Since air is used as an oxidizing medium to get the producer gas, thus energy content of producer gas is very very less 1000–1200 kCal/Nm^3. However, this gas burnt with high efficiency at about 800–900 °C temperatures if complete combustion takes place. Generally one kg biomass (10–15% moisture) produce about 2.5–3.0 Nm^3 of producer gas. The thermal conversion efficiency of the gasification process is in the range of 70–80%.

Gasification produces either producer gas or syngas, depending on the source of oxidizing media used. If air is used as a gasification agent, the products are diluted with nitrogen (as air has 79% nitrogen by volume) and gasifier generates producer gas (Table 3). However, if pure oxygen is used as a gasification agent, syngas is produced, which is rich in hydrogen and carbon monoxide. This syngas can be used as a feedstock for ethanol, methanol, naphtha, hydrogen, acetic acid, di-methyl ether, and ammonia. Syngas and producer gas can be co-fired with natural gas in conventional turbines and fuel cells or co-fired in coal-fired boilers to generate

Table 2 Requirements of air for complete combustion of biomass and its derivative

S. No.	Biomass and its derivative	Air requirement
1	Air ratio required for gasification	2.38 kg air/kg of wood
2	Air ratio required for producer gas combustion	1.15 kg air/kg of P gas
3	Air ratio required for total combustion of biomass	6.27 kg air/kg of wood

Table 3 Composition of producer gas

S. No.	Component	Percentage composition by volume
1	Carbon monoxide, CO	18–21
2	Carbon dioxide, CO_2	8–10
3	Hydrogen, H_2	14–16
4	Methane, CH_4	1–4
5	Nitrogen	50–55
6	Water vapor	4–5

electricity. Gaseous fuels can be distributed by pipeline from a gasification plant for direct use in other locations. An important advantage of gasification compared to combustion is its potential to achieve higher efficiencies (more than 75%) and lower emissions. The efficiency of a biomass-fired steam turbine system is between 20 and 25%. However, syngas-fueled engines and turbines can achieve system efficiencies in the range of 30–40%.

3.3 Applications of Producer Gas

Once you get producer gas, numbers of application are possible such as

- Thermal applications: Cooking, water boiling, steam generation, drying, etc.
- Motive power applications: Using producer gas as a fuel in Internal Combustion (IC) engines for applications such as water pumping
- Electricity generation: Electricity could be generated using producer gas in a dual-fuel mode in diesel engines or 100% producer gas in spark ignition engines.

4 Thermal Applications of Producer Gas

4.1 Gasifier-based dyeing unit

Dyeing industries need hot water, which could be easily mated by application of producer gas. By doing about 50% firewood consumption could be reduced. Apart from that, we can have good control of the “liquor temperature”. Biomass briquettes can also be used as fuel. It will replace petroleum fuels (kerosene, diesel) and have a low cost of CO_2 emissions.

4.2 Gasifier-based rubber drying units

India is the fourth largest producer of natural rubber after Thailand, Indonesia, and Malaysia. A 100 kg/h capacity gasifier could replace electricity/diesel based system used for drying crumb rubber in tunnel dryer and about 30 L diesel could be saved per hour.

4.3 Gasifier-based Namkeen units

Namkeen units used diesel for Namkeen making. In place of diesel, if gasifier system (40 kg/h capacity) is used, it would save diesel of the order of 11 L/h.

In terms of economic benefit, with an initial investment of Rs. 2.75 lakhs, the industry has been able to save Rs. 2400/day which translates into payback of just less than 120 days. It also reduces Green House gas (GHG) emission.

4.4 Gasifier for boiler application in bamboo mat factory

For the making of the bamboo mat, steam is required, which is generally met out from the waste bamboo fired boiler. Application of producer gas in place of waste bamboo fired boiler could a reduction in fuel consumption from 50–60 to 25–30 kg/h. Apart from that no need to continuously manage the fire. It will save time and increased daily production capacity (generally 2 h are required for initial pressure temperature build up).

In general, any thermal application where temperature requirement is up to 800–900 °C, producer gas could be used.

4.5 Types of Gasifier

Basically all the gasifier can be grouped into two categories, Fixed Bed, and Fluidized Bed. Fixed-bed gasifier could be subdivided into three categories, Downdraft, Updraft, and Cross–Draft. This downdraft and, updraft gasifier may be further subdivided as follows

(i) Downdraft as Throat Type and Throat Less
(ii) Updraft as Forced Draft and Natural Draft.

Irrespective of above-said classifications all the gasifier have four zones, names as drying zone (temperature varied from room temperature—160 °C); Pyrolysis zone (temperature varied from 200 to 800 °C); Oxidation zone (temperature varied from 850 to 1200 °C) and finally Reduction zone (temperature varied 900–400 °C). The sequence of these zones may change based upon design as well as operational conditions of the gasifier. Although all the gasifier has four zones, however, their positions are not fixed. It changes based upon the temperature of the reactor. For example, if any gasifier reactor length is 100 cm, then it does not mean that first 25 cm from the top would be drying zone, next 25 cm would be pyrolysis zone; further next 25 cm would be oxidation zone and finally, next 25 cm would be reduction zone. No doubt all four zones would be there, but length/size of the zone would be based upon temperature. Hence different parameter is responsible for sequences of the zone.

5 Downdraft Gasifier

In downdraft gasification process, solid biomass is fed from the top (Fig. 6a, b) and the air/oxygen from the sides, hence the biomass and gases move in the same direction and the gas is collected below the grate. At hearth zone/combustion zone, air is supplied with the help of a blower. The supply of air for gasification is controlled with valve fitted at air entry to the blower (Fig. 6b). At controlled air supply solid biomass, broken down to a combustible gas by the use of heat in an oxygen-starved environment. Heat for gasification is generated through partial combustion of the feed material. The resulting chemical breakdown of the fuel and internal reactions result in a combustible gas usually called "producer gas" (Kaupp and Goss 1984). The main combustible gases are H_2, CO, and CH_4. Overall gasification efficiency of the gasifier depends on a number of parameters such as the design of gasifier, biomass characteristics, size and shape of the biomass and operating parameters. Producer gas obtained using air as an oxidizing medium has a low calorific value about 1000–1200 kCal/Nm^3. However, the calorific value of the gas could be increased using oxygen in place of air as an oxidizing medium. In that case, gas obtained from the gasifier is called as syngas. Downdraft gasifier is more suitable for IC engine application. As here, generated gas from the gasifier has to pass through combustion zone, which has a very high temperature (850–1200 °C). At this high temperature all the impurity present in the gas cracked down and clean gas could be obtained. Typically less than 1% volatile tar-oils are produced in a throat-type downdraft gasifier. However, due to narrow size of the throat (Throat-type downdraft gasifier), smaller and wood biomass is required. Generally, one-sixth size of the throat, biomass size is required. For example, if throat diameter of the gasifier is 60 mm, then only 6 mm size biomass is needed, which makes the processing cost of the biomass very high. To overcome the above-said problems, Throat Less or Open Core downdraft gasifier has been designing and developed (Fig. 6b). The working principle of throat less downdraft gasifier is same as throat-types downdraft gasifier only difference in diameter of the gasifier reactor which, is uniform throughout the reactor. This gives the space for accepting the multi-size of biomass. However, at the same time, we have to compromise with the quality of gas. Gases obtained from throat less or Open Core downdraft gasifier is inferior in quality as compared to throat-type downdraft gasifier.

6 Updraft Gasifier

In Updraft gasifier biomass is fed from the top or side (Fig. 7a, b) while air enters the combustion zone through the grate and flows upward through the bed. The grate is mounted at the base of the gasifier, air reacts with charcoal from biomass to produce very hot CO_2 and H_2O. This CO_2 and H_2O react endothermically with char to form CO and H_2. The ascending, hot, reducing gases pyrolyze the incoming

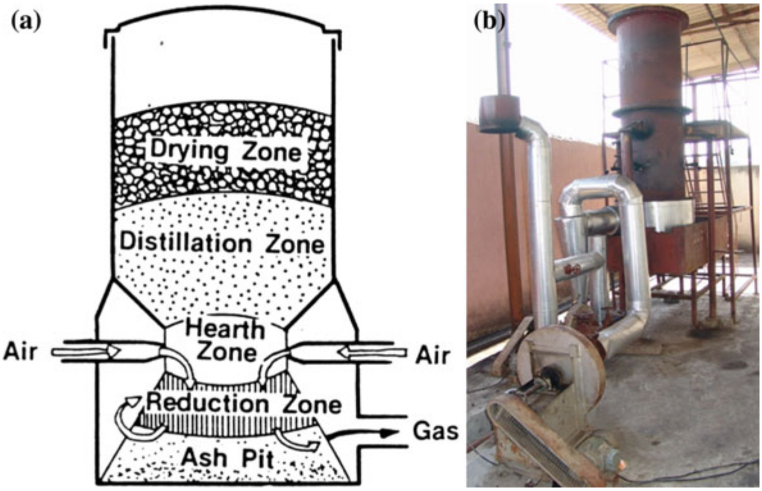

Fig. 6 **a** Throat type (Reed and Das 1988), **b** throat less or open core (Bhoi 2006)

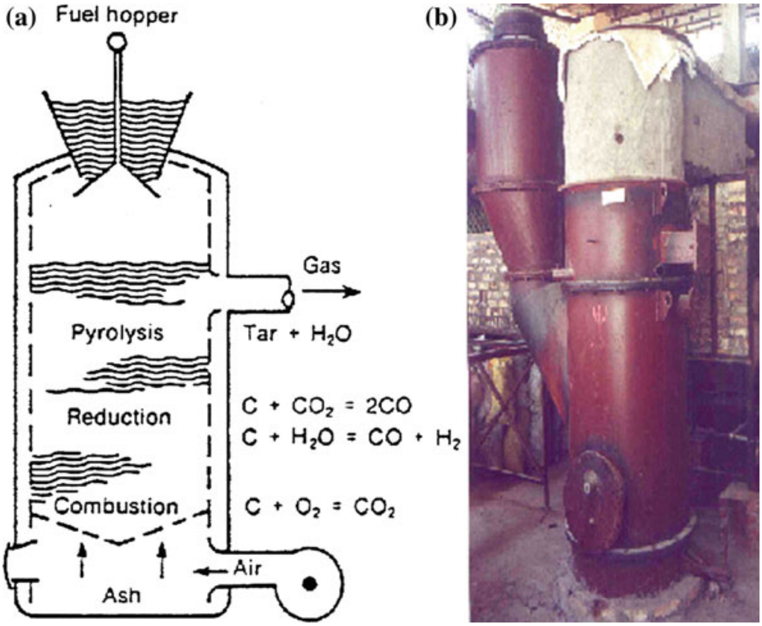

Fig. 7 **a** Forced draft (Reed and Das 1988), **b** natural draft (Patil et al. 2002)

biomass (Shrivastava 2012). Although producer gas has no ash, however, contains a higher quantity of tar and water vapor because of the passing of gas through unburnt biomass. Usually, 5–20% volatile tar-oils are produced in Updraft gasifier. The remaining heat dries the wet biomass so that none of the energy is lost as sensible heat in the gas. The advantage of updraft gasifier over other gasifier is its high conversion efficiency up to 80%. The working principle of the Natural draft gasifier is same as forced draft gasifier only difference is that it operates on chimney effect without electrical input.

7 Cross–Draft Gasifier

This type of gasifier is not so common like Downdraft and Updraft gasifier, because this type of gasifier cannot accept high volatile biomass. Although design of this type of gasifier is very simple, however, it is more suited for charcoal. In this type of gasifier biomass is filled from the top, however supply of air to the gasifier and outlet of gas is almost opposite to each other (Fig. 8). The gas is produced in the horizontal direction in front of the air nozzle and passes through a vertical grate and collected from the opposite side of air supply. Since the combustion zone and gas outlet are closer to each other, thus produced gas have very very less Tar and highly suitable for variable load gas engine (Shrivastava 2012).

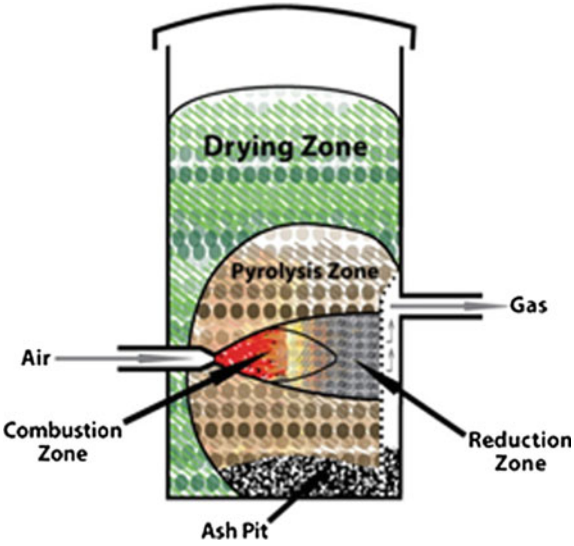

Fig. 8 Cross draft (Shrivastava 2012)

8 Other Gasifier (Modular Gasifier)

The presently used downdraft gasifiers have circular throats, which have to be dimensioned separately for each capacity of design. In addition, these gasifiers have not performed satisfactorily in the size range of more than 250 kg/h. This happens because air cannot travel up to the center of the gasifier system and between the air tuyeres, which creates hot and cold spots inside the gasifier during operation, resulting in incomplete tar cracking and high tar content in the gas. To overcome the above-mentioned problem, a modular throat-type downdraft gasifier having a rectangular throat, with suitably rounded corners to ensure uniform gas flow across the reactor section has been designed (Pathak et al. 2008). In this design, the throat of the gasifier has a square shape (module of 260–260 mm). A larger capacity gasifier can be designed by adding modules in series (Fig. 9), thus yielding the throat of a larger gasifier with a rectangular shape (260–780 mm).

9 Other Gasifier

9.1 Horizontal Gasifier

Horizontal gasifier consists of the horizontally oriented reactor (Fig. 10), grate, producer gas flaring burner as a major component. The gasifier is configured horizontally to increase the particles residence time as opposed to a vertical

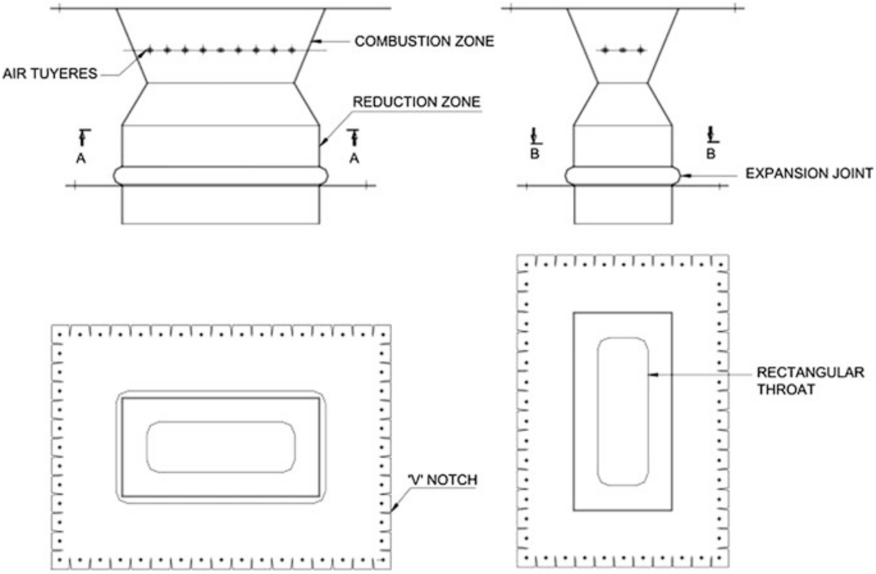

Fig. 9 Modular gasifier (Pathak et al. 2008)

Fig. 10 Horizontal gasifier (Singh et al. 2016)

fixed-bed system, where gravity forces result in lower residence time. Additionally, the enhanced particle to metal surface contact promotes heat transfer to the particle, thus increasing fuel conversion efficiency. Horizontal gasifier producer less tar and particulates matter compared to vertical updraft gasifier.

Basically, in the vertically fixed draft gasifier, biomass moves from upward to downward due to gravity which, sometimes create a problem in proper flow and attract for proper sizing of biomass. Moreover in the existing gasifier thermal zones are fixed, i.e., the residence time in a vertical gasifier is fixed (based on the travel time driven by gravity as the fuel "falls" through the unit), which may sometimes create clinker formation for biomass having higher ash content and again responsible for discontinuation of gasification process. However, vertical gasifier design is simple, requiring few moving parts, and provides ease of control. This design results in high online availability, with the exception of the time required to "clean out" the ash system.

In horizontal gasifier instead of moving the biomass, temperature zone moves (All the gasifier has four-zone named as drying, pyrolysis, reduction, and combustion). Their positions are changing as per the temperature of the gasifier rather than moving the biomass, which overcomes the limitation of vertical updraft gasifier, mainly for bridging of biomass (Singh et al. 2016).

9.2 Two-Stage gasification

All gasification design basically has four zones, namely drying, pyrolysis, combustion, and reduction. In two-stage gasification process, theses four zones are grouped in two stages. In first stage drying and pyrolysis zone reaction is taking place in one reactor; however combustion and reduction takes place in another reactor. Here producer gas produced in one reactor is partially oxidized in another reactor. As a result, due to thermal cracking, most of the tar cracked and increase the energy content of the gas. To enhance the high energy efficiency, the thermal energy present in the producer gas and the exhaust gas is being used for drying, preheating of air and for pyrolysis. The two stage gasification process offers low tar (less than 20 mg/Nm^3) and particulate matter (less than 5 mg/Nm^3).

9.3 Critical Parameters Influencing the Gasifier Performance

Performance of the gasifier depends upon the following parameters named as

- Energy content of fuel
- Fuel moisture content
- Size and shape of fuel
- Size distribution of the fuel
- Bulk density of the fuel
- Volatile matter content of the fuel
- Ash content and chemical composition
- Ultimate analysis of the fuel
- Operating conditions of the gasifier.

9.4 Performance of Gasifier

Generally, the performance of the gasifier is defined in terms of Fuel consumption rate, Specific gasification rate, Specific gas production rate, Equivalence Ratio, Gasification Efficiency, the temperature profile of gasification reactor, Flame temperature, Quantity of gas flow and Calorific value of gas. These parameters should be measured after the stable operation of the system and can be defined as:

Fuel consumption rate (FCR) This is the amount of biomass used in operating the Gasifier divided by the operating time. It could be measured by topping the gasifier after one hour of Continuous operation. Mathematically can be represented as,

$$\text{Fuel consumption rate (FCR), kg/h} = \frac{\text{Weight of biomass used in kg}}{\text{Operating time in hour}}$$

Specific gasification rate (SGR) Specific gasification rate (kg/h-m^2) could be calculated using the weight of biomass for a run, net operating period and the cross-sectional area of the reactor. As per the Kaupp and Goss (1984) for agriculture residues, the specific gasification rate varied in the range of 100–250 kg/h-m^2

$$\text{Specific gasification rate (SGR)} = \frac{\text{Weight of feed material in kg/h}}{\text{Cross-sectional area of the reactor in m}^2}$$

Specific gas production rate: (SGPR) Specific gas production rate (m^3/h-m^2) is the rate of gas production at standard temperature and pressure per unit cross-sectional area of the gasifier. $\text{SGPR} = \frac{\text{Rate of gas production in cum per hour}}{\text{Cross-sectional area of the gasifier in m}^2}$

Gasification Efficiency (*η*) Gasification efficiency is the percentage energy from biomass converted into cold producer gas (free from tar).

$$\text{Gasification efficiency } (\eta) = \frac{\text{Heating value of gas} \times \text{Volume flow rate of gas}}{\text{Heating value of gasifier fuel (Biomass)} \times \text{Fuel consumption rate}} \times 100$$

Temperature profile Temperature profile of gasifier reactor could be measured by using chromel-alumel "K" type and a Platinum rhodium "R" type thermocouple connected with Datalogger/digital temperature indicator. Since the temperature at combustion zones is generally higher, thus here "R" type thermocouple and at other places of the reactor "K" type thermocouple could be used. These thermocouples can be inserted through the probe at a different location above the grate.

Flame temperature The flame temperature could be measured by holding the "K" type thermocouple with digital temperature indicator, temperature attained at burner of different heights in the flame.

The quantity of gas flow (Q_g) Quantity of gas flow could be obtained by multiplying the area of pipe (m^2) through which gas flow with a velocity of gas flow (m/s). Mathematically can be written as $Q_g = A \times Vg$ Where, A is the area of pipe through which gas flow and, Vg is the velocity of gas flow.

Equivalence Ratio (ER) Equivalence ratio is defined as the ratio of oxygen supplied per kg biomass to the stoichiometric requirement. Equivalence ratio fixes the amount of air supplied for gasification. A value of 0.3 ER is the theoretical optimum, however, it may vary from biomass to biomass. As the ER value approaches 1.0 combustion reaction is predominant and as it tends to zero, pyrolysis is the major process.

Total Mass Flow Rate The amount of gas generated through the known amount of biomass was calculated with the help of total mass flow rate equation ($Q = \rho \times A \times V$, whereas ρ (kg/m^3) density, A (m^2) area, V (m/s) velocity).

10 Calorific Value of Gas

The calorific value of gas can be determined by using either Gas chromatograph (GC), or Junkers Gas Calorimeter. Gas chromatography is a technique that is used to separate the components of a substance. The separated material of an amount converts electric signal in the detector in the form of pick (Fig. 11a). The gaseous compounds being analyzed interact with the walls of the column, which is coated with different stationary phases. This causes each compound to pass at a different time, known as the retention time of the compound. The comparison of retention times is what gives GC its analytical usefulness and in terms of pick on the recorder (Fig. 11a). Based on pick area of different gasses, their percentage compositions in unknown calorific value gas are assigned. Caloric values of standard gases such as CO, H_2, CH_4 can be taken as 13.1, 13.2, and 41.2 MJ/m^3 respectively (1 MJ/m^3 $\approx$ 238.8459 kcal/m^3, Reed and Das 1998). Finally multiplying the percentage composition of standard gases with Caloric values and adding them will give the Caloric value of unknown gas.

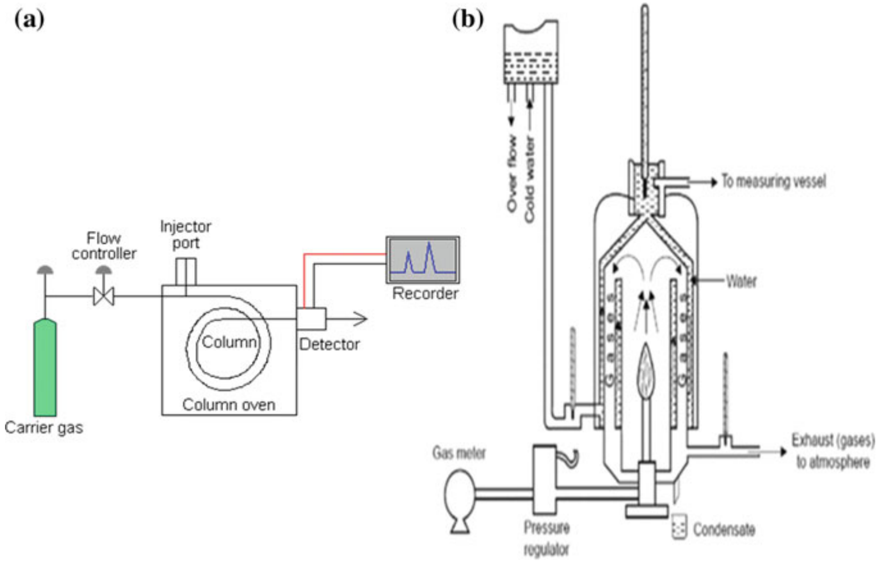

Fig. 11 **a** Gas chromatograph, **b** junkers gas calorimeter

11 Junkers Gas Calorimeter

Junker's gas calorimeter works on the Junker's principle of burning of a known volume of gas and imparting the heat with maximum efficiency to steadily flowing water and finding out of the rise in temperature of a measured volume of water (Fig. 11b). The Calorific Value of Gas = (Volume of water × Rise in Temperature)/Volume of Gas (assuming that heat capacity of water is unity). Mathematically it can be written as $CG_g = (V_w \times \rho_w \times CP_w \times \Delta T)/(V_g \times \rho_g)$.

Where, CG_g is the calorific value of gas, V_w is Volume of water collected in liters, ρ_w is density of water, CP_w is the specific heat of water, ΔT is the change in temperature of water, V_g is the volume of the burnt gas in liters, ρ_g is the density of gas burnt.

12 Properties of Producer Gas for Engine Application

Gas produced from a gasifier has a high temperature (300–450 °C) and contain impurities such as Soot, Ash, Water vapor, and Tar. The range of these impurities present in producer gas varied from the type of gasifier (Table 4). These impurities are present in sub-micron size and must be removed to acceptable levels. Acceptable levels of these impurities depend upon applications. For IC engine particulates matter should be <50 mg/N m^3 and Tar < 100 mg/N m^3. However for turbine application, Tar content in the producer gas should be <5 mg/Nm^3. Failure to remove these impurities may cause excessive wear in the engine component, carbon deposition, the filing of valve and seats and sticky of valves and rings, etc. Apart from above calorific value of producer gas should be more than 1000 kCal/Nm^3. However, it is possible to achieve the acceptable level by using suitable gas cleaning device. Particulates matter could be removed using Cyclone separators, which utilize a centrifugal force generated by a spinning gas stream to separate the particle from the raw gas. A well-designed cyclone can remove more than 95% carbonaceous fly ash particles greater than 10 microns in size.

Table 4 Tar content in different design of gasifier

S. No.	Tar	Fixed bed		Fluidized bed	
		Counter current (updraft)	Co current (downdraft)	Bubbling	Circulating
1	Mean tar content (g/Nm^3)	50	0.5	12	8
2	Tar range (g/Nm^3)	10–150	0.01–6	1–23	1–30

Sources Reed and Das (1998)

Fig. 12 Organic filter (Singh 2007)

However for removal of Tar any wet scrubbing device (such as spray tower, Centrifugal/Cyclone scrubber, Impingement scrubber, packed bed scrubber, Venture scrubber, etc.), thermal cracking or Organic filter could be used.

Organic Filter The main features of the organic filter are: It is a low-cost technology and environmentally friendly, as no waste is generated. The saturated biomass with tar could be reused as a feed to the gasifier. Fresh biomass saturated in 6–7 h. The unit (Fig. 12) consisted of a cylinder having three compartments, one for graded organic biomass like wood scrap, a second compartment for graded sawdust and a third compartment for cotton waste.

Cool gas is passed to the first compartments of the organic filter where moisture and tar were absorbed. From the first compartment, gas passed to the second compartment having sawdust where micron size particle matters were removed. If further any tar and dust are left in the producer gas passed out from first two compartments, are removed in the third compartment, which acted as a security filter.

12.1 Power Generation Using Producer Gas

Using IC engine producer gas could be used for power generation either in Dual—Fuel mode (75–80% producer gas & 20–25% diesel/bio-diesel) or 100% gas mode.

12.2 Working Principle of Dual—Fuel Based CI Engine for Power Generation

Dual-fuel operation combines the possibility of operating a diesel engine on liquid fuels such as diesel/bio-diesel and on gaseous fuels (natural gas, biogas, producer

Fig. 13 Gasifier based CI engine for dual-fuel operation (Singh 2007)

gas, etc.). It works on diesel cycle. Here gaseous fuel (primary fuel) is added to air into the engine or supplied by a supercharger (Fig. 13). The mixture of air and gaseous fuel gets compressed in the cylinder. Liquid fuel called pilot fuel injector near the Top Dead center (TDC) as a source of ignition. Gas–air mixture ignites establishing a number of flames–fronts. Basically in dual-fuel engine combustion also starts similar to Compression Ignition (CI) engine, but it is propagated by flame–fronts as in Spark Ignition (SI) engine.

12.3 Performance of Dual-fuel Engines

Duel fuel engine, produced equal power when operating on liquid fuels as with gaseous fuel. Duel fuel engine is slightly more efficient to conventional diesel engine at full load. However, the maximum output is almost same. The efficiency of dual-fuel engine in part load is slightly poor. Typical diesel engine efficiency is 41% and dual-fuel engine 38.5%.

12.4 Merits and De-Merits of Dual—Fuel Mode Power Generation

Merits

- Efficient utilization of cheap gas available from various sources and gas burns without leaving any residue (no pollution).

- Clean combustion results in reduced wear of engine parts and reduced combustion of lubrication oil.
- Easy for retrofitting with existing diesel engine without any modifications
- Plant availability higher—utility will not suffer due to nonavailability of gasifier
- Economical compared to fossil fuel—diesel.

Demerits

- Duel fuel engine has a tendency of vapor locks while using lighter fuels.
- It has a tendency of increase wear-tear due to the poor quality of gaseous fuel.
- It requires for injecting different volumes of gaseous fuel depending on their heating values and compressibility.
- Expensive cannot compete with State grid electricity.

13 Producer Gas Based Engine

The engine runs through producer gas is mainly sparked ignition engine, however operating conditions mostly based on gas derived from biomass at lower compression ratio (CR) range. Producer gas based engine gives better performance under suitable operating conditions. However due to low energy content (1000–1200 kCal/Nm^3) during operation it is derated about 40–50% and resulting loss of power about 30%. Producer gas has low flame speed as compared to gasoline, therefore improvement need to be made in ignition timing for about 30–40°, which depends on rpm and compression ratio of the engine. In the case of natural gas engine, the mixture of gasoline-air is automatically adjusted through the carburetor as well as controlled by the accelerator. But in case of producer gas based engine it is difficult to maintain as the composition of gas changes drastically over a run of gasifier. At low-speed engine, the producer gas could be used more efficiently.

A spark ignition engine requires very little/no modification to run on P gas. The cold gas efficiency of producer gas in favorable condition can be 70%. In the gasifier-engine system, losses also occur at different stages. Engine performance is expressed in terms of brake thermal efficiency. The overall efficiency of the system is the product of gasifier efficiency and brake thermal efficiency. The actual efficiency of the engine varies with design, size, and running condition. The efficiency of diesel and gasoline engines under the good condition is considered to be 30 and 20% respectively (Fig. 14). The efficiency of engine run with producer gas goes down owing to the lower density of gas–air mixture and other power losses associated with the suction of mixture in engines. Theoretically, gasoline and diesel engine operated on producer gas suffer a power loss of 30 and 20% respectively. In practice, considering a wide range of producer gas quality, a power drop ranging from 25 to 60% can be expected when diesel or gasoline engine is run with producer gas (http://cturare.tripod.com/bio.htm).

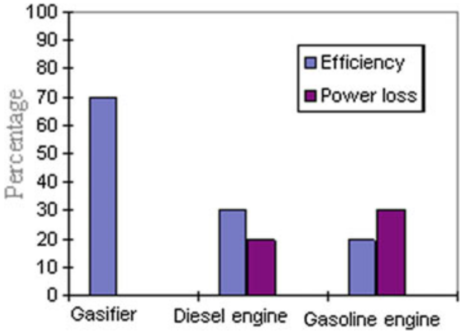

Fig. 14 Theoretical efficiency and power loss in different units of gasifier-engine system. *Source* http://cturare.tripod.com/bio.htm

14 Operational Difference Between Diesel and Gasoline Engine

There is a significant difference between diesel and spark ignition engine system with respect to its suitability for producer gas. In a diesel engine, diesel is injected at the end of the compression stroke and gets ignited immediately without any spark ignition. These will not the case with producer gas–air mixture. In fact, the diesel engine cannot operate alone on producer gas as temperature and pressure are not sufficient to ignite the gas–air mixture. Hence, during the injection of the producer gas mixture, some quantity of diesel is also injected into the combustion chamber.

15 How Producer Gas Engine Different from Natural Gas Engine

The air-to-fuel ratio of Producer gas is 1.1–1.2:1 while in Natural Gas it is 17:1, this identified for a different carburettor. Producer gas can be used in engines with higher compression ratio due to its higher octane rating. Flame speed of producer gas is higher ($\sim 20\%$), identified the setting ignition timing. Derating of the engine power is also observed which is due lower energy density of producer gas ($\sim 20\%$). Producer gas engine need different conditions in the engine cylinder and turbocharger due to lower flame temperature (about 300 K).

16 Merits and Demerits of Producer Gas Based Power Generation System

Merits

- Economically viable and can compete with State grid electricity

- Plant availability reasonably high—provided correct operation practice is adhered to
- Eco-friendly—emission from gasifier meets pollution norms and regulations.

Demerits

- Power Start-up is required were as grid is not available
- Not suitable for application if gas quality is poor (for example: low energy content and high contaminants).

17 Biomass Pyrolysis

Pyrolysis is nothing but the thermal decomposition of biomass occurring in the absence of oxygen. It is the basic chemical reaction which is happen before the combustion and gasification processes and occurs naturally. Pyrolysis of biomass generates three different energy products such as charcoal, bio-oils, and uncondensed pyro-gases in different quantities. The quantity of these products depends upon heating rate and heating temperature of reactor. Several kinds of biomass such as agricultural residues, forest residues, municipal waste, etc., could be used for Pyrolysis. The efficiency of pyrolysis process depends upon particle size of biomass. In the pyrolysis process heat transfer take place from one particle to another particle of biomass thus size of the biomass particle is very important. Pyrolysis may be either fixed-bed pyrolysis or fluidized bed pyrolysis. In fixed-bed pyrolysis, the feed material is fixed, heated at higher temperature (Fig. 15). Generally inert gas such as helium, argon, nitrogen est. is passed in the pyrolysis reactor which helps to disposal of gaseous mixture into the condenser (Asadullah 2014).

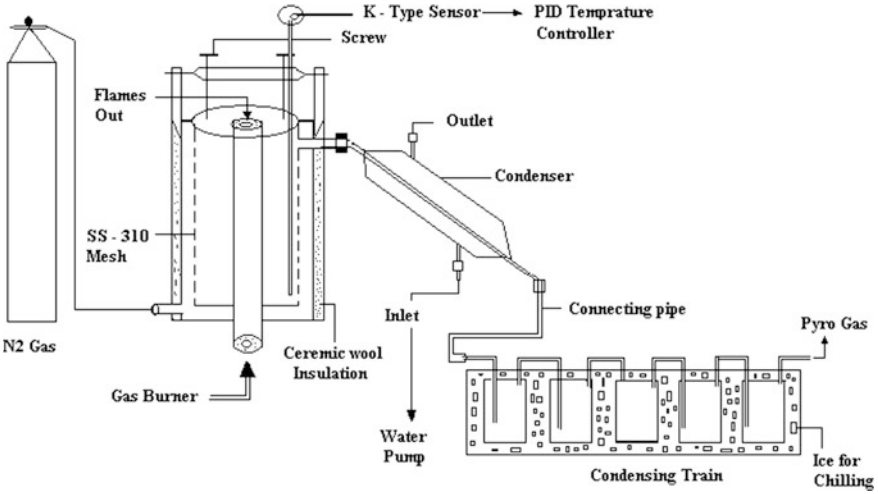

Fig. 15 Schematic of thermally heated Pyrolysis reactor (Chouhan 2010)

17.1 Pyrolysis Classification

Pyrolysis processes can be classified into Slow Pyrolysis, Fast Pyrolysis, and Flash Fast Pyrolysis. The complete thermal decomposition of the feed materials for all categories is based on heating time and heating temperature.

17.2 Slow Pyrolysis

Slow pyrolysis is being used for production of charcoal from a long time. Generally it is done at low temperatures (less than 450 °C) and low heating rates (4–8 °C/min) in the absence of air/oxygen. In this process, the residence time of vapor in the reactor is too long (5–30 min) which helps in continue to react the generated gas with each other for longer duration. As a result, formation of solid char is more compared to other component (liquids and gases). Due to low temperature and heating rate the slow pyrolysis process is not used for bio-oil production (Asadullah et al. 2013).

17.3 Fast Pyrolysis

In the fast pyrolysis process, heating rate (5–10 °C/min) and heating temperature (600–700 °C) is quite high as compared to the slow pyrolysis. Higher temperature and heating rate resulted higher formation of pyrogas which could be condensed and converted into bio-oil. Presently, in all the pyrolysis system, fast pyrolysis is the most widely used. It yields 60% wt bio-oil and takes few seconds for complete pyrolysis as well as in addition it gives 20% biochar and 20% syngas. The basic characteristics of the fast pyrolysis process are high rate of heat transfer, very short vapor residence time, rapid cooling of vapors and aerosol for high bio-oil yield and precision control of reaction temperature. The liquid product (Bio-oil) can be economically transported and easily stored (Asadullah et al. 2013). It also has potential to supply a number of valuable chemicals that offer the attraction of much higher added value than fuels.

17.4 Flash Fast Pyrolysis

The flash pyrolysis process is further advance stage of fast pyrolysis. In the case of flash fast pyrolysis heating rate and heating temperature are very high (10–15 °C/s, 800–1000 °C) and biomass residence time is very low, resulting large quantity of bio-oil production (more than 75% bio-oil). However, due to very high temperature

Table 5 Typical product yields (dry wood basis) obtained by different modes of thermo-chemical conversion of wood

Process	Conditions	Liquid, %	Char, %	Gas, %
Fast pyrolysis	Moderate temperature, short residence time particularly vapor	75	12	13
Carbonisation	Low temperature, very long residence time	30	35	35
Gasification	High temperature, long residence times	5	10	85

Source Crocker (2010)

and heating rate requires very small particle size of biomass and gas gets very short residence time (less than 1 s). This calls for long condensing trains. Flash fast pyrolysis process also has some technical limitations; thermal stability is poor as well as corrosiveness of the oil. The solids in the oil increases the viscosity over a time by catalytic action of char whereas alkali concentrated in the char dissolves in the oil which produces pyrolytic water. Typical yields obtained through different modes of thermo-chemical conversion are tabulated in Table 5.

18 Parameter Affecting the Pyrolysis Process

18.1 Moisture Content

Moisture content of the biomass is one of the important parameter for pyrlysis process. It should be maintained about 10–20% wb. High moisture in the biomass may produce low energy content of bio-oil; however less moisture in the biomass may produce only dust.

18.2 Particle Size of Feedstocks

In pyrolysis process size of the biomass particles has very important role as inside the pyrolysis reactor hear transfer take place from particle to particle. Smaller biomass particle offer more surface area compared to bigger size particles and hence help in more and uniform generation of pyrogas. Considering above 2 mm or less biomass particle found better for rapid heat transfer.

19 Conclusion

The conversion of biomass into the useful energy is the greatest contribution to the environment and society which fulfill the basic need of energy for day-to-day activities. Numbers of technologies are available to convert biomass into the energy. In this chapter, thermo-chemical conversion of biomass is discussed. Thermo-chemically biomass could be converted to energy by three ways named as Combustion, Gasification, and Pyrolysis. Combustion occurs in presence of stoichiometric oxygen, Pyrolysis in the absence of oxygen and Gasification requires partial oxidation. Compared to other available technologies, the route of thermo-chemical conversion is the simplest and most developed technology.

References

Asadullah M (2014) Biomass gasification gas cleaning for downstream applications: A comparative critical review. Renew Sustain Energ Rev 40:118–132

Asadullah M, Ab Rasid NS, Kadir SASA, Azdarpour A (2013) Production and detailed characterization of bio-oil from fast pyrolysis of palm kernel shell. Biomass Bioenergy 59: 316–324

Bhoi PR, Singh RN, Sharma AM, Patel SR (2006) Performance evaluation of open core gasifier on multi fuel. Biomass Bioenergy 30(6):575–579

Crocker M (2010) Thermal conversion of biomass to liquid fuels and chemicals, Royal Society of Chemistry

Chouhan APS (2010) Performance evaluation of Conversion process of biomass to bio-oil production through Pyrolysis technique. Ph. D. thesis submitted to Devi Ahilya University Indore

http://cturare.tripod.com/bio.htm

Kaupp A, Goss JR (1984) Small scale gas producer engine system. Published by Friedrich Vieweg & Sohn Braunschweig/Wiesbaden

Patil KN, Singh RN, Saiyed SU (2002) Case study of SPRERI natural draft gasifier installation at a ceramic industry. Biomass Bio-energy 22:497–504

Pathak BS, Patel SR, Bhave AG, Bhoi PR, Sharma AM, Shah NP (2008) Performance evaluation of an agricultural residue-based modular throat-type down-draft gasifier for thermal application. Biomass Bioenergy 32(1):72–77

Reed TB, Das A (1998) Handbook of biomass down draft gasifier engine system. IInd edition, Published by Solar Energy Research Institute, U.S. Department of Energy

Shrivastava V (2012) Design and development of downdraft gasifier for operating CI engine on dual fuel mode. M Tech thesis, submitted at Department of Mechanical Engineering National Institute of Technology Rourkela

Singh RN, Asha D, Aharwal VK (2014) Biomass as a future fuel for energy. In: Proceeding paper in recent advances in renewable energy & its application including automobiles industries at Prestige Institute of Engineering & Science, Indore, India, May 5–9

Singh RN (2007) Investigations on operation of IC engine using producer gas and non-edible plant oils and their esters in duel fuel mode. Ph. D. thesis submitted to Devi Ahilya University, Indore (MP)

Singh RN, Sharma MK, Gawade SS, Aharwal VK (2013) Reactivity of Biomass Briquettes. In: Poster presentation on Biosangam 2013-international conference on environment, health and industrial biotechnology at Motilal Nehru Institute of Technology, Allahabad

Singh RN, Balwanshi JB, Aharwal VK, Singh SP (2016) Experimental investigation of horizontal gasifier. Int J Sci Technol Soc 2(1&2):1–6

Singh RN, Vyas DK, Srivastava NSL, Narra M (2008) SPRERI experience on holistic approach to utilize all parts of Jatrophacurcas fruit for energy. Renew Energy 33:1868–1873

Singh RN, Asha D, Singh A (2017) Utilization of by-product of Mahua fruit (*Madhucaindica*) for Energy purposes. J Biofuels 8(2), July–Dec 2017

Singh A (2015) Utilization of all part of Madhucaindica (Mahua) fruit for energy. M. Tech. thesis submitted at school of energy and environmental studies, Devi Ahilya University, Indore, (unpublished)

Role of Biofuels/Biomass in Current Energy Scenario of India

Koushik Guha Biswas and Lipika Das

Abstract In recent times in India, there is a strong urge to apply technologies that will convert waste materials to conventional fossil used in transport and also into chemicals and useful resources. This advancement will help to reduce petroleum imports and reduction of greenhouse gas emissions and will use trash materials like municipal and agricultural waste mostly biomass across our country and transform them into value-added products. This calls for a need of novel group of biofuel technologies for better perspective and development of the country. One of the major feedstocks or raw materials that have come into the limelight nowadays for biofuel production is biomass. The present work tries to highlight the various biomass and biofuels and their roles with significance in perspective of Indian energy scenario.

Keywords Future fuels · Renewable energy · Biofuels · Biomass

1 Introduction

Renewable energy includes primarily all natural sources such as solar energy, wind energy, geothermal energy, bioenergy (biomass and biofuels), and hydro energy. These types of energy are very promising, and recently many reteaches are going on for its applicability in commercial scale which will reduce the dependency on conventional fossil fuels. Biofuel is a promising renewable energy which is mostly produced from various types of biomass which may include wood residues,

---

K. G. Biswas (✉)
Department of Chemical Engineering, Rajiv Gandhi Institute
of Petroleum Technology, Jais, Amethi 229304, Uttar Pradesh, India
e-mail: kbiswas@rgipt.ac.in

L. Das
Department of Chemical Engineering, Haldia Institute of Technology,
Hatiberia 721657, West Bengal, India
e-mail: lipikadas24@gmail.com

A. Sharma et al. (eds.), *Low Carbon Energy Supply*, Green Energy and Technology,
https://doi.org/10.1007/978-981-10-7326-7_10

agricultural wastes, plant wastes, and industrial and municipal wastes. This type of fuels is also known as emission less fuels as yield much less carbon dioxide (CO_2) and other greenhouse gases which can be attributed to major fluctuations in climate (Popp et al. 2014).

Low-carbon technologies cannot be considered as fully renewable as they may produce carbon emissions but less than that of orthodox fossil fuel burning technologies. Heat pump can be an ideal example of the heat which comes from the ground and is free and renewable. But on the other hand, it still needs an electric pump to function. It can be probable to create a substantial proportion of basic electricity from renewable or low-carbon technologies which are as follows.

Electricity can be generated from wind turbines, solar panels, hydral power, and photovoltaic cells.

Biomass is now the latest technology for source of energy as it can be converted to important biofuels which can be used as transportation fuels. Biomass is also accomplished by providing firm energy. Recently according to a survey, it was seen that about 32% of the total principal energy used in India is derived from biomass and around 70% of our countrymen is dependent on biomass for energy requirements.

It is quite an obvious fact that 1-day fossil fuels will seem to exhaust and there must be a secondary or backup plan for fuel requirement which can be only provided by alternative fuels like biofuels. Biomass which is the main source of alternative fuels plays a vibrant role particularly in rural areas, as it establishes the chief energy source for the most household. Energy from biomass can be utilized for several applications.

- Heat and electricity can be produced from biomass, for example, it can be used in heat as well as power plants.
- It can be used with fossil fuels to increase the effectiveness and decrease the accumulation of burning scums.
- Biomass can be converted into various fuels like methanol and ethanol which can be used as alternative transportation fuels or can be blended with fossil fuels.

1.1 Types of Biomass

Biomass basically can be classified according to its occurrence which is as follows:

a. Biomass from plants.
b. Biomass from industries.
c. Biomass from forests like wood residues.
d. Municipal wastes.
e. Biomass from organisms and plants in water.

2 Technologies Involved in Biomass Energy Production

Biomass is basically a feedstock for energy conversion which can be in the form of various chemical processes such as combustion, gasification, pyrolysis, and biochemistry as anaerobic digestion, fermentation, and transesterification. All the above techniques are used in the case-to-case basis for biomass conversion into energy.

2.1 Primary Routes for Power from Biomass

There are three main routes for biomass to power that are mostly practiced and researches are going: combustion, gasification, and anaerobic digestion.

Combustion is the method in which the biomass is utilized to harvest steam that drives the turbine. The process of combustion of biomass to produce energy can be in the form of co-firing, i.e., burning together with coal or purely burning of biomass. Gasification process includes conversion of biomass into syngas and then converting syngas to biofuels via catalytic reactions.

In case of anaerobic digestion, biomass such as kitchen waste and sewage waste is converted into energy. These biomasses are heated in the absence of air and is converted into biogas.

Another evolving road for biomass-based power is pyrolysis. This particular process involves heating of biomass at 450–600 °C in the absenteeism of air which leads to the formation of bio-oil known as the pyrolysis oil. This oil can be employed in firing the boilers.

2.2 Biomass-Based Power Production Methods

Among the various ways to produce power from biomass, the most evident is to use it to yield steam that drives a turbine. In fact, major biomass power plants in India as well as abroad follow the Rankine cycle route for biomass-based power production, although gasification and pyrolysis can also be a promising and new incipient route.

2.3 Benefits of Biomass Power

The availability of biomass is in almost all places particularly in rural areas, so this process can be used for distributed generation of power. Various renewable energy sources such as solar and wind cannot be used for baseload power generation due to their intermittency and variability. Power derived from biomass can be used in remote villages with no access to the grid but admittance to important amounts of biomass. Biomass gasification-based power production can be done at small scales (20 kW) but other energy sources like nuclear cannot be done at such small scale.

2.4 Rural Economic Upliftment

Biomass-based production is an attractive option for energy in rural areas in which utilization of biomass of agrowaste origin is done. Some of the companies are also trying to harvest energy crops for biomass-based power generation. This leads to more employment opportunities in the rural areas. Power generation from biomass is an excellent process resulting in utilization of animal and crop wastes. The feedstock can be various for bio-powers in rural areas which includes wood residues, rice husks, bagasse, etc. Any decomposition of these organic materials gives methane from which energy can be obtained after suitable conversion route. The animal business and landfills produce noteworthy volumes of methane. Biomass power can be formed frugally, at costs reasonable with grid power, if there is a good accessibility of feedstock.

3 Biomass Energy in India

- In India, around 500 million ton of biomass is manufactured and it constitutes 32% of all primary energy used.
- In recent times, biofuels in less amount are blended with conventional fossil fuels like ethanol in gasoline. This particular phenomenon has been supported by the government.
- India plans to set up biodiesel as a conventional fuel by 2020. Mostly, biodiesel is produced from transesterification reaction of animal fats and plant origin wastes. The most common feeds are jatropha, neem, and mahua.

4 Review of Research Status of Biofuels/Biomass

Swain (2014) made a study that fresh generation energy sources are of utmost importance in India and abroad. The available renewable sources have to be optimized to give maximum biofuel returns. Fossil fuels will exhaust 1 day and then renewable energies have to be utilized to make biofuels. He identified some major sources like algae, Jatropha oil, vegetable oils, cellulosic materials, corn, sugarcane, etc. He stated that algae are one of the best sources for biodiesel production. He suggested that cellulosic biofuel as a second-generation biofuel can be abundantly available raw material. This is due to the fact that traditional sources will exhaust 1 day and therefore there is a need for the implementation of future fuels. Pathak et al. (2012) also reviewed the current biofuel scenario of India and he stated that energy is the prime mover for development of economy in any country. He pointed out that the country immediately needs to establish an alternate path of energy. He had firm belief that biofuels can replace fossil fuels which calls for more detailed research and investigations. Kaushik and Singh (2012) stated that India is one of the largest energies as well as crude and petroleum products consumed in the world. The oil consumption in India is expected to reach more than 8 million barrels per day by 2035. It calls for the development of alternative sources of energy from second-generation biofuels that assume critical importance. They reflected the fact that there is a wide variance in biomass availability in India along with consumption and usage pattern, and the applicable technologies for conversion of biomass to fuel would be region specific. They pointed out that TIFAC has recently taken up the task of zone-wise mapping of the current biomass availability, their characterization, and also to assess the available technologies for their conversion into biofuel before coming up with technological recommendations. The study would also highlight the local logistics cost toward transportation. The inputs would be sourced from both secondary and primary researches including those from GIS and remote sensing. Patni et al. (2011) suggested that fossil fuels still play an important role in energy scenario of India. But there is an urgent need to develop future fuels which can sustain the economic growth of the country. Mostly, the biofuel's feedstock can give rise to crisis in food industry which has to be also kept in mind.

5 Government Incentives and Subsidies for Biomass Energy Production

The Ministry of New and Renewable Energy (MNRE) provides Central Financial Assistance (CFA) in the form of capital subsidy and financial incentives to the biomass energy projects in India (Scarlat et al. 2015).

6 Bottlenecks Faced by the Indian Biomass Industry

Biomass to Power/Heat

One of the most disadvantages of biomass plant may be the nonavailability of feedstocks, which will give rise to increase in feedstock price. Some of the other challenges may be lack of good technology for biofuel production, good regulatory framework, and poor financing mechanism.

6.1 Biomass to Transportation Fuels

Biodiesel

- Most common feedstock for biodiesel production in India is still Jatropha but there are some issues with it such as lack of skilled farmers, lack of education, lack of publicity skills, lack of long-term purchase contracts, and lack of benefits like incentives or subsidy to farmers.

Bioethanol

- The major challenge is in availability of molasses (feedstock, i.e., by-product from sugar industries) and lack of proper pricing policy.
- The Indian government make the policy regarding ethanol mixing with fuels but the state government mainly controls the movement of molasses and they put ban on transport of molasses from one state to other.
- State government also levy taxes on alcohols.

7 Conclusions

Bioenergy is basically a renewable source of energy which comes out of natural biological sources. Biofuel is the most common form of bioenergy, and mostly it is manufactured from biomass of various sources and origins. Biomass can be any organic material which has kept sunlight in the form of biochemical energy. Biofuel feedstocks can be wood waste, straw, manure, sugarcane, and many other by-products from a variety of agricultural processes. India holds a very important place in global scenario for consumption of energy as well as crude petroleum products. This calls for an immediate development of alternative fuels which can be derived from natural sources mainly from biomass.

References

Kaushik N, Singh S (2016) Opportunities for bio fuels—Indian scenario. Procedia Environ Sci 35:847–852

Pathak C, Mandalia HC, Rupala YM (2012) Biofuels: Indian energy scenario. Res J Recent Sci 1(4):88–90

Patni N, Pillai SG, Dwivedi AH (2011) Analysis of current scenario of biofuels in India specifically bio-diesel and bio-ethanol. Ahmedabad, pp 1–4

Popp J, Lakner Z, Harangi-Rákos M, Fári M (2014) The effect of bioenergy expansion: food, energy, and environment. Renew Sustain Energy Rev 32:559–578

Scarlat N, Dallemand J, Monforti-Ferrario F, Nita V (2015) The role of biomass and bioenergy in a future bioeconomy: policies and facts. Environ Dev 15:3–34

Swain KC (2014) Biofuel production in India: potential, prospectus and technology. Fundam Renew Energy Appl 1–4

Web References

http://www.ieabioenergy.com/wp-content/uploads/2013/10/MAIN-REPORT-Bioenergy-a-sustainable-and-reliable-energy-source.-A-review-of-status-and-prospects.pdf

https://www.worldenergy.org/wpcontent/uploads/2017/03/WEResources_Bioenergy_2016.pdf

https://ec.europa.eu/energy/intelligent/projects/sites/iee-projects/files/projects/documents/biomass_futures_use_of_biomass_electricity_heat_transport_fuel_en.pdf

Recent Trends of Process Intensification in Energy Domain

Koushik Guha Biswas

Abstract Process intensification which means the enhanced efficiency of a particular process was first brought into the limelight by Ramshaw in the year 1983. Basically, process intensification consists of finding out and using novel apparatus and techniques which can bring an increase in product yield or decrease in equipment size for a given production capacity. It can also bring about the decrease in energy consumption or reduction in waste production. Process intensification can be achieved through two different paths by the development of novel equipment or methods. The novel equipment can be further classified into (those for conducting chemical reactions) static mixer reactor, spinning disk reactors, etc., and (those which do not involve chemical reactions) static mixer reactor, compact heat exchangers, etc. Microreactor technology which is a boon nowadays enables the production of miniature components for chemical and biochemical systems that involve continuous flow systems usually comprising of two or more phases. The present work aims to review a complete status of process intensification in various fields of energy in India and abroad and their applications for the betterment of science and technology.

Keywords Process intensification · Heat transfer · Microreactor
Transport process · Energy · Efficiency

1 Introduction

1.1 What Does Process Intensification Means?

Process intensification (PI) simply means to increase the efficiency of a specific operation. It is basically a groundbreaking approach to plant and process design,

---

K. G. Biswas (✉)
Department of Chemical Engineering, Rajiv Gandhi Institute
of Petroleum Technology, Jais, Amethi 229304, Uttar Pradesh, India
e-mail: kbiswas@rgipt.ac.in

A. Sharma et al. (eds.), *Low Carbon Energy Supply*, Green Energy and Technology,
https://doi.org/10.1007/978-981-10-7326-7_11

development, and execution. In 1983, Ramshaw introduced the concept of process intensification and according to him, it is a device/way which can make radical changes in plant sizes leading to miniaturization of process equipment. Further, Stankiewicz and Moulijn in 2000 stated that process intensification means innovative apparatus, new treating methods, and newly built process techniques that can give higher improvements in the chemical and biochemical processing in terms of energy ingesting, plant sizes, and waste generation. Process intensification (PI) aims to decrease in plant cost, optimization of capital and energy. It has also a primary objective in terms of safety benefits by a drastic decrease in plant size. It also induces a better process in terms of energy efficiency, cost, and enhances other qualities as well. Therefore, this notion of PI is closely linked with the physical nature of the plant. PI not only encourages the betterment of processes by enhancing the prevailing technologies but also supports the growth of new technology. Nowadays microreactor technology is a live example of process intensification. The changes particularly in manufacturing technology since last 20 years have aided the invention of small components for chemical reactor technology which are termed as microreactors and microscale equipment. Microreactor technology can be generally demarcated as microstructured instruments fabricated for engineering applications such as in enhancement of reaction rates and transport processes. Due to this advancement in microreactor technology, miniature units like microheat exchangers, micromixers, and microfluidic devices for medical application are common now for commercial uses. Recently, miniaturization of process equipment has become important due to the technical and economical reason for studying fluid dynamics and transport behavior in microstructured flow systems. In microstructured flow systems, surface tension in the small passages is greatest and the intermittent flow patterns occur over a wide range of operating conditions in these channels.

1.2 Salient Features of Process Intensification

- A major shift from the batch process to continuous process.
- Newer and more advanced reactor technologies which provide high mixing and heat transfer rates can be used instead of orthodox reactors.
- Multidisciplinary methodology, which ruminates openings for the improvement of current technology along with its basic implementations.
- Enhanced process development techniques which are efficient in terms of energy consumption and environment-friendly reducing pollution.

2 Areas of Process Intensification

The methods for achieving process intensification are subdivided into multifunctional reactors (e.g., reactive distillation, reactive extraction), hybrid separations (e.g., membrane absorption, membrane distillation), methods employing supercritical fluids, dynamic (periodic) reactor operation, or methods employing substitute energy sources which include centrifugal fields, ultrasound, solar energy, microwaves, electric fields, plasma technology, etc. A flow chart (Fig. 1) shows a pictorial representation of various types of process intensification prevalent in recent times.

Some of the examples of various ways of process intensification are listed below along with the scheme of PI for different processes and systems.

- Reactor system—Spinning disk reactor, static mixer reactor, monolithic reactor, and microreactor.
- Equipments for nonreactive operations—Static mixer, compact heat exchangers, rotating packed bed, and centrifugal absorber.
- Multifunctional processes—Heat-integrated reactors, reactive separations, reactive extrusion, and fuel cells.
- Hybrid separations—Membrane adsorption, membrane distillation, and adsorptive distillation.
- Alternative energy sources—Centrifugal fields, ultrasound, solar energy, microwaves and electric fields.
- Other methods—Supercritical fluids and dynamic (periodic) reactor operation.

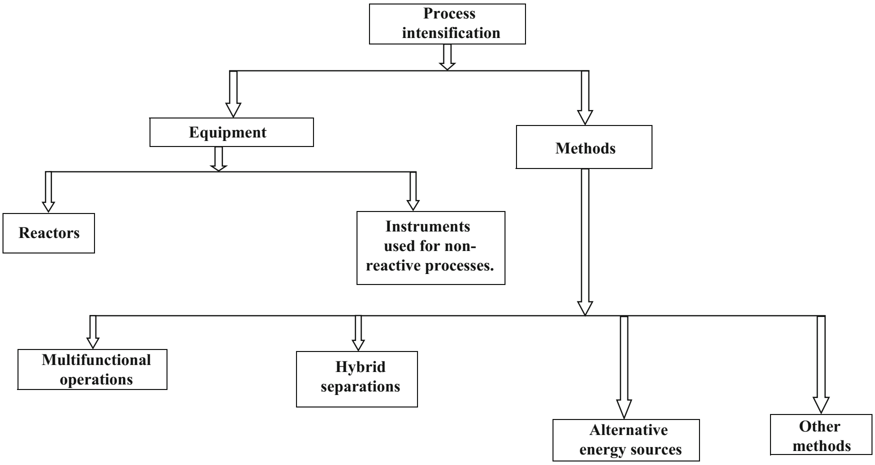

Fig. 1 Pictorial chart representing various types of process intensification

3 Review of Various Ways of Process Intensification

Some of the salient works on process intensification by past researchers have been reviewed which include the work by Brunold et al. (1989) with pulsating flow around sharp edges and to investigate the eddy mixing effect. They also studied energy loss in ducts of the rectangular and cylindrical cross-section and also reported that sharp edges either as rectangular bends or baffle inserts favor large-scale formation of eddies. This phenomenon enhances mixing manifolds even for low net flow Reynolds number but also increases energy dissipation many times. Harvey et al. (2003) performed systematic study on heat transfer and associated energy release in oscillatory flows for baffled tubes in which they took a laboratory scale heat exchanger with horizontal orientation, single pass, operating in countercurrent mode with the tube having internal diameter of 12 mm made of stainless steel of wall thickness 1 mm. The cooling medium used by them was tap water at the shell side and a mineral oil having density 840 kg/m^3. The thermal conductivity was equal to 0.137 W/m °C at the tube side which was oscillated from 2 to 10 Hz, amplitude ranging from 3.5 to 6 mm with the help of two opposite horizontal pistons connected via an operating rod and powered by an electric motor. They observed that oscillatory flow instead of steady flow resulted in high heat transfer. Investigations on the relationship between baffle thickness and spacing were performed by Ni et al. (1998) in batch operation mode with water–NaCl as a system. The pulsation frequencies and amplitudes ranging from 1 to 10 Hz and 1 to 20 mm respectively were varied. This suggested that thinner baffles favor more intense mixing while the thicker baffles lead to the eddy deformation with an optimum thickness of baffles from 2 to 3 mm. Krishna and Ellenberger (2002) performed process intensification studies using air–water system (air continuously supplied and water was taken as a batch). They considered bubble column having an internal diameter of 51 mm and height of 1050 mm for their study. They used a loudspeaker of 0.18 m as outside diameter which imparted low-frequency vibration to the water present in the column. They observed maximum bubble size reduction from 3.8 to 2.7 mm, peak volumetric mass transfer coefficient of 0.045 s^{-1} and a maximum number of smaller bubbles equal to 25 was formed which have a diameter of 0.0032 m at a frequency of 150 Hz. Ellenberger and Krishna (2002) used a 12 capillary nozzle for gas sparging having an internal diameter of 0.9 mm per capillary nozzle. They also used a membrane fitted with a piston to impart mechanical oscillation frequency 40–100 Hz and wavelength equal to 0.005 mm with air as continuous and water batch. They reported that gas holdup was enhanced almost by a factor of 2 in comparison when a single capillary gas nozzle was used. Wen and Ding (2004) took γ-Al2O3 nanoparticles and deionized water as their system and the flow was done in a copper tube to enhance the energy transport (convective heat transfer). They also observed that the increase was evident in the entrance region, and it decreased with axial distance. The improvement in the convective heat transfer was not only due to the increase of the effective thermal conductivity. Xuan and Roetzel (2000) stated that the suspended ultrafine particles in nanofluid can change transport properties and heat transfer performance. An assumption was taken by them that the nanofluid behavior was like an ordinary fluid than a complex solid–liquid mixture. They also suggested two different approaches for deriving the increased heat transfer correlation of the nanofluid. Fadzin and Lee (2014) made a numerical study on enhanced heat transfer in a 2D microchannel heat sink (MCHS) using various fluid systems. The influence of various particle volume concentration (1, 2 and 5%) of the nanoparticle on the thermal performance in the MCHS was thoroughly studied. They noted that nanofluids with low dynamic viscosity and high thermal conductivity enhanced the thermal performance. Olayiwola and Walzel (2008) investigated the impact of flow vibration in the rectangular finned channel on cross-flow transport along with convective heat transfer enhancement. Glycerol water mixture with 23 wt% of glycerol as a working fluid was used. Flow pulsation was imparted to the working fluid with the help of rubber diaphragm vibrating with the frequency of 16–54 Hz and amplitude of 0.28–0.53 mm. They observed that increasing (i.e., oscillation velocity/mean velocity) resulted in higher heat transfer for a given oscillation Reynolds number. Unsteady dynamics of Taylor bubbles rising in vertically oscillating tubes was investigated by Madani et al. (2009). They made a comparison between two pipes of I.D. 9.8 and 20 mm, vertical sinusoidal motions were imparted with frequencies ranging from 1 to 8.8 Hz. They noted that for the smaller diameter pipe, the critical acceleration (i.e., the acceleration after which the velocity started increasing) was less than the larger diameter pipe and with oscillation, and the mean rise velocity of the bubble was considerably reduced.

Balamurugan et al. (2010) explored bubble columns having two different types of internals. They took perspex pipes of I.D. 15 cm and test section length of 125 cm having 126 holes of diameter 0.2 cm and pitch of 1 cm through which gas (air) was sparged into it. They performed their work with pipes having helical springs of 0.05 and 0.1 cm as internals and the other with the nine-rod internals of 1.9 cm diameter. They have seen that using vibrating internals like spring gas, holdup enhancement of around 150% was obtained even at a higher throughput of gas superficial velocity in comparison to fixed rod internals. Investigations on pool boiling enhancement with submerged ultrasonic vibrations were done by Heffington and Glezer (2004). They selected ethanol–water (70:30) system and the ultrasonic vibrations of 1.65 MHz were applied resulting in 425% increment in water flux. They noted enhancement of nucleation rate and delayed film boiling onset and high critical heat flux with vibrations. Process intensification studies for intensifying bubble column performance by applying pulsation to the semi-batch system (i.e., air continuous and water batch) were performed by Budzyński and Dziubiński (2014). They took a column of I.D. 0.134 m and height 2.25 m which was filled with water, and the air was sparged from below with a single nozzle and experimented with three different nozzle diameters. They noted that pulsation reduced rises the velocity of bubbles, and also caused the bubbles formed at nozzle outlet to be remarkably smaller. They also observed that with an increase in pulsation frequency and amplitude, gas holdup in a column also increased. Furthermore, increase in amplitude at constant frequency was seen to have a positive relationship with gas holdup. Along with these phenomena, they found out a problem of decrease in gas holdup with an increase of water masses in bubble column at same process parameters. Kashid et al. (2007) proposed a liquid–liquid slug flow through capillaries of inner diameter 0.5, 0.75, and 1 mm as a substitute for conventional contact devices leading to process intensification. The various liquid–liquid systems used by them were succinic acid from its aqueous solution into n-butanol, iodine from its aqueous solution diffusing into kerosene, and acetic acid from kerosene into distilled water. They observed the effect of operating conditions on mass transfer coefficient. The effect of slug velocity, flow ratio, flow rates and capillary size on extraction efficiency, and mass transfer coefficient were studied and the volumetric mass transfer coefficient was found to be in the range of 0.13–0.98 (s^{-1}). They have developed a flow splitter for downstream separation of two liquid phases. A short tabular data has been given in Table 1 which shows various processes and how it has been intensified by various means.

Table 1 Tabulated description of literature survey showing various processes which have been intensified by various means

Process intensified	Means of intensification
1. Multiphase reactors	Supercritical solvents
2. Micromixing	Pulsating flows
3. Reactions for biphasic systems	Using slug flow in capillaries
4. Catalytic oxidation for deep desulfurization	T-junction microchannel reactor
5. Phosgenation processes	Column reactor having a vibrating stirring arrangement
6. Gas-phase photocatalytic oxidative dehydrogenation of cyclohexane	Fluidized bed reactor
7. Local flow parameters of two-phase flow.	Flow-induced vibration
8. Biodiesel production	Continuous oscillatory flow reactor
9. Mass transfer of wet textile	Ultrasound process
10. Slurry bubble columns	Vibration excitement
11. Dairy whey ultrafiltration	Ultrasound process
12. Mass transfer	Vibrating electrodes
13. Bubble column performance	Pulsating
14. Pulsation in two-phase flow	Wire coil insertion
15. Cross-flow filtration of polyacrylonitrile ultrafiltration membranes	Ultrasound effect
16. Mass transfer in gas–liquid dispersions	Vibration excitement
17. Gas holdup in bubble columns	Use of vibrating internals
18. Oxidation of benzyl alcohol	Using a continuous isothermal reactor under microwave irradiation
19. Gas–liquid processes	Tubular turbulent apparatus

4 Role of Process Intensification in Chemical Engineering

In chemical engineering (Gerven and Stankiewicz 2009), there is an operation like chemical reaction engineering, solids handling and processing, separation technologies along with important and broad areas such as thermodynamics, transport phenomena, and fluid mechanics. In all these areas, PI plays a pivotal role in the development and advancement of research in these areas by different means (multifunctional reactors, microreactors, etc.). A very important aspect is the synergistic relation between process intensification and process systems engineering in which PI is like a foundation stone or base from where various process systems are further revised and boosted. In this regard, PI gives an opportunity of creating a new platform for process systems engineering not only in terms of model development but also it provides space for novel instruments and their processing methods along with plant design and optimization. Even in molecular level, one can think of PI. The reason behind these is that PI offers various targets such as to enhance the efficiency of intra- and intermolecular events, to give each molecule the same treating experience and to augment the various dynamic forces in terms of increasing the surface to volume ratio, i.e., the interfacial area. Another boon in PI for chemical engineering is multifunctional reactors as well as microreactor technology. Microreactor technology allows enhancement of any transport processes (mass transfer and reaction kinetics) due to the enhanced interfacial area and contact time between the particular phases chosen for the study. This enhancement is much more than that of conventional macroreactors. The method of growth of highly active and selective catalysts, and optimization feedstock utilization (Dautzenberg and Mukherjee 2001) will lead to lessening in energy consumption per unit weight of the product and thus to a reduction in the build-up of greenhouse gas emissions. So in this regard, multifunctional reactors can be used to minimize energy and that is done by integrating several process steps into one. This includes in situ removal of products from the reaction zone. Also using multifunctional reactors series of reactions can be avoided and better reaction rate can be obtained. PI also helps in reduction of waste generation in the chemical industry. The advancements in catalyst development and progresses in reaction engineering may give a path of a new generation of multireactors which could help in disabling some of the major engineering challenges for process industries.

5 Conclusions

Process intensification is often defined in terms of its assistance to the process industries, particularly in the energy sector. A gratitude of the benefits that PI can give in terms of safety, energy saving, and improved technology will reorient the motivation behind PI. But every good thing comes with a disadvantage or limitations and there are also limitations to PI. The efficiency of the PI depends on the correct choice of techniques for vividly increasing the intensity and accelerate the process of transfer of heat, mass, and momentum within a process or operation. Despite the captivating profits of PI for the process industry, it has to be confessed that implementation has not been so successful. In the situation of an existing fully traditional and denigrated plant, it is enormously difficult to introduce untested intensified equipment. There are some concerns at one end that any breakdown will compromise the output of the whole plant, but on the other side, there are benefits of PI that are unlikely to be comprehended unless the entire process in the plant is boosted. The implementations of process intensifications transform orthodox process engineering unit operations into a radical process technology whether by integration of several unit operations or by altering inherent chemical process elements to eliminate unnecessary process blockages.

References

Balamurugan V, Subbarao D, Roy S (2010) Enhancement in gas holdup in bubble columns through use of vibrating internals. Can J Chem Eng 88:1010–1020

Brunold CR, Hunns JCB, Mackley MR, Thompson JW (1989) Experimental observations on flow patterns and energy losses for oscillatory flow in ducts containing sharp edges. Chem Eng Sci 44:1227–1244

Budzyński P, Dziubiński M (2014) Intensification of bubble column performance by introduction pulsation of liquid. Chem Eng Process Process Intensif 78:44–57

Burns JR, Ramshaw C (2001) The intensification of rapid reactions in multiphase systems using slug flow in capillaries. Lab Chip 1:10–15

Dautzenberg FM, Mukherjee M (2001) Process intensification using multifunctional reactors. Chem Eng Sci 56:251–267

Ellenberger J, Krishna R (2002) Improving mass transfer in gas–liquid dispersions by vibration excitement. Chem Eng Sci 57:4809–4815

Fadzin KA, Lee A (2014) Heat transfer enhancement in microchannel using nanofluids. Appl Mech Mater 465–466:536–540

Gerven TV, Stankiewicz A (2009) Structure, energy, synergy, times the fundamentals of process intensification. Ind Eng Chem Res 48:2465–2474

Harvey AP, Mackley MR, Seliger T (2003) Process intensification of biodiesel production using a continuous oscillatory flow reactor. J Chem Technol Biotechnol 78:338–341

Heffington S, Glezer A (2004) Enhanced boiling heat transfer by submerged ultrasonic vibrations. Sophia Antipolis, CÙte díAzur, France

Kashid MN, Harshe YM, Agar DW (2007) Liquid–liquid slug flow in a capillary: an alternative to suspended drop or film contactors. Ind Eng Chem Res 46:8420–8430

Krishna R, Ellenberger J (2002) Improving gas–liquid mass transfer in bubble columns by applying low-frequency vibrations. Chem Eng Technol 25:159–162

Madani S, Caballina O, Souhar M (2009) Unsteady dynamics of Taylor bubble rising in vertical oscillating tubes. Int J Multiph Flow 35:363–375

Ni X, Brogan G, Struthers A et al (1998) A systematic study of the effect of geometrical parameters on mixing time in oscillatory baffled columns. Chem Eng Res Des 76:635–642

Olayiwola B, Walzel P (2008) Cross-flow transport and heat transfer enhancement in laminar pulsed flow. Chem Eng Process Process Intensif 47:929–937

Wen D, Ding Y (2004) Experimental investigation into convective heat transfer of nanofluids at the entrance region under laminar flow conditions. Int J Heat Mass Transf 47:5181–5188

Xuan Y, Roetzel W (2000) Conceptions for heat transfer correlation of nanofluids. Int J Heat Mass Transf 43:3701–3707

Dye-sensitized Solar Cell Technology: Recent Development and Advancement

Ramkishore Singh

Abstract Energy is one of the essential needs for the sustainability of the society. Fast industrialization and growing population of the world have increased the demand for the energy. In the past, fossil fuels have been major sources of the energy and are being burnt for accomplishing the thermal and electrical energy demands of the society. Continuous burning of the fossil fuels has resulted in fast depletion of the fossil fuel resources and an unsustainable situation for the energy sector as well as created severe issue of the climate change. Due to the fast depletion of the fossil fuel and climate change issues, the current electricity generation technologies cannot be utilized in future. Therefore, new technologies which can run on the renewable energy sources are being developed and assessed. Solar photovoltaic is one of the renewable energy based technologies, which are suitable for the sustainability. Conventional silicon-based solar cells are expensive and suffer from the low efficiency, while dye-sensitized solar cell arose recently as a cheaper alternative to the conventional solar cells. However, they also suffer from the low conversion efficiency issue. In recent past, research in DSSC has been expedited to enhance the efficiency and reduce the overall cost of the technology. This chapter has been focused on the basic structure, working principle and the recent advancements in the different components of the DSSC.

Keywords Photovoltaic · Solar energy · Solar cell

1 Introduction

The global energy demand has increased drastically in past few decades because of rapid growth in population and increased living standards. Continuous burning of the fossil fuels, to fulfill the energy need of the society, putting enormous pressure on the

---

R. Singh (✉)
Solar Energy Division, Sardar Patel Renewable Energy Research Institute,
V.V. Nagar, Anand, Gujarat, India
e-mail: singh.ramkishore@gmail.com

A. Sharma et al. (eds.), *Low Carbon Energy Supply*, Green Energy and Technology,
https://doi.org/10.1007/978-981-10-7326-7_12

fossil fuels reserves and created severe climate change and global warming issues. Due to the climate change, different parts of the world witnessing various major problems like drought, flood, and food insufficiency. Currently, more than 40 billion tons of greenhouse gases are exhausted annually to the atmosphere and the tendency is on the rise. This GHG emission is mainly results of the high and uncontrolled use of fossil resource in energy generation. To control the emission, development of an environmentally friendly and reliable energy technology that can run on renewable energy resources is highly desirable. Hence, the demand for greener and sustainable energy production drove the scientific community to develop innovative systems able to convert renewable energy sources such as solar (Sacco et al. 2013), wind (Caduff et al. 2012) or chemical (Liu et al. 2006) into electricity.

Photovoltaic (PV) is one of the most promising technologies that convert solar energy directly into electricity. Low maintenance cost, noise-free operation and the possibility of standalone use are advantages of the technology. Moreover, utilization of solar energy reduces the global CO_2 emission similarly to other renewable sources. The solar energy, a free fuel, for generating electricity through the photovoltaic technology (a sustainable route) represents about 10,000 times the current global energy consumption (Hwang et al. 2015). This implies that present energy need of the world would be satisfied if only 0.1% surface of our planet (roughly 1% of desert areas) is covered with the PV panels of 10% efficiency (Gratzel 2001).

The solar energy not only freely available but also available abundantly, non-polluting, and unique natural renewable energy resource (Yoon et al. 2010). These fascinating facts of solar energy are pinching researchers worldwide regarding its utilization for mankind. There are over two dozen types of solar PV cells within the solar PV domain. Each of these has their own merits and demerits. Per unit cost of energy (or power) is one of the determining factors on the diffusion level of solar PV technologies. The commercially manufactured solar cells are currently based on inorganic silicon semiconductors, which will result proliferation of silicon demand in next decade and price of silicon will rise dramatically (Mishra and Bauerle 2009). Moreover, the manufacturing of crystalline silicon solar cell is quite expensive. The fabrication of wafer and the production of the poly-silicon are the main contributing costs (Powell 2015). On the other hand, the emerging solar PV technologies like Dye-Sensitized Solar Cell (DSSC) and organic PV are cheaper to manufacture because of low material cost. The materials used in DSSC are technically easier to synthesize or extracted from their natural sources (Kalowekamo and Baker 2009). Sometimes, these emerging solar PV cells are referred to as third and fourth generations of PV technology. The DSSC, hetero-junction cells, quantum dot cells, polymer solar cells, and hot carrier cells belong to the third generation solar cells (Trupke and Green 2002; Green 2001; Ludin 2014).

Despite silicon technology is currently the market leader in photovoltaic technologies, since pioneering (O'Regan and Grätzel 1991) the DSSCs have become one of the important and promising technologies in the photovoltaic field. The DSSCs have given birth to new solar cell generation and have the capacity to replace classical solid-state homo and hetero-junction devices by a new concept with a nano working electrode in the photo-electrochemical cell. The DSSC is made of following three main elements: (i) a photo-anode, (ii) an ionic conducting medium, and (iii) a counter electrode (cathode). The first one, photo-anode, is constituted by a porous semiconductor (usually TiO_2 nanoparticles) deposited on a transparent conductive oxide (TCO) glass and sensitized by dye molecules. The dye molecules absorb the incoming light, generate electrons and stimulate the injection of electrons into the oxide layer. Two properties of the oxide film that are imperative to the robust harvesting of light and the efficient production of energy should be superior electron transport characteristics and large surface area at the interface. The regeneration of dye molecules is achieved through a redox couple (usually dissolved in an organic solvent). The counter electrode usually made of a Pt thin film deposited on another TCO glass, whose main purpose is to speed up the electrolyte reduction reaction.

As anticipated above, these cells exhibit numerous advantages, namely relatively high efficiencies (about 12%) (Green et al. 2015) and low manufacturing costs. The DSSCs have unique features compared to the other solar cells, apart from being low fabrication cost, they can be made flexible and in various colors, translucent and have the ability to perform even under low (diffuse) light condition (Calogero 2013; Gong et al. 2012). Hence, these are also suitable to use indoors and as building-integrated photovoltaics, such as rollable devices for walls or windows (Gong e al. 2012; Hug 2014).

Moreover, the DSSCs can be integrated with other materials, especially those materials used in handbags and apparels.

In 2014, the global market for DSSC was valued at about 50 M$ and was estimated to increase up to 130 M$ by 2022. Currently, the most widespread areas of application are BIPV and portable charging (mainly in Europe and North America), but in near future embedded electronics, automotive and outdoor advertising are expected potential sectors in which these cells can be integrated effectively with a decisive boost in countries like China and India (GrandViewResearch 2016).

This chapter aims to explain the basic structure and functioning principle of the DSSC and recent advancements in the main components of the device to enhance the efficiency and reduce the manufacturing cost. The chapter is structured under following main sections: (i) structure and functioning of DSSC; (ii) advancements in main elements of DSSC; (iii) losses reducing strategies and (iv) conclusions. The compiled material in the chapter mainly based on the relevant scientific journal articles.

2 Structure and Functioning of DSSC

TiO_2 is generally used as photo-anode (working electrode) material and I^-/I_3^- as redox couple in most common and simple DSSC. A typical structure of a TiO_2-based DSSC is represented in Fig. 1. The five main components of the DSSC are: (i) a transparent conducting oxide (TCO) glass substrate; (ii) a wide bandgap

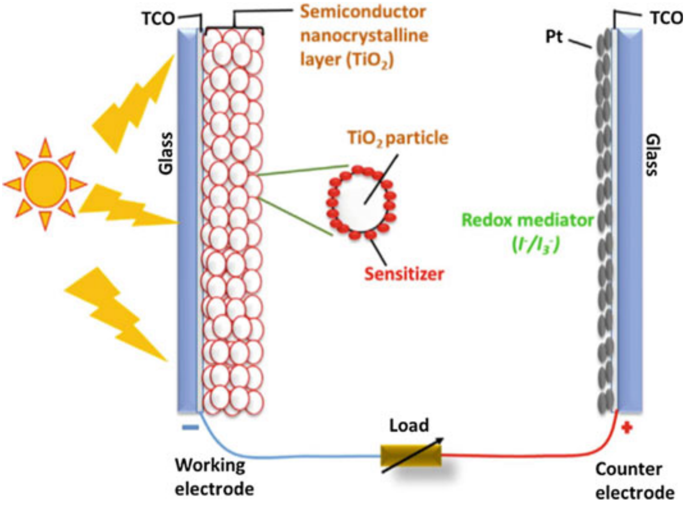

Fig. 1 Schematic illustration of the DSSC (Kumara et al. 2017)

semiconductor (usually a nanocrystalline TiO_2 film, deposited on the TCO glass substrate); (iii) a dye sensitizer anchored onto the surface of TiO_2 film; (iv) a redox mediator, a volatile electrolyte, containing iodine/triiodide ($I^{-}/I_3{}^{-}$) redox couple; and (v) a counter electrode, usually a platinum-coated TCO glass substrate.

The most important part of the DSSC is working electrode, which absorbs light. The working electrode is prepared by forming a porous network of nanocrystalline TiO_2 particles by applying nanocrystalline particles (10–20 nm) onto the TCO glass substrate and heated at 500 °C to obtain a 7–20 µm thick TiO_2 film with an internal surface area of about 1000 cm^2 per 1 cm^2. The prepared electrode with the porous network of nanocrystalline TiO_2 particles is then immersed in a dye solution for a sufficient period to facilitate the dye absorption on the TiO_2 surface. The redox mediator, a solution containing an I_3/I^{--} couple, is applied in between the two electrodes to set up the DSSC. Finally, the DSSC is illuminated through the working electrode side to generate the electrical energy (Gong et al. 2012; Narayan 2012).

Figure 2 shows the basic electron transfer process and the related potential in DSSC. When the photo-anode of the cell is exposed to the sunlight, the dye molecules are got excited by the illuminated light. These photo-excited dye molecules assist electrons moving to the conduction band of the photo-anode (TiO_2). The dye gets oxidized as the electrons reach to the conduction band. The electrons from the conduction band reach the conductive substrate after crossing the semiconductor and finally travel through the load in the external circuit. In the end, the electrons reach the counter electrode and restore the dye to the ground state after passing through the electrolyte. Oxidation of I^{-} forms $I_3{}^{-}$ ions that diffuse through the electrolyte to reach the cathode and complete the regenerative cycle by

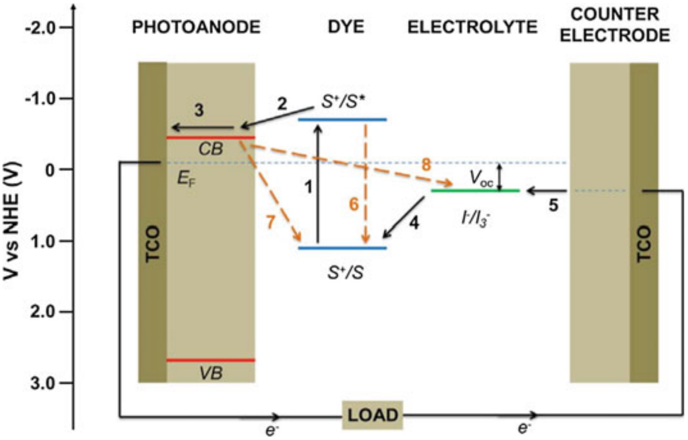

Fig. 2 Simple energy levels diagram for a Ru complexes dye DSSC, consists of TiO_2 photo-anode, I^-/I_3^- redox couple and Pt-counter electrode. Continuous and dashed arrows represent electron transfer and recombination processes respectively

transferring an electron to reduce I_3^- to I^-. For efficient operation of the device, the following two conditions are essentially required: (i) the conduction band of oxide must have lower energy than the lowest unoccupied molecular orbital (LUMO) of dye, and (ii) the energy of highest occupied molecular orbital (HOMO) should be lower than redox potential. Therefore, sensitizers are required to be designed and synthesized suitably to match the energy requirements of semiconductor and the redox couple. Generated voltage under illumination depends on the difference of the electrochemical potentials between the two contacts, i.e., the difference between the Fermi level of the mesoporous TiO_2 layer and the redox potential of the electrolyte (Nazeeruddin et al. 2011).

The efficiency of the DSSCs also degrades due to some undesirable reactions. Figure 2 also shows the processes that lead to losses in the overall efficiency of the cell. More specifically, process 6 in Fig. 2 represents efficiency loss due to direct recombination of the excited dye; and processes 7 and 8 show the recombination of injected electrons in the TiO_2 with oxidized dye and with holes in the electrolyte respectively. Technically, the last process occurs at the interface of the oxide and the electrolyte or in the exposed regions (the area where no semiconductor layer exists) of TCO, i.e., the regions exposed to the electrolyte. Generally, a compact blocking layer of semiconductor is used to restrain the recombination through second route (Cameron and Peter 2003).

The above processes in the functioning can easily be understood by expressing them into chemical reaction equations. Initially, the dye gets photo-excited absorbing sunlight (photon) by the dye sensitizer (*S*). Then, the photo-excited dye (S^*) injects an electron into the conduction band of semiconductor (TiO_2). The above processes are expressed by the Eqs. (1) and (2) respectively. The sensitizer turns to excited state $S*$ from its ground state S by absorbing a photon of energy hv (process 1 in Fig. 2).

$$S(\text{on TiO}_2) + hv \rightarrow S^*(\text{on TiO}_2) \tag{1}$$

$$S^*(\text{on TiO}_2) \rightarrow S^+(\text{on TiO}_2) + e^-(\text{on TiO}_2), \tag{2}$$

where h is Planck constant.

Despite extensive research in the area, the detailed mechanism of the injection process should be comprised fully and much more intensive research is needed to understand it clearly. For a Ru complex sensitizer attached to an oxide surface, the process occurs in a very short period of time (in the order of femtoseconds) (Kuang et al. 2006). For an efficient device, the time required for the injection process should be compared with the time taken in returning the excited state of the dye to the ground state (process 6). For typical Ru complexes DSSCs, the lifetime of the excited state of the dye is observed between 20 and 60 ns (Hagfeldt and Grätzel 2000). It is clear from the lifetime range of the excited state of the dye that the injection is an ultrafast process. The regeneration of the oxidized dye (process 4) normally completes in the microseconds. The process of the regeneration is expressed by the following reaction (3):

$$2S^+(\text{on TiO}_2) + 3\text{I}^- \rightarrow 2S(\text{on TiO}_2) + \text{I}_3^- \tag{3}$$

For life cycle of sensitizer (turnover number) over 10^8 (essential for a DSSC lifetime greater than 15 years), the lifetime of the oxidized dye must be longer than 100 s if the regeneration period is 1 µs (Wang et al. 2005).

The process of charge transportation through the mesoporous layer (process 3) completes efficiently within few milliseconds. However, further research is required to understand the process of charge transport in a better way. The oxide film may be assumed as a group of individual particles through which electrons can pass hopping. As the oxide particles are not electronically doped and surrounded by the ions in the electrolyte and hence, do not show any significant band bending and do not have an internal electric field. Further, ions in the electrolyte do charge compensate the photoinjected electrons. Consequently, electron concentration gradient appears to be a main driving force for electron transportation in the mesoporous TiO_2 film, i.e., electron transport takes place by diffusion (O'Regan et al. 1990). However, a nonlinear relation has been between the electron transport and the intensity of the incident light. The electron transport becomes much faster at higher light intensities than the lower light intensity. Recently, the electron transport has been described using multiple trapping models considering a light dependent diffusion coefficient or, more accurately, dependent on the electron concentration and Fermi level in the TiO_2 (Bisquert and Vikhrenko 2004). In the model, electrons were assumed trapped in localized states under the conduction band, from where they can escape by thermal activation. Generally, traps involved in electron transport in DSSCs are justified considering their existence either in the bulk of grain boundaries or at the oxide/electrolyte interface. However, further research and discussion are needed to understand the exact nature and position of the traps in the mesoporous TiO_2. The electron transfer reaction from the conduction band to the oxidized sensitizer (see process 7, in Fig. 2) occurs in the micro to millisecond time and follows a multi-exponential time law. The electrons' recombination in the TiO_2 with acceptors in the electrolyte is described by the lifetime (τ_n) of the electron, as shown by process 8 in Fig. 2. Under one sun intensity, the lifetimes with the I^-/I_3 are observed quite longer (in the range of 1–20 ms) than with other redox systems in the DSSC. Following equation expresses the diffused usage of the redox couple:

$$I_3^- + 2e^-(\mathrm{Pt}) \rightarrow 3I^- \tag{4}$$

In addition, while the electron flow cycle, many other undesirable side processes take place simultaneously, e.g., the recombination of injected electrons either with the oxidized dye (process 6, Fig. 2) or with I_3^- at the TiO_2 surface (process 7, Fig. 2) as per Eqs. (5) and (6), respectively, as well as non-radiation relaxation (de-excitation) of the photo-excited dye (process 8, Fig. 2) which follows Eq. (7), resulting in low photovoltaic performances of DSSCs. Conventional DSSCs consist of a mesoporous nanocrystalline TiO_2 film which possesses a large surface area but with numerous grain boundaries, which ultimately increases the recombination rates of photogenerated electron–hole pairs and consequently lowers the photovoltaic efficiency (Benkstein et al. 2003; Shahimin et al. 2005). A major condition for electricity generation with a high photovoltaic efficiency is that the electron–hole pairs should not recombine (or very rarely). Suppressing is needed to balance between the transport of charges and recombination of electron–hole pairs by using a specific architecture of semiconductor materials to accelerate electron transport and minimize recombination of electron–hole pairs by optimizing the nature, structure, and dimensions of the semiconductors. The recombination process of Eq. (5) is usually in competition with the re-reduction of the oxidized dyes by an I^- process of Eq. (3). At the same time, the processes of electron injection and regeneration described by Eqs. (2) and (3), respectively, must be kinetically more favorable than that of recombination processes of Eqs. (5) and (6), for high photocurrent and photo-voltage (Durrant et al. 2004; Wang 2012).

$$S^+(\mathrm{on\,TiO_2}) + e^-(\mathrm{TiO_2}) \rightarrow S(\mathrm{on\,TiO_2}) \tag{5}$$

The electron recombination with the molecules of the oxidized dye can compete with the process of regeneration these processes occur simultaneously, especially under actual working conditions. Actually, recombination kinetics strongly increases with the concentration of the electrons in the TiO_2 particles (O'Regan et al. 1990). For an efficient energy production, the transport time of the oxide must be lower than the lifetime of the electron. The lower transport time ensures the electron arrival at the front electrode well before the recombination.

The following equation expresses the diffusion length of the electron in terms of electron lifetime and diffusion coefficient:

$$L_n = \sqrt{\tau_n D_n} \tag{6}$$

A longer diffusion length than the film thickness is desirable to collect all the photogenerated charge carriers (Gratzel 2005).

The diffusion is a main driving force for transporting the redox mediator between the electrodes. The diffusion depends on redox mediator concentration, the distance between the electrodes and diffusion coefficient. The characteristic time for this process is greater than 1 s.

In a standard DSSC, triiodide is reduced to iodide at the counter electrode as explained by the following reaction (process 5)

$$\mathrm{I_3^-} + 2e^-(\text{on TiO}_2) \rightarrow 3\mathrm{I}^-(\text{cathode}) \tag{7}$$

This process occurs in few milliseconds. Hence, low overpotential and the rapid reaction can be ensured using the counter electrode activated by efficient catalyst like Pt.

$$S^*(\text{on TiO}_2) \rightarrow S(\text{on TiO}_2) \tag{8}$$

However, researchers continuously investigating new alternative cheaper and effective materials for the counter electrodes. The progress in the counter electrode materials is discussed in a separate section subsequently in this chapter.

3 Progress and Advancements in DSSC's Components

In the past decades, researchers have given considerable attention to develop efficient and cost-effective counter electrodes, photo-anodes from different nanostructures, dyes having larger absorption spectra and different composite materials as electrolytes. These all the elements of DSSC are critically important and influence the performance of the cell significantly. This section discusses the recent developments in these elements.

3.1 Advancement in Photo-Anode

Properties of the photo-anode largely govern the performance of the DSSCs. The photo-anode includes a mesoporous film of a metal oxide that prepared on a transparent conductive glass substrate as explained in the previous section. The mesoporous networks of wide bandgap oxide semiconductors work as electron collectors and scaffolds for loading dye molecules. Various strategies were assessed in the past to improve the DSSCs' performance by advancing the photo-anodes. Recently, an average optical transmittance and power conversion efficiency of a

DSSC with 1.2 m thick nanowire were observed 40% and 1% respectively in visible light under one sun intensity (Shin et al. 2017). The TiO_2 is commonly used material for photo-anode in the cell. As indicated previously that charge recombination between the conduction band of photoelectrode and I_3 in the electrolyte is one of the losses that lowers the overall cell performance. Treatment of TiO_2 by $TiCl_4$ is one of the solutions to inhibit the charge recombination. In some cases, photo-anode made of composite materials exhibits improved cell performance. Liu et al. (2017) has utilized poly-oxometalate(POMs)-modified TiO_2 electron-transport layer to prepare TiO_2 nanotube arrays (TNAs) photo-anode for zinc phthalocyanine (ZnPc) sensitized solar cells. The POMs/TNAs/ZnPc structure of photo-anode has improved the power conversion efficiency significantly to 45%. Use of POMs in the phthalocyanine sensitized cell prevents charge recombination. Also, electron transport process is get improved by using POMs with TiO_2 nanotube arrays. The process of electron transfer pathways in PW12-modified DSSC is shown in Fig. 3. The process of electron movement from LUMO level of phthalocyanine to conduction band of TiO_2 is an exothermic process. The exited photoelectrons in the phthalocyanine are withdrawal and moved to the TiO_2 while fabrication of TiO_2 and phthalocyanine films. The process can accelerate the separation of excited pairs of electron and hole effectively.

Marandi et al. (2017) prepared a photo-anode using hydrothermal process. The photo-anode was fabricated by spreading a layer of TiO_2 nanorods over a 20 nm nanocrystal layer on the FTO glass substrate. Growth time was manipulated to control the length and diameter of the nanorods and the corresponding thickness of the layer. The bi-layer structure possibly enhanced adsorption and sensitization in the desirable range. Also, the layer of the nanorods over the nanocrystal layer have shown better light absorption and higher power conversion efficiency of the device because of improved light scattering and traveling distance within the photo-anode. The bi-layer device could achieve a maximum efficiency of 6.2% with an enhancement of 47% than the simple nanocrystalline photo-anode device.

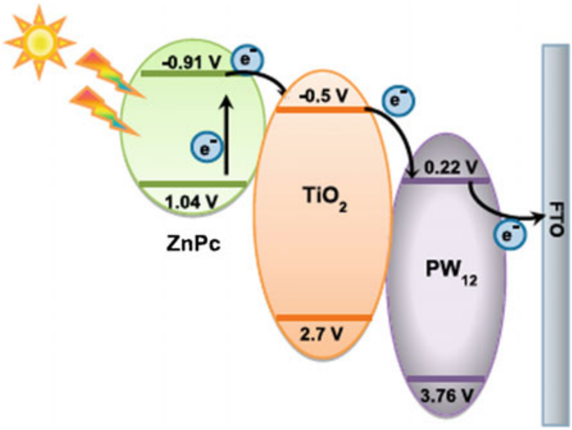

Fig. 3 Representation of electron transfer pathways in phthalocyanine sensitizer solar cells having PW12/TNAs/Pc photo-anodes (Liu et al. 2017)

The thickness of the semiconductor oxide material is crucial from performance and economic point of views in the DSSC. Fine tuning in optical, morphological, blocking behavior, and conductive properties of the semiconductor's compact layer in photo-anode could enhance the device efficiency significantly. The compact layer does not only reduce the charge recombination but also assist in the effective charge transportation. A study by Tanvi et al. (2017) showed that thin compact TiO_2 layers of thicknesses in the range 7–20 nm have not affected the optical properties but influenced the blocking behavior and therefore, the photovoltaic properties. A 7-nm thick layer prepared with 10 mM precursor concentration worked well for the best device performance. As confirmed by the impedance analysis that proper energy level position of the compact layer of the TiO_2 reduces series resistance and enhances chemical capacitance, which results in improved conductivity of the photo-anode. Recently, Nejadasad et al. (2017) used a thermal method to sensitize TiO_2 nanorods and photo-anode was prepared. The paste of TiO_2 nanoparticles prepared by the thermal method increased the efficiency of the DSSC and observed efficiency was 1.58%. Moreover, multiwall carbon nanotubes were used to replace the expensive platinum material on the counter electrode.

Niobium pentoxide (Nb_2O_5) was assessed as a promising photoelectrode material for DSSCs. Chu et al. (2017) prepared urchin-like orthorhombic Nb_2O_5 nanospheres consisting of ultrathin nano rods, by the hydrothermal method, to develop a photoelectrode. The TiO_2 modification on the urchin-like orthorhombic Nb_2O_5 nanospheres increased the photocurrent and PCE of the DSSCs. However, the impedance spectroscopy showed that charge recombination could not be reduced by the TiO_2 modification. The enhancement of dye absorption for orthorhombic Nb_2O_5 photoelectrodes is the desire to improve the performance of orthorhombic Nb_2O_5-based DSSCs. Since Nb_2O_5 exists in a multitude of crystalline polymorphic forms, good control over the preparation conditions is essentially needed for preparing good quality films. Earlier studies on Nb_2O thin films have shown that crystallization and phase formation strongly depends on post-annealing temperature (Venkataraj et al. 2002; Rosenfeld et al. 1996). The main reason for optical loses in Nb_2O_5 microstructures is volume scattering of films annealed below 900 °C and surface roughness for films annealed at this temperature (Lai et al. 2005). The structural and optical properties of the materials play a significant role when it is used as an electron blocking layer in the cell. In DSSCs the photo-excited charge carriers move through layers of different materials having lower purity (Goncalves et al. 2008). Here, the charge separation and transport are functionalized by (i) the enthalpic driving force due to the band edge difference of $\sim 0.2-0.3$ eV between the LUMO of the dye and the edge of the conduction band (CB) of nanocrystalline TiO_2 (ELUMO-ECB) (ii) the galvanic electrical potential drop across the Helmholtz layer, due to formation of a dipole between the cations and negatively charged (iodide and dye) species and (iii) the driving force arising due to HOMO of the dye and the iodide/triiodide redox potential (Cahen et al. 2000; Huang et al. 1997). A recent investigation on the effect of the Nb_2O_5 blocking layer at the working electrode/TiO_2 interface in DSSCs indicated that the cell with crystalline blocking layer demonstrated better performance than the cell with an amorphous blocking layer (Suresh et al. 2016). Suresh et al. (2017) performed an in-depth analysis of structural phase transformation due to post deposition annealing of Nb_2O_5 thin layer on a substrate of the quartz substrate and its role as hole obstructive layer at the interface of the transparent conductive surface (FTO) and titanium oxide film (TiO_2). The co-existence of orthorhombic and monoclinic phases with an interesting surface morphology is perceived at an annealing temperature of 900 °C. Nb_2O_5 blocking layer at the FTO/TiO_2 interface strongly influenced the photovoltaic parameters of the DSSC and the blocking layer in the orthorhombic phase is found to be most effective in suppressing charge recombination and delivered a maximum efficiency of 7.33%. Enhanced open-circuit voltage can be anticipated as Fermi level shifts toward the edge of the conduction band in the TiO_2 because of structural modification of the Nb_2O_5 blocking layer.

Karam et al. (2017) applied the core-shell concept to an urchin-inspired ZnO nanowire photo-anode building block as an option for improving the electron transport and minimizing electron recombination between nanowire and electrolyte. Their study showed that a 10 mm thick TiO_2 ALD shells coating in combination with 10 μm thick top layer of TiO_2 nanoparticles of 15.8 nm sized the urchin-like ZnO block improves the conversion efficiency and the open-circuit voltage (VOC) of the cell. The improvement in the conversion efficiency is seen a result of using urchin-like ZnO nanowire building block, which gives better light scattering and higher surface area with a great control of the nanowire dimensions to increase the dye loading and reduce the electron collection path. Moreover, the thin TiO_2 blocking layer decreases the recombination of charges in such a larger surface area of the nanostructure.

As previously explained in this chapter that the rate of electron transport through a porous network of the TiO_2 and the charge recombination with the redox couple of electrolyte at the interface of the photo-anode/electrolyte can effectively control the efficiency and limitations of the DSSCs. Several grain boundaries exist in the chaotic network of TiO_2 nanoparticles slow down the electron transport and increase the recombination. Low dimensional nanostructured metal oxide materials (e.g., fibers) (Rahman et al. 2011) and flakes are incorporated to enhance the electron transport. The conductivity of photo-anodes in the cells has been increased using carbon materials like graphene sheets and CNTs either as composites with TiO_2 (Singh and Nalwa 2015; Quaranta et al. 2012) or as a thin film applied on the FTO glass substrates (Brown et al. 2008). In both cases, catalytic properties for the chemical reaction presented in Eq. (4) constitute the ultimate limitation to the energy conversion efficiency (Kyaw et al. 2011).

Further, many other alternative photo-anode materials, e.g., ZnO, SnO_2, and Zn_2SnO_4 are being explored to enhance the efficiency and cost reduction. The alternative photoelectrodes material should have large surface area and/or rich surface functionality to enhance dye absorption; suitable structure and good crystallinity to facilitate the photoelectron transfer, and suitable conduction band edge positions to prevent charge recombination and high open-circuit voltage (VOC).

3.2 Advancement in the Counter Electrode

As discussed earlier in this chapter, the counter electrode is another key component, which catalyzes reduction reaction of I_3^- to I^- for regenerating the sensitizer (Hou et al. 2013; Yang and Tang 2016). Therefore, the excellent catalytic property is essential for the electrode in the device for regeneration of the oxidized species in the electrolyte.

Until now, Pt is commonly used for the counter electrode because of its superior conductivity and excellent electrocatalytic activity. The maximum efficiency (>11%) has been observed by the device, having FTO/TiO_2/N749 Dye/I–I_3 structure containing acetonitrile electrolyte and Pt-FTO counter electrode when appropriate additives are used to restrain the electron recombination and dye aggregations (Chiba et al. 2006a). The devices with the Pt counter electrode could attain charge transfer resistance within the desirable value below 1 V/cm^2 (Hagfeldt et al. 2010). Excellent electrical conductivity and lasting stability are the other desirable properties of the materials for the counter electrode. Coating of a thin layer of Pt on the FTO substrate can lower the requirement of expensive material (i.e., Pt) substantially. Despite many excellent properties, the use of Pt material for the counter electrode is still a topic of debate as the cost and stability of highly corrosive I^-/I_3^- redox couple are not in the desirable range.

To minimize the use of expensive material and to enhance the efficiency of the DSSCs, many researchers have tried alternative techniques to prepare the counter electrodes. Recently, (Chen et al. 2017) synthesized platinum nanorods (PtNRs) by electrochemical deposition (ECD) method under atmospheric environmental conditions. The prepared nanorods were used as a counter electrode with an N719 dye-sensitized TiO_2 working electrode and iodine-based electrolyte. The constructed device demonstrated a PCE of 6.58% almost 10% higher compared to 6.00% of the device with the Pt electrode prepared by the conventional sputtering method.

Many other low-cost alternative materials have been assessed for stable counter electrodes for the DSSC. Few of the researchers have reported conductive polymers (Lee et al. 2015; Li et al. 2014; Liu et al. 2014), carbon-based materials (Wu et al. 2016; Wang et al. 2016; Poudel and Qiao 2014; Yu et al. 2017), and metallic/semiconductive compounds (Shi et al. 2015; Zhu et al. 2014; Gu et al. 2014) as alternatives to Pt-counter electrode.

Recently, graphite has been identified as a potential candidate for the counter electrodes it is available abundantly at lower cost and has desirable thermal, electrical, and catalytic properties for the DSSCs. Other advantages of carbon are environmental friendliness and large surface. However, the carbon materials generally have low intrinsic electrocatalytic activity.

Nemala et al. (2017) used a low-cost liquid phase high shear exfoliation method to the prepare nanoplatelet counter electrode from natural graphite. The electrocatalytic activity, of the prepared electrode, towards I/I_3 redox mediator, was observed compared to the standard Pt electrode. Moreover, DSSCs with the GNPs counter electrode exhibited photo-conversion efficiency (PCE) around 6.23% under standard test conditions, which was close to the PCE of the device with Pt-counter electrode. Jia et al. (2017) prepared $CoSe_2$ counter electrode using another effective method known as facile electrochemical deposition. In this method, they used different deposition voltage to control the material thickness. The results of their study indicated that using the deposition at −1.1 V, to prepare the $CoSe_2$ electrode, yielded 22% higher power conversion efficiency (around 10.17%) than the Pt-counter electrode. Hence, the $CoSe_2$ can be a potential substitute for the noble Pt metal.

Many other composites of transition metal compound and carbon material were constructed and used for counter electrodes in DSSCs. Some of them are Fe_3O_4/carbon black (Bagavathi et al. 2016), Co_3O_4/mesoporous carbons (Chen et al. 2015), RuO_2/grapheme (Dao et al. 2015) and RGO/MWCNTs/NiO (Al-Bahrani et al. 2015). Results indicated that the performance of the devices based on these hybrid composites was observed much higher or comparable than that of the devices with pure transition metal compounds or pure carbon materials counter electrodes. A little interest has also been shown to use multiple transition metal compounds, especially the multiple oxide compounds, e.g., Cu_2ZnSnS_4, $Cu_2ZnSnSe_4$, $CoFeO_4$, and $NiCo_2S_4$ (Xie et al. 2017; Yuan et al. 2016; Huang et al. 2016). The results of these studies indicated that multiple transition metal compounds may demonstrate excellent performance. Further, Dong et al. (2017) explored the potential of nanosheet composite of nickel selenide/reduced graphene oxide (Ni0.85Se/rGO) for replacing the Pt counter electrode. The composite coated on the FTO using spin coating technique showed substantial electrocatalytic activity toward I_3/I. The optimal film of Ni0.85Se/rGO counter electrode yielded 9.75% power conversion efficiency. The observed efficiency was 8.15% higher compared to the Pt-based cell. Figure 4 shows the comparative performance of the DSSCs with different counter electrodes. Figure. 4 clearly indicates better performance of the counter electrodes prepared using the alternative material in comparison to the Pt-counter electrode device.

Most recently, Wang et al. (2017) synthesized NiCo2O4/carbon black ($NiCo_2O_4$/C) composite counter electrode. They have tested the performance of the electrode made of $NiCo_2O_4$/C composite and compared with the electrodes of NiO/C, Co_3O_4/C and pristine C. Their electrode yielded remarkably better PCE, 6.27%, compared to NiO/C, Co_3O_4/C and pristine C electrodes, which have demonstrated the PCEs about 5.07, 4.82, and 4.34% respectively. They have used facile solution method to prepare the composite and the material can be used to prepare flexible type counter electrode suitable for flexible DSSCs. Figure 5 shows comparative performance of the different materials.

Huang et al. (2017) have prepared a low-cost NiS-H3Mo12O40P (PMo12) composite CE. They have used periodic potential reversal technique to prepare the electrode. The composite used in the CE has demonstrated the electrocatalytic ability for I_3 reduction comparable to the Pt-based CE. Enhanced efficiency of the cell was observed because of higher electrocatalytic property and mobility of the electron of the composite material. Further, Ramar et al. (2017) reported a new

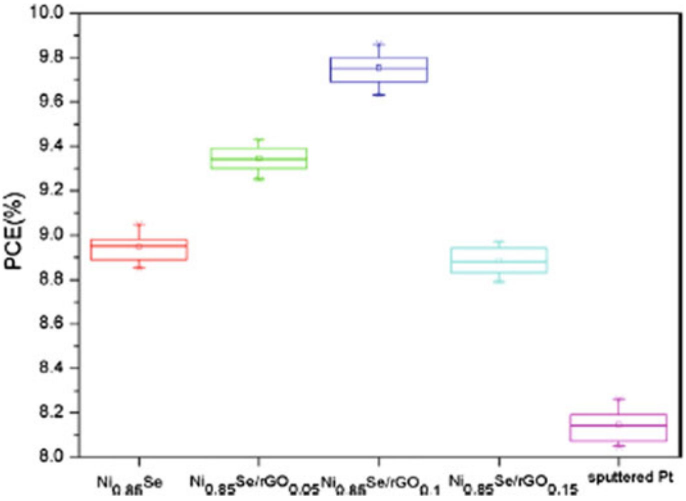

Fig. 4 Comparative PCEs of the DSSC devices using counter electrodes of different materials (Dong et al. 2017)

Fig. 5 Performance of the DSSs, under 1.5 illuminations, with different counter electrodes of an active area of 0.20 cm^2. Wang et al. (2017)

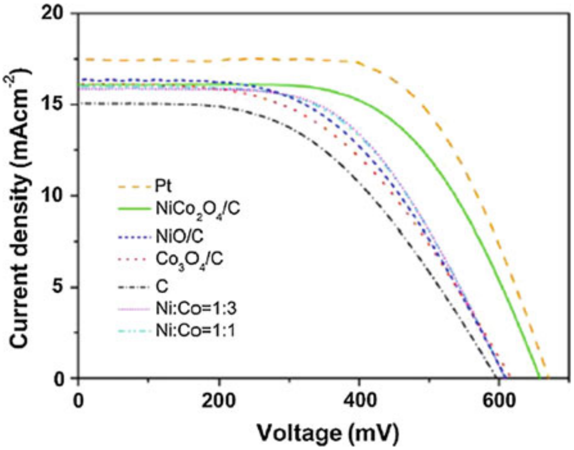

nanocomposite polyisothianaphene (PITN)/graphene, a highly efficient CE to replace the Pt. The cyclic voltammetry analysis revealed that the nanocomposite prepared in 1:4 ratio of polymer to graphene (PITN/graphene (1:4)) demonstrated a higher electrocatalytic activity than Pt. Moreover, the results of the electrochemical impedance spectroscopy and Tafel evaluation of the symmetrical cells indicated a poor charge transfer resistance and better exchange current density. In their study, the cell assembled with TiO_2 (P25) photo-anode sensitized using a dye N719, iodide/triiodide redox electrolyte and PITN/graphene (1:4) CE demonstrated higher

PCE ($\sim$5.2%) than the cell having CEs of pristine PITN (3.5%), graphene (2.5%) and sputtered Pt (4.5%).

Gemeiner et al. (2017) examined a Pt-free screen printed CE prepared from poly (3,4–ethylenedioxythiophene): polystyrene sulfonate (PEDOT: PSS) mixing with rheological agent hydroxyethyl cellulose (HEC). The CEs different percentages of the HEC and PEDOT: PSS were tested. The best performance and specific conductivity (80 S cm^{-1}) was observed with 0.03 wt% of HEC in the mixture and for a lowers thickness of 200 nm. The highest conversion efficiency of the device was achieved is 4.2%, which was around 40% lower than the device (6.9%) consisted of Pt CE.

Yuan et al. (2017) prepared, a novel sandwich-like hierarchical structure composed of reduced graphene oxide (RGO) and uniform cobalt disulfide (CoS_2) octahedrons, by a simple one-step solvothermal process, in which Co_2 cations attracted into graphene framework by the electrostatic adsorption induce the growth of octahedral CoS_2 nanoparticles between the layers of graphene. The cell assembled with the CoS_2/RGO counter electrode manifested excellent photoelectric conversion efficiency (7.69%) little higher than that of the Pt-based cell (7.38%). Recently, Wang et al. (2017) prepared an alternative three-dimensional porous vanadium nitride nanoribbon aerogels (PVNNRAs) counter electrode. The compound was prepared by hydrothermal synthesis and subsequent nitridation in ammonia/argon atmosphere as described in Fig. 6. The conversion efficiency of the DSSC with PVNNRA electrode was estimated at 7.05%, close to the Pt CE. Furthermore, the PVNNRA electrode exhibited good stability in I/I_3 redox electrolyte.

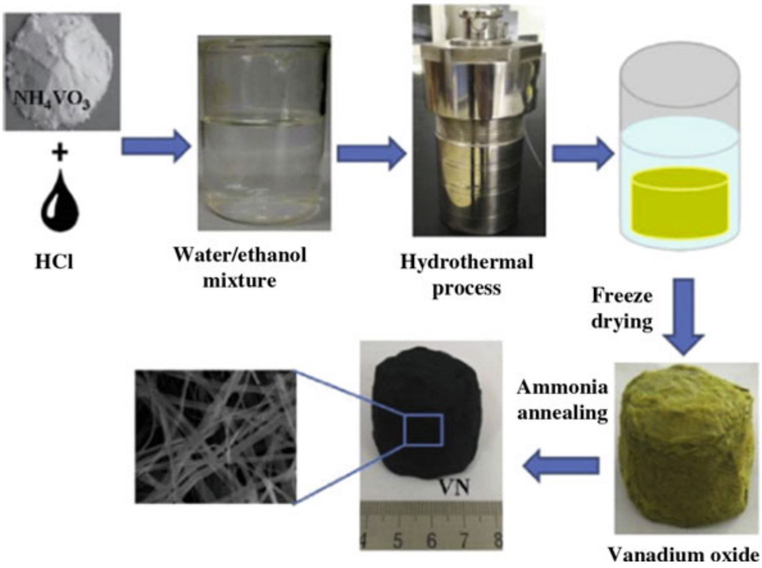

Fig. 6 Schematic preparation procedure for PVNNRAs (Wang et al. 2017)

Chen et al. (2017) prepared Cu_2ZnSnS_4-multiwall carbon nanotubes (CZTS-MWCNTs) nanohybrid Pt-free CE. The CZTS nanoparticles were synthesized by a solvothermal method, which uses an aqueous solution of composite spin coated to make the film. The power conversion efficiency of the DSSC with CZTS-MWCNTs was found to be 9.04%, which was a little higher than the conventional pure Pt-based device (8.74%). The possible electron transfer processes in different components have been demonstrated in following schematic of the electron transporting mechanisms of counter electrodes in Fig. 7. Figure 7 indicates very fast electron transfer in the CZTS-MWCNT electrode and slowest in the MWCNT.

Kim et al. (2017) prepared a core/shell structure counter electrode from carbon nanofiber/platinum nanoparticle (CNF/Pt NP) hybrid web. Their fabrication process is shown in Fig. 8. The nanofibers were prepared from polyacrylonitrile polymer and Pt precursors using coaxial electrospinning. During the process, a series of thermal treatments transformation the precursors CNF web with shell structure of NPs simultaneous. They stated that the spatial distribution of Pt NPs in the CNF increased the electrocatalytic property and the prepared CE showed a low charge transfer resistance at the interface of electrolyte and electrode.

Jayaweera et al. (2017) assessed the performance of ball milled vein graphite and floated graphite as CE materials for the DSSCs. The particle size of the vein graphite used for the CE was between 45 and 63 μm. They have used a mixture of graphite and the morpholine 5:3 ratio and a 250 μm thick layer of the mixture was prepared and sintered 350 °C. Simple ball milled graphite electrode performed 24% poorer than the ball milled floated graphite electrode. Despite 6.47% lower PCE of graphite electrode than Pt electrode, the graphite–electrodes suggested being practically attractive because of its lower cost.

There are many other studies were performed on analyzing the alternative counter electrode materials to enhance the efficiency and reduce the cost of the

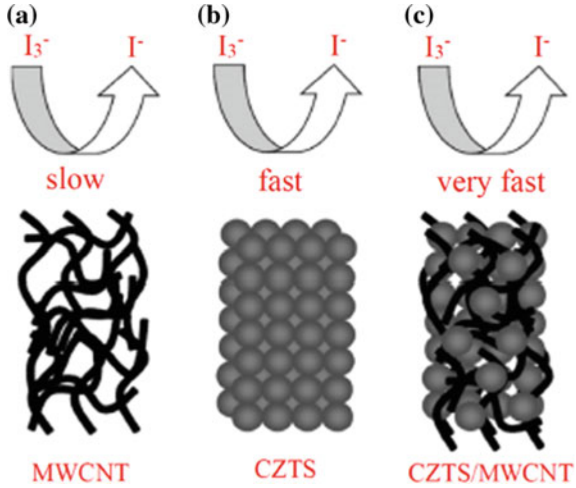

Fig. 7 The schematic of electron transporting mechanisms of CE (Chen et al. 2017)

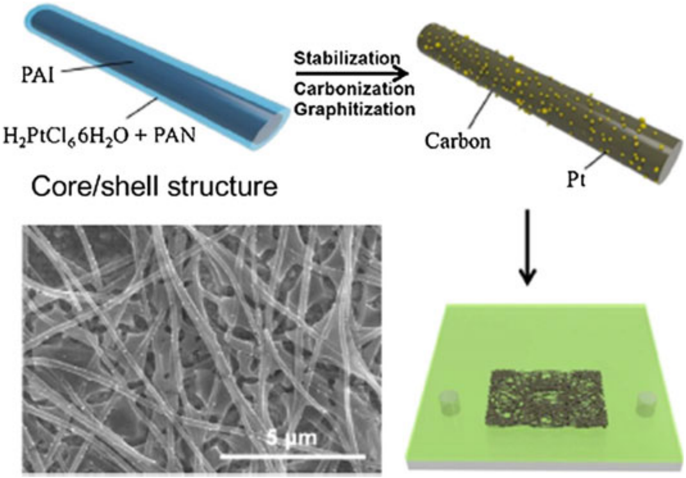

Fig. 8 Fabrication process of a core/shell structured CNF/Pt hybrid web CE (Kim et al. 2017)

DSSC devices, however, all of them cannot be included in this chapter due to the limitation of size.

3.3 Advancement in Dyes for Efficient DSSC

Among the dye sensitizers discovered, Ru(II) and Os(II) polypyridine complexes are the most efficient and commonly used sensitizers in the DSSC. However, these are expensive metal complexes with dyes and the synthesis process is a multistep and complex procedure. The introduction of the metal-free organic dyes for the DSSC was one such effort to replace the expensive metal complexes of dye sensitizers. The organic dyes have several advantages over metal complexes dyes, for example, they are simple in design, attractive colors, reduction of noble metal complexes, and higher molar extinction coefficients than the Ru(II) complexes. The organic dyes also have several disadvantages and one of which is their non-sustainability. The metal-free organic dyes are unstable, which means a tendency to degrade with time. Moreover, their manufacturing tends to be a tedious process. The dyes could be toxic, or the by-products from the manufacturing process might be environmentally hazardous. The desirable requirements of an efficient dye for DSSC application includes (Gong et al. 2012; Hagfeldt et al. 2010; Mikroyannidis 2011):

(i) it should be able to bind strongly with TiO_2 through an anchoring group so that electrons can efficiently be injected into the TiO_2 conduction band (CB). The anchoring group is either a carboxylic or a hydroxyl group;

(ii) molar absorption coefficients should be high enough to absorb solar radiation from visible to the near-IR region;
(iii) electron transfer rate from the dye sensitizer to the TiO_2 should be faster than the decay rate of the dye, and
(iv) the energy level of LUMO should be sufficiently high than the conduction band (CB) level of TiO_2 to allow for efficient charge injection into the TiO_2.
(v) the energy level of HOMO has also to be sufficiently low compared to the redox couple for efficient regeneration of the oxidized dye.

Numerous organic and inorganic dyes have been explored in the literature for the sensitizing purpose in the DSSCs. The ruthenium complexes with terpyridine moieties were the most effective sensitizers due to their wide range of light absorbing capability. These dyes can also absorb light in the near-infrared range. The performances of the DSSCs devices have been observed with these dyes. The devices using black dyes yielded PCE over 10% (Numata et al. 2013; Ozawa et al. 2016; Chiba et al. 2006), which is still not sufficient for real-world applications. Therefore, researchers are putting continuous efforts to improve the performance of the device by investigating the materials of wider absorption and suitable for absorbing an entire range of wavelength. Alteration of the ligand structure of Ru complexes is one of the routes to decrease the energy gap between HOMO and the LOMO. Onozawa-Komatsuzaki et al. (2009, 2012) altered the terpyridine ligand of black dye by replacing two terminal pyridine rings by two quinoline rings. This alteration in the ligand has shifted the LUMO potential of the dye positively and extended the absorption wavelength range of light. Eventually, the modification allows generating current utilizing the photos in the near-infrared region and enhances the incident photon to current conversion efficiency (IPCE) of the DSSC. They have observed that in the visible range devices sensitized by the Ru complexes with 2,6-bis (2-quinolinyl) pyridine ligands demonstrated poor performance compared to the devices sensitized by the black dye. The poor performance was argued as a result of a positive shift in the LUMO potentials of these Ru complexes than the black dye, which creates difficulty in the process of electron injection into the conduction band of the TiO_2. Additionally, 4-carboxyquinoline might not be appropriate for injection of the electron. Katsumata et al. (2017) tested four dye samples of the complexes of Ru synthesized with ligands of 6-(2-quinolinyl)-2,20-bipyridine. The tested samples have shown a wide range of absorption band and potential to enhance the performance of the DSSC. The extended absorption band was observed in the samples over the black dye and is a result of reduced HOMO-LUMO gap in the samples. This could be seen as a result of electron withdrawing/delocalization effects of the qionoline. Results of the study indicated that the photons in the near-IR and visible range of wavelength can be sensitized efficiently by the Ru complex with the ligands composed of both 4-carboxypyridine and 4-carboxyquinoline as well as with 6-(2-quinolinyl)-2,20-bipyridine. Hence, such kind of ligand structures has significant potential to upgrade near-IR Ru sensitizers despite the electron leakage problem from the quinoline.

Further, complex ternary oxides have been identified as potential candidates for the DSSC application due to easier controlling of chemical compositions and band structures than the binary metal oxides. Zn_2SnO_4 is one of the ternary oxides and an n-type semiconductor having a band gap of 3.6 eV. The oxide demonstrated stable properties under extreme conditions and has shown relatively high electron mobility in the range of 10–15 cm^2 V^1 s^1. The nanoparticles of the oxide have also demonstrated the potential for photovoltaic application (Kim et al. 2012), however, the PCE of the material was observed much lower than the TiO_2 because of unfavorable band structure (Wang et al. 2013; Zhao et al. 2016). A recent study showed that the oxide sensitized by the dyes having a phenylene-thiophenylene-phenylene bridge (PSP) can enhance the PCE effectively (Dou et al. 2017). Results (see Fig. 9) of the study indicate significantly higher PCE (4.68%)of a cell sensitized by optimized PSP dyes over the widely used dyes N719 and D131.

Most recently, Fang et al. (2017) synthesized and characterized three new dyes, i.e., FSD101, FSD102, and FSD103. The first two contains a dyne unit while the third one had a monogyne element. Figures 10 and 11 show the structures of the dyes and energy band diagram. The energy bandgap of the samples was estimated for the wavelength range in the absorption spectra of the dyes in DCM (Qian et al. 2016). Compared to the Fermi level of the TiO_2 (0.5 V vs. NHE), the LUMO levels of the dyes were measured sufficiently negative (i.e., −1.53, −1.32 and −1.53 V), which makes the injection of electron easier from the excited molecules of dye into the conduction band of the TiO_2. The dyes, particularly the dyne having dyes FSD101 and FSD102, with the lower energy bandgaps, could be effective sensitizers for the solar cells. The first dye sample has shown better optical, semiconductor, and electrical properties as well as higher PCE (~3.12%) than the third sample of dye (with PCE 1.55%). Also, the second tested sample has shown similar results as the first sample except a slightly lower (2.98%) PCE even though stronger electron withdrawing cyanoacrylic acid group was introduced. The difference in the performances of first and second samples was seen as a result of the poor electron

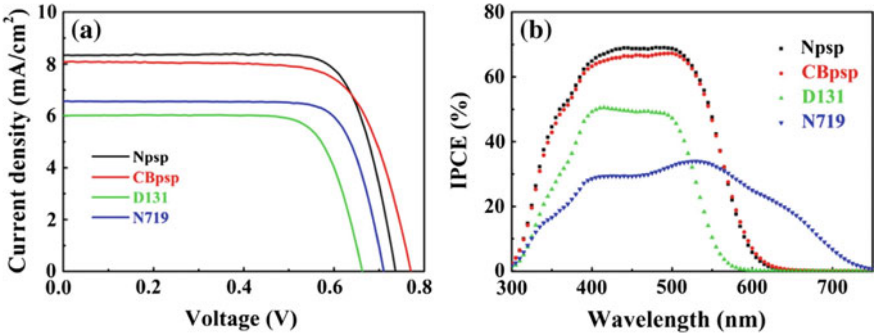

Fig. 9 Performance of Zn_2SnO_4 powder sensitized by different dyes, under AM 1.5G illumination: **a** I–V and **b** IPCE (Dou et al. 2017)

injection from the dye to the TiO_2. Many other developments in dyes have been reported in recent review articles (Prabavathy et al. 2017; Richhariya et al. 2017). Interested readers can go through the above review articles for more detail.

3.4 Advanced Electrolytes

Another component of the DSSCs is an electrolyte. The electrolyte plays an important role in the overall efficiency of the device. The electrolyte, in the DSSC, assists in the movement of the charge carriers between the electrodes and regenerated dye from internal path within itself.

In recent years, many researchers have focused on enhancing the efficiency of the devices utilizing different types of electrolytes including gel polymers (Shen et al. 2014; Benedetti et al. 2015; Bandara et al. 2015; Chou et al. 2015a; Khanmirzaei et al. 2015). The gel polymer electrolytes (GPEs) are promising

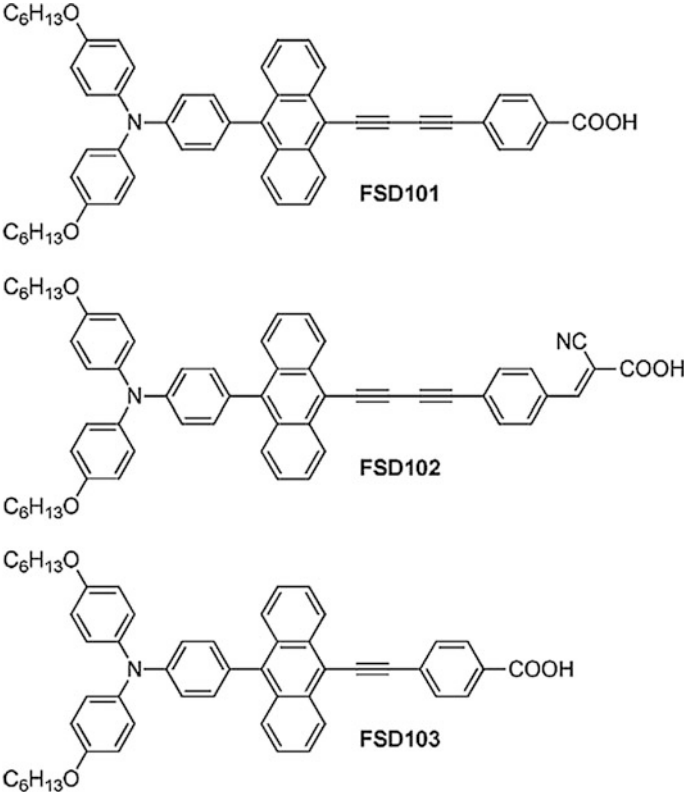

Fig. 10 Representation of molecular structures of dyes FSD101, FSD102 and FSD103 (Fang et al. 2017)

Fig. 11 Comparative energy band diagrams for FSD101, FSD102 and FSD103 (Fang et al. 2017)

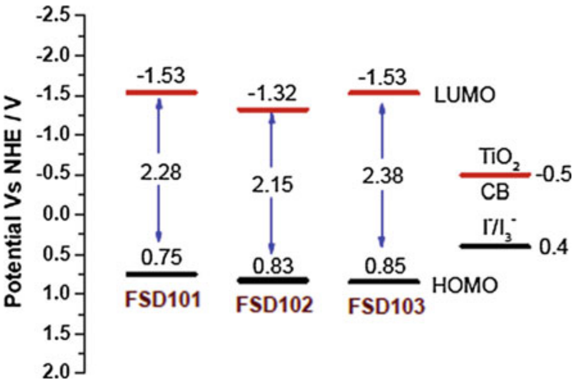

candidates for being safe and highly conductive electrolyte system to fabricate the electrical energy storage devices including solar cells and super capacitors. Biopolymers are natural, environmentally friendly, and cost-effective candidates particularly for the DSSCs (Yusuf et al. 2016). Other potential blended polymers were identified are Polyethylene oxide (PEO) and Polyvinylidene fluoride-co-hexafluoropropylene (PVdF-HFP), which can act as a host to prepare gel polymer electrolyte (GPE) of high conductivity. Fluorine's high electro-negativity and strong interaction with groups CO-C and CF2 of the respective polymers make them excellent alternatives (Prabakaran et al. 2015a, b, c). Ionic movement in the GPEs can be increased by adding NaI salt in the system. The presence of the salt provides more charge carriers (i.e., cations) and contributes to I^-/I_3^- redox couple, which eventually improves the performance of the DSSC (Mohamad et al. 2012; Lan et al. 2008; Noor et al. 2014; Huang 2006). Recently, Zebardastan et al. (2017) studied the ionic conductivities of PVdF-HFP and PEO blended GPEs using ethylene carbonate (EC) and propylene carbonate (PC) solvents in different concentrations in a range of 20% and 100 wt% of the NaI salt. The highest ionic conductivity (6.38 mS cm^{-1}) was observed with 100 wt% concentration (PP-NaI-100). The ionic conductivity of all the GEFs varies with temperature. The GEFs show the Arrhenius behavior. Moreover, the efficiency of DSSC device using the PP-NaI-100 electrolyte was observed highest (about 5.67%). Hence, the PP-NaI-100 GEF was identified as an excellent candidate for enhancing the efficiency of the DSSC. The candidate is safe and could be a cost-effective option.

Liu et al. (2017) studied NiO based p-type aqueous DSSC for different Li-ion concentrations in electrolytes. Presence of the Li-ions forms an electric field close to the surface of NiO electrode and holds back the recombination. Analysis indicated that narrowing the driving force after adding the Li-ions did not influence the process of charge injection. At the same time, improvement in the photo-voltage was observed by increasing the difference between the energy levels of the redox potential of the electrolyte and the valence band of the NiO. The average power conversion efficiency of aqueous p-DSSCs was measured 0.40%, under standard

AM 1.5 G test conditions, at the optimal concentration (1.35 M) of the Li-ions. The efficiency was almost double compared to value without Li-ions.

The performance of the DSSC can change significantly by using electrical additives in the liquid electrolyte. The additives in the electrolyte can improve the potential of the redox couple, kinetics of the recombination, semiconductor surface state and shift of the conduction band edge. Literature shows that the charge recombination rate can be reduced about 1–2 orders of magnitude by adding 4-tert-butylpyridine (TBP) and pyridine derivatives (Hagfeldt et al. 2010). Recently, various other alternative additives have been suggested because of high cost and awful odor of the TBP (He et al. 2014; Bai et al. 2008). Dehghani et al. observed an increase in the efficiency of the DSSC from 6.03% to 7.04% on using triphenylphosphate as an additive (2015). Kusama et al. tested above 20 different additives of benzimidazole for the N719 sensitized solar cells (2004). They observed improvement in the Voc and the fill factor, while the drop in the Jsc. Further, they tested over 30 different alkyl pyridines (Kusama et al. 2003) and a similar effect on the performance of the device was observed in most cases. Sun et al. (2017) tested a mixture of benzimidazole and 2-methylimidazole as a replacement of the TBP. The optimized ratio of the two compounds yielded an efficiency of 7.93% with Voc of 0.817 V, significantly higher than the device with TBP (efficiency 7.49% and Voc of 0.765 V).

4 Reduction of Reflection Losses Using Antireflection Coating

The efficiency of the solar cells also drops due to reflection losses. A fraction of the incident light on the photo-anode reflected the atmosphere as a result of reflecting properties of the glass used in the photodiode. To build a highly efficient solar cell, the losses including the reflection should be least or zero. To minimize the reflection losses, the antireflection coating (ARC) is one of the effective treatments, which are being utilized by the cell designers and researchers (Chou et al. 2015b). According to the Fresnel formula, refractive index of the ARC film should be lower than glass substrate for the effective device. For instance, if the glass substrate's refractive index is 1.52 then the desirable refractive index of the ARC film is 1.22 to eliminate the reflectance completely. Unfortunately, the material of such a low refractive index is not available until now. Consequently, a film of the low refractive index (e.g., SiO_2 film, $n = 1.35$–1.48) is used as an effective approach to reducing the reflection and scattering of the light (Lei and Yang 2010; Yeh et al. 2000).

Chen et al. (2017) deposited a solution of hydrofluosilicic acid (H_2SiF_6) and boric acid (H_3BO_3) in different concentrations on the SiO_2 ARC film for activating the photo-anodes. The film was treated using liquid phase deposition (LPD) method. The LPD-SiO_2 coating brought the refractive index of the film down, improved the transmittance and eventually a gain of 25.39% in the short

Fig. 12 Performance of the DSSC with ARC treated by a solution of hydrofluosilicic acid (H_2SiF_6) and different concentration of boric acid (H3BO3) (Chen et al. 2017)

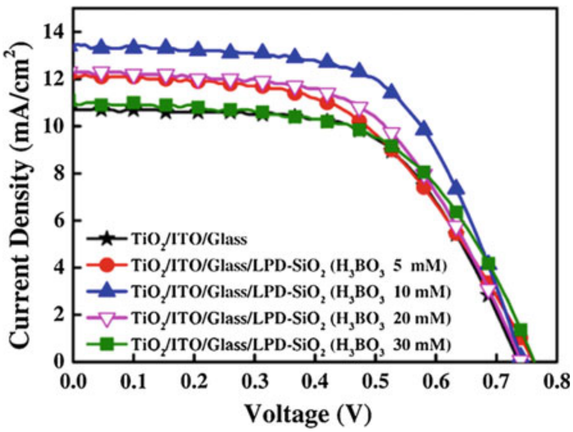

current density was measured (Fig. 12). The film treated by using a 10-mM concentration of H_3BO_3 brought the surface roughness down to 0.49 nm from 1.04, which increased the light transmittance from 91.5% to 93%. Higher transmittance enhanced the photon-absorbing efficiency of the dye and eventually enhanced the conversion efficiency of the device significantly (i.e., from 4.76% to 6.03%).

5 Conclusions

The DSSC is one of the recently emerging conversion technologies that are used for direct conversion of solar energy to the electrical energy. The DSSCs are easy to fabricate, low cost, able to harvest broad range of the solar spectrum. Their transparent and flexible features make them suitable particularly for building application. They can also work in the indoor low light environment and can be fabricated in different colors. The variation in the color and transparency make them the very attractive option as power generating windows in the buildings. Despite many attractive features, DSSCs suffer from the low conversion efficiency, expansive counter electrode, and limited options of efficient dyes. Recombination and reflective losses are major issues that restrict the conversion efficiency in the low range. In recent years, considerable research has been done for identifying alternative materials to make photo-anodes and counter electrodes cost-effective and efficient. Moreover, blocking film is mainly being used for minimizing the recombination losses while the antireflective coating is one of the options to minimize the reflective losses from the photo-anode surface.

References

Al-Bahrani MR, Ahmad W, Mehnane HF, Chen Y, Cheng Z, Gao Y (2015) Enhanced electrocatalytic activity by RGO/MWCNTs/NiO counter electrode for dye-sensitized solar cells. Nano-Micro Lett 7:298–306

Bagavathi M, Ramar A, Saraswathi R (2016) Fe3O4 carbon black nanocomposite as a highly efficient counter electrode material for dye-sensitized solar cell. Ceram Int 42:13190–13198

Bai Y, Cao Y, Zhang J, Wang M, Li R, Wang P, Zakeeruddin SM, Grätzel M (2008) High-performance dye-sensitized solar cells based on solvent-free electrolytes produced from eutectic melts. Nat Mater 7:626–630

Bandara TMWJ, Aziz MF, Fernando HDNS, Careem MA, Arof AK, Mellander BE (2015) Efficiency enhancement in dye-sensitized solar cells with a novel PAN-based gel polymer electrolyte with ternary iodides. J Solid State Electrochem 19:2353–2359

Benedetti JE, Freitas FS, Fernandes FC, Goncalves AS, Magalhes A, Nogueira AF (2015) Investigation of the structural properties of poly(ethylene oxide) copolymer as gel polymer electrolyte and durability test in dye-sensitized solar cells. Ionics 21:1771–1780

Benkstein KD, Kopidakis N, van de Lagemaat J, Frank AJ (2003) Influence of the percolation network geometry on electron transport in dye-sensitized titanium dioxide solar cells. J Phys Chem B 107:7759–7767

Bisquert J, Vikhrenko VS (2004) Interpretation of the time constants measured by kinetic techniques in nanostructured semiconductor electrodes and dye-sensitized solar cells. J Phys Chem B 108:2313–2322

Brown P, Takechi K, Kamat PV (2008) Single-walled carbon nanotube scaffolds for dyesensitized solar cells. J Phys Chem C 12:4776–4782

Caduff M, Huijbregts MAJ, Althaus H-J, Koehler A, Hellweg S (2012) Wind power electricity: the bigger the turbine, the greener the electricity. Environ Sci Technol 46:4725–4733

Cahen D, Hodes G, Grätzel M, Guillemoles JF, Riess I (2000) Nature of photovoltaic action in dye-sensitized solar cells. J Phys Chem B 104:2053–2059

Calogero G et al (2013) Synthetic analogues of anthocyanins as sensitizers for dyesensitized solar cells. Photochem Photobiol Sci 12:883–894

Cameron PJ, Peter LM (2003) Characterization of titanium dioxide blocking layers in dye-sensitized nanocrystalline solar cells. J Phys Chem B. 107:14394–14400

Chen M, Shao LL, Gao ZM, Ren TZ, Yuan ZY (2015) Cobalt oxide and nitride particles supported on mesoporous carbons as composite electrocatalysts for dye-sensitized solar cells. J Power Sources 286:82–90

Chen I-C, Wei Y-H, Tsai MC, Tseng FG, Wei SY, Wu HC, Hsieh CK (2017) High performance dye-sensitized solar cells based on platinum nanoroses counter electrode. Surf Coat Technol 320:409–413

Chen H, Wang J, Jia C, Mou J, Zhu L (2017) Highly efficient dye-sensitized solar cell with a novel nanohybrid film of Cu2ZnSnS4-MWCNTs as counter electrode. Appl Surf Sci 422:591–596

Chen CN, Wu M-J, Hsu CF, Huang JJ (2017) Antireflection coating of SiO2 thin film in dye-sensitized solar cell prepared by liquid phase deposition. Surf Coat Technol 320:28–33

Chiba Y, Islam A, Watanabe Y, Komiya R, Koide N, Han L (2006) Dye-sensitized solar cells with conversion efficiency of 11.1%. Jpn J Appl Phys 45:L638–L640

Chou HT, Hsu HC, Lien CH, Chen ST (2015a) The effect of various concentrations of PVDF-HFP polymer gel electrolyte for dye-sensitized solar cell. Microelectron Reliab 55:2174–2177

Chou CC, Tsao KY, Wu CC, Yang HT, Chen CM (2015b) Improved power conversion efficiency for dye-sensitized solar cells using a subwavelength-structured antireflective coating. Appl Surf Sci 328:198–204

Chu L, Wei L, Yu A, Qin Z, Hu R, Shu H, Luo QP, Min Y, Yang J, Li XA (2017) Effect of TiO2 modification on urchin-like orthorhombic Nb2O5 nanospheres as photoelectrodes in dye-sensitized solar cells. Solar Energy 153:584–589

Dao VD, Larina LL, Lee JK, Jung KD, Huy BT, Choi HS (2015) Graphene-based RuO2 nano hybrid as a highly efficient catalyst for triiodide reduction indye-sensitized solar cells. Carbon 81:710–719

Dong J, Wu J, Jia J, Fan L, Lin J (2017) Nickel selenide/reduced graphene oxide nanocomposite as counter electrode for high efficient dye-sensitized solar cells. J Colloid Interface Sci 498:217–222

Dou J, Li Y, Xie F, Chow TJ, Wei M (2017) Highly efficient triarylene conjugated dyes for dye-sensitized Zn2SnO4 solar cells. Solar Energy 155:1–6

Durrant JR, Haque SA, Palomares E (2004) Towards optimisation of electron transfer processes in dye sensitised solar cells. Coord Chem Rev 248:1247–1257

Fang JK, Sun T, Tian Y, Zhang Y, Jin C, Xu Z, Fang Y, Hu X, Wang H (2017) Novel diyne-bridged dyes for efficient dye-sensitized solar cells. Mater Chem Phys 195:1–9

Gemeiner P, Perinka N, Švorc L, Hatala M, Gál L, Belovičová M, Syrový T, Mikula M (2017) Pt–free counter electrodes based on modified screen–printed PEDOT:PSS catalytic layers for dye–sensitized solar cells. Mater Sci Semicond Process 66:162–169

Goncalves LM, Bermudez VD, Ribeiro HA, Mendes AM (2008) Dye-sensitized solar cells: a safe bet for the future. Energy Environ Sci 1:655–667

Gong J, Liang J, Sumathy K (2012) Review on dye-sensitized solar cells (DSSCs): fundamental concepts and novel materials. Renew Sustain Energy Rev 16:5848–5860

GrandViewResearch (2016) Dye sensitized solar cell market analysis by application (Portable charging, BIPV/BAPV, embedded electronics, outdoor advertising, automotive (AIPV)) and segment forecasts to 2022

Gratzel M (2001) Photoelectrochemical cells. Nature 414:338–344

Gratzel M (2005) Solar energy conversion by dye-sensitized photovoltaic cells. Inorg Chem 44:6841–6851

Green MA (2001) Third generation photovoltaics: ultra-high conversion efficiency at low cost. Prog Photovolt Res Appl 9:123–135

Green MA, Emery K, Hishikawa Y, Warta W, Dunlop ED (2015) Solar cell efficiency tables (version 46). Prog Photovolt Res Appl 23:805–812

Gu X, Zhang S, Qiang Y, Zhao Y, Zhu L (2014) Synthesis of Cu2ZnSnS4 nanoparticles for applications as counter electrodes of CdS quantum dot-sensitized solar cells. J Electron Mater 43:2709–2714

Gu JW, Li N, Tian LD, Lv ZY, Zhang QY (2015) High thermal conductivity graphite nanoplatelet/UHMWPE nanocomposites. Rsc Adv 5:36334–363349

Hagfeldt A, Grätzel M (2000) Molecular photovoltaics. Acc Chem Res 33:269–277

Hagfeldt A, Boschloo G, Sun L, Kloo L, Pattersson H (2010) Dye-sensitized solar cells. Chem Rev 110:6595–6663

He BL, Tang QW, Luo JH, Li QH, Chen XX, Cai HY (2014) Rapid charge-transfer in polypyrrole-single wall carbon nanotube complex counter electrodes: improved photovoltaic performances of dye-sensitized solar cells. J Power Sources 256:170–177

Hou Y, Wang D, Yang XH, Fang WQ, Zhang B, Wang HF, Lu GZ, Hu P, Zhao HJ, Yang HG (2013) Rational screening low-cost counter electrodes for dye-sensitized solar cells. Nat Commun 4

Huang SY, Schlichthorl G, Nozik AJ, Gratzel M, Frank AJ (1997) Charge recombination in dye-sensitized nanocrystalline TiO2 solar cells. J Phys Chem B 101:2576–2582

Huang Y, Lan Z, Wu J, Wang D, Hao S, Lin J (2006) Quasi-solid state dye-sensitized solar cells based on gel polymer electrolyte with poly(acrylonitrile-co-styrene)/NaI + I2. Solar Energy 80:1483–1488

Huang N, Li G, Huang H, Sun P, Xiong T, Xia Z, Zheng F, Xu J, Sun X (2016) One-step solvothermal tailoring the compositions and phases of nickel cobalt sulfides on conducting oxide substrates as counter electrodes for efficient dye-sensitized solar cells. Appl Surf Sci 390:847–855

Huang J, Yao N, Fu K, Deng X (2017) Low cost and high catalytic efficiency composite counter electrode NiS-H3Mo12O40P for dye-sensitized solar cells. Mater Lett 198:65–68

Hug H et al (2014) Bio photovoltaics: natural pigments in dye-sensitized solar cells. Appl Energy 115:216–225

Hwang S, Batmunkh M, Nine MJ, Chung H, Jeong H (2015) Dye-sensitized solar cell counter electrodes based on carbon nanotubes. ChemPhysChem 16:53–65

Jayaweera EN, Kumara GRA, Pitawala HMGTA, Rajapakse RMG, Gunawardhana N, Bandara HMN, Senarathne A, Ranasingh CSK, Huang H-H, Yoshimura M (2017) Vein graphite-based counter electrodes for dye-sensitized solar cells. J Photochemd Photobiol A Chem 344:78–83

Jia J, Wu J, Dong J, Bao Q, Fan L, Lin J, Hu L, Dai S (2017) Influence of deposition voltage of cobalt diselenide preparation on the film quality and the performance of dye-sensitized solar cells. Solar Energy 151:61–67

Kalowekamo J, Baker E (2009) Estimating the manufacturing cost of purely organic solar cells. Sol Energy 83:1224–1231

Karam C, Guerra-Nunez C, Habchi R, Herro Z, Abboud N, Khoury A, Tingry S, Miele P, Utke I, Bechelany M (2017) Urchin-inspired ZnO–TiO2 core-shell as building blocks for dye sensitized solar cells. Mater Des 126:314–321

Katsumata K, Matsui H, Yamaguchi T, Tanabe N (2017) 6-(2-Quinolinyl)-2,20-bipyridine ruthenium complexes for near-infrared sensitization in dye-sensitized solar cells. Inorg Chim Acta 463:118–125

Khanmirzaei MH, Ramesh S, Ramesh K (2015) Hydroxypropyl cellulose based non-volatile gel polymer electrolytes for dye-sensitized solar cell applications using 1-methyl-3-propylimidazolium iodide ionic liquid. Sci Rep 5

Kim DW, Shin SS, Cho IS, Lee S, Kim DH, Lee CW, Jung HS, Hong KS (2012) Synthesis and photovoltaic property of fine and uniform Zn2SnO4 nanoparticles. Nanoscale 4

Kim GH, Park SH, Birajdar MS, Lee J, Hong SC (2017) Core/shell structured carbon nanofiber/platinum nanoparticle hybrid web as a counter electrode for dye-sensitized solar cell. J Ind Eng Chem 52:211–217

Kuang DIS, Wenger B, Klein C, Moser J-E, Humphry-Baker R et al (2006) High molar extinction coefficient heteroleptic ruthenium complexes for thin film dyesensitized solar cells. J Am Chem Soc 128:4146–4154

Kumara NTRN, Lim A, Lim CM, Petra MI, Ekanayake P (2017) Recent progress and utilization of natural pigments in dye sensitized solar cells: a review. Renew Sustain Energy Rev 78:301–317

Kusama H, Arakawa H (2004) Influence of benzimidazole additives in electrolytic solution on dye-sensitized solar cell performance. J Photoch Photobio A 162:441–448

Kusama H, Konishi Y, Sugihara H, Arakawa H (2003) Influence of alkylpyridine additives in electrolyte solution on the performance of dye-sensitized solar cell. Sol Energy Mat Sol C 80:167–179

Kyaw AKK, Tantang H, Wu T, Ke L, Peh C, Huang ZH, Zeng XT, Demir HV, Zhang Q, Sun XW (2011) Dye-sensitized solar cell with a titanium-oxide-modified carbon nanotube transparent electrode. Appl Phys Lett 021107:4776–4782

Lai FC, Li M, Wang HQ, Hu HL, Wang XP, Hou JG et al (2005) Optical scattering characteristic of annealed niobium oxide films. Thin Solid Films 488:314–320

Lan Z, Wu J, Lin J, Huang M, Li P, Li Q (2008) Influence of ionic additives NaI/I2 on the properties of polymer gel electrolyte and performance of quasi-solid-state dye-sensitized solar cells. Electrochimica Acta 53:2296–2301

Lee K, Cho S, Kim M, Kim J, Ryu J, Shin KY, Jang J (2015) Highly porousnanostructured polyaniline/carbon nanodots as efficient counter electrodes for Pt-free dye-sensitized solar cells. J Mater Chem A3:19018–19026

Lei PH, Yang CD (2010) Growth of SiO2 on InP substrate by liquid phase deposition. Appl Surf Sci 256:3757–3760

Li CT, Lee CP, Fan MS, Chen PY, Vittal R, Ho KC (2014) Ionic liquid-doped poly(3, 4-ethylenedioxythiophene) counter electrodes for dye-sensitized solarcsolar cellsells: cationic and anionic effects on the photovoltaic performance. Nano Energy 9:1–14

Liu HSC, Zhang L, Zhang J, Wang H, Wilkinson DP (2006) A review of anode catalysis in the direct methanol fuel cell. J Power Sources 155:95–110

Liu WT, Fang YY, Xu P, Lin Y, Yin X, Tang G, He M (2014) Two-step electrochemical synthesis of polypyrrole/reduced grapheme oxide composites as efficient Pt-free counter electrode for plastic dye-sensitized solar cells. ACS Appl Mater Inter 6:16249–16256

Liu R, Sun Z, Zhang Y, Xu L, Li N (2017) Polyoxometalate-modified TiO2 nanotube arrays photoanode materials for enhanced dye-sensitized solar cells. J Phys Chem Solids 109:64–69

Liu H, Xiang W, Tao H (2017b) Probing the influence of lithium cation as electrolyte additive for the improved performance of p-type aqueous dye sensitized solar cells. J Photochem Photobiol, A 344:199–205

Ludin NA et al (2014) Review on the development of natural dye photosensitizer for dye sensitized solar cells. Renew Sustain Energy Rev 31:386–396

Marandi M, Goudarzi Z, Moradi L (2017) Synthesis of randomly directed inclined TiO2 nanorods on the nanocrystalline TiO2 layers and their optimized application in dye sensitized solar cells. J Alloys Compd 711:603–610

Mikroyannidis JA et al (2011) Low band gap dyes based on 2-styryl-5-phenylazopyrrole: synthesis and application for efficient dye-sensitized solar cells. J Power Sources 196:4152–4161

Mishra AFM, Bauerle P (2009) Metal-free organic dyes for dye-sensitized solar cells: from structure: property relationships to design rules. Angew Chem Int Ed 48:2474–2499

Mohamad AA, Tan WC, Alias S, Ismail AB (2012) Effect of styrene–acrylonitrile content on 0.5 M NaI/0.05 M I2 liquid electrolyte encapsulation for dye-sensitized solar cells. J Solid State Electrochem 16:2103–2112

Narayan MR (2012) Review: dye sensitized solar cells based on natural photosensitizers. Renew Sustain Energy Rev 16:208–215

Nazeeruddin Md K, Baranoff E, Grätzel M (2011) Dye-sensitized solar cells: a brief overview. Sol Energy 85:1172–1178

Nejadasad H, Zarei H (2017) The effect of carbon nanotubes on the efficiency of dye sensitized solar cells based on TiO2 nanorods. Optik 142:211–217

Nemala SS, Kartikay P, Prathapani S, Bohm HM, Bhargava P, Bohm S, Mallick S (2017) Liquid phase high shear exfoliated graphene nanoplatelets as counter electrode material for dye-sensitized solar cells. J Colloid Interface Sci 499:9–16

Noor MM, Buraidah MH, Careem MA, Majid SR, Arof AK (2014) An optimized poly(vinylidene fluoride-hexafluoropropylene)-NaI gel polymer electrolyte and its application in natural dye sensitized solar cells. Electrochim Acta 121:159–167

Numata Y, Singh SP, Islam A, Iwamura M, Imai A, Nozaki K et al (2013) Enhanced light-harvesting capability of a panchromatic Ru(II) sensitizer based on pextended terpyridine with a 4-methylstylryl group for dye-sensitized solar cells. Adv Funct Mater 23:1817–1823

Onozawa-Komatsuzaki N, Yanagida M, Funaki T, Kasuga K, Sayama K, Sugihara H (2009) Near-IR sensitization of nanocrystalline TiO2 with a new ruthenium complex having a 2,6-bis (4-carboxyquinolin-2-yl)pyridine ligand. Inorg Chem Commun 12:1212–1215

Onozawa-Komatsuzaki N, Funaki T, Kasuga K, Nakazawa Y, Sayama K, Sugihara H (2012) Synthesis and electrochemical properties of 2,6-bis(quinoline-2-yl) pyridyl ruthenium complexes as near-infrared sensitizers for dye-sensitized solar cells. Jpn J Appl Phys 51:10

O'Regan B, Grätzel M (1991) A low-cost, high-efficiency solar cell based on dye-sensitized colloidal TiO2 films. Nature 353:737–740

O'Regan B, Moser J, Anderson M, Graetzel M (1990) Vectorial electron injection into transparent semiconductor membranes and electric field effects on the dynamics of light-induced charge separation. J Phys Chem 94:8720–8726

Ozawa H, Sugiura T, Kuroda T, Nozawa K, Arakawa H (2016) Highly efficient dye sensitized solar cells based on a ruthenium sensitizer bearing a hexylthiophene modified terpyridine ligand. J Mater Chem A4:1762–1770

Poudel P, Qiao Q (2014) Carbon nanostructure counter electrodes for low cost and stable dye-sensitized solar cells. Nano Energy 4:157–175

Powell DM, Fu R, Horowitz K, Basore PA, Woodhouse M, Buonassisi T (2015) The capital intensity of photovoltaics manufacturing: barrier to scale and opportunity for innovation. Energy Environ Sci 8:3395–3408

Prabakaran K, Mohanty S, Nayak SK (2015a) Solid state dye sensitized solar cells: Eosin-Y sensitized TiO2-ZnO/PEO-PVDF-HFP-MMT electrolytes/MWCNT-Nafion (R) counter electrode. Ceram Int 41:11824–11835

Prabakaran K, Mohanty S, Nayak SK (2015b) PEO/PVdF-HFP electrolytes for natural dye sensitized solar cell applications: effect of modified nano-TiO2 on electrochemical and photovoltaic performance. J Mater Sci Mater Electron 26:3887–3897

Prabakaran K, Mohanty S, Nayak SK (2015c) Improved electrochemical and photovoltaic performance of dye sensitized solar cells based on PEO/PVDF-HFP/silane modified TiO2 electrolytes and MWCNT/Nafion (R) counter electrode. Rsc Adv 5:40491–40504

Prabavathy N, Shalini S, Balasundaraprabhu R, Velauthapillai D, Prasanna S, Muthukumarasamy N (2017) Enhancement in the photostability of natural dyes for dye-sensitized solar cell (DSSC) applications: a review. Int J Energy Res 41:1372–1396

Qian X, Shao L, Li H, Yan R, Wang X, Hou L (2016) Indolo[3,2-b]carbazole-based multi-donor–π–acceptor type organic dyes for highly efficient dye-sensitized solar cells. J Power Sources 319:39–47

Quaranta S, Gozzi D, Tucci M, Lazzarini L, Latini A (2012) Efficiency improvement and full characterization of dye-sensitized solar cells with MWCNT/anatase Schottky junctions. J Power Sources 204:249–256

Rahman M, Tajabadi F, Shooshtari L, Taghavinia N (2011) Nano particulate hollow TiO2 fibers as light scatterers in dye-sensitized solar cells: layer-by-layer selfassembly parameters and mechanism. Chemphyschem 5:966–973

Ramar A, Saraswathi R, Vilian ATE, Chen S-M, Wang F-M (2017) Polyisothianaphthene/graphene nanocomposite as a new counter electrode material for high performance dye sensitized solar cell. Synth Met 230:58–64

Richhariya G, Kumar A, Tekasakul P, Gupta B (2017) Natural dyes for dye sensitized solar cell: a review. Renew Sustain Energy Rev 69:705–718

Rosenfeld D, Schmid PE, Szeles S, Levy F, Demarne V, Grisel A (1996) Electrical transport properties of thin-film metal-oxide-metal Nb2O5 oxygen sensors. Sensor Actuat B-Chem 37:83–89

Sacco A, Rolle L, Scaltrito L, Tresso E, Pirri CF (2013) Characterization of photovoltaic modules for low-power indoor application. Appl Energy 102:1295–1302

Shahimin MM, Suhaimi S, Alahmed ZA, Chyský J, Reshak AH (2005) Materials for enhanced dye-sensitized solar cell performance: electrochemical application. Int J Electrochem Sci 10:2859–2871

Shen SY, Dong RX, Shih PT, Ramamurthy V, Lin JJ, Ho KC (2014) Novel polymer gel electrolyte with organic solvents for quasi-solid-state dye-sensitized solar cells. ACS Appl Mater Interfaces 6:18489–18496

Shi ZW, Deng D, Li L (2015) Pt-free and efficient counter electrode with nano structured CoNi2S4 for dye-sensitized solar cells. Sci Rep 1–6

Shin E, Jin S, Hong J (2017) Transparent TiO2 nanowire networks via wet corrosion of Ti thin films for dye-sensitized solar cells. Appl Surf Sci 416:353–357

Singh E, Nalwa HN (2015) Graphene-based dye-sensitized solar cells: a review. Sci Adv Mater 7:1863–1912

Sun X, Li Y, Mao H, Dou J, Wei M (2017) Towards a high open-circuit voltage by co-additives in electrolyte for high-efficiency dye-sensitized solar cells. J Power Sources 359:142–146

Suresh S, Deepak TG, Ni CS, Sreekala CNO, Satyanarayana M, Nair AS et al (2016) The role of crystallinity of the Nb2O5 blocking layer on the performance of dye-sensitized solar cells. New J Chem 40:6228–6237

Suresha S, Unni GE, Ni C, Sreedharan RS, Krishnan RR, Satyanarayana M, Shanmugam M, Pillai VM (2017) Phase modification and morphological evolution in Nb2O5 thin films and its influence in dye-sensitized solar cells. Appl Surf Sci 419:720–732

Tanvi VS, Singh A, Prakash O, Mahajan A, Debnath AK, Muthe KP, Gadkari SC (2017) Improved performance of dye sensitized solar cell via fine tuning of ultrathin compact TiO2 layer. Sol Energy Mat Sol C 170:127–136

Trupke T, Green MA (2002) Improving solar cell efficiencies by up-conversion of sub-band-gap light. J Appl Phys 92:4117–4122

Venkataraj S, Drese R, Liesch C, Kappertz O, Jayavel R, Wuttig M (2002) Temperature stability of sputtered niobium-oxide films. J Appl Phys 91:4863–4871

Wang M, Grätzel C, Zakeeruddin SM, Grätzel M (2012) Recent developments in redox electrolytes for dye-sensitized solar cells. Energy Environ Sci 5:9394–9405

Wang PWB, Humphry-Baker R, Moser J-E, Teuscher J, Kantlehner W et al (2005) Charge separation and efficient light energy conversion in sensitized mesoscopic solar cells based on binary ionic liquids. J Am Chem Soc 127:6850–6856

Wang YF, Li K-N, Xu Y-F, Rao H-S, Su C-Y, Kuang D-B (2013) Hydrothermal fabrication of hierarchically macroporous Zn2SnO4 for highly efficient dye-sensitized solar cells. Nanoscale 5:5940–5948

Wang GQ, Zhang J, Hou S, Zhang W, Zhao ZD (2016) Edge-nitrogenated graphene nanoplatelets as high-efficiency counter electrodes for dye-sensitized solar cells. Nanoscale 8:9676–9681

Wang Y, Fu N, Maa P, Fang Y, Peng L, Zhou X, Lina Y (2017) Facile synthesis of NiCo2O4/carbon black composite as counter electrode for dye-sensitized solar cells. Appl Surf Sci 417:670–677

Wang G, Hou S, Yan C, Lin Y, Liu S (2017) Three-dimensional porous vanadium nitride nanoribbon aerogels as Ptfree counter electrode for high-performance dye-sensitized solar cells. Chem Eng J 322:611–617

Wu CS, Chang T-W, Teng H, Lee YL (2016) High performance carbon blackcounter electrodes for dye-sensitized solar cells. Energy 115:513–518. (Part 1)

Xie Y, Zhang C, Yang G, Yang J, Zhou X, Ma J (2017) Highly crystalline stannite-phase Cu2XSnS4 (X = Mn, Fe Co, Ni, Zn and Cd) nano flower counter electrodes for ZnO-based dye-sensitised solar cells. J Alloy Compd 696:938–946

Yang P, Tang Q (2016) A branching NiCuPt alloy counter electrode for high-efficiency dye-sensitized solar cell. Appl Surf Sci 362:28–34

Yeh CF, Lee YC, Wu KH, Su YC, Lee SC (2000) Comprehensive investigation on fluorosilicate glass prepared by temperature-difference-based liquid-phase deposition. J Electrochem Soc 147:330–334

Yoon TP, Ischay MA, Du J (2010) Visible light photocatalysis as a greener approach to photochemical synthesis. Nat Chem 2:527–532

Yu YH, Teng IJ, Hsu YC, Huang WC, Shih CJ, Tsai CH (2017) Covalent bond grafted soluble poly (o-methoxyaniline)-graphene oxide composite materials fabricated as counter electrodes of dye-sensitised solar cells. Org Electron 42:209–220

Yuan H, Jiao Q, Zhang S, Zhao Y, Wu Q, Li H (2016) In situ chemical vapor deposition growth of carbon nanotubes on hollow CoFe2O4 as an efficient and low cost counter electrode for dye-sensitized solar cells. J Power Sources 325:417–426

Yuan H, Liu J, Jiao Q, Li Y, Liu X, Shi D, Wu Q, Zhao Y, Li H (2017) Sandwich-like octahedral cobalt disulfide/reduced graphene oxide as an efficient Pt-free electrocatalyst for high-performance dye-sensitized solar cells. Carbon 119:225–234

Yusuf SNF, Azzahari AD, Yahya R, Majid SR, Careem MA, Arof AK (2016) From crab shell to solar cell: a gel polymer electrolyte based on N-phthaloylchitosan and its application in dye-sensitized solar cells. Rsc Adv 6:27714–27724

Zebardastan N, Khanmirzaei MH, Ramesh S, Ramesh K (2017) Presence of NaI in PEO/PVdF-HFP blend based gel polymer electrolytes for fabrication of dye-sensitized solar cells. Mater Sci Semicond Process 66:144–148

Zhao T, Luo W, Deng Y, Luo Y, Xu P, Liu Y, Wang L, Ren Y, Jiang W (2016) Monodisperse mesoporous TiO2 microspheres for dye sensitized solar cells. Nano Energy 26:16–25

Zhu L, Qiang YH, Zhao YL, Gu XQ (2014) Double junction photo electrochemical solar cells based on Cu2ZnSnS4/Cu2ZnSnSe4 thin film as composite photo cathode. Appl Surf Sci 292:55–62

Photovoltaic-Assisted Thermoelectric Cooling and Heating Systems

Kashif Irshad, Khairul Habib and R. Saidur

Abstract At present, maintaining thermal comfort inside the buildings is becoming expensive and environmental unfriendly for a great majority of countries, as the mechanism of cooling air can prompt the tremendous utilization of energy and CO_2 emissions. This chapter introduces the renewable concept of photovoltaic (PV) and thermoelectric module (TEM) implemented on the building for thermal load reduction. The chapter starts by describing the basics of the PV technology and its dependent parameters, which enhances its performance. In addition, TEMs as an alternative to conventional space conditioning technology are presented. Since PV panel can power the TEMs directly and cause no harm to the environment, therefore, the numerical modeling of PV-assisted TEMs for development of energy-efficient buildings is presented. After that, different kinds of literature focusing on the application of integration of two materials, i.e., TEM and PV for thermal load reduction of buildings, are provided. Results suggested that implementation of PV-assisted TEM system reduces 5–10 °C inlet temperature with COP ranges from 0.4 to 2.5. Lastly, the challenges and future commendation of PV-assisted TEMs technologies are discussed. Thus, it was suggested that PV-assisted TEM system provides Freon free, less energy consuming, and less CO_2

K. Irshad (✉)
Mechanical Engineering Department, King Khalid University,
P.O Box: 960, Abha 6142, Kingdom of Saudi Arabia
e-mail: alig.kashif@gmail.com

R. Saidur
Research Centre for Nano-Materials and Energy Technology (RCNMET),
School of Science and Technology, Sunway University,
No. 5, Jalan Universiti, Bandar Sunway, 47500 Petaling Jaya, Malaysia
e-mail: saidur@sunway.edu.my

R. Saidur
Department of Engineering, Lancaster University, Lancaster LA1 4YW, UK

K. Habib
Department of Mechanical Engineering, Universiti Teknologi PETRONAS,
32610 Bandar Seri Iskandar, Perak Darul Ridzuan, Malaysia
e-mail: khairul.habib@utp.edu.my

A. Sharma et al. (eds.), *Low Carbon Energy Supply*, Green Energy and Technology,
https://doi.org/10.1007/978-981-10-7326-7_13

emission solution to the space conditioning problem of the building as compared to traditional air-condition system.

Keywords Thermoelectric module · Photovoltaic panel · Thermal modeling Heating and cooling · Building envelope

Abbreviations

A_{PV}	Photovoltaic cell's area (m^2)
A_{Glass}	Photovoltaic glazing's area (m^2)
C_{f}	Air duct's friction factor
C_{g}	Glass specific heat (J/kg K)
C_{P}	Air specific heat (J/kg K)
C_{w}	Wall specific heat (J/kg K)
d	Air duct hydraulic diameter (m)
D, D_{w}, D_{G}	Air duct's depth, thickness of the wall, and glass panel thickness (m)
E	Power rate of PV cells (W/m^2)
g	Gravitational acceleration (m/s^2)
G	Vertical plane's total solar radiation (W/m^2)
G	Geometric factor (cm)
G_{BR}	Beam radiation on surface (W/m^{2}h)
G_{H}	Horizontal surface global solar radiation (W/m^2 h)
G_{N}	Direct normal solar radiation (W/m^2 h)
G_{PV}	Solar radiation which arrives on the PV surface (W/m^2)
Gr_{x}	Local Grashof number
G_{TR}	Total radiation on surface (W/m^2 h)
h_{co}, h_{ci}	External and internal surfaces of PV glass panel convective heat transfer coefficients (W/m^2 K)
h_{nrwo}	External heat transfer coefficient's radiation of normal wall (W/m^2 K)
h_{nwi}, h_{nwo}	Convective heat transfer coefficient on the external and internal surfaces of normal wall (W/m^2 K)
h_{ro}, h_{ri}	Radiation heat transfer coefficients on the external and internal surfaces of PV glass panel (W/m^2 K)
h_{rwo}	Radiation heat transfer coefficient on the external surface of PV wall (W/m^2 K)
h_{wo}, h_{wi}	External and internal surfaces of PV wall convection heat transfer coefficients (W/m^2 K)
i	Interest rate
I	Input current to TEMS (A)
I_{mpp}	Current at maximum power point (A)
I_{o}	Saturation current (A)
I_{ph}	Photocurrent (A)
$I_{\mathrm{ph,ref}}$	Photocurrent obtained from a given PV cell at STC reference condition working
I_{sc}	Short circuit current

k_B	$1.3806503 \times 10^{-23}$ J/K is Boltzmann's constant
K_{TE}	Module's thermal conductance (W/K)
L	Height of PV wall (m)
$\dot{m}$	Mass flow rate (kg/s)
n	Time in years
N	Total number of elements used
n_d	Quality factor of the diode
N_{pv}	Number of cells connected in series
N_{ux}	Local Nusselt number
P_{mpp}	Power at maximum power point (W)
Pr	Prandtl number
$\mathrm{P_{TE}}$	Power input for TEM (W)
q	Value of electron's charge (-1.602×10^{-19} C)
Q_{cold}	Heat absorbed at cold surface (W)
Q_{FH}	Fourier heat
Q_{hot}	Heat released at hot surface (W)
Q_{JH}	Joule heat
Q_{PEC}	Peltier cooling
Q_{PEH}	Peltier heating
R_{TE}	Module's electrical resistance (Ω)
S_{TE}	Module's Seebeck voltage (V/K)
ΔT	$T_{hot} - T_{cold}$ (K)
T_{cold}	Cold side temperature (K)
T_{hot}	Hot side temperature (K)
T_a	Next time step's temperature (K)
T_{DB}	Next time step's dry-bulb temperature (K)
T_{in}	Next time step's interior room temperature (K)
T_{nwo}, T_{nwi}	Temperature of external and internal surfaces of normal wall (K)
T_o	Next time step's air duct outlet temperature (K)
T_P, T_e	Temperature of PV glass panel and air duct (K)
T_{pn}	P–N junction's temperature (K)
T_{ref}	298.15 (K)
T_{SKY}	Next time step's sky temperature (K)
T_w	PV wall's temperature (K)
T_{wo}, T_{wi}	Temperature of external and internal surfaces of PV wall (K)
U_j	Overall heat transfer coefficient between interlayer and indoor room (W/m^2 K)
V_a	Velocity of the air flow in the duct (m/s)
V_{in}	Voltage (V)
V_{mpp}	Maximum power point's voltage (V)
V_{oc}	Open circuit voltage
V_w	Next time step's wind velocity (m/s)
w	Width of PV wall (m)
Z	Figure of merit (K^{-1})

Greek Symbol

α	Seebeck coefficient (V/K)
α_{pv}, α_{wall}, α_{nwall}	Absorptivity of the PV cells, PV wall, and the normal wall
α_{wpv}, α_{npv}	Equivalent absorptivities of the elements with and without PV cell on the glass panel
β	Heat expansion coefficient (K^{-1})
ε	PV cell coverage's ratio
ε_o, ε_e, ε_i, ε_{te}	PV's emissivities for internal and external glass panels, the ambient, and thermoelectric module
η_0	Electrical efficiency at standard conditions
κ	Thermal conductivity (W/(cm K))
$\lambda_a, \lambda_g, \lambda_w$	Thermal conductivity of air, glass, and wall (W/m K)
μ_v	Open circuit voltage temperature coefficient (V/K)
μ_f	Short circuit current temperature coefficient (A/K)
v	Kinematic viscosity of air (m^2/s)
ξ_1, ξ_2, ξ_3	Emissivity factors
ρ	Next time step's humidity ratio
ρ, ρ_g, ρ_w	Density of air, glass, and wall (kg/m^3)
σ	Resistivity (Ω cm)
τ_{pv}, τ	External PV cell's transmissivity, glass panel's elements (without PV cell)
φ	Solar azimuth and zenith angle
x	Range of measured value

1 Introduction

The global human population is increasing rapidly over the past few centuries. It is expected that human population will reach about 9.6 billion by 2050 (World population prospects—population division—United Nations 2015). The huge population growth has resulted in a large increase in demand in the building sector. The building industry sector plays a substantial role in the worldwide resource consumption whereby about 50% of the materials taken from nature is utilized to construct diverse sorts of structures and their subordinate facilities (F. ISI, “Projekt” 2015). Besides that, nearly 47.6% of world energy is consumed in the operational process of buildings (F. ISI, “Projekt” 2015), which lead to more than 36% of CO_2 discharges (F. ISI, “Projekt” 2015) as clearly shown in Fig. 1 whereby the heating ventilation and air-conditioning system (HVAC) has revealed to be the most energy consuming devices used in the buildings for cooling and heating purposes.

In order to tackle these issues, numerous studies have been conducted worldwide to improve the energy efficiency of buildings. These techniques include renovating

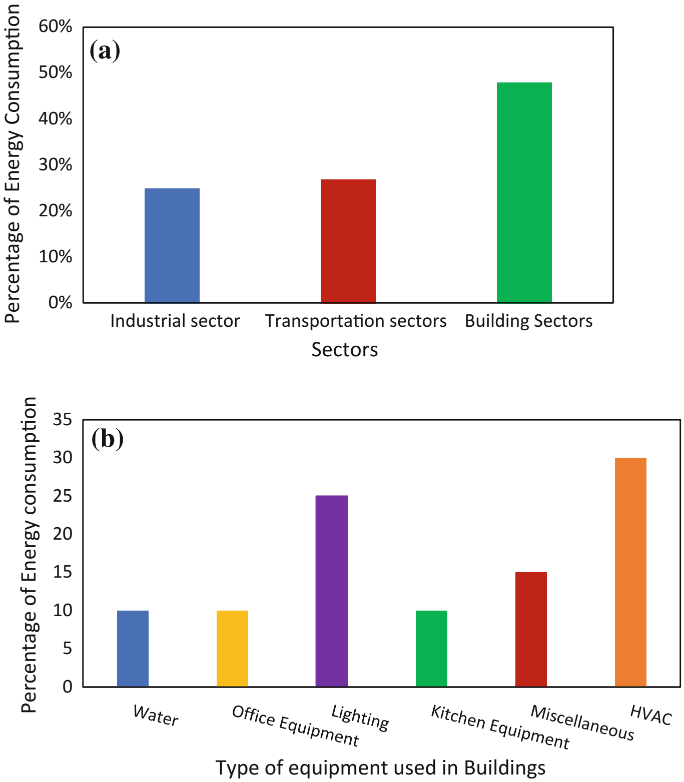

Fig. 1 **a**, **b** Energy consumption in different sectors and energy consuming equipment in buildings (F. ISI, "Projekt" 2015)

the existing structure by employing energy-efficient techniques and analyzing it technically and economically (Huang et al. 2013); life-cycle analysis (Manfren et al. 2013); new designing and construction material of building structure such as insulation materials, reflective coatings (Yu et al. 2009; Joudi et al. 2013); and thermal load reduction by managing the heating, cooling, ventilation and air-conditioning installations, and lighting systems (Goyal et al. 2013). However, HVAC system installed on the buildings utilized a significant proportion of energy from the total energy consumption in buildings (Chua et al. 2013). A market report indicates that with the rapid economic growth as well as electrification expansion, developing countries, especially Asian countries, are seeing a large increase in the demand for the HVAC equipment, and this demand will rise from $91.5 to $120 billion by 2018 (T. F. G. Inc, Critical power: Selective coordination in healthcare buildings 2015).

The current ways used to resolve the present circumstance are to use alternative energy assets. This can decrease the utilization of conventional technologies or system that consumed a lot of energy. Application of semiconductor materials along with building material such as placement of solar cells on the exterior part of the buildings has revealed that PV panel not only decreases the thermal load of the buildings but also provides energy by converting solar energy into electrical energy commonly known as the photoelectric effect. But, for the regions such as tropical climate, where both temperature and humidity stay high consistently, building that incorporated with the PV framework alone cannot reduce the warm load inside the structures. So, integration of another material knows as the thermoelectric module (TEM) alongside with the PV framework for the advancement of self-feasible air cooling framework can solve this issue. TEMs are solid semiconductor-based electronic segments, which operates on the standard of the Peltier effect, with the advantages of the helpful establishment, no moving parts, and reliable operation. But, due to the low coefficient of performance (COP), cooling capacity, and high initial cost, the area of application of TEMs is still restricted to a small region, and there is very limited research focusing on their application in full-scale building cooling applications. Thus, this chapter provides an overview of PV-assisted TEMs for cooling and heating of buildings in order to provide refrigerant free, less energy consuming, and less CO_2 emission solution to the space conditioning problem of the current building.

2 Photovoltaic Technology

Solar energy, which is available abundantly and in free forms, can be directly converted into electricity by using solar cell assembled in series over the photovoltaic panel. One of the fascinating aspects of PV panel is that it converts solar energy into electrical energy without employs any moving components or parts, and does not emit any harmful gases and independent of fossil or nuclear fuels.

2.1 Basic of Photovoltaic

The PV module consists of few numbers of solar cells that are electrically connected in series and thermally in parallel. Solar cells are made of similar types of semiconductor materials such as silicon. The PV module directly converts light energy into electrical energy. This conversion process involves two key processes. First, solar cell absorbs a light photon of the certain wavelength emitted from the sun, followed by raising an electron from lower energy band to higher energy band, and creates electron–hole pairs eventually. An electron in a higher energy band can either travel across the cell until it reaches an electrode or releases its energy as heat and return back to its orbit. So, in a second process, an electric field exists at the p–n junction and separates the hole and electron from recombining. It also acts as a diode by permitting electrons to flow out from the P side to the N side, yet not the other route around. This stream of electrons gives the current and the cell's electric

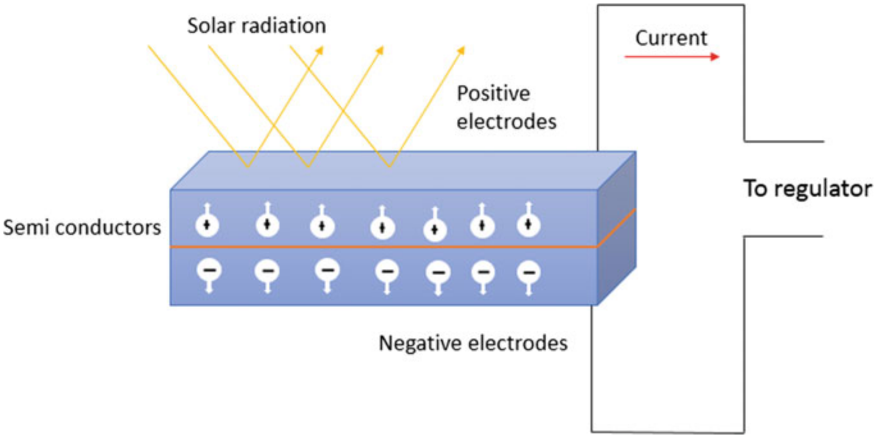

Fig. 2 Cross section view of solar cell

field causes a voltage. By putting metal contacts on the top and base of the PV cell, we can draw that the current off for outside utilization is similar as shown in Fig. 2 (Compare green energy prices and suppliers, GreenMatch.co.uk 2015).

2.2 Photovoltaic System

Although a PV module consists of many cells, which convert solar energy into electrical energy, it cannot be used solely and has to rely on a system to produce usable energy output. A PV system consists of:

(a) PV array, which comprises few modules,
(b) Charge controller to regulate the power from the PV array,
(c) Power storage system consists of deep cycle batteries,
(d) Inverter to convert the DC power from the array to AC power,
(e) Cables, sensors, and physical structure, and
(f) Backup power supply or linking to the utility grid if needed (Prasad and Snow 2005).

The remaining components of the PV system are known as balance of system (BOS), which are also very important for achieving the maximum efficiency and operation of entire system apart from the solar cell of PV module.

3 Thermoelectric Technology

The TEMs can generate a temperature difference, especially when a typical material is subjected to an electric potential (Peltier effect) (Enescu and Virjoghe 2014).

3.1 Basic of Thermoelectricity

A TEM comprises a pair of thin ceramic wafers and several P-type and N-type doped semiconductor material junctions as shown in Fig. 3. It is linked electrically in series and thermally in parallel, forming a thermoelectric couple (Shea 2007). A TEM is formed by combining several hundred of the thermoelectric couples. The P-type element has a shortage of electron while the N-type element has an excess of an electron. An electron tends to move from the P-type to the N-type element through an electrical connector. In other words, an electron is migrated from a lower energy level to a higher energy level. However, an electron tends to release energy into the environment when it moves from the N-type to the P-type element or from an upper energy level to a lesser energy level. In this manner, one face of the Peltier cooler will be warmed while the other side will be cooled (Riffat and Ma 2004).

The nature of a TEM relies on the other parameters such as the temperature variance between the cold and hot sides, the electric current applied across p–n junction, electrical and thermal conductivities of the thermocouple, and thermal

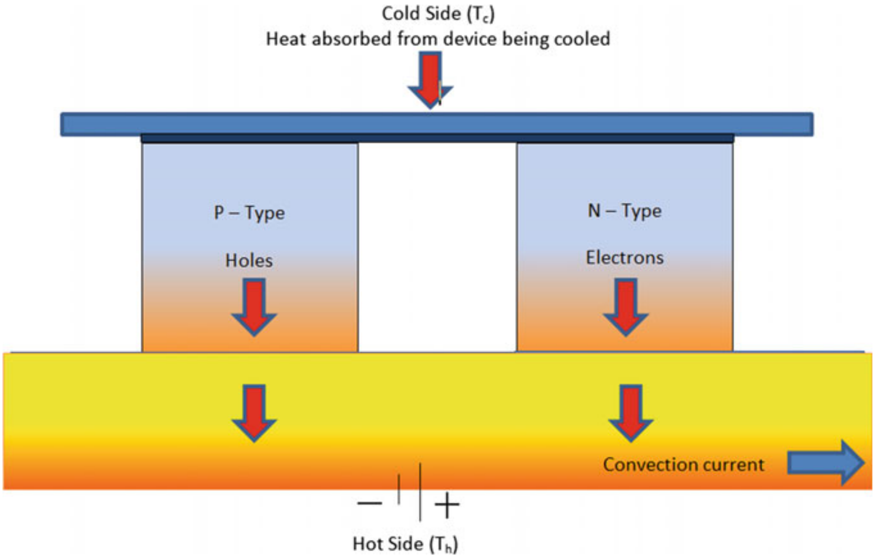

Fig. 3 Working principle of TEM

resistance of the heat sink that attached on the warm face of a TEM (Chein and Huang 2004). The maximum input electric current and cooling capacity are the two factors that can decide the number of thermal elements in a TEM (Goldsmid 2016) while the thermal efficiency of a TEM is depended on the dimensionless figure of a merit ZT value.

The dimensionless ZT value is expressed as (Rowe 1995)

$$\mathrm{ZT} = \frac{\sigma S^2}{K_\mathrm{e} + K_\mathrm{th}} T \tag{1}$$

where σ is electric conductivity, and K is thermal conductivity because of electron transport and lattice phonon. In ZT, the energy carriers such as electrons and holes are the one that can contribute to the electric conductivity (σ) and electronic thermal conductivity (K_e) while the phonons contribute to the lattice thermal conductivity (K_th) (Alam and Ramakrishna 2013).

It is very challenging to make the enhancement efforts of ZT due to the interconnection of the TE parameters. The most common methods used to optimize the TE materials are to decrease the lattice thermal conductivity K. This can be done through the introduction of the scattering centers or/and increase the power factor that can be done through optimization of the carrier concentration. The as-mentioned parameters are the function of the carrier mobility (μ), carrier effective mass (m^*), scattering factor (r), and their interconnectivity limit (ZT) to almost 1 in the large bulk materials. If the carrier concentration (n) is further increased, the Fermi energy, as well as the average energy, also increases but a high rate of increment in Fermi energy also results in a decrement of S (Pichanusakorn and Bandaru 2010). This will lead to the reduction of the power factor (σS^2) significantly. In other words, the increment of σ tends to increase the value of K, which strongly give rises to the thermal conductivity (K). Researchers always focus on providing the solution toward the major problems faced in the bulk materials properties.

It has been identified that the ZT of the TE advance materials can be enhanced using the nanostructuring approach. In other words, improvement of the density of state (DOS) is possible through the quantum confinement that will lead to the increase of the Seebeck coefficient (Fitriani et al. 2016). This enhancement method gives a solution to decouple the electrical conductivity and Seebeck coefficient. Apart from that, nanostructuring allows phonons can be distributed efficiently as compared to the electrons. This strongly contributes to the declination in the thermal conductivity (K_th) (Szczech et al. 2011). The improved ZT of the TE materials can be anticipated for nanotubes and nanowires.

4 Numerical Model of Solar-Assisted Thermoelectric System

In this section, numerical heat transfer models of the PV implemented on the wall with an air gap and TEM system are presented. To fulfill the requirement to drive the required model of the as-mentioned system, the heat conduction process is considered as a one dimension, which appeared to be at the unsteady state. The transfer of heat for PV was presumed to occur from the exterior surface of the PV to the air duct. Accordingly, three energy balance equations for heat transfer model are created as displayed below:

(a) The ratio of the PV cell coverage in the PV panel is defined as (Jie et al. 2007)

$$\varepsilon = \frac{A_{\mathrm{PV}}}{A_{\mathrm{Glass}}} \tag{2}$$

Now, calculation of the produced electrical power by the solar cell for several solar radiations and cell temperature can be done by using a model recommended by Saloux et al. (2011). The photocurrent in relation to temperature and irradiance is defined as

$$I_{\mathrm{ph}} = \frac{G}{G_{\mathrm{ref}}}\left[I_{\mathrm{ph,ref}} + \mu_{\mathrm{f}}(T - T_{\mathrm{ref}})\right] \tag{3}$$

The saturation current can be found as follows:

$$I_{\mathrm{o}} = \frac{I_{\mathrm{sc,ref}} + \mu_{\mathrm{f}}(T - T_{\mathrm{ref}})}{\exp\left[\frac{q(V_{\mathrm{oc,ref}} + \mu_{\mathrm{V}}(T - T_{\mathrm{ref}}))}{nN_{\mathrm{s}}k_{\mathrm{B}}T}\right] - 1} \tag{4}$$

The quality coefficient of a diode (n) is

$$n = \frac{q(V_{\mathrm{m,ref}} - V_{\mathrm{oc,ref}})}{N_{\mathrm{s}}k_{\mathrm{B}}T_{\mathrm{ref}}}\frac{1}{\ln\left(1 - \frac{I_{\mathrm{m,ref}}}{I_{\mathrm{sc,ref}}}\right)} \tag{5}$$

The current and voltage at the uppermost power point together with the corresponding power is determined by

$$V_{\mathrm{mpp}} = \frac{nN_{\mathrm{s}}k_{\mathrm{B}}T}{q}\ln\left(\frac{nN_{\mathrm{s}}k_{\mathrm{B}}T}{qI_{\mathrm{O}}}\frac{I_{\mathrm{SC}}}{V_{\mathrm{OC}}}\right) \tag{6}$$

$$I_{\mathrm{mpp}} = I_{\mathrm{ph}} + I_{\mathrm{O}} - \frac{nN_{\mathrm{s}}k_{\mathrm{B}}T}{q}\left(\frac{I_{\mathrm{sc}}}{V_{\mathrm{OC}}}\right) \tag{7}$$

$$P_{\mathrm{mpp}} = I_{\mathrm{mpp}}V_{\mathrm{mpp}} \tag{8}$$

The voltage of the open circuit is found as follows:

$$V_{\mathrm{OC}} = \frac{nN_{\mathrm{s}}k_{\mathrm{B}}T}{q}\ln\left(1 + \frac{I_{\mathrm{sc}}}{I_{\mathrm{O}}}\right) \tag{9}$$

(b) PV panel's energy balance

The cells of the PV affixed behind to the glass of the PV panel have a minimal thickness. Thus, the conduction of heat from the glass panel and PV cell was effective. It was also expected that the temperature was shifted consistently by *Y* direction of the PV panel as shown in Fig. 4. By assuming uniform temperature distribution along PV cell and neglecting PV cells heat capacity due to its thickness, the resulting equation of the panel can be developed as follows (Jie et al. 2007):

$$\rho_{\mathrm{g}}c_{\mathrm{g}}\frac{\partial T_{\mathrm{P}}}{\partial t} = \frac{\partial}{\partial x}\left(\lambda_{\mathrm{g}}\frac{\partial T_{\mathrm{P}}}{\partial x}\right) + \frac{\partial}{\partial z}\left(\lambda_{\mathrm{g}}\frac{\partial T_{\mathrm{P}}}{\partial z}\right) + b \tag{10}$$

whereby $b = (S_{\mathrm{c}} + S_{\mathrm{p}}T_{\mathrm{P}})/\delta$.

Heat transfer of a glass panel with the PV cell as shown in Fig. 4 is given by (Jie et al. 2007)

$$S_{\mathrm{c}} = [\alpha\tau + (1-\tau)G - E + h_{\mathrm{co}}T_{\mathrm{a}} + \xi_1 h_{\mathrm{ro}}T_{\mathrm{a}} + h_{\mathrm{ci}}T_{\mathrm{e}} + \xi_2 h_{\mathrm{ri}}T_{\mathrm{wo}}] \tag{11}$$

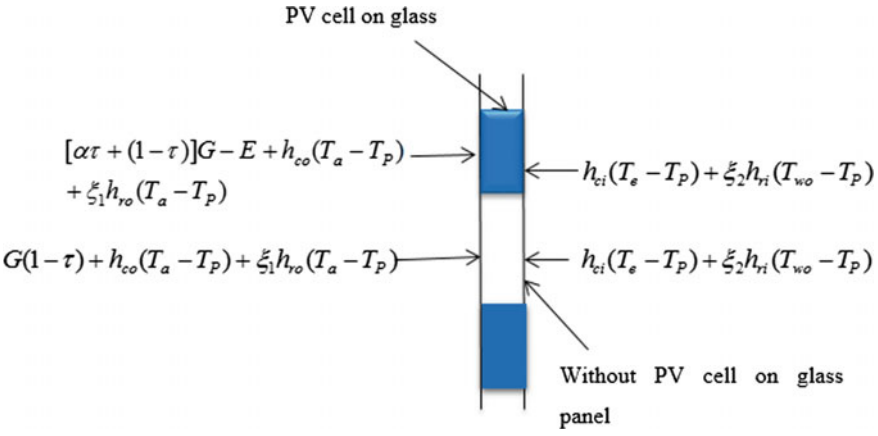

Fig. 4 Heat transfer through the glass panel with or without photovoltaic cell

$$S_{\mathrm{p}} = -(h_{\mathrm{co}} + \xi_1 h_{\mathrm{ro}} + h_{\mathrm{ci}} + \xi_2 h_{\mathrm{ri}}) \tag{12}$$

(1) Heat transfer for a glass panel without PV cell:

$$S_{\mathrm{c}} = [G(1-\tau) + h_{\mathrm{co}} T_{\mathrm{a}} + \xi_1 h_{\mathrm{ro}} T_{\mathrm{a}} + h_{\mathrm{ci}} T_{\mathrm{e}} + \xi_2 h_{\mathrm{ri}} T_{\mathrm{wo}}] \tag{13}$$

$$S_{\mathrm{p}} = -(h_{\mathrm{co}} + \xi_1 h_{\mathrm{ro}} + h_{\mathrm{ci}} + \xi_2 h_{\mathrm{ri}}) \tag{14}$$

Radiant heat transfer coefficients of the PV glass panel surface are given as

$$h_{\mathrm{ro}} = \sigma(T_{\mathrm{P}}^2 + T_{\mathrm{a}}^2)(T_{\mathrm{P}} + T_{\mathrm{a}}) \tag{15}$$

$$h_{\mathrm{ri}} = \sigma(T_{\mathrm{P}}^2 + T_{\mathrm{cold}}^2)(T_{\mathrm{P}} + T_{\mathrm{cold}}) \tag{16}$$

The emissivity factors ξ_1 and ξ_2 can be determined by

$$\frac{1}{\xi_1} = \frac{1}{\varepsilon_{\mathrm{o}}} + \frac{1}{\varepsilon_{\mathrm{e}}} - 1 \tag{17}$$

$$\frac{1}{\xi_2} = \frac{1}{\varepsilon_{\mathrm{i}}} + \frac{1}{\varepsilon_{\mathrm{te}}} - 1 \tag{18}$$

The coefficients of the convective heat transfer for the presence of the wind on both inner and external side of the panel is denoted by (Smolec and Thomas 1993)

$$h_{\mathrm{o}} = 5.7 + 3.8\ \mathrm{V} \tag{19}$$

The resulting heat transfer coefficient can be computed from

$$h_{\mathrm{i}}(X) = (N_{\mathrm{ux}} \lambda_{\mathrm{a}})/X \tag{20}$$

The required equations for turbulent and laminar boundary layer by Tsuji and Nagano (1988) are used:

$$N_{\mathrm{ux}} = 0.120(Gr_{\mathrm{x}} Pr)^{1/3} \quad \text{for turbulent boundary layer} \tag{21}$$

$$Gr_{\mathrm{x}} = g\beta \cdot (T_{\mathrm{p}} - T_{\mathrm{a}}) \cdot X^3/v^2 \tag{22}$$

$$Pr = v/\alpha_{\mathrm{a}} \tag{23}$$

(c) An inner air duct energy balance

The parameter of air for each length was studied in an air duct as shown in Fig. 5. The energy balance for the vertical direction, X in the inner part of an air duct is displayed by (Ji et al. 2007)

$$\dot{m}C_{\mathrm{P}}T_{\mathrm{e}} + h_{\mathrm{ci}}(T_{\mathrm{p}} - T_{\mathrm{e}})w \cdot \mathrm{d}X = \dot{m}C_{\mathrm{P}}(T_{\mathrm{e}} + \mathrm{d}T_{\mathrm{e}}) + h_{\mathrm{wo}}(T_{\mathrm{e}} - T_{\mathrm{wi}})w \cdot \mathrm{d}X + \rho C_{\mathrm{P}}D \cdot w \cdot \mathrm{d}X\frac{\mathrm{d}T_{\mathrm{e}}}{\mathrm{d}t} \tag{24}$$

whereby $\dot{m}$ can be considered as the air mass flow rate and is denoted by $\rho wD \cdot V_{\mathrm{a}}$.

After simplifying Eq. (24), a new equation is obtained as shown below:

$$DC_{\mathrm{p}}\rho\frac{\mathrm{d}T_{\mathrm{e}}}{\mathrm{d}t} = h_{\mathrm{i}}(T_{\mathrm{P}} - T_{\mathrm{e}}) - h_{\mathrm{wo}}(T_{\mathrm{wo}} - T_{\mathrm{e}}) - \rho V_{\mathrm{a}}DC_{\mathrm{p}}\frac{\mathrm{d}T_{\mathrm{e}}}{\mathrm{d}x} \tag{25}$$

$$V_{\mathrm{a}} = \sqrt{\frac{0.5Xg\beta(T_{\mathrm{out}} - T_{\mathrm{in}})L + (\Delta P/\rho)}{C_{\mathrm{f}}(L/d)}} \tag{26}$$

(d) Thermoelectric modules' mathematical model

The equations of cooling and heating capacity of a typical thermoelectric module comprised of four various kinds of heat like Joule heat (Q_{JH}), Peltier heating (Q_{PEH}), Peltier cooling (Q_{PEC}), and Fourier heat (Q_{FH}) are shown below (Enescu and Virjoghe 2014):

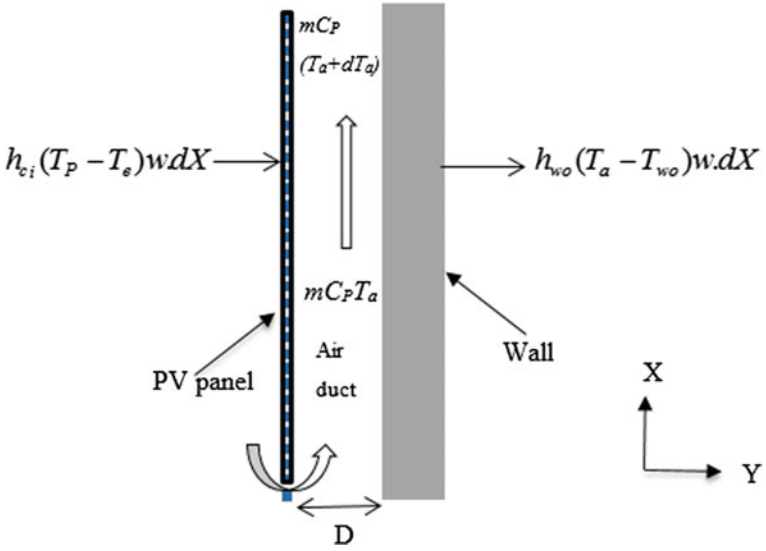

Fig. 5 Energy balance in an air duct

$$Q_{\mathrm{JH}} = I^2R \tag{27}$$

$$Q_{\mathrm{PEH}} = \alpha IT_{\mathrm{hot}} \tag{28}$$

$$Q_{\mathrm{PEC}} = \alpha IT_{\mathrm{cold}} \tag{29}$$

$$Q_{\mathrm{FH}} = K(T_{\mathrm{hot}} - T_{\mathrm{cold}}) \tag{30}$$

By combining all the as-mentioned equations, the cooling and heating capacity of a typical TEM can be expressed as

$$Q_{\mathrm{cold}} = S_{\mathrm{TE}}IT_{\mathrm{cold}} - 0.5I^2R_{\mathrm{TE}} - K_{\mathrm{TE}}\Delta T \tag{31}$$

$$S_{\mathrm{TE}} = 2N\alpha \tag{32}$$

$$R_{\mathrm{TE}} = 2N\sigma/G' \tag{33}$$

$$K_{\mathrm{TE}} = 2N\kappa G' \tag{34}$$

$$Q_{\mathrm{hot}} = S_{\mathrm{TE}}IT_{\mathrm{hot}} + 0.5I^2R_{\mathrm{TE}} - K_{\mathrm{TE}}\Delta T \tag{35}$$

$$V_{\mathrm{in}} = (S_{\mathrm{TE}} \times (T_{\mathrm{hot}} - T_{\mathrm{cold}})) + (I \times R_{\mathrm{TE}}) \tag{36}$$

Energy balance of hot and cold part is revealed as (Goldsmid 2010)

$$h_{\mathrm{TE}}A_{\mathrm{TE}}(T_{\mathrm{hot}} - T_{\mathrm{a}}) = \alpha IT_{\mathrm{h}} + 0.5I^2R - K(T_{\mathrm{hot}} - T_{\mathrm{cold}}) \tag{37}$$

$$h_{\mathrm{TE}}A_{\mathrm{TE}}(T_{\mathrm{a}} - T_{\mathrm{cold}}) = \alpha IT_{\mathrm{C}} - 0.5I^2R - K(T_{\mathrm{hot}} - T_{\mathrm{cold}}) \tag{38}$$

The resulting electrical input power of a typical TEM can be shown by (Goldsmid 2010)

$$P_{\mathrm{TE}} = \alpha I(T_{\mathrm{hot}} - T_{\mathrm{cold}}) + I^2R_{\mathrm{TE}} \tag{39}$$

$$Z = \frac{S_{\mathrm{TE}}^2}{R_{\mathrm{TE}}K_{\mathrm{TE}}} \tag{40}$$

For TEM's cooling mode, the coefficient of performance can be illustrated by

$$\mathrm{COP}_{\mathrm{TE\,cooling}} = \frac{Q_{\mathrm{cold}}}{P_{\mathrm{TE}}} \tag{41}$$

The cooling model's system coefficient of performance can be shown by

$$\mathrm{COP}_{\mathrm{TE-AD\,system}} = \frac{Q_{\mathrm{cold}}}{(P_{\mathrm{TE}} + W)} \tag{42}$$

For the case of TE-AD system, the cooling capacity, $Q_{\text{TE-AD}}$, was assessed by the following equations:

$$Q_{\mathrm{TE-AD}} = C_{\mathrm{p,air}}\dot{m}(T_{\mathrm{a}} - T_{\mathrm{out}}) \tag{43}$$

$$\mathrm{COP}_{\mathrm{TE-AD}} = \frac{Q_{\mathrm{TE-AD}}}{nP_{\mathrm{TE}}} \tag{44}$$

5 Photovoltaic-Assisted Thermoelectric Module Technologies for Building Application

In order to reduce the operational cost of the TE heating and cooling system, the TEM powered by a solar cell is introduced in the market. The PV panel converts solar energy into the direct current, which is directly utilized by TEM without using the additional equipment, i.e., inverter, batteries, etc. The typical solar thermoelectric system inside a house can be generally divided into two types such as solar TE refrigeration equipped with the air-conditioning system and building envelope system with the TE.

5.1 Building Envelope System with Thermoelectric Module

Building envelope system with the TE, which can control the thermal load (i.e., cooling and heating load) of a building, can be developed by incorporating the PV cell and TEMs over the building surface. Both PV and TE system are combined into one enclosure surface. Solar radiation falling on the building surface is converted into direct electrical energy by using PV cells (Khire et al. 2005). This electrical energy is used to provide power to TEMs. This system can work in dual mode, i.e., heating and cooling, depending upon the direction of the input electrical current.

TE-PV building wall was developed by integrating the PV unit and the TEMs as shown in Fig. 6. This system can actively control the heat flux that passes through the wall (Khire et al. 2005). The external surface of the TE-PV building wall consists of the PV unit, then an airflow channel and a TE unit. Khire et al. (2005) develop an analytical model of the TE-PV building wall system. Results show that

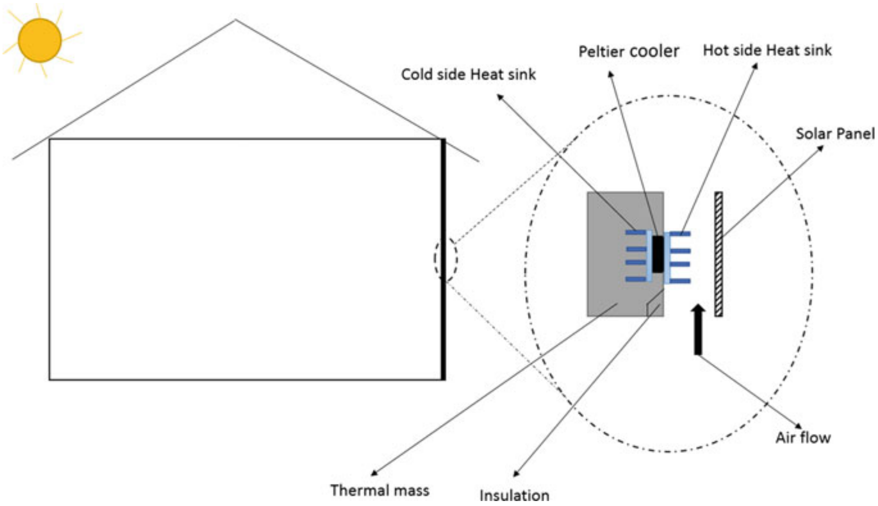

Fig. 6 TE wall building system (Khire et al. 2005)

with the increase in distribution density of the TE coolers, input power required to operate the TEMs decreases. In the majority of the TE-PV building, the wall arrangement thermal resistance of heat sink attached to the TEM plays an important role in deciding the optimal number of TEM required for that particular configuration.

Recently, Liu et al. (2015) developed an innovative solar thermoelectric radiant wall (ASTRW) system. The outcomes validate that the ASTRW reduces the thermal load of a house and gives sufficient cooling capacity for space conditioning. Cooling efficiency of ASTRW was depended on the PV installation angle and increased from 3.3 to 7.1% as the installation angle reduces from 90° to 60°. The overall efficiency of the resulting ASTRW system after incorporating with the PV (1.9%) and TE (5.5%) system. Liu et al. (2015) again tested a system (solar thermoelectric) in the cold climatic environment. The result shows that the average inner surface temperature (T_r) for the system was depended on solar irradiation intensity during daylight on a sunny winter day. At a heating capacity of 111 W/m^2 and solar radiation of about 325 W/m^2, the thermal efficiency of the ASTRW reaches 34.2% with COP of 2.3. While during overcast or raining winter's day, T_r of the system reaches 15.7 °C with a maximum COP of about 2.0 and heating capacity of 36 W/m^2 at 2 V. Finally, it was also suggested that to enhance the ASTRW system, heat dissipation from TEMs should be improved, and heat losses during night time can be reduced by closing inlet and outlet vents.

A novel active thermal insulator (ATI) window developed by Harren-Lewis et al. (2012) consists of semitransparent PV module, TEMs, and heat sink, which was used inside of building for controlling the heat transfer. The results show 67% reduction in heat gain and thermal load of building after installing the ATI window.

PV panel attached to the window reduces heat transfer rate through the window and also generates electrical energy as an additional benefit. ATI window reduces the overall thermal load of the building and can provide a possible solution for high energy consumption and environmental degradation problem. However, parameters such as air flow rate, window configuration and direction of placement, glazing thickness, and optimum number of TEMs are not reported in this study. Maneewan et al. (2004) investigated thermoelectric roof solar collector (TE-RSC) that can aid in decreasing the roof heat gain at the same time refining ventilation of house and attic. The same authors (Maneewan et al. 2005) also investigated the lab-scale model of TE-RSC. Maneewan et al. (2005) performed the numerical simulation combining TE modules with conventional roof solar collector (RSC) in order to analysis attic heat gain reduction. Results show that the yearly energy saving of electrical power is 362 kWh with the roof heat transfer reduction rate of about 3–5 W/m^2. Economic analysis showed that the internal proportion of return was 22.05%, and the payback period of the TE-RSC was 4.36 years.

Liu et al. (2014) developed an innovative solar thermoelectric cooled ceiling integrated with displacement ventilation system (STCC-DV). In STCC-DV system powered by PV system, the conventional hydronic pipe has been replaced with TEMs for dehumidification of air. The results show that input voltage and indoor and outdoor temperatures of enclosure were the factors which strongly influenced the coefficient of performance and total heat flux of the panel. The resulting total heat flux was 110 W/m^2 with COP of 1.9 only for the case of heating mode. In cooling mode, it was 60 W/m^2 and 0.9, respectively, at 4 V. However, the benefits of STCC-DV system as compared to the conventional hydronic pipe system are energy and economic savings, which are not reported in this study.

5.2 Solar Thermoelectric Refrigeration and Air-Conditioners

Conventional refrigeration and air-conditioning system consists of compressor, condenser, evaporator, and expansion valve that is considered as the energy-intensive device (Samuel et al. 2013). Vapor compression technologies using refrigerants such as Freon, R134a, etc., can cause enormous emission of greenhouse gas. As a promising non-vapor compression technology, TEM requires direct current to produce a difference in temperature (Peltier effect). Although the TE refrigeration system has less COP typically in the range of 0.4–0.6, it has a low thermodynamic efficiency of 1%. But it offers many great advantages such as silent operation, refrigerant free, high reliability, and independent on fossil resources.

Dai et al. (2003) investigated experimentally the TE refrigeration system powered by the PV panel and attained the relationship between the coefficient of performance (COP) and solar radiation intensity of a TE refrigerator. Results show that temperature differences between two sides of TEM and intensity of solar insolation were the two key parameters in which the performance of the TE refrigerator varies. At the refrigerated space, a temperature range of 5–10 °C and COP of 0.3 have been accomplished so far. Abdul-Wahab et al. (2009) successfully developed and verified the portable TE cooler experimentally, which is powered by the PV panel. The outcomes reveal that COP of 0.16 and temperature reduction from 27 to 5 °C were achieved in approximately 44 min in the refrigerated area. However, these studies (Dai et al. 2003; Abdul-Wahab et al. 2009) were carried out in a very small-scale control environment. Applications of both the system in a large real transient environment are not reported. Also, performance parameters, i.e., optimum number and input power to TEMs, air flow rate, orientation and an air gap of the PV panel, and heat sink configuration, were not examined. Atik and Çakir (2006) designed a solar-driven TE cooler for off-grid places and buildings. Results show that for enclosure size of 29 × 29 × 29 cm^3, COP of 0.9 was achieved with an indoor temperature of 4.9 °C when the ambient temperature was 17.8 °C. Atik and Yildiz (2012) investigated the performance of the domestic refrigerator equipped with the thermoelectric and PV unit. Results obtained suggested that the difference in temperature between 14.7 °C and COP of 0.58 between the internal and external of the refrigerator have been achieved. Cheng et al. (2011) investigated TEMs driven by solar by using a typical regeneration component for green building purposes. For the test room with dimension of 30 × 12 × 10 cm^3, the temperature difference between the internal and external can extend up to 16.2 °C in the cooling mode. Heat energy dissipated by the solar cell and hot side of TEMs was absorbed by cooling circulating water, thus increasing the efficiency of both the solar cell and TEMs with hot water as a by-product. However, Cheng's study did not provide any information related to the thermal comfort opinion of occupants and economic benefits of the solar-driven TEMs over grid connected TEM system. Mei et al. (1993) became the first who analytically investigated the vehicle application of PV-assisted TE air cooling framework. Results display that for reaching the cooling power of 4 kW at an ambient temperature of 38 °C, 9.5 kW electrical energy was needed. Melero et al. (2003) established a simulation framework for the air-conditioning system that has a total of 48 TEMs. These TEMs were fixed in the ceiling of a room. Outcomes demonstrate that TEMs give adequate temperature reduction in the test room that can fulfill the occupant's requirement. These outcomes reveal that TEMs can act efficiently to reduce the temperature. But experimental validation and effect of parameters, i.e., hot side temperature of TEMs, optimum input power, heat sink fin configuration and air flow rate, air gap and PV efficiency, and life-cycle cost analysis, are not presented in this study. Xi et al. (2007) reviewed the advancement and application of the PV-assisted TE system and concluded that combination of the TEC and PV cell can be used for air-conditioning purpose with less energy consumption and greenhouse gas emission (Xi et al. 2007).

As of late, Alomair et al. (2015) conducted a test to explore the air-conditioner that functioned using solar energy approach in the rustic places. There is a solid relationship between the air-conditioner's cooling capacity and the size of TEMs. It can be said that when the power of a system increases, the temperature variance between the cold and hot part also increases. However, COP is decreasing. Liu et al. (2015) suggested the special type of the air cooling equipped with warm water supply (STACHWS) system. The results uncovered that the temperature of water enormously influences the STACHWS system's performance. In the water heating and room cooling mode, the COP of STACHWS is diminishing with the increase in water temperature. Moreover, the COP in water heating mode and space cooling was 4.51. At the point when this system operates as a pump, the COP can achieve 2.59 in refrigeration mode and 3.01 in the warming mode. In other words, the STACHWS's performance can be enhanced by increasing the heat transfer resistance, input voltage, and figure of merit ZT value. Irshad et al. (2015) first performed an experiment by putting thermoelectric air pipe cooling framework (TE-AD) on the north side of the experimental chamber. The result shows indoor temperature reduction of 1.2–5.3 °C. The test room cooling performance was further explored by the combined effect of north side TE-AD system and south side photovoltaic wall (PV-W) (Irshad et al. 2017). The result uncovered that the input power is directly proportional to the cooling performance of the TE-AD system. About 1806.75 kWh/year was saved when the PV-TE-AD system was at 6 A whereby the resulting COP and cooling capacity were 1.15 and 517.24 W, respectively. Atta (2017) examined a closed space's (30 m^3) thermal performance by using the solar-powered TE cooling system. When this system was operated at 12 V and 11.2 A, about 14 °C in temperature reduction with COP of 0.72 was accomplished.

6 Challenges and Future Recommendations

The as-mentioned BAPV system has experienced some limitations, for example, sensitive to climate patterns. It relies upon different aspects, for example, installation site, solar cell temperature, and the percentage of incident solar energy that converts the cell into electricity. TEMs offer many benefits as they can operate at direct current (DC) that can be provided straightforwardly through solar cells. Notwithstanding, it is expensive, and the energy efficiency is very small in magnitude. The performance of TEMs significantly relies upon the value of ZT. Nonetheless, ZT value that falls under the limited temperature range is not sufficient because of low efficiency. This issue has limited its applications. Moreover, different elements ought to be considered other than the efficiency, for example, high output power density. At the point when the heat source volume is huge, it would not influence the cost of the heat source. It has been distinguished the TEM system faces some issues such as diffusion across various materials. If the PV is combined with the TEM system, it can produce complication in the building construction and design later. This will further increase the costing as the TEMs and PV are still new in the present market. Shortage of talent in the BIPV field also will increase the total design fees.

In future, it is important to utilize the TEM that has ZT factor greater than 2.0 to advance the performance and COP value of the PV-assisted TEM system in the thermoelectric module. Besides that, the phase change material (PCM) to reduce the air flow barrier should be considered to lower the TEMs' heat transfer resistance, especially on the hot side. The sociological investigation on the consciousness of the advantages of the PV-assisted TEMs module is mainly proposed.

7 Conclusions

The importance of changing our current scenario of utilizing energy for maintaining thermal comfort inside the building is essential to ensure our future's prosperity. Among various renewable energy techniques, solar energy can possibly take care of our issues with an abundance of free accessibility. Building applied photovoltaic system (BAPV) proves to be a good alternative in reducing thermal loads of the building with additional benefits of electrical energy production. Thermoelectric technology, which is commonly famous for heating and cooling of small application areas due to low COP, is now gaining popularity in building heating and cooling application. TEMs work on the principle of Peltier effect by converting the direct electrical current into the temperature difference, which is in a solid state. Despite having low COP values typically 0.5, TEMs provide an alternative solution to an existing high energy consuming refrigeration system such as vapor compression system with no moving parts, refrigerants free, high reliability, and flexibility in operation. The performance of TEMs was enhanced by integrating it with the energy storage materials such as PCM. Direct connectivity of the PV and TEMs can generate the temperature difference or known as Peltier effect. This can help to evolve new area of solar-powered TEM. Exploration of this area helps to develop an active building envelope system, including active wall, active window, and active ceiling. By combining the PV system and TEMs, the solar thermoelectric air-conditioner has been developed, which can be used for building cooling and heating applications.

Acknowledgements The authors of the present work feel grateful and would like to thank Ministry of Higher Education (MOHE), Malaysia for giving the funding under grant and Prototype Research Grant Scheme (PRGS) number 0153AB-L08. Besides that, we would like to thank University Teknologi PETRONAS (UTP), Malaysia as well for providing facilities.

References

Abdul-Wahab SA, Elkamel A, Al-Damkhi AM, Al-Habsi IA, Al-Rubai'ey' HS, Al-Battashi AK, Al-Tamimi AR, Al-Mamari KH, Chutani MU (2009) Design and experimental investigation of portable solar thermoelectric refrigerator. Renew Energy 34:30–34

Alam H, Ramakrishna S (2013) A review on the enhancement of figure of merit from bulk to nano-thermoelectric materials. Nano Energy 2:190–212

Alomair M, Alomair Y, Mahmud S, Abdullah HA (2015) Theoretical and experimental investigations of solar-thermoelectric air-conditioning system for remote applications. J Thermal Sci Eng Appl 7:021013

Atik K, Çakir H (2006) Directly connected photovoltaic cooling system. Elec J Mac Tech 3:33–37

Atik K, Yildiz Y (2012) An experimental investigation of a domestic type solar TE cooler. Energy Sources, Part A 34:645–653

Atta RM (2017) Solar thermoelectric cooling using closed loop heat exchangers with macro channels. Heat Mass Transf 1–14

Chein R, Huang G (2004) Thermoelectric cooler application in electronic cooling. Appl Therm Eng 24:2207–2217

Cheng T-C, Cheng C-H, Huang Z-Z, Liao G-C (2011) Development of an energy-saving module via combination of solar cells and thermoelectric coolers for green building applications. Energy 36:133–140

Chua K, Chou S, Yang W, Yan J (2013) Achieving better energy-efficient air conditioning—a review of technologies and strategies. Appl Energy 104:87–104

Compare green energy prices and suppliers, GreenMatch.co.uk (2015) [Online]. Available: http://www.greenmatch.co.uk/. Accessed: 5 Sep 2015

Dai Y, Wang R, Ni L (2003) Experimental investigation and analysis on a thermoelectric refrigerator driven by solar cells. Sol Energy Mater Sol Cells 77:377–391

Enescu D, Virjoghe EO (2014) A review on thermoelectric cooling parameters and performance. Renew Sustain Energy Rev 38:903–916

F. ISI, “Projekt” (2015) [Online]. Available: http://www.isi.fraunhofer.de/isi-de/e/projekte/archiv/bis-2012/155.php. Accessed: 5 Sep 2015

Fitriani OR, Long BD, Barma MC, Riaz M, Sabri MFM, Said SM, Saidur R (2016) A review on nanostructures of high-temperature thermoelectric materials for waste heat recovery. Renew Sustain Energy Rev 64:635–659

Goldsmid HJ (2010) Introduction to thermoelectricity. Series in materials science, vol 121. Springer, pp 7–45

Goldsmid HJ (2016) Introduction to thermoelectricity. Springer, Berlin

Goyal S, Ingley HA, Barooah P (2013) Occupancy-based zone-climate control for energy-efficient buildings: complexity vs. performance. Appl Energy 106:209–221

Harren-Lewis T, Rangavajhala S, Messac A, Zhang J (2012) Optimization-based feasibility study of an active thermal insulator. Build Environ 53:7–15

Huang Y, Niu J-L, Chung T-M (2013) Study on performance of energy-efficient retrofitting measures on commercial building external walls in cooling-dominant cities. Appl Energy 103:97–108

Irshad K, Habib K, Thirumalaiswamy N, Saha BB (2015) Performance analysis of a thermoelectric air duct system for energy-efficient buildings. Energy 91:1009–1017

Irshad K, Habib K, Basrawi F, Saha BB (2017) Study of a thermoelectric air duct system assisted by photovoltaic wall for space cooling in tropical climate. Energy 119:504–522

Ji J, Yi H, Pei G, He HF, Han CW, Luo CL (2007) Numerical study of the use of photovoltaic-Trombe wall in residential buildings in Tibet. Proc Inst Mech Eng, Part A: J Power Energy 221:1131–1140

Jie J, Hua Y, Wei H, Gang P, Jianping L, Bin J (2007) Modeling of a novel Trombe wall with PV cells. Build Environ 42:1544–1552

Joudi A, Svedung H, Cehlin M, Rönnelid M (2013) Reflective coatings for interior and exterior of buildings and improving thermal performance. Appl Energy 103:562–570

Khire RA, Messac A, Van Dessel S (2005a) Design of thermoelectric heat pump unit for active building envelope systems. Int J Heat Mass Transf 48:4028–4040

Khire RA, Messac A, Van Dessel S (2005b) Optimization based design of thermoelectric heat pump unit of active building envelope systems. Heat transfer, Part B, pp 824–90

Liu Z, Zhang L, Gong G (2014) Experimental evaluation of a solar thermoelectric cooled ceiling combined with displacement ventilation system. Energy Convers Manage 87:559–565

Liu Z, Zhang L, Gong G, Han T (2015a) Experimental evaluation of an active solar thermoelectric radiant wall system. Energy Convers Manage 94:253–260

Liu Z, Zhang L, Gong G, Luo Y, Meng F (2015b) Evaluation of a prototype active solar thermoelectric radiant wall system in winter conditions. Appl Therm Eng 89:36–43

Liu ZB, Zhang L, Gong G, Luo Y, Meng F (2015c) Experimental study and performance analysis of a solar thermoelectric air conditioner with hot water supply. Energy Build 86:619–625

Maneewan S, Khedari J, Zeghmati B, Hirunlabh J, Eakburanawat J (2004) Investigation on generated power of thermoelectric roof solar collector. Renew Energy 29:743–752

Maneewan S, Hirunlabh J, Khedari J, Zeghmati B, Teekasap S (2005) Heat gain reduction by means of thermoelectric roof solar collector. Sol Energy 78:495–503

Manfren M, Aste N, Moshksar R (2013) Calibration and uncertainty analysis for computer models—a meta-model based approach for integrated building energy simulation. Appl Energy 103:627–641

Mei VC, Chen FC, Mathiprakasam B, Heenan P (1993) Study of solar-assisted thermoelectric technology for automobile air conditioning. J Solar Energy Eng 115:200

Melero A, Astrain D, Vian J, Aldave L, Albizua J, Costa C (2003) Application of thermoelectricity and photovoltaic energy to air conditioning. In: Proceedings ICT03 22nd international conference on thermoelectrics (IEEE Cat No03TH8726), pp 627–630

Pichanusakorn P, Bandaru P (2010) Nanostructured thermoelectrics. Mater Sci Eng R Rep 67: 19–63

Prasad MD, Snow DK (2005) Designing with solar power: a source book for building integrated photovoltaics. The Images Publishing, London

Riffat SB, Ma X (2004) Improving the coefficient of performance of thermoelectric cooling systems: a review. Int J Energy Res 28:753–768

Rowe DM (1995) CRC handbook of thermoelectrics. CRC Press, Boca Raton, FL

Saloux E, Teyssedou A, Sorin M (2011) Explicit model of photovoltaic panels to determine voltages and currents at the maximum power point. Sol Energy 85:713–722

Samuel DL, Nagendra SS, Maiya M (2013) Passive alternatives to mechanical air conditioning of building: a review. Build Environ 66:54–64

Shea JJ (2007) Thermoelectrics handbook-macro to nano [book review]. IEEE Electr Instrum Mag

Smolec W, Thomas A (1993) Theoretical and experimental investigations of heat transfer in a Trombe wall. Energy Convers Manage 34:385–400

Szczech JR, Higgins JM, Jin S (2011) Enhancement of the thermoelectric properties in nanoscale and nanostructured materials. J Mater Chem 21:4037–4055

T. F. G. Inc, Critical power: selective coordination in health care buildings (2015) [Online]. Available: http://www.csemag.com/single-article/world-hvac-equipment-demand-to-reach-120billion/0f755bca9c29d64103966c8b634c361a.html. Accessed: 5 Sep 2015

Tsuji T, Nagano Y (1988) Characteristics of a turbulent natural convection boundary layer along a vertical flat plate. Int J Heat Mass Transf 31:1723–1734

World population prospects—population division—United Nations (2015) [Online]. Available: https://esa.un.org/unpd/wpp/. Accessed: 05 Sep 2015

Xi H, Luo L, Fraisse G (2007) Development and applications of solar-based thermoelectric technologies. Renew Sustain Energy Rev 11:923–936

Yu J, Yang C, Tian L, Liao D (2009) A study on optimum insulation thicknesses of external walls in hot summer and cold winter zone of China. Appl Energy 86:2520–2529

Familiarization with Energy Storage Technologies and Their Relevance for Renewable Energy (RE) Based Power Generation

Ishan Purohit, Sudhakar Sundaray and Saurabh Motiwala

Abstract This chapter familiarizes with the energy storage technologies, and its applications with respect to nonconventional energy resources. Establishing the energy-environmental interaction and associated challenges of sustainability the requirement of energy storage, energy storage technologies, global scenario, along with the techno-economics of renewable energy (focusing on solar) with storage in the current market scenario have been presented. The initiatives on energy storage to support utility scale electricity in context of India have also been highlighted.

Keywords Energy storage · EES · ESS · Renewable energy · RE

Nomenclature

AGM	Absorbed Glass Mat
CAES	Compressed Air Energy Storage
CEA	Central Electricity Authority
CAPEX	Capital Expenditure
CERC	Central Electricity Regulatory Commission
CIA	Central Intelligence Agency
CSP	Concentrating Solar Power
CUF	Capacity Utilization Factor
DLC	Double-Layer Capacitor
EES	Electrical Energy Storage
EMS	Energy Management System
ESS	Energy Storage System
EU	European Union

I. Purohit (✉)
International Finance Corporation, World Bank Group, New Delhi, India
e-mail: drishanpurohit@gmail.com

S. Sundaray
TAFE Motors and Tractors Limited, Alwar, India

S. Motiwala
Tractebel Engineering Pvt. Ltd, Gurgaon, India

A. Sharma et al. (eds.), *Low Carbon Energy Supply*, Green Energy and Technology,
https://doi.org/10.1007/978-981-10-7326-7_14

EV	Electric Vehicle
FES	Flywheel Energy Storage
GHG	Greenhouse gases
GoI	Government of India
GW	Giga Watt
Gt	Gigatonnes
HFB	Hybrid Flow Battery
IEA	International Energy Agency
IEO	International Energy Outlook
IFC	International Finance Corporation
INR	Indian Rupee
IRR	Internal Rate of Return
kW	kilo Watt
LA	Lead-acid
LCOE	Levelised Cost of electricity
Li-ion	Lithium ion
Mt	Metric ton
MW	Mega Watt
MWh	Mega Watt hour
NaS	Sodium Sulfur
NiCd	Nickel Cadmium
NiMH	Nickel Metal Hydride
NREL	National Renewable Energy Laboratory
OECD	Organisation for Economic Co-operation and Development
OLTC	On-Load Tap Changer
PCM	Phase Change Material
PHS	Pumped Hydro Storage
POSOCO	Power System Operation Corporation Limited
PV	Photovoltaic
RE	Renewable Energy
RECAI	Renewable Energy Country Attractiveness Index
REN21	Renewable Energy Policy Network for the 21st Century
RES	Renewable Energy Sources
RFB	Redox Flow Battery
RRAS	Reserves Regulation Ancillary Services
SM	Solar Multiple
SMES	Superconducting Magnetic Energy Storage
SNG	Synthetic Natural Gas
SVC	Static VAR Compensator
T&D	Transmission and Distribution
TCES	Thermo-chemical Energy Storage
TES	Thermal Energy Storage
ToD	Time-of-Day
TWh	Tera Watt hour

USD	US Dollar
US DOE	United States Department of Energy
WEO	World Energy Outlook
WRI	World Resources Institute
WTG	Wind Turbine Generator

1 Introduction

Energy consumption around the world is significantly growing from past decades. Electricity can be generated through direct or indirect ways. Primary, resources of electricity generation are classified under conventional and nonconventional. Conventional resources of electricity generation are coal, gas, oil, and large hydro whereas, nonconventional includes wind, solar, biomass, etc. Unlike the thermal energy, storing electricity is techno-economically more complex and challenging. Like accumulator, the energy storage facilitates to generate the energy at one time through any source and use it later time as per the requirement/convenience of the end user.

Sustainable energy is essential for sustainable growth of the society which is essentially based on the three core dimensions namely energy security, energy equity, and environmental sustainability. Within the improving economy and life expectancy aspects, the energy requirement per capita is growing across the globe. Our past and current energy systems are dominated by fossil fuels which produce greenhouse gases (GHG) the fundamental cause of global climate change. As per International Energy Outlook (U.S. Energy Information Administration 2016), the world net electricity generation has been estimated to reach 25.8 trillion kWh in 2020 that is approximately 30% higher than the electricity generation reported in 2012. Electricity generation around the globe is dominated by the use of coal as a resource, accounted for 40% of the total electricity generation in 2012. The share of coal is still significant in the overall electricity generation though, a continuous shift for other resources has also been noticed in past few years. As an example, nuclear and large hydro based power plants have reduced the share of coal in the overall electricity generation. These resources prove to be the environmental friendly compared to coal. As per the report of World Energy Outlook (World Energy Outlook 2016), the power sector (including heat production) accounted for 13.5 Gt of CO_2 emissions globally and that is 42% of global energy-related CO_2 emissions. Further, these emissions are the main cause of global warming so as electricity generation as well. In view of the above, to achieve the targets of limiting global temperature *below 2 °C*, a significant and rigorous transition towards clean energy resources is needed. In this aspect, renewable sources of energy play a greater role in the total energy mix. As per the annual report of Renewable Energy Network (Renewables Global Status Report 2017), world renewable power generating capacity was 2017 GW in 2015 which has been increased further with an addition of 161 GW in the year 2016. In the present scenario, solar power is taking the maximum lead (47%) in RE power followed by wind (34%) and small hydro (15%) globally.

In the year of 2016, renewable energy resources nearly have 30% share in the overall installed power generation capacity of the world and same was equivalent to supply the 24.5% of electricity globally. Out of 30%, the share of hydropower was around 16.6%.

As mentioned earlier, there is a continuous shift towards renewable energy resources globally, though these resources have certain limitations compared to their other counterparts (conventional energy resources). One of such major limitations is intermittency (i.e. the variation of the energy resource with time, season, day, location, etc.). In order to ensure adequacy and efficiency of any electro-mechanical system, the energy needs to be available on demand. Most of the time generation and consumption of electricity took place at the same time. Therefore, sufficient amount of electricity needs to be generated to meet the required demand at consumption point instantaneously. The imbalance between the supply and required demand at consumption level may create harmonics in the transmission system (electric grid) and further affects the stability and quality (voltage and frequency). An electricity supplying utility must ensure continuous and flexible power supply for consumers. If the required amount of power is not generated as per the demand the power quality will deteriorate and may cause service interruption. It is obvious from the consumer level that energy demand may vary instantaneously and energy generation source must have to respond accordingly. Therefore, to meet such challenges an accurate forecasting of the variations in demand is essential.

In view of the above, renewable resources can only meet the majority of world's power requirement if they ensure a continuous supply of energy even for variable demand irrespective of their intermittent behavior. Energy storage can play an important role in the same, however, the availability of such energy (stored) should be at affordable cost (Fig. 1).

Therefore, a power plant, must fulfill two essential functions in addition to the basic power generation, (i) to generate sufficient power (kW) when necessary (kilowatt function) and (ii) a forecasting function to assess and follow the minute-by-minute and second-by-second fluctuations in demand, using the extra power from the "kilowatt function". Renewable energy resources (without storage) such as solar and wind do not own both a kW function and a frequency control function unless they are suitably modified. However, the addition of electrical energy storage can helps renewable energy resources (solar and wind) to be equipped with a kW function and a frequency control function. As an example, Pumped hydro has been widely used to meet the shortage of electricity demand at

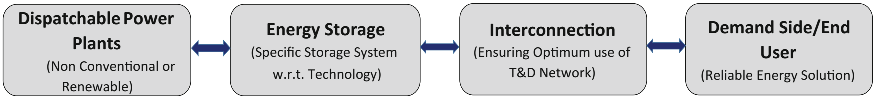

Fig. 1 Electrical system with the flexibility of energy resources

large scale. In a similar way, stationary batteries have also been used in solar and wind-based systems to support output as well as rapid response capability.

Grid-connected renewable energy generation may have several effects on the operation of the power grid. One of them is harmonics in the frequency of power supply. The reason for the same is the fluctuation in the output of renewable energy that makes system frequency control difficult, and frequency deviation too wide thus, system operation may deteriorate. In case of conventional energy generation system (e.g. thermal), frequency control is generally managed by the output change capability of the thermal generators. Most of the times thermal generators are not allowed to operate at full capacity else for most of the time that operate with some positive and negative output margin (i.e. increases and decreases in output) and same is used to adjust frequency, and this cause inefficient operation. It is expected that with increased penetration of renewable power generation, such output margins needs to be increased, and further, decreases the thermal generation efficiency even more. The developing and underdeveloped economies of the world cannot afford inefficient running of thermal power plants as it may increase the cost of energy generation and thus, affects the financial viability. Therefore, installation of energy storage systems at strategic locations (of solar and wind power plants, electric grid substations) can be a promising measure to deal with the above situations. However, the type of storage, the capacity of storage, and the point of interconnection need to be analyzed based on the systematic study of the regional electrical grid network.

The essential roles of electric energy storage in the development of smart grid are as follows:

- **Control** of power flow and mitigate congestion, or maintain the voltage in the appropriate range,
- To electrify the equipment such as Electric Vehicles (EVs) so that same could be integrated into Smart Grid. EVs are used in several countries of the world such as the US and Europe as distributed energy resource. Being a distributed energy resource EVs can also have the capability of providing load shifting function to a smart grid. Moreover, EVs are expected to be the mobile storage medium that has the capability of providing power at the time of peak demand. In view of this, policies for the promotion of electric mobility are evolving in the several countries of the world.
- Energy Storage has a key role in **Energy Management Systems (EMS)** in residential and commercial sectors. As an example of such systems (Residential/ Commercial consumers mostly change their energy consumption as per the Time of Day (TOD) tariff. Therefore utilities having TOD tariff policies will need storage system to store electricity from excess generating or cheaper energy supply source and deliver it as when required. Thus an electric storage system can allow EMS to function optimally for the time when less power needed from the grid or expensive source of supply.

Due to several global and regional driving policies of addressing climate change issues most of the developed and developing countries are increasing the RE share in their energy mix depending on the resource availability. The intermittency caused by solar and wind resources on the grid may strongly affect the power quality and grid balancing. Additionally, in order to synchronize the energy generation through several projects and simultaneous consumption the utilities enforce curtailment over the project developers which are a significant revenue loss. Further, the scheduling and forecasting of RE power have been made mandatory (in the process in several countries like India) by several countries by utilities in order to ensure maximum utilization of the transmission and distribution infrastructure and minimize energy losses due to line unavailability. RE projects have been given Must Run status by many countries, however, several countries have explored the TOD tariff model as well. One side such initiatives are encouraging RE power generation but another side there are several issues need to be addressed with increasing share of RE power on the grid. Energy storage is one of the options to address power curtailment, power balancing, enhance grid availability, improve system utilisation, and support forecasting and scheduling of dispatchable utility scale RE power.

2 Energy and Environment

Energy is the basic need of human being and explicitly required for the well-being and socioeconomic growth of the individual as well as economies of the world thus, make energy resource very significant in the overall progress. However, energy and environment are very closely linked to each other, as energy production and its consumption have certain impacts on the environment and further negative implications. Starting from the beginning, the generation process of energy/electricity (from fossil fuel based plants) releases CO_2 and other GHG emissions that are the prime sources of environmental pollution as well as global warming. The same pollutants emit if such energy sources (fossil fuel based) are even used for transportation, heating, and cooling purposes.

In view of the above countries around the world are much focused on the sustainable development as well as to ensure good quality of life for their residents. As mentioned earlier from the production stage to utilization energy has certain adverse implications on the environment. Energy-related GHG emissions approximately account for 80% of the total emissions. Electricity generation and heat production has the largest share in the same and further followed by the energy use in the transport sector.

By the end of year 2016, the world cumulative electricity production has been reported as 24,816,400 GWh out of which China produces 6,142,490 GWh followed by the USA of 4,350,800 GWh, etc. Figure 2 presents the annual energy generation of top 15 countries/regions across the globe by the year 2016. World annual GHG emissions have been reported as around 45,261.25 Mt CO_2 equivalent in which China contributes around 25.93% followed by the USA as 13.8%, EU by

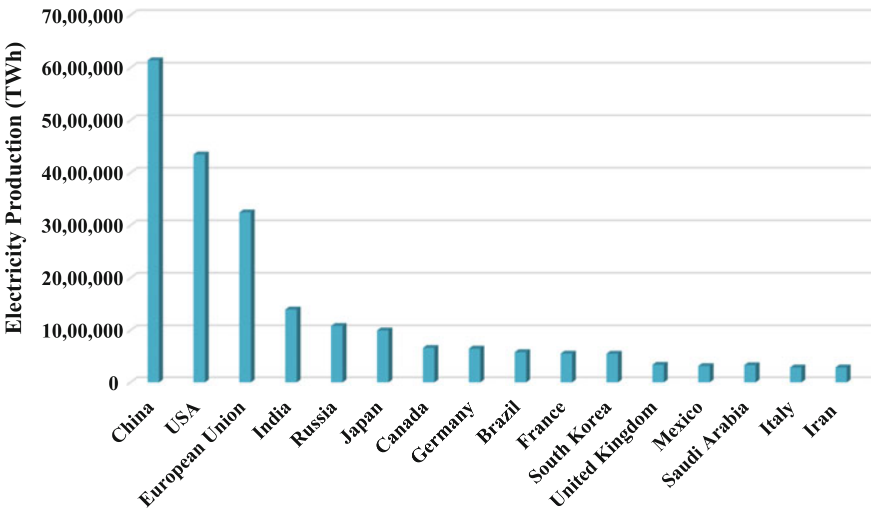

Fig. 2 Annual electricity production by top 15 countries/regions by the year 2016 (BP Statistical Review of World Energy 2017)

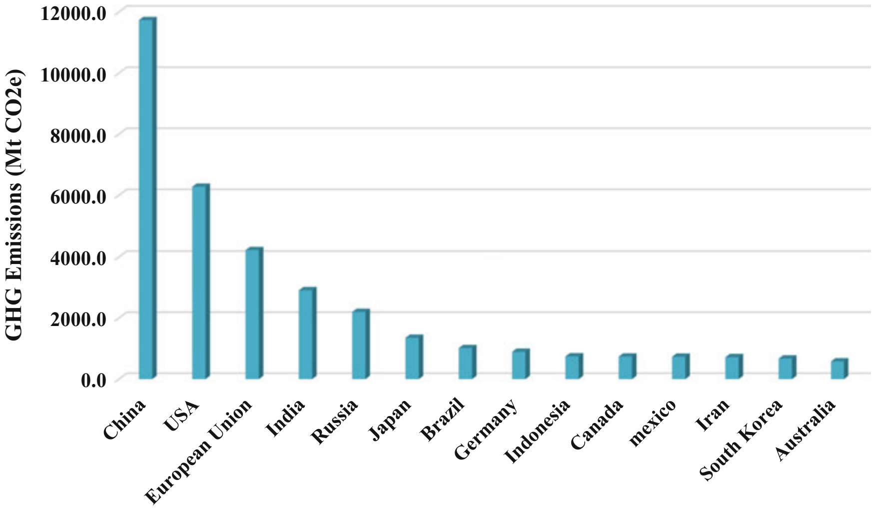

Fig. 3 Annual GHG emissions by top 15 countries/regions by the year 2013 (Wri.org 2017)

9.5% and India at 6.45%, etc. Only 10 countries produce around 70% of global GHG emissions. Figure 3 presents annual GHG emissions by top 15 countries/regions reported by World Resources Institute (Wri.org 2017). It is worth mentioning that around electricity generation singly accounts for the 25% of the overall GHG emissions. On the other hand, transport sector that consumes about 27% of energy demand only accounts for 14% of GHG emissions. Other major GHG emitter sector is industry, that consumes 28% of primary energy and is responsible for 21% of GHG emissions.

2.1 Global Power Scenario

Globally the energy markets are in transition phase due to accelerating growth and improving prosperity causing growth in energy demand especially in developing economies, particularly in Asia, rather than from traditional markets in the OECD. As per the reference case of International Energy Outlook of 2016, it has been projected that world net electricity generation increases 69% by 2040, from 21.6 trillion kWh in 2012 to 25.8 trillion kWh in 2020 and 36.5 trillion kWh in 2040. A worldwide mix of primary fuels used to generate electricity has changed a great deal over the past several decades. Coal continues to be the fuel most widely used in electricity generation, but there have been significant shifts in other generation fuels. Generation from nuclear power increased rapidly from the 1970s through the 1980s, and natural gas-fired generation increased considerably after the 1980s. As per World fact book-CIA, USA the global installed capacity of power generation has been reported as 6.301 billion kW in 2014. Figure 4 presents the world's top ten countries with their installed power generation capacities.

Reduction in the CO_2 and GHG emissions from the energy sector can be possible through two ways, (i) adopting energy efficiency measures in the generation and consumption of energy resources and, (ii) adoption of clean and green energy

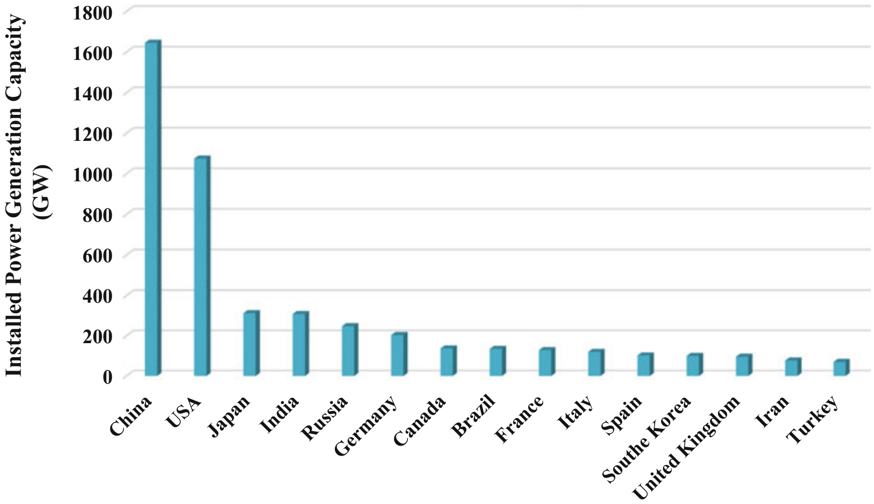

Fig. 4 World's top countries with installed power generation capacity (The World Factbook Library 2017)

resources. The first one has limited scope while the second option (adoption of clean and green energy resources) has a broader scope in long term for environmental perspective. In view of the above considerable emphasis has been given to the development of renewable energy resources from past few decades. Presently renewable energy resources are growing at the much faster rate for electricity generation compared to their other counterparts or conventional energy resources. The growth rate of 2.9% per year has been estimated for the same from 2012 to 2040. With this growth rate (2.9%/year) the share of electricity generation from renewables will increase from 22% in 2012 to 29% in 2040. The non-hydropower renewables accounted for 5% of total world electricity generation in 2012. As per the IEO report, it is expected that until the year of 2040 the share of the same will be 14% due to the growth coming from wind power especially.

In 2015, 147 GW renewables added into global RE generating capacity and the cumulative capacity became 1,849 GW, which is 9% higher over 2014. The contribution of solar and wind together is about 77% of all renewable capacity, where hydropower is 19% (REN 2016).

Figure 5 presents the RE generation capacity in world's top ten countries.

Renewable-based power generation is the prime focus of the countries around the world, to meet their goals regarding the reduction of GHG emissions. Installed capacity and market for renewable energy projects are continuously growing and significant addition to the overall power generation has been reported in past few years. As an example, in the year of 2015 wind-based projects accounted for the 63 GW of power generation. With innovative technologies, better forecasting models and decreasing cost of solar-based power generation is giving a strong competition to the existing conventional options. The reported installed capacity of solar-based power generation reaches 229 GW in the year 2015 and that is 100

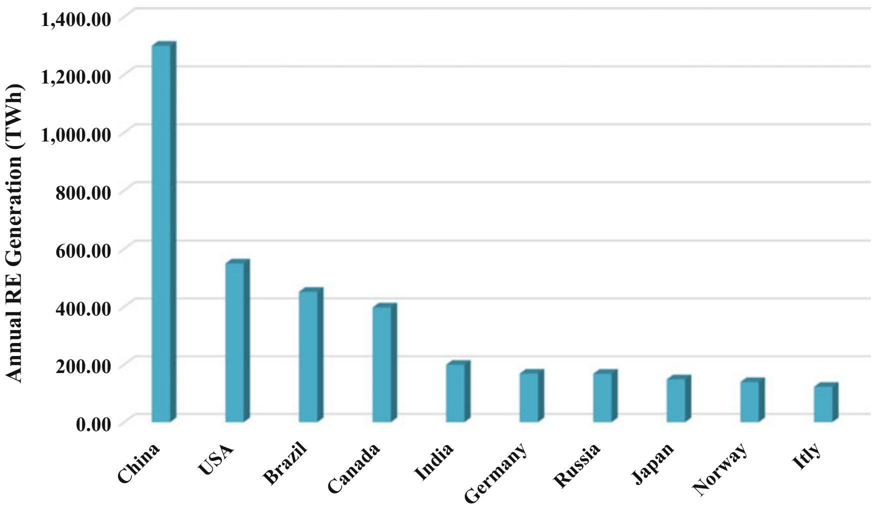

Fig. 5 World's top countries with RE generation capacity (range from 2014 to 2016) (Renewables Global Status Report 2017)

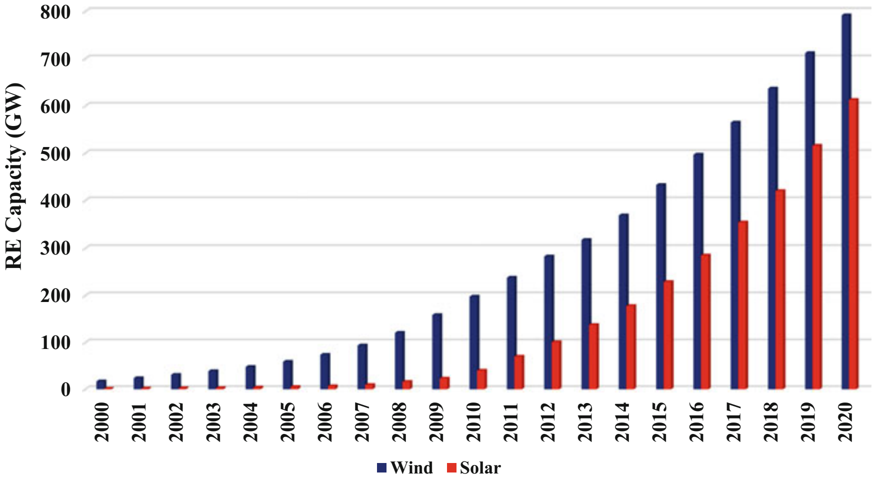

Fig. 6 Global wind and solar installations in Gigawatts (GW)—installed and projected capacity (Fi-powerweb.com 2017)

times higher than the capacity in the year 2000. Figure 6 presents the global pattern of implemented and projected RE capacity (Wind and Solar) till the year 2020. Several countries are operating the RE power share from 10 to 50% of cumulative power mix depending on the availability of respective renewable energy resource.

2.2 Power Scenario in India

India is the world's third-largest producer and fourth largest consumer of electricity. At present, the utility electricity sector in India has one National Grid with an installed capacity of 329.23 GW. The RE power plants (including hydro) constituted 30.8% of total installed capacity. As per Central Electricity Authority (2017), during the fiscal year 2016–17, the gross electricity generated by utilities in India was 1,236.39 TWh and the total electricity generation (utilities and non-utilities) in the country was 1,433.4 TWh however the gross electricity consumption was 1,122 kWh per capita in the year 2016–17. The per capita electricity consumption is low compared to many countries despite cheaper electricity tariff in India. Figure 7 presents the year wise growth of power generation capacity in India.

India's RE sector has been ranked third in the Renewable Energy Country Attractiveness Index (RECAI) with China at second and the US on top. At present, around 57% contribution in cumulative power capacity belongs to coal followed by large hydro. The RES contributes around 20% capacity in India. Figure 8 presents the share of various power generating sources in Indian context by end of April

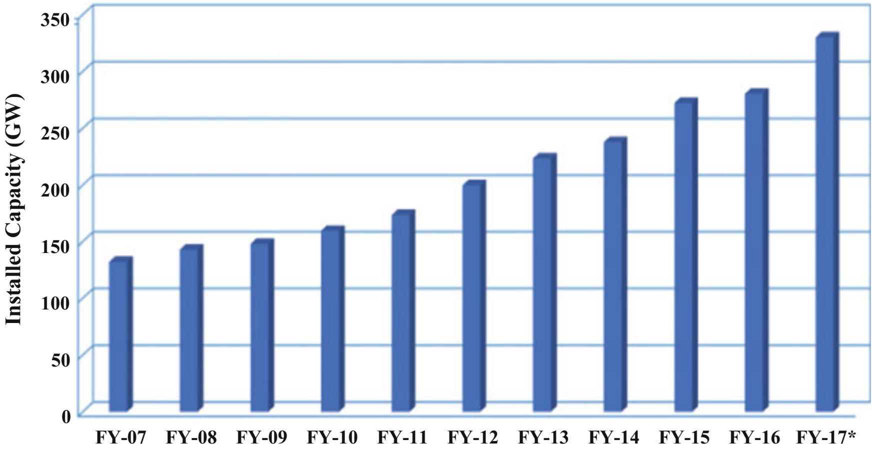

Fig. 7 The growth of Indian power sector (from FY 2007 to 2017*) (Power Market Overview and Trends 2017)

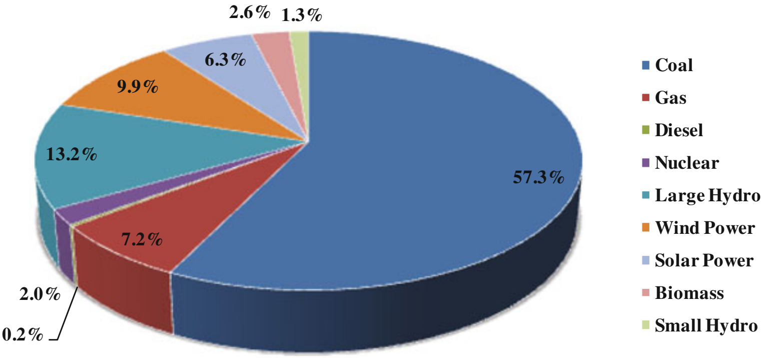

Fig. 8 Installed capacity by source in India as on 30th April 2018 (All India Installed Capacity (in MW) of Power Stations 2018)

2018. The government of India (GoI) has upscaled the target of RE-based power generation to 175 GW by the year 2022; including 100 GW of solar power, 60 GW of wind power, 10 GW of biopower and 5 GW from small hydro resources. GoI has announced that no new coal-based capacity addition is required for next 10 years till 2027 except 50 GW under different stages of construction and likely to come online between 2017 and 2022. The government intends to achieve 40% cumulative electric power capacity from non-fossil fuel sources by 2030.

3 Electricity and the Role of Energy Storage

RE power projects are one of the promising options to limit the consumption of fossil fuels and a corresponding reduction in the GHG emissions from the energy (electricity generation) sector. Due to the concerns of climate change, initiatives taken by several countries on developing regulatory frameworks. Wind and Solar power generation under RE have taken a shape in the overall energy mix. The solar electricity generation through photovoltaic route has taken the edge over concentrating solar power (CSP) generation route. However, with the provision of thermal energy storage CSP plants may prove as much attractive option to generate power for 24 h a day. Irrespective of CSP (with storage), both the wind and solar PV have variable and uncertain thus lack displaceability around the globe. Though, the growing installed capacity of wind and solar projects raised the concerns regarding reliability and stability of electricity grid. Such intermittent nature of RE resources and increased share in overall energy generation motivate the stakeholders around the world to explore energy storage options and their integration into the existing systems. However, the potential role of storage in the electric grid will depend on its technical as well as economic viability. Therefore in terms of economic viability, choice of storage as an option in RE projects required a detailed comparison with the competitive options such as demand response, transmission, flexible generation as well as improved operations.

Smooth and efficient operation of the electric grid is only possible if supply and demand of electricity are kept in proportion or equal at any given moment. To ensure the same, constant adjustment of the supply even for an instant change in the demand side is needed. Major causes of instant change in the demand side include a daily pattern of human activity, the instant requirement of commercial as well as industrial segments and unexpected changes from overloading of equipment. Provision of energy storage can play a crucial role in this and will in the balanced and flexible operation of the electric grid.

The electricity generated through power projects need to be stored for the required time period in order to utilize them either for direct supply of electricity to the connected loads or support utility grid during disturbances. Different energy storage technologies are used to store electrical energy in different forms suitable for different applications as shown in Fig. 9.

Following are the key area of concern from the integration of RE power projects to an existing network (i.e. grid) with their increasing capacity.

- Balancing of Power
- Curtailments, and
- Generation Reserves

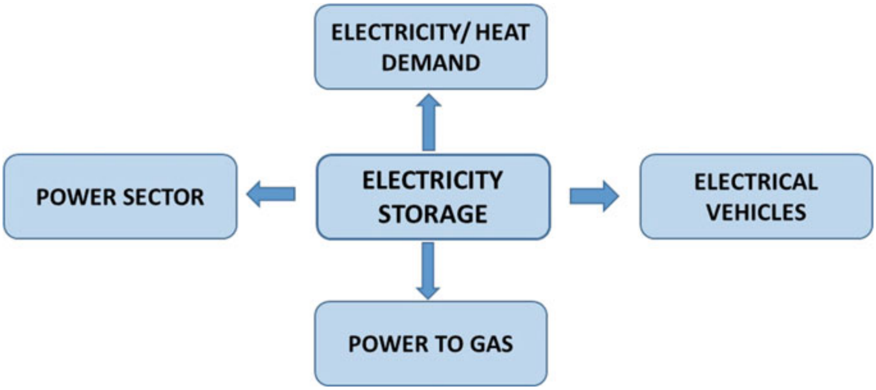

Fig. 9 Various options for storing electricity produced from variable RE

3.1 Balancing of Power

In power system, the key requirement is to keep the system in balance. At present, due to increase in percentage share of renewables in the grid, power balancing becomes cumbersome. As a consequence, different technical issues erupt and those are categorized depending on the duration for which the particular technical issue remains in the grid. On short time scales (i.e. milliseconds to minutes), the challenges are primarily related to power quality issues, such as stability of voltage and frequency in the grid. On medium time scales (i.e. minutes to hours), the scheduled production must meet the planned demand. On longer timescales (i.e. weeks to seasons), the production and transmission capacity should be able to meet the electricity demand in all parts of the grid network over the year, otherwise, loads must be curtailed to keep the system in balance. Figure 10 presents the electricity demand and supply pattern through a wind power project, however, the pattern of energy delivered by a solar and wind power project has been presented in Fig. 11.

Electric grids are usually designed for large controllable electric generation and use three-phase planning process to ensure the generation of power in accordance with the demand. Since grid can only store a small fraction of power generated due to low storage capacity, there must be a balance between supply and demand of electricity. Such practice (balance between demand and supply) helps to avoid a blackout or other cascading problems (Steen et al. 2014). However, to maintain such balancing with the intermittent sources is always a challenge as they disrupt the conventional methods for planning the daily operation of the electric grid. Fluctuation of power due to an intermittent resource over multiple time horizons, forcing the grid operator to adjust its day-ahead, hour-ahead, and real-time operating procedures as presented in Fig. 12.

The most prominent challenges of an electrical distribution system are voltage rise and overloading of system components. However, the other issues may also arise from fluctuation in electricity production due to varying wind speed and cloud

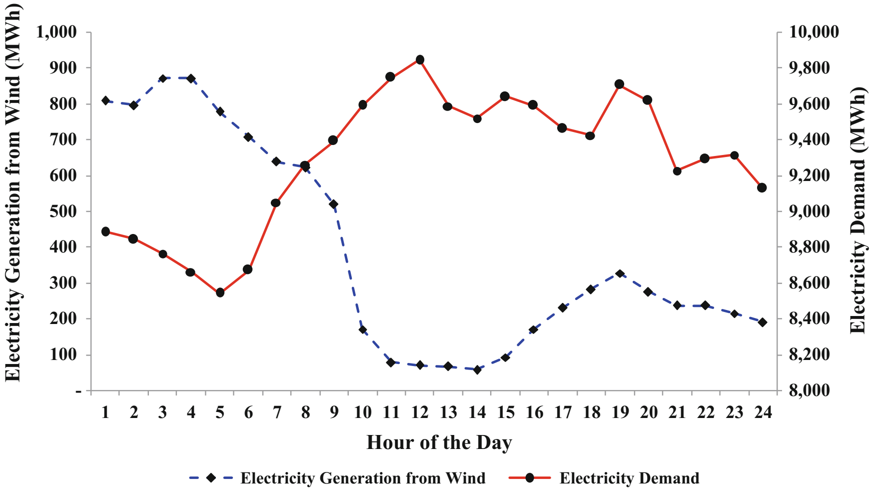

Fig. 10 Electricity generation (hourly) from wind power plants versus electricity demand in Gujarat (on January 28, 2011) (Gujarat State Load Dispatch Centre)

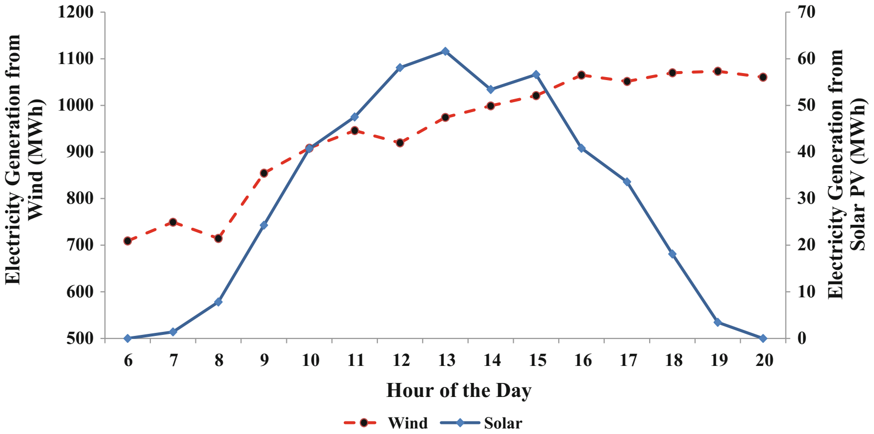

Fig. 11 Hourly average electricity generation from Wind and Solar on June 18, 2012 in Kutch, Gujarat, India (Gujarat State Load Dispatch Centre)

movements in the wind and solar-based power generation respectively. The sudden rise in the voltage usually happens when the electricity generated exceeds the local demand, causing the electricity to flow in opposite direction compared to normal operation. The flow of power in reverse direction may also affect the protection system and cause overloading in system components.

To deal with the above problems different approaches has been adopted. These include reinforcement in the distribution grid, demand-side management; energy

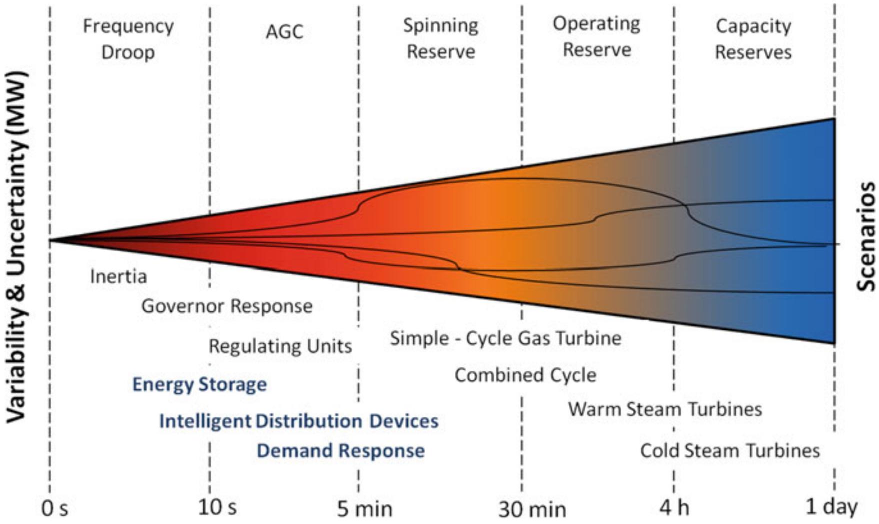

Fig. 12 The growth of variability and uncertainty with time and associated resources and reserves available to maintain power-balance (National Load Dispatch Centre, Government of India)

storage, energy curtailment, reactive power compensation and coordinated on-load tap changer (OLTC) control. The capacity of wind and solar PV plants that can be installed in a distribution system without affecting the reliability and performance of the system depends on the design of the distribution system and on the load profile. A high mismatch between the electricity generation and demand creates more difficulties for large-scale penetration of renewable energy projects. On the other hand, systems with relatively better load matching can ensure higher penetration. Designing of a system for high peak demand can facilitate more share of solar and wind power than the systems designed for a low peak demand. Despite these concerns, the length of the distribution grid (long distances between the customer and the Substation) will also experience higher fluctuations (a rise) in the voltage level, compared to a grid with shorter distances.

- The transmission system is the basic component of the high end electricity grid. In the perspective of efficient transmission, the placement of generators needs to be closely placed with the load as much as possible. Large-scale addition of solar and wind power in the electric grid can have the following causes in the utilization of transmission system. The optimal locations of power plants may change the optimal sites for wind and solar power plants are often not the sites where power plants have traditionally been placed.

Increased transmission capacity can be used for smoothing variations in the production patterns from wind and solar power.

The generation pattern of solar and wind are such that with an increase in a geographical distance, i.e. grid of large transmission network, results in smaller variations in aggregated production. The expansion of transmission capacity is also essential for better utilization of hydro and gas-based power plants to manage during demand and supply mismatch.

The abrupt change in power generation from RE (Solar and wind) power projects creates a sudden mismatch in power supply and demand, which creates instability in the grid. Though the solar power generation over a day follows an inverse "U" pattern, the generation from wind power plant is very much variable in nature and it shows much inconsistency over the year as well as on two consecutive days. The gas-based power plants and hydropower plants are considered as a most prominent option as spinning reserves due to their ability to respond immediately to the power demand. The gas-based power plants cannot be utilized fully due to a shortage of gas. A day-ahead planning is also required for the same depending on the resource availability. The abnormal behavior of solar PV and Wind Turbine Generator (WTG) based power generation is shown in Figs. 13 and 14 below operational projects in the state of Gujarat, India. Day-by-day the requirement for power balancing is increasing due to increase in penetration of more renewable-based power which is intermittent in nature.

Sufficient reactive power ensures the flow of voltage and power efficiently. With the increase in the share of renewable energy based power, reactive power demand increases. As an example, the addition of wind generators may require the installation of synchronous condensers, STATCOMs and static VAr (volt-ampere reactive) compensators (SVCs) for managing required voltage levels near wind farms. There is a possibility that, areas of the power system may become congested. In this case, an additional reactive power support will be required, however; issues may arise for the procurement of such addition reactive power support. Therefore, planning for additional reactive power support and its operational framework is critically important.

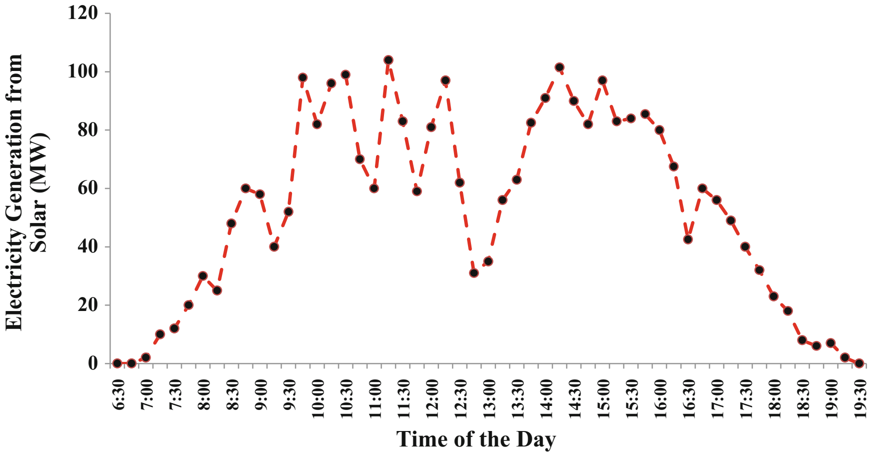

Fig. 13 Hourly solar power generation curve on April 11, 2011 in Gujarat, India (Report on Green Energy Corridors 2012)

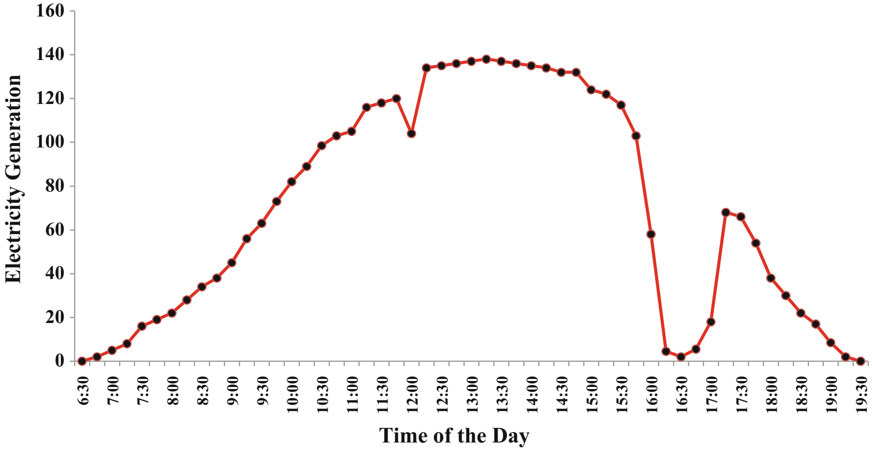

Fig. 14 Hourly solar power generation curve on April 13, 2011, in Gujarat, India (Report on Green Energy Corridors 2012)

3.2 Power Congestion

In several countries including India, RE power projects operate with 'must run' status. In practice, power plants with must run status, not to be considered in selecting generators based on the preferential tariff. However, in past curtailment of wind power in the state of Tamil Nadu, India was experienced during high wind seasons to avoid power congestion and power imbalance in the grid. It was also observed that solar power plants also suffering from power curtailment during peak generation hours in the state of Rajasthan and Tamil Nadu, India. The most prominent cause of power curtailment was an issue of power congestion in the transmission line and no provision for energy storage. Power congestion is a technical issue which needs to be addressed with a coordinated approach. Figure 15 shows a typical indicative generation pattern of a solar PV plant on the clear sunny day as well as a cloud passing day. Variable generation is an issue from power balancing point of view, whereas power congestion leads to curtailment of solar power during peak generation hours. In both the cases, energy storage of suitable capacity will be an effective solution to support grid as well as utilization of power, loss due to curtailment.

Recently, GoI took initiatives for development of solar PV power projects along with Battery Energy storage and solar-wind hybrid projects. In both the cases, the plant load factor increases significantly and utilization of power evacuation infrastructure increases which ultimately help in improving techno-economics of the power plant. Figure 16 shows a pictorial representation of the benefits of solar PV power plant with storage.

There must be separate feed-in-tariff for renewable with storage power plants as the cost of electricity from storage is higher due to the high cost of the storage

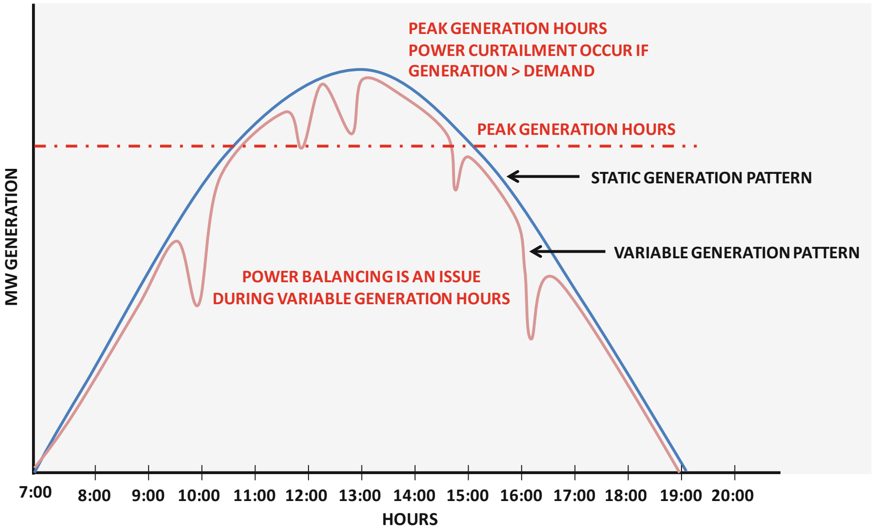

Fig. 15 Typical energy generation pattern of a solar PV plant

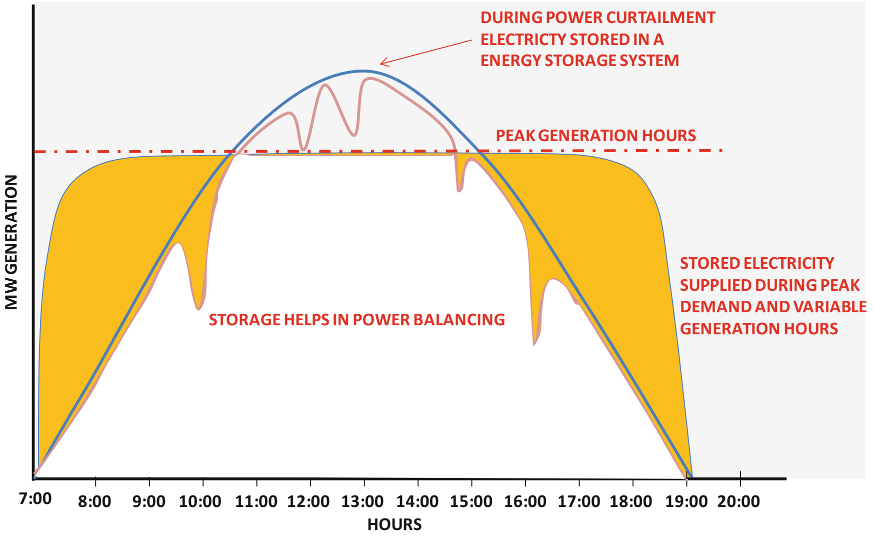

Fig. 16 Benefits of solar PV plant with energy storage

system and technical losses associated with energy storage system and power conversion device. Whether the tariff of renewable with storage will attract developers or not is yet to be seen but it is believed that the economy of scale in near future will bring down the cost of storage.

3.3 Generation Reserves

To manage the intermittency and variability in the generation of power from renewable energy resources generation, supplementary services such as flexible generation and energy storage will be required. Hydropower and gas-based power plants are considered as good spinning reserves for balancing of power. Therefore, a coordinated planning of gas-based thermal power plants with that for RE development may also be proved as one option. However, the provision of such supplementary services and the success of its implementation will hinge on the incentives and market signals provided to such generators.

The energy storage systems such as Pumped Hydro Storage, Compressed Air Energy Storage, flywheel, Supercapacitor, Hydrogen storage, Batteries (Lead-Acid, Lithium-ion, NaS), etc., are also being considered globally as the measures to handle the issues pop up due to the variability of renewable energy based power generation. Different types of energy storage technologies are suited for various grid conditions depending upon their power density, energy density, discharge time, and response time, etc. In India, Central Electricity Regulatory Commission (CERC), Govt. of India has released the regulations on Ancillary Services Operations-2015 and POSOCO has prepared the detailed procedure for ancillary services operations. As per the regulation, all the generating stations that are the regional entities and whose tariff is determined or adopted by CERC for their full capacity shall provide Reserves Regulation Ancillary Services (RRAS).

3.3.1 Time Shifting

To meet the yearly increasing energy demand the power sector utilities constantly required an increment in the supply capacity and addition of transmission/ distribution lines Cost of electricity generation can be reduced by storing electricity at off-peak times, for example at night, and discharging it at peak times. In such case, a large gap in demand between peak and off-peak may become beneficial even with the additional cost of storing electricity. Use of storage to decrease the gap between daytime and night-time may allow generation output to become flattered, that leads to an improvement in operating efficiency and cost reduction in fuel. This is the reason that many utilities constructed pumped hydro-based power plants, and have recently begun installing large-scale batteries at substations. The RE power critically depends on the availability of individual RE resources, and energy generation in excess not demanded by the connected loads is curtailed. Therefore, high-grade energy (electricity) can be effectively utilized by storing surplus electricity and using it during hours of peak demand or peak price. A schematic of the uses of electrical energy storage in the grid (depending on the frequency and duration of use) is presented in Fig. 17.

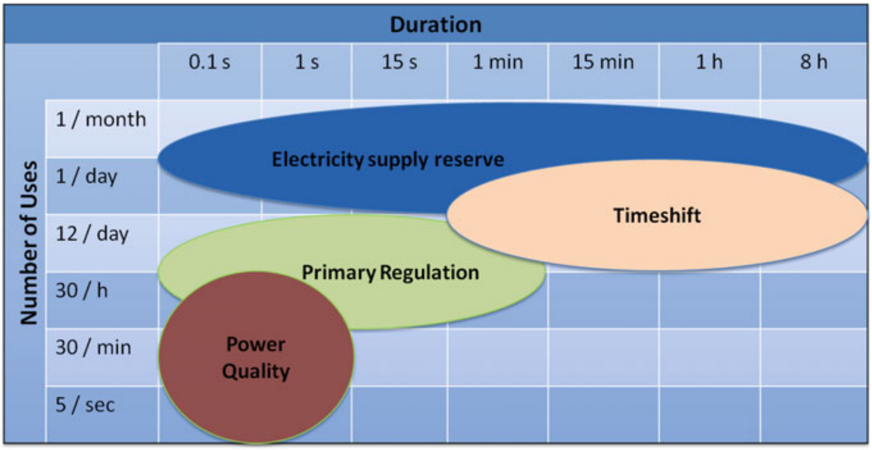

Fig. 17 Uses of electrical energy storage in grid depending on the frequency and duration of use (A white paper on "Electrical Energy Storage" by International Electrotechnical Commission 2011)

4 Energy Storage Applications—Relevance

The relevance of available energy storage technologies has been found in the services of energy generation, transmission, distribution and utilization. The form of energy storage and the geographical location varies with the requirements. Some typical energy storage technology applications referred from technology roadmap for energy storage developed by IEA are listed in Table 1.

Large-scale storage of energy enables the efficient running of the electrical grid and thus has benefits in terms of lower prices, fewer emissions and reliable supply of power. The use of storage in renewable energy based power generation also helps in improving the quality of power (in terms of frequency regulation) and also, allows companies to supply power when it is economical and optimally efficient. The storage-based RE projects also provide an uninterruptible source of power for critical infrastructure and services.

5 Energy Storage Technologies

There is a wide variety of energy storage technologies some of them are in regular practice and else once are in the emerging stage, with certain advantages, disadvantages thus make them applicable to a limited range of applications. Different energy storage concepts are employed globally that have a broader overview of life cycles costs, efficiencies, and energy densities (size and weight). Classification of all such energy storage technologies is shown in Fig. 18. However, the capability of

Table 1 Key characteristics of storage systems for applications in the energy system (Technology Roadmap 2014)

Application	Size (MW)	Discharge duration	Cycles (typical)	Response time
Seasonal storage	500–2000	Days to months	1–5 per year	Day
Arbitrage	100–2000	8–24 h	0.25 to 1 per day	>1 h
Frequency regulation	1–2000	1–15 min	20–40 per day	1 min
Load following	1–2000	15 min–1 day	1–29 per day	<15 min
Voltage support	1–40	1 s–1 min	10–100 per day	Millisecond to second
Black start	0.1–400	1–4 h	<1 per year	<1 h
Power congestion	10–500	2–4 h	0.14–1.25 per day	>1 h
Demand shifting and peak reduction	0.001–1	Minutes to hours	1–29 per day	<15 min
Off-grid	0.001–0.01	3–5 h	0.75–1.5 per day	<1 h
Variable supply resource integration	1–400	1 min to hours	0.5–2 per day	<15 min
Spinning reserve	10–2000	15 min–2 h	0.5–2 per day	<15 min

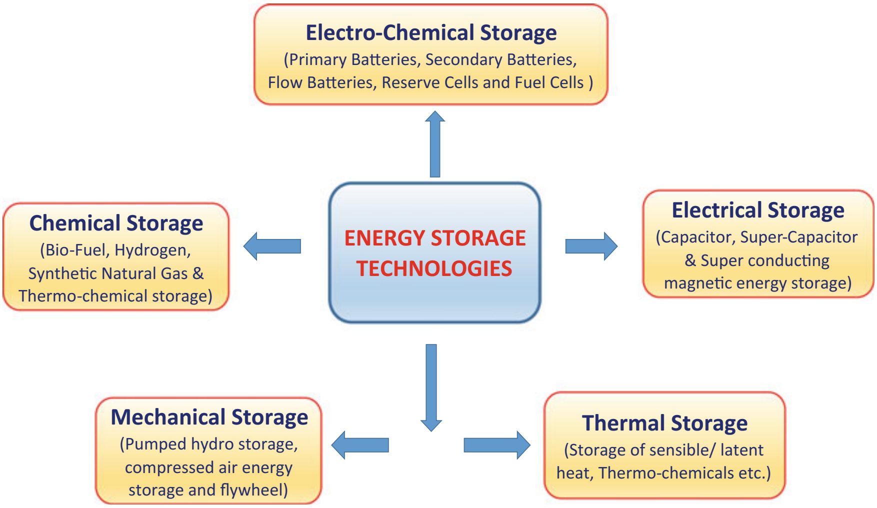

Fig. 18 A schematic of energy storage technologies

each technology to meet high power and high energy demand has become the subject and focus area of many studies.

Energy storage applications are classified into two broad categories: power and energy applications. Energy storage system designed for power application has the capacity to store a small amount of energy per kW of rated power output, and require high power output for the relatively short period (from several seconds to 15 min). Energy storage system designed for energy application has large energy capacity with discharge durations up to many hours.

Energy storage technologies have also been presented in the following section briefly.

5.1 Electrochemical Energy Storage System

Electrochemical energy storage systems work on the principle of conversion of chemical energy into electrical energy. During this conversion process mostly two reaction partners undergo a chemical process. The energy of this reaction is then available as an electric current at a defined voltage and time. Major examples of electrochemical storage technology involve:

- Electrochemical batteries and
- Electrochemical capacitors

Electrochemical cells and batteries can be classified into four categories based on the principle of operation namely, primary cell or battery, secondary cell or battery, reserve cell, and fuel cell. A second useful classification refers to discharge depth; either shallow or deep cycle batteries. Deep cycle batteries have fewer thick plates in structure, are suitable for renewable applications. The third classification refers to the characteristic of the electrolyte in the battery (flooded or wet and sealed). Flooded or wet batteries are widely used in renewable applications. There are two varieties of sealed batteries; the Gel and Absorbed Glass Mat (AGM) for renewable applications. Transportation and micro power (stationary/portable) generation including wind and solar energy utilization are among the important application areas of electrochemical energy storage systems. Each electrochemical storage technology is described below.

5.1.1 Primary Cell or Battery

A primary battery generally is not rechargeable. Most primary cells utilize electrolytes, which are contained in the absorbent material or a separator. The type of electrolyte as aqueous and non-aqueous might categorize the primary batteries. Aqueous batteries contain water-based electrolyte solutions.

5.1.2 Secondary Cell or Battery

A secondary cell or battery is recharged by passing current through the circuit in the opposite direction to the current during discharge. Rechargeable battery systems can be separated by the electrolyte type into two groups. They have both aqueous and non-aqueous electrolytes, which are based on water and solvents respectively. The key options are presented as below:

Lead-Acid Battery

Lead-acid batteries are used in the world at larger scale compared to other type of batteries. These batteries are being used in both mobile and stationary applications. The frequently used applications of these batteries include emergency power supply systems, standalone systems with PV, battery systems for mitigation of output fluctuations from solar and wind power plants and as starter batteries in vehicles. The typical service life of lead-acid batteries is 3–15 years (with a maximum of 1,500 cycles of life) and have the cycle efficiency around 75–90%. In brief, lead-acid batteries offer a mature and well-researched technology at relatively lower costs.

Various types of lead-acid are: vented and sealed housing versions (called valve regulated lead-acid batteries, VRLA), flooded, sealed, AGM, etc. Presently, the costs for stationary batteries are comparably higher, much higher than the starter kind of batteries due to their mass production. The major advantages of lead-acid batteries are, a favorable cost/performance ratio, easy recyclability, and a simple charging technology; however, a decrease of usable capacity with high power is one of the disadvantages of these batteries. However, For example, if a battery is discharged in one hour, only about 50–70% of the rated capacity is available.

Lithium-Ion Battery (Li-Ion)

The lithium-ion battery is one of the important storage technology for portable and mobile applications (e.g., laptop, cell phone, electric bicycle, and electric car) since the year of 2000. These have high cell voltage up to 3.7 V. It means that the number of cells in series with the associated connections and electronics can be reduced to obtain the target voltage. For example, one lithium-ion cell can replace three NiCd or NiMH cells (which have a cell voltage of only 1.2 V). These batteries have an advantage in terms of high gravimetric energy density and the prospect of large cost reductions through mass production.

Li-ion batteries have an overall share of 50% in the small portable devices market. However, there are still some challenges for developing these batteries at large-scale. Major hindrances in the same are high cost of packaging and internal overcharge protection circuits. Lithium-ion battery generally owns high charging

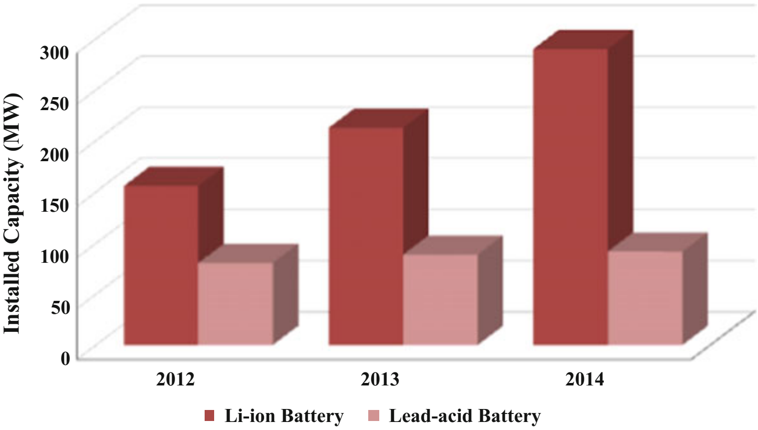

Fig. 19 Global installed capacity of lead-acid and Li-ion batteries (Global Energy Storage Market Overview and Regional Summary Report 2015)

and discharging efficiency, mostly in the range of 85–98%. Discharging time from seconds to weeks makes them a very flexible and universal storage technology. Since lithium-ion batteries are currently expensive, they can only compete with lead-acid batteries in those applications those require shorter discharge times (e.g., as primary control backup). Further, research on lithium-ion battery technology is ongoing and focus is on the development of cathode materials. Globally installed capacities of lead-acid andlLi-Ion batteries until the year of 2014 is presented in Fig. 19.

Nickel Cadmium and Nickel Metal Hydride Battery (NiCd, NiMH)

Nickel cadmium (NiCd) battery is in commercial use since 1915. Nickel-based batteries have a higher power and slightly greater energy density, higher the number of cycles compared to Lead-acid batteries. From the technical point of view, NiCd battery is capable of performing well even at low temperatures in the range of −20 to −40 °C. Due to the toxicity of Cadmium, these batteries are presently only used for stationary applications in Europe.

Another type (NiMH) batteries were also developed to replace the NiCd batteries due to their similar properties except for the maximal nominal capacity (which is still ten times less compared to NiCd and Lead-acid). Furthermore, NiMH battery has a much higher energy density (Wh/kg) as compared to NiCd and Lead-acid batteries. In portable and mobile applications sealed NiMH batteries are being replaced by the Lithium-ion batteries. Presently the Hybrid vehicles are mostly uses sealed NiMH batteries, because of their robust nature and comparably safer use than Lithium-ion batteries. The present cost of NiMH batteries is similar to the Lithium-ion batteries.

Sodium Sulfur Battery (NaS)

Sodium Sulfur (NaS) battery consists of liquid (molten) Sulfur at the positive electrode and liquid (molten) Sodium at the negative electrode. The active materials are separated by a solid beta alumina ceramic electrolyte. The battery temperature is kept between 300 and 350 °C to keep the electrodes molten. NaS batteries usually have a typical life of around 4,500 cycles and a discharge time of 6.0–7.2 h. They usually have efficiency up to 75% with fast response time. These qualities enable NaS batteries to be economically used in combined power quality and time shift applications with high energy density. The NaS battery technology has been demonstrated in Japan for 270 MW of installed capacity. The largest reported NaS battery storage installation is 34 MW/245-MWh for wind power stabilization in northern Japan. Germany, France, USA, and UAE also have NaS batteries in operation. The major limitation of these batteries is to maintain their operating temperature. A heat source is required to maintain the temperature which uses the battery's own stored energy thus partially reducing its performance. Since 1990, NaS batteries are being manufactured by one company in Japan, with a minimum packaged module size of 50 kW and with typically 300–360 kWh of energy capacity. The use of the single module is not possible as 20 modules are combined into one battery. The minimal commercial power and energy range is on the order of 1 MW and 6.0–7.2 MWh. These batteries are suitable for applications with daily cycling as the response time is in the range of milliseconds. It is worth mentioning that NaS batteries closely meet the requirements of Utilities for grid stabilization.

5.1.3 Flow Batteries

Flow batteries work on the principle of charging and discharging in the active masses of the electrodes. These can be classified into redox flow batteries and hybrid flow batteries. Storage of energy is taking place in one or more electroactive species which are dissolved in liquid electrolytes. These electrolytes are stored in external tanks and pumped through the electrochemical cell that converts chemical energy directly into electricity and vice versa. The power of flow batteries is measured on the basis of their size and design of the electrochemical cell whereas the energy depends on the volume of the tank where the electrolyte is placed. Originally developed by NASA in the early 70s as EES for long-term space flights, flow batteries can be fitted to a wide range of stationary applications. Flow batteries are now in the focus of storing energy for durations of hours or days with a power of up to several MW.

5.1.4 Reserve Cell

A reserve cell or battery is often used for long storage. Reserve batteries are assembled without electrolyte and the active chemicals of the cell are segregated and isolated until required. They can be reliably stored under a variety of adverse conditions that would compromise the performance of fully activated cells.

5.1.5 Fuel Cell

Fuel cells are electrical generation devices, which mainly use the chemical energy of hydrogen or another fuel to unleash a fuel's latent chemical energy and convert to produce electricity. Fuel cells work like batteries. They, however, do not run down or need recharging, also produce electricity and heat if fuel is supplied. A fuel cell is composed of an anode, a cathode, and an electrolyte membrane. Hydrogen is passed through the anode and oxygen through the cathode. The hydrogen molecules are split into electrons and protons at the anode. The protons pass through the electrolyte membrane, while the electrons are forced through a circuit, generating an electric current and excess heat. The protons, electrons, and oxygen combine to produce water molecules at the cathode side.

5.2 Chemical Energy Storage System

Chemical energy is stored in the chemical bonds of atoms and molecules, which can only be seen when it is released in a chemical reaction. After the release of chemical energy, the substance is often changed into entirely different substance. Primarily, chemical energy storage focuses on Hydrogen and Synthetic Natural Gas (SNG) as secondary energy carriers. These two gases have a considerable impact on the storage of electrical energy in large quantity. Chemical energy storage system uses excess electricity to produce hydrogen via electrolysis process. There are different ways of using hydrogen as an energy carrier, either as pure hydrogen or as SNG after the production. The overall efficiency of hydrogen and SNG is low compared to other storage technologies such as PHS and Li-ion. It may be noted that chemical energy storage is the only concept which allows storage of a large amount of energy, i.e. Terra Watt hour range, and for a greater period even for the seasonal storage.

Biofuels can also be used as a chemical energy storage system, and further classified as first-generation, second-generation, and third-generation biofuels. As an example, biofuels such as biodiesel, straight vegetable oil, alcohol fuels, or biomass can be used to replace hydrocarbon fuels through a series of chemical processes. These processes convert the carbon and hydrogen of coal, natural gas plants, and animals and other organic wastes into short hydrocarbons. A significant research work on this aspect is underway.

5.3 Electrical Energy Storage Systems

5.3.1 Capacitor

Electrical Energy Storage Systems can be categorized as electrostatic including Capacitors and Supercapacitor, and magnetic/current energy storage system. Brief descriptions for the same are provided in the following paragraphs.

Energy storage using capacitor is the most direct method to store electricity. A capacitor consists of two metal plates separated by a non-conducting layer called a dielectric. One plate of the capacitor is charged with direct current, the other plate will have induced in it a charge of the opposite sign. Capacitors stores energy on the surfaces of metalized plastic film or metal electrodes. Its worth mentioning that the energy density of the capacitors is very low, which can deliver or accept high currents, however, only for an extremely short period.

5.3.2 Supercapacitor

Supercapacitors are also known as, electrochemical double-layer capacitors (DLCs), and is known from last 60 years. They act as the gap fillers between classical capacitors used in electronics and general batteries, because of their nearly unlimited cycle stability and extremely high power capability as well as their many orders of magnitude higher energy storage capacity when compared to traditional capacitors. This technology has a large development potential that may lead to much greater capacitance and energy density than conventional capacitors. Thus enabling compact designs. Other main features of supercapacitor are (i) extremely high capacitance values, of the order of many thousand Farads, and (ii) the possibility of very fast charging and discharging. These capacitors have extraordinarily low inner resistance. Such features are not available with conventional batteries. Other advantages of supercapacitor include durability, high reliability, no maintenance, long life and operation over a wide temperature range and in diverse environments (hot, cold, and moist).

5.4 Superconducting Magnetic Energy Storage (SMES)

Superconducting magnetic energy storage (SMES) systems work on the electrodynamic principle, in which, the energy is stored in the magnetic field created by the flow of direct current in a superconducting coil, that is kept below its superconducting critical temperature. The main component of this storage system is a coil made up of superconducting material. Additional components include power conditioning equipment and a cryogenically cooled refrigeration system.

The major advantage of SMES is the very quick response time due to which the demanded power can be available almost instantaneously. These systems also have high overall round-trip efficiency (85–90%) and the very high power output with a quick response time and can be provided for a short period. SMES systems do not have a moving part and their overall reliability crucially depends on the refrigeration system. In principle, the energy can be stored indefinitely if the cooling system is operational, however, longer storage times are restricted by the energy demand of the refrigeration system. Large SMES systems with (more than 10 MW power) are mainly used in particle detectors for high-energy physics experiments and nuclear fusion. Till date only a few, small SMES systems are commercially available and the same are primarily used for power quality control in manufacturing plants such as microchip fabrication process.

5.4.1 Mechanical Energy Storage

Mechanical energy storage is classified by working principles as follows: pressurized gas, forced springs, kinetic energy, and potential energy. The most useful advantage of mechanical energy storage is that they can readily deliver the energy whenever required for mechanical works. Mechanical energy storage methods are easily adaptable to convert and store energy from water current, wave, and tidal sources. They mainly comprise of flywheel, pumped hydro storage, and compressed air energy storage Technologies.

5.4.2 Compressed Air Energy Storage (CAES)

Compressed air (compressed gas) energy storage technology has been used since the nineteenth century for different industrial applications. Air is the most abundant storage medium due to its availability. Compress air is used as the storage medium and kept in the underground structure or an above-ground system of vessels or pipes. Typical underground storage options are caverns, aquifers or abandoned mines. On the basis of requirement, the stored compressed air is mixed with natural gas, burned and expanded in gas turbine cycle. However, if the heat released during compression is dissipated by cooling and not stored, the air must be reheated prior to expansion in the turbine. This process is called adiabatic CAES and generally has low round-trip efficiency (below 50%). Adiabatic technology is well proven and has high reliability and can start without external power input. The advantage of CAES is its large capacity and disadvantages are low round-trip efficiency and geographic limitation of the location of use. Presently, only two adiabatic CAES systems are in operation globally. The first CAES power plant was built in, Germany in the year 1978. It works with a round-trip efficiency of approximately 41%. The second CAES plant (110 MW) was commissioned in 1991 in McIntosh (Alabama, USA). In this plant a, recuperate was used to recover heat from the exhaust of the gas turbine thus, a higher round-trip efficiency of 54% is achieved. Both of the CAES systems use off-peak electricity for air compression and are operated for peak saving daily.

5.4.3 Flywheel Energy Storage (FES)

Flywheel Energy Storage system stores energy (rotational energy) in an accelerated rotor (a massive rotating cylinder). The main components of a flywheel energy storage system include rotating body/cylinder (comprised of a rim attached to a shaft) in a compartment, the bearings, and the transmission device (motor/generator mounted onto the stator). The energy is stored in the flywheel by keeping the rotating body at a constant speed. An increase in the speed results in the higher amount of energy stored. Electricity is used to accelerate the flywheel. And that is supplied by a transmission device. If the flywheel's rotational speed is reduced electricity may also be extracted from the system by the same transmission device. The first version of Flywheels uses a large steel rotating body on mechanical bearings, however advanced FES systems have rotors made of high-strength carbon filaments, suspended by magnetic bearings, and spinning at speeds from 20,000 to over 50,000 rpm in a vacuum enclosure. The main features of flywheels are the excellent cycle stability and a long life, little maintenance, high power density and the use of the environmentally inert material. However, Flywheels have a high level of self-discharge due to air resistance and bearing losses and suffer from low current efficiency. Presently, flywheels are commercially used for power quality in industrial and UPS applications, mainly in a hybrid configuration. Efforts are being made to optimize flywheels for long-duration operation (up to several hours) as power storage devices for use in vehicles and power plants.

5.5 Pumped Hydro Storage (PHS)

The conventional pumped hydro energy storage system uses works between two water reservoirs that are kept at different levels. During the lower demand period the excess energy is used to pump water from the lower to the upper reservoir (charging) and during the hours of higher power demand, the water flows back from the upper to the lower reservoir through a hydro turbine that is coupled with a generator to produce electricity (discharging). Different configurations can be used in the case of pumped hydro energy storage. As an example high dam can be used as pumped hydro storage plant (upper reservoir). On the other hand for the lower reservoir, flooded mine shafts, other underground cavities, and the open sea are also technically possible. The main applications are for energy management via time shift, namely non-spinning reserve and supply reserve. PHS has historically been used by electric utilities to reduce total generation cost by time shifting and to control grid frequency. The first hydro storage plants were built in Italy and

Switzerland in the year of 1890s. Later (By 1933) PHS plants with reversible pump-turbines have also been developed. Typical discharge time of PHS plants varies from few hours to a few days. PHS plants have very high efficiencies; in the range of 70–85%. Advantages of PHS are longer useful life and practically unlimited cycle stability of the installation. The main limitations includes; the dependence on topographical conditions and large land use.

5.6 Thermal Energy Storage System

TES systems are suitable systems to store heat or cold in a storage medium at a temperature for further usage, under different conditions such as temperature, place, or power. TES systems are applicable in several industrial and residential purposes, such as space heating or cooling, process heating and cooling, hot water production, or electricity generation. TES system can be classified into three different categories, such as sensible heat, latent heat, absorption, and adsorption system. In RE power segment TES is mainly used in CSP (i.e. solar thermal) power projects to increase operating hours. In TES system, mainly molten salt (a mixture of $NaNO_3$ and KNO_3) is used as the storage material. Figure 20 presents two tanks based TES system of a parabolic trough collector based CSP project.

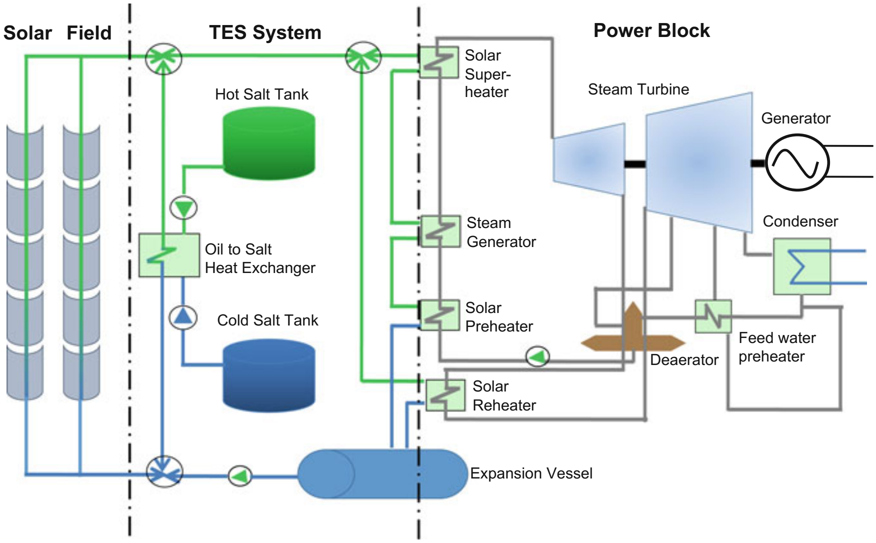

Fig. 20 Schematic view of TES system with parabolic trough-based CSP project (Electric Power Research Institute (EPRI) 2010)

5.6.1 Sensible Heat Storage System

Sensible heat storage leads temperature changes in the process. The storage capacity of sensible heat storage systems depends on the specific heat capacity and the mass of the medium used. The storage medium can be in different phases as a liquid (water, molten salt or thermal-oil), solid (stone, concrete, metal, or the ground), or liquid with solid filler material (molten salt/stone).

5.6.2 Latent Heat Storage System

Latent heat storage involves the process of phase change of storage medium during charging and discharging. Latent heat storage use phase change materials (PCMs) as storage media. Thermal conductivity (k) is a key instrument in latent heat system. However, the density and the enthalpy at the phase transition are also important as they determine to the capacity of the volumetric storage. Both organic (paraffin), inorganic, and bio-based PCM’s (salt hydrates) can be used in latent heat storage systems.

5.6.3 Absorption and Adsorption Storage System

In the absorption and adsorption storage system the heat is not stored directly as sensible or latent heat but by means of a chemical process. Therefore, this kind of thermo-chemical storage is one of the indirect ways to store heat. Absorption and adsorption are two good examples of this process, which consumes and releases heat in charging and discharging mode respectively. High energy density (approximately 1000 MJ/m^3) resulting in a small volume of material is taken into account as the main advantage of sorption energy storage. Absorption systems can also act as heat pumps for cooling as well as heating possible.

6 Deployment of Energy Storage

As per US DoE, globally the total energy storage capacity operational today has reached 74 GW. Out of which more than 68 GW is Pumped Hydro Storage. The installed energy storage system capacity is much more but all of them are not operational. The operational capacity of energy storage systems is very low as compared to the installed intermittent renewable energy (solar and wind) generation capacity until the end of the year 2016. Figure 21 shows worldwide operational energy storage projects capacity breakup based on technology type. Till date the mechanical storage comprises more than 90% of global market share (mainly in pumped hydro); however, the thermal and electrochemical storage options are picking the market due to increasing share of RE power in the overall energy mix.

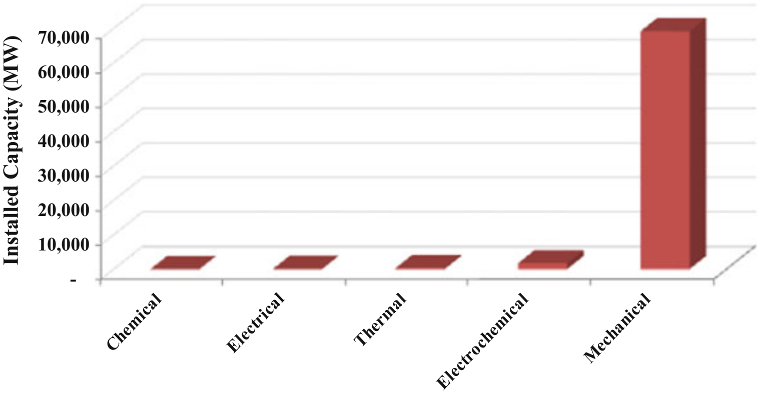

Fig. 21 The global market share of energy storage technologies (Energystorageexchange.org 2017)

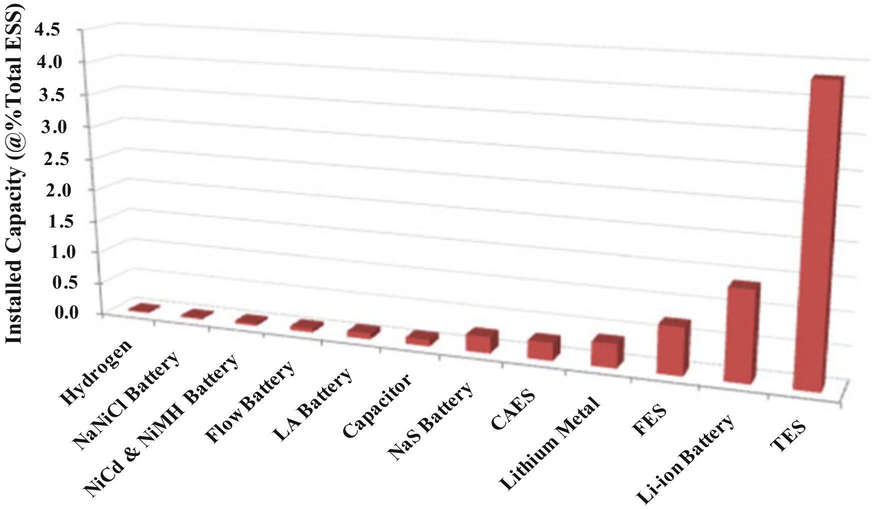

Fig. 22 The percentage share of different energy storage technologies in total installed capacity (Energystorageexchange.org 2017)

Figure 22 presents market share of different energy storage technologies (except pumped hydro storage) globally as per the energy storage database of USDoE 2016.

Pumped hydro storage has a maximum contribution of more than 90%, followed by thermal energy storage and Li-ion battery. The contribution of each other storage technologies is below 1%. The application of PHS is time shifting, power quality, and emergency supply. Thermal energy storage is mostly used in CSP plants for time shifting and power quality. The use of Li-ion battery storage technology is for power quality and grid network efficiency. Battery technologies are also used for time shifting application in case of the off-grid renewable energy system.

It is important to notice the installed capacity of energy storage systems in the countries having more renewable specifically solar and wind-based power generation. Figure 23 shows the installed capacity of energy storage systems as a percentage of installed RE capacity in major countries such as China, Denmark, Germany, India, Italy, Japan, Spain, and the USA by end of the year 2016.

Depending on the type of RE projects different countries has adopted relevant energy storage technology options to address the power quality. This is very important from the point of view of the nature of the RE resource to select and optimize the suitable storage option; for example, in Spain, thermal energy storage is widely adopted due to the availability of higher direct normal irradiance and installed CSP projects. Figures 24 and 25 relate the energy storage scenario along with the type of RE mix over top RE major countries of the globe.

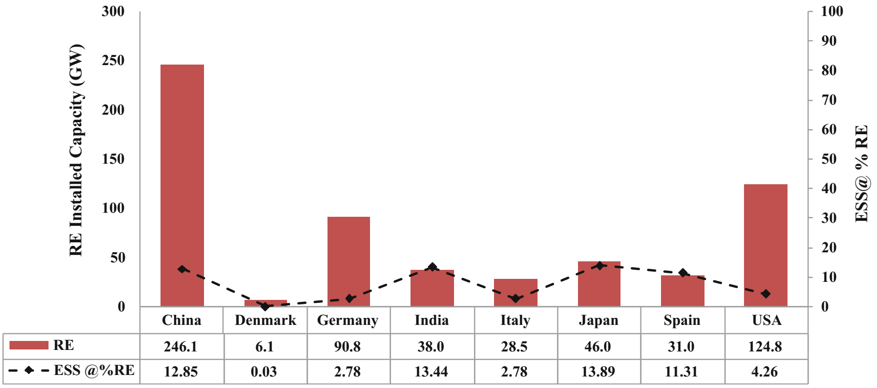

	China	Denmark	Germany	India	Italy	Japan	Spain	USA
🟥 RE	246.1	6.1	90.8	38.0	28.5	46.0	31.0	124.8
– ◆ – ESS @%RE	12.85	0.03	2.78	13.44	2.78	13.89	11.31	4.26

Fig. 23 Installed energy storage over top RE major countries (Energystorageexchange.org 2017)

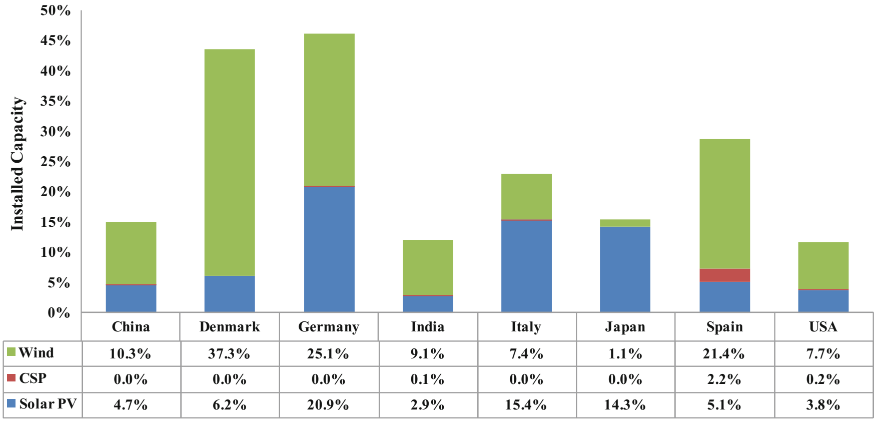

	China	Denmark	Germany	India	Italy	Japan	Spain	USA
🟩 Wind	10.3%	37.3%	25.1%	9.1%	7.4%	1.1%	21.4%	7.7%
🟥 CSP	0.0%	0.0%	0.0%	0.1%	0.0%	0.0%	2.2%	0.2%
🟦 Solar PV	4.7%	6.2%	20.9%	2.9%	15.4%	14.3%	5.1%	3.8%

Fig. 24 RE resource and technology wise installed capacity (Energystorageexchange.org 2017)

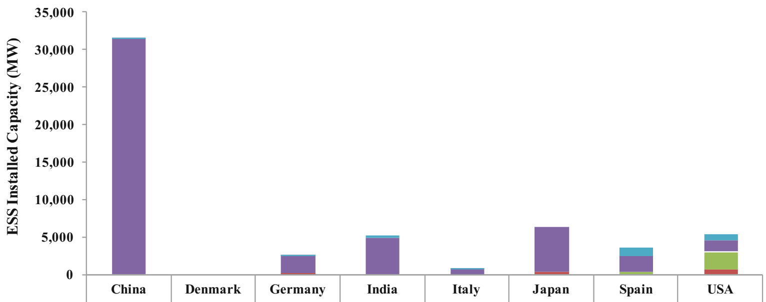

	China	Denmark	Germany	India	Italy	Japan	Spain	USA
Thermal Energy Storage	51.5		1.5	226.2	5.1		1,131.7	815.0
Mechanical Energy Storage	31,514.0	-	2,379.6	4,850.0	730.0	6,140.0	2,013.4	1,497.9
Electrical Energy Storage	-	-	-	15.0	-	-	350.0	2,348.0
Electrochemical energy storage	53.3	1.6	131.6	15.1	56.2	254.6	8.1	656.8
Chemical Energy Storage	-	-	12.7	-	1.2	-	-	-

Fig. 25 Technology wise installed capacity of energy storage in top RE major countries (Energystorageexchange.org 2017)

Annexure 1 presents the list of representative conventional power generation projects comprising energy storage across the globe. However, the representative global projects of renewable energy comprising relevant energy storage technologies are presented in Annexure 2.

7 Energy Storage Scenario in India

India has aggressive targets for shifting to renewable energy (i.e.175 GW installed capacity by the year 2022 in which 100 GW of solar and 60 GW of wind power), which at present is unscheduled and affecting the smooth operation of the electric grid. These challenges can only be met by the use of energy storage technologies. In India, several programs have been launched in the past few years (Smart Grids and Electric Vehicles missions, and programs on decentralized electrification and rural microgrids) necessitates the use of energy storage in the future energy strategy of the country.

7.1 Existing Legal/Regulatory and Policy Framework

Following key legal and regulatory initiatives are being explored by GoI to push energy storage sector:

- National Electric Mobility Mission (NEMM): The Govt. of India launched National Electric Mobility Mission in April 2015. The target of 6–7 million Electric Vehicles by 2022 in the country has been set under the mission.

- Net Metering Policy: Net energy metering is a type of Distributed Generation that allows customers with an eligible power generator to offset the cost of their electric usage with energy they export to the grid. So far most of the Indian States have released net metering policies which give the consumer a provision to install Rooftop PV at their premises. Recent technology development also allows utilization of solar power during grid outage with the help of hybrid inverter and battery energy storage technology.
- Renewable Energy Targets: the GoI has already set aggressive targets of 175 GW of renewable energy with 100 GW coming from solar, 60 GW by wind, 10 GW by biomass and 5 GW by small hydro by 2022. Integration of renewable energy will require energy storage technologies.
- National Smart Grid Mission: Ministry of Power has approved National Smart Grid Mission (NSGM) which has set aggressive targets for Microgrids which will require energy storage technologies.

7.2 Recent Initiatives for Deployment of Energy Storage Systems

Recently following initiatives have been taken by GoI to implement energy storage facilities with utility scale RE power supply:

- Recently, the Ministry of New and Renewable Energy, GoI has set up a task force to draft a National Energy Storage Mission for the country.
- A 10 MW Li-ion based battery energy storage project at Jhajjar, Haryana: A joint project by Panasonic and AES, which will provide reliability and backup to the manufacturing facility, while demonstrating grid stability and renewable integration services in the region.
- A 10 MW Li-ion based battery energy storage project at TPDDL's facilities: A joint project by Mitsubishi Corporation, AES, and TPDDL. The energy storage system will contribute to stabilizing the grid network of TPDDL, which delivers power to over 7 million customers across the Northern and Northwestern regions of Delhi. The project implementation work started in January 2018.
- CEA has claimed 100 GW of PHES will eventually be constructed in the country, with 10 GW planned to come online in the next 5 years.
- Over last two years, the tenders for utility scale solar storage projects aggregating more than 60 MWh, floated by SECI and NTPC (National Thermal Power Corporation) and NLC (Neyveli Lignite Corporation) across the states of Andhra Pradesh, Karnataka and Andaman & Nicobar Islands have been scrapped.
- In March 2018, both NTPC and NLC have retendered solar plus battery projects of cumulative 45 MW capacity in Andaman & Nicobar Islands.

- In recent past, the MNRE, NISE and other PSUs had taken up few demonstration projects to analyze solar thermal storage projects. However, those projects have not been effective to be scaled up to a commercial level.
- A solar wind hybrid project of 160 MW with battery storage will come up in Andhra Pradesh. The project shall be funded by World Bank with SECI as owner and off-taker of the project.
- Recently, SECI has called for the bids of 2000 MW Wind Solar Hybrid project. Which shows positive sign for storage integration in near future looking at the operational aspects.
- SECI has invited bids for grid-Connected 2 MW Solar PV and 0.5 MW Wind Hybrid Power Plant with 1 MWh Energy Storage System at village—Rangreek, district—Lahaul-Spiti in the State of Himachal Pradesh.
- On the sidelines to promote electric vehicles in the country, the NITI Ayog has already suggested a three stage strategy to promote the manufacturing of batteries in India.
- The India Energy Storage Alliance (IESA) estimates Indian energy storage market to grow up to 200 GWh by 2022 which could invite investments up to $ 6 billion in manufacturing of storage devices.

8 Drivers and Barriers

The key drivers that affect the development of energy storage technologies worldwide are

- **Renewable Energy Integration**
  One of the main drivers of energy storage is the growing share of renewable power in the grid. Earth has huge potential for power generation from solar and wind resources. On the other hand, electricity generation from solar and wind resources has already become cheaper to many conventional sources of power generation. Development of software and hardware tools for forecasting and scheduling of renewable power generation becomes renewable power management better. The challenges of grid integration emerge with large-scale deployment of renewable. The severities of the challenges depend upon the strength of grid network in the region. Medium and large-scale Energy Storage Systems will play a major role in power quality improvement through time shifting and peak shaving.
- **Electricity Demand and Supply Gap**
  Many regions in the world are energy deficit and peak deficit. Energy storage can play a major role to reduce the demand and supply gap. During peak periods when demand is higher than supply, storage could fill the gap and compensate power plants operated to meet base demand and avoid the expensive source of power generation. During the off-peak period when demand is less than supply and generation is from intermittent sources, electrical energy can be stored to

utilize during peak hours. On the contrary, from the Consumers' point of view, storage can lower electricity cost since it can store electricity bought at low prices during off-peak and use it or sell it during peak hours.

- **Electrification Through Microgrid or Off-Grid**
  Electrification through microgrid or off-grid will play an important role in solving the issue of energy access in underdeveloped regions. Microgrids can operate in parallel or in island mode to utility power grid. Energy storage is a vital component of the off-grid and microgrid system for reliable power supply.
- **Electric Vehicles**
  Battery Energy Storage technology is the vital component of Electric Vehicles. Electric vehicles can also act as virtual power plants and can help in supplying power to the grid during peak hours and can charge during off-peak hours.
  At present the barriers to large-scale deployment of energy storage technologies are as follows:

  - The high cost of energy storage technologies,
  - Lack of studies on potential assessment of different energy storage technologies so the renewable energy resource planning,
  - Non-enforcement of ToD Tariff in different countries,
  - The absence of local manufacturing potential at present to support immediate demand for large-scale grid storage,
  - Lack of operational experiences for many energy storage technologies in different countries,
  - The issue of safety, storage, and transportation.

9 Techno-economics of Energy Storage (W.R.T. Solar Projects)

Electrical energy storage technologies can be used for the applications with short discharge time, medium discharge time and long discharge time. For the applications having short discharge time DLC, SMES, and FES technologies are used. The energy-to-power ratio for such technologies is less than 1 (e.g., a capacity of less than 1 kWh of a system with a power of 1 kW). As mentioned earlier, FES can be used for larger capacities—electrochemical energy storage, and: LA, Li-ion, and NaS batteries are best suitable for medium discharge time storage applications (Table 2).

The technology of the different electrochemical techniques is relatively similar. They are available in the range of kW to MW and kWh to MWh compared to other storage technologies. Typical discharge times are up to several hours, with an energy-to-power ratio of between 1 and 10 (e.g., between 1 and 10 kWh for a 1 kW system). Batteries can be tailor-made to the requirements of an application: balances may be made for high energy or high power density, fast charging behavior or long

Table 2 Specific technical inter-comparison of different electrical energy storage technologies

Discharge time	Energy-to-power ratio	Energy storage technologies
Short discharge time (seconds to minutes)	<1	Double-layer capacitors (DLC)
		Superconducting magnetic energy storage (SMES)
		Flywheel energy storage (FES)
Medium discharge time (minutes to hours)	Between 1 and 10	Flywheel energy storage
		Larger capacities—electrochemical energy storage such as Lead-Acid (LA), Lithium-ion (Li-ion) and Sodium Sulfur (NaS) batteries
Long discharge time (days to months)	>10	Hydrogen (H_2)
		Synthetic Natural Gas (SNG)
Between medium and long discharge times	Between 5 and 30	Pumped hydro storage (PHS)
		Compressed air energy storage (CAES)
		Redox flow batteries

life, etc. H_2 and SNG technologies are being used for long discharge time storage applications. The energy-to-power ratio of such systems is comparably higher (greater than 10). PHS, CAES, and Redox flow batteries are well situated for medium and long discharge times. Similar to H_2 and SNG systems, these electrical energy storage technologies have external storage tanks. However, the energy densities are rather low, that limits the energy-to-power ratio to values to the range of 5–30. Table 2 presents the discharge time and energy-to-power ratio of different energy storage technologies practically in use.

The cost of different energy storage technologies, its efficiency and cycle lifetime are key aspects of technology adoption. The cost of different storage technologies varies across geographies due to the issue of availability locally and system size. There are various studies, depicts kW or kWh cost of different storage systems.

9.1 Utility Scale Solar PV Projects

In this section, as a case study LCOE of a Solar PV system with both Lead-acid and Li-ion batteries have been worked out. The assumptions for LCOE estimation is listed in Table 3.

Considering the above assumptions and without any battery storage system, the LCOE turns around to be USD 0.068/kWh. A similar calculation is carried out considering both Lead-acid and Li-ion storage batteries for 5 MW capacity for the duration of half an hour and more. A sensitivity analysis is carried out to have a clear picture of the impact on LCOE and IRR due to a reduction in present battery cost and increase in a number of storage hours, which showed in Figs. 26, 27, 28 and 29.

Table 3 List of assumptions

Parameters	Values/description	Remarks
PV system capacity	50 MW AC and 60 MW DC	
PV system cost	USD 74,242/MWp	As per Present Market Price
Annual energy generation	1.664MU/MWp	As per CERC (Tariff Order of CERC)
O&M cost of PV plant	USD 19,697/MWp	As per CERC
Plantlife	25 years	As per CERC
Interest rate	13%	As per CERC
Loan repayment period	12 years	As per CERC
Storage capacity	5 MW (10% @50 MW)	–
Lead-acid Battery replacement period	Once in 5 years	As per Manufacturer Warranty
The present cost of Lead-acid Battery	USD 1.06/Wh	International Finance Corporation (2017)
Li-ion Battery replacement period	Once in 13 years	As per Manufacturer Warranty
The present cost of Li-ion Battery	USD 0.85/Wh	International Finance Corporation (2017)
DoD	50%	As per Manufacturer's recommendation
Lead-acid Battery efficiency	75%	As per Manufacturer's recommendation
Li-ion Battery efficiency	85%	As per Manufacturer's recommendation
Inverter replacement year	Once in 13 years	As per Manufacturer's recommendation
Foreign exchange	1 USD = 66 INR	Present rate
Electricity tariff	USD 0.985	

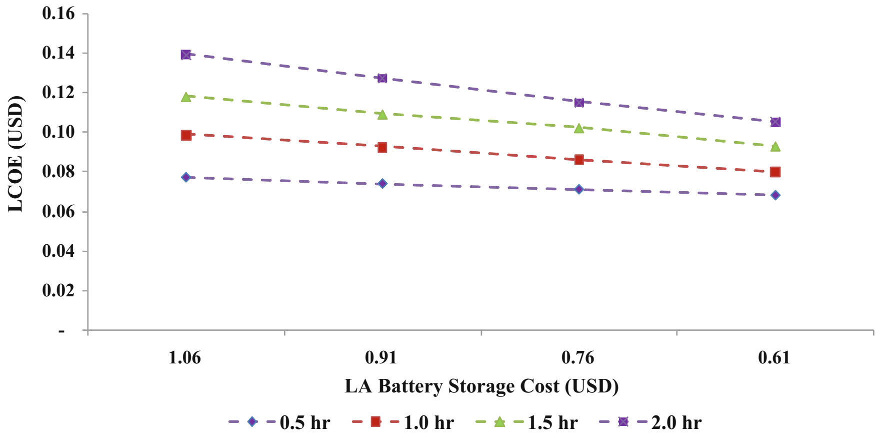

Fig. 26 LCOE for different hours of storage and capital cost of lead-acid battery

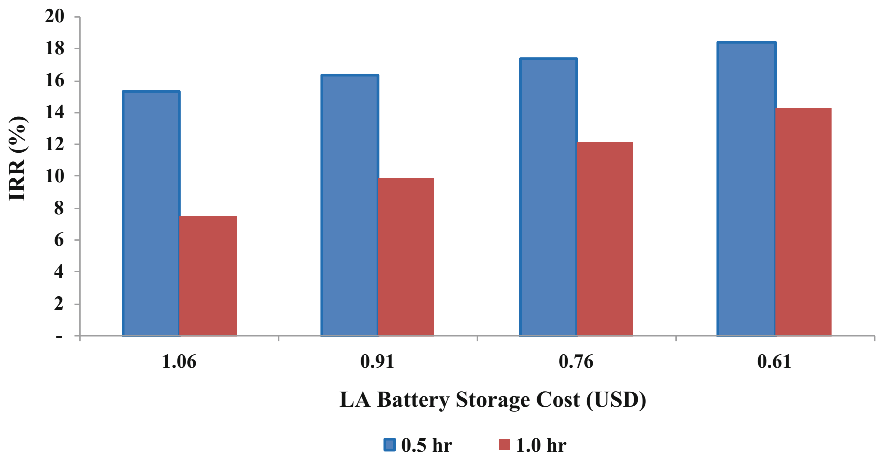

Fig. 27 IRR for different hours of storage and capital cost of lead-acid battery

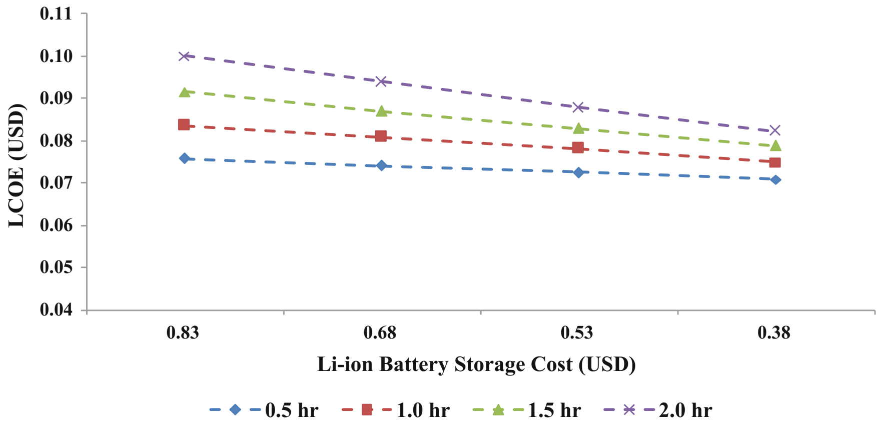

Fig. 28 LCOE for different hours of storage and capital cost of Li-ion battery

9.2 Utility Scale CSP Projects

In this section, as a case study, LCOE of a Concentrated Solar Power Plant with and without thermal energy storage has been worked out. The assumptions for the analysis are listed in Table 4.

Considering the above assumptions and without any storage, the LCOE turns around to be USD 0.202/kWh. A similar calculation is carried out for an different combination of Solar Multiple (SM) and Thermal Energy Storage (TES) hours as shown in Figs. 30 and 31. The System Advisor Model software tool of NREL is

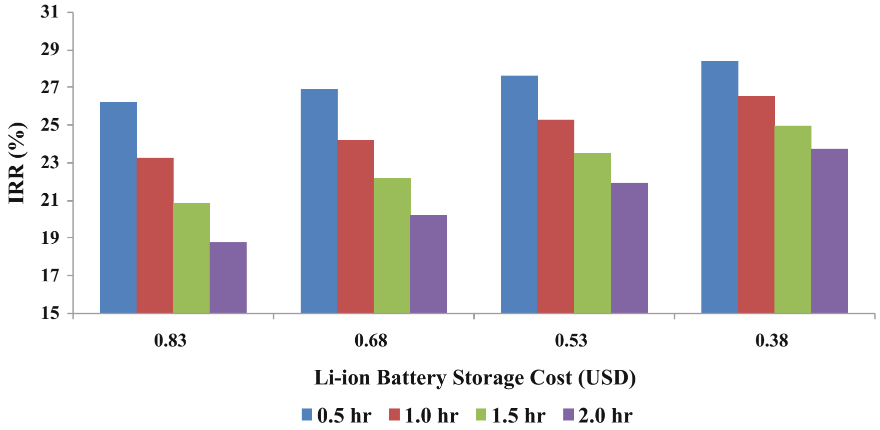

Fig. 29 IRR for different hours of storage and capital cost of Li-ion battery

Table 4 List of assumptions

Parameters	Values/Description	Remarks
CSP plant capacity	1 MW	
Capital cost	USD 1,818,182/MWp	As per "Tariff Order of CERC" and "Sundaray and Kandpal" (2013)
Plantlife	25 years	As per CERC
Interest rate	13%	As per CERC
Loan repayment period	12 years	As per CERC
Storage capacity	3–12 h	
Foreign exchange	1 USD = 66 INR	Present rate

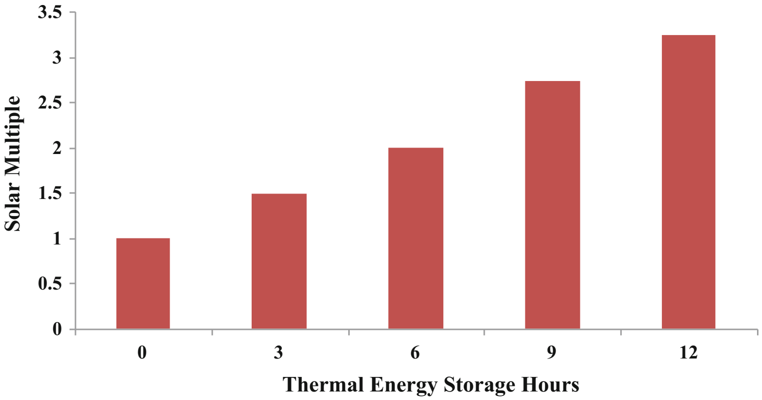

Fig. 30 An optimum combination of solar multiple and thermal energy storage hours

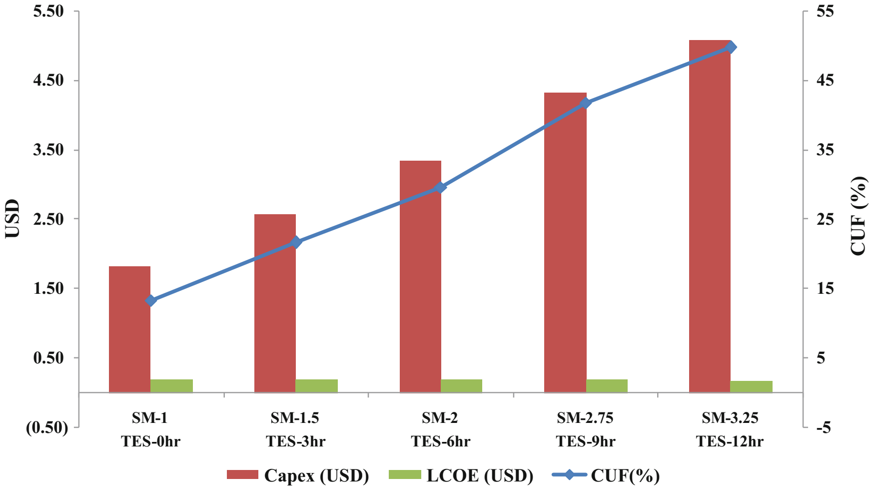

Fig. 31 CUF, CAPEX and LCOE for different SM and TES hours

used for the analysis (Purohit and Purohit 2010, 2015, 2017; Sharma et al. 2017; Purohit et al. 2013).

10 Future of Energy Storage Technologies

In the current scenario, at the global level, the main options for large-scale energy storage are pumped hydro storage followed by the batteries. The favorable cost economics of storage may open the dimension of electrical vehicles as mainstream. Energy storage technologies have significant potential to support sustainable development in emerging economies by accelerating the quality and reliability of electricity supply along with the optimized integration of RE power. The state of art EES technologies have wide range of technological characteristics. With a suitable combination of technologies, EES can meet most technical requirements for different power system and network operations. However, apart from pumped hydro storage most of the EES technologies are economically not much viable or mature enough for implementation at large scale. In several countries, the successful transformation of the energy system is increasingly being linked with development and deployment of EES. It is projected by several market research reports that there is significant optimism which comprises sufficient improvements in the energy storage which could be achieved in next 5–8 years.

This is well established that electrical energy storage could play a pivotal role in future low-carbon electrical systems, balancing inflexible or intermittent supply with demand. Both the conventional electricity generation industry, DER and intermittent renewable energy supply systems required the electric energy storage for reduction of the challenges they are facing. The energy storage technologies have various applications, ranging from large-scale generation and transmission-related systems to distribution network and even customer/end-user sites. The energy storage is also proved as a feasible option in multiple grid applications; that can ensure the reliability and resilience of the network and deliver energy more efficiently. However, at present stage, high capital costs of EES systems and several other various markets and regulatory barriers are hindering the required deployment of the technology at large scale. EES technologies are vigorous if both the transition to a new energy mix and global decarbonization are to succeed. As more and more electricity from fluctuating RE flows through power lines, grids must become increasingly flexible to prevent blackouts. Multiple market drivers suggest that electrical energy storage systems are going to be essential for future power systems within the next decade. However, the deployment of the EES technologies is proceeding at very different rates around the world with respect to prevailing resource, technology and regulations, etc.

Annexure 1

List of global representative conventional power projects with energy storage

S. No.	Technology classification	Installed capacity (MW)	Country of installation	Reason for installation
1	Lead-acid battery	10.0	US	Uninterrupted power supply during grid disturbances
2	NiCd, NiMH	27.0	US	In the event of a generation or transmission-related outage, it can provide 27 MW of power for 15 min. That's enough time to start up local generation when there is problem with the power plants
3	Pumped Hydro Storage	3,003.0	US	This project is used for time shifting application. It pumps water to an elevated reservoir at night and lets it run back down to generate electricity during the day
4	Compressed Air Energy Storage	321.0	Germany	The 321-MW plant utilizes nuclear-sourced night-time power for compression and produces peak power during the day via a natural gas turbine

(continued)

(continued)

S. No.	Technology classification	Installed capacity (MW)	Country of installation	Reason for installation
5	Flywheel Energy Storage	400.0	UK	EFDA JET Fusion Flywheel Annual consumption is very dependent on whether JET is operational or in shutdown. The peak of consumption here is during a 300 s JET pulse—where over 300 MW of electrical power is pulled from the grid, and up to 400 MW is supplied from two large flywheels located in Culham, U.K. However, this is only for 30 s, every 20–30 min
6	Liquid: water or thermo-oil. Solid: concrete or the ground	90.0	US	This is a Generation Storage system in which water is chilled at off-peak and stored in a thermal energy storage tank. The following day during peak, chilled water is pulled from the tank to chill the inlet air of the gas turbine, resulting in increased output. System is weather dependent, with full 90 MW output at 95 °F. System offers increased MWs for capacity and/or ancillary services beginning at temperatures above 59 °F, with highest performance at highest temperatures

Annexure 2

List of global representative RE based (CSP, Solar PV and Wind) power projects with energy storage (Tables 5 and 6)

Table 5 Global CSP projects with thermal energy storage (all based on PTC technology)

Project Name	Country	Year	Key parameters	Capacity	TES description
Andasol-1	Spain	2008	Solar Resource: 2,136 kWh/m^2/year Estimated Electricity Generation: 1,58,000 MWh/year	49.9 MW with Steam Rankine Cycle	Storage type: 2- tank indirect 28,500 tons of molten salt (60% $NaNO_3$ + 40% KNO_3) Storage capacity: 7.5 h
Andasol-2	Spain	2009	Solar Resource: 2,136 kWh/m^2/year Estimated Electricity Generation: 1,58,000 MWh/year	49.9 MW with Steam Rankine Cycle	Storage type: 2- tank indirect 28,500 tons of molten salt (60% $NaNO_3$ + 40% KNO_3) Storage capacity: 7.5 h
Andasol-3	Spain	2011	Solar Resource: 2,200 kWh/m^2/year Estimated Electricity Generation: 1,75,000 MWh/year	50.0 MW with Steam Rankine Cycle	Storage type: 2- tank indirect Storage capacity: 7.5 h
Arcosol 50	Spain	2011	Solar Resource: 2,097 kWh/m^2/year Estimated Electricity Generation: 1,75,000 MWh/year	49.9 MW with Steam Rankine Cycle	Storage type: 2- tank indirect 28,500 tons of molten salt (60% $NaNO_3$ + 40% KNO_3) Storage capacity: 7.5 h
Arenales	Spain	2013	Solar Resource: NA Estimated Electricity Generation: 1,66,000 MWh/year	50.0 MW with Steam Rankine Cycle	Storage type: 2- tank indirect Molten salt (60% $NaNO_3$ + 40% KNO_3) Storage capacity: 7 h

(continued)

Table 5 (continued)

Project Name	Country	Year	Key parameters	Capacity	TES description
Aste 1A	Spain	2012	Solar Resource: 2,019 kWh/m^2/year Estimated Electricity Generation: 1,70,000 MWh/year	50.0 MW with Steam Rankine Cycle	Storage type: 2- tank indirect Molten salt (60% $NaNO_3$ + 40% KNO_3) Storage capacity: 8 h
Aste 1B	Spain	2012	Solar Resource: 2,019 kWh/m^2/year Estimated Electricity Generation: 1,70,000 MWh/year	50.0 MW with Steam Rankine Cycle	Storage type: 2- tank indirect Molten salt (60% $NaNO_3$ + 40% KNO_3) Storage capacity: 8 h
Astexol II	Spain	2012	Solar Resource: 2,052 kWh/m^2/year Estimated Electricity Generation: 1,70,000 MWh/year	50.0 MW with Steam Rankine Cycle	Storage type: 2- tank indirect Molten salt (60% $NaNO_3$ + 40% KNO_3) Storage capacity: 8 h
Bokpoort	South Africa	2016	Solar Resource: NA Estimated Electricity Generation: 2,30,000 MWh/year	50.0 MW with Steam Rankine Cycle	Storage type: 2- tank indirect Molten salts Storage capacity: 9.3 h - 1,300 MWh-t
Casablanca	Spain	2013	Solar Resource: NA Estimated Electricity Generation: 1,60,000 MWh/year	50.0 MW with Steam Rankine Cycle	Storage type: 2- tank indirect Molten salt (60% $NaNO_3$ + 40% KNO_3) Storage capacity: 7.5 h
Crescent Dunes Solar Energy Project	United States	2015	Solar Resource: 2,685 kWh/m^2/year Expected Electricity Generation: 5,00,000 MWh/year	110.0 MW with Steam Rankine Cycle	Storage type: 2- tank indirect Storage capacity: 10 h
Extresol-1	Spain	2010	Solar Resource: 2,168 kWh/m^2/year	50.0 MW with Steam Rankine Cycle	Storage type: 2- tank indirect 28,500 tons of molten salt

(continued)

Table 5 (continued)

Project Name	Country	Year	Key parameters	Capacity	TES description
			Expected Electricity Generation: 1,58,000 MWh/year		(60% $NaNO_3$ + 40% KNO_3) Storage capacity: 7.5 h—1,010 MWh-t
Extresol-2	Spain	2010	Solar Resource: 2,168 kWh/m^2/year Expected Electricity Generation: 1,58,000 MWh/year	49.9 MW	Storage type: 2-tank indirect 28,500 tons of molten salt (60% $NaNO_3$ + 40% KNO_3) Storage capacity: 7.5 h—1,010 MWh-t
Extresol-3	Spain	2012	Solar Resource: 2,168 kWh/m^2/year Expected Electricity Generation: 1,58,000 MWh/year	50.0 MW	Storage type: 2- tank indirect 28,500 tons of molten salt (60% $NaNO_3$ + 40% KNO_3) Storage capacity: 7.5 h—1,010 MWh-t
KaXu Solar One	South Africa	2015	Solar Resource: NA Expected Electricity Generation: 3,30,000 MWh/year	100.0 MW with Steam Rankine Cycle	Storage type: 2- tank indirectMolten salts Storage capacity: 2.5 h
Khi Solar One	South Africa	2016	Solar Resource: NA Expected Electricity Generation: 1,80,000 MWh/year	50.0 MW with Steam Rankine Cycle	Saturated Steam Storage capacity: 2 h
La Florida	Spain	2010	Solar Resource: NA Estimated Electricity Generation: 1,75,000 MWh/year	50.0 MW with Steam Rankine Cycle	Storage type: 2- tank indirect 29,000 tons of molten salt (60% $NaNO_3$ + 40% KNO_3) Storage capacity: 7.5 h

(continued)

Table 5 (continued)

Project Name	Country	Year	Key parameters	Capacity	TES description
Manchasol-1	Spain	2011	Solar Resource: 2,208 kWh/m^2/yearExpected Electricity Generation: 1,58,000 MWh/year	49.9 MW	Storage type: 2- tank indirect 28,500 tons of molten salt (60% $NaNO_3$ + 40% KNO_3) Storage capacity: 7.5 h
Manchasol-2	Spain	2011	Solar Resource: 2,208 kWh/m^2/yearExpected Electricity Generation: 1,58,000 MWh/year	50.0 MW	Storage type: 2- tank indirect 28,500 tons of molten salt (60% $NaNO_3$ + 40% KNO_3) Storage capacity: 7.5 h
Solana Generating Station	United States	2013	Solar Resource: NA Expected Electricity Generation: 9,44,000 MWh/year	250.0 MW with Steam Rankine Cycle	Storage type: 2- tank indirect Molten salts Storage capacity: 6 h
Termesol 50	Spain	2011	Solar Resource: 2,097 kWh/m^2/year Expected Electricity Generation: 1,75,000 MWh/year	49.9 MW with Steam Rankine Cycle	Storage type: 2- tank indirect 28,500 tons of molten salt (60% $NaNO_3$ + 40% KNO_3) Storage capacity: 7.5 h
Termosol 1	Spain	2013	Solar Resource: NA Estimated Electricity Generation: 1,80,000 MWh/year	50.0 MW with Steam Rankine Cycle	Storage type: 2- tank indirect Molten salt (60% $NaNO_3$ + 40% KNO_3) Storage capacity: 9 h
Termosol 2	Spain	2013	Solar Resource: NA Estimated Electricity Generation: 1,80,000 MWh/year	50.0 MW with Steam Rankine Cycle	Storage type: 2- tank indirect Molten salt (60% $NaNO_3$ + 40% KNO_3) Storage capacity: 9 h

Table 6 Global solar PV and wind projects with electrical storage

S. No.	Project Name	Country	Technology type	Rated power in kW	Duration (hr)	Service/Use
1	Shiura Wind Park	Japan	Valve Regulated Lead-acid Battery	4,500	2.33	Renewables Capacity Firming
2	Cowessess First Nation High Wind and Storage Project	Canada	Lithium-ion Battery	400	1.87	Renewables Capacity Firming Time Shift Power Quality
3	Wind Energy Institute of Canada Durathon Battery	Canada	Sodium-nickel-chloride Battery	1,000	2.0	Renewables Capacity Firming
4	Notrees Battery Storage Project—Duke Energy	United States	Lithium-ion Battery	36,000	0.67	Electric Energy Time Shift
5	AES Laurel Mountain	United States	Lithium-ion Battery	32,000	0.25	Frequency Regulation
6	MID Primus Power Wind Energy Storage Demonstration—Renewables Firming	United States	Zinc Bromine Flow Battery	250	4.0	Renewables Energy Time Shift
7	The Zhangbei Project—State Grid/Sparton Resources	China	Vanadium Redox Flow Battery	2,000	4.0	Renewables Energy Time Shift
8	Guodian Hefeng Beizhen Wind Farm: VFB	China	Vanadium Redox Flow Battery	2,000	2.0	Onsite Renewable Generation Shifting
9	Pillar Mountain Wind Project—Xtreme Power	United States	Advanced Lead-acid Battery	3,000	0.25	Electric Supply Reserve Capacity—Spinning
10	Santa Rita Jail Smart Grid—Alameda County RDSI CERTS Microgrid Demonstration	United States	Lithium Ion Phosphate Battery	2,000	2.0	Electric Bill Management
11	Kaheawa Wind Project—Younicos	United States	Advanced Lead-acid Battery	1,500	0.4	Ramping
12	Kaheawa Wind Power Project II—Younicos	United States	Advanced Lead-acid Battery	10,000	0.75	Electric Supply Reserve Capacity—Spinning
13	XCEL MinnWind Wind-to-Battery Project—NGK	United States	Sodium sulfur Battery	1,000	7.2	Frequency Regulation
14	Falköping Substation Smart Grid—ABB	Sweden	Lithium-ion Battery	75	1.0	Distribution upgrade due to solar
15	Graciosa Project	Portugal	Lithium Ion Titanate Battery	6,000	0.53	Distribution upgrade due to solar

(continued)

Table 6 (continued)

S. No.	Project Name	Country	Technology type	Rated power in kW	Duration (hr)	Service/Use
16	Smart ZAE Flywheel Project	France	Flywheel	100	1.0	Electric Bill Management with Renewables
17	Tozzi Energy Storage System—TESS	Italy	Sodium-nickel-chloride Battery	35	3.0	Renewables Energy Time Shift
18	Isle of Muck Microgrid System	United Kingdom	Lead-acid Battery	45	3.67	Onsite Renewable Generation Shifting
19	Isle of Rum Microgrid System	United Kingdom	Lead-acid Battery	45	3.67	Onsite Renewable Generation Shifting
20	Isle of Eigg Electrification Project	United Kingdom	Lead-acid Battery	60	3.67	Onsite Renewable Generation Shifting
21	140 MW Wind Park with 1 MW Power to Gas System	Germany	Hydrogen Storage	1,000	27.0	Renewables Capacity Firming
22	Cape Barren Island Hybrid System	Australia	Electrochemical	163	1.0	Onsite Renewable Generation Shifting
23	Clear Creek Flywheel Wind Farm Project	Canada	Flywheel	5,000	0.10	Distribution upgrade due to wind
24	Gapado Island, Jeju Smart Grid Project	Korea, South	Lithium-ion Battery	1,000	1.0	Distribution upgrade due to wind
25	Yeongheung Wind-Farm Energy Storage System	Korea, South	Lithium-ion Battery	4,000	4.0	Onsite Renewable Generation Shifting
26	Tomamae Wind Farm	Japan	Vanadium Redox Flow Battery	4,000	1.50	Renewables Capacity Firming
27	Hawi Wind Farm BESS	United States	Lithium Ion Titanate Battery	1,000	15.0	Renewables Capacity Firming
28	Carthage Water & Electric Plant	United States	Advanced Lead-acid Battery	100	2.27	Distribution upgrade due to solar

(continued)

Table 6 (continued)

S. No.	Project Name	Country	Technology type	Rated power in kW	Duration (hr)	Service/Use
29	Kennedy Energy Park	Australia	Lithium-ion Battery	4,000	1.0	The 4 MWh Energy Storage System is a part of 43.2 MW Wind, 1 MW Solar PV and Battery Storage hybrid project. The project is expected to be commissioned by end of year 2018.

Annexure 3

List of operational energy storage projects in India

S. No.	Project name	Technology type	Rated power in kW	Duration (h)	Service/Use
1	India One Solar Thermal Plant	Heat Thermal Storage	1,000	16.0	Renewable Energy Time Shift Renewable Capacity Firming
2	Tehri Pumped Storage Hydroelectric Power Plant	Open-loop Pumped Hydro Storage	1,000,000	n/a	Electric Energy Time Shift Electric Supply Capacity
3	Sun-carrier Omega Net Zero Building in Bhopal	Vanadium Redox Flow Battery	45	6.67	Onsite Renewable Generation Shifting
4	Diwakar CSP Plant	Molten Salt Thermal Storage	100,000	4.0	Renewable Capacity Firming Renewable Energy Time Shift
5	NagarjunaSagar Pumped Hydro Station Tail Pond Project	Open-loop Pumped Hydro Storage	700,000	8.0	Electric Energy Time Shift Electric Supply Capacity

(continued)

(continued)

S. No.	Project name	Technology type	Rated power in kW	Duration (h)	Service/Use
6	Giga Capacitor Hyperadad Test Project (IL)	Electrochemical Capacitor	15,000	10.0	Renewable Energy Time Shift Distribution upgrade due to solar Stationary Transmission/Distribution Upgrade Deferral
7	30 kW Flow Battery by Imergy Power Systems at Global Academy of Technology College	Vanadium Redox Flow Battery	30	4.0	Microgrid Capability Onsite Power Onsite Renewable Generation Shifting Renewable Capacity Firming
8	SardarSarovar Pumped Storage Power Station	Open-loop Pumped Hydro Storage	1,450,000	n/a	Electric Energy Time Shift Electric Supply Capacity
9	Bhira Pumped Storage Hydro Plant	Open-loop Pumped Hydro Storage	150,000	n/a	Electric Energy Time Shift Electric Supply Capacity
10	Ghatghar Pumped Storage Hydroelectric Power Plant	Open-loop Pumped Hydro Storage	250,000	n/a	Electric Energy Time Shift Electric Supply Capacity
11	Kadamparai Hydroelectric Pumped Storage Power Plant	Open-loop Pumped Hydro Storage	400,000	n/a	Electric Energy Time Shift Electric Supply Capacity
12	Purulia Pumped Storage Hydroelectric Power Plant	Open-loop Pumped Hydro Storage	900,000	6.0	Electric Energy Time Shift Electric Supply Capacity
13	Clique Solar Thermal HVAC System	Chilled Water Thermal Storage	175	48.0	Onsite Renewable Generation Shifting Electric Bill Management with Renewable
14	Gram Power KharedaLakshmipura Microgrid	Lead-acid Battery	40	n/a	Renewable Capacity Firming Onsite Renewable Generation Shifting Electric Supply Capacity Microgrid Capability

(continued)

(continued)

S. No.	Project name	Technology type	Rated power in kW	Duration (h)	Service/Use
15	KVK Energy Solar Project	Molten Salt Thermal Storage	100,000	4.0	Renewable Capacity Firming Renewable Energy Time Shift
16	Gujarat Solar One	Molten Salt Thermal Storage	25,000	9.0	Renewable Capacity Firming Renewable Energy Time Shift

References

All India Installed Capacity (in MW) of Power Stations (April 2018) Central Electricity Authority (CEA). Available at: http://www.cea.nic.in/reports/monthly/installedcapacity/2018/installed_capacity-04.pdf. Accessed 18 May 2018

Analysis of actual generation data collected from Gujarat State Load Dispatch Centre

BP Statistical Review of World Energy (2017) BP p.l.c., London. Source—https://www.bp.com/content/dam/bp/en/corporate/pdf/energy-economics/statistical-review-2017/bp-statistical-review-of-world-energy-2017-full-report.pdf

Electric Power Research Institute (EPRI) (June 2010) Solar thermocline storage systems: preliminary design study. Electric Power Research Institute, Palo Alto, CA

Energystorageexchange.org (2017) DOE global energy storage database. Source—https://www.energystorageexchange.org/. Accessed 25 July 2017

Fi-powerweb.com. (2017) Wind energy and solar. Installed GW capacity—global and by country. Source—http://www.fi-powerweb.com/Renewable-Energy.html

Global Energy Storage Market Overview & Regional Summary Report (2015) Mawson ACT: Energy Storage Council. Available at: https://neca.asn.au/sites/default/files/media/state_nsw/News%20&%20Views/ESC%20Global%20Energy%20Storage%20Report_2015.pdf

International Electrotechnical Commission (2011) A white paper on "Electrical Energy Storage"

International Finance Corporation (2017) Report energy storage trends and opportunities in emerging markets under ESMAP. Source—https://www.ifc.org/wps/wcm/connect/ed6f9f7f-f197-4915-8ab6-56b92d50865d/7151-IFC-EnergyStorage-report.pdf?MOD=AJPERES

POSOCO-National Load Dispatch Centre, Government of India

Power Market Overview and Trends (2017) Indian Brand Equity Foundation. Source—https://www.ibef.org/download/Power_-_January_2017.pdf

Power Sector Report by Central Electricity Authority (January 2017) Source—http://www.cea.nic.in/reports/monthly/executivesummary/2017/exe_summary-01.pdf

Purohit I, Purohit P (2010) Techno-economics of concentrating solar power in India. Energy Policy 38(6):3015–3029

Purohit I, Purohit P (2015) Inter-comparability of solar radiation databases in Indian context. Renew Sustain Energy Rev 50(2015):735–747

Purohit I, Purohit P (2017) Technical and economic potential of concentrating solar thermal power generation in India. Renew Sustain Energy Rev 78(2017):648–667

Purohit I, Purohit P, Shekhar S (2013) The potential of concentrating solar power in North-Western parts of India. Energy Policy 62:157–175

Renewables 2017 Global Status Report. REN21 Secretariat, Paris. Available at: http://www.ren21.net/wp-content/uploads/2017/06/17-8399_GSR_2017_Full_Report_0621_Opt.pdf

Renewables Global Status Report (2016) REN21 Secretariat, Paris. Available at: http://www.ren21.net/wp-content/uploads/2016/05/GSR_2016_Full_Report_lowres.pdf

Renewables Global Status Report (2017) REN21 Secretariat, Paris. Source—http://www.ren21.net/wp-content/uploads/2017/06/17-8399_GSR_2017_Full_Report_0621_Opt.pdf

Report on Green Energy Corridors (2012) Vol-I. Power Grid Corporation of India Ltd, Gurgaon. Source—http://re.indiaenvironmentportal.org.in/files/file/Report-Green%20Energy%20corridor.pdf

Sharma C, Sharma A, Purohit I, Mullick SC, Kandpal TC (2017) Comparison of solar radiation data sources for design and performance appraisal of CSP systems in India. Int J Ambient Energy (Online available)

Steen D, Joel G, Göransson L, Nursbo S, Brolin M (2014) Challenges of integrating solar and wind into the electricity grid, systems perspectives on renewable power. Source—http://publications.lib.chalmers.se/records/fulltext/210515/local_210515.pdf

Sundaray S, Kandpal TC (2013) Preliminary feasibility evaluation of solar thermal power generation in India. Int J Sustain Energy

Tariff Order of Central Electricity Regulatory Commission, Govt. of India for Financial Year 2016–17. Source—http://www.cercind.gov.in/2016/orders/SORE.pdf

Technology Roadmap (2014). Energy storage. International Energy Agency, Paris. Source—https://www.iea.org/publications/freepublications/publication/TechnologyRoadmapEnergystorage.pdf

The World Factbook Library (2017) Source—https://www.cia.gov/library/publications/the-world-factbook/rankorder/2240rank.html

U.S. Energy Information Administration (2016) International energy outlook. U.S. Energy Information Administration, Washington, DC. Source—https://www.eia.gov/outlooks/ieo/pdf/0484(2016).pdf

World Energy Outlook (2016) International Energy Agency, Paris, France. Source—https://www.iea.org/publications/freepublications/publication/WorldEnergyOutlook2016ExecutiveSummaryEnglish.pdf

Wri.org. (2017) CAIT—Country Greenhouse Gas Emissions Data. World Resources Institute. Available at: http://www.wri.org/resources/data-sets/cait-country-greenhouse-gas-emissions-data. Accessed 7 Aug 2017

Thermal Storage Technologies for Space Cooling and Heating

Behzad Rismanchi, Sheikh Khaleduzzaman Shah, Tshewang Lhendup and Lu Aye

Abstract Storing thermal energy is not a new concept; harvesting ice for summer applications and the ice trade was a nineteenth-century industry. Thermal storage technologies enable excess thermal energy to be stored and used later. Balancing of energy demands between day and night (daily storage) or winter and summer (seasonal storage) and reducing the peak demands are the example benefits of thermal storage technologies. This chapter presents short-term cold thermal energy storage technologies and seasonal thermal energy storage technologies, and discusses their operational strategies. Full storage operation, partial storage with demand limiting and load levelling operating strategies are discussed.

Keywords Coolth storage · Heat storage · Ice · Chilled water
Borehole heat exchanger

1 Introduction

Currently, 65% of the energy used for space conditioning is in the form of electricity. Most of this electricity is generated from brown and black coal which is the single most significant contributor to greenhouse gas (GHG) emissions. In Australia, 200 Mt of $CO_{2\text{-e}}$ or 37% of national GHG emission in 2007 was from electricity generation (Department of Climate Change 2009). Furthermore, the electricity demand for space heating and cooling is increasing due to increasing number of buildings associated with an increase in population. With the growing population, the demand for the space heating and cooling will continue to rise, and therefore, it is a paramount importance to utilise the resources to their best performance and use renewable energy sources such as solar thermal energy wherever

---

B. Rismanchi · S. K. Shah · T. Lhendup · L. Aye (✉)
Renewable Energy and Energy Efficiency Group, Department of Infrastructure Engineering, Melbourne School of Engineering, The University of Melbourne, Melbourne, VIC 3010, Australia
e-mail: lua@unimelb.edu.au

A. Sharma et al. (eds.), *Low Carbon Energy Supply*, Green Energy and Technology,
https://doi.org/10.1007/978-981-10-7326-7_15

possible to limit the increased use of fossil fuels and associated GHG emissions. Countries have committed to the United Nations Framework Convention on Climate Change (UNFCCC) to reduce GHG emissions by the next decade (Department of Environment 2012). This GHG emission reduction will require a concerted effort to change the approach to energy consumption. Hence, a realistic and cost-effective measure to minimise GHG emission is necessary to achieve the above target. If alternative low carbon ways of heating, ventilation and air-conditioning (HVAC) were used, then a substantial reduction in GHG emissions and the carbon footprint could occur. Therefore, there is a need to look for alternative technologies which have lower energy consumption for space heating and cooling. While renewable energy is an alternative that is environmentally friendly, one of the issues is its intermittent availability. Most of the renewable energy sources are not available continuously. However, the building's heating and cooling load vary. Moreover, the peak loads and the availability of the energy sources may not match. Therefore, storage of energy is necessary to enable the system to match the demand. Reserving coolth and thermal energy for later use are not new technologies; for many years, natural ice was harvested from caves or frozen rivers to preserve food during the summer. Also, natural hot water from hot water spring was used during the cold days.

2 Cold Thermal Energy Storage (CTES) Systems

Cold thermal energy storage (CTES) systems are primarily utilised to transfer the energy consumption from peak to off-peak hours, this is especially beneficial when the primary source of energy is electricity. Therefore, they also referred to as "off-peak cooling" systems. In most of the regions, the off-peak hours are nighttimes when the ambient temperature is lower and thus less energy is required compared to the conventional cooling systems that run on demand during the daytime. It is reported that storing coolth is cheaper than storing electricity to produce cooling (MacCracken 2010).

CTES systems are used in the industry in different configurations. Some focused on storing the coolth using the thermal mass of the building, and the technique is known as pre-cooling where the cooling system starts operating early in the morning before the occupants arrive. This technique is the best on office buildings (Morgan and Krarti 2007). CTES is also used during transport of temperature-sensitive products (Cabeza et al. 2002; Kowata et al. 2002). Designers should consider selecting a CTES system when any of the following criteria are applied.

- The maximum cooling demand is substantially higher than the average cooling load. This is true for most of the nonindustrial facilities.

- The electricity price structure includes high demand charges, a significant difference between peak and off-peak rates, or special rebates or incentives for coolth storage installations.
- An existing space cooling system is undergoing expansion.
- An existing tank suitable for coolth storage use is available.
- Space cooling is needed for an application in a remote region.
- Capacity of electricity available at the site is limited.

The performance of a CTES system defined by its coefficient of performance (COP) is equal to the ratio of the net rate of cooling over the required power. The chiller and compressor type and configuration define the nominal COP of the system. However, the actual COP of the system is calculated using the fieldwork measurements, where the power consumption and net cooling demand is recorded over a predefined period. The COP of the chiller depends directly on the chilled water temperature. Comparing to the standard operation, the chiller used to produce ice would have a lower COP (Beggs and Ward 1992).

CTES systems have been applied in commercial and industrial scales for the past few decades, and thus substantial information, guidelines and standards relating to these systems are available. The American Society of Heating, Refrigerating and Air-conditioning Engineers (ASHRAE) has summarised the techniques and different geometries in a handbook (ASHRAE 2007).

CTES systems are categorised into three types: Chilled Water storage (CWS), Ice Thermal Storage (ITS) and eutectic salt systems (Hasnain 1998b). Details about each type will be presented in this chapter. Among these types, the CWS and ITS systems are used more commonly. The primary features of these storage systems are presented in Table 1. The main advantage of ITS system is the required storage volume compared with the other two systems. However, the COP of the ITS system is lower. Therefore, the optimum system sizing and configuration would depend on the localised parameters such as the climate conditions, electricity price, peak hours and the system setup.

2.1 Chilled Water Storage (CWS) Technique

In a conventional system configuration, the chiller provides the chilled water based on the demand that is directly used in the building. In a CTES system, the chilled water is stored in storage tanks for later use. It is a mature technology that has been used for shifting energy consumption from the peak hours to the off-peak hours (Mackie and Reeves 1988). During the past decade, different types of CWS have been developed and utilised in the field to provide the required cooling load. Often a complex tank and piping configuration is required to store the chilled water. The primary challenge in the design of the storage tank is to avoid mixing the chilled stored water with the return water. Some of the available configurations are tank series, labyrinth, multiple tanks with an empty tank, baffle, membrane and thermally stratified systems (Fig. 1).

Table 1 Primary features of cold storage systems (Hasnain 1998b; Incropera and DeWitt 2002; Washington State University 2003)

Parameter	Chilled water	Ice storage	Eutectic salt
Specific heat (kJ kg^{-1}K^{-1})	4.19	2.04	–
Latent heat of fusion (kJ kg^{-1})	–	334	80–250
Chiller type	Standard water cooled	Low-temperature secondary coolant	Standard water cooled
Chiller cost per kW ($)	57–85	57–142	57–85
Tank volume (m^3 kWh^{-1})	0.089–0.169	0.019–0.023	0.048
Storage installed cost ($ kWh^{-1})	8.5–28	14–20	28–43
Charging temperature (°C)	4–6	(−6)–(−3)	4–6
Chiller charging COP (–)	5.0–6.0	2.7–4.0	5.0–6.0
Discharge temperature (°C)	1–4 above charging	1–3	9–10
Discharge fluid	Water	Secondary coolant	Water
Tank interface	Open tank	Closed system	Open tank
Maintenance	High	Medium	Medium

2.2 *Ice Thermal Storage (ITS) System*

Among CTES systems, the use of ice is the most common due to the required space. The high latent heat of fusion of ice [h_{fg} = 334 kJ kg^{-1} (Incropera and DeWitt 2002)] makes it suitable to store a high volume of energy in a smaller tank. According to the statistical data in the early 90s, around 1,500–2,000 units of CTES systems were utilised in the United States with the majority being used in the office buildings, hospitals and schools. Among the installed systems, the ITS systems had the largest share ($\sim$80%) followed by the CWS system ($\sim$15%) (Potter et al. 1995). By employing ice, the greater part of the base load can be stored for further use (ASHRAE 2007). If we consider a temperature gradient of 15 °C between the supply and return for an ITS and CWS system, the CWS system would need around 6 times larger volume to store the same amount of energy (cooling) (see Eq. (1)).

$$\begin{gathered} Q_{\text{ice}} = Q_{\text{water}} \Rightarrow m_{\text{ice}}(c_{\text{p}}\Delta T + h_{\text{fg}}) = m_{\text{water}}c_{\text{p}}\Delta T \\ V_{\text{ice}}970(4.19 \times 15 + 334) = V_{\text{water}}1000 \times 4.19 \times 15 \Rightarrow V_{\text{water}} = 6.1V_{\text{ice}} \end{gathered} \tag{1}$$

The ITS system has been mainly utilised in buildings where it is utilised during the peak hours of the day, like office buildings, schools or stores. In most of the cases, ITS system would help to downsize the HVAC system components;

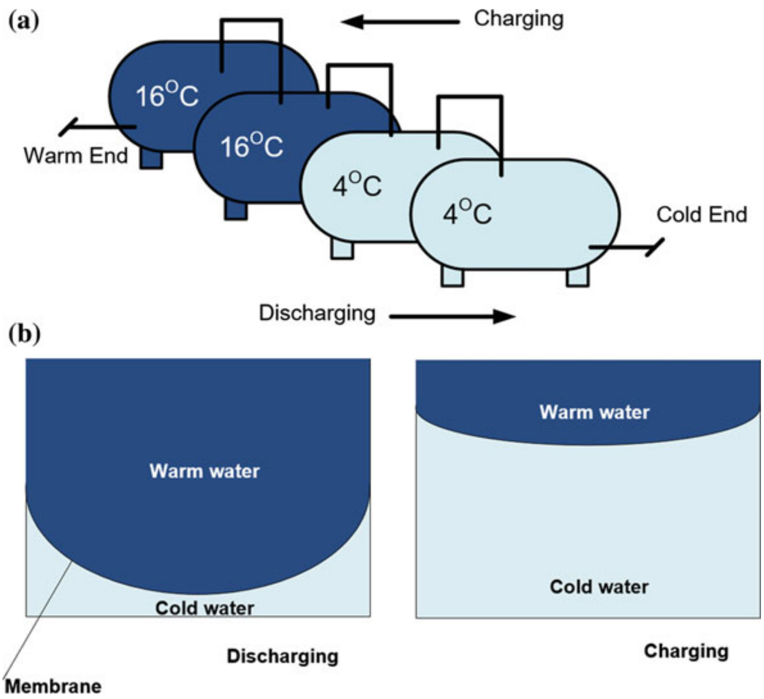

Fig. 1 **a** Series tank and **b** membrane tank. Adapted from Yau and Rismanchi (2012)

this means smaller ducting system and air handling units (AHUs) are required that would provide more usable space. Comprehensive reviews on the thermal energy storage systems are available in the literature (Zalba et al. 2003; Saito 2002; Yau and Rismanchi 2012). The limitation of ITS system is the storage temperature as well as the supply chilled water from the chiller. The chiller must produce chilled water with lower temperature (−6 to −3 °C) compared to the regular operation that requires special working fluid to prevent freezing.

The ITS systems are categorised into four main types, ice harvesting, ice-on-coil, ice slurry or encapsulated ITS systems (Dorgan and Elleson 1994), based on the charging and discharging mechanism. An alternative categorisation is based on the system components medium, and they can be defined as dynamic types, where the ice is formed out of the storage tank and is moved to the reservoir, or the static type, where the ice is formed directly inside the storage tank (Ho and Tu 2008).

Ice Harvester System

The ice harvester system has an open insulated storage tank and a vertical plate surface that is placed on top of the tank. In the charging process, a layer of ice is formed on the surface of the plate. The process continued until required ice thickness is achieved and the thickness could vary between 8 and 10 mm. A hot gas would then feed to the evaporator causing the ice in contact with the plates to melt

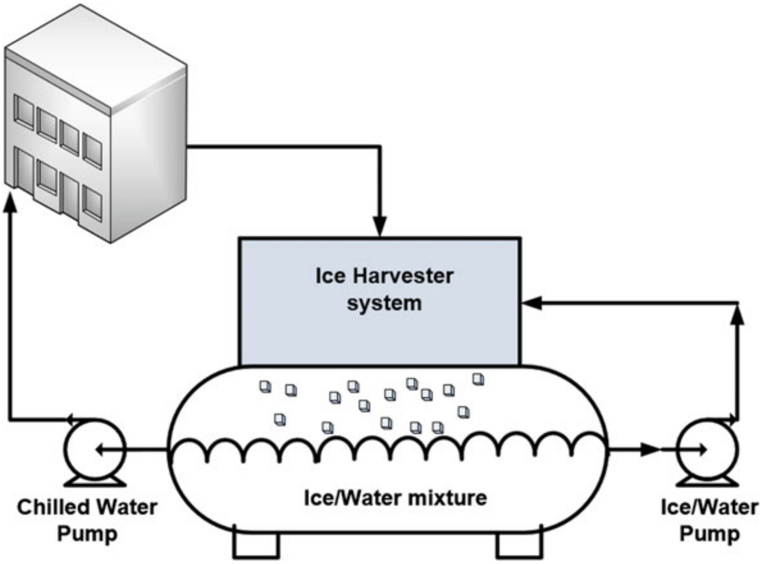

Fig. 2 Schematic diagram of a typical ice harvester system. Adapted from Yau and Rismanchi (2012)

and fall into the storage. Therefore, this system is classified as a dynamic ITS. Figure 2 shows an ice harvester system.

Encapsulated Ice Storage System

An encapsulated ice storage system comprises large steel or concrete tank filled with series of plastic capsules of water (spheres or rectangular) immersed in a secondary coolant such as ethylene glycol. The capsules are made of a high-density polyethylene that is able to withstand the pressure due to the water expansion. The size and shape of the capsules vary based on the storage capacity. The rectangular capsules are found from 0.017 to 0.0042 m^3, and spheres are from 75 to 100 mm (Dorgan and Elleson 1994). During the charging period, a low-temperature solution (−6 to −3 °C) passes through the tank and from ice inside the capsules.

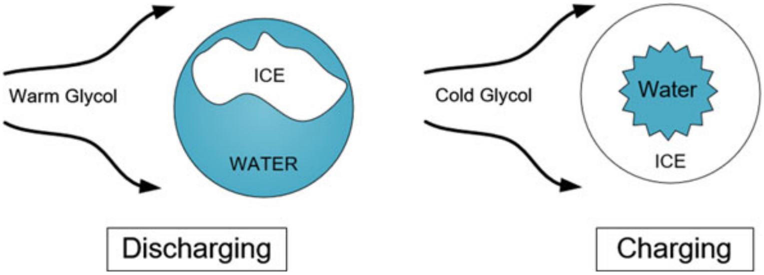

Fig. 3 Charging and discharging cycle of encapsulated ITS system. Adapted from Yau and Rismanchi (2012)

Figure 3 demonstrates the charging and discharging cycles (Erek and Dincer 2009; Fang et al. 2010).

Ice-on-Coil Storage System

The ice-on-coil ITS has two variants: external melt and internal melt ice-on-coil. The external melt is also known as ‘ice builder’ as the ice is shaped on the outer surface of the coils submerged in the storage tank full of water (Lee and Jones 1996a, b), whereas on internal melt ice-on-coil ITS, the heat transfer fluid passes through winding coils submerged in tanks filled with water. On the external melt system, the ice thickness varies from 40 to 65 mm based on the system configuration. High charging temperature (−7 to −3 °C) forms a thinner layer compared to the lower charging temperatures (−12 to −9 °C).

3 Operation Storage Strategies

The stored energy in the TES system can be kept for short-term for daily usage or can be kept for long-term for seasonal usage. The short-term operation strategies are generally categorised into two methods: full storage or partial storage. The most cost-effective mode of operation is defined based on the system configuration, source availability energy price structure and capital costs of equipment.

3.1 Short-Term Operation Strategy

The short-term storage strategy is categorised into full storage and partial storage strategies. In the full storage operating strategy, the required cooling load is fully stored during the off-peak hours (normally during the nighttimes). While in the partial storage strategy, only part of the required cooling is stored during the off-peak hours. This means in the full storage strategy the chiller does not require to work during the peak hours, while on the partial storage strategy the base cooling load will be provided from the storage system and the fluctuations should be supplied by the chiller during the peak hours. The chiller size in the partial storage strategy is normally smaller than the required chiller for the full storage strategy. This gives designers the flexibility to choose the proper system.

The partial storage strategy is further categorised based on the energy demand in two categories: load levelling (chiller works at full load continuously) and demand limiting operations (the chiller’s work is controlled to minimise the energy cost). Figure 4 shows the difference in the previously mentioned strategies.

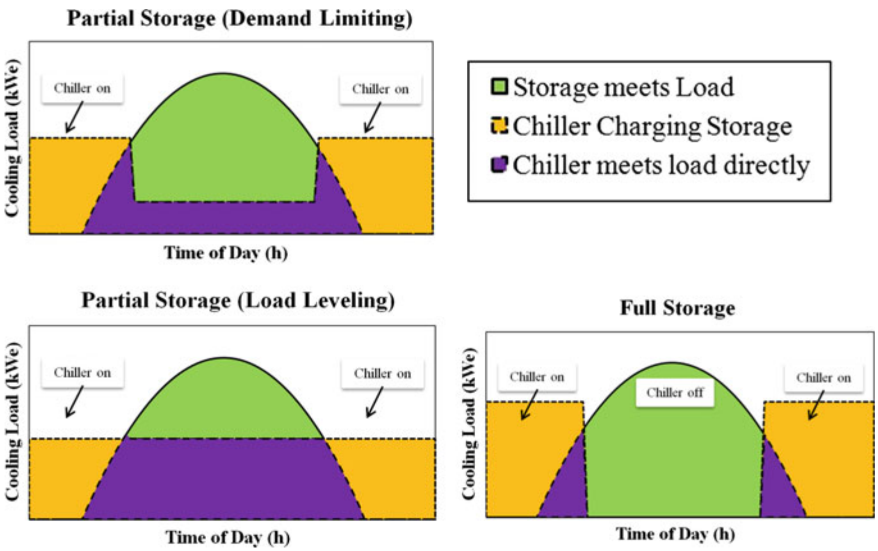

Fig. 4 Comparison of different operating strategies of CTES system. Adapted from Dorgan and Elleson (1994), Yau and Rismanchi (2012)

3.2 Seasonal Thermal Energy Storage (STES) System

Seasonal thermal energy storage (STES) systems store the heat (/cooling) in large quantities in one season to be used in another season. In some cases, STES systems are coupled with heat pumps and solar collectors to enhance the overall effectiveness of the systems. The performance of a STES system depends on their storage capacity, long-term stability and life cycle costs. The main parameters affecting the performance are stored temperature, heat losses, the interval of storage, type of storage medium, etc. (Rad and Fung 2016). The ground as a storage medium is most promising technology due to its large scale and comparatively low cost (Nordell 2000). There are commonly two types of storage medium such as solid, e.g. soil or rock, and liquid, e.g. water (Dincer et al. 1997).

There are four types of long-term thermal storage medium for space heating: hot water tank storage (HWTS), water gravel thermal pit storage (WGPS), aquifer thermal energy storage (ATES) and borehole thermal energy storage (BTES). In HWTS system, reinforced concrete or steel is usually used to construct the storage tank and water is used as a storage medium. This system has a low heat loss but the cost is relatively high due to ground construction and insulation works (Garg et al. 1985).

The water and gravel are used as media storage in WGPS system. This system has insulation on sides and on the top, which makes it the second most expensive approach after HWTS. The operating temperature is kept below 95 °C based on construction materials (Nielsen 2003). On the other hand, the ATES system is recognised as a porous media saturated with water, sand, gravel or sandstone, etc. (Sanner 1999).

ATES system has separate warm and cold well(s). For injecting or extracting heat from the storage media, two or more wells are drilled into the aquifer. This system is usually used for district cooling or heating applications (Andersson et al. 2003) and it is not suitable for small-scale application such as a single-family house (Hasnain 1998a) due to which requiring large site especially storage volume is more than 100,000 m^3 (Schmidt et al. 2003).

On the BTES system, ground itself is used as a medium of heat or coolth storage. In a seasonal BTES case, vertical or horizontal channels are carved into the field for injecting or extracting the heat. The channel's depth depends on the borehole heat load, ground temperature, thermal conductivity of the ground and groundwater level (Terziotti et al. 2012). The advantage of this system is the availability of ground as the storage medium and the requirement of less space for storage heat, and storage capacity (space) can be easily extended.

Table 2 summarised the distinct parameters for these four STES technologies. As can be seen from the table, the most dominant factors when designing an STES are cost and system capacity. In many cases, a large-scale system for a community is more economically feasible compared to small-scale individual systems (Fisch et al. 1998, Lhendup 2013).

Borehole Heat Exchangers

In BTES system, the ground is used as a storage medium to store the excess heat of summer to be used in winter for space heating. In this system, vertical or horizontal boreholes are used as channels to exchange heat between the building and the storage medium. In general, the vertical boreholes perform better than horizontal as they require less space and less excavation. Normally, length of vertical boreholes varies from 30 to 100 m with 3–4 m gaps (Schmidt et al. 2003). In the BTES, single U-tube, double U-tube or concentric pipes are used in ducts for exchange the heat as shown in Fig. 5. The U-tube material is usually made of synthetic material such as high-density polyethylene. A mixture of water and ethanol (or glycol) is generally used as the heat transfer medium. The grout is used for filling the borehole, which normally is of bentonite, quartz with sand or water mixture. The thermal conductivity of borehole depends on the local condition. A number of research have been conducted on heat transfer properties of grout based on fundamental theories (Bennet et al. 1987), measurements in the laboratories (Paul 1996) and field works (Austin 1998). Some of the common thermal conductivities are bentonite (0.8–1.0 W m^{-1}K^{-1}), stagnate water (0.6 W m^{-1}K^{-1}), thermal enhance grout with quartz (1.0–1.5 W m^{-1}K^{-1}) and water saturated quartz sand (1.5–2.0 W m^{-1}K^{-1}) (Rad and Fung 2016).

In BTES, heat extracted from the ground is generally higher than the natural heat injected to ground (Lazzarin 1986). Therefore, the ground needs to be charged artificially via solar collectors to maintain the balance between supply and demand with consideration of thermal losses (Fahlén and Karlsson 2003). The charged and

Table 2 Summary of different types of seasonal thermal energy storage system (Rad and Fung 2016; Hesaraki et al. 2015; Schmidt et al. 2003)

Category	HWTS	WGPS	BTES	ATES
Storage medium	Water	Gravel water	Ground material	Water–sand/gravel
Heat storage capacity (kWh/m^3)	60–80	30–50	15–30	30–40
Storage volume for (1 m^3 water equivalent)	1	1.3–2	3–5	2–3
Geological requirement	– Stable ground conditions – Preferably no groundwater – 5–15 m deep	– Stable ground conditions – Preferably no groundwater – 5–15 m deep	– Drillable ground – Preferably groundwater – 30–100 m deep – High heat capacity – High thermal conductivity	– Natural aquifer layer with high hydraulic conductivity – Low or no natural groundwater flow – Aquifer thickness 20–50 m
Advantages	– Instal any location – High heat capacity – Easy to instal	– More cost-effective than the HWTS – Leaving natural aquifer untouched	– Can be used for both heating and cooling – Suitable for small and large application	– Cost-effective – Low maintenance
Limitations	– High cost – High thermal loss – Corrosion	– High cost – Small stratification – Leakage	– Not feasible for all locations with groundwater flow – High initial cost	– Require specific climate condition – High thermal loss – Clogging effects

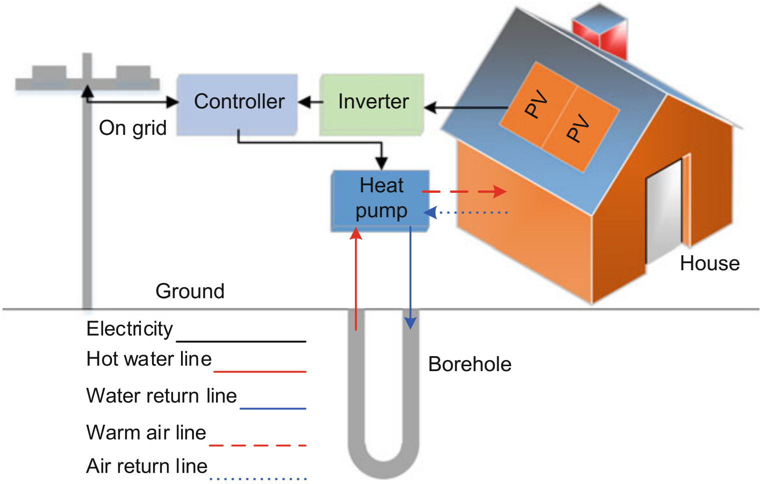

Fig. 5 An example of BTES coupled with heat pump powered by grid-connected PV array

discharged storage temperatures of BTES vary from 2 to 20 °C and −3 to 6 °C, respectively. To upgrade the heating capacity of the system, the BTES is normally coupled with a heat pump to upgrade the supply to higher temperatures. By this method, the borehole depth can be reduced from around 7 to 4.5 m (Chiasson and Yavuzturk 2003). Due to heat dissipation under the ground, the first 3–5 years of the BTES is considered as the operational start-up time after which the heat loss will be reduced and the system performance will be improved (Pavlov and Olesen 2012).

4 Summary/Conclusions

Short-term thermal storage technologies for space cooling and long-term thermal storage technologies for space heating have been presented. These technologies enable excess coolth or heat to be stored and use later. Balancing of electricity demands between day and night (daily storage) or winter and summer (seasonal storage) could be achieved by applying them. Reducing the peak energy demands is also one of the benefits of thermal storage technologies. Full coolth storage operation which eliminates the daytime electricity requirements for the chillers, partial storage operating strategies for limiting the demand and for levelling the load have been presented and discussed. Different types of STES system have been summarized and description of BTES technology for space heating also has been provided.

References

Andersson O, Hellström G, Nordell B (2003) Heating and cooling with UTES in Sweden-current situation and potential market development. In: Proceedings of the 9th international conference on thermal energy storage, Warsaw, Poland, 1–4 Sept 2003

ASHRAE (2007) Thermal storage. In: ASHRAE handbook: HVAC applications. American Society of Heating, Refrigerating and Air Conditioning Engineers (ASHRAE), Inc., Atlanta, GA

Austin WA III (1998) Development of an in situ system for measuring ground thermal properties. Oklahoma State University, Stillwater, Oklahoma

Beggs CB, Ward IC (1992) Ice storage: design study of the factors effecting installations. Build Serv Eng Res Technol 13:49–59

Bennet J, Claesson J, Hellström G (1987) Multipole method to compute the conductive heat flows to and between pipes in a composite cylinder. Husbyggnadsteknik, Tekniska högsk, Lund University of Technology

Cabeza LF, Roca J, Nogués M, Zalba B, Marín JM (2002) Transportation and conservation of temperature sensitive materials with phase change materials: state of the art. In: IEA, ECES IA Annex 17, Advanced thermal energy storage techniques—feasibility studies and demonstration projects, 2nd Workshop, Ljubljana, Slovenia

Chiasson AD, Yavuzturk C (2003) Assessment of the viability of hybrid geothermal heat pump systems with solar thermal collectors. ASHRAE Trans 109(2):487–500

Department of Climate Change (2009) Australian national greenhouse accounts: national inventory by economic sector 2007. Department of Climate Change, Commonwealth Government of Australia, Canberra

Department of Environment (2012) Submission under the Kyoto protocol: quantified emission limitation or reduction objective. Department of Environment, Commonwealth Government of Australia, Canberra

Dincer I, Dost S, Li X (1997) Performance analyses of sensible heat storage systems for thermal applications. Int J Energy Res 21(12):1157–1171

Dorgan CE, Elleson JS (1994) Design guide for cool thermal storage. American Society of Heating, Refrigerating and Air-Conditioning Engineers, Atlanta, GA

Erek A, Dincer I (2009) Numerical heat transfer analysis of encapsulated ice thermal energy storage system with variable heat transfer coefficient in downstream. Int J Heat Mass Transf 52(3–4):851–859. https://doi.org/10.1016/j.ijheatmasstransfer.2008.06.024

Fahlén P, Karlsson F (2003) Improving efficiency of hydronic heat pump heating systems. In: The 21st international congress of refrigeration, Washington, USA, January, 2003

Fang GY, Wu SM, Liu X (2010) Experimental study on cool storage air-conditioning system with spherical capsules packed bed. Energy Build 42(7):1056–1062. https://doi.org/10.1016/j.enbuild.2010.01.018

Fisch MN, Guigas M, Dalenback JO (1998) A review of large-scale solar heating systems in Europe. Sol Energy 63(6):355–366. https://doi.org/10.1016/S0038-092x(98)00103-0

Garg H, Mullick S, Bhargava A (1985) Chemical energy storage. In: Solar thermal energy storage. Springer, Berlin, pp 292–427

Hasnain SM (1998a) Review on sustainable thermal energy storage technologies. Part I: Heat storage materials and techniques. Energy Convers Manag 39(11):1127–1138. https://doi.org/10.1016/S0196-8904(98)00025-9

Hasnain SM (1998b) Review on sustainable thermal energy storage technologies. Part II: Cool thermal storage. Energy Convers Manag 39(11):1139–1153. https://doi.org/10.1016/S0196-8904(98)00024-7

Hesaraki A, Holmberg S, Haghighat F (2015) Seasonal thermal energy storage with heat pumps and low temperatures in building projects—a comparative review. Renew Sustain Energy Rev 43:1199–1213. https://doi.org/10.1016/j.rser.2014.12.002

Ho CD, Tu JW (2008) Evaluation of a recirculation scheme for ice storage melting with air as the working fluid. Heat Transfer Eng 29(3):295–305. https://doi.org/10.1080/01457630701758088

Incropera FP, DeWitt DP (2002) Introduction to heat transfer, 4th edn. Wiley, New York

Kowata H, Sase S, Ishii M, Moriyama H (2002) Cold water thermal storage with phase change materials using nocturnal radiative cooling for vegetable cooling. In: World renewable energy congress WII, Cologne, Germany

Lazzarin R (1986) Solar assisted absorption or motor driven heat pump with earth seasonal storage, Part 1. Accessed 27.11.16

Lee AHW, Jones JW (1996a) Laboratory performance of an ice-on-coil, thermal-energy storage system for residential and light commercial applications. Energy 21(2):115–130. https://doi.org/10.1016/0360-5442(95)00095-X

Lee AHW, Jones JW (1996b) Modeling of an ice-on-coil thermal energy storage system. Energy Convers Manag 37(10):1493–1507. https://doi.org/10.1016/0196-8904(95)00224-3

Lhendup T (2013) Development of an inter-seasonal thermal storage system, PhD thesis, Infrastructure Engineering, The University of Melbourne, Australia

MacCracken M (2010) Energy storage providing for a low-carbon future. ASHRAE J 52(9):28

Mackie EI, Reeves G (1988) Stratified chilled water storage tank design guide. Electric Power Research Institute, Paolo Alto, CA

Morgan S, Krarti M (2007) Impact of electricity rate structures on energy cost savings of pre-cooling controls for office buildings. Build Environ 42(8):2810–2818. https://doi.org/10.1016/j.buildenv.2005.11.010

Nielsen K (2003) Thermal energy storage: a state-of-the-art. https://www.sintef.no/globalassets/upload/smartbygg/wp3/thermal-energy-storage.pdf. Accessed 27.11.16

Nordell B (2000) Large-scale thermal energy storage. In: Proceedings WinterCities' 2000, Energy and Environment, 14 February, Lulea, Sweden, 1–10

Paul ND (1996) The effect of grout thermal conductivity on vertical geothermal heat exchanger design and performance. Master thesis, South Dakota State University, Brookings, SD

Pavlov GK, Olesen BW (2012) Thermal energy storage—a review of concepts and systems for heating and cooling applications in buildings: Part 1—Seasonal storage in the ground. HVAC&R Res 18(3):515–538

Potter RA, Weitzel DP, King DJ, Boettner DD (1995) ASHRAE RP-766: study of operational experience with thermal storage systems. ASHRAE Trans 101:549–557

Rad FM, Fung AS (2016) Solar community heating and cooling system with borehole thermal energy storage—review of systems. Renew Sustain Energy Rev 60:1550–1561. https://doi.org/10.1016/j.rser.2016.03.025

Saito A (2002) Recent advances in research on cold thermal energy storage. Int J Refrig 25(2):177–189. https://doi.org/10.1016/S0140-7007(01)00078-0

Sanner B (1999) High temperature underground thermal energy storage: state-of-the-art and prospects. Lenz. http://www.iea-eces.org/files/a12summary.pdf. Accessed 27.11.16

Schmidt T, Mangold D, Müller-Steinhagen H (2003) Seasonal thermal energy storage in Germany. In: ISES solar world congress, 19.06.2003

Terziotti L, Sweet M, McLeskey J (2012) Modeling seasonal solar thermal energy storage in a large urban residential building using TRNSYS 16. Energ Build 45:28–31

Washington State University (2003) Thermal energy storage. Energy efficiency fact sheet. Washington State University Cooperative Extension Energy Program

Yau YH, Rismanchi B (2012) A review on cool thermal storage technologies and operating strategies. Renew Sustain Energy Rev 16(1):787–797. https://doi.org/10.1016/j.rser.2011.09.004

Zalba B, Marin JM, Cabeza LF, Mehling H (2003) Review on thermal energy storage with phase change: materials, heat transfer analysis and applications. Appl Therm Eng 23(3):251–283. https://doi.org/10.1016/S1359-4311(02)00192-8

Solar Passive Technique to Meet Energy Challenges in Building

Alok Kumar Maurya and Mahendra Joshi

Abstract Electricity consumption is increasing day by day; as per the world energy outlook 2011, this demand will increase by 53% from 2008 to 2035. As per the electric holding company, 52% of the energy is utilized alone in heating ventilation and air conditioning in domestic buildings. This increasing demand has to be cut short. Expanding utilization of energy has prompted natural contamination bringing about a worldwide temperature alteration and ozone layer depletion. Solar passive techniques employed will help to meet the energy demands of the building. These techniques in the building incorporate the natural process for heating or cooling to achieve balanced indoor condition. The solar passive technique can reduce the energy load in the building by 50–70%. Incorporation of these strategies would absolutely lessen our reliance on artificial means for thermal solace and limit the ecological issues because of excessive utilization of energy and other natural resources and subsequently will evolve build form, which will be more natural responsive, more sustainable, and more natural cordial of tomorrow.

Keywords Solar passive · Energy · H.V.A.C · Thermal comfort

1 Introduction

In developing countries, many of residences, offices, and commercial space are made without taking the sufficient consideration of the climate. Such spaces may have poor indoor climate which affects health, work efficiency, and comfort. As expectations for everyday comforts rise, people start to install the cooling or heating

---

A. K. Maurya (✉)
Ansal School of Architecture, Dr. A.P.J. Abdul Kalam Technical University Lucknow, Lucknow, India
e-mail: ar.alokmaurya@gmail.com

M. Joshi
School of Architecture, B.B.D University Lucknow, Lucknow, India
e-mail: iitmahe@gmail.com

A. Sharma et al. (eds.), *Low Carbon Energy Supply*, Green Energy and Technology,
https://doi.org/10.1007/978-981-10-7326-7_16

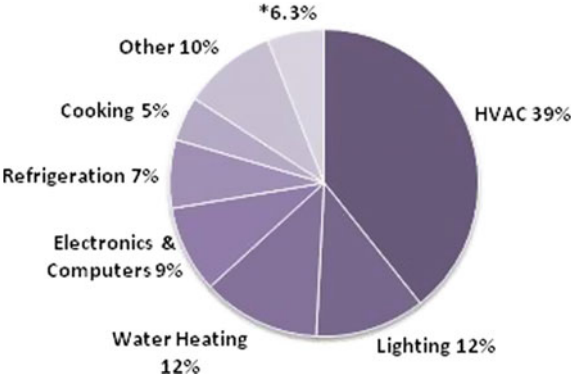

Fig. 1 Residential building total energy end use (2006) (DOE 2008)

equipment to enhance the indoor climate and to maintain desired indoor environment, this equipment consumes a large amount of power.

Globally, energy consumption develops by 53% in the vicinity of 2008 and 2035 in the reference case, with much of the increase driven by strong economic growth in the developing nations especially China and India. China and India represent half of the anticipated increment in world energy use throughout the following 25 years. In 2008, China and India jointly utilized almost of 21% energy globally available (The international energy outlook 2011). As per the electric holding company, 52% of the energy is consumed in the residential sector and in this amount of energy, most of the energy is used in HVAC and lighting.

Technical advancement in the mechanical cooling, heating, ventilation, and lighting has lead to improvement in the indoor environment and increase work efficiency. But these mechanical instruments run on the energy and most of the energy (electrical) is generated by the non-renewable sources. Figure 1 shows residential building total energy end use. Nonrenewable energy sources are depleting very fast which are making the architect and designer community to think about an ingenious method to reduce the energy dependency to make the healthier environment.

Fossil fuel emits greenhouse gas; this fossil fuel powers the mechanical equipment which is cools or heats up the space. It is foolish to run these equipments on fossil fuel after knowing that it harms us. This has caused architects, engineers, and planners to stimulate the interest toward the adoption of passive techniques for buildings to reduce the energy load in the building.

2 Passive Techniques

Passive technique in the building incorporates the natural process for heating or cooling to achieve balanced indoor condition. Conduction, convection, and radiations are the natural process of heat flow which is adopted in the building to maintain the desired indoor habitable conditions.

Table 1 Basic cooling strategies for hot and dry climate (Sharma 2003)

Minimize external load due to climate	Minimize internal heat load	Removal of heat	Provision of additional cooling
Reduction of penetration of the direct sun	Reduction of casual gains	Ventilation	Earth contact building
Reduction of conduction of heat through walls/roof			Evaporative cooling
Reduction of infiltration of outside hot air			Radiative cooling

Table 2 Basic heating strategies for cold climate (Sharma 2003)

Maximize heat gain from climate	Resist Heat loss	Provision of additional heating
Increase in penetration of the direct sun	Increase thermal resistance	Provision of a large window on South and west side (In northern hemisphere)
Trapping heat	Decrease air exchange rate	Sunspaces

In hot and dry conditions, reducing heat gain and removal of excess heat gain are desired to achieve the favorable indoor environment. In cold climate, to achieve habitable indoor condition, we have to maximize heat gain and resist heat loss.

The initial step to accomplish passive cooling in a building is to minimize the unwanted thermal loads. Usually, there are two types of thermal loads:

1. Exterior loads due to the climate.
2. Internal loads due to cooking, electrical or mechanical apparatus, and people Tables 1 and 2 shows basic cooling and heating strategies.

2.1 *Passive Cooling*

Passive cooling systems are minimum costly methods for cooling a building which augments the proficiency of the building envelope with no utilization of mechanical equipment. It depends on natural heat sinks to expel heat from the building. These techniques drive cooling straightforwardly from evaporation, convection, and radiation without utilizing any electrical gadgets in between. These techniques depend upon the daily climate changes in temperature and relative humidity.

Passive cooling can be done by the following means:

- 2.1.1 Natural ventilation,
- 2.1.2 Windows and shading,
    - 2.1.2.1 Overhangs, louvers, and awnings;
    - 2.1.2.2 Brise soleil; and
    - 2.1.2.3 Roof shading;
- 2.1.3 Wind towers,
- 2.1.4 Earth air tunnels,
- 2.1.5 Evaporative cooling,
- 2.1.6 Desiccant cooling, and
- 2.1.7 Courtyard effect.

2.1.1 Natural Ventilation

Outdoor breeze forces air inside the building through the opening by the push-and-pull effect of positive pressure at the windward side and negative pressure (suction) at leeward side. To gain maximum ventilation in the building, windows should be placed in opposite pressure zones. Figure 2 shows natural ventilation within the building.

Natural ventilation can reduce energy consumption within the building to fair limits. Figure 3 shows natural ventilation potential—HVAC savings.

2.1.2 Windows and Shading

Roughly, 40% of unwanted solar radiation comes through the window in a home. This solar radiation can be controlled by the solar film as it can reflect 80% of the incoming solar radiation (Cooling Your Home Naturally 1994).

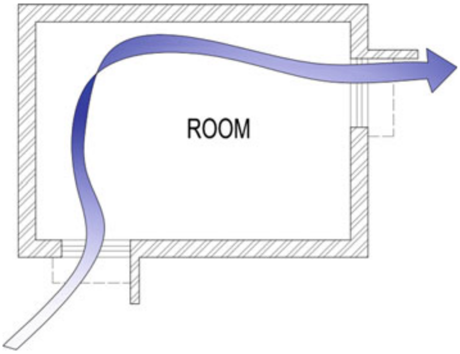

Fig. 2 Natural ventilation within the building [author]

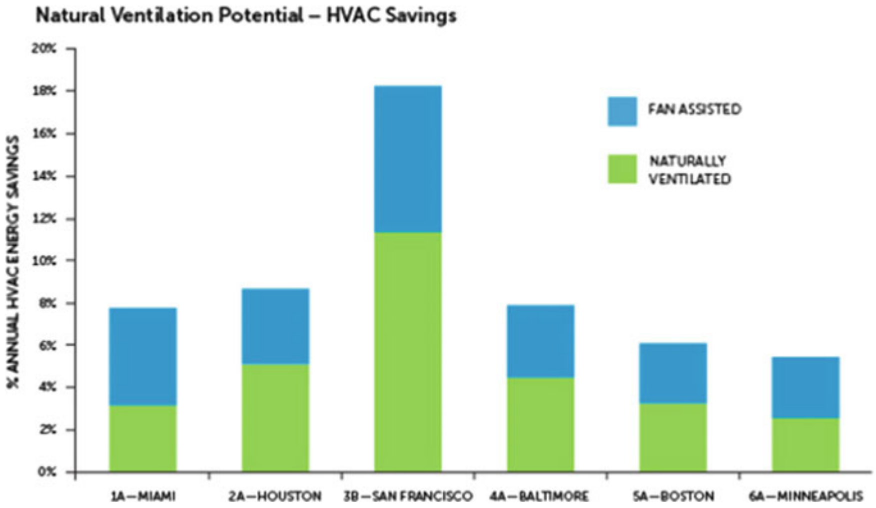

Fig. 3 Natural ventilation potential—HVAC savings (http://www.payette.com/research-project/naturally-ventilated-healthcare-1)

Shading devices reduce the solar radiation falling on the exposed surface of buildings, which reduces the heat gain and cooling load drastically. Shading the window can significantly enhance the indoor climate of the building.

A solar shading device can reduce the indoor temperature by 2.5–4.5 °C. Further, the temperature can be reduced by up to 4.5–6.8 °C by incorporating insulation and controlled air circulation rate (Kumar et al. 2005).

2.1.2.1 Overhangs, Louvers, and Awnings

Properly designed and placed shading device can significantly lessen building heat gain and cooling necessities and enhance the characteristic lighting nature of building inside. Shading devices are designed on the basis of the solar path, altitude, and its inclination toward a particular building facade. Figure 4 shows different solar shading devices.

2.1.2.2 Brise Soleil

Brise soleil is a sun breaker outside the windows, openings, or spread over the entire surface of a building's facade. Many conventional techniques exist for reducing the heat gain and sun glare, for example, lattices, pierced screens, as used at the Tāj Mahal, or blinds of split bamboo as used in Japan, shades utilized outside the windows that are comparable essentially to Venetian blinds.

Figure 5 shows concrete brise soleil.

2.1.2.3 Roof Shading

Shading the roof is a vital technique for decreasing heat gain. Heat gain through the terrace can be reduced by providing roof cover of vegetation, earthen pot, mud phuska, or canvas. Shading gave by outer means should not interfere with evening or night time cooling.

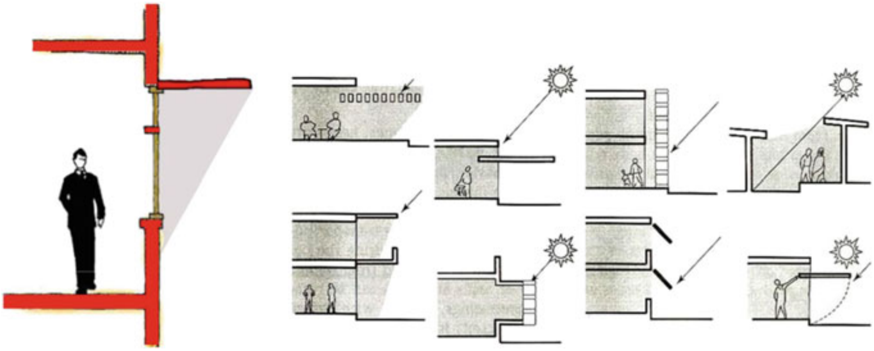

Fig. 4 Solar shading devices (Kamal 2010)

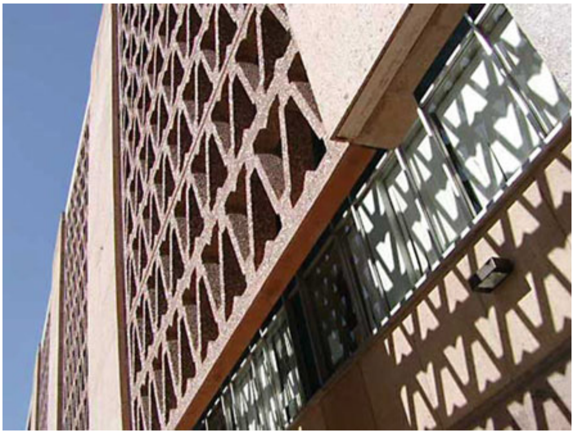

Fig. 5 Concrete brise soleil (https://www.britannica.com/technology/brise-soleil)

At many places, the mass of water is stored on the rooftop. During summer season, this water is covered by moveable reflective and insulating material. At daytime, this insulating material keeps away the solar radiation from water mass and water absorbs the heat from the room beneath and keeps the temperature cool within the room. During the night, this movable insulating material is moved from the water mass which allows the water mass to dissipate the heat. Figure 6 shows roof shading by roof pond.

Inverted earthen pots are laid closely on the entire surface of the roof which provides a large surface for the radiative emission. Inverted pots trap the heat within itself which acts as an insulating material, and this encumbers the heat gain in the room. This technique makes the roof unusable. In some cases, broken ceramic tiles or china mosaics are laid over the roof which increases the reflection of incident solar radiation. Figure 7 shows roof shading by inverted earthen pots.

Roof shading of deciduous plants and creepers is one of the better alternatives. Transpiration process from the plants and vegetation lowers the temperature of the

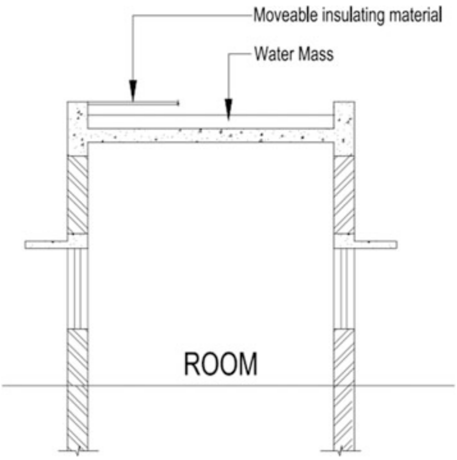

Fig. 6 Roof shading by roof pond [author]

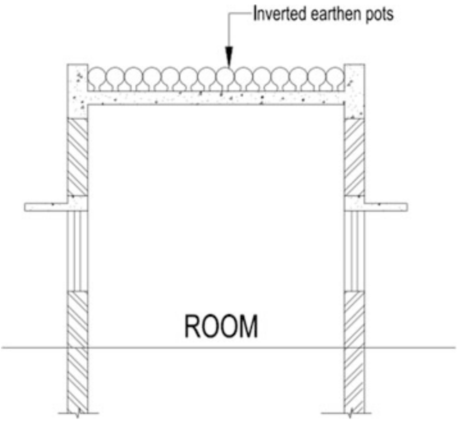

Fig. 7 Roof shading by inverted earthen pots [author]

rooftop to a level than that of the daytime air temperature. Figure 8 shows roof shading by vegetation.

Shading roof by white canvas is one of the less expensive and efficient ways to reduce the heat gain from the terrace. White canvas maximizes the reflectance and minimizes the heat gain from the roof. Figure 9 shows the roof shading by white canvas.

2.1.3 Wind Towers

In a wind tower, the hot surrounding air enters the tower through the openings at top of the tower, gets cooled, and in this way air gets heavier and sinks down. The opening of the rooms, i.e., inlet and outlet, forces air to get circulated. Draft of a

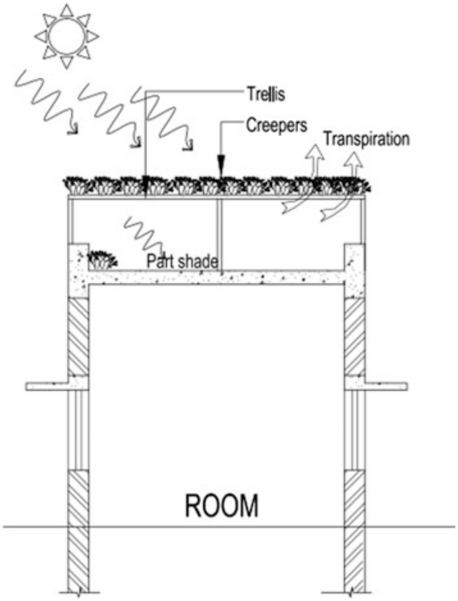

Fig. 8 Roof shading by vegetation [author]

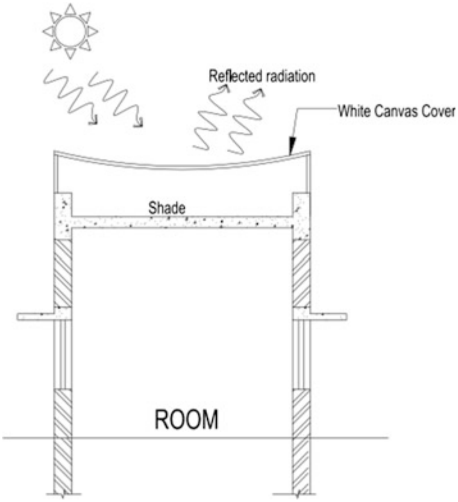

Fig. 9 Roof shading by white canvas [author]

cool air is created within the room when an inlet is provided with the outlet on the other side of the room. After a whole day of heat exchange, the wind tower becomes warm in the evening.

In the night, this phenomenon gets reversed, and the cooler ambient air comes in contact with the bottom of the tower through the rooms; it gets heated up by the warm surface of wind tower and begins to rise due to buoyancy, and thus an air flow is maintained in the reverse direction. Figure 10 shows the concept of wind tower.

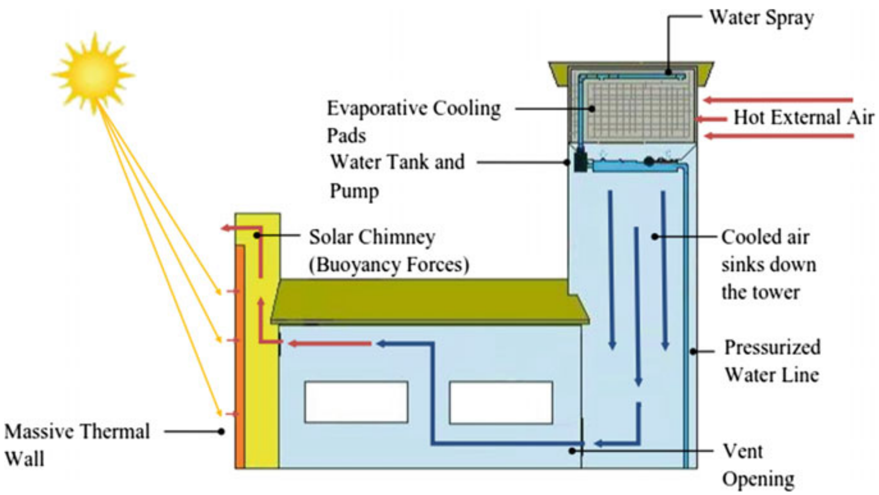

Fig. 10 Concept of wind tower (Hughes et al. 2017)

The modern wind towers decrease the electrical energy consumption of the buildings, especially during the peak times, between 20 and 80%. In evaporative cooling type wind towers (at inlet water spray is provided to cool down the air), the outlet air was 10 °C cooler than the inlet air in the summer days (Dehghani-sanij et al. 2015).

2.1.4 Earth Air Tunnels

In this method, air is allowed to pass through the underground pipe system which is buried 1–3 m down below the earth surface. This system is used for both cooling and heating. After 2–3 m depth, the temperature of earth remains constant, i.e., at this level, in summer, the temperature is cooler than the outer surface and in winter vice versa (Benhammou et al. 2015). Figure 11 shows one-dimensional model of the earth–air heat exchanger system.

Air coming out from the earth air tunnel has been noticed a significant drop of 5–6 °C in temperature during summers, using five air changes with 100-mm-diameter and 210-mm-length pipe (Tiwari et al. 2014).

2.1.5 Evaporative Cooling

It cools the space by evaporating water. It is effective in hot and dry climatic zones where relative humidity is low. Its concept of working is by using the sensible heat of air to evaporate the water, thereby cooling the air, resulting in cool indoor space.

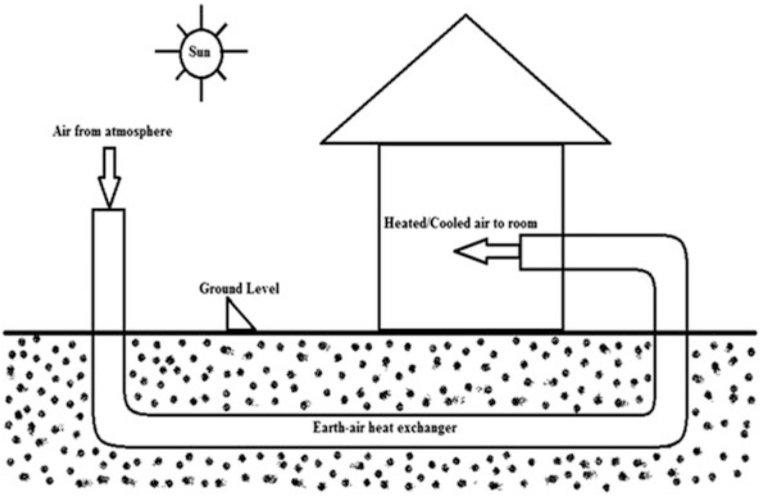

Fig. 11 One-dimensional model of the earth–air heat exchanger system (Bisoniya 2015)

As per the Amer, it is one of the most significant, efficient, and oldest ways to cool down the indoor space approximately by 9.6 °C (Amer 2006).

In Iran, Turkey, and the Middle East, this technique is combined with wind tower to channelize the cool air to pass over the water pad or water cistern to cool the air and to generate a refreshing effect in the indoor space. Evaporative cooling technique is extensively used in the form of the desert cooler. Desert cooler works on the same principle; it consists of a fan, water, evaporative pads, and pump.

Passive down drought system in which water cellulose pad or water cistern is provided at the top, which can maintain the indoor temperature by 29–30 °C with 6–9 number of air changes, whereas outdoor temperature is 43–44 °C (Kamal 2012).

Roof surface evaporative cooling is also one of the evaporative cooling techniques in which water is sprayed over the suitable water retaining material like water-resistant slab, gunny bags, etc.

2.1.6 Desiccant Cooling

In the desiccant cooling framework, desiccant salts or mechanical dehumidifiers are utilized to accomplish the coveted level of humidity in the surroundings. Silica gel, alumina gel, and activated alumina are some of the examples of dehumidifiers. The desiccants used may be regenerated by solar energy. Air is forced to flow over the unit area containing desiccants which assimilate the moisture and dries the air adiabatically. This method works efficiently in warm and humid climate.

The desiccant cooling system is composed of the four primary parts, desiccant wheel as a dehumidifier, heat recovery wheel, evaporative cooling as a humidifier, and solar evaporative tube collector as a heat source.

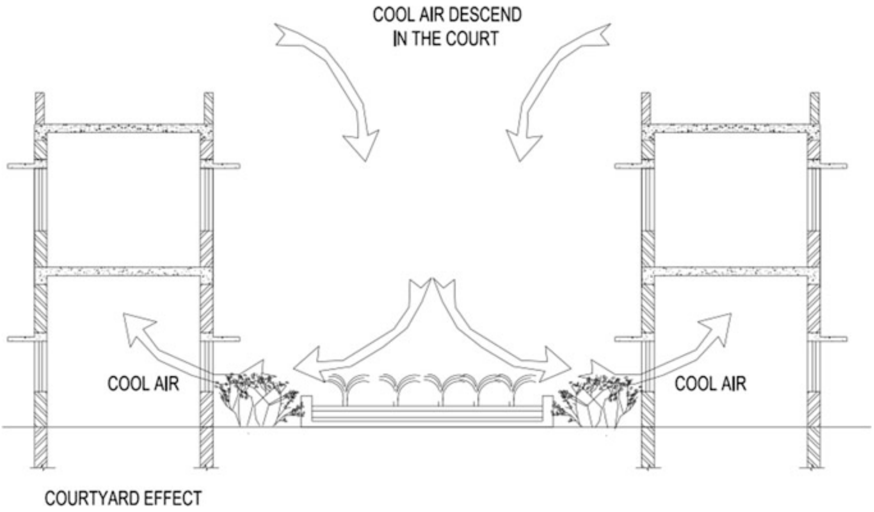

Fig. 12 Courtyard effect [author]

2.1.7 Courtyard Effect

Localized heating within structures might be lessened to a huge degree by using the thermal interaction due to the difference in temperature of the courtyard and the building core contingent on the proportion of courtyard, wind, speed, and direction. Figure 12 shows courtyard effect.

In some vernacular practice, courtyards are incorporated with water body and trees, which adds to humidity, evaporative cooling, and mutual shade.

2.2 Passive Heating

Solar passive heating is eco-friendly. In this technique, no electricity, no fossil fuel is consumed and no harmful emission is released to the environment. It is the cleanest way to heat an indoor space without consuming too much of electricity or fossil fuel.

The passive solar system may not replace mechanical ways of heating an indoor space but it can reduce dependency on them. It can reduce dependency on mechanical means 2–5% without any extra cost. The inclusive solar passive system can reduce dependency on mechanical way by 25–75% but it needs large initial investment.

In the passive solar technique, building materials are to collect, store, and distribute solar energy by conduction, convection, and radiation.

There are mainly three types of passive solar heating systems:

2.2.1 Direct gain,
2.2.2 Indirect gain, and
2.2.3 Isolated gain.

2.2.1 Direct Gain

For this situation, solar radiation is specifically transmitted through glazing into the room for thermal heating. Amid the day, the entire building structure gathers, assimilates, and stores the heat and discharges the heat during the evening for thermal heating as appeared in Fig. 13.

Double glazing ought to be utilized as a part of a request to reduce heat loss from indoor to outdoor air, and windows ought to be secured by insulation around evening time to take care of a similar issue. The air cavity reduces the warmth exchange by conduction since air is a poor conductor. This demonstrates a diminishment of 9% in heat gain up and a lessening of 28% in loss can be accomplished by utilizing double-glazed system when compared with the single-glazed system (Gupta and Tiwari 2016).

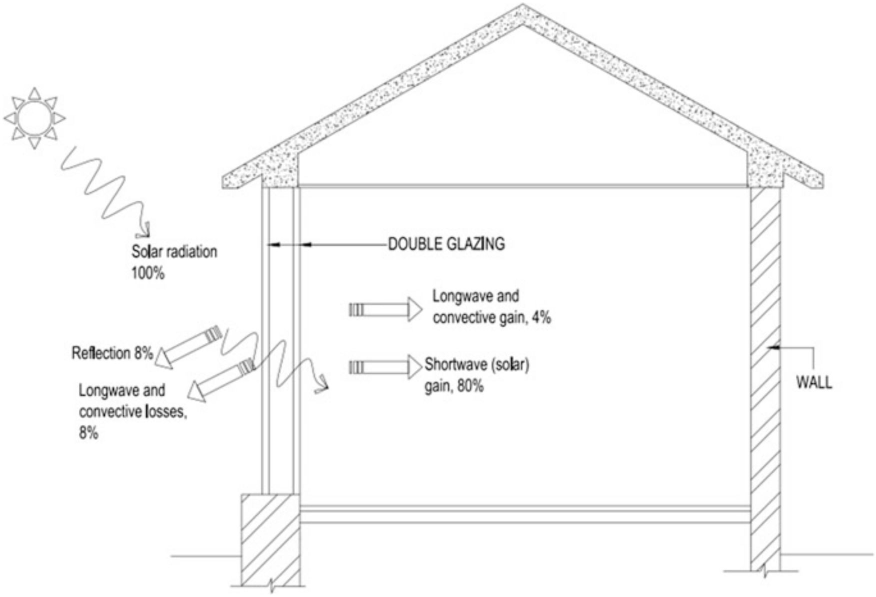

Fig. 13 Direct gain [author]

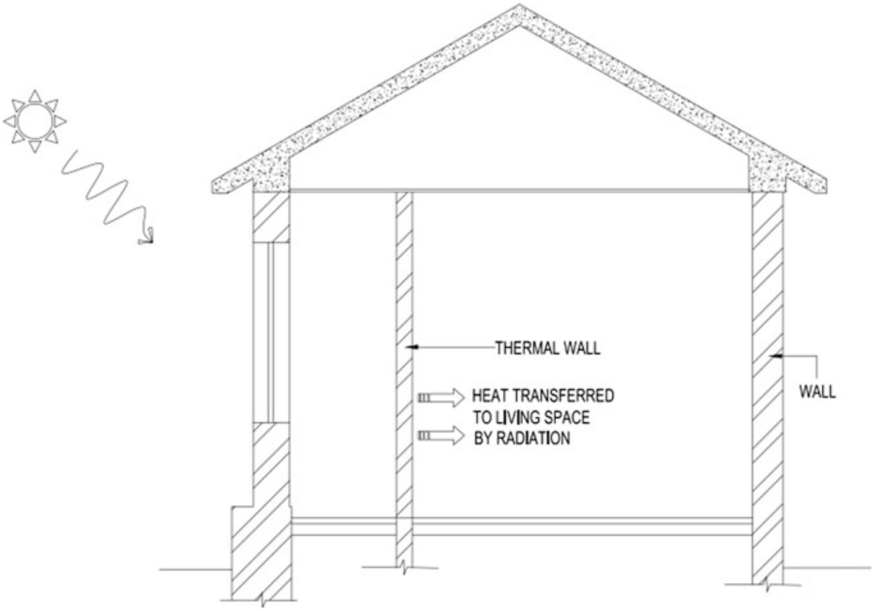

Fig. 14 Indirect gain [author]

2.2.2 Indirect Gain

In this method, solar radiation is allowed to enter the room through the glazing and is stored in thermal mass. Stored heat is transferred to the indoor space by conduction and convection. It includes Trombe wall and water wall. Figure 14 shows an indirect gain.

Heat flow within the space depends upon the thickness, surface area, surface treatment, and thermal properties of the thermal mass in which heat is stored. Dark-colored thermal mass is preferred to promote absorption of solar radiation and it maximizes the efficiency.

The passive heating technique reduces heating demands by 25% annually (Liu and Feng 2011).

2.2.3 Isolated Gain (Solarium or Sunspace)

A sunspace is a room intended to catch heat. Vertical windows catch the heat simply like the direct and indirect pickup system. The same brickwork or water drums are utilized as thermal mass. Distribution is accomplished through roof and floor vents, windows/entryways, and fans. The sunspace is isolated from the rest of the home using windows or doors. This ensures the home against the sun's fluctuating temperatures. Figure 15 shows sunspace.

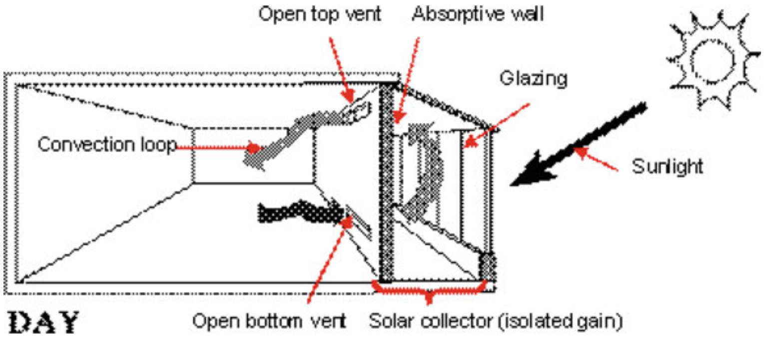

Fig. 15 Sunspace (https://uwaterloo.ca/systems-design-engineering/passive-solar-hybrid-convection-system)

2.3 Daylighting

Daylight is the light source that our eyes have acclimatized to utilize. It is present for most of the working day everywhere. Daylight is made out of a spectral power distribution (SPD) of electromagnetic radiation in the visible wavelength range (380–780 nm). Daylight has two parts, viz., daylight and skylight. Daylight is the immediate segment of light originating from the sun, which is variable in nature and makes glare and shadow. Then again, the skylight is a diffuse segment of light originating from the Skydome. Skylight is very relentless and does not make glare and shadow.

While designing the building, daylight must be taken into the account at the initial stage. The position of the window and orientation of the building is one the most important parts while designing for the daylight. Furthermore, the light coming to a specific point inside a building comprise direct daylight, diffuse light, externally reflected light from the ground, building surface and internally reflected light from ceilings, walls, and so forth.

The ratio of indoor illumination (Ei) to the corresponding outdoor illumination (Eo) in percentage is called as Daylight Factor (D.F.) Table 3 shows recommended daylight factors:

Table 3 Recommended daylight factors (Bhavesh et al. 2016)

Building	Area/activity	Daylight factor (%)
Dwellings	Kitchen	2.5
	Living room	0.625
	Study room	1.9
Schools	Classroom	1.9–3.8
	Laboratory	2.5–3.8
Offices	General	1.9
	Drawing	3.75
	Inquiry	0.625–1.9

$$\text{D.F.} = \text{Ei}/\text{Eo} \times 100$$

Amount of the daylight available, occupancy pattern, and control system can affect the energy saving within the building. Electric lighting consumes 35–50% of the electricity (http://www.wbdg.org/resources/daylighting). A good design in which daylighting is considered well can save electric by 75% used in the electrical lighting of that particular space (http://www.facilitiesnet.com/energyefficiency/article/Harnessing-Daylight-For-Energy-Savings-Facilities-Management-Energy-Efficiency-Feature–4267).

Another medium of daylighting is light shelves and solar tubes which add a quality of daylighting in the room.

Figures 16 and 17 show solar tube and light shelf, respectively.

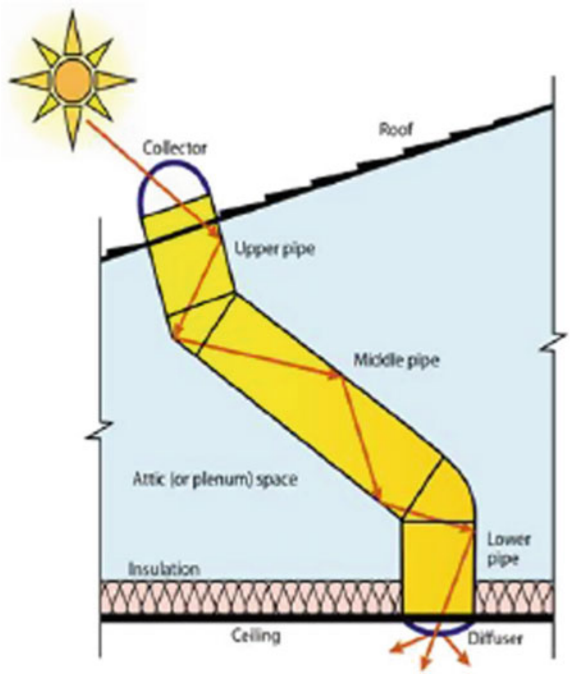

Fig. 16 Solar tube (https://www.nrc-cnrc.gc.ca/ci-ic/article/v16n1-10)

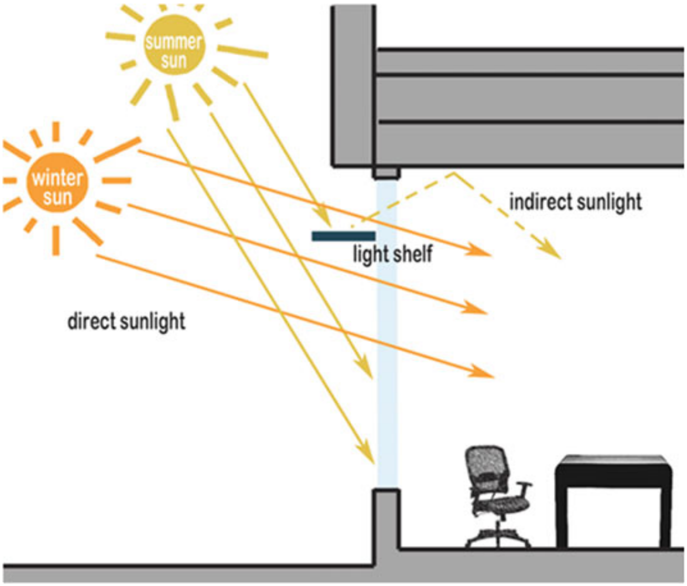

Fig. 17 Light shelf (https://www.nrc-cnrc.gc.ca/ci-ic/article/v16n1-10)

2.4 *Other Technique*

Other than above mentioned techniques, there is some of the method or solution which can be used in building to lower down the energy demand within the building.

2.4.1 External Cladding, Color, and Texture

Color, texture, and external cladding play important role in building these factors or elements can reduce the heat gain and vice versa. Smoothly finished and light-hued surface like a wall reflects more light and heat, while rough finished surface makes self-shading and increase the area of re-radiation. Dull shades of outer wall retain more radiation, which increases heat gain. Lighter shades of the surface have high emissivity, resulting in low heat gain, so these shades can be utilized in the warmer realm.

Tables 4 and 5 explain the effect of the color of the external wall in the different climatic zones of India.

Table 4 Effect of the color of external surface on room temperatures for hot, dry, warm, and humid climate (http://vincesarmy.blogspot.in/2014/11/daniels-review-light-shelves-unite-and.html)

Color (Absorptive, emissivity)	Ahmadabad (Hot and dry)					Mumbai (Warm and humid)				
	Yearly min (°C)	Yearly max (°C)	Yearly avg (°C)	H_{25}^{Y} (h)	H_{30}^{Y} (h)	Yearly min (°C)	Yearly max (°C)	Yearly avg (°C)	H_{25}^{Y} (h)	H_{30}^{Y} (h)
White Painted surface (0.3, 0.9)	20.6	42.2	29.7	7140	3908	24.5	34.6	29.6	8605	3350
White washed surface (0.4, 0.9)	20.8	42.5	30.0	7319	4123	24.8	34.9	29.8	8667	3654
Dark gray surface (0.9, 0.9)	21.9	44.0	31.1	7830	5599	26.0	36.1	30.9	8760	5535
Cream surface (0.4, 0.5)	21.2	43.0	30.4	7498	4739	25.3	35.30	30.2	8760	4320
Red surface (0.6, 0.9)	21.2	43.1	30.4	7498	4739	25.2	35.4	30.2	8760	4412

Table 5 Effect of color of external surface on room temperatures for composite and moderate climate (http://vincesarmy.blogspot.in/2014/11/daniels-review-light-shelves-unite-and.html)

Color (Absorptive, emissivity)	Nagpur (Composite)					Pune (Moderate)				
	Yearly min (°C)	Yearly max (°C)	Yearly avg (°C)	H_{25}^{Y} (h)	H_{30}^{Y} (h)	Yearly min (°C)	Yearly max (°C)	Yearly avg (°C)	H_{25}^{Y} (h)	H_{30}^{Y} (h)
White Painted surface (0.3, 0.9)	20.4	40.1	29.2	7067	2975	22.0	34.4	27.4	7078	1926
White washed surface (0.4,0.9)	20.7	40.3	29.5	7220	3139	22.3	34.7	27.7	7319	1957
Dark gray surface (0.9,0.9)	22.2	41.7	30.9	7923	4408	23.7	35.9	28.8	8171	2682
Cream surface (0.4, 0.5)	21.4	40.9	30.1	7494	3715	23.0	35.2	28.2	7894	2172
Red surface (0.6,0.9)	21.3	40.9	30.1	7494	3687	22.9	35.2	28.1	7864	2140

H_{25}^{Y}: Number of hours for which room temperature exceeds 25 °C in a year
H_{30}^{Y}: Number of hours for which room temperature exceeds 30 °C in a year
Min minimum, *max* maximum, *avg* average

2.4.2 Insulation

Walls, floors, roof, etc. are the building components by which heat gain or heat loss occurs. By installing proper insulation internally or externally, heat gain or loss can be regulated. Properly insulated building helps in maintaining the room temperature, i.e., during winter, it prevents heat loss and during summer it reduces heat gain. The insulated material is a bad conductor of heat; it creates baffle between exterior and interior surface, i.e., cool exterior warm interior during winter and warm exterior and cool interior during summer.

As insulation is important in both climates, viz., warm and cold climate, less energy is required for maintaining the comfortable temperature in the building throughout the year. Resisting heat flow is the working principle of the insulating material which is measured by *R*-value (the higher the *R*-value, the greater the insulation). As per the type of material, density and thickness, *R*-value changes. *R*-value is affected by thermal bridging. Thermal bridging is unwanted heat flow from the exterior to the interior through joints, studs, and rafters. To gain the best insulation, thermal bridging must be avoided.

Cellulose, cotton, fiberglass, mineral wool, perlite, rockwool, sheep wool, PUF (Polyurethane foam), thermocool, etc. are some of the materials which can be used for insulation purpose. Figure 18 shows cellulose insulation. Table 6 shows R-value of the different insulating materials.

Fig. 18 Cellulose insulation (https://energy.gov/energysaver/insulation-materials)

Table 6 The *R*-value of the different insulating materials (https://energy.gov/energysaver/insulation-materials)

S. No.	Insulating materials	*R*-value
1.	Cellulose	R-3.5
2.	Fiberglass	R-11 to R-38
3.	Plastic fiber insulation	R-3.8 to R-4.3
4.	Cotton	R-3.4
5.	Sheep's wool	R-3.5
6.	Polyurethane	R-5.5 to R-6.5
7.	Vermiculite and perlite insulation	R-2.4

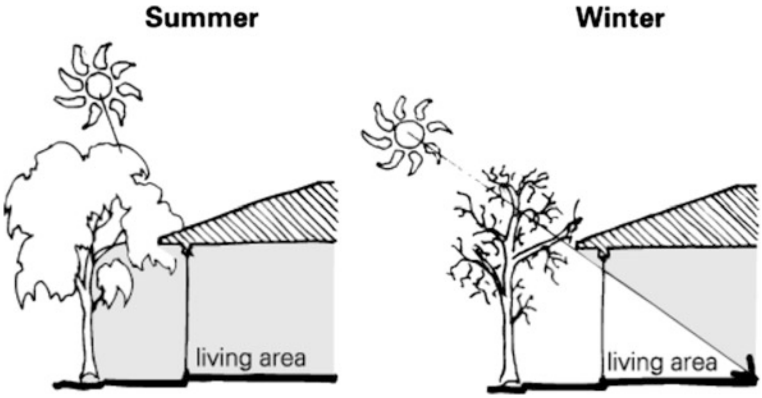

Fig. 19 Shading by deciduous trees in summer and winter (http://www.yourhome.gov.au/passive-design/shading)

2.4.3 Vegetation

Trees or landscape area can reduce the solar radiation falling on the surface by shading, and it adds to evaporative cooling by evapotranspiration process. Trees can control or channelize air movements which are responsible for advected heat. The deciduous plant can be planted on the eastern and western side (in the northern hemisphere) which will cut off the summer harsh solar radiation and will allow winter sun rays in the room. Figure 19 shows shading by deciduous trees in summer and winter (http://www.yourhome.gov.au/passive-design/shading).

Landscape area or urban park reduces or eliminates the urban heat island effect. Reducing the urban heat island reduces the cooling load in the building.

The tree can dissipate 65% of the heat generated, by evapotranspiration process, and 17% reduction in building cooling active evaporation by trees. 50% wind speed reduction by shade trees yielded 7% reduction in heating energy in winter (Coder 2011).

3 Conclusion

With an increment of energy, utilization of air conditioning recommends a more significant examination of the urban condition and the effect on structures and additionally to an amplified use of passive cooling procedures. Proper research ought to go for better understanding microclimate around structures and to comprehend and depict comfort necessities under transient conditions. Theoretical studies have demonstrated that the utilization of all the above strategies in structures may diminish their cooling load up to 50–70%.

In today's engineering, it is presently fundamental for architects and building specialists to consolidate aloof passive solar methods in structures as an intrinsic piece of the plan and compositional expression and they ought to be incorporated reasonably from the start. Incorporation of these strategies would absolutely lessen our reliance on artificial means for thermal solace and limit the ecological issues because of excessive utilization of energy and other natural resources and subsequently will evolve build form, which will be more natural responsive, more sustainable, and more natural cordial of tomorrow.

References

Amer EH (2006) Passive options for solar cooling of buildings in arid areas. Energy 31:1322–1344

Atwa M (2016) Architectural design with environmental solutions as a scope for sustainability: achieving energy efficiency in buildings passively

Benhammou M, Draoui B, Zerrouki M, Marif Y (2015) Performance analysis of an earth-to-air heat exchanger assisted by a wind tower for passive cooling of buildings in arid and hot climate. Energy Convers Manage 91:1–11

Bhavesh P, Dnyaneshwar P, Mukul P, Pratik P, Abhishek D (2016) Study of solar passive techniques suitable for building in Mumbai Region

Bisoniya TS (2015) Design of earth–air heat exchanger system. Geoth Energy 3:18

Coder KD (2011) Identified benefits of community trees and forests

Cooling Your Home Naturally (1994) DOE/CH10093-221 FS 186, October 1994, p 2

Dehghani-sanij AR, Soltani M, Raahemifar K (2015) A new design of wind tower for passive ventilation in buildings to reduce energy consumption in windy regions

DOE (2008) 2008 Buildings energy data book, Section 2.1.5

Gupta N, Tiwari GN (2016) Review of passive heating/cooling systems of buildings, p 307

http://www.yourhome.gov.au/passive-design/shading. Accessed on 20 Feb 2018

http://vincesarmy.blogspot.in/2014/11/daniels-review-light-shelves-unite-and.html. Accessed on 22 Feb 2018

http://www.payette.com/research-project/naturally-ventilated-healthcare-1. Accessed 10 Feb 2018

http://www.payette.com/research-project/naturally-ventilated-healthcare-1. Accessed 10 Feb 2018

http://www.wbdg.org/resources/daylighting

http://www.facilitiesnet.com/energyefficiency/article/Harnessing-Daylight-For-Energy-Savings-Facilities-Management-Energy-Efficiency-Feature–4267

https://energy.gov/energysaver/insulation-materials. Accessed on 20 Feb 2018

https://www.nrc-cnrc.gc.ca/ci-ic/article/v16n1-10. Accessed on 22 Feb 2018

https://www.britannica.com/technology/brise-soleil

https://uwaterloo.ca/systems-design-engineering/passive-solar-hybrid-convection-system

Hughes BR, Calautit JKS, Shazhad SS (2017) Adapting buildings to meet the energy challenge. http://www.energy.leeds.ac.uk/uploads/documents/104_Hughes%20-%20paper.pdf. Accessed 16 Feb 2018

https://www.mipandl.org/ees/EES_PassiveSolarHeat.pdf Accessed on 14th May 2018

Kamal MA (2010) A study on shading of buildings as a preventive measure for passive cooling and energy conservation in buildings. Int J Civ Environ Eng 20 http://ijens.org/102406-5252%20IJCEE-IJENS.pdf. Accessed 10 Feb 2018

Kamal MA (2012) An overview of passive cooling techniques in buildings: design concepts and architectural interventions. Acta Tech Napocen Civ Eng Architect 55:84–97

Kumar R, Garg SN, Kaushik SC (2005) Performance evaluation of multi-passive solar applications of a non air-conditioned building. Int J Environ Technol Manage 5(1):60–75

Liu YW, Feng W (2011) Integrating passive cooling and solar techniques into the existing building in South China. Adv Mater Res 368–373:3717–3720

Sharma A (2003) Climatic responsive energy efficient passive techniques in buildings

The international energy outlook 2011

Tiwari GN, Singh V, Joshi P, Shyam D, Deo A, Prabhakant D et al (2014) Design of an earth air heat exchanger (EAHE) for climatic condition of Chennai, India. Open Environ Sci 8:24–34

Fuel Cell: Fundamental, Classification, Application, and Environmental Impact

Anand Singh, Prashant Baredar, Hitesh Khare and Anil Kumar

Abstract In this chapter, an outline of fuel cell technology is being discussed with its advantages, disadvantages, and classification. The application of fuel cell is being done in comprehensive areas such as stationary electrical energy generation, fuel cell energy for transportation, and portable electrical energy generation. Fuel cell environmental impact based on stationary power generation, transportation system is discussed.

Keywords Fuel cell · Environmental · Portable power · Transportation system Stationary power

1 Introduction

Fuel cell (FC) is a standing device in which electrochemical cell transforms chemical energy into electrical energy (Wilberforce et al. 2016). It produces electricity within the cell through chemical reactions between a hydrogen fuel and an oxidant, activated with electrolyte (Wang et al. 2017). The wandering of reactants in the cell, the response yields drift out, while the electrolyte remnants inside. Fuel cells operate until essential reactant and oxidant flows are sustained. For automotive applications cleaner source of energy has a wide range of operations, and the fuel

---

A. Singh
Electrical and Electronics Department, Lakshmi Narain College of Technology,
Bhopal 462021, Madhya Pradesh, India
e-mail: anand24883singh@gmail.com

P. Baredar (✉) · A. Kumar
Energy Centre, Maulana Azad National Institute of Technology, Bhopal 462003,
Madhya Pradesh, India
e-mail: prashant.baredar@gmail.com

H. Khare
Mechanical Engineering Department, Technocrats Institute of Technology,
Bhopal 462021, Madhya Pradesh, India

A. Sharma et al. (eds.), *Low Carbon Energy Supply*, Green Energy and Technology,
https://doi.org/10.1007/978-981-10-7326-7_17

cell has sophisticated energy storage capability (Fuel cell Today 2012). In advanced countries, R&D on fuel cell is being funded for more than half a century initially to combat the rise in oil prices and later to combat the global warming. Billions of dollars have been spent in most of these countries. It is difficult to get the exact figures from the earliest years. However, some data are available for the more recent years (WEFORUM 2017). For example, USA announced $41.9 million (2009, DOE) in Recovery Act funding to quicken fuel cell commercialization and arrangement with diligence subsidizing another ~$54 million (totaling ~$96 million) with the definite objective of instantaneous disposition of up to 1,000 fuel cell systems in backup electrical power, material supervision, and combined heat and power uses. The bulk of the currency has been spent on fuel cell deployment. As expected, the level of research funding in India has been abysmally low even though fuel cell research has been continuing in this country for more than 25 years Jürgen (Garche and Jörissen 2017). India's policy on fuel cells and financial support are driven largely by four agencies, viz., MNRE, DST, DAE, and CSIR. Under its NMITLI program, CSIR has provided a total budgetary support of about Rs. 20 Crore during 2004–2013 for the development of different fuel cell technologies. MNRE is a major supporter of hydrogen and fuel cell research in the country for some epochs (MNRE 2017). It has supported nearly Rs. 5.0 crores during Eleventh Five Year Plan (2007–2012) and Rs. 1.00 crores during Twelfth Five Year Plan(2012–2017) for developing these technologies. MNRE guidelines state that financial assistance for R&D projects counting the skill authentication and parade projects that include an organization with industry/civil society administrations should habitually be partial to 50% of the project charge. However, for any suggestion from educational institutions, government/non-profit exploration administrations, and NGOs, the ministry may provide up to 100% funding. Private educational institutions should adhere to positive situations for availing project grants from the ministry (MNRE 2017).

1.1 Fuel Cell Principle

Fuel cell works on the principle of energy but is not at all like a battery; an energy unit does not rundown or requires reviving. It delivers energy as power and warmth insofar as fuel is provided (Wikipedia 2017). It comprises of an anode and a cathode with electrolyte sandwiched between them (USDE 2014). Oxygen disregards one cathode and hydrogen over the other, producing electrical energy, a limited amount of thermal energy, and water. Figure 1 shows the basic principle of the fuel cell.

1. Separation into a proton and an electron, till a hydrogen particle (from the fuel source) is in contact with the negative anode catalyst layer.
2. The conservative proton passes through the electrolyte.

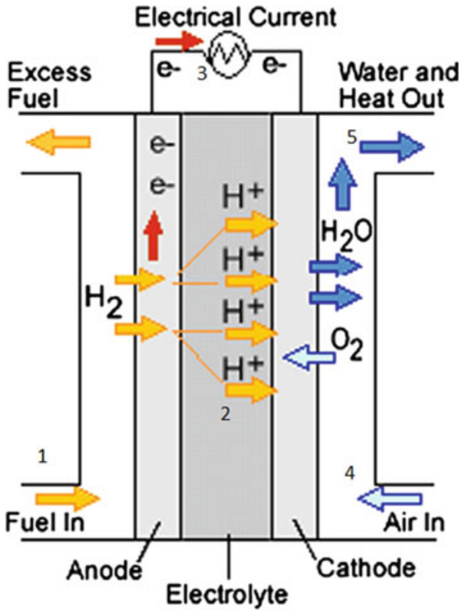

Fig. 1 Fuel cell principle (Wanga et al. 2011)

3. The FC current through the external circuit, electron passes.
4. The circuit allocations the electrons to the positive cross of the electrolyte coating tie and assembly an oxygen section.
5. Generating water and an inadequate extent of thermal energy in the positive cathode ingredient varnish.

1.2 Advantages of Fuel Cells

Fuel cells possess advantages over conventional power sources such as internal combustion engines or batteries (The next galaxy 2017 and Your article library 2017). Although fuel cells' characteristics are valid for some applications and rest are common.

1. No harmful gas emission—no emission except water at the tailpipe as no fossil fuels are used by the vehicle on fire.
2. Zero Pollution Lifelong—As hydrogen is derived from a renewable source and the automobiles can be made completely from renewable resources just as any other automobile can be.
3. No oil mandatory—in any of the components of a fuel cell vehicle as electric vehicle at its core.

4. Dispersed fuel making—is possible as it is relatively simple and much more economical than gasoline. It leads to less transportation, and more options for fuel sourcing are possible.
5. Higher efficiency—than either gasoline or diesel is conceivable with a hydrogen fuel cell in vehicles.
6. Silent process—means no noise pollution as an electric vehicle is without a burning producer.
7. Low heat options - for fuel cells are being traveled by the military for sensitive operations and stealth applications.
8. Longer range than the buck and weight than do current and anticipated battery technologies as pound-for-pound, cost-for-cost contrasts.
9. Almost zero maintenance, but occasional failure of a cell within a cell stack as fuel cells are built of modular units without moving portions.

1.3 Disadvantages of Fuel Cell

The fuel cell energy has estimable benefits, but not absolutely preferable, clean, and inexpensive energy source for most governments and companies, are volatile batteries in gaseous state (The next galaxy 2017; Your article library 2017). It is beneficial than other sources but has various risks and drawbacks also (CEF 2017). Some of the disadvantages of hydrogen energy include the following:

1. Affluent but these cells are being handmade and there are automakers (17 so far) who are excited to drip with mass manufactures as fuel cells are rather modest units that lend themselves to easy mechanization in production.
2. As hydrogen is created, complete reforming is not as unsurprisingly possible as other sources of fuel—specifically some biofuels and clean power.
3. When complete life succession of hydrogen as a fuel is painstaking electrolysis is inefficient and a net energy loss overall.
4. As associated to accusing battery EV batteries it takes moderately shorter time but longer to refuel and start compared to gas or diesel engines. Refilling a hydrogen fuel cell takes more time than impelling gasoline.
5. Hydrogen fuel cell although at highest efficiency, at an exact core temperature often “rise up” to get to heat before producing enough power flow to operate a vehicle.
6. On output ratio, FCs are higher than the batteries but density/mile ratio is minor.
7. The platinum catalyst makes this common fuel cell technology expensive, replacements are being searched.

2 Classification of Fuel Cells

The fuel cells are in developing phase (Fuel Cell Today 2012) and can be classified as

- Varied categories (types of fuel and oxidant)
- The type of electrolyte,
- The hotness of procedure,
- The reactants are nourished to the cell by interior or outside manifolds, etc. (USDE 2014; Tomczyk 2006).

The nethermost collective prearrangement of fuel cells founded on the type of electrolyte:

(1) Phosphoric acid fuel cell (PAFC)
(2) Solid oxide fuel cell (SOFC)
(3) Alkaline fuel cell (AFC)
(4) Proton-exchange membrane fuel cell (PEMFC or PEFC).
(5) Molten carbonate fuel cell (MCFC).

2.1 Phosphoric Acid (PAFC)

Figure 2a shows the PAFC that uses liquefied phosphoric acid as an electrolyte, the principal fuel cells to be commercialized have enhanced expressively in stability, performance, and cost (Chen et al. 2016). PAFCs produce energy more than 40% productivity and closely 85% of the vapor generated is used for cogeneration. Working system temperatures are in the range of 300–400 °F (150–200 °C). The liquid phosphoric acid soaked in a matrix is the electrolyte (Pareta et al.). PAFCs has a tolerance of about 1.5% a CO concentration that enhances the choice of fuel they can use (Chen et al. 2015). Sulfur should be removed in case of gasoline being used.

2.2 Proton Exchange Membrane Fuel Cell (PEMFC)

PEM fuel cells recognized as PEM and are shown in Fig. 2b. PEMFC is a type of FC being developed for stationary FC power generation, portable FC, and transport applications as well (Cheng and Liu 2015). Functioning at quite low temperatures (about 175 °F or 80 °C), at high power density, can differ their output to meet shifts in energy demand and are suited for applications in vehicles where quick startup is required (Eddine et al. 2014; Guerrero et al. 2015). Thin PEM is a plastic sheet that

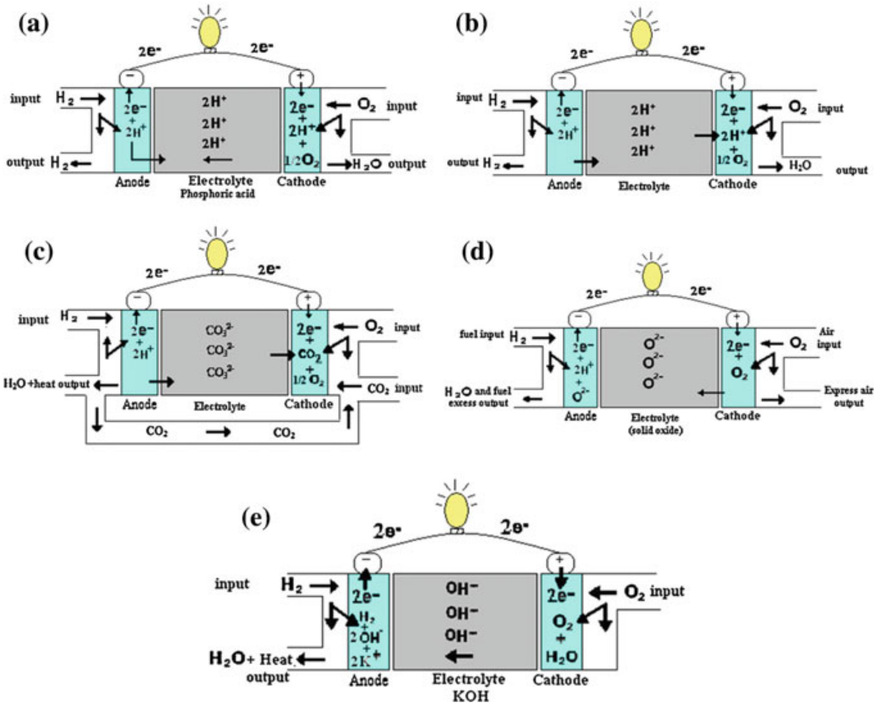

Fig. 2 Classification of fuel cell **a** PAFC **b** PEMFC **c** MCFC **d** SOFC **e** AFC (Mekhilefa et al. 2012)

allows hydrogen ions to pass through it. The solid organic polymer flour sulfonic acid is the electrolyte. The solid electrolyte has benefits because it reduces corrosion and management problems (Sutharssan et al. 2017).

2.3 *Molten Carbonate Fuel Cell (MCFC)*

The MCFC uses a watery solution of lithium saturated in a medium for an electrolyte and, sodium and/or potassium carbonates, Fig. 2c (Goo et al. 2016). The high efficiencies of fuel-to-electricity operating at 1200 °F or 650 °C with 85% cogeneration are around 60%. Because of this high temperature required for enough conductivity, moral metallic catalysts for the cell's electrochemical corrosion and decrease methods are not required (Discepoli and Desideri 2014). MCFCs have been worked on hydrogen, natural gas, propane, CO, landfill gas, nautical diesel, and replicated coal gasification yields (Devianto et al. 2016; Chiodo et al. 2016). 10–2 MW MCFCs have been tested for electric service applications. The high working temperatures are advantageous for flouting of carbon bonds due to higher efficiency an in larger hydrocarbon fuels as the higher adeptness and tractability to use more fuels and inexpensive catalysts are increased (Verda and Sciacovelli 2012).

2.4 Solid Oxide Fuel Cell (SOFC)

The FC with high energy procedures for industrial and large-scale essential energy generating plant SOFC are used as shown in Fig. 2d (Andrea et al. 2017). A solid oxide system utilizes hard ceramic material of solid zirconium oxide, at 1800 °F or 1000 °C, making efficacies up to 60 and 85% cogeneration and production up to 100 kW. SOFC utilization in motor vehicles are being established as fuel cell auxiliary power units (APUs) in Europe. Solid oxide fuel cells operate at 80–100 °C of all fuel cell systems (Cebollero et al. 2017; Cinti and Desideri 2015). These high temperatures abridge scheme formation. As the electrolyte is solid the cell can be molded in an assortment of arrangements by approving interior reforming easing the growth of cogeneration systems along with mixture energy systems as coating rounds for gas turbines and/or steam cycles (Chatrattanawet et al. 2017). As shown in Fig. 2, the electrolyte, yttria-stabilized zirconia is supported by the cathode constructed from lanthanum manganite surrounded by the anode, nickel cermet's. Fuel gas enters from the outer surface of the tube and air enters the cell from the inner surface (Dimitrova and Mar 2017). The prime focus is on reducing industrial cost, refining system integration, and dropping the working temperature to the range of 55–75 °C. The lower working temperature would unmoving deliver the compensations of internal reforming while reducing the physical problems related with the very high-temperature process. Systems based on SOFCs are being measured for a variety of purposes ranging from small applications such as housing energy systems and automobile supplementary energy units, where the basic gasoline dispensation requirements related with SOFCs are appealing to large utility-scale uses, which benefit from the high efficiencies obtained by assembly SOFC systems with vapor turbines and/or steam cycles (Emı et al. 2017). To form a fuel cell system tools labeled must be coupled with a variety of support subsystems, which yield useful energy from willingly obtainable fuels.

2.5 Alkaline Fuel Cell (AFC)

The AFC, also known as the bacon FC is one of the most established FC machineries as shown in Fig. 2e (Ariyanfar et al. 2011). AFCs chomp hydrogen and clean oxygen creating clean water, heat, and power. NASA has used AFC in Apollo-series missions, and on the space shuttle on space missions, these cells can realize energy generating productivities of up to 70%. Their working temperature is 150–200 °C (300–400 °F) using an aqueous solution of alkaline potassium

Table 1 Electrochemical reactions in fuel cells (Devianto et al. 2016; Chatrattanawet et al. 2017; Fuel cell Today 2012)

Fuel cell	Anode reaction	Cathode reaction	Overall reaction
PAFC	$H_2 \rightarrow 2H + 2e^-$	$1/2O_2 + 2H^+ + 2e^- \rightarrow H_2O$	$H_2 + 1/2\,O_2 \rightarrow H_2O$
PEMFC	$H_2 \rightarrow 2H + 2e^-$	$1/2O_2 + 2H^+ + 2e^- \rightarrow H_2O$	$H_2 + 1/2O_2 \rightarrow H_2O$
MCFC	$H_2 + CO_3^{2-} \rightarrow H_2O + CO_2 + 2e^-$	$1/2O_2 + CO_2 + 2e^- \rightarrow CO_3^{2-}$	$H_2 + 1/2\,O_2 + CO_2(\text{cathode}) \rightarrow H_2O + CO_2(\text{anode})$
SOFC	$H_2 + O^{2-} \rightarrow H_2O + 2e^-$	$1/2\,O_2 + 2e^- \rightarrow O^{2-}$	$H_2 + 1/2\,O_2 \rightarrow H_2O$
AFC	$H_2 + 2OH^- + 2e^- \rightarrow 2H_2O + 2e^-$	$2H_2O + O_2 + 4e^- \rightarrow 4OH^-$	$2H_2 + O_2 \rightarrow 2H_2O$

Table 2 Comparison of different types of fuel cells (USDE 2014; Tomczyk 2006)

Fuel cell ➡	AFC	PEMFC	PAFC	MCFC	SOFC
Electrolyte	Aqueous potassium hydroxide	Sulphonated organic polymer	Phosphoric acid	Molten lithium/sodium potassium carbonate	Yttria-stabilized zirconia (YSZ)
Operating temperature	60–90 °C	70–100 °C	150–220 °C	600–700 °C	650–1000 °C
Charge carrier	OH^-	H^+	H^+	CO_3^{2-}	O^{2-}
Anode	Nickel or precious metal	Platinum	Platinum	Nickel/Chromium Oxide	Nickel/Yttria-stabilized zirconia
Cathode	Platinum (Pt) or Lithiated NiO	Platinum	Platinum	Nickel Oxide (NiO)	Strontium doped lanthanum manganite
Co-generation heat	None	Low quality	Acceptable for many applications	High	High
Electrical efficiency	60	40–45	40–45	50–60	50–60
Fuel sources	H_2	H_2	H_2	H_{2-}, CO Natural gas	H_{2-}, CO Natural gas
Application	• Military • Space	• Backup power • Portable power • Distributed generation •Transportation • Specialty vehicles	• Distributed generation	• Electric utility • Distributed generation	• Auxiliary power • Electric utility • Distributed generation
Advantages	• Cathode reaction earlier in alkaline electrolyte, clues to high enactment • Low price mechanisms	• Solid electrolyte decreases weathering and electrolyte organization problems • Low temperature • Fast start-up	• Sophisticated temperature enables CHP • Increased acceptance to fuel impurities	• High efficiency • Fuel suppleness • Can use a variety of catalysts • Appropriate for CHP	• Extraordinary efficiency • Fuel flexibility • Can use a variety of catalysts • Hard electrolyte • Appropriate for CHP & CHHP • Hybrid/GT cycle
Disadvantages	• Sensitive to CO_2 in fuel and air • Electrolyte management	• Expensive catalysts • Sensitive to fuel impurities • Low temperature waste heat	• Pt catalyst • Long start-up time • Low current and power	• High-temperature corrosion and breakdown of cell mechanisms • Stretched start-up time • Low power density	• High-temperature corrosion and failure of cell components • High-temperature operation needs long start-up time and limits

hydroxide saturated in a matrix as the electrolyte (Song and Zhang 2014). The cathode reaction is quicker in the alkaline electrolyte which is beneficial and some enterprises are examining ways to reduce costs and improve operating flexibility (An et al. 2013). They typically have a cell output from 300–5 kW. Table 1 shows the anode, cathode, and overall electrochemical reaction of different types of fuel cells. Table 2 shows the comparison of different types of fuel cells.

3 Mathematical Modeling of Fuel Cell (FC)

The conversion of chemical energy of a fuel (hydrogen) and an oxidant (air or oxygen) into electrical power is through a fuel cell (Tanni and Iqbal 2014). The model shown in Fig. 3 characterizes working at insignificant circumstances of temperature and pressure. The corresponding circuit can be modified varying limitations of based on the polarization curve. The movement of negative current into the stack is vetoed by using anode (Mathworks 2017).

The fuel cell voltage is given by

$$V_{\mathrm{hfc}} = E_{\mathrm{op}} - \left\{ N_{\mathrm{hfc}} \times A \times \ln\left(\frac{i_{\mathrm{hfc}}}{i_0}\right) \times \frac{1}{\frac{\mathrm{ST_d}}{3} + 1} \right\} - \left(R_{\mathrm{int}} \times i_{\mathrm{hfc}}\right) \tag{1}$$

where V_{hfc} is the FC voltage (V) i_{hfc} is the FC current (A), E_{op} is the FC open circuit voltage (V), A is the FC Tafel slope (V), N_{hfc} is the number of FCs, i_0 is the exchange current (A), $\mathrm{ST_d}$ is the FC reply time at 95% of the final value (s), and R_{int} is the FC internal resistance (ohm) (Singh et al. 2017).

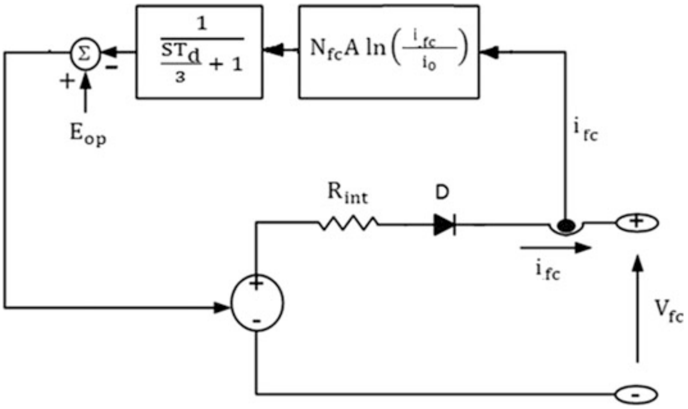

Fig. 3 Electrical circuit diagram of fuel cell (Souleman et al. 2009)

$$E_{\mathrm{op}} = K_{\mathrm{c}} \times E_{\mathrm{nerst}} \tag{2}$$

where E_{nerst} is the Nernst voltage (V) K_{c} is the voltage constant at the nominal condition.

$$i_{\mathrm{o}} = \frac{z \times F \times k \times (P_{\mathrm{H_2}} + P_{\mathrm{O_2}})}{R \times h} \times \mathrm{e}^{\left(\frac{-\Delta G}{R \times T}\right)} \tag{3}$$

where R is the gas constant [8.3145 J/(mol K)], F is the Faraday constant [96485 an s/mol], z is the amount of moving electrons ($z = 2$), ΔG is the start energy barrier (J), T is the temperature of process (K), h is the Planck's constant (6.626×10^{-34} Js), $P_{\mathrm{O_2}}$ is the FC air partial pressure (atm), $P_{\mathrm{H_2}}$ is the FC fuel partial pressure (atm), and k is the Boltzmann's constant (1.38×10^{-23} J/K).

$$A = \frac{R \times T}{z \times \alpha \times F} \tag{4}$$

where α is the coefficient of charge transfer (Mathworks 2017)?

$$\mathrm{UtH_2} = \frac{60000 \times R \times T \times i_{\mathrm{hfc}}}{z \times F \times P_{\mathrm{ffuel}} \times V_{\mathrm{ffuel}} \times x\%} \tag{5}$$

where $\mathrm{UtH_2}$ is the FC utilization of hydrogen, P_{ffuel} is the FC supply pressure of fuel (atm), V_{ffuel} is the FC fuel flow rate (l/min), $x\%$ is the percentage of hydrogen in the fuel (%).

$$\mathrm{UtO_2} = \frac{60000 \times R \times T \times i_{\mathrm{hfc}}}{z \times F \times P_{\mathrm{fair}} \times V_{\mathrm{fair}} \times y\%} \tag{6}$$

In the above equation, $\mathrm{UtO_2}$ is the utilization of oxygen, P_{fair} is the supply pressure of air (atm), V_{fair} is the airflow rate (l/min), $y\%$ is the percentage of oxygen in the oxidant (%).

50% oxygen utilization by the fuel cell is the nominal condition (Milewski and Lewandowski 2014). The partial pressures of hydrogen, oxygen, and water vapor are determined as follows as in (7), (8), and (9):

$$P_{\mathrm{H_2}} = (1 - \mathrm{UtH_2}) \times x\% \times P_{\mathrm{ffuel}} \tag{7}$$

$$P_{\mathrm{O_2}} = (1 - \mathrm{UtO_2}) \times y\% \times P_{\mathrm{fair}} \tag{8}$$

$$P_{\mathrm{H_2O}} = \{w + (2 \times y\% \times \mathrm{UtO_2})\} \times P_{\mathrm{fair}} \tag{9}$$

$$w = \text{Percentage of water vapor in the oxidant}(\%)$$

Knowing the partial pressures of gases, the Nernst voltage equation is given as

$$E_{\text{nernst}} = 1.229 + \left\{(T - 298) \times \frac{-44.43}{zF}\right\} + \left\{\frac{RT}{zF} \times \ln\left(P_{\text{H}_2} \times \sqrt{P_{\text{O}_2}}\right)\right\} \quad (10)$$

For $T > 373$ K

$$E_{\text{nernst}} = 1.229 + \left\{(T - 298) \times \frac{-44.43}{zF}\right\} + \left\{\frac{RT}{zF} \times \ln\left(\frac{P_{\text{H}_2} \times \sqrt{P_{\text{O}_2}}}{P_{\text{H}_2\text{O}}}\right)\right\} \quad (11)$$

where

$$P_{\text{H}_2\text{O}} = \text{Partial pressure of water vapor (atm)}$$

The stack output voltage is represented by the following equation:

$$V = E_{\text{oc}} - \{N_{\text{fc}} \times A \times \ln(i_0)\} - R_{\text{int}} \quad (12)$$

4 Review Analysis of Fuel Cell Energy System

The fuel cell (FC) technology is another conventional energy unit due to its higher efficiency, hygienic process, and cost-effective supply of energy required by the consumers (Wang et al. 2005). The legalized models through experiments were approved on a 500-W Avista Labs SR-12 PEM fuel cell stack. Finished model results shown by the models can predict the energy response of the fuel cell stack below steady state as well as at momentary conditions. The temperature response of the fuel cell stack forecasts the use of fuel cell control-related studies.

Wolfgang Fried et al. (2004) present the governing equations of the transient behavior of a PEM and its influence of the operating conditions along with current density on internal parameters, especially the ohmic resistance.

(Pasricha and Shaw 2006) provide a relatively simple, physically motivated, dynamic model of a fuel cell. The dynamic model is obtained by extending a stationary current–voltage depiction to comprise temperature dependence, and by dynamically showing the temperature of the membrane. They validated model performance using investigational data collected from a 500-W fuel cell (Chiu et al. 2004). In this paper, an effort is defined to mend the small-signal modeling of a PEM fuel cell's dynamic presentation as an preliminary step toward examining internal design modifications and/or external controller strategies to improve its transient response. They recognized from the simulation results that the model significantly improves the transient response of PEMFC. Bucci et al. (2007) developed an automatic testing system and performed both the static and dynamic representation of PEMFC stack and the data obtained is used for the amalgamation of a dynamic model of a stack of PEMFC, which has been endorsed through experimental measures.

Na and Gou (2008) deliberate a dynamic PEMFC model and a design for a nonlinear control for PEMFCs by feedback linearization to delay the cell stack life. The feedback linearization is practical to the PEMFC arrangement so that the deviation can be kept as small as conceivable during turbulences or load distinctions. The nonlinear control strategy has been prompted in MATLAB. According to the results, the nonlinear controller has better transient responses than the linear controller under load deviations.

Tanrioven and Alam (2006) author presented the modeling, control, and simulation of 5 kW PEMFC-based energy supply system for residential applications, also a proportional–integral (PI)-type controller is proposed to satisfy the system desires for voltage and power. They concluded from simulation results that suitable dynamic responses are obtained from the proposed control structure. They inveterate by the power-quality estimation that the bus voltage harmonics meet the IEEE-519 requests for all home uses.

Andújar et al. (2011), in this work, constructed and verified a hybrid system involvinga fuel cell and a battery. They determined that the whole system works efficiently under changed load power values such as 12 V-DC, 48 V-DC, and 230 V-AC. Hua et al. (2007) established a dynamic model and then made a 600 W prototype hybrid power generation scheme consisting of fuel cells, lead-acid batteries, and a DC/DC converter. They applied a digital signal processor (DSP) for the system control and verified the results through experiments. They concluded that the hybrid power system increases the peak power capacity and provides a stable output with the addition of a power converter and appropriate controls.

Thounthong et al. (2008) display a novel control algorithm for utilizing a PEMFC mainly for future electric automobile applications as a source and batteries as a balancing source for distributed power generation system. The structure used was FC system current, battery bank current, and battery SOC cascade control. The small-scale devices of a 500 W, 40-A PEMFC and a 48 V, 33 Ah battery bank were used for the offered control procedure during motor drive cycles and they showed excellent performances (Prema Kumar et al. 2012). In this work, the load behavior of SOFC was analyzed and it was observed that the fluctuations due to load distinctions occupied attention by the SOFC output voltages in the electrical energy system. The SOFC can supply power-preserving inverter voltage as desired, reducing effluence and the cost of energy.

Ariyanfar et al. (2011) offered a 100 W alkaline fuel cell with mobile electrolyte and its marginal apparatus was intended. The offered model uses GAMS codes to find optimum beliefs of the cost model, electrochemical and heat transfer equations. The electrolyte flow rate, inlet and outlet temperatures, pressure drop, heat exchanger areas as parameters that effect on cell concert and total cost. They found that running cost is more effective than the fixed cost.

5 Applications of Fuel Cells

Fuel cell is categorized into three comprehensive sectors: stationary electrical power generation, energy for transportation, and portable electrical power generation.

5.1 *Stationary Power Generation*

Stationary FC today is defined as a unit which provides electricity (and sometimes heat) without movement of the system. When the generation exceeds the demand, hydrogen can be stored via electrolysis on water (Blain 2007). During high load time, the demand exceeds generation, the stored hydrogen retained within the fuel cell can be used to meet the demand. A stationary power generation application of fuel cells focuses on two main markets shown in (Fig. 4). A fuel cell is used for dispersed generation. Keeping the fuel cell close to the assigned center, transmission and distribution cost could be avoided then reduced. To join on isolated websites certain as development sites, military camps yet short village well accepted than DG sets.

Emergency or auxiliary furnish at hospitals, academic establishments, and so on may stand met using a fuel cell. Combined heat and power (Wilberforce et al. 2016), energy produced from the fuels cells operating at high temperatures, like SOFC and MCFC, provide industrial process heat or generate extra energy retaining waste heat boilers and steam turbines. It is an important occasion to increase the efficiency of the electrical power plant.

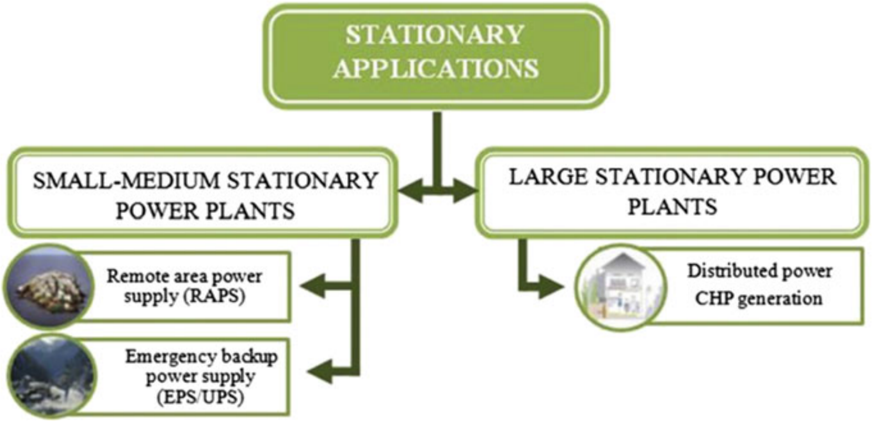

Fig. 4 Stationary applications for fuel cells (Wilberforce et al. 2016)

5.2 Transportation Power

Development of particular vehicles devours huge quantities of fossil fuel and their emissions significantly lower the air quality (Amjad et al. 2010). To discourse these difficulties, investigating alternative sources of power is done. Almost all of the major automobile manufacturers are designing and testing fuels being done by Mazda, Honda, Nissan, Volkswagen, Hyundai, Toyota, General Motors, Ford, Chrysler, BMW, and Suzuki shown in Fig. 5 (Gooeyrabinski 2017). Fuel cell-powered automobiles contain many scarcer parts to a variety of noise than in an IC engine that burns fuel, the only noise from a fuel cell-powered automobile is

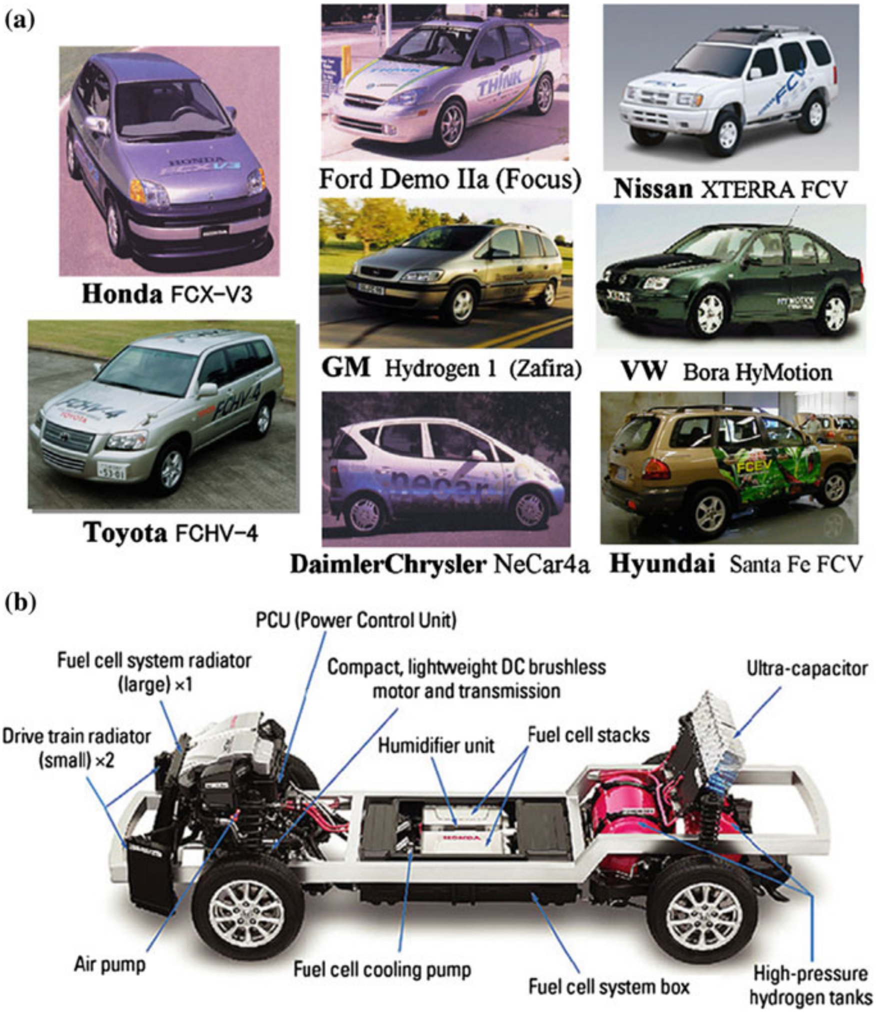

Fig. 5 Fuel cell car (**a**) and layout of the Honda FCX Powertrain (**b**) (Wanga et al. 2011)

from the compressor. Fuel cell-powered vehicles do not require any CI Engine (Aftabuzzaman and Mazloumi 2011). Less maintenance is required as there are no moving parts. Fuel cell automobiles are more reliable due to scarcer progressions to failure as shown in Fig. 6 (Greencarreports 2017). The biggest drawback is that water is needed to produce power and can freeze below 32 °F damaging the membrane and other components (Ahluwalia et al. 2011). Draining the water from the stack before shutting down the vehicle or using new coolant systems and/or block heaters are the solutions to this problem. Solutions to address this problem includes producing fuel cells commercially. The largest fuel cell uses their sixth-generation FC Velocity-HD6 modules power bus fleet in the world, which operates 20 buses (Ahluwalia et al. 2012). Greenhouse gas productions are compact by about 2000 tons per year. Many other nations use fuel cell-powered buses counting Brazil, Japan, Spain, Czech Republic, Australia, and the United States of America.

5.3 Portable Power

Fuel cell performance since ancient in the form of power portable electronic devices, (e.g., cellular phones, laptops yet other low power appliances, especially among military operations). It is used as a substitute for primary or rechargeable batteries. Instead of charging for long, a small cartridge of methanol can be replaced by an ink size cartridge of the printer. The efficiency of FC is always higher as

Fig. 6 Fuel cell bus (**a**); and one of the DaimlerChrysler fuel cell buses (**b**) (Wanga et al. 2011)

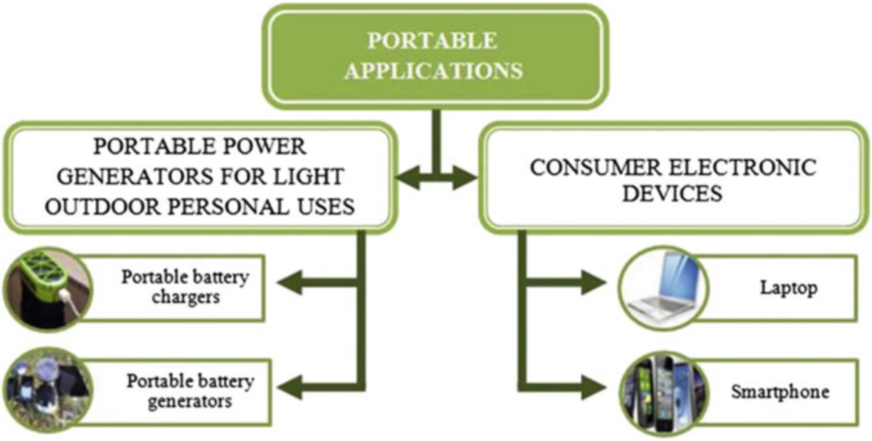

Fig. 7 Portable applications for fuel cells (Wilberforce et al. 2016)

linked with predictable electrical energy system and other distributed power generation systems as it is beneficial due to zero emanation, quick fitting and gives respectable opportunities for cogeneration processes as shown in Fig. 7.

6 Environmental Impact

Decrease in greenhouse gas emissions by fuel cells that use hydrogen, deliver high air feature (Suleman et al. 2015). The decrease of NO_X, SO_2, and CO_2 finished variation of coal, oil, and ordinary gas-fired producing capacity with Connecticut with a fuel cell as follows (Sharma and Strezov 2017).

This resources that for each megawatt of predictable fossil fuel generation ability substituted with capability from a fuel cell:

- Normal reductions of NO_X discharges would be compact by 11,213 lbs;
- SO_2 discharges would be compact by 9,373 lbs, and
- CO_2 discharges would be compact by approximately 7.2 million lbs.

At 40 MW, average reductions of NO_X discharges would be compact by 224 tons; SO_2 emissions would be compact by 187 tons, and CO_2 emissions would be condensed by roughly 144 thousand tons. With a CHP use and pretentious extra increased efficiency from abridged transmission line losses; these yearly emission decreases could be crumpled (Lee et al. 2015). Table 3 shows the Emission Declines by Fuel Cell Technology (lb/MWh) and Table 4 shows the Budding Average Annual Emissions Decline for each megawatt of predictable fossil fuel cohort replaced with volume from a fuel cell.

Table 3 Emission declines by fuel cell technology (lb/MWh) (CHFCC 2017)

GHG emissions ↓	Coal power plant converted fuel cells plant	Oil-power plant converted fuel cells plant	Gas-power plant converted fuel cells plant	Average emissions reductions after fuel cell plant
NO_X	2.53	2.4	0.31	1.28
SO_2	1.79	4.12	0.021	1.07
CO_2	1,106–1,524	832–1,340	255–763	824

Table 4 Probable average annual emissions decline for every megawatt of predictable fossil fuel generation substituted with volume from a fuel cell (CHFCC 2017)

GHG emissions ↓	1 MW	40 MW
NO_X	11,213 lbs	224 tons
SO_2	9,373 lbs	187 tons
CO_2	7,218,240 lbs	144,365 tons

Table 5 Automobile emissions comparison (grams/mile) (CHFCC 2017)

GHG emissions ↓	Emissions after predictable gasoline-powered passenger cars	Emissions after predictable gasoline drove light trucks	Emissions after conventional diesel transit buses	Emissions after hydrogen fuel cells
NO_X	0.95	1.22	12.5	0
SO_2	0.007	0.0097	0.0214	0
CO_2	369	511	2,242.7	0

The use of fuel cells for transport applications will decrease emission for traveler automobiles and mass transportation as 61% of transport reliefs GHG emissions. These automobiles are responsible for 28% of all GHG emissions in Connecticut, likened to 22% nationwide (Ito 2017). Conventional diesel transport buses emit noteworthy amounts of GHG have the budding for the supreme energy investments using fuel cell applications associated with most other transport uses. A comparison of automobile emissions is shown in Tables 5 and 6. Figure 8 shows the conservational impact of fuel cell bus and Fig. 9 shows the well-to-wheels greenhouse gas emission.

Table 6 Automobile emissions evaluation (grams/mile) potential annual emission decreases per automobile using hydrogen fuel cell impulsion systems (pounds/year) (CHFCC 2017)

GHG emissions ↓	Possible emission decreases per year after replacement of a gasoline-fueled passenger car	Possible emission decreases per year after replacement of a gasoline-fueled light truck	Possible emission decreases per year after replacement of a predictable diesel transit bus
NO_X	26.2	37.7	1,019.9
SO_2	0.192	0.299	1.746
CO_2	10,169	15,772	182,984

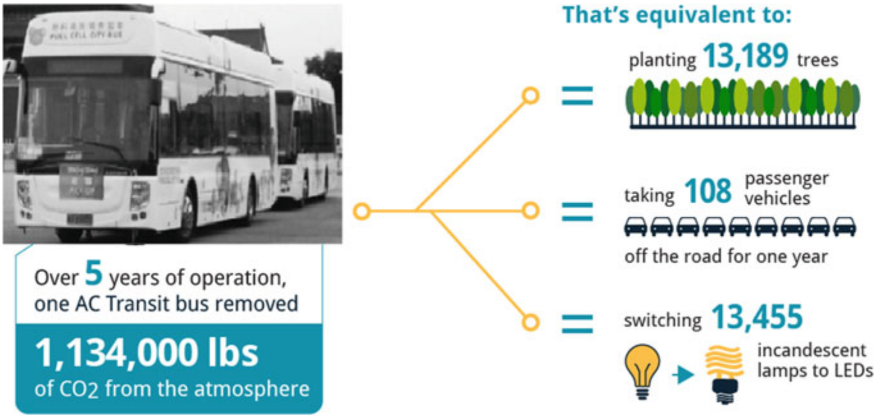

Fig. 8 Environmental impact of fuel cell bus (Liangfei et al. 2009)

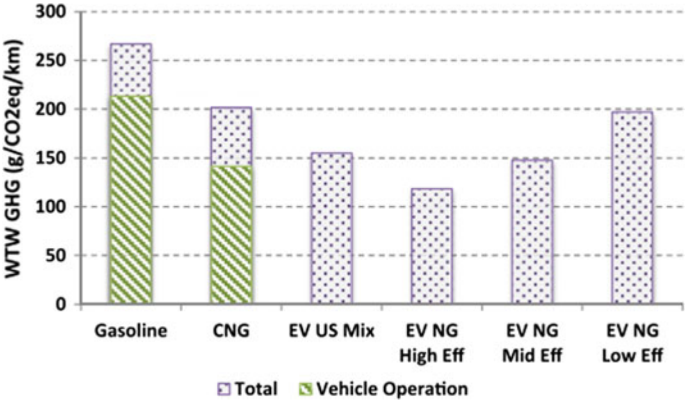

Fig. 9 Well-to-wheels greenhouse gas emission (Curran et al. 2014)

This accepts hydrogen-produced fuel cell automobiles running on hydrogen fashioned from renewable resources removing all GHG emissions associated to predictable fossil fuel-powered automobiles (Duclos et al. 2017). Supplementary of one traveler vehicle, light truck or transit bus can result in yearly emission decreases shown in the following tables.

7 Conclusion

This chapter presents a basic overview of the fuel cell technology along with advantage, disadvantages, applications, classification, and review of the fuel cell. The classification of fuel cell such as PAFC, PEMFC, AFC, MCFC, and SOFC is described. Fuel cell is categorized on the basis of stationary power generation, power for transportation, and portable power generation. The usage of fuel cells particularly that employ hydrogen, better-quality air and concentrated GHG emissions is explained Replacement of coal, oil, and natural gas-fired producing capability by fuel cell (fueled by natural gas) technology would result in the decrease of NO_X, SO_2, and CO_2, Fuel cell with other energy sources offers more advantages such as high energy efficiency, zero emission, quick installation, and delivers for cogeneration processes.

References

Aftabuzzaman M, Mazloumi E (2011) Achieving sustainable urban transport mobility in post peak oil era. Transp Policy 18(5):695–702

Ahluwalia RK, Wang X, Kwon J, Rousseau A, Kalinoski J, James B, Marcinkoski J (2011) Performance and cost of automotive fuel cell systems with ultra-low platinum loadings. J Power Sources 196(10):4619–4630

Ahluwalia RK, Hua TQ, Peng JK (2012) On-board and Off-board performance of hydrogen storage options for light-duty vehicles. Int J Hydrogen Energy 37(3):2891–2910

Amjad S, Neelakrishnan S, Rudramoorthy R (2010) Review of design considerations and technological challenges for successful development and deployment of plug-in hybrid electric vehicles. Renew Sustain Energy Rev 14(3):1104–1110

An L, Chai ZH, Zeng I, Tan P, Zhao TS (2013) Mathematical modeling of alkaline direct ethanol fuel cells. Int J Hydrogen Energy 38:1467–1475

Andújar JM, Segura F, Durán E, Rentería LA (2011) Optimal interface based on power electronics in distributed generation systems for fuel cells. Renew Energy 36:2759–2770

Ariyanfar L, Ghadamian H, Roshandel R (2011) Alkaline fuel cell (AFC) engineering design, modeling and simulation for UPS provide in laboratory application. In: World renewable energy congress, pp 1227–1234

Blain L (2007) Honda set to release hydrogen fuel cell car—and home fuelling station. Retrieved Oct. 2014 from http://www.gizmag.com/honda-fuel-cell-fcx/8394/

Bucci G, Ciancetta F, Fiorucci E, Vegliò F (2007) An experimental approach to the modeling of PEM fuel cells in dynamic conditions. In: IEEE conference on power tech, pp 1094–1099

Cebollero JA, Lahoz R, Larrea A (2017) Tailoring the electrode-electrolyte interface of Solid Oxide Fuel Cells (SOFC) by laser micro-patterning to improve their electrochemical performance. J Power Sources 360:336–344

CEF (2017) http://www.conserve-energyfuture.com/advantages_disadvantages_hydrogenenergy.php. Accessed on 04-8-17

Chatrattanawet N, Saebea D, Authayanun S (2017) Performance and environmental study of a biogas-fueled solid oxide fuel cell with different reforming approaches. Energy, 1–10

Chen X, Wang Y, Cai L, Zhou Y (2015) Maximum power output and load matching of a phosphoric acid fuel cell-thermoelectric generator hybrid system. J Power Sources 294:430–436

Chen X, Wang Y, Zhao Y, Zhou Y (2016) A study of double functions and load matching of a phosphoric acid fuel cell/heat-driven refrigerator hybrid system. Energy 101:359–365

Cheng S, Liu J (2015) Nonlinear modeling and identification of proton exchange membrane fuel cell (PEMFC). Int J Hydrogen Energy 40:9452–9461

CHFCC (2017) http://chfcc.org/resources/fuel-cell-information-database/fuel-cell-environmental-impact/. Accessed on 02-8-17

Chiodo V, Zafarana G, Maisano S, Freni S, Galvagno A (2016) Molten carbonate fuel cell system fed with biofuels for electricity production. Int J Hydrogen Energy 41:18815–18821

Chiu LY, Diong B, Gemmen RS (2004) An improved small-signal model of the dynamic behavior of PEM fuel cells. IEEE Trans Ind Appl 40(4):970–977

Cinti G, Desideri U (2015) SOFC fuelled with reformed urea. Appl Energy 154:242–253

Curran SJ, Wagner RM, Graves RL, Keller M, Green JB Jr. (2014) Well-to-wheel analysis of direct and indirect use of natural gas in passenger vehicles. Energy 75:194–203

Devianto H, Sasongko D, Sempurna FI, Nurdin I (2016) Effect of gas composition produced by gasification, on the performance and durability of molten carbonate fuel cell (MCFC), J Nat Gas Sci Eng, 35:896–905

Dimitrova Z, Mar F (2017) Environomic design for electric vehicles with an integrated solid oxide fuel cell (SOFC) unit as a range extender chal. Renew Energy 112:124–142

Discepoli G, Desideri U (2014) Modeling the performance of MCFC for various fuel and oxidant compositions. Int J Hydrogen Energy 9:1–9

Duclos L, Lupsea M, Mandil G, Svecova L, Thivel PX, Laforest V (2017) Environmental assessment of proton exchange membrane fuel cell platinum catalyst recycling. J Clean Prod 142:2618–2628

Eddine N, Aoul H, Khochemane L (2014) Bond graph modeling approach development for fuel cell PEMFC systems. Int J Hydrogen Energy 39:15224–15231

Emı P, De Miranda V, Ven SA (2017) Direct utilization of carbonaceous fuels in multifunctional SOFC anodes for the electro synthesis of chemicals or the generation of electricity. Int J Hydrogen Energy 2:13927–13938

FCT (2012) Fuel cell today. www.fuelcelltoday.com/media/1637138/fc_basics_technology_types.pdf. Accessed on 30-7-17

Friede W, Raël S, Davat B (2004) Mathematical model and characterization of the transient behavior of a PEM fuel cell. IEEE Trans Power Electron 19(5):1234–1241

Garche J, Jörissen L (2017) Applications of fuel cell technology: status and perspectives. https://www.electrochem.org/dl/interface/sum/sum15/sum15_p39_43.pdf. Accessed on 04-8-17

Goo M, Lee C, Sae H, Jang S, Ae S, Seo H, Hee S, Chul H, Han J, Woo S, Hyun S (2016) Effects of vibrations in marine environments on performance of molten-carbonate fuel cells. Int J Hydrogen Energy 41:18732–18738

Gooeyrabinski (2017). https://gooeyrabinski.com/category/hydrogen-fuel-cell-cars/. Accessed on 04-8-17

Greencarreports (2017). http://www.greencarreports.com/news/1036494_delivery-begins-for-largest-deployment-of-fuel-cell-buses-in-the-world. Accessed on 04-8-17

Guerrero N, Cisneros M, Gervasio D, Francisco J, Robles P (2015) Approaches to polymer electrolyte membrane fuel cells (PEMFCs) and their cost. Renew Sustain Energy Rev 52:897–906

Hua C-C, Huang C-L, Chiu H-C (2007) Research on dynamic response of hybrid power source systems with PEMFCs and lead-acid batteries. In: IEEE power conversion conference, Nagoya, pp 739–744

Ito H (2017) Economic and environmental assessment of phosphoric acid fuel cell-based combined heat and power system for an apartment complex Energy Information Administration of US Environmental Protection Agency of US. Int. J. Hydrogen Energy (42) 15449–15463

Lanzini A, Madi H, Chiodo V, Papurello D, Maisano S, Santarelli M (2017). Dealing with fuel contaminants in biogas-fed solid oxide fuel cell (SOFC) and molten carbonate fuel cell (MCFC) plants : degradation of catalytic and electro-catalytic active surfaces and related gas puri fi cation methods. Prog. Energy Combust Sci 61:150–188

Lee YD, Ahn KY, Morosuk T, Tsatsaronis G (2015) Environmental impact assessment of a solid-oxide fuel-cell-based combined-heat-and-power-generation system. Energy (79):455–466

Mathworks (2017) Mathwork. http://in.mathworks.com/help/physmod/sps/powersys/ref/fuelcellstack.html;jsessionid=1e11811f007e92bb926b5a09d191. Accessed on 02-8-17

Mekhilefa S, Saidur R, Safari A (2012) Comparative study of different fuel cell technologies. Renew Sustain Energy Rev 16:981–989

Milewski J, Lewandowski J (2014) Mathematical modeling of a molten carbonate fuel cell for CO_2 separation. Recent researches in energy, environment and sustainable development, 122–127

MNRE (2017). http://mnre.gov.in/mnre-2010/new-technologies/chemical-energy/. Accessed on 04-8-17

Na WK, Gou B (2008) Feedback-linearization-based nonlinear control for PEM fuel cells. IEEE Trans Energy Convers 23(1):179–190

Pasricha S, Shaw SR (2006) Dynamic PEM fuel cell model. IEEE Trans Energy Convers 21(2): 484–490

Prema Kumar N, Nirmala Kumari K, Rosalina KM (2012) Modeling design of solid oxide fuel cell power system for distributed generation applications. Int J Adv Res Comput Eng Technol 1(9): 46–51

Sharma A, Strezov V (2017) Life cycle environmental and economic impact assessment of alternative transport fuels and power-train technologies. Energy 133:1132–1141

Singh A, Baredar P, Gupta B (2017) Techno-economic feasibility analysis of hydrogen fuel cell and solar photovoltaic hybrid renewable energy system for academic research building. Energy Convers Manag 145:398–414

Song X, Zhang D (2014) Bimetallic Ag e Ni/C particles as cathode catalyst in AFCs (alkaline fuel cells). Energy 70:223–230

Souleman NM, Tremblay O, Dessaint LA (2009) A generic fuel cell model for the simulation of fuel cell vehicles. IEEE 1722–1729

Suleman F, Dincer I, Agelin-Chaab M (2015) Environmental impact assessment and comparison of some hydrogen production options. Int J Hydrogen Energy 40:6976–6987

Sutharssan T, Montalvao D, Kang Y, Wang W, Pisac C, Elemara H (2017) A review on prognostics and health monitoring of proton exchange membrane fuel cell, Renew Sustain Energy Rev, 75:440–450, November 2015

Tanni MA, Iqbal MT (2014) Modeling and control of a grid connected PAFC system. Int J Energy Sci 4(3):69–76

Tanrioven M, Alam MS (2006) Modeling, control, and power quality evaluation of a PEM fuel cell-based power supply system for residential use. IEEE Trans Ind Appl 42(6):1582–1589

Thenextgalaxy (2017). https://thenextgalaxy.com/10-disadvantages-and-advantages-of-hydrogen-fuel-cells/. Accessed on 04-8-17

Thounthong P, Rael S, Davat B (2008) Control algorithm of fuel cell and batteries for distributed generation system. IEEE Trans Energy Convers 23(1):148–155

Tomczyk P (2006) Short communication MCFC versus other fuel cells—characteristics, technologies and prospects. J Power Sources 160:858–862

USDE (2014) U.S. Department of Energy/Fuel Cell Technologies Program. https://energy.gov/sites/prod/files/2014/03/f9/fc_comparison_chart_0.pdf

Verda V, Sciacovelli A (2012) Optimal design and operation of a biogas fuelled MCFC (molten carbonate fuel cells) system integrated with an anaerobic digester. Energy 47:150–157

Wang C, Nehrir MH, Shaw SR (2005) Dynamic models and model validation for PEM fuel cells using electrical circuits. IEEE Trans Energy Convers 20(2):442–451

Wang Y, Leung DYC, Xuan J, Wang H (2017) A review on unitized regenerative fuel cell technologies, part B: unitized regenerative alkaline fuel cell, solid oxide fuel cell, and micro fluidic fuel cell. Renew Sustain Energy Rev 75:775–795

Wanga Y, Chen KS, Mishler J, Cho SC, Adroherv XC (2011) A review of polymer electrolyte membrane fuel cells: technology, applications, and needs on fundamental research. Appl Energy 88:981–1007

WEFORUM (2017). https://www.weforum.org/agenda/2015/06/how-fuel-cells-are-transforming-energy-markets/. Accessed on 04-8-17

Wikipedia (2017) Fuel cell. https://en.wikipedia.org/wiki/Fuel_cell. Accessed on 04-8-17

Wilberforce T, Alaswad A, Palumbo A, Dassisti M, Olabi AG (2016) Advances in stationary and portable fuel cell applications. Int J Hydrogen Energy 41:16509–16522

Xu L, Li J, Hua J, Li X, Ouyang M (2009) Adaptive supervisory control strategy of a fuel cell/battery-powered city bus. J Power Sources 194:360–368

Yourarticlelibrary (2017). http://www.yourarticlelibrary.com/fuel/fuel-cell-advantages-and-disadvantage-of-fuel-cell/12358/. Accessed on 04-8-17

Shallow Geothermal Energy: An Emerging Technology

Guillermo Andres Narsilio and Lu Aye

Abstract Shallow geothermal energy systems use the upper few metres of the ground below the surface to provide space heating and cooling efficiently. Well-designed systems render year-round coefficient of performance (COP) of about four or more. In closed-loop geothermal systems, high-density polyethylene (HDPE) or cross-linked polyethylene (PEX) pipes are embedded in trenches, boreholes or into geostructures (e.g. piles) to form ground heat exchangers (GHEs), whose function is to access this sustainable geothermal energy. A large proportion of electricity worldwide is generated from fossil fuels. Substituting commonly used electric heating and cooling systems with shallow geothermal ones could significantly decrease peak energy consumption and greenhouse gas emissions given their high COPs and high primary energy ratios. This chapter summarises the fundamental principles of the technology, the various factors that affect the thermal performance of different types of GHEs and their impacts on the capital and operating costs of geothermal systems. In addition, this chapter provides an overview of what the future might hold in terms of using geostructures with a dual purpose, as load-bearing-buried structures and as GHEs. Consideration is given to common design methods and an example is presented using a simplified design method. The chapter highlights the importance of directing additional efforts in research and development of the performance of ground loop systems.

Keywords Ground-coupled heat pumps · Energy efficiency · Ground heat exchangers · Sustainability · Greenhouse gas emission reduction

---

G. A. Narsilio
Geotechnical Engineering, Department of Infrastructure Engineering, Melbourne School of Engineering, The University of Melbourne, Melbourne, VIC 3010, Australia

L. Aye (✉)
Renewable Energy and Energy Efficiency Group, Department of Infrastructure Engineering, Melbourne School of Engineering, The University of Melbourne, Melbourne, VIC 3010, Australia
e-mail: lua@unimelb.edu.au

A. Sharma et al. (eds.), *Low Carbon Energy Supply*, Green Energy and Technology,
https://doi.org/10.1007/978-981-10-7326-7_18

1 Introduction

The previous chapters have let readers see that there exists and will continue to persist for some time, an inexorable increase in global energy demand driven by world population growth and the desire to pursuit a higher 'quality of life'. Indeed, the human population and associated annual energy consumption per capita have grown at exponential rates since the industrial revolution (Glassley 2010). This growing demand may be satisfied by either increasing energy supply, for example, by using the low-carbon energy supply technologies such as the ones presented in this book (or by finding new ways to exploit once uneconomical oil and gas reservoirs) or by good management and reducing demand for energy. Better yet, the energy and environmental dilemma may be addressed by a combination of these two sides of the equation, increasing energy supply while reducing (deaccelerating really) demand. Finding renewable energy sources with low greenhouse gas emissions and using energy-efficient technologies help tackling both sides of the energy problem. Therefore, the long(er)-term solution relies on slowing down and hopefully reducing global energy demand and the use of fossil fuels.

Geothermal energy is a vast and adaptable resource that can help satisfying the aforementioned needs. Geothermal energy can be used for power generation as well as for the provision of space heating, space cooling and hot water to residential, commercial and industrial buildings (de Moel et al. 2010; Glassley 2010; Johnston et al. 2011).

If one put aside those volcanic regions where geothermal energy is readily available near the surface, then geothermal energy can be harnessed in two different forms (Fig. 1). The first form generates electricity with turbines that use the heat extracted using water from kilometre deep boreholes that reach strata where temperatures exceed 175 °C. This heat source has tremendous potential, and steady progress has been made to aim producing electricity on a commercial scale. The other form, which is well established outside Australasia, uses the ground to provide year-round efficient space heating and cooling, and sometimes domestic hot water as well (Amatya et al. 2012; Banks 2008; Brandl 2006; Preene and Powrie 2009; Loveridge and Powrie 2014). This chapter focuses on the latter form, also known as *ground source heat pump (for heating), ground-coupled heat pump (for heating and cooling), geoexchange* or often times just referred to as *shallow geothermal energy* technology.

Shallow geothermal energy technology can contribute to lower or smoothing peak electricity demand. This shift in reducing demand instead of increasing supply has driven industry and researchers around the world in developing analytical and numerical models to help predict, and thus design and optimise, these systems. For the geotechnical and geoenvironmental community, this concerns the thermo-geomechanical response of the ground to the exchange of heat, and the pursuit of smaller, cheaper and more efficient ground heat exchangers (GHEs) since the main barrier to shallow geothermal systems is usually high initial capital costs associated with the drilling needed for the installation of GHEs. Professor Brandl in

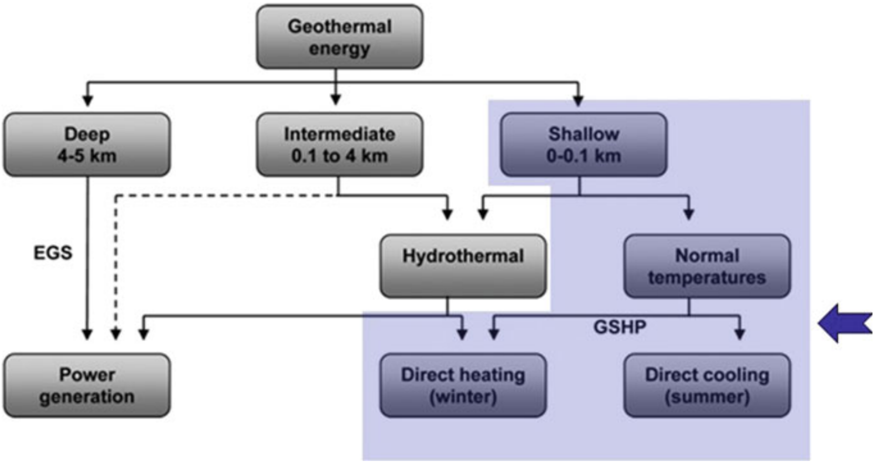

Fig. 1 Geothermal energy: power generation versus heating and cooling. This chapter focuses on the latter technology

his Rankine Lecture (Brandl 2006) promoted the use of any geostructure in contact with the ground (e.g. structural piles) to be used as GHEs. Current trends in research points towards using not only piles as heat exchangers (i.e. energy piles or energy foundations), but retaining walls, tunnel linings, parking lots and even roads. This strategy may significantly reduces the capital costs of geothermal systems. GHE research has accelerated in the past 5–10 years. During this time, two complementary research efforts have been pursued. One focused on the geomechanical considerations of using load-bearing geostructures; and another focused purely on the thermal performance, in order to better understand and maximise the energy transfer between the ground and the GHEs (thus potentially reducing drilling costs).

For an effective shallow geothermal system design, the thermal performance of GHEs should be predicted accurately. A summary of the most commonly used existing analytical solutions and some of the most practical numerical models for simulation of vertical GHEs can be found in Loveridge et al. (2018). In this chapter, we introduce the technology and present key aspects related to the current design of GHEs and recent developments in this area.

2 Shallow Geothermal Energy Systems

In *shallow geothermal energy* systems, the ground within a few tens of metres from the surface is used as a heat sink in summer and/or as a heat source in winter for cooling and heating buildings (Fig. 2) (Johnston et al. 2011; Narsilio et al. 2014). Within about 100–200 m of the surface, the ground temperature is typically close to

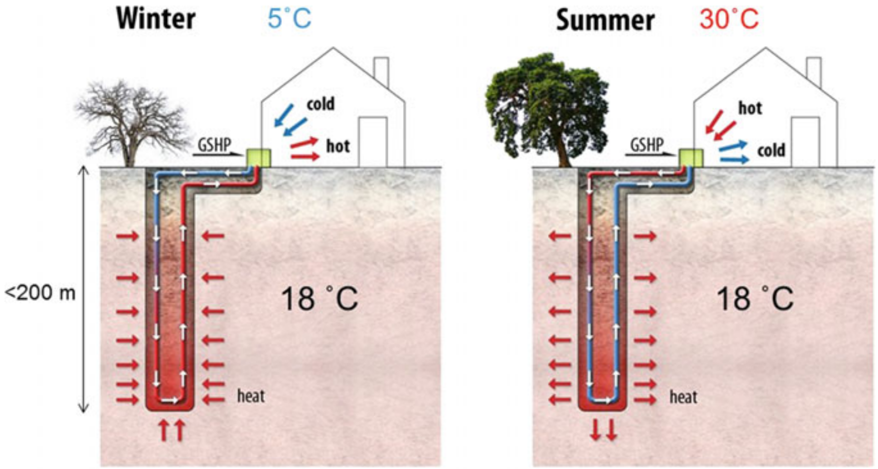

Fig. 2 Schematic of a shallow geothermal energy system in heating (winter) and cooling (summer) modes. Typical temperatures of a temperate climate. Figure not to scale

the mean atmospheric temperature, much below the 175 °C temperatures normally required for power generation.

To illustrate this important feature of shallow geothermal energy systems, Fig. 3 shows ground temperatures measured for approximately 2 years at an experimental site in Parkville, Victoria (the University of Melbourne's main campus in Australia). The figure depicts the naturally occurring ground temperatures variations at the site. While the ambient air temperature in Melbourne varied between 2.3 and 41.1 °C over the 2 years shown in Fig. 3, below about 10 m, the ground temperature was relatively constant at 18.6 °C, making the ground a good sink or source of heat throughout the year (Colls 2013; Colls et al. 2012).

To illustrate this important feature of shallow geothermal energy systems, Fig. 3 shows ground temperatures measured for approximately 2 years at an experimental site in Parkville, Victoria (the University of Melbourne's main campus in Australia). The figure depicts the naturally occurring ground temperatures variations at the site. While the ambient air temperature in Melbourne varied between 2.3 and 41.1 °C over the 2 years shown in Fig. 3, below about 10 m, the ground temperature was relatively constant at 18.6 °C, making the ground a good sink or source of heat throughout the year (Colls 2013; Colls et al. 2012).

In general, ground temperature is influenced by solar radiation and ambient air temperature up to approximately 5–10 m of depth depending on the soil and/or rock conditions. Daily and seasonal temperature fluctuations can be significant. Bellow these depths, the average thermal gradient arises primarily from the heat within the Earth's core, and is between 20 and 30 °C increase per kilometre (Banks 2008). As a result, the ground temperature within the first couple of hundred metres below the ground surface is considered constant for all practical purposes and is in principle close to the local mean annual ambient air temperature. Consequently, the ground

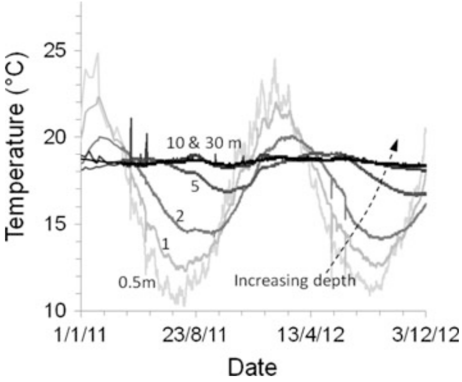

Fig. 3 Measured ground temperatures (at selected depths) over time in Parkville, Victoria (Australia). Data from Colls (2013)

tends to be warmer than the ambient air during winter and cooler during summer. This statement is true regardless of geology and location (except for volcanic regions where the Earth's ground heat fluxes are stronger).

3 Key Components

In shallow geothermal energy systems, three key components can be identified: (i) the primary circuit, (ii) the ground-coupled heat pump (GCHP), and (iii) the secondary circuit. These two main circuits are connected via the ground-coupled heat pump. The primary or ground circuit comprises the ground heat exchanger (GHE) system. The GHE system is in close contact with the ground to facilitate extraction or rejection of heat via the selected carrier fluid. The secondary circuit is located within the building or industrial process that requires to be heated or cooled, and where this thermal energy is distributed.

The GCHP interfaces between these two circuits. In winter, the GCHP extracts heat from the carrier fluid circulating in the ground loops (typically water), it upgrades the heat, and it delivers it to the building that requires heat. The return cooled fluid is reinjected into the ground loops to heat up again and complete the cycle. In summer, the reverse happens with the GCHP extracting unwanted heat from the building and rejecting it to the ground. Thus, the GCHP moves and upgrades heat between the building and the ground via GHEs, and it does so very efficiently due to the year-round narrow temperature range of the ground closer to applied loads.

Both circuits should be carefully designed considering the technical specifications of the link between the two (i.e. the ground-coupled heat pump). A brief description of the primary circuit, as the main component that differentiates shallow geothermal systems from other more common heating and cooling systems, and the basic functioning principles of heat pumps are included next. Fewer details are included in this chapter regarding the secondary circuit, because in most cases, it is treated and designed following standard guidelines common to air-source heat pumps and other conventional heating and cooling systems.

3.1 Primary Circuit: Ground Heat Exchangers (GHEs)

Either open- or closed-loop systems can be used when designing a shallow geothermal system (Preene and Powrie 2009). In open-loop systems groundwater is used directly as the heat transfer fluid, while in closed-loop systems a heat transfer fluid is circulated through absorber pipes embedded into the ground.

Open-loop systems can be used in sites boosting certain ground permeability and geochemistry (mineralogy) (among other considerations); closed-loop systems do not typically require any particular hydrogeological conditions and can be implemented almost anywhere since the circulating fluid is never in direct contact with the ground. In contrast, groundwater is pumped out of the ground and it is returned after heat has been exchanged in open-loop systems. Therefore, care must be taken in selecting the location of the return system, so that the groundwater intake temperature is not adversely affected. When hydrogeological conditions are favourable and large volumes of water can be handled, open-loop systems present major advantages over closed ones: they can be simpler and more efficient. However, clogging or bio-fouling in the wells and heat exchangers are some of the operational problems that open systems are prompted to. The temperature fluctuations cause minerals to dissolve and to re-precipitate leading to clogging (Brandl 2006). Additionally, maintenance costs tend to be higher in open-loop systems due to the use of submersible pumps. Given the potential environmental and operational concerns associated with open-loop systems, and the potential for widespread adoption of closed-loop systems, this chapter focuses on the latter.

Ground heat exchangers (GHEs) are typically designed in close-loop systems to be placed vertically or horizontally. HDPE or PEX pipe loops can be placed in (i) small diameter vertical boreholes that are between 30 and 200 m in depth (typically 100 m) (Fig. 4a), (ii) in trenches between approximately 1 and 2 m in depth, typically outside the footprint of the building to be serviced (Fig. 4b) or (iii) in any structure of residential, commercial and industrial buildings that are in intimate contact with the ground (e.g. the foundations) (Fig. 4c).

Typical borehole GHEs contain one or more U-shaped loops made of HDPE or PEX pipes and thermo-fused fittings. These are generically known as “absorber pipes” (Fig. 4). The heat is transferred between the ground and the heat carrier fluid contained in the absorber pipes primarily by conduction through the ground, the grout and the pipe walls. Convective heat transfer then dominates within the carrier fluid in the absorber pipes. In the case of horizontal GHEs, either U-shaped loops or “slinky” configurations are normally employed. The slinky configuration maximises the length of absorber pipe per linear metre of trench (Fig. 4b).

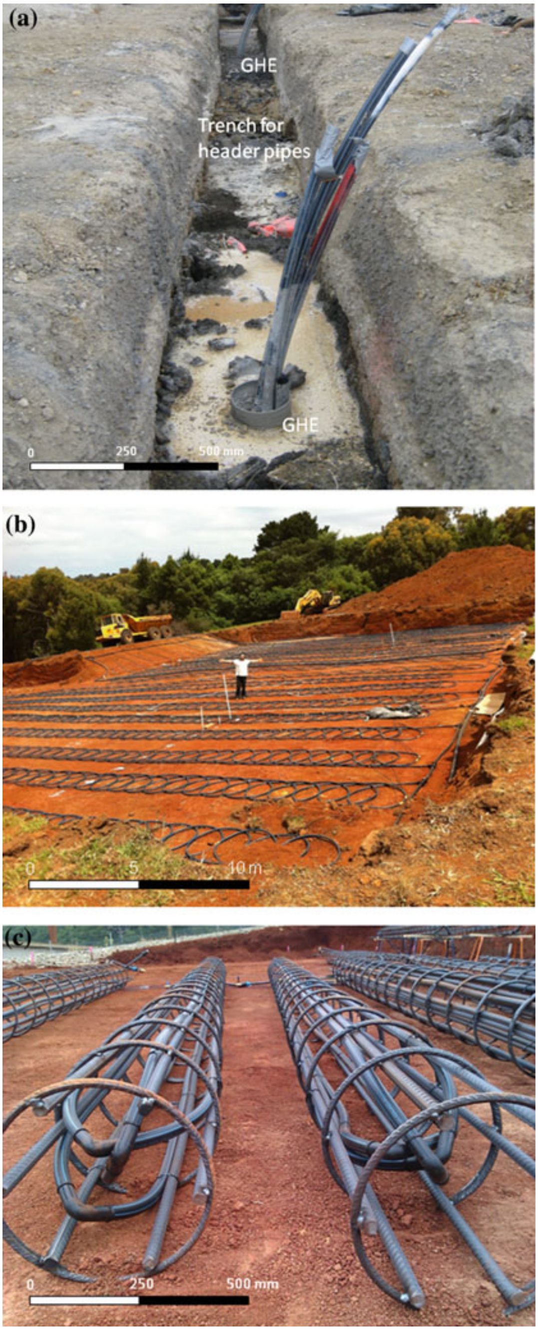

Fig. 4 Primary circuit. Examples of different types of closed-loop ground heat exchangers (GHEs) before backfilling/grouting/concreting: **a** vertical borehole GHEs, **b** horizontal Slinky™ GHEs, **c** energy piles

Vertical systems are inherently more efficient than horizontal systems because the latter are more susceptible to daily and seasonal temperature variations. As a result, horizontal systems require more land to accommodate and longer lengths of pipe. However, under certain conditions, the time shift that exists in the ground temperature at relatively shallow depths (e.g. 2 m depth in Fig. 3—typical depth of GHE in horizontal systems) may become beneficial. In addition, a horizontal system is normally more cost-effective than a vertical system, and it is the preferred option when there is indeed enough surface land available. While a horizontal geothermal system may be less efficient to operate, the increased running costs is typically lower by the cost savings arising from cheaper horizontal trenching. However, depending on soil conditions, if battering is required for trenching, the total cost of groundworks may become larger than vertical drilling, in which case a shallow geothermal energy system with vertical GHEs may result more cost-effective than with horizontal GHEs. For a detailed analysis of the cost of vertical GHEs systems, refer to Lu et al.'s works and references cited therein (Lu et al. 2017a, b).

Environmental risks and mineral precipitation issues are clearly minimised or eliminated in closed GHE systems since the heat transfer fluid is kept isolated from the ground. Furthermore, licenses to extract groundwater are not required as it is the case in Australia for open-loop systems (Johnston 2012), this is valid in Australia, but readers should check their local legislation.

The heat transfer fluid is typically water. However, when sub-freezing temperatures are expected to be reached when the geothermal heating, ventilation and air-conditioning (HVAC) system operates in heating mode, a water-antifreeze solution is used instead (e.g. a mix of water with methanol, ethanol or propylene glycol); sub-freezing temperature is not common in Australia and in other temperate climates, but common in Northern Europe, Korea, parts of China and North America.

3.2 Ground-Coupled Heat Pumps (GCHPs) and Fluid Circulation Pumps

When operating in heating mode, the set temperature is typically higher than the ground temperature. The use of a cooler source, the ground, to heat a building apparently contradicts the second law of thermodynamics. Heat pumps use electrical or mechanical work to cleverly upgrade the thermal energy to adequate levels and to overcome this apparent contradiction.

A schematic representation of a heat pump is shown Fig. 5. Let us explore the basic operating principles in heating mode. In general, heat transfer occurs when there exists a temperature and/or phase change in a material. Heat transfer associated with phase changes is substantially larger than the ones that correspond to only temperature changes. The refrigerants (working fluids) used in heat pumps change phases from liquid to gas or vice versa at suitable operating temperatures and pressures, achieving efficient heat transfer.

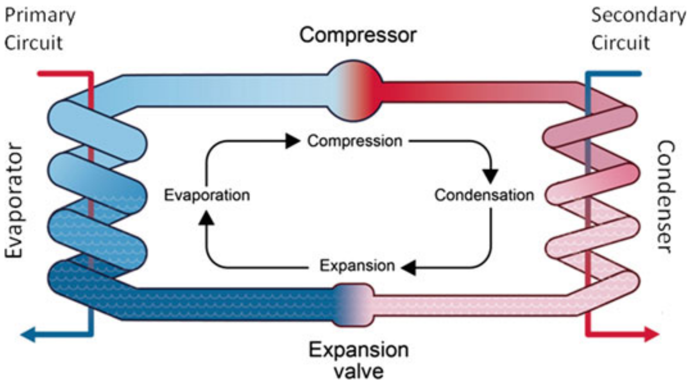

Fig. 5 Schematic representation of a heat pump cycle in heating mode

In Fig. 5, relatively “cool” refrigerant in *liquid* state receives, via an internal heat exchanger, heat from the relatively “warm” water or water-antifreeze solution that comes from the ground loops (i.e. the primary circuit acts as a heat source). At this “evaporator”, the *liquid* refrigerant becomes *vapour*, cooling the water or water-antifreeze solution in the process. The “cooled” heat transfer fluid of the primary circuit is reinjected into the GHE to be warmed up again by the ground. The refrigerant temperature must be lower than that of the water arriving from the GHEs (so heat flows to it). The refrigerant boiling point must be below the entering water temperature at relatively low pressure. Next, the now warm(er) refrigerant *vapour* is compressed, which further increases the temperature of the refrigerant vapour. The much hotter, high-pressure refrigerant vapour leaving the compressor is hotter than the secondary circuit (i.e. the heat sink), and thus heat flows from the refrigerant to the building and eventually condenses at high pressure (see “condenser” in the figure). The now *liquid* refrigerant is still at much higher temperature and pressure than at which it boiled. So, the hot *liquid* refrigerant is depressurised as it passes through an expansion valve, returning the pressure and temperature of the liquid to its original conditions prior to the evaporator to restart the cycle. In cooling mode, the process is reversed: the condensation of the refrigerant heats the heat transfer fluid in the primary circuit, which is re-cooled by the ground.

GCHPs require energy input mainly to the compressor but also to circulation pumps that move the fluid within the primary circuit. However, the heat output is typically much larger than the energy input required: GCHPs typically produce about 3.5–5.5 kWh of thermal energy for every 1 kWh of electricity used. The ratio of these values defines a “coefficient of performance” or COP. GCHP COPs of between 3.5 and 5.5 are typical and higher than yearly average air-source heat pumps’ COPs (Southard et al. 2014). This is inherently true because heat pump COP increases with decreasing temperature difference between the heat sink and the heat source (Banks 2008), and these temperature differences fluctuate significantly more when air is used as the heat sink/source, as opposite to the ground (Fig. 3).

Therefore, GCHPs are generally and inherently more energy efficient than air-source heat pumps since the averaged ground temperature is always closer to the set ambient building temperature than the external ambient air is.

3.3 Secondary Circuit: Distribution of Heating and/or Cooling

The secondary circuit distributes the thermal energy generated by the GCHP, for instance, throughout buildings (space heating and cooling), greenhouses (heating), ice data centres (cooling), dewatering (heating), ice rinks (cooling), aquatic centres (heating), among others. The distribution systems can use either water, air or refrigerant as the transfer medium. In residential applications, the use of airflow and return ducts under the floor or ceiling or in both are common; as well as the use of radiators or fan coil units mounted close to locations of high thermal loads (e.g. near windows) when water instead of air is the heat transfer fluid of choice. Hydronic heating in the floor slab is also common. Proper fresh air intakes typically form part of the secondary circuit to maintain good and healthy air quality.

The distribution schemes are the same as for conventional heating, ventilation and air-conditioning (HVAC) systems, for which standard references exist. However, it is worth noting that the GCHP's output air or water temperatures may be marginally lower than that from other conventional HVAC systems, therefore, the design of ducting and piping in the secondary circuit must take into consideration this difference.

The heating and cooling loads of a building can also be estimated following well-established procedures found in the HVAC literature. The main factors influencing the computation of heating and cooling include climate, construction forms and orientations, building envelope (materials used in the building), the effects of solar radiation and shading, ventilation, internal lights and appliances, occupancy and building use and purpose. Designers and engineers have the opportunity to control some of these factors, particularly for new builds, in such a way that heating and cooling demands are reduced and if possible, balanced, so that the GCHP systems are more cost-effective to install and operate.

4 Design: An Overview and Simplified Approach

The design approach for shallow geothermal systems may be multidisciplinary, and includes the following: (i) the estimation of thermal demands, (ii) the selection of GCHPs and configuration and (iii) the design of the layout, number and length of GHEs and header manifold and (iv) the design of the distribution system. The installation is considered complete with the commissioning of the system. Johnston (2012) summarises this process and presents a simplified approach which is are briefly described next.

4.1 Thermal Load

Standard HVAC guidelines can be followed to estimate the thermal demand to be satisfied by the shallow geothermal system. Best practices include the hourly or daily estimation of thermal loads. Peak thermal load design may lead to unnecessarily expensive and overdesign of the GHE system. Thermal load estimation procedures and software that follow the recommendations set by ASHRAE *Handbook of Fundamentals* (ASHRAE 2012) or by ACCA *Manual J* or *Manual* J_{AE} are recommended (IGSHPA 2011).

4.2 GCHP Selection and GHE Configurations

The selection of a GCHP or cluster of GCHPs involves the consideration of a number of factors. When heating loads to be satisfied by the geothermal system are much higher than the cooling loads, a moderate over-sizing of the GCHP(s) of about 10–15% may be justified; however, the GCHP(s) should not be oversized by more than 25% of the design cooling load (IGSHPA 2011).

Once a GCHP (or cluster of GCHPs) is chosen, the designer must carefully inspect its specifications. The key factors to inspect may include (Johnston 2012):

- The entering water temperature (EWT) to the GCHP and the leaving water temperature (LWT): If the LWT is close to sub-zero (Celsius) temperature at the lowest design heating conditions, then an antifreeze solution is required in the primary circuit. The potential for freeze heaving of the ground must be also considered in this case.
- The COP of the GCHP: It varies with EWT which is the temperature at which the heat transfer fluid returns from the ground loops. One would attempt to maximise COP. COP increases with the length of the ground loops, so here the designer must balance GHE installation costs (primarily driven by drilling and earthwork costs, directly proportional to pipe length) against the target predominant operating COP.
- The flow rate of the heat transfer fluid in the ground loops: One must find a balance between pipe diameters that render turbulent flow (to maximise heat transfer) and that minimises head loses (to avoid requiring a bigger circulation pump).
- The characteristics of the thermal output: e.g. output temperature and airflow for a ducting distribution system; output water temperature and flow characteristics for a hydronic system.

Refer to the *ASHRAE Handbook* (ASHRAE 2012) for more details on other factors that may need to be considered but whose discussion is beyond the scope of this chapter.

4.3 GHE Layout and Total Length

Depending on the size of the land available for the shallow geothermal installation, one must decide on the type of GHE system to use, either vertical or horizontal. In addition, in newly built buildings with significant foundations that may include large diameter piles, one must consider converting them into energy piles, a practice that is not currently common (except for perhaps in Switzerland) but is becoming promising and the focus of further R&D given the potentially reduced capital costs involved (Lu and Narsilio 2018).

Commercial buildings with large foundations would typically require to satisfy high thermal loads, for which horizontal systems are usually not adequate. However, horizontal systems are usually a more cost-effective alternative than vertical GHEs in the case of residential buildings (CGC 2010), provided that there is inadequate land space available. If not, vertical systems or a combination of both vertical and horizontal systems may be considered.

Once a decision is made on a vertical or horizontal GHE system, then the total length of the ground loop is determined. This total length of pipe is then distributed into a number of borehole GHEs or trench GHEs, whose number is established by also deciding on the length of each borehole or trench. Land and local earthwork machinery availability would play a role in these decisions; however, as a first approximation, designers may consider a thermal yield of approximately 40–60 W m^{-1} of vertical GHE or of 10–30 W m^{-2} of horizontal GHE to initially estimate the length and number of vertical or horizontal GHEs required, respectively. These are the rule of thumbs and as such should only be used as an initial guide and never for the final design. A proper GHE length design is influenced by a number of factors that affect the thermal performance of GHEs such as hydrogeological conditions, thermal properties of the ground and their variability, borehole/trench size, loop orientation, location, thermal properties of the backfill or grout, pipe sizes and spacing and most importantly, the actual thermal loads to be satisfied and the ratio of heating to cooling energy demand. The Canadian GeoExchange Coalition (CGC) and the International Ground Source Heat Pump Association (IGSHPA) offer design manuals that contain more refined methods of loop design (CGC 2010; IGSHPA 2011). Commercial software tools are also available for this purpose, including GLD, GLHEPRO, EED, 4EE and TRNSYS among others. Infinite source line model, finite line source model and cylindrical line source model are some of the models on which the commercial software are based.

The method summarised by IGSHPA to estimate the lengths of GHE loop can be used here to demonstrate the general principles of design. When in heating mode, the total length L of vertical boreholes with single U-shaped loops can be estimated as (IGSHPA 2011):

$$L = \frac{Q_{\mathrm{h}}\left(\frac{\mathrm{COP}_{-1}}{\mathrm{COP}}\right)\left(R_{\mathrm{b}} + R_{\mathrm{g}}F_{\mathrm{h}}\right)}{T - \left(\frac{\mathrm{EWT}_{\mathrm{min}} + \mathrm{LWT}_{\mathrm{min}}}{2}\right)} \tag{1}$$

where Q_h is the GCHP heating capacity at design heating conditions, T is the far-field ground temperature at the site, COP is the coefficient of performance at design conditions, R_b represents the borehole thermal resistance, R_g is the ground thermal resistance, F_h represents the proportion of the time the GCHP has to run to provide the heat required during the design heating month (also known as run fraction), $\mathrm{EWT_{min}}$ is the design entering water temperature (to the GCHP), and $\mathrm{LWT_{min}}$ is the leaving water temperature. The $\mathrm{LWT_{min}}$ controls the minimum temperate of the heat transfer fluid reinjected into the ground. For temperature climates and whenever possible, $\mathrm{LWT_{min}}$ should be kept sufficiently above 0 °C otherwise a water-antifreeze solution instead of just plain water is needed in the GHEs.

GCHP manufactures usually provide Q_h and COP as a function of $\mathrm{EWT_{min}}$ and $\mathrm{LWT_{min}}$ as part of pump's technical specifications. On the other hand, the use of the building indicates the value for F_h. R_b can be estimated in a number of different ways, IGSHPA uses the following formula (IGSHPA 2011):

$$R_\mathrm{b} = \frac{1}{\mathrm{SF_b} k_\mathrm{grout}} + \frac{\ln(d_\mathrm{o}/d_\mathrm{i})}{4\pi k_\mathrm{p}} \tag{2}$$

where k_grout is the grout thermal conductivity, d_o and d_i are the outer and inner diameters of the ground loop pipes, k_p is the grout thermal conductivity, and $\mathrm{SF_b}$ is a dimensionless shape factor that captures the effects of pipe separation within the ground loop in relation to the diameter of the borehole d_b and the pipe outer diameter d_o. Table 1 can be used to estimate parameters α and β, so that $\mathrm{SF_b}$ can be found as:

$$\mathrm{SF_b} = \alpha(d_\mathrm{b}/d_\mathrm{o})^{\beta} \tag{3}$$

Table 1 Coefficients for $\mathrm{SF_b}$ (IGSHPA 2011; Johnston 2012; Narsilio et al. 2012)

Configuration	α	β
	20.10	−0.9447
	17.44	−0.6052
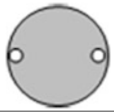	211.91	−0.3796

The ground thermal resistance can be estimated as:

$$R_g = \frac{\ln(d_g/d_b)}{2\pi k_g} \tag{4}$$

where d_g is the diameter of the ground around the borehole GHE affected by its operation, where little change in temperature is observed in the long term (usually taken as approximately 5 m), and k_g is the ground thermal conductivity.

Let us use a residential building in Melbourne, Australia to exemplify the estimation of the total length of GHE required to satisfy the typical peak heating demand of 15 kW based on the simplified approach outlined above and first presented by Johnston (2012). Readers can also compare these results against those obtained from the use of the mobile application 'geothermal' (Fig. 6), which are derived based on IGSHPA and ASHRAE methodologies. Once again, the results from the mobile application should only be used as a guide for pre-design and not for the actual design of these systems.

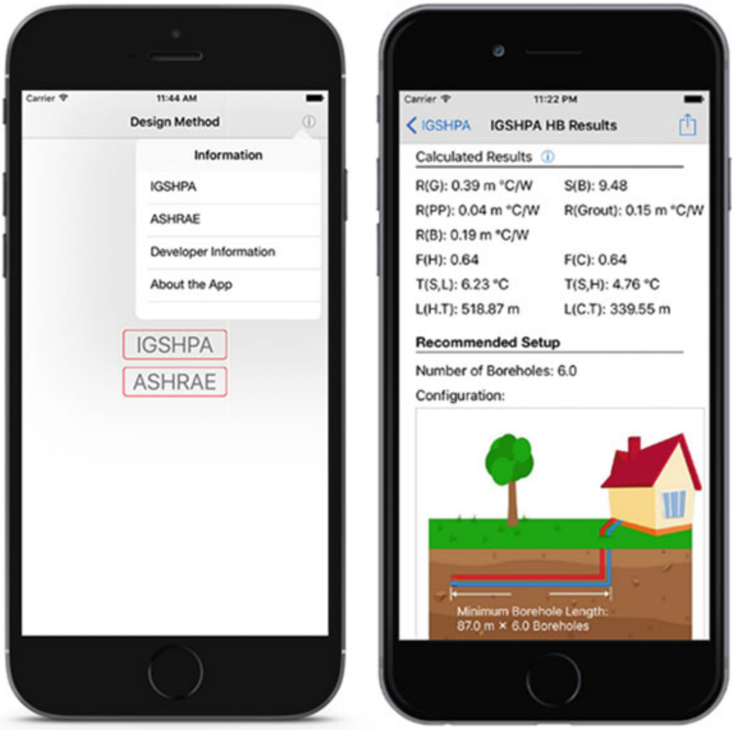

Calculated Results

R(G): 0.39 m °C/W S(B): 9.48

R(PP): 0.04 m °C/W R(Grout): 0.15 m °C/W

R(B): 0.19 m °C/W

F(H): 0.64 F(C): 0.64

T(S,L): 6.23 °C T(S,H): 4.76 °C

L(H.T): 518.87 m L(C.T): 339.55 m

Recommended Setup

Number of Boreholes: 6.0

Configuration:

Minimum Borehole Length:
87.0 m × 6.0 Boreholes

Fig. 6 Screenshot of the mobile application 'geothermal' and GHE total length results for a geothermal system *Source* http://geothermalapp.com

Vertical borehole GHEs containing single U-shaped loops will be considered. The borehole diameter is set at 114.3 mm (4.5 in.) and the HDPE pipe outer diameter is selected at 25 mm with an standard dimension ratio (SDR) of 11 (i.e. wall thickness of 2.27 mm). Thermal testing of the HDPE, the ground and the grout reveal thermal conductivities of 0.45, 1.15 and 2.2 (W m^{-1} K^{-1}) respectively. To satisfy the 15 kW peak heating demand, a 15 kW capacity GCHP is selected. Its manufacturer's technical specifications show that the GCHP operates at a COP of 4 when the EWT_{min} is 7 °C and the LWT_{min} is 4 °C. Assuming a working family living in this residential building, a run fraction of 0.6 is chosen for this example. For Melbourne, the far-field ground temperature is approximately 18 °C (Fig. 3). Following Eqs. (1) through (4), with the input variables summarised above, the required total GHE length L is calculated at approximately 310 m. This total length can be distributed into 3 vertical GHEs of just over 100 m in depth each, 5 m apart. Since more drilling companies are able to drill 50 m boreholes, another option to consider is spreading the total length of GHE into 6 vertical GHE boreholes of just over 50 m in depth, again with a 5 m spacing provided that there is enough land availability.

The ratio of heating to cooling energy exchanged with the ground must be also considered. For cases with balanced heating and cooling loads (i.e. the heat in kWh extracted from the ground in winter is approximately equal to that rejected to the ground in summer), then no correction is necessary. However, for thermally unbalanced cases (e.g. more heat is extracted from the ground than it is rejected in a yearly basis) then a gradual overall increase or decrease of the ground temperature could be expected. Since COP is (amongst other factors) a function of the ETW, this longer term ground temperature variations may reduce the shallow geothermal system efficiency and even cause problems associated with ground overheating or ground heaving due to freezing if the thermal imbalance is not properly accounted for. Continuing with the Melbourne residency example, if 20 and 12 MWh were the total yearly heating and cooling energy extracted and rejected from/to the ground, respectively, then an unbalanced ground load correction factor of 1.1 would be required following the IGSHPA design method. This translates to an increase of the total GHE length to approximately 342 m. The variation to the total GHE length is directly proportional to the thermal imbalance, thus the previous suggestion to engineer the buildings to render balanced thermal loads.

The method exemplified above for heating mode is similar to that followed to estimate the total GHE loop length in cooling mode. Designers must select the critical length to be used in the final design. Using the EED software with the input data of the aforementioned example, a ground loop design with 6 vertical GHEs, 5 m apart in a 2 × 3 grid pattern, rendered a total GHE length L of 286 m (i.e. 6 GHEs to approximately 48 m). The use of double U-shaped loops would reduce this total length to about 242 m, representing a saving of an entire 48 m-deep vertical GHE over the single U-shaped loop choice.

5 Energy Geostructures

Energy geostructures are foundations or other buried geotechnical structures which have absorber pipes embedded so that they can have a dual purpose, structural as well as thermal. Effectively, the addition of HDPE pipes converts these buried structures into ground heat exchangers that form part of a shallow geothermal system. Therefore, the need for construction of special-purpose GHEs is removed or minimised in an attempt to reduce capital costs for the system (Lu and Narsilio 2018; Loveridge et al. 2018), however cost savings may not always be achieved (Park et al. 2015).

Piles are the most common type of energy geostructure. Energy piles were first trialled in the 1980s in northern Europe (Brandl 2006). Their application has expanded in time (e.g. Amis and Loveridge 2014; Amatya et al. 2012), but their numbers are still small compared to the total shallow geothermal installations worldwide. Demonstration projects using walls, tunnel linings and slabs as ground heat exchangers soon followed the first pile installations (Adam and Markiewicz 2009) and a number of new initiatives are being considered, for example for the AUD 11 billion Melbourne Metro Rail Project in Australia (Narsilio et al. 2016a, b), in the Seoul Metro in Korea, and in the Paris and Torino Metro Projects in Europe. However, these types of energy geostructures are less common than piles since the embedment of geothermal pipe loops may not be as straightforward to achieve in real-life projects, and design methods are just in their infancy.

Energy pile shallow geothermal systems tend to incur lower capital costs than traditional vertical GHEs systems such as boreholes (Lu and Narsilio 2018; CIBSE 2013). In terms of design, given the geometrical resemblance to borehole GHEs, ‘traditional’ thermal design methods can be adapted for use with piles (e.g. Pahud 2007; Eskilson 1987). However, as pointed by Loveridge and Powrie (2013a) and Loveridge et al. (2018), there remain some limitations of such approaches. Additionally, approaches for the geotechnical design of piles subject to thermal changes are under development (e.g. Mimouni and Laloui 2014; Loria and Laloui 2016). By contrast, there are not any standard design and analysis approaches for other structures, thus every project must proceed on a case by case basis, typically using complex detailed numerical schemes (Narsilio et al. 2016a, b; di Donna and Barla 2016; Nicholson et al. 2014) or analytical solutions highly constrained by underlying assumptions not always applicable. The proliferation of underground infrastructure, particularly for public transport (e.g. metro tunnels, sewage tunnels, underground train stations) has prompted the desire to take advantage of these structures to harness thermal energy from the ground. While energy-piled foundations are typically used to provide renewable heat to the buildings they support, for train stations’ retaining walls and tunnel linings converted into special GHEs, the user of the heat may be a third party. The inclusion of third parties places additional logistical, legal and bureaucratic barriers for the adoption of the technology. It is only through a holistic, multidisciplinary and multi-sectoral approach which can see this and many other low-carbon and energy-efficient technologies integrated in future infrastructure and construction developments.

Research into the application of energy geostructures has focused in two main areas; (i) the geomechanical effects of using buried bearing structures also as heat exchangers and thermal batteries (e.g. Bourne-Webb et al. 2009; Stewart and McCartney 2014); (ii) the thermal performance of these structures and the pursuit of energy efficiency maximisation (e.g. Loveridge and Powrie 2013b; Bidarmaghz et al. 2016b; Bidarmaghz and Narsilio 2016). Both these areas have the aim of minimising uncertainty and risk in design, facilitating reduction in capital costs and hence an increase in technology uptake.

Designers must ensure that the heat pump and the energy geostructures operate within an acceptable temperature range to (i) protect the structure from extreme temperature changes that may impact on the geotechnical performance, and (ii) ensure that the heat pump operates within its optimal efficiency range. The upper bound temperature limits will depend on the heat pump, typically about 40–45 °C, the lower bound is generally taken as 0–2 °C to avoid ground freezing (GSHPA 2012), although lower fluid temperatures can potentially be tolerated (Loveridge 2012; Loveridge et al. 2012). A detailed review of recent research on energy geostructures in both these areas can be found in Loveridge et al. (2018), covering analysis approaches and the field and model scale testing that has been used to inform those approaches.

5.1 *Energy Piles*

A key difference between energy piles and typical vertical borehole GHEs is that for the former, the number of piles, configuration and length are not primarily designed to fulfil the (thermal) loads of the building, but rather for its geomechanical structural stability. This leaves little room for optimisation of the geothermal ground loop design, as the main design parameters, like the pile (i.e. GHE) length and separation, are pre-determined. Therefore, the provision of 100% of the heating and cooling energy required (thermal load) cannot be guaranteed and instead a hybrid system must often be used, to complement the produced geothermal energy using auxiliary means (Bidarmaghz et al. 2016a; Narsilio et al. 2015). The design challenge here is to maximise the thermal energy that the geothermal system can provide using the already designed energy piles. Currently, there exist limited design approaches.

Some integrated building simulation software packages allow analyses of all components of a ground-coupled heat pump system from the in ground components to the delivery of heating and cooling, e.g. EnergyPlus (Fisher et al. 2006) or TRNSYS (Klein et al. 2017). Ground-coupled heat pump models were reviewed by Do and Haberl (2010) and found they are typically aimed at borehole heat exchanger design, but a standalone implementation of TRNSYS for application to energy piles is available (Pahud 2007). In addition, a range of analytical solutions are used to determine the changes in temperature for a given thermal demand. This allows to determine the amount of energy that is available within certain temperature limits. Given that fast runtimes are required to process thermal load input data, which may vary on an hourly basis and cover the service life (i.e. decades), analytical solutions may be preferred over numerical solutions. However, some numerical tools have been implemented with sufficient computational efficiency that they provide reasonable alternatives (e.g. Pahud 2007) including the use of advanced machine learning techniques (Makasis et al. 2018).

To simplify the thermal problem most analysis approaches separate the temperature change into a number of zones for which different solutions are applied, the change in circulating fluid temperature, ΔT_f, can be given by:

$$\Delta T_{\mathrm{f}} = \Delta T_{\mathrm{ground}} + \Delta T_{\mathrm{pile}} + \Delta T_{\mathrm{pipe}} \tag{5}$$

If analytical techniques are adopted then the ground temperature change is calculated using a transient temperature response function (G_{g}) calculated at the pile wall (i.e. at $r = r_{\mathrm{b}}$, where r_{b} is the radius of the pile):

$$\Delta T_{\mathrm{ground}} = \frac{q}{2\pi\lambda_{\mathrm{g}}} G_{\mathrm{g}}(t, r) \tag{6}$$

where k_{g} is the ground thermal conductivity (W m^{-1} K^{-1}), q is the applied thermal power (W m^{-1}) and t is the elapsed time (s). The temperature response function or G-function can take a number of different forms as summarised in Table 2.

G-functions are temperature response functions originally developed for borehole heat exchangers by Eskilson (1987) using the superposition borehole model (SBM), and are now adopted more generally to describe any function that relates the temperature change in the ground surrounding a vertical GHE to the applied thermal load q (Loveridge et al. 2018). G-functions are typically expressed as a dimensionless form of Eq. (6), which is as follows:

$$\Phi = G_{\mathrm{g}}(Fo, r^{*}) \tag{7}$$

where Φ is the dimensional temperature response, $\Phi = 2\pi k_{\mathrm{g}} \Delta T / q$, Fo is the Fourier number or dimensionless time with $Fo = \alpha_{\mathrm{g}} t / r_{\mathrm{b}}^{2}$ and $r*$ is a dimensionless geometry factor, often expressed as radial coordinate divided by heat exchanger length, α_{g} is the ground thermal diffusivity. Full details of these solutions are not included here since they are readily available in the literature (Bourne-Webb et al. 2016a).

All the models assume that the ground is homogeneous and isotropic, with no initial temperature gradient and no groundwater flow. Such factors are known to affect the temperature changes around vertical ground heat exchangers (e.g. Signorelli et al. 2007; Bidarmaghz et al. 2016b), but are more difficult to account for by analytical means. G-functions are normally plotted for a constant q (Fig. 7), but as q varies in actual routine operation it is necessary to use some form of temporal superposition and/or load aggregation (Claesson and Javed 2011) to

Table 2 Summary of types of *G*-function that can be used with piles

Model	Reference	Description	Comments
Infinite Line Source (ILS)	Carslaw and Jaeger (1959)	Infinitely long and thin heat source. Homogeneous medium	Infinite length implies that long-term steady-state behaviour is neglected
Infinite (Hollow) Cylindrical Source (ICS)	Carslaw and Jaeger (1959), Ingersoll et al. (1954), Kakaç and Yener (2008), Bernier (2001)	Assumes an infinitely long hollow cylinder which acts as a heat source embedded in a homogeneous medium	Long-term steady-state behaviour is neglected. Gives larger temperature changes than the ILS at short time periods. Is equivalent at longer time periods
Superposition Borehole Model (SBM)	Eskilson (1987)	Uses numerically exact calculation based on a finite line heat source, with superposition for multiple boreholes	Calculated numerically. SBM *G*-functions must be pre-programmed into software codes for different combinations of multiple boreholes. Widely used approach
Analytical Finite Line Source (FLS)	Eskilson (1987), Zeng et al. (2002), Lamarche and Beauchamp (2007)	Using a mirrored virtual line sink approach to simulate the ground surface, these *G*-functions provide an analytically exact version of SBM	The mid-depth or the average temperature of the GHE is used as the reference temperature. Recent works focuses on simplifying the math (Claesson and Javed 2011)
Solid Cylinder Model (SCM)	Man et al. (2010)	Heat flow into and out of the heat exchanger is simulated. The model has been presented in both infinite and finite forms	Studies by Loveridge and Powrie (2013b) suggest that the SCM may provide a sensible upper bound for piles, providing the finite version of the model is used
Pile *G*-Functions	Loveridge and Powrie (2013b)	Derived numerically based on SBM. *G*-functions presented as upper and lower bound solutions	The functions typically fall between the SCM and the log linear simplification of the FLS

Source Loveridge et al. (2018)

determine the overall temperature change, $\Delta T(t)$ resulting from $q(t)$ over the lifetime of a geostructure.

The most frequently adopted type of *G*-function is the SBM and other finite line source (FLS) approaches which are readily implemented in accessible borehole design software that is sometimes used for piles. However, this approach has not been extensively validated for piles and may over predict induced temperature

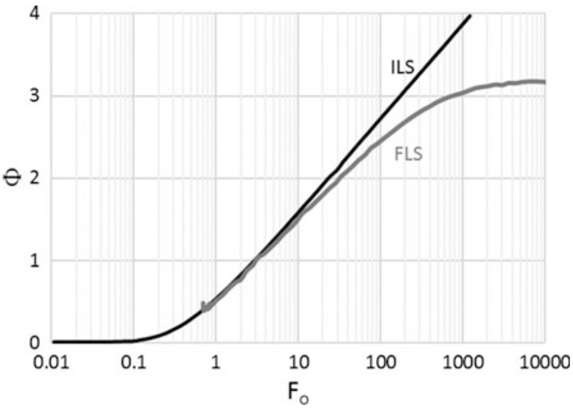

Fig. 7 Example of a *G*-function for an infinite line source (ILS) model and a finite line source (FLS) model (aspect ratio 33)

changes due to the short length of piles (e.g. Wood et al. 2010). Nevertheless, this limitation would be conservative. Following a similar approach to the SBM, Loveridge and Powrie derived upper and lower bound G-functions based on pile geometries rather than on a line source (Loveridge and Powrie 2013b). This newer approach was only validated on short-term thermal response tests of small diameter piles and awaits longer term validation and critical assessment for larger diameters.

The absence of appropriate field data sets to validate models and help assign the most appropriate boundary conditions also remains a barrier to further development. Despite the fact that analytical solutions have been developed to capture the thermal performance of GHEs, most of the assumptions bring limitations. Numerical models solving the governing heat transfer equations have surged in an attempt to overcome such limitations. This includes 1D finite difference models (e.g. Gehlin and Hellström 2003) and finite element (FE) models in 2D (e.g. Austin et al. 2000; Sharqawy et al. 2009) and 3D (e.g. Bidarmaghz 2014; Ozudogru et al. 2014; Signorelli et al. 2007; Narsilio et al. 2018).

5.2 *Energy Walls*

Despite energy wall case studies been in operation for over a decade, very limited published analyses exist, with most relying solely on numerical simulations (ICConsulten 2005; Soga et al. 2014; Bourne-Webb et al. 2016b; di Donna et al. 2017; Coletto and Sterpi 2016). There exists, however, two other approaches, but not widely adopted: (i) Sun et al. (2013) have proposed an analytical solution based on heat conduction. Many assumptions used in the analysis of energy piles have been used in this model, with the addition of a convective heat transfer boundary condition for the inside face of a retaining wall. The model was tested against full numerical simulations and a limited dataset from the Shanghai Museum of Nature History (Sun et al. 2013); (ii) Kurten et al. (2015) applied an approach based on electrical analogy and uses numerical computation of a sequence of “thermal” resistances. This model has been validated against full numerical simulations and model scale laboratory tests (Kürten et al. 2015).

5.3 Energy Tunnels

Tunnel linings with embedded geothermal pipe loops are also relatively rare, thus there is no routine design and analysis practice yet. Numerical simulation is the most common approach to assess temperature changes and heat transfer rates. Studies have been conducted in both two (Franzius and Pralle 2011) and three dimensions (Nicholson et al. 2014; Bidarmaghz et al. 2017; di Donna and Barla 2016). The structure internal boundary condition is very important, as the air inside the tunnel can be used as a heat source together with the ground (Zhang et al. 2014), as well as the effect of groundwater impacting on the energy efficiency of energy tunnels (di Donna and Barla 2016; Bidarmaghz and Narsilio 2018; Barla et al. 2016). Analytical solutions have also been proposed (e.g. Zhang et al. 2013).

6 Summary/Conclusion

Well-designed shallow geothermal energy systems represent a highly effective, sustainable, and economic technology for space heating and cooling, as well as for domestic hot water (but there are competitive alternatives to the latter). This is particularly important to address and help to mitigate the consequences of climate change. This emerging technology has a growth rate of 10% per annum over recent years in some parts of the world, however, the capital costs of installation need to be reduced to increase penetration in emerging markets. In localities where the shallow geothermal industry is just being established, the installation costs are still high. To have a mature shallow geothermal industry providing efficient, clean heating and cooling for our buildings it is imperative that engineers, architects, developers, regulators, politicians and the general public are educated, trained and accredited. There exists a relatively good understanding of the technologies associated with the “above-ground” components of shallow geothermal energy systems. While these can always be improved further, the best opportunity to reduce costs may lie on the “below-ground” components of geothermal energy systems. The use of structures as GHEs is a clever attempt at this aim and is gaining traction worldwide. Current GHE design methods were briefly discussed and references to full descriptions provided. In contrast, these guidelines do not yet exist for energy geostructures but academic references in this developing front were included in this chapter. In order to address this shortcoming, an increasing number of (geotechnical and mechanical) research groups are undertaking a number of research and demonstration projects to understand how effective the technology is under a range of different conditions. Research and development are being directed to more appropriate guidelines for the design and operation of a variety of GHEs types and configurations.

References

Adam D, Markiewicz R (2009) Energy from earth-coupled structures, foundations, tunnels and sewers. Geotechnique 59(2):229–236

Amatya B, Soga K, Bourne-Webb P, Amis T, Laloui L (2012) Thermo-mechanical behaviour of energy piles. Geotechnique 62(6):503–519

Amis T, Loveridge F (2014) Energy piles and other thermal foundations for GSHP—developments in UK practice and research. REHVA Eur HVAC J 32–35

Ashrae (2012) American Society of heating refrigeration and air-conditioning engineers handbook. ASHRAE

Austin WA, Yazuzturk C, Spitler JD (2000) Development of an in-situ system for measuring ground thermal properties. ASHRAE Trans 106(1):365–379

Banks D (2008) An introduction to thermogeology: ground source heating and cooling. Wiley-Blackwell

Barla M, Di Donna A, Perino A (2016) Application of energy tunnels to an urban environment. Geothermics 61:104–113

Bernier MA (2001) Ground-coupled heat pump system simulation. ASHRAE Trans 107:605–616

Bidarmaghz A (2014) 3D Numerical modelling of vertical ground heat exchangers. In: Melbourne School of Engineering. The University of Melbourne, Australia

Bidarmaghz A, Narsilio GA (2016) Shallow geothermal energy: emerging convective phenomena in permeable saturated soils. Géotechn Lett 6(2):119–123

Bidarmaghz A, Narsilio GA (2018) Heat exchange mechanism in tunnel GHE systems. Geomech Energy Environ. in press

Bidarmaghz A, Makasis N, Narsilio GA, Francisca FM, Carro Pérez ME (2016a) Geothermal energy in loess. Environ Geotech 3(4):225–236

Bidarmaghz A, Narsilio GA, Johnston IW, Colls S (2016b) The importance of surface air temperature fluctuations on long-term performance of vertical ground heat exchangers. Geomech Energy Environ 6:35–44

Bidarmaghz A, Narsilio GA, Buhmann P, Moormann C, Westrich B (2017) Thermal interaction between tunnel ground heat exchangers and borehole heat exchangers. Geomech Energy Environ 10:29–41

Bourne-Webb PJ, Amatya B, Soga K, Amis T, Davidson C, Payne P (2009) Energy pile test at Lambeth College, London: geotechnical and thermodynamic aspects of pile response to heat cycles. Geotechnique 59(3):237–248

Bourne-Webb P, Burlon S, Javed S, Kürten S, Loveridge F (2016a) Analysis and design methods for energy geostructures. Renew Sustain Energy Rev 65:402–419

Bourne-Webb PJ, Bodas Freitas TM, Da Costa Gonçalves RA (2016b) Thermal and mechanical aspects of the response of embedded retaining walls used as shallow geothermal heat exchangers. Energy Build 125:130–141

Brandl H (2006) Energy foundations and other thermo-active ground structures. Geotechnique 56(2):81–122

Carslaw HS, Jaeger JC (1959) Conduction of heat in solids. Second Edition, Oxford University Press

CGC (2010) Design and installation of residential ground source heat pump systems. Canadian GeoExchange Coalition

CIBSE (2013) Ground source heat pumps TM51:2013. Chartered Institute of Building Services Engineers, London, UK

Claesson J, Javed S (2011) An analytical method to calculate borehole fluid temperatures for time-scales from minutes to decades. ASHRAE Trans 117(2):279–288

Coletto A, Sterpi D (2016) Structural and geotechnical effects of thermal loads in energy walls. Proc Eng 158:224–229

Colls S (2013) Ground heat exchanger design for direct geothermal energy systems. In: Department of Infrastructure Engineering, Melbourne School of Engineering. PhD thesis, The University of Melbourne, Melbourne, Australia, p 476

Colls S, Johnston I, Narsilio G (2012) Experimental study of ground energy systems in Melbourne, Australia. Aust Geomech 47(4):21–26

de Moel M, Bach PM, Bouazza A, Singh RM, Sun JO (2010) Technological advances and applications of geothermal energy pile foundations and their feasibility in Australia. Renew Sustain Energy Rev 14(9):2683–2696

di Donna A, Barla M (2016) The role of ground conditions on energy tunnels' heat exchange. Environ Geotech 3(4):214–224

di Donna A, Cecinato F, Loveridge F, Barla M (2017) Energy performance of diaphragm walls used as heat exchangers. Proc Inst Civil Eng Geotech Eng 170(3):232–245

do SL, Haberl JS (2010) A review of ground coupled heat pump models used in whole-building computer simulation programs. In: Proceedings of the 17th symposium for improving building systems in hot and humid climates, Austin Texas, August 24–25, 2010

Eskilson P (1987) Thermal analysis of heat extraction boreholes. Department of Mathematical Physics, University of Lund

Fisher DE, Rees SJ, Padhmanabhan SK, Murugappan A (2006) Implementation and validation of ground-source heat pump system models in an integrated building and system simulation environment. HVAC&R Res 12(sup1):693–710

Franzius JN, Pralle N (2011) Turning segmental tunnels into sources of renewable energy. Proc Inst Civil Eng Civil Eng 164(1):35–40

Gehlin SEA, Hellström G (2003) Influence on thermal response test by groundwater flow in vertical fractures in hard rock

Glassley W (2010) Geothermal energy: renewable energy and the environment. CRC Press, Florida, USA

GSHPA (2012) Thermal pile design installation and materials standards, Issue 1.0. Ground Source Heat Pump Association, Milton Keynes, UK, p. 85

Icconsulten (2005) Wirtschaftliche optimierung von tunnelthermieabsorberanlagen, grundlage-nuntersuchung und planungsleitfaden. 23.12.2005. Rev 1, 84 pp

Igshpa (2011) Ground source heat pump residential and light commercial: design and installation guide. International Ground Source Heat Pump Association, Oklahoma State University

Ingersoll LR, Zobel OJ, Ingersoll AC (1954) Heat conduction with engineering, geological and other applications. McGraw-Hill, New York

Johnston IW (2012) Geothermal energy using ground source heat pumps. In: New Zealand geothermal workshop 2012 proceedings, p 8

Johnston IW, Narsilio GA, Colls S (2011) Emerging geothermal energy technologies. KSCE J Civil Eng 15(4):643–653

Kakaç S, Yener Y (2008) Heat conduction, 4th Edition, Taylor and Francis Group, Boca Raton FL, USA

Klein SA, Beckman WA, Mitchell JW, Duffie JA, Duffie NA, Freeman TL, Mitchell JC, Braun JE, Evans BL, Kummer JP, Urban RE, Fiksel A, Thornton JW, Blair NJ, Williams PM, Bradley DE, McDowell TP, Kummert M, Arias DA, Duffy MJ (2017) TRNSYS 18: a TRaNsient SYstem Simulation program, the Solar Energy Laboratory, University of Wisconsin, Madison

Kürten S, Mottaghy D, Ziegler M (2015) Design of plane energy geostructures based on laboratory tests and numerical modelling. Energy Build 107:434–444

Lamarche L, Beauchamp B (2007) A new contribution to the finite line-source model for geothermal boreholes. Energy Build 39(2):188–198

Loria AFR, Laloui L (2016) The interaction factor method for energy pile groups. Comput Geotech 80:121–137

Loveridge F (2012) The thermal performance of foundation piles used as heat exchangers in ground energy systems. In: Proceedings of. University of Southampton

Loveridge F, Powrie W (2013a) Pile heat exchangers: thermal behaviour and interactions. Proc Inst Civil Eng Geotech Eng 166(2):178–196

Loveridge F, Powrie W (2013b) Temperature response functions (G-functions) for single pile heat exchangers. Energy 57:554–564

Loveridge F, Powrie W (2014) 2D thermal resistance of pile heat exchangers. Geothermics 50:122–135

Loveridge F, Amis T, Powrie W (2012) Energy pile performance and preventing ground freezing. In: Proceedings of the 2012 international conference on geomechanics and engineering (ICGE'12), vol 1, Seoul, August, 2012

Loveridge F, McCartney J, Narsilio GA, Sanchez M (2018) Energy geostructures: a review of analysis approaches, in situ testing and model scale experiments. Geomech Energy Environ

Lu Q, Narsilio GA (2018) Economic analysis of utilising energy piles for residential buildings. Energy (under review)

Lu Q, Narsilio GA, Aditya GR, Johnston IW (2017a) Cost and performance data for residential buildings fitted with GSHP systems in Melbourne Australia. Data Brief 12:9–12

Lu Q, Narsilio GA, Aditya GR, Johnston IW (2017b) Economic analysis of vertical ground source heat pump systems in Melbourne. Energy 125:107–117

Man Y, Yang H, Diao N, Liu J, Fang Z (2010) A new model and analytical solutions for borehole and pile ground heat exchangers. Intl J Heat Mass Transfer 53:(13–14):253–2601

Makasis N, Narsilio GA, Bidarmaghz A (2018) A machine learning approach to energy pile 756 design. Comput Geotech 97:189–203

Mimouni T, Laloui L (2014) Towards a secure basis for the design of geothermal piles. Acta Geotech 9(3):355–366

Narsilio G, Johnston I, Colls S, Bidarmaghz A, Valizadeh-Kivi A, Neshastehriz S (2012) Direct geothermal energy research and demonstration projects for Victoria, Australia In: Choi C-K (ed) Proceedings of the 2012 world congress on advances in civil, environmental, and materials research (ACEM'12), pp 2433–2446

Narsilio GA, Johnston IW, Bidarmaghz A, Colls S, Mikhaylovaa O, Kivi A, Aditya R (2014) Geothermal energy: introducing an emerging technology. In: Horpibulsuk S, Chinkulkijniwat A, Suksiripattanapong C (eds) Advances in civil engineering for sustainable development (ACESD 2014), pp 1–14, Suranaree University of Technology, Nakhon Ratchasima, Thailand

Narsilio GA, Francisca FM, Ferrero H, Bidarmaghz A, Serrano C, Carro Perez M, Makasis N, Delacoste E (2015) Geothermal energy in loess: a detailed numerical case study for Cordoba, Argentina. In: Manzanal D, Sfriso AO (eds) Proceedings of the XV Pan-American conference on soil mechanics and geotechnical engineering, XV PCSMGE 2015, pp 704–711, 15–18 November 2015, https://doi.org/10.3233/978-1-61499-603-3-704, Buenos Aires, Argentina

Narsilio GA, Bidarmaghz A, Disfani M, Makasis N (2016a) Geothermal exchange feasibility study—stage 2, p 59. Report to the Melbourne Metro Rail Authority, Victorian Government

Narsilio GA, Bidarmaghz A, Disfani M, Makasis N, Johnston I (2016b) Geothermal exchange feasibility study—stage 1, p 60. Report to the Melbourne Metro Rail Authority, Victorian Government

Narsilio GA, Bidarmaghz A, Johnston IW, Colls S (2018) Detailed numerical modelling of ground heat exchangers based on first principles. Comput Geotech (Accepted 5 May 2017)

Nicholson DP, Chen Q, Silva MD, Winter A, Winterling R (2014) The design of thermal tunnel energy segments for Crossrail, UK. Proc Inst Civil Eng—Eng Sustain 167(3):118–134

Ozudogru T, Olgun C, Senol A (2014) 3D numerical modeling of vertical geothermal heat exchangers. Geothermics 51:312–324

Pahud D (2007) PILESIM2, Simulation tool for heating/cooling systems with heat exchanger piles or borehole heat exchangers, user manual. Lugano, Switzerland, Scuola Universitaria Professionale della Svizzera Italiana

Park S, Sung C, Jung K, Sohn B, Chauchois A, Choi H (2015) Constructability and heat exchange efficiency of large diameter cast-in-place energy piles with various configurations of heat exchange pipe. Appl Therm Eng 90:1061–1071

Preene M, Powrie W (2009) Ground energy systems: from analysis to geotechnical design. Geotechnique 59(3):261–271

Sharqawy MH, Mokheimer EM, Badr HM (2009) Effective pipe-to-borehole thermal resistance for vertical ground heat exchangers. Geothermics 38(2):271–277

Signorelli S, Bassetti S, Pahud D, Kohl T (2007) Numerical evaluation of thermal response tests. Geothermics 36(2):141–166

Soga K, Qi H, Rui Y, Nicholson D (2014) Some considerations for designing GSHP coupled geotechnical structures based on a case study. In 7th international congress on environmental geotechnics (7ICEG2014), Melbourne, 10–14th November, 2014

Southard LE, Liu X, Spitler JD (2014) Performance of the HVAC systems at the ASHRAE headquarters building—part 1. ASHRAE J 56(9):1–10

Stewart MA, McCartney JS (2014) Centrifuge modeling of soil-structure interaction in energy foundations. ASCE J Geotech Geoenviron Eng 140(4):04013044-1-11

Sun M, Xia C, Zhang G (2013) Heat transfer model and design method for geothermal heat exchange tubes in diaphragm walls. Energy Build 61:250–259

Wood CJ, Liu H, Riffat SB (2010) Comparison of a modelled and field tested piled ground heat exchanger system for a residential building and the simulated effect of assisted ground heat recharge. Intl J Low Carbon Technol 5(3):137–143

Zeng HY, Diao NR, Fang Z (2002) A finite line-source model for boreholes in geothermal heat exchangers. Heat Transfer - Asian Res 31(7):558–567

Zhang G, Xia C, Sun M, Zou Y, Xiao S (2013) A new model and analytical solution for the heat conduction of tunnel lining ground heat exchangers. Cold Reg Sci Technol 88:59–66

Zhang G, Xia C, Yang Y, Sun M, Zou Y (2014) Experimental study on the thermal performance of tunnel lining ground heat exchangers. Energy Build 77:149–157

Shale Gas: A Futuristic Non-conventional Energy Resource

Gunjan Kumar Agrahari and Sudha Agrahari

Abstract Global energy security is a major goal for rapid industrial progress. However, meeting the demand of energy and continuing the pace of industrial growth in future would depend on the sustainable economic development and simultaneously addressing the global climate change concerns. It is, therefore, necessary that alternate energy sources with reduced environmental footprints are discovered and developed on a commercial scale. In this scenario, shale gas could clearly be a "game-changing" resource that could transform the global energy market and contribute significantly to the national energy security of different countries. Various countries are considering the shale gas as a means to strengthen their energy security as well as an opportunity to reduce greenhouse gas emissions. However, the unconventional shale gas is present in low permeable rock formations. The extraction and production of shale gas as an economically profitable venture had so far, been difficult, with only the United States exploiting it at large scale. With the innovations in technology, and continuous improvements and advancements in production techniques such as hydraulic fracturing and horizontal drilling, shale gas is emerging as an attractive futuristic source of energy. The advanced technology has, therefore, made it possible to explore the shale reserves and its commercial extraction safe. Nonetheless, the worldwide development of shale gas-based energy production units would depend on collaboration and cooperation among different countries. The stakeholders having common energy goals can harness this futuristic energy resource after formulating a comprehensive framework that addresses various social, legal, environmental, geophysical, engineering, and technological challenges.

G. K. Agrahari (✉)
Department of Chemical Engineering, Engineering Science Division,
Rajiv Gandhi Institute of Petroleum Technology, Jais Campus, Amethi 229304, India
e-mail: gagrahari@rgipt.ac.in

S. Agrahari
Department of Geology and Geophysics, Indian Institute of Technology Kharagpur,
Kharagpur 729302, West Bengal, India
e-mail: sudha@gg.iitkgp.ernet.in

A. Sharma et al. (eds.), *Low Carbon Energy Supply*, Green Energy and Technology,
https://doi.org/10.1007/978-981-10-7326-7_19

Keywords Shale gas · Unconventional energy · Fracturing technologies
Geophysical reservoir characterization · Environmental challenges

1 Introduction

The natural gas trapped within the pores of sedimentary geological rock formations (known as shale plays) and produced by employing horizontal drilling and hydraulic fracturing technologies is commonly known as shale gas. Shale plays are both source and reservoir for unconventional shale oil or gas or both in combined form. The shale gas is found as adsorbed on the organic matter (kerogen), mostly thermogenic in origin (Löhr et al. 2015). The type of hydrocarbon would depend on the organic matter from which the deposits have been formed, and to the extent of maturation level. It can also be present as the free gas within the fractures or voids naturally found in the rocks. Shale deposits are largely found in fluvial, marine, and lacustrine environs, and are capable of holding a high amount of organic substances such as algae plants and marine organisms, which are cracked to generate hydrocarbons. In contrast, conventional natural gas reservoirs are formed by partial migration of these hydrocarbons below the structural and stratigraphic traps. The natural thermal processes carried over the buried organic substances lead to the maturation of these matters to unconventional oil or gas deposits. The unconventional shale gas, which is predominantly methane, is different from the conventional hydrocarbons with respect to the rock sources from which it is obtained. In addition to dominant methane, small volumes of ethane, propane, and butane can also be present in the shale gas. The structural complexities determining the shale matrices play a role in making these rocks either as seal, or reservoir. The shale gas thus formed is evaluated with respect to certain geological parameters; the important ones are thickness and areal extent of shale rocks, organic matter, thermal processes, mineralogy, natural faults, and adjacent underground water containing formations (Löhr et al. 2015).

The shale rocks are widely spread on the Earth's surface. The gas obtained from shale rocks is different from the conventional natural gas in the sense that shale formation rocks are dense sedimentary clay stones with low porosity and permeability compared to natural gas formations. Porosity in the shale rocks, in general ranges from 2 to 8%, rarely going beyond 14%, whereas permeability falls in the nanodarcy range (https://www.thomaswhite.com/wp-content/uploads/2012/08/img-shale-gas-the-fuel-for-future.jpg. Accessed on Feb 18, 2018). Due to the low porosity and very low permeability, extraction and production of gas from shale reservoirs is possible only after mechanically stimulating these dense rocks. With the applications of novel drilling and fracturing methods, the commercial production of gas from shale formations has become economically beneficial, thereby ushering an era of gas-based energy demands, that is being regarded as the game changer in the energy market (Shaffer et al. 2013). Since sustainable economic and industrial growth in future would depend on meeting the demand of energy and simultaneously addressing the global climate change concerns, it is necessary that alternate energy sources are discovered and developed on a commercial scale. With improvements in production technology, shale gas is emerging as an attractive future energy resource and by the year 2035, it is estimated to be nearly 90% of the total gas production in the United States of America (US) (Rahm and Riha 2012). As per the report published by The U.S. Energy Information Administration (USEIA), it is estimated that shale gas reserves throughout the world add 47% to the global technically recoverable natural gas resources; with 7299 TCF of shale gas and 345 billion barrels of shale oil in 41 countries (Brittingham et al. 2014). This huge shale deposit has the potential to achieve a drastic reduction in toxic emissions from conventional energy resources. The major countries such as US, China, and EU nations have been embarking on projects to extract the trapped gas from underground reservoirs. The profitable extraction of shale gas, however, depends on effectively addressing the concerns of negative environmental impacts that are associated with the commercial production. The energy policy drafted by a leading European think tank analyzes the possibility of adopting shale gas as a tool to transit into the era of low-carbon emission (Helm 2011).

2 Historical Perspective

As early as nineteenth century, shale gas production was attempted, however because of huge costs involved, the commercial production had to wait till the emergence of hydraulic fracturing techniques that could attain huge production volumes. The United States (US) is the pioneer country to extract shale gas for commercial use. William Hart is regarded as the pioneering person who drilled the first commercial gas well in 1821 in the shale formations located in the state of New York in the US. Floyd Farris and J. B. Clark were the two engineers who initiated the hydraulic fracturing technology in the year 1920 (https://www.thomaswhite.com/wp-content/uploads/2012/08/img-shale-gas-the-fuel-for-future.jpg. Accessed on Feb 18, 2018). The technology soon enabled large-scale gas production, and with further research and improvement, the shale gas field development was initiated in the states of Kentucky, Michigan, Ohio, and Indiana. With an average production ranging from 5 to 6 billion m^3 per year, these locations became the primary source of gas by the end of the twentieth century with gas occurring at shallow levels (Fig. 1).

During the 1940s decade, exploration and extraction were carried out at large scale in America. Hydraulic fracturing technique was employed in the Klepper play in Kansas State, and also in Oklahoma and Texas by several companies, followed by large-scale fracking in the decades to follow. Comprehensive research was also conducted in the subsequent years to enhance the production efficiencies of these plays. The “Eastern Project” conceived by the Energy Research Center (Morgantown) and supported by the US Department of Energy in 1976, conducted investigations on hydraulic fracturing to explore the various unconventional

Fig. 1 Sedimentary shale rock (https://www.thomaswhite.com/wp-content/uploads/2012/08/img-shale-gas-the-fuel-for-future.jpg. Accessed on Feb 18, 2018)

hydrocarbon resources (https://www.thomaswhite.com/wp-content/uploads/2012/08/img-shale-gas-the-fuel-for-future.jpg. Accessed on Feb 18, 2018). The starting of Mitchell Energy & Development Company in the 1980s by George P. Mitchell was a significant milestone in the commercial production of shale gas. The other prominent corporations during that period that were engaged in the exploration and production of shale gas included *BP, Royal Dutch Shell, Total, Statoil, Apache, Devon Energy,* and *Noble Energy*. The leader of these corporations was *Chesapeake Energy* of Oklahoma. The company possessed several plays and was a shareholder in Barnett, Fayetteville, Bossier, Haynesville, and also Marcellus Shales (https://www.thomaswhite.com/wp-content/uploads/2012/08/img-shale-gas-the-fuel-for-future.jpg. Accessed on Feb 18, 2018).

3 Shale Gas Production: Current Status

Various estimates and projections report that in the US the gas is so abundant that it will soon replace the natural gas, and make the US a gas exporter from her current status of fossil fuel importer. There is enough resource in the US that can last for this century. The immediate outcome would be on energy prices globally, with implications on European and Chinese energy supplies. It is estimated that beyond the year 2020, global energy players such as Europe, Russia, and India would also become leading gas producers besides the US. Shale gas is expected to add 7299 trillion cubic feet (TCF) to the global gas deposits by the year 2035 when the consumption would increase threefold. This figure is much higher with respect to the projected 6614 TCF of gas obtainable from conventional reserves. Except for the US which has become self-sufficient in gas production, other countries are dependent on exports to meet their energy needs. This leads to fluctuations in global energy prices. However, many of these countries have their own shale reserves which are at various stages of exploitation, and product development. The US with considerable shale gas reserves is undoubtedly the current global leader with significant impact on gas market prices. In the year 2013, the shale gas made up to 35% of the total natural gas production in the US. The main shale plays (geographic production regions) in the US are located in Barnett, Eagle Ford, Fayetteville, Haynesville, Marcellus, and Woodford (Shaffer et al. 2013; Brittingham et al. 2014). The production from these plays has led to the generation of a large number of jobs and have made huge contributions to the nation's GDP (Cooper et al. 2016). This has also resulted in the decline of energy prices over the world and turned the country from a gas importer to its exporter. With the falling prices of gas positively impacting the overall economic prospects, the new industrial and investment opportunities came up in the US and significant investments were achieved in chemicals and manufacturing sectors. It is projected that the country would become a leading hub of commodities manufacturing with $72 billion of investment by 2020, and creation of one million jobs by 2025 (Brittingham et al. 2014; Cooper et al. 2016).

In China, a government study estimates that the country has the largest shale gas reserves in the world (Chang et al. 2012). It is projected that the total gas reserves—at 25.08 trillion m^3, are nearly 200 times the annual consumption. A large part of China's shale gas reserves is located in the geographic regions of Sichuan and Tarim (Xinjiang) basins in the southwestern and northwestern China (Chang et al. 2012). The country has set a target of 60 billion m^3 of shale gas production by 2020. Once exploited, this gas can drastically reduce the Chinese import burdens and her dependence on coal. In Europe, the rocky geographic region extending from Poland across the planes of Northern Europe, and from under the North Sea to Britain comprises of shale gas reserves (Helm 2011). However, there are some key issues to be resolved before Europe matches to US production level of shale gas. The European regions have not been extensively seismically surveyed with regards to shale gas exploration. Moreover, a complex regulatory framework is required prior to its commercial extraction which can address the issues of land ownership, property rights, resource planning, and utilization of water resources. It is expected that Europe would become a major player in shale gas production beyond 2020 (Helm 2011).

4 Technologies for Shale Gas Production

The most widely used method for shale gas production is hydraulic fracturing which is employed for extracting the gas from shale plays. A combination of several techniques—high volume fracturing, horizontal drilling, and slickwater fracturing using chemicals, which are generally adopted in American shale plays, have made the commercial production viable and profitable. Formation stimulation is another fracturing technique that does not use water-based fracturing fluids.

These stimulation techniques use explosives, or foams instead of water. In this section, we briefly discuss the common hydraulic fracturing technique which is predominantly used by major companies over the world.

4.1 Hydraulic Fracturing

In this technique, a liquid is employed to fracture the geological rock formations underneath which the gas is trapped. The fracturing fluid is pumped into the borewell at sufficiently high pressure so that the rock gets fractured at the end of the borehole. The pressure should be high enough to overcome the strength of the rock. Water is commonly employed as the pumping liquid, however, gelled crude oil, and gelled kerosene have also been used in the past. With the development of clay stabilizing agents, foams, and gelling agents, water-based aqueous fluids such as brine have become the choice for base fracturing fluid in the vast majority of fracturing operations. In high-temperature wells, gel stabilizers, and cross-linking agents are added to increase the viscosity of aqueous fracturing fluids.

The properties of shale plays vary with respect to their location, exhibiting unique characteristics for each play. This makes imperative to design and develop specific fracture technology for a particular play, which can be achieved by introducing a fracturing fluid into a specific composition suitable with regards to the operational characteristics of the play. Fracturing techniques using slickwater (see Sects. 4.2, 4.3), CO_2, N_2, or carbon dioxide foam have also been used in the plays across North America. Often a solid material, mainly consisting of sand, or ceramic is added to the fluid. This solid material is known as proppant and it is added to achieve the desired permeability. Slickwater is suitable for brittle rocks, whereas proppant addition is required for ductile reservoirs. Carbon dioxide fluids are also used in place of water to enhance the energy of gas expansion, which reduces the flowback time. In general, the frac fluid is made up of base fluid, additive chemicals, and proppant, with sometimes compressed N_2 or CO_2 added to enhance its energy to recover the fluid and reduce water consumption. In several places, water is not preferred as a base fluid because, in certain formations, it can be a disadvantage to gas production because of the specific mineral composition in that play. In several plays, the interaction between the rock and water-based fluid softens the rock which leads to embedment of the proppant and its reduced conductivity. In other rocks, excess water from the frac fluid can get trapped in the under-saturated formations because of the capillary retention (Gandossi and Estorff 2015). This phenomenon, known as water blocking, results in the loss of gas production due to the decrease in the gas permeability.

4.2 Hydraulic Fracturing Employing Water as the Base Fluid

Since water-based fluids are dominantly used for hydraulic fracturing, the technique is discussed in detail here. In this technique, water is mixed with friction reducing compounds. The technique called as slickwater fracturing is the widely adopted common method for good stimulation in shale gas production. Water is mixed with silica sand and other chemical additives to enhance the resistance to friction, and bacterial growth. A description of fluid additives is given in Table 1 (Arthur et al. 2008). Water makes to 98% or more in the frac fluid, with an overall concentration of additives in the range 0.5–2% (Fig. 2).

Table 1 Additives in fracturing fluid

Additive type	Main compound	Purpose	Common use of main compound
Acid	Hydrochloric acid or muriatic acid	For the fracturing of shale formations, acids are used to clean cement from casing perforations and drilling mud clogging natural formation porosity if any prior to fracturing fluid injection (dilute acids concentrations are typically about 15% acid)	Swimming pool chemical and cleaner
Biocide	Glutaraldehyde	Fracture fluids typically contain gels which are organic and can, therefore, provide a medium for bacterial growth. Bacteria can break down the gelling agent reducing its viscosity and ability to carry proppant. Biocides are added to the mixing tanks with the gelling agents to kill these bacteria	Cold sterilant in healthcare industry
Breaker	Sodium chloride	Chemicals that are typically introduced toward the later sequences of a frac job to “break down” the viscosity of the gelling agent to better release the proppant from the fluid as well as enhance the recovery or “flow back” of the fracturing fluid	Sodium chloride is also used as a food preservative
Corrosion Inhibitor	N,n-dimethylformamide	Used in fracture fluids that contain acids; inhibits the corrosion of steel tubing, well casings, tools, and tanks	Used as a crystallization medium in pharmaceutical industry

(continued)

Table 1 (continued)

Additive type	Main compound	Purpose	Common use of main compound
Crosslinker	Borate salts	There are two basic types of gels that are used in fracturing fluids; linear and cross-linked gels. Cross-linked gels have the advantage of higher viscosities that do not break down quickly	Non-CCA wood preservatives and fungicides
Friction reducer	Petroleum distillate or mineral oil	Minimizes friction allowing fracture fluids to be injected at optimum rates and pressures	Cosmetics including hair, make-up, nail, and skin products
Gel	Guar gum or hydroxyethyl cellulose	Gels are used in fracturing fluids to increase fluid viscosity allowing it to carry more proppant than a straight water solution. In general, gelling agents are biodegradable	Guar gum is a food-grade product used to increase the viscosity and elasticity of foods such as ice cream, and salad dressings
Iron control	Citric acid	A sequestering agent that prevents precipitation of metal oxides	Citric acid is used to remove lime deposits. Lemon juice is approximately 7% citric acid
KCl	Potassium chloride	Added to water to create a brine carrier fluid	Low sodium table salt substitute
Oxygen scavenger	Ammonium bisulfite	Oxygen present in fracturing fluids through the dissolution of air causes the premature degradation of the fracturing fluid, oxygen scavengers are commonly used to bind the oxygen	Used in cosmetics
Proppant	Silica, quartz sand	Proppants consist of granular material, such as sand, which is mixed with the fracture fluid and is used to hold open the hydraulic fractures allowing the gas or oil to flow to the production well	Playbox sand, concrete or mortar sand
Scale inhibitor	Ethylene glycol	Additive to prevent precipitation of scale (calcium carbonate precipitate)	Automotive antifreeze and de-icing agent
Surfactant	Naphthalene	Used to increase the viscosity of the fracture fluid	Household fumigant (found in mothballs)

Source ALL Consulting, Tusla, Oklahoma online publication (presented without modification) (Arthur et al. 2008)

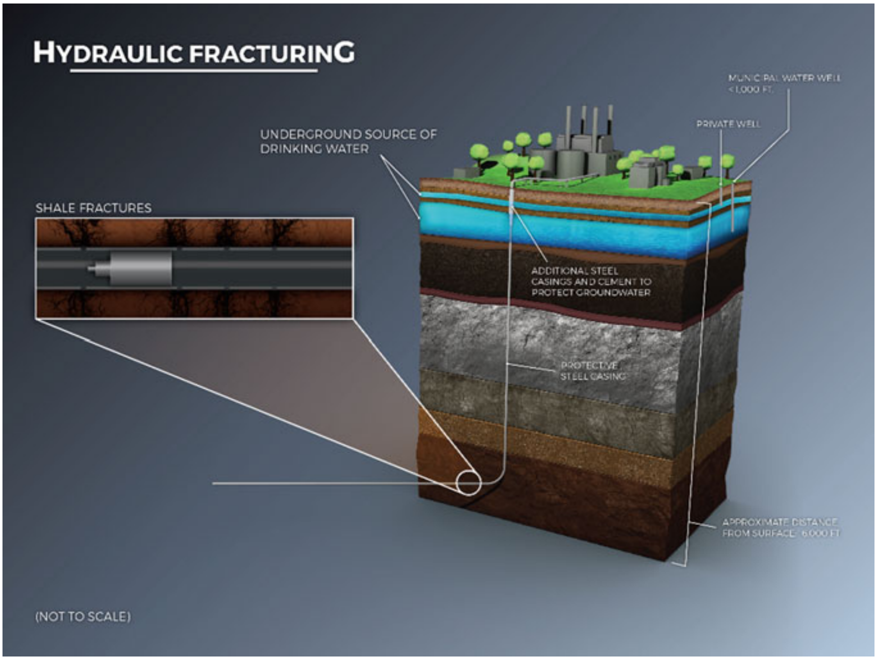

Fig. 2 Representation of stimulation of a shale gas reservoir by hydraulic fracturing technique. *Source* U.S. Department of Energy website—https://energy.gov; USDW—Underground source of drinking water

4.3 Slickwater Fracturing

Slickwater with low viscosity would form low width fractures. This results in long fractures with complex network and enhanced reservoir-to-wellbore connectivity (Gandossi and Estorff 2015). However, there is some drawback associated with slickwater. This fluid has the problem of settling of proppants, as it is a poor proppant carrier. Therefore, high pumping rates are required to maintain the necessary flow velocities in order to minimize the settling problem. Settling of proppant sand inside the equipment, or pipes may cause termination of fracturing process prematurely, leading to a loss in production. To overcome the problem of proppant settling, linear gel and cross-linked systems are added, however, this can decrease the required fracture complexity. In contrast, the advantages of slickwater fluids include lower damage of gel, higher stimulated reservoir volume, reduced cost with improved fracture containment (Mohanty et al. 2012).

In many cases, polymers are added to enhance fluid viscosity, friction reduction, and improving the properties of linear gels added to the fluid. High viscosity fluids are known as "linear fracturing fluids". Different types of polymers are added to water. These polymers are in dry powdered form. When these are added to water they get swelled producing a viscous gel. The rationale for forming the gel is to enhance the transport properties of proppant carrying frac fluid. Guar, hydroxypropyl guar, hydroxyethyl cellulose, carboxymethyl hydroxypropyl guar, and carboxymethyl hydroxyethyl cellulose are some common polymers used for gel formation (NSCEP 2004). Linear gels form thick filter cakes over the lower permeability rocks and are very effective in controlling the fluid loss. However, these gels are ineffective in high permeable rocks. To improve the overall fracturing performance cross-linked fluids are employed. Borate ions are used to crosslink the hydrated polymers. Such fluids have shown considerably improved performances in low, as well as high permeable shale formations, exhibiting high proppant transport, stable fluid rheology at high temperatures (300 °F), reduced loss of fluid, and improved cleanup (Gandossi and Estorff 2015).

4.4 Fracturing Using Viscoelastic Surfactant Gel Fluids

In viscoelastic surfactant (VES) gel fluids, surfactants are added and mixed with inorganic salts, to offer improved viscosity, proppant transport, and elasticity. The VES technology is further classified into sub-categories—worm-like micelles, lamellar structures or vesicles depending on the structure formed in the system (Gandossi and Estorff 2015). Micelles are formed in the fluid with the increase in surfactant concentrations in water. These micelles interact with each other because of the ionic forces. The ionic forces can further be increased with the addition of electrolytes or other salts and surfactants. Biocides, as well as additional clay control compounds and flow back surfactants, are not required in the VES technology.

Several new fracturing technologies such as zipper fracturing, cavitation hydro-vibration fracturing, hydra-jet fracturing, exothermic hydraulic fracturing, hydraulic fracturing enhanced by water pressure blasting have also been developed and described elsewhere (Gandossi and Estorff 2015; Yu and Sepehrnoori 2013; East LE Jr et al. 2004; Al-Nakhli et al. 2013; Huang et al. 2011).

5 Geophysical Characteristics of Shale Plays

The geophysical characterization of shale gas resource plays is quite different from the conventional reservoir characterization (Chopra et al. 2012). Shale gas formations are both the source rocks and reservoir rocks, and, therefore, migration is not necessary. Due to nearly zero permeability, it forms its own seal. In general, the shale gas is trapped in the form of free gas in natural fractures and intergranular porosity, in the form of sorbed gas into kerogen and clay particle surfaces, or in the form of dissolved gases in kerogen and bitumen (Curtis 2002). However, in the conventional reservoir, there exists a trap where the hydrocarbons are migrated but they develop at a different place. On the contrary, shale gas plays cover larger areas and contain varying amounts of hydrocarbons throughout that area. This is the reason that shale gas reservoirs require wider characterization (Duey 2012).

In order to map the geological surfaces and seismic stratigraphic relationships, and major faults and subtle structural trends, standard or conventional geophysical workflows continue to be significant in unconventional plays as well. The shale gas reservoir characterization workflows follow the similar methodology, for example, poststack attributes, such as coherence and curvature, are being successfully applied for mapping discontinuities and structural trends that may impact drilling, completion, or production (Close et al. 2012). Seismic is not only used as a tool for mapping structures in shale gas and unconventional plays. Its functioning has evolved far more than that. This is the only remotely sensed predrill data available, therefore 3D seismic data can be utilized in the planning of well sites by locating the intersect zones or “sweet spots” that are expected to have good gas storage. A well-defined well location allows optimal stimulation (i.e., the appropriate combination of lithological compressibility and rigidity, and an absence of major barriers to stimulated fracture propagation) (Close et al. 2012).

Well, logs contribute significantly to shale gas production since it links geology, geophysics, and petroleum engineering. Well, logs are utilized in the exploration phase for the identification of lithology, mineral types and compositions, total organic carbon (TOC), porosity, permeability, gas content, and the potential resources quantity. However, in the development stage, well logs data are used to calculate various parameters of geological and engineering purposes for horizontal drilling and production. These are used in hydraulic fracturing stimulation by estimation of the mechanical properties and determining the orientation and magnitude of the in-situ stress (Zhang et al. 2015).

The logging curves belonging to shale gas reservoirs indicate “three high and two low” phenomenon (Deng and Wang 2015). Acoustic wave and resistivity cross-plot method is the key technique for evaluation of shale gas by the application of logging curve combination technique. Due to the presence of rich hydrocarbons, dual laterolog resistivity logging of shale gas shows a low value. Higher values are indicated in acoustic time curve for shale gas. Acoustic time for shale is between sandstone and mudstone. In the presence of cracks and rich organic matter, the acoustic time curve shows even higher values. Natural gamma-ray and neutron porosity logs show high value for shale. The presence of organic matter enhances the radioactivity, which is indicated as high values in gamma-ray log curve. Furthermore, the shale consists of huge amount of clay shale, high irreducible water saturation, rich kerogen and natural gas as indicated in neutron porosity log. The density log curve indicates a low value for shale gas, however, in presence of cracks and rich organic matter the density log values are even smaller. The shale density is higher than coal and lower than sandstone.

The productivity of shale gas reservoir depends on the organic richness (TOC), maturation ($R_{0\%}$), thickness, gas-in-place, permeability, mineralogy, brittleness, and pore pressure of shale gas reservoirs (Chopra et al. 2012). Along with this the depth of the shale gas formation also plays a significant role as it will influence the economics of the gas recovery.

The core analyses for some reservoirs indicate a different correlation of TOC for silica-rich and clay-rich rocks. In such situations, two probable interpretations are being considered. For silica-rich rocks, TOC indicates a positive correlation with quartz content and a negative correlation with clay content. On the contrary, clay-rich rocks have a poor and negative correlation with clay and quartz contents, but positive correlation with calcite content (Zhu et al. 2011). Sample analysis results are used to predict the level of maturity (LOM) by computing the vitrinite reflectance ($R_0\%$). The LOM values vary from 6 or 7 to 12 depending on the type of organic matter. The reservoirs having LOM values close to 7 indicates the onset of maturity for an oil-prone kerogen and 12 points toward the onset of overmaturity for oil-prone kerogen.

6 Challenges and Issues

This is fundamentally important that a new energy resource should be environmentally clean, affordable, safe, and should be competitive in the market. Shale gas is projected to be the dream fuel of the future. Such debates have been carried out to discuss the sustainability criterion that is necessary for the shale gas to qualify as a futuristic clean source of energy. The development of new engineering methods for extraction has significantly reduced the production costs. The gas extraction has been made possible by applying sophisticated seismic mapping techniques to locate the gas spots, precisely followed by horizontal drilling and fracking process. During the fracking process, a huge amount of fresh water and toxic chemicals are required leading to depletion of water resources, and generation of wastewater. Other problems include leakage of methane from the underground rocks and adverse effects on the drinking water table. Shale gas is, however, regarded as a benign energy source compared to the currently dominant coal-based power plants. Coal exploitation is energy intensive and is associated with larger toxic emissions such as methane, ash, SO_x, and NO_x. The thermal efficiency of coal-fired power plants is low, require huge capital expenditure in mining and transportation of coal, and the loss of energy during transmission is high (Cooper et al. 2016). The huge shale gas deposits worldwide offer a vast opportunity to tap this resource to the benefit of society. The exploration and extraction techniques for producing shale gas should, therefore, be developed in such a way so that the risks associated with conventional energy resources can be minimized.

6.1 Water Management Issues

Production of shale is associated with a large number of threats to the environment because a huge amount of nearby fresh water is required for fracturing the shale to allow hydrocarbons reach the surface. A study conducted by World Resources

Institute (WRI) in several countries estimated that nearly 38% of the area of shale reserves is located in arid regions, with 386 million people inhabiting these regions (Reig et al. 2014). The report further states that 19% reserves are located in areas of high or extremely high seasonal variability. Nearly 15% areas of shale reserves are exposed to high or extremely high drought severity. The major environmental and social challenges would be crucial in framing policies for the commercial production of shale gas. Moreover, the limited freshwater availability for shale gas production would also have to compete with the irrigational, municipal, and industrial demands in many countries. Variations in hydrological conditions with respect to spatial and seasonal changes across shale plays, or within plays, occur throughout the year and can lead to uncertainties in predicting the demand for freshwater for hydraulic fracturing and drilling (Reig et al. 2014). These uncertainties can adversely affect the business of the companies. Public concerns and stress on freshwater resources can also threaten a company's social license to operate. Furthermore, because of social and environmental impacts government regulations can change thereby affecting the short- and long-term investments.

Shale gas production leads to the generation of high salinity water that comes to the surface from the underground formations. Flowback water from the hydraulic fracturing, as well as the formation water, comprise the waste stream of water called as produced water (Shaffer et al. 2013). Flowback water generally returns during the initial weeks of fracturing whereas formation water is continuously obtained during a well's lifetime. Approximately 8000–15,000 m^3 of water may be consumed during drilling and fracturing of a shale gas well, e.g., as per historical data, median water use during good development in Texas region of US can range over 11,000–22,000 m^3, whereas in Marcellus shale region this can range over 8000–27,000 m^3. There are many factors which govern the management of water during good development. Depending on the volume and water quality, legal framework of the region, geological characteristics of shale play, and the availability of resources the management of water can be carried out. In the US where large-scale production of shale gas has been achieved, currently, a huge amount ($\sim$98%) of produced water is injected underground. This is done in order to maintain pressure within the geological formations. Small portions (of higher quality) are also discharged to surface water sources, for livestock watering, and for irrigating the farmlands. More recently, this water can be cleaned and employed for reuse in the good development.

The quality of produced water during good development is very poor. For carrying out hydraulic fracturing of shale formations, a fracturing fluid is prepared by mixing water with certain chemicals, and sand. The chemicals used in this fluid are highly toxic and corrosive (see Sect. 4). Moreover, certain bacterial killing compounds are also added to the fluid which is highly hazardous and is a concern from the perspective of public health. If the shale plays are located near to drinking water sources, or if the produced water is disposed of without proper treatment, there is a likelihood of contamination of water sources meant for public consumption. Conventional wastewater treatment plants are inadequately equipped to control a number of toxic compounds such as bromides, naturally occurring radionuclides (NORMs), biocides (glutaraldehyde and quaternary ammonium chloride), etc., contained in produced water. In such plants, various chemical treatment agents can unwantedly react with dissolved impurities resulting in the formation of undesirable byproducts. Besides huge chemical doses can lead to overloading of these plants and finally to the improper quality of treated water. The discharge of such water to natural streams can adversely affect the marine ecosystem, and increase the toxicity levels of natural water. Moreover, during hydraulic fracturing, the fracturing fluid can leak through fissures and find a way to the underground water reservoirs, or surface water. The chances of surface water contamination through this route are very low because the shale plays are located very deep.

6.2 Geotechnical Issues

Shale plays and reservoirs can often be located close to groundwater aquifers. Hazardous chemicals are used during fracture stimulation which can contaminate the aquifer water (Cooke 2012). Methane can seep into groundwater sources through leaks in the fracture-stimulated wells. It can also leak through fugitive emissions from flowback water, or through equipment and pipeline leakages. There can also be natural thermogenic emissions of methane from the hydrocarbon sources across faults within the earth. There are other issues of induced seismicity —because of the injection of huge amounts of fracturing fluid. The high water volumes penetrating near "critical fault", can cause the fault to slip thereby resulting in an earthquake. The injected water should be flowed backward from the fractures prior to the occurring of gas flow. The flowback fracturing water dissolved may be contaminated with methane and salts, as well as traces of radioactive substances. This water needs to be disposed of as per existing environmental regulations. Another geological issue pertains to tectonic stresses. Several shale plays exist in regions known for extensional tectonic stresses (Cooke 2012). This can affect the development of shale wells because a higher level of stresses adversely impacts the stimulated reservoir volumes resulting in high costs of well. Various geological parameters and techniques of drilling and fracturing should be evaluated by the exploration groups in the regions of shale formations.

6.3 Environmental Issues

Since the year 2009, many environmental impact studies have been conducted to assess the direct impact of hydraulic fracturing. Shale gas (a source for electricity generation) is considered as an attractive replacement for coal-based power plants with expected reductions in greenhouse gas (GHG) emissions. The coal-fired power plants generated 1514 TWh electricity in the year 2012 in the US, which is significantly lesser compared to 2016 TWh generated in 2007. In the same period, gas-based generation rose from 897 to 1226 TWh which included power generated from shale gas as well as natural gas, with CO_2 emissions during electricity production decreasing to 2029 Mt from 2426 Mt (Stamford and Azapagic 2014). Researchers generally agree on the lower life cycle GHG emissions and related effects on climate for shale gas electricity, compared to coal-fired power plants (Cooper et al. 2016). Global warming potential, which is an indicator of climate change impact, has been reported in the range 412–1102 g CO_2 eq. per kWh in different studies, for shale gas-based electricity generation. The same value of the potential for coal-based electricity generation has been reported in the range 837–1130 g CO_2 eq. per kWh (MacKay and Stone 2013).

Methane emission is a potential threat that can increase the climate impact of shale gas. Fugitive emissions of methane occur during shale gas production. The sources of methane can be leakage from various production machinery and equipment, pipelines, and produced water, as well as venting of the gas during the gas development process. Methane is regarded as a menace during shale gas production because as per some studies, emissions nearing to 12% of total gas produced can nullify the benefits obtainable from shale gas compared to coal (Howarth et al. 2011). There are, however, certain mitigation strategies that can be employed to reduce methane emissions. The fugitive methane gas can be separated from wastewater without it being vented away for further use. Leakages can be located by the use of sophisticated cameras (BP p.l.c 2012).

Besides methane, there are several other emissions associated with shale gas production. These pollutants include NO_x, few hydrocarbons, and other volatile organics. Some fine silica particles are also released in the atmosphere. One of the major hazardous gases released is hydrogen sulfide (H_2S). The corrosive H_2S can corrode equipment and pipelines and is also a potential threat to human health. It is speculated that chemicals used in the fracturing fluid, and activity of some microorganisms in the formations could be the possible reason behind the H_2S release. Another environmental problem that has been identified during shale gas extraction relates to photochemical oxidants creation potential (POCP). This problem of photochemical smog, is primarily the result of VOC emissions, either during the sweetening process or from equipment. This drastically reduces the environmental benefits of using shale gas as it can possibly be 98 times worse than natural gas and 18 times worse than the coal power in the extreme scenario (Cooper et al. 2016).

During the gas development process, large chunks of land covered with natural vegetation are subjected to a land-use change which can increase the climate change impact of shale gas (Bond et al. 2014). As per an estimate, the development of shale gas production units on grassland can release 1.21 g CO_2 eq. per MJ of gas, compared to 13.41 g CO_2 eq. per MJ emissions from developments on peat soil (Cooper et al. 2016). Moreover, the huge amount of land area is required to establish a production unit which may lead to the possible destruction of natural forests, and adversely affecting the local ecosystem.

7 Conclusion

Shale gas as an alternative energy resource can have useful effects on the national economy with regards to benefits for industries, and generation of employment. This can lead to the development of fracturing and stimulating technologies, which, however, require huge capital inflow and technical know-how. It is imperative that the governments invest high expenditures on research prior to commercializing the extraction of shale gas and establishing it as an unconventional resource that is economically viable with profitable revenue earnings. The major environmental challenges have to be addressed before commissioning of production. However, other conventional energy resources such as coal, and oil are also associated with the issues of ecological contamination, air pollution, and seismic effects, and therefore environmental impacts of shale gas exploration and extraction have to be evaluated with respect to existing conventional energy production methods. The national government would be required to frame detailed and comprehensive policy and regulatory structure to address the various challenges.

Shale gas is an abundantly available energy resource with huge potential benefits for future energy security goals, but the diverse nature of the geography and geology of shale sources, as well as different energy needs of various countries, make it difficult to formulate a standard worldwide policy framework. However, considering the potential benefits of the unconventional resource and its positive effects on global energy security, proper collaboration and cooperation between countries as well as other stakeholders, such as industries, academic research groups, local inhabitants, and environmental groups can lead to the development of long-term standard procedures that can be implemented in different countries. The key to successful establishment of shale gas as a viable and futuristic energy resource would depend on international collaboration which is required to implement a comprehensive strategy for creating research and development infrastructure, addressing geophysical, and engineering issues for developing sustainable and cost-effective extraction technologies, as well as meeting the various social and environmental challenges in order to ensure unhindered long-term energy production.

References

Al-Nakhli AR, Abass HH, Al-Ajwad HA, Kwak HT, Al-Harith AM, Al-Otaibi A (2013) Unconventional gas stimulation by creating synthetic sweetspot. In: SPE unconventional gas conference and exhibition. Society of Petroleum Engineers, Muscat, Oman

Arthur JD, Bohm B, Coughlin BJ, Layne M (2008) Hydraulic fracturing considerations for natural gas wells of the fayetteville shale. In ALL Consulting: Tulsa, OK, US. https://steinlevy.com/files/20120606155241-NYLJ%20Reprint.pdf. Accessed on 18th Feb 2018

Bond CE, Roberts J, Hastings A, Shipton ZK, João EM, Kyzy JT, Stephenson M (2014) Life-cycle assessment of greenhouse gas emissions from unconventional gas in Scotland. ClimateXChange, Glasgow, Scotland, UK

BP p.l.c (2012) Unconventional gas and hydraulic fracturing: issue briefing. BP p.l.c., London

Brittingham MC, Maloney KO, Farag AM, Harper DD, Bowen ZH (2014) Ecological risks of shale oil and gas development to wildlife, aquatic resources and their habitats. Environ Sci Policy 48:11034–11047

Chang Y, Liu X, Christie P (2012) Emerging shale gas revolution in China. Environ Sci Technol 46:12281–12282

Chopra S, Sharma RK, Keay J, Marfurt KJ (2012) Shale gas reservoir characterization workflows. In: SEG Las Vegas 2012 annual meeting, Las Vegas, US

Close D, Perez M, Goodway B, Purdue G (2012) Integrated workflows for shale gas and case study results for the Horn River basin, British Columbia, Canada. Lead Edge 31(5):556–569

Cooke D (2012) A brief review of geoscience issues associated with shale gas development in Australia. University of Adelaide/Australian School of Petroleum, and ZDAC Geophysical Technologies, Australia

Cooper J, Stamford L, Azapagic A (2016) Shale gas: a review of the economic, environmental, and social sustainability. Energy Technol 4:772–792

Curtis JB (2002) Fractured shale gas systems. AAPG Bull 86:1921–1938

Deng X, Wang X (2015) Research status of shale gas evaluation methods. IOSRJEN 5(6):52–54

Duey R (2012) Geophysics has a role in shale plays. In: Center for wave phenomena. Department of Geophysics, Colorado School of Mines, Colorado, US

East LE Jr, Grieser W, McDaniel BW, Johnson B, Jackson R, Fisher K (2004) Successful application of hydrajet fracturing on horizontal wells completed in a thick shale reservoir. In: SPE eastern regional meeting. Society of Petroleum Engineers, Charleston, West Virginia

Gandossi L, Estorff UV (2015) An overview of hydraulic fracturing and other formation stimulation technologies for shale gas production. Joint Research Centre: European Union

Helm D (2011) Shale gas and the low carbon transition in Europe. demosEUROPA–Centre for European Strategy: Warsaw, Poland

Howarth RW, Santoro R, Ingraffea A (2011) Methane and the greenhouse-gas footprint of natural gas from shale formations. Clim Change 106:679–690

https://www.thomaswhite.com/wp-content/uploads/2012/08/img-shale-gas-the-fuel-for-future.jpg. Accessed on 18th Feb 2018

Huang B, Liu C, Fu J, Guan H (2011) Hydraulic fracturing after water pressure control blasting for increased fracturing. Int J Rock Mech Min Sci 48(6):976–983

Löhr SC, Baruch ET, Hall PA, Kennedy MJ (2015) Is organic pore development in gas shales influenced by the primary porosity and structure of thermally immature organic matter? Org Geochem 87:119–132

MacKay DJC, Stone TJ (2013) Potential greenhouse gas emissions associated with shale gas extraction and use. In: Department of energy & climate change, G. O. UK., Ed. London

Mohanty KK, Gaurav A, Gu M (2012) Improvement of fracturing for gas shales 07122-38 FINAL, Austin, Texas

NSCEP (2004) Evaluation of impacts to underground sources of drinking water by hydraulic fracturing of coaled methane reservoirs. In: N. S. C. f. E. P., Ed. United States Environmental Protection Agency, Washington, DC

Rahm BG, Riha SJ (2012) Toward strategic management of shale gas development: Regional, collective impacts on water resources. Environ Sci Policy 17:12–23

Reig P, Luo T, Proctor JN (2014) Global shale gas development: water availability and business risks. Washington, DC, USA

Shaffer DL, Chavez LHA, Ben-Sasson M, Castrillón SR-V, Yip NY, Elimelech M (2013) Desalination and reuse of high-salinity shale gas produced water: drivers, technologies, and future directions. Environ Sci Technol 47:9569–9583

Stamford L, Azapagic A (2014) Life cycle environmental impacts of UK shale gas. Appl Energy 134:506–518

Yu W, Sepehrnoori K (2013) Optimization of multiple hydraulically fractured horizontal wells in unconventional gas reservoirs. J Pet Eng 1–16

Zhang Y, Jin S, Jiang H, Wang Y, Jia P (2015) Review of well logs and petrophysical approaches for shale gas in Sichuan Basin, China. Open Pet Eng J 8(Suppl 1: M9):316–324

Zhu Y, Liu E, Martinez A, Payne MA, Harris CE (2011) Understanding geophysical responses of shale-gas plays. Lead Edge 30(3):332–338

Energy Awareness and Education: Needs and Challenges of Developing Low-Carbon Societies

Saurabh Mishra

Abstract World's growing energy demands have exacerbated the problem of rising carbon footprints around the globe. There has been a growing consensus that carbon emission can be contained and treated through socio-technical transitions. However, the prime challenge which is faced, at large, is to frame a vision beyond the approach of simply being satiated with containing the carbon levels and role reversals. Educating and making people aware about benefits of post-carbon societies both at the individual as well as global level in terms of wealth and job creations with an added accrual achieving sustainability can help to build integrated techno-societal low-carbon transition. Engaging the societies in the restructuring of energy can be combed out by rejuvenation of the prevalent societal heuristics. Education and awareness have an undoubted pivotal role in inducing behavioral changes, within the various level of stakeholders, in the society. To develop targeted energy-literate and empathized community, the idea should be engraved in designs which are focused upon proliferating awareness and also converting that awareness into societal practice. Conceptual schemata of societal entities can be trained and made energy transition-ready state by addressing and initiating an interaction within societies.

Keywords Energy awareness · Carbon footprints · Socio-technical transitions
Societal heuristics · Low-carbon societies

1 Building Low-Carbon Societies

World's growing energy demands have exacerbated the problem of rising carbon footprints around the globe. This has in fact led to induce the widespread occurrences of climate change impacts nowadays. Melting glaciers, rising sea levels along with aggravated (like never before) pollution levels have coaxed us untir-

---

S. Mishra (✉)
Rajiv Gandhi Institute of Petroleum Technology, Jais, Amethi, U.P, India
e-mail: smishra@rgipt.ac.in

A. Sharma et al. (eds.), *Low Carbon Energy Supply*, Green Energy and Technology,
https://doi.org/10.1007/978-981-10-7326-7_20

ingly. Yet the world has not much got over the choice of convenience. Low-carbon technologies their development, growth, and usage stand berated against the conventional energy replenishes. Climate change has in itself begun to breed the next biggest challenge against development agenda and policies (World Bank 2010; UNDP 2007). Abatement of carbon in energy utilization has often been recognized and summoned in the vision of world agencies in an effort to avoid flushing of the threshold limit of carbon footprint (Anderson and Bows 2008).

Building low-carbon cities have long being endured in vision. There has been a growing consensus that carbon emission can be contained and treated through socio-technical transitions. Over the past two decades, there has evolved a convincing work and opinion that low-carbon technologies transition and adoption is a slow process, which involves a great deal of contribution from a wide variety of areas including culture and belief systems (Kemp et al. 2007). Building low-carbon societies face a multitude set off a challenge on economic, technical, political, cultural, ethical, and infrastructural front. It is for sure, pretty visible that a large-scale societal maneuver is the only key to success. Stakeholders at all levels need to empathize with the cause. For change begets but resistance. Especially, by the end users of technologies. Vogue becomes an important agent in deferring the transition between technologies along with lack of awareness, knowledge, and education in society. Citizens of every society are indispensable cordons, who adorn roles across a vivid range of panorama; most important of the roles being the consumer of technology. Low-carbon societies are solely dependent on consumer habits and choices. Formation of low-carbon societies has a dual-pronged approach: (1) Containment and role reversals and (2) Technology transition and acceptability.

Containment and role reversals are the more popular and adapted approach by the societies; it includes—protecting and proliferating natural carbon sinks, viz., forests and wetlands (DFID 2009; Urban et al. 2011) and changing consumption patterns within the concurrent technologies. This helps to empathize and motivate societies to contribute to the collective well-being and global environment concerns. On the other hand, technology transition and acceptability stand plagued by doubts, viz., credibility, sustainability, financial implications, political agendas, misconstrued fathoms, lack of social vision, technological cohesion, and solidarity. Framing the vision beyond the approach of simply containing and role reversal is the prime challenge which is faced today at large.

Educating and making people aware about benefits of post-carbon societies both at the individual as well as global level in terms of wealth and job creations with an added accrual achieving sustainability can help to build integrated techno-societal low-carbon transitional vision. Governments and leaderships also need to pitch in the effort by shifting the focus on imposing limitations for exploring finite natural resources and pressing the lesser accelerator on economic growth. Thereby implicating policy of just/fair and equitable all-round human development, managing and reducing carbon footprints giving birth to—carbon redounding socio-technical regimes—“stable and ordered configurations of technologies, actors, and rules that represent the basis for social and economic practices" and includes "a complex web of technologies, producer companies, consumers and markets, regulations, infrastructures and cultural values" (Berkhout et al. 2010).

2 Capacity Building for Low-Carbon Societies

Societies need to be educated and made aware while preparing to transform to—clean energy/technology adoption. Capacity building is an important measure in making the opportunities grow within the societies, maturing them to the low-carbon ready status. Brewing "understanding abilities", within stakeholders through knowledge dissemination would help to generate empathy within societies. This would open a plethora of gates toward competency and skills acquisition; paving way for new job opportunities and economic as well as human and ecological excellence. Societal patterns and stakeholder configurations (such as user–producer relations and interactions, intermediary organizations, public authorities, etc.) are mutually dependent on and co-evolve with each other (Rohracher and Späth 2014). Hence, capacity building for achieving low-carbon societies serves as a cardinal affair at hand.

There is a popular view that societal capacity building through particular attention to knowledge management, reflection, and learning (Collins and Ison 2009; Tschakert and Dietrich 2010; Tanner et al. 2012) is important for mitigating climate change through low-carbon societies. Thus, impetrating community-level action is a potent resource for influencing energy and low-carbon behavior change (McKenzie-Mohr 2000; Middlemiss 2008; Peters and Jackson 2008; Heiskanen et al. 2009). But, current learning-based approaches are upfront with the various challenges as—"our existing methodological toolbox is sparsely equipped to facilitate and sustain such adaptive and anticipatory learning in the face of complex risks and uncertainties" (Tschakert and Dietrich 2010).

Engaging the societies in the restructuring of energy can be combed out by rejuvenation of the prevalent societal heuristics. Development of these new heuristics should aim to seek utmost compatibility in formulating—socio-technical and cultural empathy, toward low-carbon transitions. Targeted and deliberated efforts focused in spirit on achieving societal maneuver by acting upon stakeholders through motivation, improving habits, making low-carbon choices, framing clean energy attitudes and consumption patterns—would illuminate important dynamics having normative implications upon society. Geels (2002) in his effort to depict technological transition has proposed seven dimensions (Fig. 1) of the socio-technical regime: technology, user practices, and application domains (markets), the symbolic meaning of technology, infrastructure, industry structure, policy, and techno-scientific knowledge. The representation of multi-level perspective is not limited to being ontological reality mapping, but it is an analytical and heuristic framework decrypting the technological transition in society.

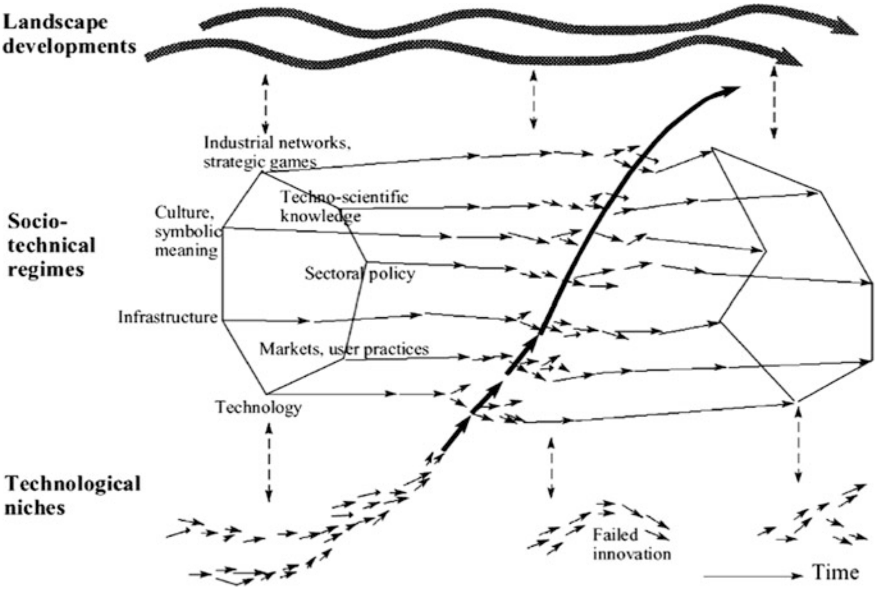

Fig. 1 Depicting the heuristics of social-technical transition (Geels 2002)

It is pertinent to note that technological transition in societies is a process which does not spring up as a surprise, it is a result of the continuous, deliberate, and stepwise process of reconfiguration of societal normative and vision. It, therefore, is not sudden and independent action, but the conflation of series of adaptations in which the older norms give way to the newer ones (Van den Ende and Kemp 1999; Summerton 1994). Traditionally, it has been expounded that existing systems have strong institutional interdependencies. Systems here could be described as "socio-technical configurations where technologies, institutional arrangements (for example, regulation, norms), social practices and actor constellations (such as user-producer relations and interactions, intermediary organizations, public authorities, etc.) mutually depend on and co-evolve with each other" (Rohracher and Späth 2014). Further, these can be decoded as socio-technical systems which have deeply intertwined characteristics which form-configurations that work (Rip and Kemp 1998). This sets up a dire task when capacity building (for low-carbon technologies) in societies is upfront; stakeholders prefer incremental innovations in existing systems as compared to reconfiguring the system as a whole (Markard and Truffer 2006, 2008). Hence, induction of a sea change can only be brought up if the alternative socio-technical systems form and stand their own independent coexisting structures within the society. When these new systems gain dominance over the older ones by exhibiting higher performance and sustainability indicators they are apt to be termed as "sustainability transitions" (Geels 2006a, b).

3 Social Learning and Knowledge Dissemination

The long history in energy consumption, patterns, and its transitions that the world stands witness to has been propelled by the need that the humans have encountered through their resolve to better evolve and develop (Bashmakov 2007). The recent critical need the human race is faced with is to reduce the carbon footprints and yet map the progress of civilization. As per the WEO special report (Fig. 2), the world's energy-related world carbon dioxide emission is slated to attain a rise from 32.2 billion metric ton in 2012 to 35.6 billion metric ton in 2020 and to 43.2 billion metric ton in 2040; an increase of 34% over the projection period.

The larger portion of these emissions continues to be attributed with developing non-OECD nations, many of which continue to rely heavily on fossil fuels to meet the fast-paced growth of energy demand. The scenario has almost remained the same in the context since the last report of WEO in 2016 (Fig. 3). Fourth Assessment Report of the Intergovernmental Panel on Climate Change (IPCC 2007) calls for an urgent reduction in carbon emissions by the inevitable restructuring of the socio-technical systems. Restructuring of social systems needs awareness and knowledge dissemination to happen successfully at a meta-scale. Society being a heterogeneous entity requires a multifarious and meticulous approach to be trained and made compatible with the new socio-technical systems.

Social learning theories have formed the backbone of the solution of imbibing societal changes through education and awareness. Sorensen's (1996) useful definition of learning within societies can be characterized as—a combined act of discovery and analysis, of understanding and giving meaning, and of tinkering and the development of routines. In order to make an artifact work, it has to be placed, spatially, temporally, and conceptually. It has to be fitted into the existing, heterogeneous networks of machines, systems, routines, and culture.

Fig. 2 World energy-related carbon dioxide emissions by fuel type, 1990–2040 in billion metric ton (International Energy Outlook Special Report, 2016, Fig. ES-8, p 06). *Source* U.S. Energy Information Administration

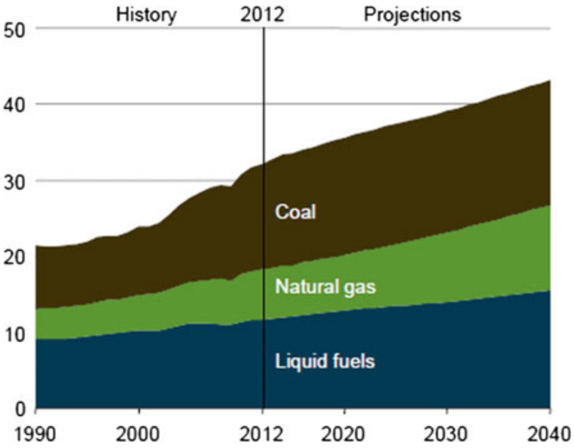

Fig. 3 Energy-related carbon dioxide emissions by country (Energy-Climate Map, World Energy Outlook Special Report, 2013, Fig. 1.11, p 30)

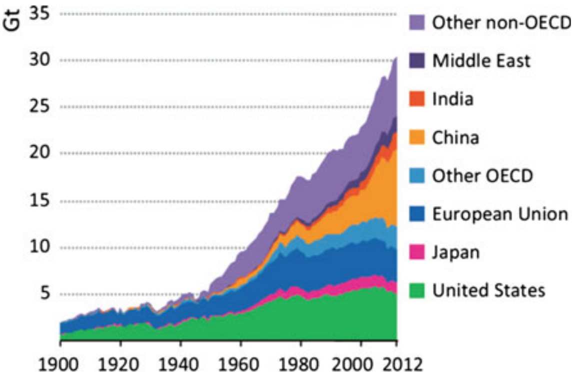

Arnstein's ladder of citizen engagement (Arnstein 1969) has been the most celebrated and trusted theory of the times. It has even been the fundamental contributor toward many other developed approaches on the similar lines. The concept of citizen participation needs to be reoriented not only just in terms of their participation but also in the manner of social learning, associated importance, and nature of the problem for which the socio-technical transformation reaps the solution. For this to understand the socio-technical regime becomes pertinent, which Geels (2002) explains as the interlinking of three different dimensions such as (a) network of actors and social groups, (b) regulative, normative, and cognitive rules, and (c) material and technical elements. Thus, develop an empowered, energy-literate, and empathized community, the idea should be engraved in designs which are focused upon proliferating awareness and also converting that awareness into societal practice.

Darby (2003, 2006a, b) delineates that energy awareness and education can be understood in terms of social learning theories, such that emphasis is laid on experimental and contextual elements of learning through informal interactions. Thereby stressing upon valuable knowledge conversion to action within societal groups by acting with communities instead of acting upon communities (e.g., Butcher et al. 2008; Adger 2003). In community sustainability projects aimed at inducing energy literacy among social groups, schools, and various education centers in accrual of their populace (Hart 1993; 1997; Zografakis et al. 2008) along with community's learned voices (mavens) and leadership (Barnett et al. 2009) form main actors of bring about the change. Social theories of practice have also been instrumental in suggesting ways of societal transformations. Reckwitz (2002) has explained practice theory as the existence of a practice depends upon the specific interconnectedness of many elements—forms of bodily activities, mental activities, things and their use, background knowledge in the form of understanding, know-how, and notions of competence, states of emotion, and motivational knowledge.

4 Inducing Behavioral Impact in Societies

Education and awareness have an undoubted pivotal role in inducing behavioral changes within the various level of stakeholders in the society. Education empowers an individual and in the denouement, the society is also empowered. United Nations (2005) has conferred that—education in addition to being a human right, is a prerequisite for achieving sustainable development and an essential tool for good governance, informed decision-making and the promotion of democracy. Therefore, education for sustainable development strengthens the capacity of individuals to make judgments and choices in favor of sustainable development. Building low-carbon societies is a key toward achieving energy sustainability.

The lack of energy knowledge can be regarded as being illiterate and innumerate (Newborough and Probert 1994, 1991). Also, the United Nations Commission on Environment Development (1992) had stressed that at school level—the teachers and their students should be exposed to concepts and methods of sustainable development. Compulsory primary and secondary level education and exposure to energy could produce more energy-literate society. Inducing energy sustainability culture and impact within societies is more powerful than pure technological advancements; “Energy squandering could be better remedied by education and legislation rather than advanced technological solutions. The probability of achieving sustainable future increases with the energy literacy of our society” (Newborough and Probert 1994). Thus, societies can be trained by education to instill energy thrift and efficient behavior and attitudes (Zografakis et al. 2007).

Behavioral models have also been helpful in understanding the why and how of consumer behavior toward new energy technologies and their adaptions. Attitude–behavior models have sought to express the engagement of an individual in a behavior based on their beliefs and ideas relating to the issues in question. In this continuation, the theory of reasoned action explains that people in society are guided in shaping their attitude and behavior by the antecedents (Fishbein and Ajzen 1975). While in real life, the consumer’s behavior does not conform to this theory; it is static and socially isolated from other fellow mates within the in society (Spaargaren and Van Vliet 2000). Ajzen (1991), in his theory of planned behavior, has impressed that norms in combination with social will are the underlying current which exercises control over an individual’s behavior and attitude. Wenger’s (1998, 2002) social theory of learning explains “communities of practice” as the group of “people who share a concern, a set of problems, or a passion about a topic, and who deepen their knowledge and expertise in this area by interacting on an ongoing basis”.

Pathway for capacity building and impacting behavioral changes in societies toward achieving a low-carbon status (Fig. 4) can be said to be largely dependent upon four basic tenets, viz., (1) Interactions, (2) Opportunities, (3) Knowledge, and (4) Empathy. Interactions within the social work well to construct/modify social heuristics positively by-exchange of opinion, tinkering, consumptions patterns, habit formations, motivation, etc. Opportunity creation by highlighting the

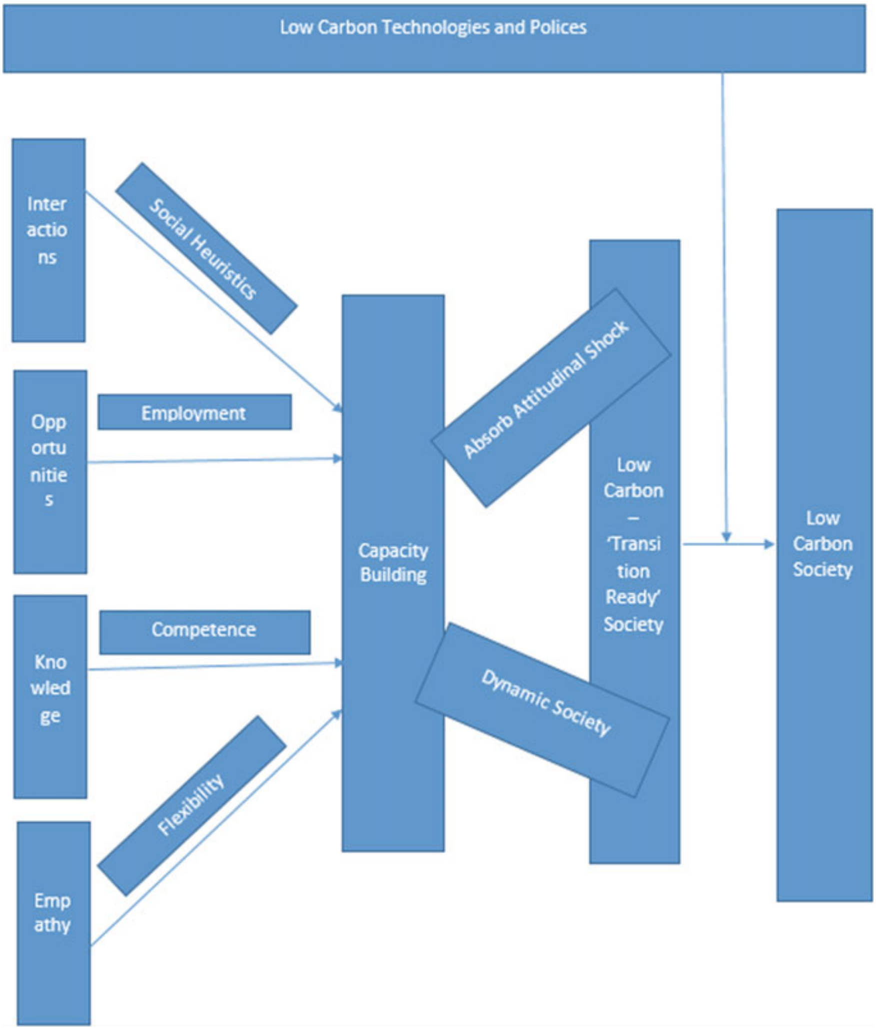

Fig. 4 Capacity building and socio-technical transition toward low-carbon societies

economic advantages of low-carbon technologies, along with skill acquisition and sectoral job openings would serve to empower the society to better embrace the technological change. Knowledge dissemination by engaging all academic and research institutions at a higher level along with primary and secondary education induction can play a game changer role and imbibe competence amongst social entities at all levels. Empathy is the most important component in the fast-moving information-bombarded world. Most of the policies and technological maneuvers fall flat even in the face of convincing evidence in their favor due to the lack of empathy.

Sensitization of people is also of extreme importance, to induce flexibility and adaptability to the change, without which the society behaves as indifferent and convenient oriented block.

5 Conclusion

Learning is imperative for building low-carbon societies. Knowledge dissemination should be such that it does not offer an attitudinal shock to the present and future stakeholders. Therefore, linking with all kinds of academic and research institutions at a very basic level should mark the initiation of the process. There should be theoretical (classroom) learning which is duly supported by experimental (real-time) exposure; imbuing the seeds of—"socio-technical transition-ready communities and societies". The ever-increasing gap between the awareness and knowledge of the consumers and the low-carbon market and policies can strongly —"inhibit the diffusion of carbon-saving technologies despite their apparent environmental and economic advantages" (Unruh 2000). This clearly earmarks that technology, policies, and the users/stakeholders should work to achieve a sync and trust mechanism. As Glad (2012) puts it, social learning should be symphonized with the following ingredients: user access to technology (physical and cognitive), communication (between users), trust (in technology and between users), social roles (of users), and co-production of technology. The future of building low-carbon societies heavily delegates upon user-technology partnership interactions within societies. The rigid understanding and convenience-based structure should burn and give way to flexibility. Schema of societal entities can be constructed as—"energy transition-ready". This change in heuristics should be dynamic in nature; static or "objective" transition-based approach would only conclude in another lock for future transitions. Thus, the demand of the world today is to spearhead a socio-technical transition such that the societal structure now and in future can embrace new technologies and be better facilitated.

References

Adger W (2003) Social capital collective action and adaptation to climate change. Econ Geogr 79(4):387–404

Ajzen I (1991) The theory of planned behavior. Organ Behav Hum Decis Process 50:179–211

Anderson K, Bows A (2008) Reframing the climate change challenge in light of post-2000 emission trends. Phil Trans R Soc A 366:3863–3882

Arnstein S (1969) A ladder of citizen participation. J Am Inst Planners 35:216–224

Barnett J, Brook Lyndhurst OLR (2009) The diffusion of environmental behaviors: the role of influential individuals in social networks, an investigation into the notion of 'green' mavens, with a view to identifying specific opportunities for communications and policy, report to DEFRA

Bashmakov I (2007) Three laws of energy transitions. Energy Policy 35(7):3583–3594

Berkhout F, Verbong G, Wieczorek AJ, Raven R, Lebel L, Bai X (2010) Sustainability experiments in Asia: innovations shaping alternative development pathways? Environ Sci Policy 13:261–271

Butcher H, Banks S, Henderson H, Robertson J (2008) Critical community practice. Oxford University Press

Collins K, Ison R (2009) Jumping off Arnstein's ladder: social learning as a new policy paradigm for climate change adaptation. Environ Policy Governance 19(6):358–373

da Graca Carvalho M, Bonifacio M, Dechamps P (2011) Building a low carbon society. Energy (Oxford), 36(4):1842–1847

Darby S (2003) Awareness, action and feedback in domestic energy use. Unpublished D. Phil thesis, Environmental Change Institute, University of Oxford

Darby S (2006a) The effectiveness of feedback on energy consumption. A review for DEFRA of the literature on metering, billing and direct displays. Environmental Change Institute, University of Oxford

Darby S (2006b) Social learning, household energy practice and public policy: lessons from an energy-conscious village. Energy Policy 34:2929–2940

DFID (Department for International Development) (2009) Eliminating world poverty: building our common future. DFID White Paper, London

Fishbein M, Ajzen I (1975) Belief, attitude, intention and behaviour: an introduction to theory and research. Addison-Wesley, Reading, MA

Geels FW (2002) Technological transitions as evolutionary reconfiguration processes: a multi-level perspective and a case-study. Res Policy 31:1257–1274

Geels FW (2006a) The hygienic transition from cesspools to sewer systems (1840–1930): the dynamics of regime transformation. Res Policy 35:1069–1082

Geels FW (2006b) System innovations and transitions towards sustainability: challenges for innovation theory, 14

Glad W (2012) Housing renovation and energy systems. Build Res Inf 40(3):274–289

Hart R (1993) Action research: the critical role of children's environmental education in community-based sustainable development. Educ Dev Bull 4(2)

Hart R (1997) Children's participation: the theory and practice of involving young citizens in community development and environmental care. UNICEF, New York and Earthscan, London

Heiskanen E, Johnson M, Saastamoinen M, Vadovics E (2009) How does consumer behaviour change? Examples from energy conservation. Future of the consumer society, Tampere, Finland

IPCC 2007 Climate change 2007: synthesis report. In: Team CW, Pachauri RK, Reisinger A (eds) Contribution of working groups I, II and III to the fourth assessment report of the intergovernmental panel on climate change. IPCC, Geneva, Switzerland

Kemp R, Rotmans J, Van Asselt M (2007) Assessing Dutch energy transition policy: how does it deal with dilemmas of managing transitions? J Environ Plan Policy Manage 9(3):315–331

Markard J, Truffer B (2006) Innovation processes in large technical systems: market liberalization as a driver for radical change? Res Policy 35:609–625

Markard J, Truffer B (2008) Technological innovation systems and the multi-level perspective: towards an integrated framework. Res Policy 37:596–615

McKenzie-Mohr D (2000) New ways to promote pro environmental behavior: promoting sustainable behavior: an introduction to community-based social marketing. J Soc Issues 56(3): 543–554

Middlemiss L (2008) Influencing individual sustainability: a review of the evidence on the role of community-based organisations. Int J Environ Sustain Dev 7(1):78–93

Newborough M, Probert D (1994) Purposeful energy education in the UK. Appl Energy 48:243–259

Newborough M, Getvoldsen P, Probert D (1991) Primary- and secondary level energy education in the UK. Appl Energy 40:119–156

Peters M, Jackson T (2008) Community action a force for social change? Some conceptual observations, RESOLVE working paper series, 01–08, University of Surrey

Reckwitz A (2002) Toward a theory of social practices: a development in culturalist thinking. Eur J Soc Theory 5(2):243–263

Rip A, Kemp R (1998) Technological change. In: Rayner S, Malone EL (eds) Human choice and climate change—Resources and technology. Battelle Press, Columbus. Printer Publisher Ltd., London, New York, pp 327–399

Rohracher H, Späth P (2014) The interplay of urban energy policy and socio-technical transitions: the eco-cities of graz and freiburg in retrospect. Urban Stud 51(7):1415–1431

Sorensen KH (1996) Learning technology, constructing culture: socio-technical change as social learning, STS working paper no. 18/96, Centre for Technology and Society, University of Trondheim, Trondheim

Spaargaren G, Van Vliet B (2000) Lifestyles, consumption and the environment: the ecological modernization of domestic consumption. Environ Polity 9:50–76

Summerton J (ed) (1994) Changing large technical systems. Westview Press, Boulder

Tanner T, Lockwood M, Seballos F (2012) Learning to tackle climate change. Institute of Development Studies, Brighton

Tschakert P, Dietrich KA (2010) Anticipatory learning for climate change adaptation and resilience. Ecol Soc 15(2):11

UN (2005) United Nations, Economic and Social Council, UNECE Strategy for education for sustainable development, CEP/AC.13/2005/3/Rev.1

UNCED (1992) United nations commission on environment development. The global partnership for environment and development: a guide to Agenda 21. Rio de Janerio, Brazil, 3–14 June 1992 https://sustainabledevelopment.un.org/content/documents/Agenda21.pdf

UNDP (2007) Human development report 2007/2008 fighting climate change: human solidarity in a divided world. United Nations Development Programme, New York

Unruh GC (2000) Understanding carbon lock-in. Energy Policy 28:817–830

Urban F, Mitchell T, Silva Villanueva P (2011) Issues at the interface of disaster risk management and low carbon development. Clim Dev 3(3):259–279

Van den Ende J, Kemp R (1999) Technological transformations in history: how the computer regime grew out of existing computing regimes. Res Policy 28:833–851a

Wenger E (1998) Communities of Practice—learning, meaning and identity. Cambridge University Press, Cambridge

Wenger E, McDermott R, Snyder WM (2002) Cultivating communities of practice. Harvard Business School Press, Boston, MA

World Bank (2010) World Development Report (2010) Development and climate change. World Bank, Washington, D.C.

Zografakis N, Dasenakis D, Katantonaki M, Kalitsounakis K, Paraskaki I (2007) Strengthening of energy education in Crete. In: Proceedings of SECOTOX conference and the international conference on environmental management, engineering, planning and economics, Skiathos, 24–28 June, pp 2933–2938

Zografakis N, Menegaki AN et al (2008) Effective education for energy efficiency. Energy Policy 36:3226–3232